



# CORAL REEF RESEARCH METHODS

EDITED BY: Shashank Keshavmurthy, James Davis Reimer and  
Nina Yasuda

PUBLISHED IN: Frontiers in Marine Science



# frontiers

## Frontiers eBook Copyright Statement

The copyright in the text of individual articles in this eBook is the property of their respective authors or their respective institutions or funders. The copyright in graphics and images within each article may be subject to copyright of other parties. In both cases this is subject to a license granted to Frontiers.

The compilation of articles constituting this eBook is the property of Frontiers.

Each article within this eBook, and the eBook itself, are published under the most recent version of the Creative Commons CC-BY licence.

The version current at the date of publication of this eBook is CC-BY 4.0. If the CC-BY licence is updated, the licence granted by Frontiers is automatically updated to the new version.

When exercising any right under the CC-BY licence, Frontiers must be attributed as the original publisher of the article or eBook, as applicable.

Authors have the responsibility of ensuring that any graphics or other materials which are the property of others may be included in the CC-BY licence, but this should be checked before relying on the CC-BY licence to reproduce those materials. Any copyright notices relating to those materials must be complied with.

Copyright and source acknowledgement notices may not be removed and must be displayed in any copy, derivative work or partial copy which includes the elements in question.

All copyright, and all rights therein, are protected by national and international copyright laws. The above represents a summary only. For further information please read Frontiers' Conditions for Website Use and Copyright Statement, and the applicable CC-BY licence.

ISSN 1664-8714

ISBN 978-2-83250-888-6

DOI 10.3389/978-2-83250-888-6

## About Frontiers

Frontiers is more than just an open-access publisher of scholarly articles: it is a pioneering approach to the world of academia, radically improving the way scholarly research is managed. The grand vision of Frontiers is a world where all people have an equal opportunity to seek, share and generate knowledge. Frontiers provides immediate and permanent online open access to all its publications, but this alone is not enough to realize our grand goals.

## Frontiers Journal Series

The Frontiers Journal Series is a multi-tier and interdisciplinary set of open-access, online journals, promising a paradigm shift from the current review, selection and dissemination processes in academic publishing. All Frontiers journals are driven by researchers for researchers; therefore, they constitute a service to the scholarly community. At the same time, the Frontiers Journal Series operates on a revolutionary invention, the tiered publishing system, initially addressing specific communities of scholars, and gradually climbing up to broader public understanding, thus serving the interests of the lay society, too.

## Dedication to Quality

Each Frontiers article is a landmark of the highest quality, thanks to genuinely collaborative interactions between authors and review editors, who include some of the world's best academicians. Research must be certified by peers before entering a stream of knowledge that may eventually reach the public - and shape society; therefore, Frontiers only applies the most rigorous and unbiased reviews.

Frontiers revolutionizes research publishing by freely delivering the most outstanding research, evaluated with no bias from both the academic and social point of view. By applying the most advanced information technologies, Frontiers is catapulting scholarly publishing into a new generation.

## What are Frontiers Research Topics?

Frontiers Research Topics are very popular trademarks of the Frontiers Journals Series: they are collections of at least ten articles, all centered on a particular subject. With their unique mix of varied contributions from Original Research to Review Articles, Frontiers Research Topics unify the most influential researchers, the latest key findings and historical advances in a hot research area! Find out more on how to host your own Frontiers Research Topic or contribute to one as an author by contacting the Frontiers Editorial Office: [frontiersin.org/about/contact](https://frontiersin.org/about/contact)



# CORAL REEF RESEARCH METHODS

Topic Editors:

**Shashank Keshavmurthy**, Biodiversity Research Center, Academia Sinica, Taiwan

**James Davis Reimer**, University of the Ryukyus, Japan

**Nina Yasuda**, The University of Tokyo, Japan

**Citation:** Keshavmurthy, S., Reimer, J. D., Yasuda, N., eds. (2022).

Coral Reef Research Methods. Lausanne: Frontiers Media SA.

doi: 10.3389/978-2-83250-888-6

# Table of Contents

- 06 Editorial: Coral Reef Research Methods**  
James Davis Reimer, Nina Yasuda and Shashank Keshavmurthy
- 11 Quantifying Coral Reef Resilience to Climate Change and Human Development: An Evaluation of Multiple Empirical Frameworks**  
Ashley H. Y. Bang, Chao-Yang Kuo, Colin Kuo-Chang Wen, Kah-Leng Cherh, Ming-Jay Ho, Nien-Yun Cheng, Yen-Chia Chen and Chaolun Allen Chen
- 23 High Clonality and Geographically Separated Cryptic Lineages in the Threatened Temperate Coral, *Acropora pruinosa***  
Supisara Pipithkul, Sota Ishizu, Akifumi Shimura, Hiroyuki Yokochi, Satoshi Nagai, Hironobu Fukami and Nina Yasuda
- 32 Genome-Wide SNP Data Revealed Notable Spatial Genetic Structure in the Deep-Sea Precious Coral *Corallium japonicum***  
Kenji Takata, Fumihito Iwase, Akira Iguchi, Hideaki Yuasa, Hiroki Taninaka, Nozomu Iwasaki, Kouji Uda, Tomohiko Suzuki, Masanori Nonaka, Taisei Kikuchi and Nina Yasuda
- 42 Genetic Structure of the *Goniopora lobata* and *G. djiboutiensis* Species Complex Is Better Explained by Oceanography Than by Morphological Characteristics**  
Nina Yasuda, Yuko F. Kitano, Hiroki Taninaka, Satoshi Nagai, Takuma Mezaki and Hiroshi Yamashita
- 54 In vitro Symbiosis of Reef-Building Coral Cells With Photosynthetic Dinoflagellates**  
Kaz Kawamura, Satoko Sekida, Koki Nishitsuji, Eiichi Shoguchi, Kanako Hisata, Shigeki Fujiwara and Noriyuki Satoh
- 65 Corrigendum: In vitro Symbiosis of Reef-Building Coral Cells With Photosynthetic Dinoflagellates**  
Kaz Kawamura, Satoko Sekida, Koki Nishitsuji, Eiichi Shoguchi, Kanako Hisata, Shigeki Fujiwara and Noriyuki Satoh
- 70 Spatial Autocorrelation Analysis Using MIG-seq Data Indirectly Estimated the Gamete and Larval Dispersal Range of the Blue Coral, *Heliopora coerulea*, Within Reefs**  
Daniel Frikli Mokodongan, Hiroki Taninaka, La Sara, Taisei Kikuchi, Hideaki Yuasa, Yoshihisa Suyama and Nina Yasuda
- 81 In situ Estimation of Coral Recruitment Patterns From Shallow to Mesophotic Reefs Using an Optimized Fluorescence Imaging System**  
Hagai Nativ, Federica Scucchia, Stephane Martinez, Shai Einbinder, Alex Chequer, Gretchen Goodbody-Gringley and Tali Mass
- 93 Application of RNA Interference Technology to Acroporid Juvenile Corals**  
Ikuko Yuyama, Tomihiko Higuchi and Michio Hidaka

- 100** *Phylogeography of Blue Corals (Genus Heliopora) Across the Indo-West Pacific*  
Hiroki Taninaka, Davide Maggioni, Davide Seveso, Danwei Huang, Abram Townsend, Zoe T. Richards, Sen-Lin Tang, Naohisa Wada, Taisei Kikuchi, Hideaki Yuasa, Megumi Kanai, Stéphane De Palmas, Nipphon Phongsuwan and Nina Yasuda
- 114** *Its What's on the Inside That Counts: An Effective, Efficient, and Streamlined Method for Quantification of Octocoral Symbiodiniaceae and Chlorophyll*  
Rosemary Kate Steinberg, Emma L. Johnston, Teresa Bednarek, Katherine A. Dafforn and Tracy D. Ainsworth
- 125** *Comparison of Standard Caribbean Coral Reef Monitoring Protocols and Underwater Digital Photogrammetry to Characterize Hard Coral Species Composition, Abundance and Cover*  
Erick Barrera-Falcon, Rodolfo Rioja-Nieto, Roberto C. Hernández-Landa and Edgar Torres-Irineo
- 138** *A Comparison of Size, Shape, and Fractal Diversity Between Coral Rubble Sampled From Natural and Artificial Coastlines Around Okinawa Island, Japan*  
Giovanni D. Masucci, Piera Biondi and James D. Reimer
- 146** *Underwater Light Characteristics of Turbid Coral Reefs of the Inner Central Great Barrier Reef*  
Ross Jones, Mari-Carmen Pineda, Heidi M. Luter, Rebecca Fisher, David Francis, Wojciech Klonowski and Matthew Slivkoff
- 168** *Novel Mitochondrial DNA Markers for Scleractinian Corals and Generic-Level Environmental DNA Metabarcoding*  
Chuya Shinzato, Haruhi Narisoko, Koki Nishitsuji, Tomofumi Nagata, Noriyuki Satoh and Jun Inoue
- 177** *Endosymbiont Communities in Pachyseris speciosa Highlight Geographical and Methodological Variations*  
Sudhanshi S. Jain, Lutfi Afik-Rosli, Bar Feldman, Ismael Kunning, Oren Levy, Ralph R. Mana, Benjamin J. Wainwright and Danwei Huang
- 189** *Integrated Population Genomic Analysis and Numerical Simulation to Estimate Larval Dispersal of Acanthaster cf. solaris Between Ogasawara and Other Japanese Regions*  
Mizuki Horoiwa, Takashi Nakamura, Hideaki Yuasa, Rei Kajitani, Yosuke Ameda, Tetsuro Sasaki, Hiroki Taninaka, Taisei Kikuchi, Takehisa Yamakita, Atsushi Toyoda, Takehiko Itoh and Nina Yasuda
- 201** *Bacterial Communities in Coral Offspring Vary Between in situ and ex situ Spawning Environments*  
Jia-Ho Shiu, Che-Hung Lin, Aziz Jabir Mulla, Viet Do Hung Dang, Chia-Ling Fong and Yoko Nozawa
- 212** *A Protocol for Extracting Structural Metrics From 3D Reconstructions of Corals*  
Eoghan A. Aston, Stephanie Duce, Andrew S. Hoey and Renata Ferrari

**226** *Consideration of Genetic Structure in the Ecologically or Biologically Significant Marine Areas Criteria: A Review of Convention on Biological Diversity Regional Workshops and A Case Study of Coral Reef Conservation Planning*

Takehisa Yamakita, Fumiaki Sodeyama, Akira Iguchi, Yuko F. Kitano, Kosuke M. Teshima, Akifumi Shimura, Aki Nakabayashi, Satoshi Nagai, Takashi Nakamura, Hiroaki Aizawa and Nina Yasuda

**240** *Fine Intervals are Required When Using Point Intercept Transects to Assess Coral Reef Status*

Chao-Yang Kuo, Cheng-Han Tsai, Ya-Yi Huang, Wei Khang Heng, An-Tzi Hsiao, Hernyi Justin Hsieh and Chaolun Allen Chen





## OPEN ACCESS

## EDITED AND REVIEWED BY

John Hiscott,  
Istituto Pasteur Italia Cenci Bolognetti  
Foundation, Italy

## \*CORRESPONDENCE

James Davis Reimer  
jreimer@sci.u-ryukyu.ac.jp  
Nina Yasuda  
ninayausda@gmail.com  
Shashank Keshavmurthy  
coralresearchtaiwan@gmail.com

This article was submitted to  
Coral Reef Research,  
a section of the journal  
Frontiers in Marine Science

## SPECIALTY SECTION

RECEIVED 23 November 2022  
ACCEPTED 29 November 2022  
PUBLISHED 13 December 2022

## CITATION

Reimer JD, Yasuda N and  
Keshavmurthy S (2022) Editorial: Coral  
reef research methods.  
*Front. Mar. Sci.* 9:1105688.  
doi: 10.3389/fmars.2022.1105688

## COPYRIGHT

© 2022 Reimer, Yasuda and  
Keshavmurthy. This is an open-access  
article distributed under the terms of  
the [Creative Commons Attribution  
License \(CC BY\)](#). The use, distribution  
or reproduction in other forums is  
permitted, provided the original  
author(s) and the copyright owner(s)  
are credited and that the original  
publication in this journal is cited, in  
accordance with accepted academic  
practice. No use, distribution or  
reproduction is permitted which does  
not comply with these terms.

# Editorial: Coral reef research methods

James Davis Reimer<sup>1,2\*</sup>, Nina Yasuda<sup>3\*</sup>  
and Shashank Keshavmurthy<sup>4\*</sup>

<sup>1</sup>Molecular Invertebrate Systematics and Ecology Lab, Faculty of Science, University of the Ryukyus, Okinawa, Japan, <sup>2</sup>Tropical Biosphere Research Center, University of the Ryukyus, Okinawa, Japan, <sup>3</sup>Aquatic Conservation Laboratory, Department of Ecosystem Studies, Graduate School of Agricultural and Life Sciences, The University of Tokyo, Tokyo, Japan, <sup>4</sup>Biodiversity Research Center, Academia Sinica, Nangang, Taiwan

## KEYWORDS

research methods, coral reef, ecology, physiology, molecular ecology

## Editorial on the Research Topic Coral reef research methods

## 1 Introduction

Coral and coral reefs are facing increasing existential threats to their existence as a result of stress from human-accelerated climate change and other various human pressures (Hughes et al., 2017; Le Nohäic et al., 2017; Hughes et al., 2019). Due to these increasing threats, there has been increase in the activity of researchers to understand the effects of various stressors, and also into examinations of how to mitigate and conserve corals and coral reef ecosystems into the future.

To accomplish such research, scientists employ various methodologies and techniques as part of their research protocols. However, often these methods and techniques are not standardized (Hughes et al., 2003), and in addition potentially important sampling schemes and/or effective methods may be overlooked (Weinberg, 1981; Plaisance et al., 2011; Alzate et al., 2014; McLachlan et al., 2020; Thurber et al., 2022), thus missing chances to increase the potential efficacy of the research being performed.

This special issue, “Coral Reef Research Methods”, is a collection of 20 original research papers. These papers can be broadly divided into three categories: 1) introductions to and explanations of new methods of coral reef research, 2) verifications of useful methods, including comparisons of old and new methodologies, and 3) exploratory papers examining the previously unexamined taxa or ecosystems, which can also provide insights into sampling schemes, research designs, and general coral reef biogeographic patterns. Here, in this editorial, we summarize the 20 papers included in this Research Topic, and add thoughts on the potential future directions of coral reef research methodologies.

## 2 Introductions to and explanations of new methods of coral reef research

Just over one-third of the papers (=7/20) in this Research Topic introduce novel methods for investigating coral reefs. These new methods range from ecological survey and field methodologies to *in vitro* and laboratory protocols, and are each briefly introduced below.

One of the chief struggles many coral reef researchers have faced is how to quantify and obtain meaningful data from the complex and often highly rugose structure of coral reefs. Included in this Research Topic are three different methods, each aiming to make the acquisition of field data from the intricate morphology of coral reef ecosystems easier and more accurate. A primary example is shown by [Aston et al.](#), who have developed protocols for extracting structural metrics from three-dimensional reconstructions of corals. Importantly, their results indicate that even a simple metric such as scleractinian coral colony diameter combined with morphotaxa information can explain the large majority of sheltering provisions of the colony. As well, six of seven morphotaxa appear to have similar habitat provisioning characters. These results indicate that despite the complex structure of individual coral colonies, calculations of habitat space may be governed by common rules, hinting at the development of powerful future ecological analytical methods; this paper represents an important step in this direction.

Similarly, [Masucci et al.](#) compared the size, shape, and fractal diversity of coral rubble from natural and artificial coastlines around Okinawa, Japan. The methodology utilizes free software and images, and was able to clearly discern between rubble from natural and artificial coastlines. With an increase in coastal armoring ([Masucci & Reimer, 2019](#)), and the importance of coral rubble in the provisioning of habitat space for infaunal organisms ([Masucci et al., 2021](#)), this method promises to become an important tool in environmental monitoring of coral reefs.

Recently, mesophotic coral ecosystems (MCEs) have been investigated in increasing detail, particularly with respect to the ecology, physiology, reproduction, and molecular ecology of scleractinian corals. [Nativ et al.](#) have optimized a protocol for the fluorescence imaging estimation of *in-situ* coral recruitment patterns from shallow to mesophotic depths. As dive and observation times are limited in MCEs, development and optimization of protocols such as their FluorIS method is timely. As this non-invasive method is based on a single camera, and increases speed over past methodologies, the understanding of coral recruitment patterns in MCEs should become more accessible into the future.

The remaining four papers in this subsection of this Research Topic span the bridge between *in situ* data collection and laboratory methods.

For example, [Steinberg et al.](#) have developed a new method for quantifying the endosymbiotic Symbiodiniaceae (=zooxanthellae) counts and chlorophyll concentrations for octocorals. While such methods already exist for Scleractinia, much less studies have applied these methods to octocorals and other anthozoans that are often major components of coral reefs to increase biodiversity ([Epstein and Kingsford, 2019](#)), and our understanding of even their basic biology lags behind that of Scleractinia. Efforts like [Steinberg et al.](#) are a welcome addition to better understand the total biodiversity of coral reefs.

Assessing coral diversity is one of the biggest challenges facing conservation efforts of coral reef ecosystems, particularly given the incredibly high diversity of these ecosystems ([Knowlton et al., 2010](#)), and also the ever-increasing loss of biodiversity ([De'ath et al., 2012](#)). [Shinzato et al.](#) provide new environmental DNA (eDNA) primer sets to better assess reef-building coral species *via* 12S and cytochrome oxidase subunit 1 (COI) sequences, and their initial analyses indicate high scleractinian specificity and utility. With the rapid development of the eDNA field, these primer sets should aid future efforts to more rapidly and accurately monitor coral reefs.

Conducting experiments on endosymbiotic zooxanthellae in culture has been severely limited by the inability to successfully establish *in vitro* cultures for the large majority of Symbiodiniaceae ([Santos et al., 2001](#); [Chakravarti and Van Oppen, 2018](#); [Wang et al., 2021](#)), and thus there are major gaps in our understanding of the cellular mechanisms of these symbionts. [Kawamura et al.](#) successfully developed an *in vitro* line of Symbiodiniaceae in symbiosis with coral cells for future experimentation and manipulation, representing a critical step forward in our ability to examine these keystone symbionts.

Finally, [Yuyama et al.](#) applied RNA interference technology involving gene knockdown to understand and modify the expression of genes involved in stress tolerance level and fluorescence emission in coral juveniles, providing an important molecular tool for future analyses of coral planulae and polyps.

## 3 Verifications of useful methods, including comparisons of old and new methodologies

Ecological research on coral reefs has a comparatively long history with the field of coral reef science, with numerous papers published through time. Despite this, there are still basic issues regarding standardizing monitoring and survey techniques. In this Research Topic, four articles (one-fifth of the total; 4/20 papers) have examined the verification and improvement of current methods, or compared more newly developed methods with older methods, as outlined below.

[Kuo et al.](#) have suggested improvement to one of the Point Intercept Count (PIC) methodology of examining coral reef

benthos *via* the proposing sampling at finer intervals than has been standard. In general, PIC examines the presence or absence of taxa at set intervals, often of 50 cm or 1 m, but the findings of Kuo et al. based on research from Taiwan suggest finer scale intervals of 10cm may be needed to more accurately obtain benthic community data.

Yamakita et al. applied the Ecologically or Biologically Significant Marine Areas (EBSA) concept from the Convention on Biological Diversity (CBD) to examine results in Japanese coastal waters considering coral cover change in association with climate change and including genetic diversity data of Scleractinia and blue corals. While such examinations are usually performed on charismatic or endangered megafauna, they can be equally applicable to other organisms. Their results indicated relative importance of temperate areas for the first time which was not obvious in the traditional assessments, but also highlighted sampling bias in the form of a general lack of data from warm temperate Japan, demonstrating the need for more in-depth genetic analyses of coral reef organisms.

Bang et al. compiled data from four different methods of resilience analyses on coral reefs in southern Taiwan, and compared results. While there was little agreement among the different datasets with each other, or with general baseline data, all indicated high resilience in the region, possibly due to the well-known occurrence of local upwelling. Surprisingly, “the most successful assessments were those that empirically quantified ecological processes and local factors with only a few indicators, rather than broader approaches that measured many indicators”, indicating that future, well-chosen datasets may provide broad analytical power in examining coral reef resilience.

Barrera-Falcon et al. compared coral data from an underwater digital photogrammetry protocol (UWP) of coral reefs in Cozumel, the Caribbean, with other, more commonly utilized methods including Point Intercept (PT), video transects (VT), and the Atlantic and Gulf Rapid Reef Assessment (AGRRA) protocol. Their results highlighted the sensitivity of the UWP method to colony abundance, species richness, smaller-sized species, and consistently returned a lower percentage coverage than other methods. As more researchers are increasingly using photogrammetry-based methods, such comparisons carry importance in understanding how best integrate these new methods into datasets.

## 4 Exploratory papers examining the previously unexamined taxa or ecosystems

Finally, just under half of the papers (=9/20) in this Research Topic can be broadly classified as “exploratory” research, newly investigating coral reef ecosystems or taxa. While such papers

may not be methods-based papers in the strictest sense, much can be learned from the methodologies and experimental designs they employ. Below, we briefly outline these papers.

Turbid inner bays and inshore reefs have drawn considerable attention because of terrestrial runoff and poor water quality (GBRMPA, 2020). Jones et al. examined the underwater spectral characteristics of inshore reefs on the Great Barrier Reef, and suggest that light monitoring frameworks are needed to better understand the threats to these ecosystems, particularly given their comparatively higher frequencies of turbidity events.

One common component of deeper reefs and turbid areas in the Indo-Pacific is the scleractinian genus *Pachyseris* (see DeVantier and Turak, 2017). Jain et al. examined the Symbiodiniaceae community associated with *Pachyseris* in the turbid reefs of Singapore and more pristine reefs of Papua New Guinea, finding notable differences in Symbiodiniaceae genera between locations, and highlighting the need to account for local environmental conditions in sampling schemes. Similarly, Shiu et al. demonstrated “spawning environments do not affect the bacterial composition in maternal colonies, but influence that of the offspring” in scleractinian corals, yet another indication of the importance of taking local conditions into account.

As shown by these studies, sampling designs are of great importance in biodiversity research. Recent advances in genetic analyses have enabled researchers to reveal cryptic genetic lineages in many different coral organisms (Bongaerts et al., 2011; Ladner and Palumbi, 2012; Yasuda et al., 2014; Nakabayashi et al., 2019; Richards et al., 2018). However, available local information sometimes causes confusion in the distribution of cryptic species and lineages. Taninaka et al. and Pipithkul et al. demonstrated population genetic and phylogeographic analyses covering wide ranges of coral distributions are promising and can provide important cues for patterns of speciation and diversification as well as the existence of possible past refugia. Likewise, population genetic analyses across different morphological species may indicate unexpected oceanographic boundaries (Yasuda et al.). Finally, Takata et al. examined fine-scale next-generation spatial genetic structure of the precious coral *Corallium japonicum*, showing up to dispersal scale of 11 km, thus demonstrating the need for conservation management at small and local scales.

Estimating larval dispersal ranges in ecological time-scales is critical for conservation and management, including in designing effective Marine Protected Areas, as many corals and coral reef organisms have pelagic larval dispersal. As such, there are many research papers on meta-population genetic structures of coral reef organisms based on population genetics and phylogeographic approaches. However, one of the issues that larval dispersal estimates based on genetic approaches have is that estimated meta-population genetic structures do not only reflect larval dispersal that occurred on ecological time scales but including structures that occurred during evolutionary time-

scales. Horoiwa et al. estimated the population genetic structure of the Crown-of-Thorns starfish *Acanthaster cf. solaris* across the Ogasawara and Kuroshio regions, finding that they were homogeneous through oceanic larval dispersal simulation, indicating direct migration of larvae from the Kuroshio region and Ogasawara is physically difficult and thus implicating stepping-stone migration patterns. This study highlighted the importance of assessing larval dispersal by multiple methods to accurately understand the time scales of larval dispersal when considering conservation management.

Mokodongan et al. empirically demonstrated dispersal distances in blue corals (*Heliopora* spp.) estimated by the intercept of spatial autocorrelation analyses well agreed with the dispersal distance directly estimated in the field using settlement tiles. The study also compared more traditional (microsatellite markers) and newer (genome-wide SNPs data using MIG-seq analyses) methods and demonstrated estimated dispersal distance did not change between the two methods, although more samples were required when using microsatellite analyses.

## 5 Thoughts on potential future directions of coral reef research methodologies and conclusions

The twenty contributions to this Research Topic span a wide range of fields, and summarizing the findings is a difficult task. Still, we can identify some general trends. Firstly, methodologies of coral reef research are becoming increasingly powerful and complex, yet are becoming easier to use, with results indicating broad general rules and trends that may yet emerge. In short, development and utilization of new methods will lead to an increasing rate of fundamental changes in our understanding of coral reef ecosystems. We can expect the future of coral reef science, despite facing the threats of climate change and increasing local stressors, to be one of key discoveries and advances in knowledge and conservation. Secondly, many of these original papers in the current collection demonstrate the importance of local conditions. Knowledge of small-scale settings and more holistic characterization of entire ecosystems will allow coral reef

researchers to learn from success stories and unique settings, providing yet more information for the fight to protect coral reefs into the future.

## Author contributions

SK, NY, and JR wrote, edited, and approved the final draft of the paper.

## Funding

NY was supported by the Japan Society for the Promotion of Science (grant numbers 17H04996, 19H03212, Grant-in-Aid for Research Fellows: 19J21342) and JSPS Bilateral Joint Research (JPJSBP120209929). SK is supported by a Postdoctoral Fellowship from Academia Sinica and the National Science and Technology Council (NSTC), Taiwan.

## Acknowledgments

Editors acknowledge all the authors who submitted their work to make this special issue a success.

## Conflict of interest

The authors declare that the research was conducted in the absence of any commercial or financial relationships that could be construed as a potential conflict of interest.

## Publisher's note

All claims expressed in this article are solely those of the authors and do not necessarily represent those of their affiliated organizations, or those of the publisher, the editors and the reviewers. Any product that may be evaluated in this article, or claim that may be made by its manufacturer, is not guaranteed or endorsed by the publisher.

## References

- Alzate, A., Zapata, F. A., and Giraldo, A. (2014). A comparison of visual and collection-based methods for assessing community structure of coral reef fishes in the tropical Eastern Pacific. *Rev. Biología Trop.* 62, 359–371. doi: 10.15517/rbt.v62i0.16361
- Bongaerts, P., Riginos, C., Hay, K. B., van Oppen, M. J., Hoegh-Guldberg, O., and Dove, S. (2011). Adaptive divergence in a scleractinian coral: physiological adaptation of *Seriatopora hystrix* to shallow and deep reef habitats. *BMC Evolutionary Biol.* 11 (1), 1–15. doi: 10.1186/1471-2148-11-303
- Chakravarti, L., and Van Oppen, M. (2018). Experimental evolution in coral photosymbionts as a tool to increase thermal tolerance. *Front. Mar. Sci.* 5, 227. doi: 10.3389/fmars.2018.00227
- De'ath, G., Fabricius, K. E., Sweatman, H., and Puotinen, M. (2012). The 27-year decline of coral cover on the Great Barrier Reef and its causes. *Proc. Natl. Acad. Sci. U. S. A.* 109, 17995–17999. doi: 10.1073/pnas.1208909109
- DeVantier, L., and Turak, E. (2017). Species richness and relative abundance of reef-building corals in the Indo-West Pacific. *Diversity* 9, 25. doi: 10.3390/d9030025



- Epstein, H. E., and Kingsford, M. J. (2019). Are soft coral habitats unfavourable? a closer look at the association between reef fishes and their habitat. *Environ. Biol. Fishes* 102, 479–497. doi: 10.1007/s10641-019-0845-4
- GBRMPA (2020). Position statement. water quality. Available at: <https://elibrary.gbrmpa.gov.au/jspui/handle/11017/3683>.
- Hughes, T. P., Baird, A. H., Bellwood, D. R., Card, M., Connolly, S. R., Folke, C., et al. (2003). Climate change, human impacts, and the resilience of coral reefs. *Science* 301 (5635), 929–933. doi: 10.1126/science.1085046
- Hughes, T. P., Barnes, M. L., Bellwood, D. R., Cinner, J. E., Cumming, G. S., Jackson, J. B. C., et al. (2017). Coral reefs in the Anthropocene. *Nature* 546, 82–90. doi: 10.1038/nature22901
- Hughes, T. P., Kerry, J. T., Connolly, S. R., Baird, A. H., Eakin, C. M., Heron, S. F., et al. (2019). Ecological memory modifies the cumulative impact of recurrent climate extremes. *Nat. Clim. Chang* 9, 40–43. doi: 10.1038/s41558-018-0351-2
- Knowlton, N., Brainard, R. E., Fisher, R., Moews, M., Plaisance, L., and Caley, M. J. (2010). “Coral reef biodiversity,” in *Life in the world's oceans: Diversity, distribution, and abundance*. Ed. A. D. McIntyre (Chichester: Wiley-Blackwell), 65–79.
- Ladner, J. T., and Palumbi, S. R. (2012). Extensive sympatry, cryptic diversity and introgression throughout the geographic distribution of two coral species complexes. *Mol. Ecol.* 21 (9), 2224–2238. doi: 10.1111/j.1365-294X.2012.05528.x
- Masucci, G. D., Biondi, P., and Reimer, J. D. (2021). Impacts of coastal armouring on rubble mobile cryptofauna at shallow coral reefs in Okinawa, Japan. *Plankton Benthos Res.* 16 (4), 237–248. doi: 10.3800/pbr.16.237
- Masucci, G. D., and Reimer, J. D. (2019). Expanding walls and shrinking beaches: loss of natural coastline in Okinawa Island, Japan. *PeerJ*. 7, e7520. doi: 10.7717/peerj.7520
- McLachlan, R. H., Price, J. T., Solomon, S. L., and Grottoli, A. G. (2020). Thirty years of coral heat-stress experiments: A review of methods. *Coral Reefs*, 39(4):885–902. doi: 10.1007/s00338-020-01931-9
- Nakabayashi, A., Yamakita, T., Nakamura, T., Aizawa, H., Kitano, Y. F., Iguchi, A., et al. (2019). The potential role of temperate Japanese regions as refugia for the coral *Acropora hyacinthus* in the face of climate change. *Sci. Rep.* 9, 1892. doi: 10.1038/s41598-018-38333-5
- Le Nohaïc, M. L., Ross, C. L., Cornwall, C. E., Comeau, S., Lowe, R., and Schoepf, V. (2017). Marine heatwave causes unprecedented regional mass bleaching of thermally resistant corals in northwestern Australia. *Sci. Rep.* 7, 14999. doi: 10.1038/s41598-017-14794-y
- Plaisance, L., Caley, M. J., Brainard, R. E., and Knowlton, N. (2011). The diversity of coral reefs: what are we missing? *PLoS One* 6 (10), e25026. doi: 10.1371/journal.pone.0025026
- Richards, Z. T., Yasuda, N., Kikuchi, T., Foster, T., Mitsuyukii, C., Stat, M., et al (2018). Integrated evidence reveals a new species in the ancient blue coral genus *Heliopora* (Octocorallia). *Scientific Reports*. 8(1):1–4.
- Santos, S. R., Taylor, D. J., and Coffroth, M. A. (2001). Genetic comparisons of freshly isolated versus cultured symbiotic dinoflagellates: Implications for extrapolating to the intact symbiosis. *J. Phycol.* 37 (5), 900–912. doi: 10.1046/j.1529-8817.2001.00194.x
- Thurber, R. V., Schmeltzer, E. R., Grottoli, A. G., Woesik, R., Toonen, R. J., Warner, M., et al. (2022). Unified methods in collecting, preserving, and archiving coral bleaching and restoration specimens to increase sample utility and interdisciplinary collaboration. *PeerJ* 10, e14176. doi: 10.7717/peerj.14176
- Wang, J., Chen, J., Wang, S., Li, F., Fu, C., and Wang, Y. (2021). Monoclonal culture and characterization of Symbiodiniaceae C1 strain from the scleractinian coral *Galaxea fascicularis*. *Front. Physiol.* 11. doi: 10.3389/fphys.2020.621111
- Weinberg, S. (1981). A comparison of coral reef survey methods. *Bijdragen tot Dierkunde* 51 (2), 199–218.



# Quantifying Coral Reef Resilience to Climate Change and Human Development: An Evaluation of Multiple Empirical Frameworks

Ashley H. Y. Bang<sup>1†</sup>, Chao-Yang Kuo<sup>1†</sup>, Colin Kuo-Chang Wen<sup>2</sup>, Kah-Leng Cherh<sup>3</sup>, Ming-Jay Ho<sup>1</sup>, Nien-Yun Cheng<sup>1,4</sup>, Yen-Chia Chen<sup>1</sup> and Chaolun Allen Chen<sup>1,2,5\*</sup>

<sup>1</sup> Biodiversity Research Center, Academia Sinica, Taipei, Taiwan, <sup>2</sup> Department of Life Science, Tunghai University, Taichung, Taiwan, <sup>3</sup> Sprouts Nature Education, Taichung, Taiwan, <sup>4</sup> Institute of Marine Biology, National Taiwan Ocean University, Keelung, Taiwan, <sup>5</sup> Department of Life Science, National Taiwan Normal University, Taipei, Taiwan

## OPEN ACCESS

### Edited by:

Nina Yasuda,  
University of Miyazaki, Japan

### Reviewed by:

Lyndon Mark DeVantier,  
Coral Reef Research, Australia  
Hironobu Fukami,  
University of Miyazaki, Japan

### \*Correspondence:

Chaolun Allen Chen  
cac@gate.sinica.edu.tw

<sup>†</sup>These authors have contributed  
equally to this work

### Specialty section:

This article was submitted to  
Coral Reef Research,  
a section of the journal  
Frontiers in Marine Science

**Received:** 25 September 2020

**Accepted:** 15 December 2020

**Published:** 13 January 2021

### Citation:

Bang AHY, Kuo C-Y, Wen CK-C,  
Cherh K-L, Ho M-J, Cheng N-Y,  
Chen Y-C and Chen CA (2021)  
Quantifying Coral Reef Resilience to  
Climate Change and Human  
Development: An Evaluation of  
Multiple Empirical Frameworks.  
*Front. Mar. Sci.* 7:610306.  
doi: 10.3389/fmars.2020.610306

The integrity of coral reefs has increasingly been threatened by human development and climate change. As a result, the concept of ecological resilience – an ecosystem's capability to resist and recover from environmental stressors – has become an important aspect of coral reef conservation. In this study, coral reef resilience was quantitatively scored in Kenting National Park (KNP), Taiwan, using four different assessment frameworks: the first uses the opinions of local reef experts, the second includes metrics specific to the local reef context, the third combines the previous two approaches, and the fourth relies solely on ecological metrics from biodiversity surveys. To evaluate the accuracy of each assessment, the resulting resilience scores were compared with historical coral recovery rates, which served as a proxy for resilience. While each approach to measuring resilience has its merits and drawbacks, the picture of resilience became clearest when a few key indicators were included to reflect core ecosystem processes. Trends in resilience scores varied depending on the makeup of the assessment's indicators, and there was little correlation between the baseline metrics measured using different data collection methods. However, all resilience assessment trends indicated that KNP's Nanwan area is high in resilience. This is likely due to the effects of local tidally-induced upwelling, which significantly relieve the growing thermal stress placed on surrounding coral communities. Ultimately, the most successful assessments were those that empirically quantified ecological processes and local factors with only a few indicators, rather than broader approaches that measured many indicators. These findings are particularly relevant for reef managers to consider as they develop and employ resilience-based management strategies.

**Keywords:** coral reef conservation, ecological resilience, resilience assessment, marine protected areas, Taiwan

## INTRODUCTION

Coral reefs are facing threats ranging from local to global scales: destructive fishing and water pollution degrades the integrity of local ecosystems (Meng et al., 2008), while climate change and ocean acidification hinders the survival and growth of coral communities worldwide [reviewed in Anthony (2016)]. During the recent third global bleaching event in 2014–2017, anomalously

warm sea surface temperatures led to the loss of one-third of the Great Barrier Reef's coral cover (Hughes et al., 2018). Coral reproduction output was severely inhibited over the following year, further hindering the recovery of coral communities (Heron et al., 2016). Such disturbances will continue to increase in both frequency and severity in the future, making coral reef conservation more crucial than ever. From a management standpoint, understanding both the historic and future responses of corals to these stressors is critical to identifying areas of resilience for coastal and marine conservation (Roche et al., 2018).

Ecological resilience was first defined by Holling (1973) as the ability of an ecological system to absorb change and disturbance while maintaining system stability. Since then, the concept of resilience has been expanded upon by other authors, whereby the resilience of a system is predicated on its return time to a stable state following a disturbance [reviewed in Gunderson (2000)]. Within coral reefs, the idea that a system can return to an alternative stable state following a disturbance has also been established, balancing a baseline state of coral cover dominance with a second, macroalgae-dominated state (Mumby et al., 2007). More recently, McClanahan et al. (2012) adapted this definition to further highlight two key components of reef resilience: resistance and recovery, both of which are tangible and relevant to management strategies (Nyström et al., 2008).

The concept of resilience to global environmental change has been a cornerstone of recent coral reef ecosystem management strategies, leading to the development of numerous frameworks for its quantification (hereon referred to as resilience assessments) (Anthony et al., 2014; Standish et al., 2014). Seeing as the management outcomes may be influenced by the definition of resilience applied, the present study uses the definition from McClanahan et al. (2012), which others have also adopted in their resilience assessments on reef systems (e.g., Cinner et al., 2013; Anthony et al., 2014; Maynard et al., 2015).

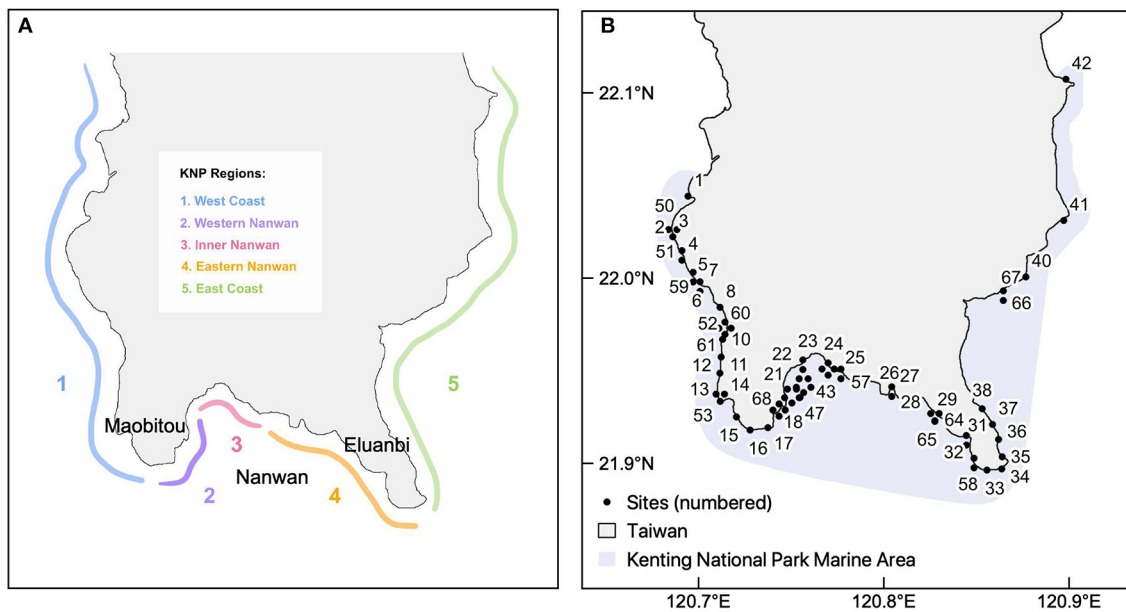
Typically, resilience is scored based on a set of indicators that represent aspects of ecosystem states, functions, or processes (Lam et al., 2017). These indicators range from being broad and standardized to localized and fine-scale (Lam et al., 2020). Reef resilience was first quantified in by the IUCN in 2009 (Obura and Grimsditch, 2009). The framework, which applies 61 indicators, is one of the most comprehensive standardized assessments to date (Obura and Grimsditch, 2009). Subsequent studies have used a wide variety of metrics, data collection methods, and scopes [reviewed in Lam et al. (2017)], ranging from field-based surveys of ecological processes (e.g., Gibbs and West, 2019) to the Bayesian modeling of historical reef data (e.g., van Woesik, 2013).

Resilience quantification has only recently been incorporated into management strategies, and thus there are few long-term datasets that monitor resilience (Standish et al., 2014). Some resilience assessments have instead utilized existing long-term reef monitoring datasets, particularly coral cover, as proxies or indicators for resilience (Cinner et al., 2013; Mumby et al., 2014; Lam et al., 2017; Guest et al., 2018). Following disturbances, reefs with high coral cover are believed to have high resilience, as the remaining population has tolerated past stressors and

is able to populate the next generation of recruits (Maynard et al., 2010). Coral cover data have been collected for decades to describe reef status and measure recovery from disturbances, making it ideal for use in quantifying resilience (West and Salm, 2003; Adjerooud et al., 2009; Sweatman et al., 2011). In particular, recovery rates calculated from coral cover have shown to be suitable instantaneous proxies for ecological resilience and recoverability (Lam et al., 2020).

On the other hand, a single indicator may not capture the multifaceted factors that underlie resilience, such as structural complexity, anthropogenic stressors, and ecosystem processes (Darling et al., 2019; Lam et al., 2020). To include these aspects, many resilience assessments include a wide variety of indicators extending beyond direct measures of coral population (Lam et al., 2017). Assessments also range in scope depending on the intended outcome and application. Broad-scope assessments, which have the advantage of being practical and accessible, typically utilize simplified scoring systems to qualitatively assess complex metrics (Lam et al., 2017; Gibbs and West, 2019; Obura and Grimsditch 2009). Some resilience assessments have also been tailored to suit the local environmental setting by starting with a previously established set of indicators and adding or removing indicators accordingly (Maynard et al., 2015; Gibbs and West, 2019). This approach makes use of existing taxonomically-specific survey data, hence improving the assessment's spatial and temporal resolution and rigor (Lam et al., 2017). Additionally, the inclusion of indicators that specifically represent the reef's capacity for resistance and recovery on a local level has been identified as a crucial component of effective resilience quantification (Maynard and Mcleod, 2012).

Despite the many resilience frameworks in existence, it is unclear whether the wide range of approaches yield similar resilience scores and conservation outcomes when applied to the same reef system. To address this gap, our study quantified the resilience of coral reefs in Kenting National Park (KNP), Taiwan, using four different frameworks. KNP is Taiwan's oldest established marine national park, and possesses high heterogeneity in environmental, biological, and anthropogenic factors that influence reef resilience across five park regions (Meng et al., 2008; Keshavmurthy et al., 2019) (**Figure 1A**). The reefs of KNP have demonstrated historical resilience to the impacts of climate change due to a variety of factors: (a) high genetic connectivity of corals within the West Pacific and South China Sea; (b) local tidally-influenced upwelling that ameliorates the effects of thermal stress; and (c) association with thermal-tolerant Symbiodinaceae (Chen and Keshavmurthy, 2009; Keshavmurthy et al., 2019). While these unique factors all contribute to the resilience of KNP's reefs to various climate change impacts, there has yet to be a quantitative assessment of resilience within this region. The four assessments used in this study apply a range of approaches and data collection methods, which are evaluated for the extent of overlap, or lack thereof, in resulting resilience scores and management implications. This investigation ultimately sheds light on which approaches allow for a practical yet accurate evaluation of resilience for direct application in reef management.



**FIGURE 1 |** The five geographical regions of the Kenting National Park in southern Taiwan (A) and the 68 study sites (black points) (B).

## MATERIALS AND METHODS

### Study Area

Located on the southernmost tip of Taiwan's Hengchun Peninsula, Kenting National Park (KNP) lies at the intersection of currents from the Bashi Channel, South China Sea, and Pacific Ocean. It is influenced by seasonal typhoon paths that approach Taiwan, mainly from the southeast [Dai, 1993; reviewed in Keshavmurthy et al. (2019)]. A section of the southern coast of KNP, Nanwan (meaning South Bay in Chinese, **Figure 1A**), is sheltered from typhoons and has highly localized tidally-induced upwelling throughout the year. This effect circulates cooler currents toward the surface and contributes to the high degree of ecological heterogeneity within KNP (Lee et al., 1999a,b). Additionally, KNP has a very low tidal range, with the difference between high and low tide in KNP being approximately one and a half meters.

In total, the park encompasses 152 km<sup>2</sup> of coastal waters, managed through four zoning types: protected, landscape, recreation, and general use (Chen et al., 2017). This zoning system was established in 1984 and last updated in 2014 (Ho et al., 2016). Overall, the marine park provides habitats for over 300 coral species, 1,015 reef fish species, and 146 shellfish species (Dai, 1997, 2018). KNP is also a very popular tourist destination in Taiwan; several hundreds of thousands of visitors partake in recreational water sports and land-based tourist activities annually in KNP, particularly in Nanwan (Chen et al., 2017). Western Nanwan also houses a nuclear power plant, which has been expelling hot water effluent onto the surrounding reefs since its construction in 1985 (Keshavmurthy et al., 2012). Consequently, corals within the power plant's vicinity are constantly exposed to temperatures 2–3°C higher than other park

areas (Keshavmurthy et al., 2012, 2019). These local factors make KNP a unique system to study both anthropogenic and ecological influences on reef resilience.

### Biodiversity Field Surveys

The following indicators were measured through a comprehensive biodiversity survey conducted in the summer of 2014: coral species richness and diversity (Simpson's index), coral recruitment [referring to the abundance of juvenile corals <5 cm in size, see Obura and Grimsditch (2009)], fish biomass, and macroalgae cover (see **Supplementary Table 1** for more detail). The biodiversity surveys were conducted at 68 reef sites in KNP, which were selected to represent coral communities along the coast at a high-resolution scale and reduce selection bias. Fifty-two sites were surveyed at 6-m depth, one at 10-m depth, nine at 15-m depth, and six at 25-m depth (**Figure 1B**). At each depth, the biological indicators were surveyed along a 60-m long transect haphazardly placed along the depth contours.

To survey adult coral assemblage composition and the abundance of coral recruitment, the 60-m transect was divided into four 10-m transects with 5-m intervals between transects. The same 60-m transect was divided into two 25-m transects with 5-m intervals to survey macroalgae abundance. Adult coral assemblage composition data were collected using the line intercept transect (LIT) method, coral recruitment was recorded along four 10-m × 0.5-m belt transects, and macroalgae abundance was measured using point intercept transects (PIT) at 0.5-m intervals along each 25-m transect [modified from the Reef Check protocol, see Hodgson et al. (2006)]. *Corals of the World* (Veron and Stafford-Smith, 2000) and *Scleractinia of Taiwan I*



and II (Dai and Horng, 2009a,b) were used as guides to identify coral species.

The relative biomass of fish was surveyed along the 60-m transect, divided into two 30-m long sections, using the underwater visual census method (English and Wilkinson, 1997). Fish abundances and the body lengths were recorded in each 30-m by 5-m by 5-m belt transect. *Marine Fishes in Kenting National Park* (Chen and Kwang, 2010) was used as a guide to identify each fish to the species level. The abundance of fish in KNP were not substantially affected by the time of day at which the survey was conducted. The relative biomass of total fish at each site was estimated by summing the cubed body length of each fish. Each of the biological indicators was either directly scored from one (lowest resilience) to five (highest resilience), or the field measurements were statistically scaled from 1 to 5. This combined scoring/scaling method has been commonly used in frameworks that apply both field-based and evaluative scoring methods (Obura and Grimsditch, 2009; McClanahan et al., 2012).

## Expert Opinion Workshop

In addition to the biodiversity survey data, resilience indicators were also scored via a workshop held with local coral reef experts. The expert opinion workshop capitalized on the multidecadal knowledge of reef experts and their holistic understanding of complex factors influencing coral reef resilience. They were asked to score 11 resilience indicators outlined in the evidence-based framework of McClanahan et al. (2012): coral diversity, coral recruitment, fish biomass, macroalgae, fishing pressure, resistant coral species, temperature variability, nutrients (pollution), sedimentation, physical human impacts, and coral disease (Table 1). The local reef experts scored the indicators for the same 68 sites on a 5-point Likert scale, with one denoting low resilience conditions and five denoting high resilience conditions as in the biodiversity surveys (McClanahan et al., 2012). Participants were also provided with detailed descriptions of scoring criteria from the IUCN's resilience assessment framework (Obura and Grimsditch, 2009, see **Supplementary Table 2**). Since Taiwanese coral reef ecology is a relatively small discipline, only four local experts possessed the requisite knowledge to perform the comprehensive evaluation required for the assessment. Though having so few workshop participants may have enhanced individual bias and uncertainty, this reason should not prevent resilience studies from being carried out in historically understudied reefs such as KNP.

## Additional Resilience Indicators

The local coral reef experts consulted in the resilience scoring workshop also recommended the removal of six resilience indicators from the original McClanahan et al. (2012) framework and subsequent substitution with indicators that were more relevant to the local context. The indicators removed were: coral disease, resistant coral species, physical human impacts, temperature variability, nutrients, and sedimentation. These indicators were substituted with: bleaching susceptibility, human gravity [a measure of human accessibility to reefs, calculated by dividing the population of the nearest human settlement by the squared travel time to the reef site, see Cinner et al. (2018)],

**TABLE 1 |** Summary of indicators (marked with an "x") used in four assessments: (1) workshop-scored indicators, (2) localized indicators and biodiversity survey metrics, (3) combined indicators from Assessments 1 and 2, (4) biodiversity survey metrics only.

Indicator	Assessment			
	1	2	3	4
Coral diversity*	x	x	x	x
Total fish biomass*	x	x	x	x
Macroalgae cover*	x	x	x	x
Coral recruitment*	x	x	x	x
Fishing pressure*	x	x	x	
Coral species richness		x	x	x
Typhoon exposure		x	x	
Bleaching susceptibility		x	x	
Tidally-induced upwelling		x	x	
Tourism		x		
Human gravity		x		
Resistant coral species	x		x	
Temperature variability	x		x	
Nutrients (pollution)	x		x	
Sedimentation	x		x	
Physical human impacts	x		x	
Coral disease	x		x	
Total	11	11	15	5

Indicators marked with an asterisk (\*) were quantified using two methods: the expert opinion workshop (Assessment 1) and the biodiversity survey (Assessments 2, 3, and 4).

tourism, coral species richness, typhoon exposure, and tidally-induced upwelling (see **Supplementary Tables 3, 4** for detailed explanation on indicator substitution).

The six additional indicators were quantified using existing data to produce scores for each site on the same scale as the previous indicators. Bleaching susceptibility was quantified by consulting coral reef experts to assign a bleaching sensitivity score (on a scale of one to five) for each coral genus within KNP. A site-specific bleaching susceptibility score was then calculated by multiplying the abundance of each genus by its sensitivity score. Human gravity was calculated from data from Taiwanese government reports on the populations of the nearest town to each reef site (Taiwan Ministry of the Interior, 2019). Similarly, the level of tourism at each site was quantified by the number of annual tourists visiting the nearest tourist landmark (Taiwan Ministry of the Interior, 2017). Coral species richness was calculated from the biodiversity survey dataset (see section Biodiversity field surveys). Typhoon exposure was scored by ranking each site for their geographic exposure to the two major typhoon paths influencing KNP (Dai, 1991; Kuo et al., 2011, 2012; Keshavmurthy et al., 2019). Lastly, tidally-induced upwelling data was adapted from previous measurements taken in KNP (Lee et al., 1999a,b) to score each site for its level of upwelling. Each of the indicators was scaled on a range of one to five, with one indicating low resilience conditions and five indicating high resilience conditions.

**TABLE 2 |** Overview of different resilience assessments and comparison of approach types.

Brief description	Assessment			
	1	2	3	4
	Expert opinion workshop	Indicators tailored to local context	Includes all indicators	Biodiversity survey data
Qualitative data	x		x	
Quantitative data		x	x	x
Anthropogenic indicators	x	x	x	
Locally-specific indicators		x	x	

Each assessment feature is marked with an "x".

## Resilience Assessment Frameworks

The four frameworks that were used to quantify resilience apply different combinations of indicators and data types (Table 1, further described below). In total, 17 resilience indicators were measured through quantitative or qualitative surveys and employed across the four frameworks (Tables 1, 2 and Supplementary Table 1). For each assessment, the resilience score for each site was calculated by averaging the scaled scores of the resilience indicators. Although some studies have explored the use of weighting systems for indicators (Maynard et al., 2010; Ladd and Collado-Vides, 2013; Gibbs and West, 2019), there is no clear evidence that implementing weighting schemes is effective (Maynard and Mcleod, 2012). Studies that have tested indicators under a variety of weighting systems have also showed that the resulting management actions and derived outcomes were largely unaffected by the weighting (Gibbs and West, 2019). Thus, the indicators in our resilience assessments were equally weighted.

Assessment 1, the most generalized assessment approach, followed the protocol of the evidence-based framework of McClanahan et al. (2012) and used the 11 indicators scored in the expert opinion workshop (Table 1).

Assessment 2 adapted the framework from McClanahan et al. (2012) by incorporating the additional indicators that were reflective of the local context in KNP and quantified empirically. The indicators in this assessment were scored from the biodiversity surveys rather than the expert opinion workshop. A total of 11 indicators were used in this assessment, applying the six substitutions suggested by the local reef experts (Table 1).

Assessment 3 addressed the holistic approach applied in frameworks such as the IUCN's by using as many indicators as possible to calculate resilience (Obura and Grimsditch, 2009). Fifteen of the 17 total indicators measured were applied in this assessment, excluding the human gravity and tourism indicators to avoid redundancy with the physical human impacts indicator. This approach combined both the quantitative field

data and qualitative workshop data described in the previous two assessment frameworks (Table 1).

Assessment 4 contrasts with Assessment 3 by focusing solely on characterizing resilience using field measurements of parameters indicative of a few key biological reef processes [as in Ladd and Collado-Vides (2013); Maynard et al., 2015, etc.]. Resilience was calculated from the five metrics directly measured in the biodiversity survey: coral diversity, species richness, coral recruitment, fish biomass, and macroalgae cover (Table 1).

Coral recovery rate, calculated as the difference between coral cover in 2010 and 2016, was used to evaluate the outcomes of the resilience assessments (see Supplementary Table 1). The 2010 to 2016 timespan encompasses a period of rapid reef recovery between two major typhoon disturbances in KNP: Typhoon Morakot (2009) and Meranti (2016) (Kuo et al., 2011, 2012; Keshavmurthy et al., 2019). Multidecadal coral cover data for this period were obtained from the Long-Term Ecological Research (LTER) project, which recorded data at eight sites in KNP (Kuo et al., 2012; Keshavmurthy et al., 2019).

## Spatial and Statistical Data Processing

Resulting resilience scores were classified into quartiles for comparison between assessments (Gibbs and West, 2019). The Kruskal-Wallis test (KW test) was used to test whether mean resilience scores differed significantly, and the Kolmogorov-Smirnov test (KS test) was used to conduct pairwise comparisons of resilience scores from each assessment. The extent to which scores from the expert opinion workshop and the field surveys overlapped was evaluated by calculating the Pearson's correlation coefficient (PCC) for indicators that were measured in both datasets (i.e., coral diversity, coral recruitment, macroalgae cover, fish biomass, and fishing pressure). All statistical data processing was carried out in R v.3.5.1 (R Core Team, 2020).

Spatial trends of relative resilience scores were analyzed on QGIS v3.8.1 (QGIS Development Team, 2020). The Moran's I index was calculated to test the null hypothesis that scores were randomly distributed throughout the study area. Scores from each assessment were then interpolated along a 500-m coastal buffer zone using the inverse distance weighting tool. The buffer zone was extended in parts of Nanwan, where study sites were >500 m from the shore. Coral recovery rates were also interpolated within this region for spatial comparison with resilience scores. Resilience scores were also compared with coral recovery rates for statistical correlation via the Pearson's correlation coefficient.

## RESULTS

### Biodiversity Field Surveys

The ecological survey yielded over 21,000 data points on benthic composition, fish, macro-invertebrates, and coral recruitment (see Supplementary Table 5 for regional summary statistics and Supplementary Table 1). The west coast of KNP had the highest regional average of coral diversity (average = 0.876, Simpson's diversity index), though diversity was relatively high in all park regions barring the east coast (average = 0.738, Supplementary Table 5). Between 2010 and 2016, Western

**TABLE 3 |** Summary of resilience scores generated from the localized and generalized assessments.

Assessment	Mean	Minimum	Maximum	St. Dev.
1	3.21	2.66	3.88	0.30
2	3.36	2.39	3.97	0.31
3	3.40	2.81	3.95	0.27
4	3.32	2.28	4.28	0.50

**TABLE 4 |** *P*-values from the Kolmogorov-Smirnoff test comparing distributions of resilience scores in Assessments 1–4.

Assessment	1	2	3
2	<b>9.63e-5</b>		
3	<b>2.04e-4</b>	0.74	
4	<b>9.90e-3</b>	0.24	<b>0.046</b>

Bolded values indicate a significant difference ( $p < 0.05$ ).

Nanwan had the highest mean living coral cover in 2016 (average = 61.0%) and the west coast had the lowest (average = 26.5%). The highest coral species richness was concentrated in Inner Nanwan (average = 47.1 species at each site), where the relative biomass of total fish (average = 643,600 cm<sup>3</sup>) was also the highest. The east coast had the lowest coral species richness (average = 27.4 species at each site) and the lowest relative biomass of total fish (average = 155,000 cm<sup>3</sup>).

## Resilience Scores and Indicators

Resilience scores from the four assessments ranged between 2.28 and 4.28 at each site (Table 3), with the lowest and highest mean scores being 3.21 (Assessment 1) and 3.40 (Assessment 3). There were no significant differences between the average resilience score of each assessment and the group mean (KW test  $\chi^2 = 271$ ,  $df = 237$ ,  $p = 0.0639$ ), though pairwise comparisons of assessments indicated significant differences in the distributions of four out of the six pairs (Table 4). There was little to no correlation in the indicators measured in both qualitative and quantitative surveying methods (Table 5). Coral diversity had the strongest correlation between the two datasets, but this was only moderate (PCC = 0.423, Table 5). Macroalgae cover had virtually no correlation between the two measurement methods (PCC = 0.042), while the others had correlation coefficients ranging from 0.141 to 0.396 (Table 5).

The breakpoints for resilience quartiles were 3.09 (25%), 3.31 (50%), and 3.55 (75%). Only six sites (39, 43, 45, 51, and 52) were grouped into in the same resilience quartile by all four assessments (Table 6). Fifteen sites were grouped into in the same quartile by three out of the four assessments, nine of which were classified as high resilience (4th quartile). In contrast, more than half of the sites ( $n = 38$ ) were classified into three or even four different quartiles.

In all four assessments, the spatial distribution of resilience scores had a highly significant tendency toward clustering (Moran's Index,  $I = 0.261$ ,  $p < 0.001$ ). Most of the sites in

**TABLE 5 |** Pearson's correlation coefficient for indicators scored by both qualitative (expert opinion workshop) and quantitative (biodiversity field survey) methods.

Indicator	Coral diversity	Coral recruitment	Total fish biomass	Macroalgae cover	Fishing pressure
Correlation coefficient	0.423	0.141	0.312	0.042	0.396

Values range from  $-1$  to  $1$ , with  $0$  indicating no correlation.

Inner Nanwan (i.e., around sites 21–25) and part of Eastern Nanwan (i.e., sites 28 and 29) were identified as high resilience areas by all assessments, while the sites off the east coast of KNP (sites 35–42) generally had mid-to-low resilience (Figure 2). Other areas in KNP had spatial patterns of resilience that varied depending on the assessment (Figure 2). The two peninsulas of KNP, Eluanbi and Maobitou, had relatively high resilience in Assessment 1 (Figure 2A), but mid-level resilience in Assessment 3 and 4 (Figures 2C,D) and low resilience in Assessment 2 (Figure 2B). The west coast of KNP had mostly low resilience in Assessments 1 and 3, but very high resilience in Assessment 4. The resilience of western Nanwan reefs was interpreted differently by each assessment: high resilience by Assessment 1, mid/low by Assessments 3 and 4, and very low by Assessment 2.

## Coral Recovery Rates

The highest coral recovery rates were found in the innermost parts of Nanwan (mean recovery rate of 494.3%, see Supplementary Table 5), which is also where all resilience assessments identified high resilience reefs (Figure 3). Recovery rates were also relatively high off the southwestern coast of Hengchun Peninsula and in eastern Nanwan (mean recovery rate of 115.2%). The lowest site-based recovery rates were near Eluanbi and the nuclear power plant in western Nanwan (Figure 3) and the lowest regional recovery rate was along the east coast (mean recovery rate of  $-38.6\%$ ). These spatial patterns of coral cover recovery were most closely replicated in Assessments 2 and 4 (Figures 2B,D, 3). The resilience pattern of Assessment 1 largely lacked similarity to those of the coral recovery rates, particularly in Eluanbi and western Nanwan (Figures 2A, 3). Lastly, Assessment 3 classified Maobitou as low resilience and Eluanbi as relatively high resilience, which is the opposite of the coral recovery rate trends (Figures 2C, 3). Based on a visual comparison of spatial trends in coral recovery rates and the resilience scores, assessment performance can be ranked from high to low accuracy as follows: 4, 2, 1, 3 (Figures 2, 3). From a statistical correlation standpoint, the assessments rank 2, 4, 3, 1 (Pearson's correlation coefficient: 0.368, 0.310, 0.283, 0.147, respectively).

## DISCUSSION

This study is the first to investigate how resilience scores are affected by different assessment approaches. We tested four resilience assessment frameworks to score resilience in KNP, Taiwan, yielding unique insights into ecological resilience

**TABLE 6 |** Comparison of resilience quartiles between the four assessments at each site, where: Q1 (red, low resilience) is <3.09, Q2 (orange) is 3.09–3.31, Q3 (yellow) is 3.31–3.55, and Q4 (green, high resilience) is >3.55.

Site	Assessment			
	1	2	3	4
1	2.70	3.33	3.11	3.97
2	2.94	3.17	3.13	3.26
3	2.94	3.15	3.11	3.19
4	2.94	3.39	3.32	3.81
5	2.94	3.40	3.32	3.83
6	2.91	3.59	3.19	3.58
7	2.66	3.56	3.00	3.51
8	2.85	3.53	3.27	3.73
9	2.94	3.23	3.22	3.51
10	3.03	3.56	3.50	4.22
11	3.09	3.97	3.52	4.28
12	3.09	3.59	3.32	3.56
13	3.30	3.15	3.14	2.69
14	2.88	3.02	3.07	3.16
15	3.30	2.85	3.47	3.42
16	3.21	2.77	3.28	3.17
17	3.24	3.07	3.41	3.29
18	3.12	2.90	3.22	3.33
19	3.39	2.62	3.11	3.03
20	3.64	3.41	3.84	3.73
21	3.73	2.97	3.50	3.31
22	3.30	3.52	3.56	3.52
23	3.18	3.04	3.37	2.97
24	3.30	3.63	3.69	3.93
25	3.12	3.77	3.58	3.87
26	2.91	3.21	3.09	2.81
27	2.94	3.33	3.18	3.07
28	3.06	3.59	3.53	3.66
29	3.61	3.46	3.70	3.29
30	3.06	3.37	3.17	2.44
31	3.18	3.72	3.46	3.19
32	3.21	3.24	3.38	2.93
33	3.27	3.40	3.54	3.09
34	3.27	3.26	3.43	2.76
35	3.30	3.29	3.52	2.87
36	3.30	3.26	3.48	2.83
37	3.21	3.37	3.31	2.40
38	3.07	3.43	3.36	2.63
39	3.76	3.74	3.87	4.09
40	3.12	3.71	3.46	3.11
41	2.91	3.53	3.32	2.72
42	2.91	3.34	3.18	2.28
43	3.82	3.72	3.88	4.03
44	3.82	3.50	3.74	3.55
45	3.70	3.58	3.77	3.85
46	3.88	3.32	3.66	3.25
47	3.57	3.17	3.58	3.34
48	3.88	3.52	3.95	4.13

(Continued)

**TABLE 6 |** Continued

Site	Assessment			
	1	2	3	4
49	3.79	3.40	3.86	3.85
50	2.88	3.29	3.21	3.63
51	2.88	3.05	3.02	3.07
52	2.68	3.05	2.94	2.92
53	2.91	3.04	3.07	3.13
54	3.21	3.08	3.22	3.53
55	3.16	2.39	2.81	2.58
56	3.48	3.48	3.54	3.38
57	3.18	3.75	3.54	3.70
58	3.06	3.39	3.33	2.67
59	3.15	3.63	3.37	3.45
60	3.03	3.45	3.28	3.44
61	3.12	3.47	3.38	3.42
62	3.39	3.92	3.90	3.76
63	3.39	3.92	3.92	3.77
64	3.45	3.94	3.95	4.12
65	3.45	3.58	3.73	3.34
66	2.93	3.36	3.16	2.34
67	3.18	3.34	3.23	2.30
68	3.24	2.89	3.20	2.86

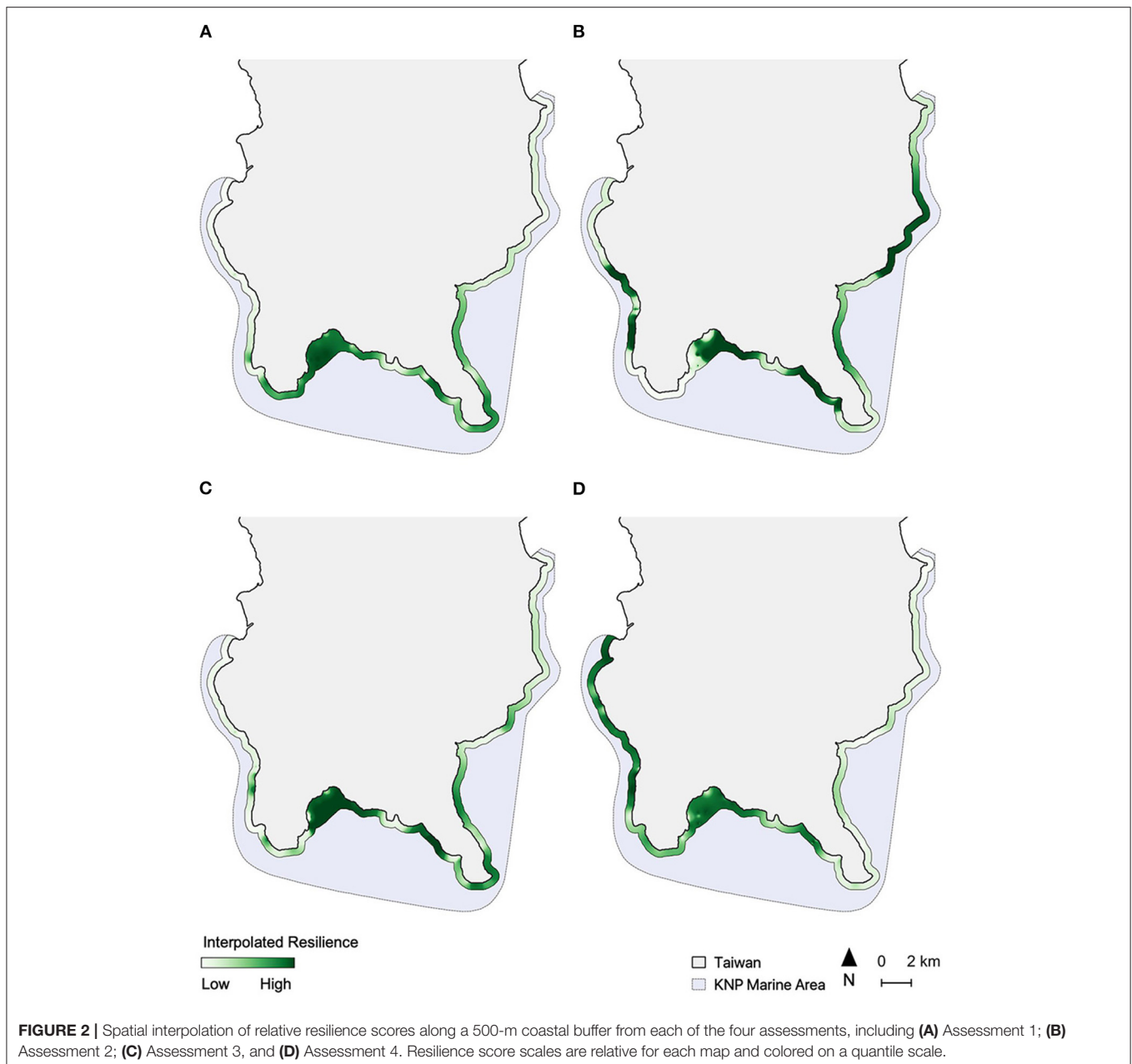
quantification. The study also highlights the importance of *in-situ* quantitative studies on ecological processes, which have shown to be more reliable indicators of resilience than qualitatively-assessed indicators.

## Influence of Indicator Selection on Resilience Scores

Our analysis demonstrated that Assessments 2 and 4 generally showed resilience trends with better consistency than did the broader-scale and qualitative Assessments 1 and 3. The substantial variation in scores between assessments can largely be attributed to differences in indicator selection. In many of the studied sites, indicators were scored similarly in the expert opinion workshop and biodiversity survey, but the overall resilience score and quartile ranking varied depending on the assessment's set of indicators. For instance, all four assessments were in general consensus with low scores for coral recruitment, fish biomass, tourism, and human impacts at western Nanwan sites (e.g., sites 18, 19, 54). Yet, overall resilience scores diverged due to the inclusion of other indicators in some assessments that detracted from the overall similarities. Incorporating sedimentation, nutrient pollution, and coral disease in Assessments 1 and 3 increased the resilience scores at these sites, while scores remained low in Assessments 2 and 4 without these indicators. This example illustrates how the inclusion of different indicators can influence the final resilience score of a site despite the core ecological processes conferring the same level of resilience.

The method of data collection can also lead to large differences in resilience scores, as seen in the weak correlation between

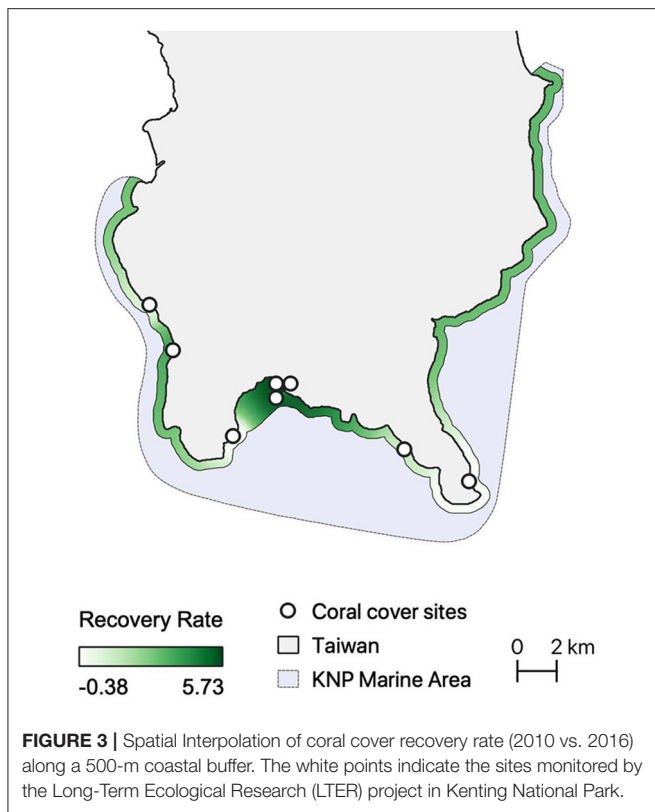




the datasets of five indicators measured in both the expert opinion workshop and biodiversity survey. This lack of overlap highlights the discrepancies between qualitative, opinion-based scoring and empirical, field-based scoring in the context of resilience quantification. Our use of an expert opinion workshop incites the assumption that the experts are both accurate and relatively consistent with one another, though a certain degree of dissonance amongst individual opinions is unavoidable (Lam et al., 2020). The large majority of similar studies quantified their indicators through field surveys resembling our biodiversity surveys (e.g., Cinner et al., 2013; Maynard et al., 2015; Hock et al., 2017), suggesting that this approach may be more suitable for resilience assessments than expert scoring. The opinions of experts, however, are still valuable in shaping the framework

approach and indicator selection [as in Gibbs and West (2019)] and offering insight into the validity of quantified resilience scores (McClanahan et al., 2012).

Previous resilience studies have shown that assessment outcomes are sensitive to the number of indicators used, in which more indicators do not necessarily lead to a better portrayal of resilience (Lam et al., 2020). The incremental importance of each indicator diminishes as the total number of indicators increases, and scores thus tend to revert to the group average (Maynard and Mcleod, 2012; McClanahan et al., 2012). Indeed, we found that the assessment that applied the most indicators had the least reliable outcome: Assessment 3 included a combination of different data collection methods using 17 diverse indicators, yet yielded the least congruous results (Figure 2). Therefore, the



inclusion of more indicators and data types in the hopes of “covering all the bases” is not necessarily beneficial when it comes to quantifying reef resilience (McClanahan et al., 2012; Mumby et al., 2014).

## Strengths of a Localized and Succinct Approach

The success of Assessment 4, which consisted of five indicators that characterize ecological processes, suggests that resilience can be modeled relatively well with a few key indicators. It may thus be redundant to include anthropogenic drivers that are already reflected in baseline ecological and environmental indicators. Including such indicators, like pollution, fishing, or even typhoon exposure, may introduce a level of bias or error that outweighs the indicator’s marginal contribution to resilience modeling. Like many prior resilience studies, the succinct approach of Assessment 4 has shown success because it places ecosystem processes and biodiversity at the focal point of resilience (Hughes et al., 2005). Other resilience assessments conducted on similar spatial scales have also successfully calculated relative resilience without factoring in anthropogenic indicators (e.g., Maynard et al., 2015).

Furthermore, the assessments in our study that utilized empirically measured field data (Assessments 2 and 4) performed better than did those that used qualitative data derived from expert opinion (Assessments 1 and 3). Resilience assessments, therefore, need not stray too far from traditional biodiversity surveys, which capture aspects of baseline ecological functions at a high resolution (Lam et al., 2017). Since the diversity of species

and functional groups have been established as key supporters of ecosystem resilience, metrics that quantify these features are important components of resilience assessments (Walker et al., 1999; Gunderson, 2000).

Existing historical reef monitoring programs can easily be adapted to suit resilience frameworks, as demonstrated in our study (Bachtar et al., 2019; Gibbs and West, 2019). These are important considerations to keep in mind when designing future resilience assessments, especially to maximize the use of time, energy, and funding resources. The inclusion of locally-relevant indicators in Assessment 2 contributed to its success in portraying resilience, particularly because the level of influence of each indicator is dependent on the environmental setting (Maynard and Mcleod, 2012). However, this approach is limited in that not all reefs have high-resolution, long-term monitoring data for multiple resilience indicators. Field survey data represent a single time point, while scoring conducted via expert opinions capitalizes on the multidecadal, holistic knowledge of its scorers (Lam et al., 2017).

Despite the four assessments having diverging trends, all four identified KNP’s Nanwan region, particularly Inner Nanwan, as high resilience areas. This is likely driven by the effects of tidally-influenced upwelling, which provides significant year-round cooling effects to relieve thermal stress placed on the coral communities (Keshavmurthy et al., 2019). This effect is particularly strong in Inner and Western Nanwan, where maximum summer temperature fluctuations can range from 4 to 5°C within 2 h (Keshavmurthy et al., 2019). Additionally, Nanwan is sheltered from direct damage from oncoming typhoons, but is simultaneously well-positioned to benefit from the dissipation of warm surface waters by cool storm surges induced by the typhoons (Keshavmurthy et al., 2019). A combination of these unique local environmental effects contributes to the consistent identification of Nanwan as a high resilience region in all assessments.

One important caveat of the present study was that our proxy for resilience, coral cover, is just one metric that characterizes a complex ecological concept. There are other aspects of reef dynamics, such as coral assemblage composition, that cannot be captured by coral cover, yet also contribute to the holistic picture of resilience. However, we currently do not have additional data to expand our resilience assessment analysis and instead have endeavored to provide an initial overview given the data constraints. In the coming years, we hope to conduct more comprehensive surveys in KNP and work toward a more sophisticated portrayal of resilience.

## Toward a Better Resilience Assessment

Our results show that while each approach to measuring resilience has its merits and drawbacks, the picture of resilience becomes clearest when a few key indicators are included to reflect core ecosystem processes and locally-relevant factors. The assessment that included as many indicators as possible was less successful at capturing resilience than was the one that concisely quantified key ecological processes, thus suggesting that “less is more” when it comes to selecting the number of indicators in a resilience assessment. We also found that individual indicator

selection is a critical component of the framework design that is highly influential over scoring outcomes. As such, it is important to thoroughly consider the resilience framework's design within the context of specific reef management goals and the local environmental setting.

Some studies assert the need for a standardized resilience scoring system that can be applied across all reefs (e.g., Hodgson et al., 2015), but this comes with the loss of crucial factors such as local specificity. The exclusion of metrics that characterize the unique mechanisms governing the ecosystem's shifts to alternative stable states, a key aspect in recent resilience concepts, may lead to an inaccurate portrayal of resilience (Petraitis and Dudgeon, 2016; Lam et al., 2020). Resilience assessments must also be adapted to complement the scale at which management strategies are being implemented (Lam et al., 2020). The findings produced from our analysis of different frameworks approaches and data collection methods support this notion, which can be further explored in future resilience assessments.

In our study, each approach interpreted resilience in KNP's reefs differently, but the high degree of dissonance was largely ameliorated through cross-checking areas with their resilience quartile classifications. The application of multiple approaches or data collection methods can thus be an effective way to ascertain a more holistic and accurate portrayal of reef resilience. Overall, when employed with careful planning and consideration, resilience assessments are a powerful tool for enacting practical conservation strategies. Our holistic snapshots of reef health and relative resilience to environmental changes makes these frameworks highly valuable to coral reef ecologists, managers, and policymakers alike.

## DATA AVAILABILITY STATEMENT

The raw data supporting the conclusions of this article will be made available by the authors, without undue reservation.

## REFERENCES

- Adjeroud, M., Michonneau, F., Edmunds, P. J., Chancerelle, Y., Lison de Loma, T., Penin, L., et al. (2009). Recurrent disturbances, recovery trajectories, and resilience of coral assemblages on a South Central Pacific reef. *Coral Reefs* 28, 775–780. doi: 10.1007/s00338-009-0515-7
- Anthony, K. R. N. (2016). Coral reefs under climate change and ocean acidification: challenges and opportunities for management and policy. *Annu. Rev. Env. Resour.* 41, 59–81. doi: 10.1146/annurev-environ-110615-085610
- Anthony, K. R. N., Marshall, P. A., Abdulla, A., Beeden, R., Bergh, C., Black, R., et al. (2014). Operationalizing resilience for adaptive coral reef management under global environmental change. *Glob. Change Biol.* 21, 48–61. doi: 10.1111/gcb.12700
- Bachtiar, I., Suharsono, A. D., and Neviaty, P. Z. (2019). Practical resilience index for coral reef assessment. *Ocean Sci. J.* 54, 117–127. doi: 10.1007/s12601-019-0002-1
- Chen, C. A., and Keshavmurthy, S. (2009). Taiwan as a connective stepping-stone in the Kuroshio triangle and the conservation of coral ecosystems under the impacts of climate change. *Kuroshio Sci.* 3, 15–22.
- Chen, J.-P., and Kwang, T.-S. (2010). *Marine Fishes in Kenting National Park, 1st Revised Edn.* Kenting: Kenting National Park Headquarters.

## AUTHOR CONTRIBUTIONS

All authors contributed to the conception and design of the study. CC, CW, C-YK, K-LC, M-JH, N-YC, and Y-CC conducted the field data collection. AB conducted the data processing and analysis and wrote the first draft of the manuscript. AB, CC, CW, C-YK, and K-LC contributed to manuscript revisions. All authors have read and approved of the submitted version.

## FUNDING

Research for this project funded by a Research Fellows Grant from the Fulbright Program and the Foundation for Scholarly Exchange (Fulbright Taiwan) awarded to AB, the Academia Sinica Postdoctoral Fellowship awarded to C-YK, and the Long-Term Ecological Research grant from Kenting National Park Headquarters to CC.

## ACKNOWLEDGMENTS

Many thanks to the lab members of Coral Reef Evolutionary and Ecological Genetic Laboratory of the Biodiversity Research Center, Academia Sinica, for providing logistical support and conducting fieldwork for the long-term ecological research (LTER) and reef surveys of the Kenting National Park (KNP), Taiwan. We thank Aichi Chung and Chieh Wei for contributing their expertise to the generalized resilience assessment workshop. We also thank Noah Last of Third Draft Editing for his English language editing.

## SUPPLEMENTARY MATERIAL

The Supplementary Material for this article can be found online at: <https://www.frontiersin.org/articles/10.3389/fmars.2020.610306/full#supplementary-material>

- Chen, Y.-J., Cai, Y.-L., and Zhang, Q.-H. (2017). *Monitoring Survey of Fishing Resource of Kenting National Park (In Chinese)*. Kenting: Kenting National Park Headquarters.
- Cinner, J. E., Huchery, C., Darling, E. S., Humphries, A. T., Graham, N. A. J., Hicks, N. M., et al. (2013). Evaluating social and ecological vulnerability of coral reef fisheries to climate change. *PLoS ONE* 8:e74321. doi: 10.1371/journal.pone.0074321
- Cinner, J. E., Maire, E., Huchery, C., MacNeil, A., Graham, N. A. J., Mora, C., et al. (2018). Gravity of human impacts mediates coral reef conservation gains. *Proc. Natl. Acad. Sci. U.S.A.* 115, e6116–e6125. doi: 10.1073/pnas.1708001115
- Dai, C.-F. (1991). Reef environment and coral fauna of southern Taiwan. *Atoll. Res. Bull.* 354, 1–24. doi: 10.5479/si.00775630.354.1
- Dai, C.-F. (1993). Patterns of coral distribution and benthic space partitioning on the fringing reefs of Southern Taiwan. *Mar. Ecol.* 14, 185–204. doi: 10.1111/j.1439-0485.1993.tb00479.x
- Dai, C.-F. (1997). Assessment of the present health of coral reefs in Taiwan. *Status of Coral Reefs in the Pacific*. UNH Sea Grant CP-98-01. Honolulu, HI: University of Hawaii, 123–131.
- Dai, C.-F. (2018). “Coastal and shallower water ecosystem,” in *Regional Oceanography of Taiwan Version II*, ed S. Jan (Taipei: National Taiwan University Press), 263–299.

- Dai, C.-F., and Horng, S. (2009a). *Scleractinia of Taiwan I. The Complex Group*. Taipei: National Taiwan University.
- Dai, C.-F., and Horng, S. (2009b). *Scleractinia of Taiwan II. The Robust Group*. Taipei: National Taiwan University.
- Darling, E. S., McClanahan, T. R., Maina, J., Gurney, G. G., Graham, N. A. J., Januchowski-Hartley, F., et al. (2019). Social–environmental drivers inform strategic management of coral reefs in the Anthropocene. *Nat. Ecol. Evol.* 3, 1341–1350. doi: 10.1038/s41559-019-0953-8
- English, S. A., and Wilkinson, C. R. (1997). *Survey Manual for Tropical Marine Resources*, 2nd Edn. Townsville, QLD: Australian Institute of Marine Science.
- Gibbs, D. A., and West, J. M. (2019). Resilience assessment of Puerto Rico's coral reefs to inform reef management. *PLoS ONE* 14:e0224360. doi: 10.1371/journal.pone.0224360
- Guest, J. R., Edmunds, P. J., Gates, R. D., Kuffner, I. B., Andersson, A. J., Barnes, B. B., et al. (2018). A framework for identifying and characterising coral reef “oases” against a backdrop of degradation. *J. Appl. Ecol.* 55, 2865–2875. doi: 10.1111/1365-2664.13179
- Gunderson, L. H. (2000). Ecological resilience – in theory and application. *Ann. Rev. Ecol. Syst.* 31, 425–439. doi: 10.1146/annurev.ecolsys.31.1.425
- Heron, S. F., Maynard, J. A., van Hooidek, R., and Eakin, C. M. (2016). Warming trends and bleaching stress of the world's coral reefs 1985–2012. *Sci. Rep.* 6:e38402. doi: 10.1038/srep38402
- Ho, M.-J., Cheng, N.-Y., Chen, Y.-C., Kuo, C.-Y., Wen, C. K.-C., Cherh, K.-L., et al. (2016). Investigating current status of benthic ecology in the Kenting National Park Marine zones, Taiwan. *J. Nat. Park.* 26, 46–56.
- Hock, K., Wolff, N. H., Oritz, J. C., Condie, S. A., Anthony, K. R. N., Blackwell, P. G., et al. (2017). Connectivity and systemic resilience of the great barrier reef. *PLoS Biol.* 15:e2003355. doi: 10.1371/journal.pbio.2003355
- Hodgson, D., McDonald, J. L., and Hosken, D. J. (2015). What do you mean, ‘resilient’? *Trends Ecol. Evol.* 30, 503–506. doi: 10.1016/j.tree.2015.06.010
- Hodgson, G., Kiene, W., Mihaly, J., Liebeler, J., Shuman, C., and Maun, L. (2006). *A Guide to Coral Reef Monitoring. Instruction Manual*. Pacific Palisades, CA: Reef Check Foundation, 1–86.
- Holling, C. S. (1973). Resilience and stability in ecological systems. *Annu. Rev. Ecol. Syst.* 4, 1–23. doi: 10.1146/annurev.ecol.04.11.0173.000245
- Hughes, T. P., Bellwood, D. R., Folke, C., Steneck, R. S., and Wilson, J. (2005). New paradigms for supporting the resilience of marine ecosystems. *Trends Ecol. Evol.* 20, 380–386. doi: 10.1016/j.tree.2005.03.022
- Hughes, T. P., Kerry, J. T., Baird, A. H., Connolly, S. R., Dietzel, A., Eakin, C. M., et al. (2018). Global warming transforms coral reef assemblages. *Nature* 556, 492–496. doi: 10.1038/s41586-018-0041-2
- Keshavmurthy, S., Hsu, C.-M., Kuo, C.-Y., Meng, P.-J., Wang, J.-T., and Chen, C. A. (2012). Symbiotic communities and host genetic structure of the brain coral *Platygyra verweyi*, at the outlet of a nuclear power plant and adjacent areas. *Mol. Ecol.* 21, 4393–4407. doi: 10.1111/j.1365-294X.2012.05704.x
- Keshavmurthy, S., Kuo, C.-Y., Huang, Y.-Y., Carballo-Bolaños, R., Meng, P.-J., Wang, J.-T., et al. (2019). Coral reef resilience in Taiwan: lessons from long-term ecological research on the coral reefs of Kenting National Park. *J. Mar. Sci. Eng.* 7:388. doi: 10.3390/jmse7110388
- Kuo, C.-Y., Meng, P.-J., Wang, J.-T., Chen, J.-P., Chiu, Y.-W., Lin, H.-J., et al. (2011). Damage to the reefs of Siangjiao Bay marine protected area in Kenting National Park, Taiwan during Typhoon Morakot. *Zool. Stud.* 50:85. Available online at: <http://hdl.handle.net/11455/71637>
- Kuo, C.-Y., Yuen, Y. S., Meng, P.-J., Ho, P.-H., Wang, J.-T., Liu, P.-J., et al. (2012). Recurrent disturbances and the degradation of hard coral communities in Taiwan. *PLoS ONE* 7:e44364. doi: 10.1371/journal.pone.0044364
- Ladd, M. C., and Collado-Vides, L. (2013). Practical applications of monitoring results to improve managing for coral reef resilience: a case study in the Mexican Caribbean. *Biodiv. Cons.* 22, 1591–1608. doi: 10.1007/s10531-013-0493-5
- Lam, V. Y. Y., Doropoulos, C., Bozec, Y., and Mumby, P. J. (2020). Resilience concepts and their application to coral reefs. *Front. Ecol. Evol.* 8, 1–14. doi: 10.3389/fevo.2020.00049
- Lam, V. Y. Y., Doropoulos, C., and Mumby, P. J. (2017). The influence of resilience-based management on coral reef monitoring: a systematic review. *PLoS ONE* 12:e0172064. doi: 10.1371/journal.pone.0172064
- Lee, H.-J., Chao, S.-Y., and Fan, K.-L. (1999a). Flood-ebb disparity of tidally induced recirculation Eddies in a semi-enclosed basin: Nan Wan Bay. *Cont. Shelf Res.* 19, 871–890. doi: 10.1016/S0278-4343(99)00060-0
- Lee, H.-J., Chao, S.-Y., Fan, K.-L., and Kuo, T.-Y. (1999b). Tide-induced eddies and upwelling in a semi-enclosed basin: Nan Wan. *Estuarine Coastal Shelf Sci.* 49, 775–787. doi: 10.1006/ecss.1999.0524
- Maynard, J. A., Marshall, P. A., Johnson, J. E., and Harman, S. (2010). Building resilience into practical conservation: identifying local management responses to global climate change in the southern great barrier reef. *Coral Reefs* 29, 381–391. doi: 10.1007/s00338-010-0603-8
- Maynard, J. A., McKagan, S., Raymundo, L., Johnson, S., Ahmadi, G. N., Johnston, L., et al. (2015). Assessing relative resilience potential of coral reefs to inform management. *Biol. Conserv.* 192, 109–119. doi: 10.1016/j.biocon.2015.09.001
- Maynard, J. A., and Mcleod, K. (2012). *How-to-Guide for Conducting Resilience Assessments*. Available online at: [https://www.reefresilience.org/pdf/How-to\\_Guide\\_Final.pdf](https://www.reefresilience.org/pdf/How-to_Guide_Final.pdf) (accessed January 2, 2020).
- McClanahan, T. R., Donner, S. D., Maynard, J. A., MacNeil, M. A., Graham, N. A. J., Maina, J., et al. (2012). Prioritizing key resilience indicators to support coral reef management in a changing climate. *PLoS ONE* 7:e42884. doi: 10.1371/journal.pone.0042884
- Meng, P. J., Lee, H. J., Wang, J. T., Chen, C. C., Lin, H. J., Tew, K. S., et al. (2008). A long-term survey on anthropogenic impacts to the water quality of coral reefs, southern Taiwan. *Environ. Pollut.* 156, 67–75. doi: 10.1016/j.envpol.2007.12.039
- Mumby, P. J., Chollett, I., Bozec, Y. M., and Wolff, N. H. (2014). Ecological resilience, robustness and vulnerability: how do these concepts benefit ecosystem management? *Curr. Opin. Environ. Sust.* 7, 22–27. doi: 10.1016/j.cosust.2013.11.021
- Mumby, P. J., Hastings, A., and Edwards, H. J. (2007). Thresholds and the resilience of Caribbean coral reefs. *Nature* 450, 98–101. doi: 10.1038/nature06252
- Nyström, M., Graham, N., Lokrantz, J., and Norström, A. (2008). Capturing the cornerstones of coral reef resilience: linking theory to practice. *Coral Reefs* 27, 795–809. doi: 10.1007/s00338-008-0426-z
- Obura, D., and Grimsditch, G. (2009). “Resilience Assessment of coral reefs—Assessment protocol for coral reefs, focusing on coral bleaching and thermal stress.” in *IUCN Working Group on Climate Change and Coral Reefs* (Gland: IUCN). Available online at: [https://www.icriforum.org/wp-content/uploads/2019/12/resilience\\_assessment\\_final.pdf](https://www.icriforum.org/wp-content/uploads/2019/12/resilience_assessment_final.pdf)
- Petraitis, P. S., and Dudgeon, S. R. (2016). Cusps and butterflies: multiple stable states in marine systems as catastrophes. *Mar. Freshwater Res.* 67, 37–46. doi: 10.1071/MF14229
- QGIS Development Team (2020). ‘QGIS Geographic Information System’, *Open Source Geospatial Foundation Project*. Available online at: <http://qgis.osgeo.org> (accessed December 5, 2020).
- R Core Team (2020). *R: A Language and Environment for Statistical Computing*. R Foundation for Statistical Computing, Vienna, Austria. Available online at: <https://www.R-project.org/> (accessed November 8, 2020).
- Roche, R. C., Williams, G. J., and Turner, J. R. (2018). Towards developing a mechanistic understanding of coral reef resilience to thermal stress across multiple scales. *Curr. Clim. Change Rep.* 4, 51–64. doi: 10.1007/s40641-018-0087-0
- Standish, R. J., Hobbs, R. J., Mayfield, M. M., Bestelmeyer, B. T., Suding, K. N., Battaglia, L. L., et al. (2014). Resilience in ecology: abstraction, distraction, or where the action is? *Biol. Conserv.* 177, 43–51. doi: 10.1016/j.biocon.2014.06.008
- Sweatman, H., Delean, S., and Syms, C. (2011). Assessing loss of coral cover on Australia's great barrier reef over two decades, with implications for longer-term trends. *Coral Reefs* 30, 521–531. doi: 10.1007/s00338-010-0715-1
- Taiwan Ministry of the Interior (2017). *Fourth Comprehensive Review of Kenting National Park (In Chinese)*. Kenting: Kenting National Park Headquarters.
- Taiwan Ministry of the Interior (2019). *Number of Households and Population by Village. Dataset (In Chinese)*. Available online at: <https://data.moi.gov.tw/MoiOD/Data/DataList.aspx> (accessed September 26, 2019).

- van Woesik, R. (2013). Quantifying uncertainty and resilience on coral reefs using a Bayesian approach. *Environ. Res. Lett.* 8, 1–8. doi: 10.1088/1748-9326/8/4/044051
- Veron, J. E. N., and Stafford-Smith, M. (2000). *Corals of the World*. Townsville: Australian Institute of Marine Science.
- Walker, B., Kinzig, A., and Langridge, J. (1999). Plant attribute diversity, resilience, and ecosystem function: the nature and significance of dominant and minor species. *Ecosystems* 2, 95–113. doi: 10.1007/s100219900062
- West, J. M., and Salm, R. V. (2003). Resistance and resilience to coral bleaching: implications for coral reef conservation and management. *Conserv. Biol.* 17, 956–967. doi: 10.1046/j.1523-1739.2003.02055.x

**Conflict of Interest:** The authors declare that the research was conducted in the absence of any commercial or financial relationships that could be construed as a potential conflict of interest.

Copyright © 2021 Bang, Kuo, Wen, Cherh, Ho, Cheng, Chen and Chen. This is an open-access article distributed under the terms of the Creative Commons Attribution License (CC BY). The use, distribution or reproduction in other forums is permitted, provided the original author(s) and the copyright owner(s) are credited and that the original publication in this journal is cited, in accordance with accepted academic practice. No use, distribution or reproduction is permitted which does not comply with these terms.





# High Clonality and Geographically Separated Cryptic Lineages in the Threatened Temperate Coral, *Acropora pruinosa*

Supisara Pipithkul<sup>1</sup>, Sota Ishizu<sup>2</sup>, Akifumi Shimura<sup>2</sup>, Hiroyuki Yokochi<sup>3</sup>, Satoshi Nagai<sup>4</sup>, Hironobu Fukami<sup>1\*</sup> and Nina Yasuda<sup>1\*</sup>

<sup>1</sup> Department of Marine Biology and Environmental Sciences, Faculty of Agriculture, University of Miyazaki, Miyazaki, Japan,

<sup>2</sup> Graduate School of Agriculture, University of Miyazaki, Miyazaki, Japan, <sup>3</sup> Department of Fisheries, School of Marine Science and Technology, Tokai University, Shimizu-ku, Japan, <sup>4</sup> Research Center for Aquatic Genomics, National Research Institute of Fisheries Science, Yokohama, Japan

## OPEN ACCESS

### Edited by:

Tamotsu Oomori,  
University of the Ryukyus, Japan

### Reviewed by:

David A. Paz-García,  
Centro de Investigaciones Biológicas  
del Noroeste (CIBNOR), Mexico  
Chuya Shinzato,  
The University of Tokyo, Japan

### \*Correspondence:

Hironobu Fukami  
hirofukami@cc.miyazaki-u.ac.jp  
Nina Yasuda  
Nina27@cc.miyazaki-u.ac.jp

### Specialty section:

This article was submitted to  
Coral Reef Research,  
a section of the journal  
Frontiers in Marine Science

**Received:** 15 February 2021

**Accepted:** 16 April 2021

**Published:** 14 May 2021

### Citation:

Pipithkul S, Ishizu S, Shimura A,  
Yokochi H, Nagai S, Fukami H and  
Yasuda N (2021) High Clonality  
and Geographically Separated Cryptic  
Lineages in the Threatened  
Temperate Coral, *Acropora pruinosa*.  
Front. Mar. Sci. 8:668043.  
doi: 10.3389/fmars.2021.668043

*Acropora pruinosa* is a threatened zooxanthellate scleractinian coral that is distributed in the temperate areas along the coastline of Japan and the northern area of the South China Sea. Since *A. pruinosa* propagates both asexually and sexually, assessing clonal diversity and genetic connectivity among populations is important for conservation. In addition, high morphological variations in the field create confusion during species identification. To examine the existence of hidden genetic lineages, clonality, and genetic connectivity of *A. pruinosa* for conservation, we applied microsatellite analysis. Clustering analysis indicated two distinct geographically separated genetic lineages: one is distributed in the west, and the other is distributed in the east. The two lineages co-existed in Nishidomari, Kochi. There was no obvious difference in morphological characteristics between the two lineages. Although the factors influencing the observed distribution patterns remain unknown, there is a possibility that the two lineages might have diverged somewhere in the north-western Kyushu and north-eastern Pacific coast habitats in the past, and then periodically colonized the current habitats. A low clonal diversity was observed in most of the populations, indicating a high rate of asexual reproduction associated with their branching morphologies. In addition, there are strong genetic structuring in this species, indicating weak connectivity among populations. These results indicated a low larval dispersal potential among populations and that populations are basically sustained by a high rate of clone propagation and self-seeding. The existence of cryptic lineages and genetically isolated populations with high clonality emphasized the importance of conservation of *A. pruinosa*.

**Keywords:** scleractinia, temperate coral, biodiversity, cryptic lineages, clonality, asexual reproduction, morphological variation

## INTRODUCTION

Coral reefs provide habitat, shelter, and food for many marine organisms, helping with nutrient recycling in the ocean and other ecosystem services (Principe et al., 2011). In Japan, the distribution of coral communities stretches from the south-western areas toward the eastern part of the Japan mainland (Nishihira, 2004). However, coral communities have been threatened by ocean

acidification, climate change, and human activities (Goldberg and Wilkinson, 2004), and reef-building coral species are now listed to be threatened or vulnerable species (IUCN, 2020). Thus, basic knowledge for the proper conservation planning for coral species is needed. Most coral species can reproduce both asexually and sexually and disperse from their natal populations to cause genetic connectivity among different populations during pelagic larval period. Genetic diversity and clonality assessment may also play a vital role in predicting the adaption of populations to climate and environment changes (Gorospe et al., 2015). Thus, information about clonality, genetic diversity, and genetic connectivity between populations is required for the protection of species. In this context, the molecular population genetic approach, which is one of the promising methods for examining the clonality and genetic structure of species, can provide useful information for conservation purposes (O'Brien, 1994).

*Acropora pruinosa* is a hermatypic coral with an arborescent growth form (underwater photos in Figure 1). Veron (1992) suggested that this species is presumably endemic to the Japan mainland and Hong Kong. This unusual and limited distribution as well as sudden decrease of *A. pruinosa* population in some areas (Nanto et al., 2009; Nomura, 2009) led the species to be listed in the Japanese Red list<sup>1</sup> (Ministry of the Environment, 2017). *Acropora pruinosa* is a hermaphrodite and broadcast-spawning species. This coral species releases its gametes into the water column once a year in summer, approximately  $106 \pm 10$  min after sunset (Suzuki and Fukami, 2012). After fertilization of gametes in the water column, larvae of *A. pruinosa* move to the surface and float in the ocean for 3–10 days before settling on the ocean floor (Iwase et al., 2009). Larvae of *A. pruinosa* have a high settlement rate, and usually settle on places slightly exposed to sunlight (Iwase et al., 2009). The overall early life ecology is quite similar to that of other *Acropora* spp. (Iwase et al., 2009) and it exhibits genetic connectivity among different populations (e.g., Nakabayashi et al., 2019).

Similar to other coral species, *A. pruinosa* has a high morphological diversity, especially in terms of the thickness and length of branches, causing confusion in species delimitation. This species is often confused with *Acropora tumida* in Japan; arborescent or caespitose colonies with thicker and robust branches have been identified incorrectly as *A. tumida* (Nishihara and Veron, 1995). Sugihara et al. (2015) showed that real *A. tumida* exhibits a corymbose colony form but not an arborescent or caespitose colony form like *A. pruinosa*. Examining possible hidden lineages using molecular markers and comparisons between morphologies and genetically different lineages are of great importance for determining conservation units.

The aims of this study were to provide useful information to conserve the threatened reef-building species, *A. pruinosa*; assess the clonality, genetic diversity, and genetic structure of *A. pruinosa* to examine the existence of possible hidden lineages; assess the concordance between genetically distinct lineages and morphological characteristics; and to examine connectivity among different populations of *A. pruinosa*. To this end, we

applied codominant, highly polymorphic microsatellite markers by collecting samples from most of the Japanese habitats of *A. pruinosa*.

## MATERIALS AND METHODS

### Coral Sampling and Genotyping

In total, 331 small fragment colonies (about 5–10 cm long) of *A. pruinosa* were collected by SCUBA diving from 17 temperate sites along the Kuroshio and Tsushima currents covering most of the species' distribution in Japan from 2009 to 2015 (Table 1 and Figure 1). A small fragment (about 5 mm) of each coral sample was collected and preserved in CHAOS solution for DNA extraction (Fukami et al., 2004). Coral samples were collected from independent colonies that are mutually distantly apart whenever possible. However, the distance between the sampled colonies varied depending on the size of the population, and the shortest distance between colonies was about 1 m in a small population, such as the Enashi population (E). The rest of the samples were bleached for morphological examination.

Genotypes of the corals were determined using 9 microsatellite loci (Shinzato et al., 2014; van Oppen et al., 2016). Nine loci were amplified independently and then mixed into 3 PCR product sets using different dyes and non-overlapping loci size: Plex 1 includes 8346m3, 8499m4, and 10366m5; Plex 2 includes 441m6 and 7961m4, and Amil 2-2; and Plex 3 includes Amil 2-10, Amil 2-12, and Amil 2-23. The total PCR reaction volume was 8.14  $\mu$ l, including 1  $\mu$ l of template DNA, 0.07  $\mu$ l of each 50 mM primer, 4  $\mu$ l of master mix (GoTaq® Promega), and 3  $\mu$ l of water. The PCR program was 95°C for 5 min, followed by 40 cycles at 95°C for 30 s, 40°C for 30 s, 72°C for 30 s, and a final extension step at 72°C for 5 min.

The PCR products were diluted by 20, 50, 100, 200, 400, and 800 times depending on the quality of the samples after electrophoresing on agarose gel. For each sample, 1  $\mu$ l of the diluted PCR product was added to 14  $\mu$ l of highly deionized formamide containing 0.2  $\mu$ l of the GeneScan-600 ZX (LIZ) size standard (Applied Biosystems, Foster City, CA, United States) for genotyping on an Applied Biosystems 3730xl DNA analyzer (GeneMapper ver. 6, Applied Biosystems) into determine the allele sizes of all samples. All the genotyping loci were manually checked and modified. Wherever there was ambiguously, we re-extracted genomic DNA and re-amplified it for accurate genotyping.

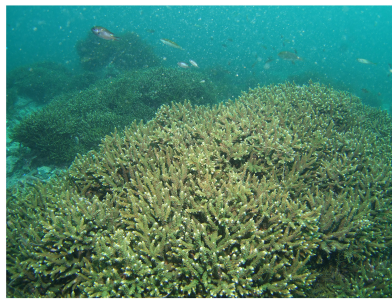
### Clonal and Genetic Diversity and Identifying the Two Cryptic Lineages

We analyzed the clonal structure of each population, Nei's genetic diversity, and Shannon index based on 9 microsatellite loci by Genodive and then calculated the probability of identity using GenAlex ver. 6.51b2 (Peakall and Smouse, 2006, 2012). This software was used to identify possible clones and clonal diversity in each population (asexually reproduced by fragmentation) and all the clonal samples except for one genet, which was excluded from the subsequent population genetic analyses. We then

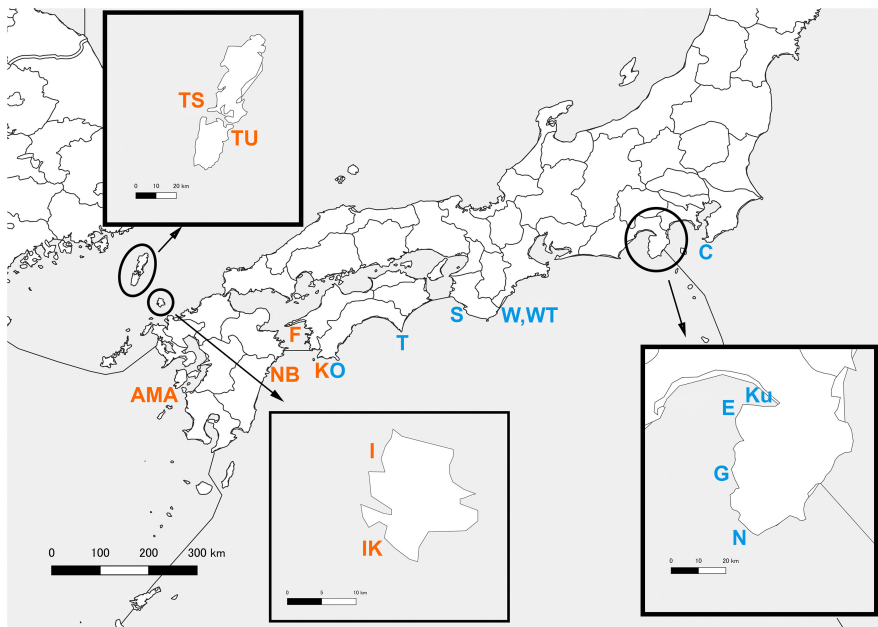
<sup>1</sup>[https://www.env.go.jp/nature/kisho/sango\\_tokusei.html](https://www.env.go.jp/nature/kisho/sango_tokusei.html)



(West lineage)



(East lineage)



**FIGURE 1** | Sampling location map with the underwater photographs of *A. pruinosa* in this study.

measured observed heterozygosity and expected heterozygosity to estimate genetic diversity in each population.

We used STRUCTURE software (Pritchard et al., 2000; Falush et al., 2003, 2007; Hubisz et al., 2009), using the admixture model without any prior information. We used the following settings to assign each individual to a pre-defined number of hypothetical clusters ( $K$ ): a burn-in of 100,000 chains followed by 100,000 Markov chain Monte Carlo replications. We performed ten independent runs for each  $K = 1$  to 10 to confirm convergence. We used STRUCTURE HARVESTER (Earl and VonHoldt, 2012) to estimate delta  $K$  and applied CLUMPAK (Kopelman et al., 2015) to calculate and visualize the coefficient of ancestry for each sample across 10 runs for the most likely values of  $K$  (Delta  $K$ ).

We conducted principal coordinates analysis (PCoA) of 13 populations ( $N > 7$ ) including Futagose and Otaura of Tsushima, Hongu and Kouze of Iki island, Amakusa, Ehime, Kochi, Shirahama, Takatomi, Fukuro Bay, Kuzura, Tago, and Nakagi using GenAlex 6.51b2 (Peakall and Smouse, 2012) to visualize the

genetic relationship among different populations and to confirm the result of STRUCTURE analysis.

## Morphological Examinations

We measured the following morphological characteristics: thickness of branch under 1 cm from the tip, and outer and inner diameters of the axial corallite (**Supplementary Figure 1**). We also counted the septal number of axial corallites and observed the radial corallites and structure of the coenosteum (**Supplementary Table 2**). Vernier caliper was used to measure the branch thickness, and a digital microscope VHX-1000 (Keyence) was used for all others. We randomly chose 44 samples and collected 2 or 3 sets of data per 1 sample, according to the number of their branches. We calculated the average, standard deviation, and maximum and minimum values over all samples and within each cryptic lineage. We also analyzed the data with a non-parametric statistical method, Mann-Whitney-Wilcoxon Rank Sum, to test if there is a significant difference between two lineages.

**TABLE 1 |** List of the sample site, population name, latitude (in the northern hemisphere), longitude (in the eastern hemisphere), sample size (n), number of genet in each population, number of genet divided by sample size (N. Genets/n), cumulative probability of identity of the 9 microsatellite markers (PI), Nei's genetic diversity, mean observed heterozygosity ( $H_o$ ), mean expected heterozygosity ( $H_e$ ), fixation index ( $F_{IS}$ ), and Shannon index, which was corrected for sample size (shc), and the sampling date for all populations (yyyy/mm) of *Acropora pruinosa*.

Sampling site	Population	Latitude (N°)	Longitude (E°)	Sample size (n)	Number of genet	N. Genets/N. sample	PI	Nei's genetic diversity	$H_o$	$H_e$	$F_{IS}$	shc	Sampling date
Tsushima (Futagose), Nagasaki	TS	34°25' 02"	129°16' 12"	18	7	0.389	5.3E-05	0.725	0.698	0.469	−0.488	0.83	2010/09
Tsushima (Otaura), Nagasaki	TU	34°16' 26"	129°19' 56"	11	7	0.636	3.7E-04	0.818	0.762	0.430	−0.772	1.077	2010/09
Iki (Hongu), Nagasaki	I	33°49' 23"	129°40' 28"	20	11	0.550	5.7E-04	0.884	0.556	0.348	−0.598	1.161	2010/09
Iki (Kouze), Nagasaki	IK	33°46' 09"	129°39' 17"	22	17	0.773	5.5E-05	0.952	0.458	0.392	−0.168	1.651	2010/09
Amakusa (Haruhae), Kumamoto	AMA	32°10' 50"	130°01' 15"	35	27	0.771	2.2E-05	0.978	0.449	0.480	0.065	1.832	2009/10
Nobeoka (Shimaaura), Miyazaki	NB	32°39' 45.2"	131°48' 38.9"	2	2	1.000	1.5E-04	1	0.278	0.458	0.375	nan	2015/07
Ehime	F	33°06' 13"	132°28' 25"	15	15	1.000	3.6E-06	1	0.437	0.512	0.146	nan	2009/08
Nishidomari, Kochi	KO	32°46' 41"	132°43' 55"	20	11	0.550	3.3E-04	0.916	0.364	0.373	0.024	1.167	2009/08
Takegashima, Tokushima	T	33°32' 33"	134°18' 58"	20	4	0.200	6.8E-04	0.284	0.583	0.365	−0.597	0.403	2009/09
Shirahama, Wakayama	S	33°41' 26.6"	135°20' 06"	14	11	0.786	1.3E-05	0.956	0.657	0.487	−0.349	1.459	2009/05
Takatomi, Wakayama	W	33°28' 57"	135°45' 30"	21	8	0.381	6.7E-03	0.567	0.417	0.262	−0.592	0.833	2009/05
Fukuro Bay, Wakayama	WT	33°28' 34"	135°46' 22"	24	14	0.583	1.2E-03	0.92	0.238	0.251	−0.052	1.296	2009/06
Kuzura, Shizuoka	Ku	35°01' 23"	138°52' 08"	14	13	0.929	2.1E-04	0.989	0.427	0.394	−0.084	1.96	2009/08
Enashi, Shizuoka	E	35°01' 25"	138°47' 60"	34	6	0.176	1.2E-03	0.369	0.611	0.366	0.669	0.479	2009/08
Tago, Shizuoka	G	34°48' 23"	138°45' 39"	26	13	0.500	9.7E-04	0.868	0.333	0.310	−0.074	1.177	2010/07
Nakagi, Shizuoka	N	34°36' 26"	138°49' 25"	24	12	0.500	1.4E-04	0.92	0.750	0.458	−0.638	1.168	2009/10
Tateyama, Chiba	C	34°59' 30"	139°49' 34"	11	6	0.545	3.3E-04	0.727	0.630	0.415	−0.518	0.915	2009/08

## Genetic Connectivity Among Different Populations

To assess genetic connectivity of the samples from different populations, we calculated global  $F_{ST}$  as well as pairwise  $F_{ST}$  of 13 populations ( $N > 7$ ) including Futagose and Otaura of Tsushima, Hongu and Kouze of Iki island, Amakusa, Ehime, Kochi, Shirahama, Takatomi, Fukuro Bay, Kuzura, Tago, and Nakagi using GenAlex ver. 6.51b2 (Table 2). We also calculated global  $F_{ST}$  for eastern and western cryptic lineages.

## RESULTS

### Clonal and Genetic Diversity of *A. pruinosa*

We found a relatively high proportion of asexual reproduction in each *A. pruinosa* population; clonal diversity using the 9 resemblance microsatellites loci ranged from 84 to 337 (Genotyped raw data available in Supplementary Table 1). The probability of identity averaged 0.00076 and ranged from 0.0067 (Takatomi, Wakayama) to 0.0000036 (Ehime) (Table 1). Thus, we assumed that the 9 microsatellite markers cannot be used to completely identify clones, but the possible error rate is still ignorable and thus is powerful enough to estimate clonality and genetic diversity in each population in this study. High frequencies of asexual reproduction with a small number of genets compared to the number of individuals were especially found in Tsushima, Iki, Amakusa, Kochi, Takegashima, Takatomi, Fukuro Bay, Enashi, Tago, Nakagi, and Tateyama. Nei's genetic diversity of each population showed the lowest value (0.284) at Takegashima and then Enashi, which indicated that each genet within a population contains quite similar genes, when comparing to other populations. Observed and expected heterozygosity ranged from 0.238 to 0.762 and 0.251 to 0.512 (Table 1).

### Cryptic Lineages Found in *A. pruinosa*

The STRUCTURE analysis revealed delta  $K = 2$ , and there were two distinct cryptic lineages within Japanese populations of *A. pruinosa* (Figure 2A). The distribution of the two lineages clearly corresponded to the geographic regions: western (Tsushima, Iki, Amakusa, Nobeoka, Ehime) and eastern (Takegashima, Shirahama, Takatomi, Fukuro Bay, Kuzura, Enashi, Tago, Nakagi, Tateyama) lineages, and the two co-existed in Kochi. The PCoA also clearly suggested a distinction between western and eastern populations, and the Kochi population showed more resemblance to the population of the eastern lineage than to that of the western lineage (Figure 2B).

### Morphological Examinations

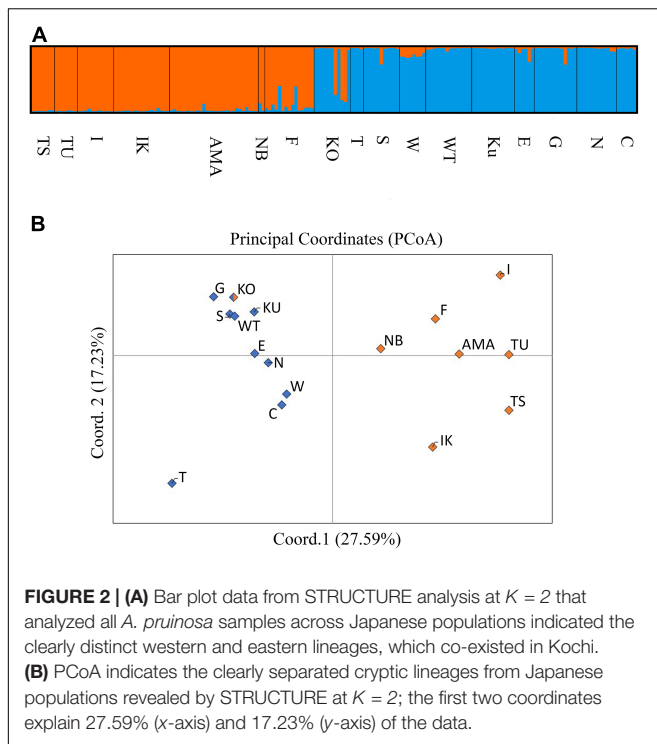
We measured the inner and outer diameters of axial corallites and the thickness of branches under 1 cm from the tip. The average lengths of all samples were 998 (S.D  $\pm$  149.3), 2,076 (S.D  $\pm$  243.0), and 3,076 (S.D  $\pm$  673.8)  $\mu$ m for inner diameter of axial corallites, outer diameter of corallite, and the thickness of branches under 1 cm from the tip, respectively (Supplementary Table 2). The lengths of the inner diameter ranged from 730 to 1,678  $\mu$ m, and those of the outer diameter ranged from 1,630 to 3,011  $\mu$ m; the thickness of branches under 1 cm from the tip ranged from 2,047 to 5,780  $\mu$ m. The averages of the inner and outer diameters of axial corallites, and the thickness of branches under 1 cm from the tip for the western lineage were 1021.2 (S.D  $\pm$  156.7), 2071.4 (S.D  $\pm$  219.6), and 3628.6 (S.D  $\pm$  721.3), respectively, while those for the eastern lineage were 962.3 (S.D  $\pm$  130.5), 2082.5 (S.D  $\pm$  277.1), and 3823.7 (S.D  $\pm$  579.8), respectively (Supplementary Table 2).

The septal number of axial corallites was 11.7 (S.D  $\pm$  1.2) for all samples, and 12.0 (S.D  $\pm$  1.3) for the western lineage, and 11.5 (S.D  $\pm$  1.1) for the eastern lineage (Supplementary Table 2). In all samples, six primary septa were distinct with nearly 2/3 to 1 radius of inner diameter. In all samples, radial corallites usually

**TABLE 2 |** Pairwise  $F_{ST}$  values (below) and  $P$  value (above) of the 13 Japanese populations of *Acropora pruinosa*.

Lineage		West	West	West	West	West	West	West/East	East	East	East	East	East	East
	Site	TS	TU	I	IK	AMA	F	KO	S	W	WT	Ku	G	N
West	TS		0.0016*	0.0001**	0.0001**	0.0001**	0.0001**	0.0001**	0.0001**	0.0001**	0.0001**	0.0001**	0.0001**	0.0001**
West	TU	0.2113		0.0007**	0.0002**	0.0006**	0.0004**	0.0001**	0.0001**	0.0003**	0.0001**	0.0001**	0.0001**	0.0003**
West	I	0.3097	0.2309		0.0001**	0.0001**	0.0001**	0.0001**	0.0001**	0.0001**	0.0001**	0.0001**	0.0001**	0.0001**
West	IK	0.1961	0.2282	0.3595		0.0001**	0.0001**	0.0001**	0.0001**	0.0001**	0.0001**	0.0001**	0.0001**	0.0001**
West	AMA	0.1517	0.1130	0.1627	0.1559		0.0001**	0.0001**	0.0001**	0.0001**	0.0001**	0.0001**	0.0001**	0.0001**
West	F	0.1889	0.1273	0.1717	0.2124	0.0684		0.0001**	0.0001**	0.0001**	0.0001**	0.0001**	0.0001**	0.0001**
West/East	KO	0.3524	0.3113	0.3540	0.3288	0.2271	0.1689		0.0015*	0.0001**	0.0001**	0.0001**	0.0001**	0.0001**
East	S	0.2971	0.2613	0.2815	0.3190	0.1967	0.1443	0.1082		0.0001**	0.0001**	0.0042*	0.0001**	0.0010*
East	W	0.3772	0.3393	0.3809	0.3128	0.2774	0.2938	0.3351	0.2538		0.0001**	0.0001**	0.0001**	0.0001**
East	WT	0.3806	0.3786	0.4098	0.3576	0.2705	0.2619	0.1819	0.1868	0.3096		0.0001**	0.0001**	0.0001**
East	Ku	0.2867	0.3025	0.2960	0.3234	0.2227	0.1853	0.2017	0.0824	0.2960	0.2244		0.0001**	0.0005**
East	G	0.3884	0.3625	0.3805	0.3426	0.2471	0.2618	0.1647	0.1721	0.3348	0.1737	0.1769		0.0001**
East	N	0.3065	0.2990	0.3549	0.2791	0.2010	0.2253	0.2529	0.1722	0.3207	0.3005	0.1745	0.2374	

\*\* means statistically significant at  $P$ -value  $< 0.001$ , and \* means  $P$ -value from 0.001 to 0.01 after Bonferroni correction.



had 6 primary septa with nearly 2/3 to 1 radius of inner diameter, and the coenosteum was reticulate.

After Mann-Whitney-Wilcoxon Rank Sum test to compare the two lineages, we found the  $P$ -values for the inner and outer diameters of axial corallites, the thickness of branches under 1 cm from the tip, and septal number of axial corallites to be 0.980, 0.584, 0.011, 0.926, respectively, suggesting a significant difference for only the thickness of branches under 1 cm from the tip. However, the range of the thickness of branches under 1 cm from the tip overlapped between the eastern and western lineages, indicating that the thickness of branches under 1 cm from the tip alone could not distinguish the two species (Supplementary Table 3).

## Genetic Connectivity

The global  $F_{ST}$  among all populations based on 9 microsatellite loci was large ( $F_{ST} = 0.245$ ,  $P < 0.001$ ). Pairwise  $F_{ST}$  values among 13 populations were also high, even within the same lineage; in the western lineage, pairwise  $F_{ST}$  values ranged from 0.0684 ( $P < 0.001$  between F and AMA) to 0.3595 ( $P < 0.001$  between I and IK), and in the eastern lineage, pairwise  $F_{ST}$  values ranged from 0.0824 ( $P = 0.0042$  between S and Ku) to 0.3096 ( $P < 0.001$  between W and WT). All the  $F_{ST}$  values for all populations were statistically significant ( $P < 0.01$ ) after Bonferroni correction (Table 2).

## DISCUSSION

This study provided basic important information for conservation of the threatened reef-building coral species

*A. pruinosa*; a relatively high proportion of asexual reproduction and low genetic diversity in each population, weak genetic connectivity among populations, presence of eastern and western cryptic genetic lineages were observed in Japan. All these facts emphasize the threatened status of *A. pruinosa*, highlighting the importance of effective conservation management of the species.

## Two Eastern and Western Cryptic Lineages Found in *A. pruinosa*

Principal coordinates analysis and STRUcTURE results revealed the existence of two genetically different lineages distributed in the east and west and co-existed in Kochi. While there was a significant difference in the thickness of branches under 1 cm from the tip between the eastern and western lineages, it was not possible to distinguish the lineages using this morphological trait alone because there was a substantial overlap in the thickness of branches under 1 cm from the tip between the two lineages. Recently, Taguchi et al. (2020) reported that *A. pruinosa* in Nishidomari, Kochi, where is the same sampling site in our study, had two different chromosome number, 28 and 29, in the same embryo. This difference might reflect the two genetically different lineages, but further detailed microscopic examination of morphology, ecological and physiological experiments will be required to determine the species status of the eastern and western lineages of *A. pruinosa*.

The existence of genetically separated cryptic lineages and their distribution are enigmatic. One possible explanation is that two distinct refugia, such as the north-eastern (somewhere in the eastern Pacific coast) and north-western (somewhere in the western Kyushu area) refugia, resulted in the distinct genetic lineages during the past climate change. *A. pruinosa* is a temperate coral that has a relatively higher tolerance to cold temperature than other coral species, including the widely distributed (tropical to temperate) species *Acropora hyacinthus* and *Acropora solitaryensis* (Higuchi et al., 2015). *A. pruinosa* is not distributed in subtropical areas in Japan. This trait of adapting well to cold temperature suggests that *A. pruinosa* might survive in colder habitats, such as the refugia in the north-eastern (Pacific) and north-western (western Kyushu) habitats, during the past warming period when corals suffered from coral bleaching in the warmer areas due to elevated water temperature. After such a warming period, the distribution of the species might expand to the southwest and southeast again to the current locations with time. Population genetic analysis on Japanese turban shell *Turbo cornutus* also showed a similar distribution of two distinct mitochondrial haplotype clusters, one of which is distributed along the Tsushima current to the west and the other is distributed along the Kuroshio current to the east. The two types also co-existed in the Seto Inland Sea (Kojima et al., 1997). The authors suggested that the two distinct lineages might have formed by two geographically separated refugia in the Japan Sea (western Kyushu) and on the Pacific coasts during the past climate change. Gene flow through a narrow strait called the Kanmon Strait resulted in the co-existence of the two types in the Seto Inland



Sea (Kojima et al., 1997). Similarly, in *A. pruinosa*, the co-existence of the western and eastern lineages in Kochi and western lineage in Nobeoka and Ehime might be attributed to gene flow through the Kanmon Strait from the north-western refugia.

## Clonal Structure, Genetic Diversity and Connectivity of *A. pruinosa*

A high ratio of asexual reproduction was found in *A. pruinosa*. Despite the similar habitats and sexual reproductive biology with *A. hyacinthus* and *A. solitaryensis* (Iwase et al., 2009), *A. pruinosa* showed a higher ratio of asexual reproduction than *A. hyacinthus* (Nakabayashi et al., 2019) and *A. solitaryensis* (Noreen et al., 2013). It is likely that coral growth form is associated with the ratio of asexual reproduction; the arborescent growth form is more fragile to environmental factors than the corymbose or tabular form (Wallace, 1999).

In addition to the high clonality, we found a low genetic diversity of *A. pruinosa* in each population, indicating that this species will be vulnerable to environmental changes. Furthermore, the limited genetic connectivity of *A. pruinosa* among populations suggests that each population is highly depends on local reproduction (self-recruitment), including asexual reproduction, implying a higher risk of local extinction in the future in the face of climate change.

*Acropora pruinosa* has a more limited genetic connectivity than other *Acropora* species, such as *Acropora digitifera* (Nakajima et al., 2010), *A. solitaryensis* (Noreen et al., 2013), and *A. hyacinthus* (Nakabayashi et al., 2019), despite having a similar early life ecology and the same larval dispersal duration (Iwase et al., 2009) to these species. It is possible that the arborescent morphological character, associated with a high frequency of asexual reproduction (fragmentations) of *A. pruinosa*, might be responsible for the limited genetic connectivity among populations. Laboratory experiments examining the fecundity of fragmented arborescent form *A. formosa* (= *Acropora muricata*) indicated that there is a trade-off of energy between reproduction and survival (Okubo et al., 2007). The high frequency of asexual reproduction in the arborescent *A. pruinosa* leads to a lower number of sexually reproduced larvae that disperse among different populations, resulting in the limited genetic connectivity of *A. pruinosa*.

## Conservation

This study revealed that the threatened status of *A. pruinosa* is much more serious than expected due to the overall low genetic diversity and the existence of cryptic lineages (possibly different species). Whether the two cryptic lineages are different species or not, genetically different lineages with different evolutionary histories should be conserved separately to sustain genetic and biodiversity as they might have adapted to different environments. Thus, the existence of two separated cryptic lineages emphasized the importance of more precise conservation because cryptic lineages would have different heat tolerance capacities and might respond differently to

climate change. Although we need more detailed morphological, ecological, and physiological analyses of the two lineages to examine species boundaries, our results cast a doubt on the “unusual distribution” of a single species, *A. pruinosa*. Given that we found distinct cryptic lineages and limited larval dispersal of *A. pruinosa*, even within Japan, it will be worth examining if *A. pruinosa* in geographically separated Hong Kong is really the same species. If *A. pruinosa* in Hong Kong is a genetically distinct endemic species, it requires more attention for conservation.

The overall low genetic diversity and high rate of asexual reproduction and self-seeding across the Japanese populations suggested that *A. pruinosa* is potentially vulnerable to environmental changes in the future because a low genetic diversity limits the ability of populations to adapt and evolve in response to climate changes and there is a low chance of replenishment by recruitment from other neighboring populations (Nei et al., 1975; Spielman et al., 2004). Alternatively, the high rate of clonal growth might be an important reproductive strategy for the preservation of the genetic diversity of populations or for the maintenance of population persistence during poor sexual recruitment periods (Baums et al., 2006).

## CONCLUSION

This study unveiled evolutionary distinct cryptic lineages of the threatened coral species *A. pruinosa* that are distributed in the east and west of the temperate Japanese coast. These two lineages might have resulted from the eastern and western refugia during the past climate change. This study also demonstrated a much higher ratio of asexual reproduction and more limited connectivity of *A. pruinosa* among different populations than other *Acropora* spp. Even though *A. pruinosa* (arborescent form) has almost the same early life ecology (spawning period, pelagic larval duration, and larval behavior) as other *Acropora* spp., a much higher rate of asexual reproduction and limited connectivity were found for this species than for the corymbose or tabular form *Acropora* spp., highlighting the importance of coral growth form on meta-population structure. All these information emphasize the threatened status of *A. pruinosa*, requiring urgent and effective conservation to avoid extinction in the face of climate change.

## DATA AVAILABILITY STATEMENT

The original contributions presented in the study are included in the article/**Supplementary Material**, further inquiries can be directed to the corresponding authors.

## AUTHOR CONTRIBUTIONS

HY, HF, and NY conceived the study. HY and HF collected the samples. SI and HF conducted morphological



analysis. SP, SI, AS, SN, and NY conducted molecular experiment. SP and NY analyzed the data and drafted the manuscript. All authors checked and edited the final manuscript.

## FUNDING

This study was supported by a research grant from the Kuroshio Biological Research Foundation, Grant-in-Aid for Young Scientists (A) (17H04996), the Program to Disseminate Tenure Track System in University of Miyazaki, and the Environment Research and Technology Development Fund (4RF-1501), Ministry of the Environment, Japan.

## REFERENCES

- Baums, I. B., Miller, M. W., and Hellberg, M. E. (2006). Geographic variation in clonal structure in a reef-building Caribbean coral, *Acropora palmata*. *Ecol. Monogr.* 76, 503–519.
- Earl, D. A., and VonHoldt, B. M. (2012). STRUCTURE HARVESTER: a website and program for visualizing STRUCTURE output and implementing the Evanno method. *Conserv. Genet. Resour.* 4, 359–361. doi: 10.1007/s12686-011-9548-7
- Falush, D., Stephens, M., and Pritchard, J. K. (2003). Inference of population structure using multilocus genotype data: linked loci and correlated allele frequencies. *Genetics* 164, 1567–1587.
- Falush, D., Stephens, M., and Pritchard, J. K. (2007). Inference of population structure using multilocus genotype data: dominant markers and null alleles. *Mol. Ecol. Notes* 7:4. doi: 10.1111/j.1471-8286.2007.01758.x
- Fukami, H., Budd, A. F., Levitan, D. R., Jara, J., Kersanach, R., and Knowlton, N. (2004). Geographic differences in species boundaries among members of the *Montastraea annularis* complex based on molecular and morphological markers. *Evolution* 58, 324–337. doi: 10.1111/j.0014-3820.2004.tb01648.x
- Goldberg, J., and Wilkinson, C. (2004). “Global threats to coral reefs: coral bleaching, global climate change, disease, predator plagues, and invasive species,” in *Status of Coral Reefs of the World: 2004*, ed. C. Wilkinson (Townsville, AU: Australian Institute of Marine Science), 67–92.
- Gorospe, K. D., Donahue, M. J., and Karl, S. A. (2015). The importance of sampling design: spatial patterns and clonality in estimating the genetic diversity of coral reefs. *Mar. Biol.* 162, 917–928. doi: 10.1007/s00227-015-2634-8
- Higuchi, T., Agostini, S., Casareto, B. E., Suzuki, Y., and Yuyama, I. (2015). The northern limit of corals of the genus *Acropora* in temperate zones is determined by their resilience to cold bleaching. *Sci. Rep.* 5:18467. doi: 10.1038/srep18467
- Hubisz, M. J., Falush, D., Stephens, M., and Pritchard, J. K. (2009). Inferring weak population structure with the assistance of sample group information. *Mol. Ecol. Resour.* 9, 1322–1332. doi: 10.1111/j.1755-0998.2009.02591.x
- IUCN (2020). *The IUCN Red List of Threatened Species. Version 2020-3*. Available online at: <https://www.iucnredlist.org> (accessed February 07, 2021).
- Iwase, F., Nakano, S., Aki, H., Okada, N., and Shimizu, R. (2009). Field test on breeding technique of the zoogamy for *Acropora tumida*. *J. Jpn. Soc. Civil Eng.* 65, 1216–1220. doi: 10.2208/kaigan.65.1216
- Kojima, S., Segawa, R., and Hayashi, I. (1997). Genetic differentiation among populations of the Japanese trurban shell Turbo (Batillus) cornutus corresponding to warm currents. *Mar. Ecol. Prog. Ser.* 150, 149–155.
- Kopelman, N. M., Mayzel, J., Jakobsson, M., Rosenberg, N. A., and Mayrose, I. (2015). CLUMPAK: a program for identifying clustering modes and packaging population structure inferences across K. *Mol. Ecol. Resour.* 15, 1179–1191.
- Ministry of the Environment (2017). *The Japanese Red list of Coral Species (in Japanese)*. Available online at: [https://www.env.go.jp/nature/kisho/sango\\_tokusei.html](https://www.env.go.jp/nature/kisho/sango_tokusei.html) (accessed December 18, 2020).
- Nakabayashi, A., Yamakita, T., Nakamura, T., Aizawa, H., Kitano, Y. F., Iguchi, A., et al. (2019). The potential role of temperate Japanese regions as refugia for the coral *Acropora hyacinthus* in the face of climate change. *Sci. Rep.* 9:1892. doi: 10.1038/s41598-018-38333-5
- Nakajima, Y., Nishikawa, A., Iguchi, A., and Sakai, K. (2010). Gene flow and genetic diversity of a broadcast-spawning coral in northern peripheral populations. *PLoS One* 5:e11149. doi: 10.1371/journal.pone.0011149
- Nanto, C., Kishimoto, T., and Ueno, S. (2009). Changes in *Acropora tumida* community in Kuzura, Sugura Bay, Central Japan and effects of fences for protecting the coral. *Bull. Inst. Oceanic Res. Develop. Tokai Univ.* 30, 13–20.
- Nei, M., Maruyama, T., and Chakraborty, R. (1975). The bottleneck effect and genetic variability in populations. *Evolution* 29, 1–10. doi: 10.1111/j.1558-5646.1975.tb00807.x
- Nishihara, M., and Veron, J. E. N. (1995). *Hermatypic Corals of Japan*. Tokyo: Kaiyusha.
- Nishihira, M. (2004). “Hermatypic coral of Japan,” in *Coral Reefs of Japan*, eds Japan Coral Reef Society and The Ministry of Environment of Japan (Japan: Ministry of Environment), 10–13.
- Nomura, K. (2009). Recent changes in coral communities in Kushimoto, the southernmost part of Honshu, Japan. *J. Jpn. Coral Reef Soc.* 11, 39–49. doi: 10.3755/jcrs.11.39
- Noreen, A. M. E., Van Oppen, M. J. H., and Harrison, P. L. (2013). Genetic diversity and differentiation among high-latitude broadcast-spawning coral populations disjunct from the core range. *Mar. Ecol. Prog. Ser.* 491, 101–109. doi: 10.3354/meps10480
- O'Brien, S. J. (1994). A role for molecular genetics in biological conservation. *Proc. Natl. Acad. Sci. U.S.A.* 91, 5748–5755. doi: 10.1073/pnas.91.13.5748
- Okubo, N., Motokawa, T., and Omori, M. (2007). When fragmented coral spawn? Effect on size and timing on survivorship and fecundity of fragmentation in *Acropora formosa*. *Mar. Biol.* 151, 353–363. doi: 10.1007/s00227-006-0490-2
- Peakall, R., and Smouse, P. E. (2006). GENALEX 6: genetic analysis in Excel. Population genetic software for teaching and research. *Mol. Ecol. Notes* 6, 288–295. doi: 10.1111/j.1471-8286.2005.01155.x
- Peakall, R., and Smouse, P. E. (2012). GenAlEx 6.5: genetic analysis in excel. Population genetic software for teaching and research—an update. *Bioinformatics* 28, 2537–2539. doi: 10.1093/bioinformatics/bts46
- Principe, P. P., Bradley, P., Yee, S. H., Allen, P. E., and Campbell, D. E. (2011). *Quantifying Coral Reef Ecosystem Services*. North Carolina: U.S. Environmental Protection Agency, Office of Research and Development, Research Triangle Park.
- Pritchard, J. K., Stephens, M., and Donnelly, P. (2000). Inference of population structure using multilocus genotype data. *Genetics* 155, 945–959.
- Shinzato, C., Yasuoka, Y., Mungpakdee, S., Arakaki, N., Fujie, M., Nakajima, Y., et al. (2014). Development of novel, cross-species microsatellite markers for *Acropora* corals using next-generation sequencing technology. *Front. Mar. Sci.* 1:11. doi: 10.3389/fmars.2014.00011
- Spielman, D., Brook, B. W., Briscoe, D. A., and Frankham, R. (2004). Does inbreeding and loss of genetic diversity decrease disease resistance? *Conserve. Genet.* 5, 439–448.

## ACKNOWLEDGMENTS

We are thankful for Ms. Ritsuko Kubota for helping with sequencing. The following helped with sampling in the field: Eriko Hatakeyama, Midori Kogi, Masanobu Sanpei, Muneyoshi Okabe, Ryuji Yamaguchi, Keiichi Nomura, Takuma Mezaki, and Kaoru Sugihara.

## SUPPLEMENTARY MATERIAL

The Supplementary Material for this article can be found online at: <https://www.frontiersin.org/articles/10.3389/fmars.2021.668043/full#supplementary-material>

- Sugihara, K., Nomura, K., Yokochi, H., Shimoike, K., Kajiware, K., Suzuki, G., et al. (2015). *Zooxanthellate Scleractinian Corals of Tanegashima Island, Japan*. Tsukuba: Center for Environmental Biology and Ecosystem Studies, National Institute for Environmental Studies.
- Suzuki, G., and Fukami, H. (2012). Evidence of genetic and reproductive isolation between two morphs of subtropical-dominant coral *Acropora solitaryensis* in the non-reef region of Japan. *Zool. Sci.* 29, 134–140.
- Taguchi, T., Tagami, E., Mezaki, T., Vacarizas, J. M., Canon, K. L., Avila, T. N., et al. (2020). Karyotypic mosaicism and molecular cytogenetic markers in the scleractinian coral *Acropora pruinosa* Brook, 1982 (Hexacorallia, Anthozoa, Cnidaria). *Coral Reefs* 39, 1415–1425. doi: 10.1007/s00338-020-01975-x
- van Oppen, M. J. H., Underwood, J. N., Muirhead, A. N., and Peplow, L. (2016). Ten microsatellite loci for the reef-building coral *Acropora millepora* (Cnidaria, Scleractinia) from the Great Barrier Reef, Australia. *Mol. Ecol. Notes* 7:3. doi: 10.1111/j.1471-8286.2006.01610.x
- Veron, J. E. N. (1992). Conservation of biodiversity: a critical time for the hermatypic coral of Japan. *Coral Reefs* 11, 13–21. doi: 10.1007/BF00291930
- Wallace, C. C. (1999). *Staghorn Corals of the World: A Revision of the Coral Genus Acropora*. Collingwood: CSIRO Publishing.
- Conflict of Interest:** The authors declare that the research was conducted in the absence of any commercial or financial relationships that could be construed as a potential conflict of interest.

Copyright © 2021 Pipithkul, Ishizu, Shimura, Yokochi, Nagai, Fukami and Yasuda. This is an open-access article distributed under the terms of the Creative Commons Attribution License (CC BY). The use, distribution or reproduction in other forums is permitted, provided the original author(s) and the copyright owner(s) are credited and that the original publication in this journal is cited, in accordance with accepted academic practice. No use, distribution or reproduction is permitted which does not comply with these terms.



# Genome-Wide SNP Data Revealed Notable Spatial Genetic Structure in the Deep-Sea Precious Coral *Corallium japonicum*

Kenji Takata<sup>1</sup>, Fumihito Iwase<sup>2</sup>, Akira Iguchi<sup>3</sup>, Hideaki Yuasa<sup>4</sup>, Hiroki Taninaka<sup>5</sup>, Nozomu Iwasaki<sup>6</sup>, Kouji Uda<sup>7</sup>, Tomohiko Suzuki<sup>7</sup>, Masanori Nonaka<sup>8</sup>, Taisei Kikuchi<sup>9</sup> and Nina Yasuda<sup>10\*</sup>

<sup>1</sup> Graduate School of Agriculture, University of Miyazaki, Miyazaki, Japan, <sup>2</sup> Shikoku Marine Life Laboratory, Otsuki, Japan,

<sup>3</sup> Geological Survey of Japan, National Institute of Advanced Industrial Science and Technology (AIST), Tsukuba, Japan,

<sup>4</sup> Department of Life Science and Technology, School of Life Sciences and Technology, Tokyo Institute of Technology,

Ookayama, Japan, <sup>5</sup> Interdisciplinary Graduate School of Agriculture and Engineering, University of Miyazaki, Miyazaki,

Japan, <sup>6</sup> Faculty of Geo-Environmental Science, Ritssho University, Kumagaya, Japan, <sup>7</sup> Laboratories of Biochemistry, Faculty

of Science, Kochi University, Kochi, Japan, <sup>8</sup> Okinawa Churashima Research Center, Okinawa Churashima Foundation,

Motobu, Japan, <sup>9</sup> Parasitology, Faculty of Medicine, University of Miyazaki, Miyazaki, Japan, <sup>10</sup> Department of Marine Biology and Environmental Sciences, Faculty of Agriculture, University of Miyazaki, Miyazaki, Japan

## OPEN ACCESS

### Edited by:

Tamotsu Oomori,  
University of the Ryukyus, Japan

### Reviewed by:

Chuya Shinzato,  
The University of Tokyo, Japan  
Federica Costantini,  
University of Bologna, Italy

### \*Correspondence:

Nina Yasuda  
nina27@cc.miyazaki-u.ac.jp

### Specialty section:

This article was submitted to  
Coral Reef Research,  
a section of the journal  
Frontiers in Marine Science

**Received:** 13 February 2021

**Accepted:** 19 May 2021

**Published:** 24 June 2021

### Citation:

Takata K, Iwase F, Iguchi A,  
Yuasa H, Taninaka H, Iwasaki N,  
Uda K, Suzuki T, Nonaka M, Kikuchi T  
and Yasuda N (2021) Genome-Wide  
SNP Data Revealed Notable Spatial  
Genetic Structure in the Deep-Sea  
Precious Coral *Corallium japonicum*.  
Front. Mar. Sci. 8:667481.  
doi: 10.3389/fmars.2021.667481

Estimating the spatial extent of gamete and larval dispersal of deep-sea coral species, is challenging yet important for their conservation. Spatial autocorrelation analysis is useful for estimating the spatial range of dispersal of corals; however, it has not been performed for deep-sea coral species using genome-wide single nucleotide polymorphisms (SNPs). In this study, we examined the spatial genetic structure of a deep-sea coral species—the Japanese red coral, *Corallium japonicum*, sampled off the coast of Kochi, which lies to the southwest of the Shikoku Island in Japan; the Kochi region suffers from over-harvesting because of its high commercial value. We also examined the power of detecting significant spatial genetic structure by changing the number of loci and the proportion of missing data using both *de novo* analysis and mapping analysis. Similar results were obtained for both *de novo* and mapping analysis, although a higher number of loci were obtained by the mapping method. In addition, “many SNPs with a lot of missing data” was generally more useful than “a small number of SNPs with a small amount of missing data” to detect significant fine-scale spatial genetic structure. Our data suggested that more than 700 neutral SNPs were needed to detect significant fine-scale spatial genetic structure. The maximum first distance class that can detect significant spatial genetic structure within Kochi for the *C. japonicum* population was less than 11 km, suggesting that the over-harvesting of *C. japonicum* within a diameter of approximately 11 km in the Kochi area should be avoided, because this can cause the local extinction of this species.

**Keywords:** precious coral, spatial genetic structure, spatial autocorrelation, conservation, larval dispersal, deep-sea coral

## INTRODUCTION

Deep-sea corals play an important role in increasing the biodiversity of the deep-sea by providing complex habitat structures for other species (Roberts et al., 2006). Some of them are also one of the most valuable marine resources with high economic value, as despite their limited supply, they are used as raw material for jewelry, especially in China and Taiwan (Tsounis et al., 2010). In Japan, three deep-sea coral species (*Corallium japonicum*, *Pleurocorallium elatius*, and *Pleurocorallium konojoj*) are harvested and used to produce jewelry as precious corals in Kochi, Kagoshima, Okinawa, and Ogasawara Islands (CITES, 2007, 2009). Precious corals have low fecundity rate (Nonaka et al., 2015), slow growth rate (Luan et al., 2013), and are highly threatened by poaching and overexploitation (Iwasaki, 2019). The Ministry of the Environment, Japan, has listed the three coral species as critically endangered species in the Red List (Ministry of the Environment Government of Japan, 2017).

The diametric and linear growth rate of the Japanese red coral *C. japonicum* is only 0.2 mm and 2–6 mm per year, respectively (Luan et al., 2013), with a maximum growth of up to 30 cm (Iwasaki et al., 2009), implying that it has a high longevity. *Corallium japonicum* is a gonochoristic broadcast spawning species (Kishinouye, 1904); thus, the size of a population and connectivity among different populations can be defined by the extent of larval dispersal. Defining population boundaries is important for conservation of a species, although it is particularly problematic in marine species (Berry et al., 2012), especially long-lived sessile species (Ayre and Hughes, 2000). Moreover, the pelagic larval dispersal duration (PLD) for most deep-sea coral species, including *C. japonicum*, is unknown (Waller, 2005), which further challenges the estimation of the extent of spatial larval dispersal.

Spatial genetic structure (SGS) based on a sufficient number of loci can examine the extent of genetic interactions between continuously distributed populations and can serve as an indicator for estimating the spatial extent of a population, i.e., a minimum and critical unit for conservation of a species (Epperson, 2005; Schwartz and McKelvey, 2009). In the Mediterranean Sea, SGS analyses of the red coral *Corallium rubrum* that was found at depths shallower than 50 m have suggested the presence of a marked genetic structuring within a few meters (Costantini et al., 2007); another analysis revealed an estimated patch size of less than 40 cm for this species (Ledoux et al., 2010; Costantini et al., 2018), indicating that self-recruitment appears to be crucial for the maintenance of the populations of red coral species (Ledoux et al., 2010). To the best of our knowledge, however, there is no previous study on SGS analysis for deep-sea marine species due to the difficulty in obtaining global positioning system (GPS) information for marine species, especially deep-sea species, and the unavailability of sufficient and suitable markers for SGS.

Multiplexed inter simple sequence repeat (ISSR) genotyping by sequencing (MIG-seq) can detect a moderate number of single nucleotide polymorphisms (SNPs) from putatively neutral loci adjacent to microsatellite regions using polymerase chain reaction (PCR) and high-throughput technology. This method

is relatively easy, cost-effective, and can be performed even without a reference genome. Because MIG-seq is a PCR-based method, low concentration and/or low-quality DNA that is often extracted from deep-sea coral species (Eguchi et al., 2020) can be used. Furthermore, previous studies on octocoral species have demonstrated that MIG-seq analysis is useful for uncovering the genetic structures and lineages that were undetectable using a small number of traditional genetic markers, including microsatellite loci and mitochondrial DNA (Richard et al., 2018; Takata et al., 2019).

There is always a trade-off between the number of SNPs obtained and the number of missing data per locus when using high-throughput analysis, such as restriction site-associated DNA sequence (RAD-seq) (Miller et al., 2007). Therefore, maintaining a balance between the number of SNPs and the ratios of missing data per locus is important for conducting accurate genetic analysis, although much information is not available for SGS analysis (Shafer et al., 2017); thus, the robustness of using a reference genome for detecting SGS using MIG-seq analysis has never been empirically examined.

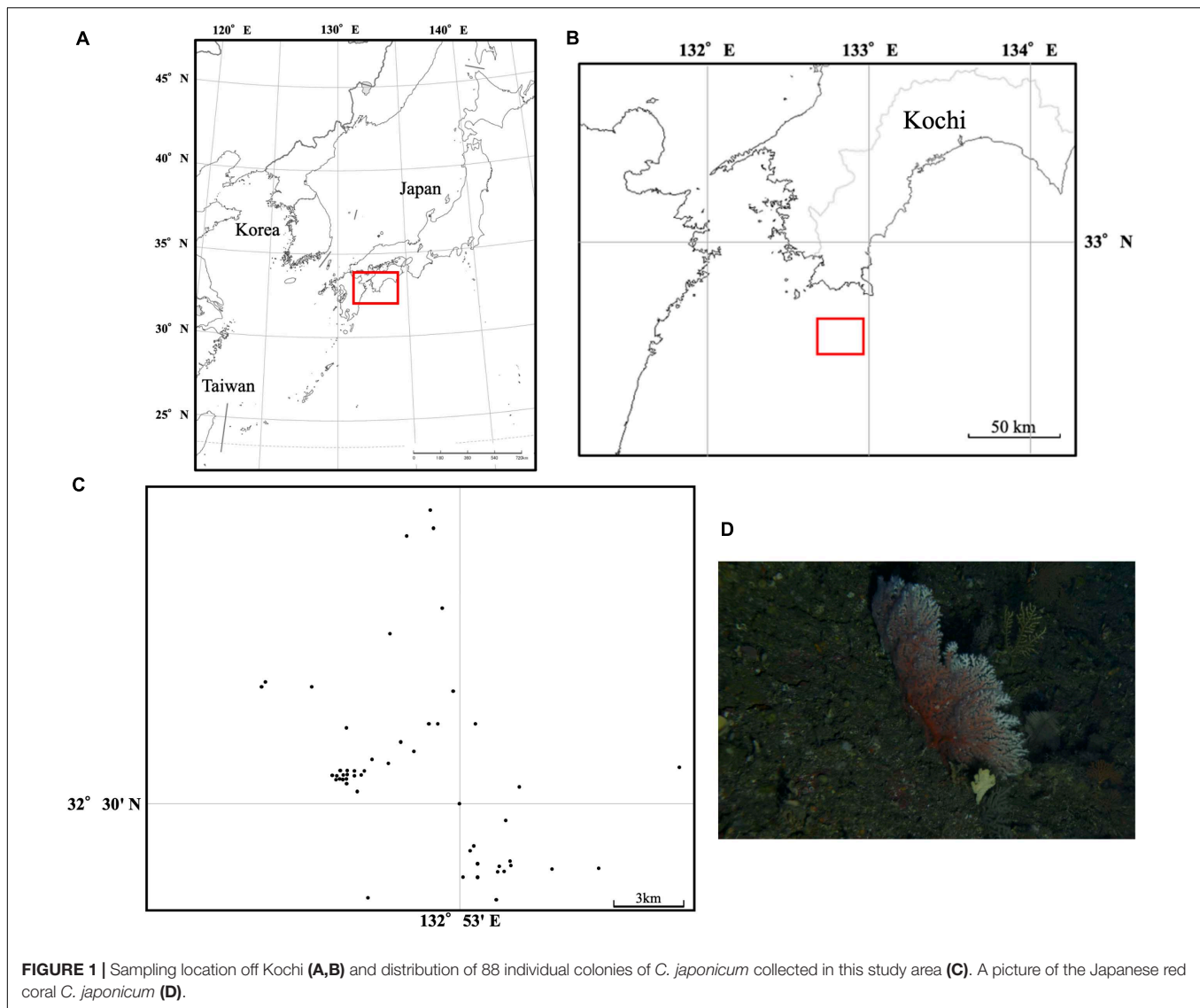
In this study, we (1) examined the robustness of detecting SGS by changing the number of loci and the proportion of missing data using both in *de novo* analysis and mapping methods, and (2) revealed the extent of *C. japonicum* (Japanese red coral) population (in terms of larval dispersal) in one of the most important fishing grounds, Kochi.

## MATERIALS AND METHODS

### Coral Sampling and DNA Extraction for MIG-Seq Analysis

We exhaustively sampled 88 individual colonies of *C. japonicum* using a traditional coral net, and GPS information for each coral was recorded based on the ship locations at which fishermen started drawing the nets off the coast of Kochi in Japan from 2011 to 2014 (Figure 1). The horizontal distance at which each coral was sampled was approximately 18 km × 18 km; the maximum distance between the colonies was 18.6 km. The depth at which each coral was sampled was similar (100–140 m), and, thus, we only considered horizontal distance among the samples. Almost 1 cm of coral fragment from each sample was collected and preserved in 99.5% ethanol until genomic DNA extraction.

The genomic DNA was extracted using a modified heat alkaline method (Nakabayashi et al., 2019; Takata et al., 2019). We used the MIG-seq method (Suyama and Matsuki, 2015) to obtain genome-wide SNP data. MIG-seq amplifies putatively neutral, anonymous genome-wide ISSR regions (Gupta et al., 1994; Zietkiewicz et al., 1994) using a simple 2-step PCR procedure. We used eight pairs of multiplex ISSR primers (MIG-seq primer set 1, Suyama and Matsuki, 2015) with the Multiplex PCR Assay Kit Ver. 2 (TaKaRa Bio Inc., Otsu, Shiga, Japan) for the first PCR; we used a total reaction volume of 7 µL in a T100™ Thermal Cyclerr (Bio-Rad) with the following conditions: initial denaturation at 94°C for 1 min, followed by 27 cycles of 94°C for 30 s, 38°C for 1 min, 72°C for 1 min, and final extension at 72°C for 10 min. The samples were indexed



**FIGURE 1 |** Sampling location off Kochi (A,B) and distribution of 88 individual colonies of *C. japonicum* collected in this study area (C). A picture of the Japanese red coral *C. japonicum* (D).

in the second PCR, which was performed with PrimeSTAR GXL DNA polymerase (TaKaRa Bio Inc., Otsu, Shiga, Japan) using a total of 12  $\mu$ L reaction volume in a thermal cycler under the following conditions: 21 cycles of 98°C for 10 s, 54°C for 15 s, and 68°C for 1 min. The PCR products were mixed and pooled and run on an agarose gel; the gel extraction of the PCR products that were 350–800 bp in length was performed. The gel-extracted DNA samples were sequenced using MiSeq (sequencing control software v2.0.12, Illumina) with the MiSeq Reagent v3 150 cycle kit (Illumina). Image analysis and base calling were performed using the real-time analysis software v1.17.21 (Illumina).

## Field Study Permissions

The samples were collected under the Kochi Prefecture sampling permit (Sa 401, Sa 412, and Sa 423) and Okinawa Prefecture sampling permit (Oki 21-131).

## Data Analysis

To eliminate low-quality reads and primer sequences from the raw data, we used the FASTX-toolkit version 0.0.14 (fastq\_quality\_filter)<sup>1</sup> with a fastq-quality-filter setting of  $-q\ 30\ -p\ 40$ . We removed adapter sequences for the Illumina MiSeq run from both the 5' end (GTCAGATCGGAAGAGCACACGTCTGAACTCCAGTCAC) and the 3' end (CAGAGATCGGAAGAGCGTCGTGTAGGG AAAGAC) using Cutadapt version 1.13 (Martin, 2011), and we excluded short reads of less than 80 bp.

For *de novo* analysis, the quality-filtered sequence data were demultiplexed and filtered using Stacks v1.46 (Catchen et al., 2011; Catchen et al., 2013). We used Stacks v. 1.4 (Catchen et al., 2013) to stack the reads and extract the SNPs. First, we used Ustacks with the following settings: “minimum depth of coverage required to create a stack (m)” = 3, “maximum distance

<sup>1</sup>[http://hannonlab.cshl.edu/fastx\\_toolkit/index.html](http://hannonlab.cshl.edu/fastx_toolkit/index.html)



allowed between stacks (M)" = 1, and "maximum distance allowed to align secondary reads to primary stacks (N)" = 1; deleveraging (d) and removal (r) algorithms were also enabled. Second, we used Cstacks with the following settings: "number of mismatches allowed between sample loci when building the catalog (n)" = 4, followed by the Sstacks. We created different SNP sets using the population software implemented in Stacks v. 1.4 by restricting data analysis: the minimum percentage of individuals required to process a locus across all data (r) was set at 0.5–1.0 (0.1 increments), and all SNPs per locus were used. For all of these analyses, we used the following parameters: "the minimum minor allele frequency required to process a nucleotide site at a locus (min\_maf)" = 0.01, and "the maximum observed heterozygosity required to process a nucleotide site at a locus (max\_obs\_het)" = 0.99.

For mapping analysis, we used the Burrows-Wheeler Aligner (BWA) program, specifically, the BWA-MEM algorithm (Li and Durbin, 2009). The SAM files were converted into BAM output files, which were subsequently sorted and indexed; the quality and mapping percentages per scaffold in these files were then checked. The SAM files were then used to perform SNP calling in the software Gstacks implemented in Stacks v. 2.2 (Catchen et al., 2013; Rochette and Catchen, 2017).

For the reference genome sequencing of *C. japonicum*, we used one specimen of target species collected off Shiraho, Okinawa, Japan, in 2011, using remotely operated vehicle. We extracted DNA from this specimen by using the DNeasy Blood and Tissue Kit (Qiagen, Hilden, Germany) following the manufacturer's instructions. Using the Nextera XT DNA Sample Prep Kit (Illumina), we sequenced the genome of *C. japonicum* and obtained paired-end (2 × 300 bp) reads. The adapter sequences in the reads were filtered using Cutadapt version 1.9.1 software (Martin, 2011); the reads with poor-quality bases (Q < 20) and those with lengths < 40 bp were excluded. We assembled these reads using SPAdes version 3.9.0 (Bankevich et al., 2012) with the following parameters: -k 21, 33, 55, 77, 99, and 127. Then, we retained contig sequences with coverage between 1 × to 24 × and removed sequences artificially produced by genome assembly software using Purge Haplotigs with the setting: -l 1 -m 3 -h 24 (Roach et al., 2018).

We used Gstacks option (-rm, -pcr, -duplicates) in Stacks v. 2.2 to remove PCR duplicates by randomly discarding all but one pair of each set of reads. We used the population software to prepare different datasets for subsequent analyses. We changed the ratio of missing data (r; proportion of shared SNPs among samples) ranging from 0.5 to 1 (0.1 increments). For all of these analyses, we also used the following parameters: "the minimum minor allele frequency required to process a nucleotide site at a locus (min\_maf)" = 0.01, and "the maximum observed heterozygosity required to process a nucleotide site at a locus (max\_obs\_het)" = 0.99. BayeScan v 2.1 (Narum and Hess, 2011) was used to detect possible SNPs under natural selection with a default setting.

Indicators of genetic diversity, nucleotide diversity ( $\pi$ ) and heterozygosity ( $H_E$ ), and inbreeding coefficient ( $F_{IS}$ ) were calculated using the population software and data from *de novo* and mapping were compared based

on Mann-Whitney U test. Hardy-Weinberg equilibrium (HWE) was examined for both the *de novo* (2,280 SNPs with  $r = 0.5$ ) and mapping (892 SNPs with  $r = 0.9$ ) datasets using GeneAEx ver. 6.5 (Peakall and Smouse, 2012).

## Spatial Autocorrelation Analysis

To detect SGS, we used GenAEx ver. 6.5 (Peakall and Smouse, 2012), which calculates a pairwise genetic and pairwise geographical distance matrix to generate an autocorrelation coefficient (indicated as  $r_s$ ; the correlation value between the genetic and geographic distance in this manuscript; see **Figure 4**) for a given distance class. Each distance class is bound by an upper and lower value (e.g., 0–1 km). All pairwise comparisons within a geographic range given the distance class are used to test the null hypothesis that the genotype pairs are randomly distributed within the geographic range. Spatial autocorrelation analysis superimposed the 95% confidence interval for the null hypothesis of a random SGS on the correlogram. Under restricted gene flow, and in the absence of selection, we will observe positive significance (the  $r_s$  value is higher than the 95% confidence interval for the null hypothesis of random SGS) at short distance classes, indicating that the geographically close individuals tend to have closer genotypes. Subsequently, the autocorrelation coefficient will decline through zero (here we define this point as x-intercept, see **Figure 4**) and become negative. This x-intercept provides an estimate of the extent of the positive genetic structure only if a positive significant SGS was found.

Currently, two complimentary analyses of significant SGS are often used (Peakall et al., 2003; Underwood et al., 2007): the first one uses x-intercepts (conservative permutation test using relatively short distance class). The intercept reflects the population size that is useful for the conservation of a species and for accurately assessing genetic diversity (Diniz-Filho and Telles, 2002). The second one relies on more powerful permutation tests and the use of the maximum first distance class that can detect significant SGS. This is because a single correlogram can be strongly influenced by the interactions between the extent of genetic structure and distance class sizes, together with the number of samples existing within that geographic range (Peakall et al., 2003; Underwood et al., 2007). In this study, we calculated both the x-intercepts and the maximum first distance class, but the maximum significant first distance class was regarded as the maximum range of gamete and larval dispersal.

The number of permutation tests was set to 9,999 for each analysis. We tested 15 different distance classes from 1 to 15 km using different ratios of missing data per locus for *de novo* ( $r = 0.5$ – $0.9$ ; 1.0 failed) and mapping ( $r = 0.5$ – $1.0$ ) analyses. To estimate the minimum number of SNPs that can detect significant SGS, we used  $r$  values (at intervals of 0.01) 0.7–0.8 and 0.9–1.0 for *de novo* and mapping analyses, respectively. We used the PGD spider ver 2.0.8.3 (Lischer and Excoffier, 2011) to convert SNP data file formats.

## RESULTS

### Detection of SNPs

A total of 23,991,966 raw reads with an average of 272,636 reads per sample ( $SD = 92,029.33$ ,  $SE = 147.81$ ) were obtained for the 88 sampled corals, and after filtering out the low-quality reads, 23,828,764 reads remained. We obtained 16,679,162 reads with an average of 189,536 reads per individual ( $SD = 61,902.56$ ,  $SE = 122.51$ ) after two-step filtering. We obtained *de novo* reference genome assemblies using paired-end short reads of *C. japonicum* and the amount of sequence data used for assembly, total assembly size, number of sequences, percentage of gaps, N50 value, longest and minimum sequence lengths are available in **Supplementary Table 1**. The mean value of GC contents of the *de novo* genome sequences were 38.3%, which is almost similar to that for other anthozoan genomes (Shinzato et al., 2011). Single sharp peaks on the histograms of the GC contents also support the low contamination level of this assembly (**Supplementary Figure 1**). However, caution should be warranted for the usage of the *C. japonicum* genome assembly, as no low-coverage sequences were not removed by Purge Haplotigs, DNA sequences from bacterial contaminants and other organisms might be also included in the *C. japonicum* genome assembly (**Supplementary Figure 2**).

We identified 0–2,280 SNPs by *de novo* analysis and 132–5,884 SNPs by mapping analysis (**Figure 2**). We detected 3–15 times more SNPs by mapping analysis than by *de novo* analysis when comparing with the same missing data ratio ( $r$ ). BayeScan

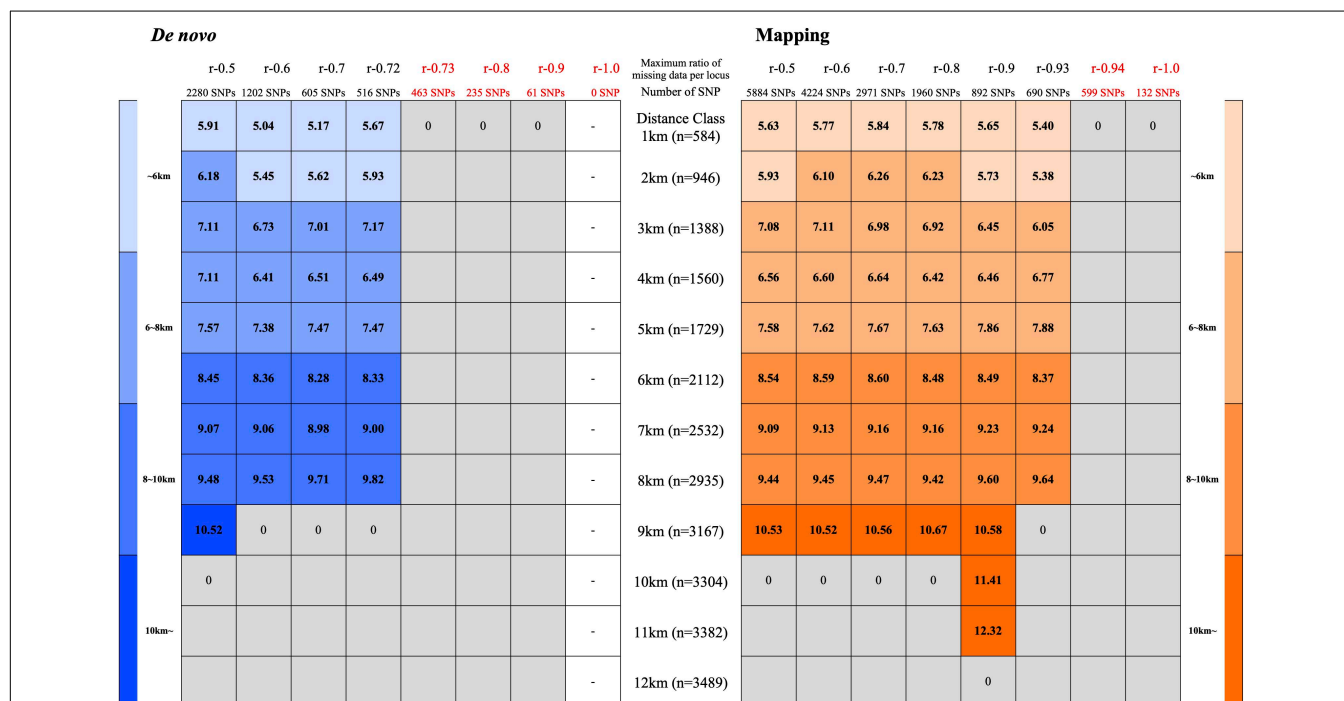
indicated that all the SNPs were neutral ( $q > 0.05$ ).  $F_{IS}$  (variant positions) values were significantly higher ( $P > 0.05$ ) in *de novo* analysis than in mapping analysis (**Figure 3**). The number of SNPs that deviated from HWE was 1,813 out of 2,280 SNPs (79.5%) for *de novo* analysis and 223 out of 892 SNPs (25.0%) for mapping analysis.

### Spatial Autocorrelation Analysis

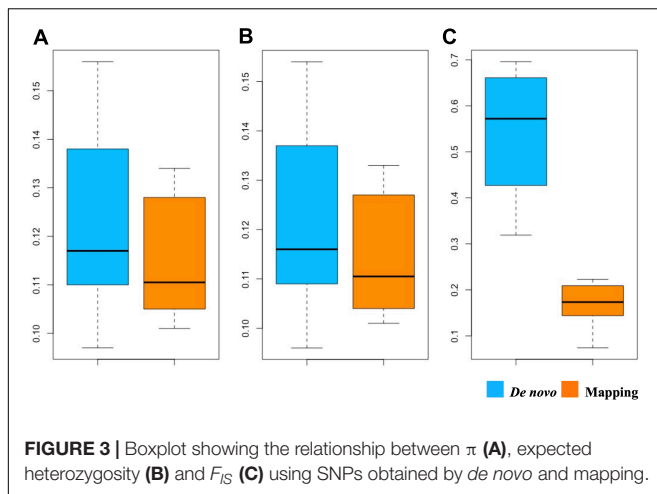
Spatial autocorrelation analysis was performed with 15 different classes of distance (1–15 km) using different ratios of missing data and numbers of SNPs based on both *de novo* analysis and mapping analysis.

Overall, when using a sufficient number of loci ( $>700$  SNPs, **Figure 2** and **Supplementary Table 2**), both *de novo* analysis and mapping analysis showed similar results (**Figure 2** and **Supplementary Table 2**); the maximum distances up to which the significant genetic structure detected were 11 km for the mapping analysis and 9 km for *de novo* analysis. However, the mapping analysis detected a wider range of significantly positive structures for the x-intercepts (summarized in **Figure 2** and **Supplementary Table 2**); the range of x-intercepts was from 5.04 km ( $r = 0.6$ ) to 10.52 km ( $r = 0.5$ ) for the *de novo* analysis and from 5.63 km ( $r = 0.5$ ) to 12.32 km ( $r = 0.9$ ) for the mapping analysis (**Figure 2** and **Supplementary Table 2**).

The correlograms based on *de novo* analysis ( $r = 0.5$ , 2,280 SNPs) and mapping analysis ( $r = 0.9$ , 892 SNPs) indicated similar results (**Figure 4**). When using the 2 km distance class, the correlation values were positive and significant up to 4 km and



**FIGURE 2 |** Outcomes of spatial genetic autocorrelation analysis with the different distance classes (1–15 km) using different ratios of missing data per locus ( $r = 0.5$ – $1.0$ ;  $r = 1.0$  for *de novo* was failed). Note that the x-intercepts were converted to zero when the correlation was not significantly different from zero and shown in gray. The color counter reflects the size of the x-intercept (lighter colors indicate smaller x-intercept values).



significantly negative from 8 km with an x-intercept of 6.18 km (*de novo* analysis, **Figure 4A**) and positive and significant up to 2 km and significantly negative from 8 km with an x-intercept of 5.73 km (mapping analysis, **Figure 4C**). When using the 5 km distance class, the correlation values were positive and significant up to 5 km, and negative and significant from 10 to 15 km, with an x-intercept of 7.57 km (*de novo* analysis, **Figure 4B**) and 7.86 km (mapping analysis, **Figure 4D**). The correlograms (including most correlograms in our data) show oscillations of high and low autocorrelation for negative and significant  $r_s$  values (**Figure 4**), indicating chaotic spatial patterns of genetic relatedness of *C. japonicum* at these scales. Such positive autocorrelation in a short distance class indicates limited larval dispersal within the sampling site (Peakall et al., 2003).

## The Number of SNPs Required for Detecting SGS

To examine the minimum number of SNPs required to detect significant SGS, analysis was performed at  $r = 0.7$ – $0.8$  for *de novo* analysis and  $r = 0.9$ – $1.0$  for mapping analysis with an interval of 0.01. *De novo* analysis could detect significant SGS when using  $> 516$  SNPs ( $r = 0.72$ ), while the mapping data could detect significant SGS when using  $> 690$  SNPs ( $r = 0.93$ ), indicating that more than 700 neutral SNPs obtained by MIG-seq are sufficient to detect significant SGS in our *C. japonicum* dataset (**Figure 2** and **Supplementary Table 3**).

## DISCUSSION

Estimating the spatial extent of gamete and larval dispersal is important for defining the size of a population and assessing the conservation management unit of marine organisms, although it has been challenging, especially for deep-sea organisms whose spawning period and PLD are unknown. In this study, we showed that both *de novo* analysis and mapping analysis are useful for detecting significant SGS when using a sufficient number of loci ( $> 700$  SNPs), although mapping analysis has more advantages in obtaining a larger number of SNPs with a lower ratio of missing

data. Furthermore, we demonstrated that the size of *C. japonicum* population that withstands frequent gamete and larval dispersal is within an area of less than 11 km off the Kochi area.

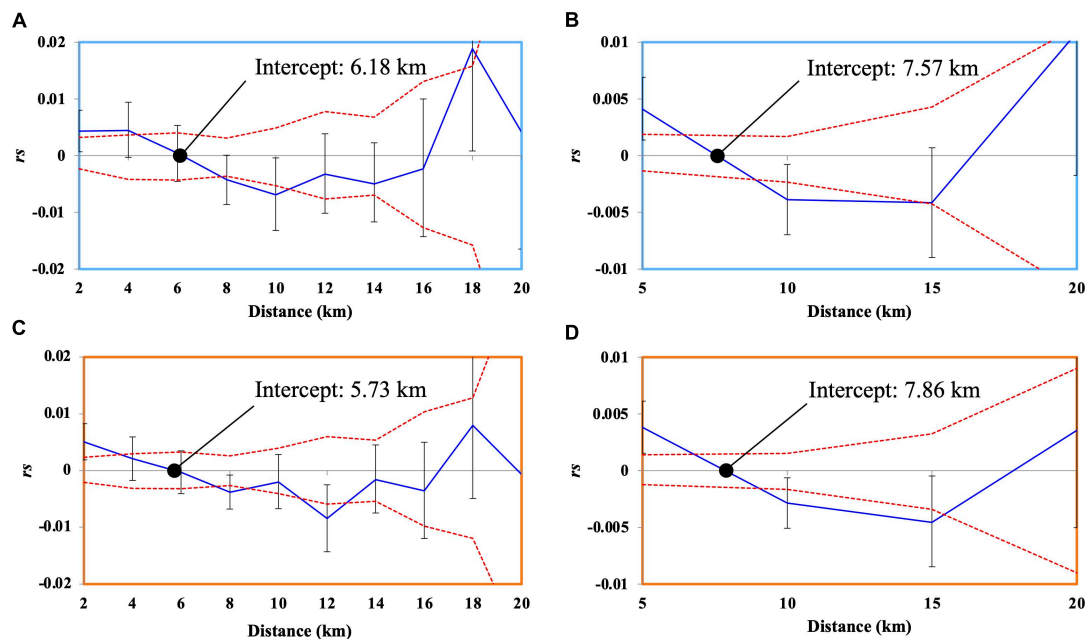
## Robustness of Detecting SGS Using *de novo* Analysis and Mapping Analysis in MIG-Seq Analysis

Many population genetic inferences based on high-throughput sequence data are influenced by bioinformatic pipelines on population genetic parameters, but this field has received little attention (Shafer et al., 2017). Thus, a comparative analysis of the robustness of different parameter settings for *de novo* analysis and mapping analysis to detect SGS would help fill the knowledge gap. This study suggests that significant SGS and comparative results with the mapping method can be obtained even without reference genome sequence data when a sufficient number of loci is used ( $> 700$  SNPs).

All genetic diversity statistics,  $F_{IS}$ , were higher in *de novo* analysis than in mapping analysis. A larger number of SNPs significantly deviated from HWE in *de novo* analysis than in mapping analysis. Mapping analysis using reference genome sequences has more advantages in distinguishing repetitive and/or duplicated regions from real SNPs than *de novo* analysis. It is likely that some of the SNPs obtained by *de novo* analysis included some repetitive and/or duplicated regions that resulted in higher genetic diversity and inbreeding coefficient. Similar to the present study, Shafer et al. (2017) also calculated summary statistics to confirm the validity of the results obtained by *de novo* and mapping analyses based on the RAD-seq data. They reported that mapping on a close reference genome detected more SNPs and reduced  $F_{IS}$ . In the present study, we found that the mapping analysis could detect a wider spatial extent of positive significant structure (up to 11 km) when using a moderate number of SNPs with a lower proportion of missing data ( $r = 0.9$ ). Arnold et al. (2013) showed that the summary statistics can deviate from true values and biases subsequent to population genetic analysis. Therefore, it is also possible that a higher proportion of missing data in *de novo* analysis failed to detect significant SGS. As previously recommended by Shafer et al. (2017), we also conclude that employing reference-based approaches wherever possible is preferable.

## Balance Between the Number of Loci and the Ratio of Missing Data for SGS Analysis

In high-throughput sequencing of reduced representation libraries, it is difficult to choose between “a large number of SNPs with a lot of missing data” and “a small number of SNPs with a small amount of missing data.” Although a few studies have examined the impact of missing data obtained by RAD-seq on population genetics (Arnold et al., 2013; Buerkle and Gompert, 2013) and phylogenetic analysis (Roure et al., 2013; Huang and Knowles, 2016), to the best of our knowledge, the present study is the first to empirically examine the balance between the number of SNPs and the ratio of missing data for SGS analysis using MIG-seq data.



**FIGURE 4 |** Correlograms showing the spatial autocorrelation  $r_s$  (here “ $r_s$ ” is used instead of “ $r$ ” that is generally used for correlation coefficient of spatial autocorrelation analysis to avoid confusion with the ratio of missing data per locus “ $r$ ”) across as a function of distance, 95% confidence interval about the null hypothesis of a random distribution of *C. japonicum*, and 95% confidence error bars about  $r_s$  as determined by bootstrapping. Autocorrelation for distance class size of **(A)** 2 km using *de novo* (2,280 SNPs), **(B)** 5 km using *de novo* (2,280 SNPs), **(C)** 2 km using mapping method (892 SNPs), and **(D)** 5 km using mapping method (892 SNPs).

Significant SGS was detected when using > 516 SNPs ( $r = 0.72$ ) for *de novo* analysis and 690 SNPs ( $r = 0.93$ ) for mapping analysis, indicating that approximately > 700 SNPs are necessary to detect significant SGS using MIG-seq data. Our results imply that choosing “a large number of SNPs with a lot of missing data” is more efficient than choosing “a small number of SNPs with a small amount of missing data” to detect significant SGS. Spatial autocorrelation analysis examines genetic relatedness among different individuals. Examining the relative genetic distance among such genetically close kinships may require a relatively large number of SNPs, even with relatively high missing data. In phylogenetic analysis, even though missing data have adverse effects, such as decreasing resolving power and the detection of multiple substitutions (Roure et al., 2013), empirical studies have suggested that a large number of SNPs despite a large amount of missing data has a higher resolution in providing phylogenetic inferences (Rubin et al., 2012; Wagner et al., 2013).

Although a sufficient number of loci is important for detecting significant SGS, a smaller ratio of missing data in mapping analysis ( $r = 0.9$ ) can detect significant SGS in a wider geographical range, implying that missing data may also slightly influence the robustness of detecting significant SGS.

## Gamete and Larval Dispersal of *C. japonicum* Estimated by SGS Analysis

Spatial autocorrelation analysis is a theoretically well-established method to estimate the extent of dispersal of target species (e.g., Epperson and Li, 1996). Spatial autocorrelation analysis

of *C. japonicum* based on MIG-seq loci revealed a pattern of significant positive local genetic structure, suggesting that proximate *C. japonica* colonies are genetically more similar than the distant colonies. Generally, the first x-intercept of the correlogram provides an estimate of the extent of positive genetic structure that is interconnected by dispersal (Peakall et al., 2003); it is also proposed to be used for deciding the management unit for conservation and to establish sampling strategies (Diniz-Filho and Telles, 2002). However, the x-intercept is largely dependent on the interaction among pre-defined distance-class size, unknown genetic structure, and the associated number of samples per distance class (Peakall et al., 2003). As suggested by Peakall et al. (2003), we examined the maximum first distance class by calculating SGS using different distance classes. We interpreted the distance class at which the estimation of  $r$  was no longer significant enough to serve as the maximum extent of the *C. japonicum* population that was formed by gamete and larval dispersal in the Kochi area. In the present study, we detected 11 km of significant maximum SGS with (mapping method  $r = 0.9$ , 892 SNPs) indicating that the spatial extent of gamete and larval dispersal occurred within this scale.

The SGS (<11 km) estimated for *C. japonicum* was larger than that of another Coralliidae coral *Corallium rubrum* (< 40 cm) that was revealed using microsatellite loci in a previous study (Ledoux et al., 2010; Costantini et al., 2018). Differences in habitat environments could be attributed to this difference; *C. japonicum* lives in a relatively open continental shelf deep-sea, while the *C. rubrum* sampled



in Costantini et al. (2007, 2018) and Ledoux et al. (2010) lived in a shallow, semi-closed cave. Further SGS studies using *C. rubrum* specimens obtained from deep water (e.g., deeper than 100 m, Costantini et al., 2010, 2013) would be useful to test this hypothesis. Alternatively, it is possible that broadcast spawner *C. japonicum* (Kishinouye, 1904) has more gamete and larval dispersal potential than the brooder *C. rubrum* (Lacaze-Duthiers, 1864). Generally, broadcast spawners have greater dispersal potential than brooding coral species (e.g., Nishikawa et al., 2003). Similarly, a brooder scleractinian coral in shallow water, *Seriatopora hystrix* (Fan et al., 2002), has significant SGS within 100 m (Underwood et al., 2007), which is also a smaller scale of dispersal than that of *C. japonicum*. In contrast, another brooding coral, but with a relatively long larval dispersal period (*Pocillopora damicornis*, 100 days) (Hariri et al., 2002), has larger SGS (60 km, Thomas et al., 2014), indicating that the reproductive strategy alone cannot predict the spatial genetic extent.

Our data suggest the extent of a population of *C. japonicum* off Kochi is less than 11 km and intensive coral sampling within 11 km in diameter would result in failure of local reproduction and subsequently cause local extinction. Although different locations may have different environmental conditions and local coral densities, a population size of 11 km in the main coral fishing ground (relatively high coral density in Kochi (Cannas et al., 2019)) implies that the extent of a population in other areas with a lower population density may be smaller than 11 km.

## CONCLUSION

In this study, we demonstrated that both *de novo* and mapping analyses using MIG-seq are effective in detecting significant SGS for *C. japonicum* populations when a sufficient number of loci (>700 SNPs) are used. Mapping analysis is preferred, as it is more robust in detecting SGS by using accurate SNPs data with lesser missing data. The results suggest that avoiding intensive coral fishing within 11 km is important for the conservation of *C. japonicum* in the Kochi area. Collectively, the findings of this study provide important implications for the development of conservation strategies for *C. japonicum*. Further spatial genetic analysis of deep-sea species using genome-wide SNPs would be useful to understand undetectable dispersal that is important for marine conservation.

## DATA AVAILABILITY STATEMENT

The datasets presented in this study can be found in online repositories. The names of the repository/repositories and accession number(s) can be found below: DDBJ (accession: DRA011567 and DRA010782), Figshare (<https://doi.org/10.6084/m9.figshare.13678735.v2>).

## AUTHOR CONTRIBUTIONS

NY conceived the study. FI, NI, KU, and TS collected the samples. FI, NI, and MN conducted the morphological analysis. KT and TK conducted the molecular experiments. AI and NI sequenced the draft genome. KT, AI, HY, HT, TK, and NY analyzed the data. KT and NY drafted the manuscript. All authors have checked and edited the final manuscript.

## FUNDING

This study was supported by a Grant-in-Aid for Young Scientists (A) (17H04996), a Grant-in-Aid for Research Fellows (19J21342), Grant-in-Aid for Scientific Research (C) (17K07274), Grant-in-Aid for Scientific Research (A) (20254934) and the Sumitomo Foundation Fiscal 2018 Grant for Basic Science Research Projects.

## ACKNOWLEDGMENTS

We are grateful to Mr. Masao Nakano, Yoshihiko Niiya, and Katsuhiko Fujita for their assistance with the collection of samples in Kochi. We thank Akemi Yoshida and Eriko Nagahiro for their help in the data analysis.

## SUPPLEMENTARY MATERIAL

The Supplementary Material for this article can be found online at: <https://www.frontiersin.org/articles/10.3389/fmars.2021.667481/full#supplementary-material>

**Supplementary Figure 1** | Mean value of the GC contents of *Corallium japonicum* collected in Okinawa using a Nextera XT DNA Sample Prep Kit (Illumina).

**Supplementary Figure 2** | A graph showing coverage read-depth of *Corallium japonicum*.

**Supplementary Table 1** | Summary of sequence assembly of *Corallium japonicum*.

**Supplementary Table 2** | Outcomes of spatial genetic autocorrelation calculated with the different first distance classes (1–15 km) using different ratios of missing data per locus ( $r=0.5-1.0$ ). The correlation  $r_s$  (here, “ $r_s$ ” is used instead of “ $r$ ,” which is generally used to represent the correlation coefficient of spatial autocorrelation analysis to avoid confusion with the ratio of missing data per locus “ $r$ ”), is shown for the first distance class in each analysis along with the number of pairwise comparisons “ $n$ ” for the calculation of “ $r_s$ ,” and the upper (U) and lower (L) bounds for the 95% confidence interval for the null hypothesis of no spatial structure ( $r_s = 0$ ), and the upper (Ur) and lower bounds (Lr) for  $r$ , as determined by bootstrap resampling, the probability  $P$  of a one-tailed test for positive autocorrelation, and the estimated  $x$ -intercept. Note that the  $x$ -intercepts were converted to zero when the  $r_s$  was not significantly different from zero.

**Supplementary Table 3** | Outcomes of spatial genetic autocorrelation calculated with the different first distance sizes of 1–15 km using  $r$ -values at intervals of 0.01 between 0.7–0.8 and 0.9–1.0 for the *de novo* and mapping analysis, respectively.

**Supplementary Table 4** | Genpop format file for *de novo* analysis ( $r=0.5$ ).

**Supplementary Table 5** | Genpop format file for mapping analysis ( $r=0.9$ ).

**Supplementary Table 6** | Geographic Distance of each sample (km).



## REFERENCES

- Arnold, B., Corbett-Detig, R. B., Hartl, D., and Bomblies, K. (2013). RADseq underestimates diversity and introduces genealogical biases due to nonrandom haplotype sampling. *Mol. Ecol.* 22, 3179–3190. doi: 10.1111/mec.12276
- Ayre, D. J., and Hughes, T. P. (2000). Genotypic diversity and gene flow in brooding and spawning corals along the Great Barrier Reef, Australia. *Evolution* 54, 1590–1605. doi: 10.1111/j.0014-3820.2000.tb00704.x
- Bankevich, A., Nurk, S., Antipov, D., Gurevich, A. A., Dvorkin, M., Kulikov, A. S., et al. (2012). SPAdes: a New Genome Assembly Algorithm and Its Applications to Single-Cell Sequencing. *J. Comput. Biol.* 19:5. doi: 10.1089/cmb.2012.0021
- Berry, O., England, P., Marriott, R. J., Burrage, C. P., and Newman, S. J. (2012). Understanding age-specific dispersal in fishes through hydrodynamic modeling, genetic simulations and microsatellite DNA analysis. *Mol. Ecol.* 21, 2145–2159. doi: 10.1111/j.1365-294X.2012.05520.x
- Buerkle, A. C., and Gompert, Z. (2013). Population genomics based on low coverage sequencing: how low should we go? *Mol. Ecol.* 22, 3028–3035. doi: 10.1111/mec.12105
- Cannas, R., Follesa, M. C., Cau, A., Cau, A., and Friedman, K. (2019). *Global Report on the Biology, Fishery and Trade of Precious Corals*. FAO Fisheries and Aquaculture Circulation no. 118. Rome, FAO.
- Catchen, J. M., Amores, A., Hohenlohe, P., Cresko, W., and Postlethwait, J. H. (2011). Stacks: building and genotyping loci de novo from short-read sequences. *G3* 1, 171–182. doi: 10.1534/g3.111.000240/-/DC1
- Catchen, J., Hohenlohe, P. A., Bassham, S., Amores, A., and Cresko, W. A. (2013). Stacks: an analysis tool set for population genomics. *Mol. Ecol.* 22, 3124–3140. doi: 10.1111/mec.12354
- CITES. (2007). *Inclusion of all Species in the Genus Corallium in Appendix ii of Cites. This Taxon Comprises 26 Closely Related Species. Consideration of Proposals for Amendment of Appendices i and ii. CITES cop14 inf. 36*. Netherlands. Available online at: <https://www.cites.org/sites/default/files/common/cop/14/inf/E14i-36.pdf> (accessed January 19, 2021).
- CITES. (2009). *Consideration of Proposals for Amendment of Appendices i and ii. CITES cop15 prop. 21, 1*. Available Online at: <https://www.cites.org/sites/default/files/eng/cop/15/prop/E-15-Prop-21.pdf> (accessed January 19, 2021).
- Costantini, F., Carlesi, L., and Abbiati, M. (2013). Quantifying spatial genetic structuring in mesophotic populations of the precious coral *Corallium rubrum*. *PLoS One* 8:e61546. doi: 10.1371/journal.pone.0061546
- Costantini, F., Fauvelot, C., and Abbiati, M. (2007). Fine-scale genetic structuring in *Corallium rubrum*: evidence of inbreeding and limited effective larval dispersal. *Mar. Ecol. Prog. Ser.* 340, 109–119. doi: 10.3354/meps340109
- Costantini, F., Rugui, L., Cerrano, C., and Abbiati, M. (2018). Living upside down: patterns of red coral settlement in a cave. *PeerJ* 6:e4649. doi: 10.7717/peerj.4649
- Costantini, F., Taviani, M., Remia, A., Pintus, E., Schembri, P. J., and Abbiati, M. (2010). Deep-water *Corallium rubrum* (L., 1758) from the Mediterranean Sea: preliminary genetic characterization. *Mar. Ecol.* 31, 261–269. doi: 10.1111/j.1439-0485.2009.00333.x
- Diniz-Filho, J. A. F., and Telles, M. P. C. (2002). Spatial autocorrelation analysis and the identification of operational units for the conservation in continuous populations. *Conserv. Biol.* 16, 924–935. doi: 10.1046/j.1523-1739.2002.00295.x
- Eguchi, K., Oguri, E., Sasaki, T., Matsuo, A., Nguyen, D. D., Jaitrong, W., et al. (2020). Revisiting museum collection in the genomic era: potential of MIG-seq for retrieving phylogenetic information from aged minute dry specimens of ants (Hymenoptera: formicidae) and other small organisms. *Myrmecol. News* 30, 151–159. doi: 10.25849/myrmecol.news\_030:151
- Epperson, B. K. (2005). Estimating dispersal from short distance spatial autocorrelation. *Heredity* 95, 7–15. doi: 10.1038/sj.hdy.6800680
- Epperson, B. K., and Li, T. (1996). Measurement of genetic structure within populations using Moran's spatial autocorrelation statistics. *Proc. Natl. Acad. Sci. U. S. A.* 93, 10528–10532. doi: 10.1073/pnas.93.19.10528
- Fan, T. Y., Li, J. J., Le, S. X., and Fang, L. S. (2002). Lunar periodicity of larval release by pocilloporid corals in Southern Taiwan. *Zool. Stud.* 41, 288–294.
- Gupta, M., Chyi, Y. S., Romero-Severson, J., and Owen, J. L. (1994). Amplification of DNA markers from evolutionarily diverse genomes using single primers of simple-sequence repeats. *Theoret. Appl. Genet.* 89, 998–1006. doi: 10.1007/BF00224530
- Harii, S., Kayanne, H., Takigawa, H., Hayashibara, T., and Yamamoto, M. (2002). Larval survivorship, competency periods and settlement of two brooding corals, *Helipora coerulesa* and *Pocillopora damicornis*. *Mar. Biol.* 141, 39–46.
- Huang, H., and Knowles, L. L. (2016). Unforeseen consequences of excluding missing data from next-generation sequences: simulation study of RAD sequences. *Syst. Biol.* 56, 400–411. doi: 10.1093/sysbio/syu046
- Iwasaki, N. (2019). “Asian regional report on the biology, fishery and trade of precious and semi-precious corals” in *Global Report On The Biology, Fishery And Trade Of Precious Corals*, eds Cannas, R., Follesa, M. C., Cau, A., Cau, A., and Friedman, K. (Rome: FAO Fisheries and Aquaculture Circulation), 191–254.
- Iwasaki, N., Hasegawa, H., Suzuki, T., and Yamasa, M. (2009). “Biology of Japanese Corallium and Paracorallium” in *Proceedings of the 1st International Workshop on Corallium Science, Management, and Trade*, eds Bruckner, A.W., and Roberts, G.G. (Silver Spring, MD: NOAA Technical Memorandum NMFS-OPR-43 and CRCP-8), 68–70.
- Kishinouye, K. (1904). Notes on the natural history of corals. *J. Imper. Fish. Bureau* 14, 1–32.
- Lacaze-Duthiers, H. D. (1864). On the formation of coral (*Corallium rubrum*). *Q. J. Sci.* 1, 614–623.
- Ledoux, J. B., Garrabou, J., Bianchimani, O., Drap, P., Feral, J. P., and Aurelle, D. (2010). Fine-scale genetic structure and inferences on population biology in the threatened Mediterranean red coral, *Corallium rubrum*. *Mol. Ecol.* 19, 4204–4216. doi: 10.1111/j.1365-294X.2010.04814.x
- Li, H., and Durbin, R. (2009). Fast and accurate short read alignment with Burrows–Wheeler transform. *Bioinformatics* 25, 1754–1760. doi: 10.1093/bioinformatics/btp324
- Lischer, H. E., and Excoffier, L. (2011). PGDSpider: an automated data conversion tool for connecting population genetics and genomics programs. *Bioinformatics* 28, 298–299. doi: 10.1093/bioinformatics/btr642
- Luan, N. T., Rahman, M. A., Maki, T., Iwasaki, N., and Hasegawa, H. (2013). Growth characteristics and growth rate estimation of Japanese precious corals. *J. Exp. Mar. Biol. Ecol.* 441, 117–125. doi: 10.1016/j.jembe.2013.01.012
- Martin, M. (2011). Cutadapt removes adapter sequences from high-throughput sequencing reads. *EMBnet J.* 17, 10–12. doi: 10.14806/ej.17.1.200
- Miller, M. R., Dunham, J. P., Amores, A., Cresko, W. A., and Johnson, E. A. (2007). Rapid and cost-effective polymorphism identification and genotyping using restriction site associated DNA (RAD) markers. *Genome Res.* 17, 240–248. doi: 10.1101/gr.5681207
- Ministry of the Environment Government of Japan. (2017). *Marine Species Red List In Japanese*. Available Online at: <http://www.env.go.jp/press/files/jp/106407.pdf> (accessed January 19, 2021).
- Nakabayashi, A., Yamakita, T., Nakamura, T., Aizawa, H., Kitano, Y. F., Iguchi, A., et al. (2019). The potential role of temperate Japanese regions as refugia for the coral *Acropora hyacinthus* in the face of climate change. *Sci. Rep.* 9:1892. doi: 10.1038/s41598-018-38333-5
- Narum, S. R., and Hess, J. E. (2011). Comparison of FST outlier test for SNP loci under selection. *Mol. Ecol. Resour.* 11, 184–194. doi: 10.1111/j.1755-0998.2011.02987.x
- Nishikawa, A., Katoh, M., and Sakai, K. (2003). Larval settlement rates and gene flow of broadcast-spawning (*Acropora tenuis*) and planula-brooding (*Stylophora pistillata*) corals. *Mar. Ecol. Prog. Ser.* 256, 87–97. doi: 10.3354/meps256087
- Nonaka, M., Nakamura, M., and Muzik, K. (2015). Sexual reproduction in precious corals (Coralliidae) collected in the Ryukyu Archipelago. *Pac. Sci.* 69, 15–46. doi: 10.2984/69.1.2
- Peakall, R., and Smouse, P. E., (2012). GenAlEx 6.5: genetic analysis in Excel. Population genetic software for teaching and research- an update. *Bioinformatics* 28, 2537–2539. doi: 10.1093/bioinformatics/bts460
- Peakall, R., Ruibal, M., and Linenmayer, D. (2003). Spatial autocorrelation analysis offers new insights into gene flow in the Australian bush rat, *Rattus fuscipes*. *Evolution* 57, 1182–1195. doi: 10.1111/j.0014-3820.2003.tb00327.x
- Richard, Z. T., Yasuda, N., Kikuchi, T., Foster, T., Mitsuyuki, C., Stat, M., et al. (2018). Integrated evidence reveals a new species in the ancient blue coral genus *Helipora* (Octocorallia). *Sci. Rep.* 8, 15875. doi: 10.1038/s41598-018-32969-z

- Roach, M. J., Schmidt, S. A., and Borneman, A. R. (2018). Purge Haplotigs: allelic contig reassignment for third-gen diploid genome assemblies. *BMC Bioinf.* 19:460. doi: 10.1186/s12859-018-2485-7
- Roberts, J. M., Wheeler, A. J., and Freiwald, A. (2006). Reefs of the deep: the biology and geology of cold-water coral ecosystems. *Science* 312, 543–547. doi: 10.1126/science.1119861
- Rochette, N. C., and Catchen, J. M. (2017). Deriving genotypes from RAD-seq short-read using Stacks. *Nat. Protoc.* 12, 2640–2659. doi: 10.1038/nprot.2017.123
- Roure, B., Baurain, D., and Philippe, H. (2013). Impact of missing data on phylogenies inferred from empirical phylogenomic data sets. *Mol. Biol. Evol.* 30, 197–214. doi: 10.1093/molbev/mss208
- Rubin, B. E. R., Ree, R. H., and Moreau, C. S. (2012). Inferring phylogenies from RAD sequence data. *PLoS One* 7:e33394. doi: 10.1371/journal.pone.0033394
- Schwartz, M. K., and McKelvey, K. S. (2009). Why sampling scheme matters: the effect of sampling scheme on landscape genetic results. *Conserv. Genet.* 10, 441–452. doi: 10.1007/s10592-008-9622-1
- Shafer, A. B. A., Peart, C. R., Tusso, S., Maayan, I., Brelsford, A., Wheat, C. W., et al. (2017). Bioinformatic processing of RAD-seq data dramatically impacts downstream population genetic inference. *Methods Ecol. Evol.* 8, 907–917. doi: 10.1111/2041-210X.12700
- Shinzato, C., Shoguchi, E., Kawashima, T., Hamada, M., Hisata, K., and Tanaka, M. (2011). Using the *Acropora digitifera* genome to understand coral responses to environmental change. *Nature* 476, 320–323. doi: 10.1038/nature10249
- Suyama, Y., and Matsuki, Y. (2015). MIG-seq: an effective PCR-based method for genome-wide single-nucleotide polymorphism genotyping using the next-generation sequencing platform. *Sci. Rep.* 5:16963. doi: 10.1038/srep16963
- Takata, K., Taninaka, H., Nonaka, M., Iwase, F., Kikuchi, T., Suyama, Y., et al. (2019). Multiplexed ISSR genotyping by sequencing distinguishes two precious coral species (Anthozoa: Octocorallia: Coralliidae) that share a mitochondrial haplotype. *PeerJ* 7:e7769. doi: 10.7717/peerj.7769
- Thomas, L., Kendrick, G. A., Stat, M., Travaille, K. L., Shedrawi, G., and Kennington, W. J. (2014). Population genetic structure of the *Pocillopora damicornis* morphospecies along Ningaloo Reef, Western Australia. *Mar. Ecol. Prog. Ser.* 513, 111–119. doi: 10.3354/meps10893
- Tsounis, G., Rossi, S., Grigg, R., Santangelo, G., Bramanti, L., and Gili, J. M. (2010). “The exploitation and conservation of precious corals,” in *Oceanography and Marine Biology: An Annual Review*, eds Gibson, R. N., Atkinson, R. J. A., and Gordon, J. D. M. (Boca Raton, FL: CRC Press), 161–212.
- Underwood, J. N., Smith, L. D., van Oppen, M. J. H., and Gilmour, J. P. (2007). Multiple scales of genetic connectivity in a brooding coral on isolated reefs following catastrophic bleaching. *Mol. Ecol.* 16, 771–784. doi: 10.1111/j.1365-294X.2006.03187.x
- Wagner, C. E., Keller, I., Wittwer, S., Selz, O. M., Mwaiko, S., Greuter, L., et al. (2013). Genome-wide RAD sequence data provide unprecedented resolution of species boundaries and relationships in the Lake Victoria cichlid adaptive radiation. *Mol. Ecol.* 22, 787–798. doi: 10.1111/mec.12023
- Waller, R. G. (2005). “Deep-water Scleractinia (Cnidaria: Anthozoa): current knowledge of reproductive processes” In *Cold-Water Corals And Ecosystems*, eds Freiwald, A., Roberts, J. M. (Springer-Verlag, Berlin Heidelberg), 691–700.
- Zietkiewicz, E., Rafalski, A., and Labuda, D. (1994). Genome fingerprinting by simple sequence repeat (SSR)-anchored polymerase chain reaction amplification. *Genomics* 20, 176–183. doi: 10.1006/geno.1994.1151

**Conflict of Interest:** The authors declare that the research was conducted in the absence of any commercial or financial relationships that could be construed as a potential conflict of interest.

Copyright © 2021 Takata, Iwase, Iguchi, Yuasa, Taninaka, Iwasaki, Uda, Suzuki, Nonaka, Kikuchi and Yasuda. This is an open-access article distributed under the terms of the Creative Commons Attribution License (CC BY). The use, distribution or reproduction in other forums is permitted, provided the original author(s) and the copyright owner(s) are credited and that the original publication in this journal is cited, in accordance with accepted academic practice. No use, distribution or reproduction is permitted which does not comply with these terms.



# Genetic Structure of the *Goniopora lobata* and *G. djiboutiensis* Species Complex Is Better Explained by Oceanography Than by Morphological Characteristics

Nina Yasuda<sup>1\*</sup>, Yuko F. Kitano<sup>1,2†</sup>, Hiroki Taninaka<sup>3</sup>, Satoshi Nagai<sup>4</sup>, Takuma Mezaki<sup>5</sup> and Hiroshi Yamashita<sup>6</sup>

## OPEN ACCESS

### Edited by:

Hajime Kayanne,  
The University of Tokyo, Japan

### Reviewed by:

Yuichi Nakajima,  
Okinawa Institute of Science  
and Technology Graduate University,  
Japan

David A. Paz-García,  
Centro de Investigación Biológica del  
Noroeste (CIBNOR), Mexico

### \*Correspondence:

Nina Yasuda  
nina27@cc.miyazaki-u.ac.jp

<sup>†</sup>These authors have contributed  
equally to this work and share first  
authorship

### Specialty section:

This article was submitted to  
Coral Reef Research,  
a section of the journal  
Frontiers in Marine Science

**Received:** 07 August 2020

**Accepted:** 21 May 2021

**Published:** 01 July 2021

### Citation:

Yasuda N, Kitano YF, Taninaka H,  
Nagai S, Mezaki T and Yamashita H  
(2021) Genetic Structure of the  
*Goniopora lobata* and *G. djiboutiensis*  
Species Complex Is Better Explained  
by Oceanography Than by  
Morphological Characteristics.  
*Front. Mar. Sci.* 8:592608.  
doi: 10.3389/fmars.2021.592608

<sup>1</sup> Department of Marine Biology and Environmental Science, Faculty of Agriculture, University of Miyazaki, Miyazaki, Japan, <sup>2</sup> Biodiversity Division, National Institute for Environmental Studies, Tsukuba, Japan, <sup>3</sup> Interdisciplinary Graduate School of Agriculture and Engineering, University of Miyazaki, Miyazaki, Japan, <sup>4</sup> Fisheries Resources Institute, Japan Fisheries Research and Education Agency, Yokohama, Japan, <sup>5</sup> Kuroshio Biological Research Foundation, Kochi, Japan, <sup>6</sup> Fisheries Technology Institute, Japan Fisheries Research and Education Agency, Ishigaki, Japan

Species delimitation of closely related corals is often challenging due to high intraspecific morphological variation and phenotypic plasticity with a lack of characteristic features and scarcity of relevant molecular markers. *Goniopora* spp. are one such coralline group, and the species status of *Goniopora lobata* and *Goniopora djiboutiensis*, an Indian and Pacific Ocean hermatypic coral species complex, has been questioned on the basis of previous molecular and morphological analyses. To further examine the species boundaries between *G. lobata* and *G. djiboutiensis* in Japan, specimens collected from areas spanning from Ryukyu Island to temperate Japanese regions were morphologically identified based on traditional morphological descriptions. Then, the genetic structure of the *G. lobata* and *G. djiboutiensis* species complex was examined using six newly developed microsatellite markers. The majority of the collected specimens had intermediate morphologies, and a STRUCTURE analysis using the LOCPRIOR model based on typical *G. lobata* and *G. djiboutiensis* morphology indicated that there were no genetic differences between these morphologies. On the other hand, STRUCTURE analysis based on oceanographic regions revealed that there was a genetic break between the temperate and subtropical regions. This weak genetic break corresponded with the Kuroshio-associated barrier, which prevents larval transport between subtropical and temperate regions. This study confirms that the current morphological identification criteria for *G. lobata* and *G. djiboutiensis* do not match the existing genetic boundaries and thus the two should be regarded as a species complex. This study also highlighted the robustness of using a multi-locus population genetic approach, including a geographic context, to confirm the species boundaries of closely related species.

**Keywords:** microsatellite markers, species delimitation, coral reefs, biodiversity, Kuroshio Current

## INTRODUCTION

Species are the fundamental units of biodiversity and are worth consideration in the conservation of ecosystems. However, the delimitation of some closely related taxa, including corals, is often challenging due to the fact that coral skeletons exhibit high phenotypic plasticity under different environmental conditions. The paucity of effective molecular tools for coral identification, together with frequent hybridization and possible reticulate evolution, has long hindered the classification of many reef-building corals (Todd, 2008). The delimitation of coral species is essential for conservation because one-third of all coral species are now facing the threat of extinction globally (Carpenter et al., 2008). In Japan, corals in subtropical areas have experienced mass bleaching because of elevated water temperatures, whereas some corals have reportedly migrated to and expanded in temperate areas (Yamano et al., 2011). Therefore, studies on the genetic connectivity between subtropical and temperate areas of coral species are important to understand such phenomena. However, no study has investigated the genetic connectivity of coral species between subtropical and temperate areas, except for *Acropora* (Nakabayashi et al., 2019). Moreover, no study has focused on other coral species, possibly because the identification of coral species in the field is challenging.

Corals belonging to the genus *Goniopora* are widely distributed across the Indian and Pacific Oceans, including subtropical and temperate areas in Japan, and have few skeletal characteristics in addition to highly variable skeletal and polyp morphologies. There are 15 nominal species in the genus *Goniopora* found in Japan (Nishihira and Veron, 1995). Veron (1993) reported that one of the relatively common species, *Goniopora lobata*, is distributed in both subtropical and temperate areas (up to Tatayama) and is very difficult to identify accurately, especially in temperate areas where skeletal variations are primarily correlated with non-reef environments. Kitano et al. (2013) reported the existence of many intermediate morphologies between closely related *G. lobata* and *G. djiboutiensis* species in Japan. *G. djiboutiensis* is less common than *G. lobata*, and its distribution overlaps with that of *G. lobata*, especially in subtropical areas (Veron, 1993; Nishihira and Veron, 1995). The first comprehensive genetic approach to delineate the species covering this whole genus was conducted in the Red Sea (Terraneo et al., 2016). The authors of the aforementioned study found discordance among genetic, morphological, and micromorphological data related to *G. lobata* and *G. djiboutiensis*, wherein *G. lobata* and *G. djiboutiensis* shared common alleles and thus could not be delineated using genetic markers including a mitochondrial region, the internal transcribed spacer (ITS) region, and the calmodulin (CalM) and ATPase $\beta$  genes (ATP $\beta$ ). Based on this molecular and morphological evidence, the aforementioned authors questioned the species status of *G. lobata* and *G. djiboutiensis*, although the study was ultimately inconclusive.

Although species delimitation analysis is often attempted via a phylogenetic approach, population genetic approaches considering the geographic contexts of processes driving population divergence and speciation have proven to be

more effective in identification of species boundaries in some phylogenetically complex groups (Medrano et al., 2014; Nakabayashi et al., 2019). Thus, further genetic studies using a multi-locus population genetic approach may help to confirm the species boundary between *G. lobata* and *G. djiboutiensis*. In this study, *G. lobata*-like and *G. djiboutiensis*-like specimens were collected from a wide range of coral habitats in Japan, including different oceanographic regions (subtropical and temperate regions) separated by an ocean current system. Six novel polymorphic microsatellite markers for *Goniopora* spp. were developed to analyze the genetic structures of the *G. lobata* and *G. djiboutiensis* species complex. Then, the specimens were comprehensively studied based on traditional morphological descriptions, ITS sequences, and microsatellites to reveal the species boundaries between *G. lobata* and *G. djiboutiensis*.

## MATERIALS AND METHODS

### Sample Collection

Owing to the fact that species identification of living colonies is difficult in the field, *G. lobata*- and *G. djiboutiensis*-like samples were collected from 15 areas spanning from Ryukyu Island to temperate regions of Japan (Table 1 and Figure 1). Samples (100–500 cm<sup>3</sup>) were collected using a hammer and chisel. A small portion of each coral sample (<1 cm<sup>3</sup>) was preserved in CHAOS solution (Fukami et al., 2004) to dissolve proteins for DNA analyses, and the remnants of the samples were bleached for morphological analyses. Total genomic DNA was extracted from colonies of the samples using the method outlined by Fukami et al. (2004). The skeletal specimens are retained either in University of Miyazaki (MUFS) or in Seto Marine Biological Laboratory (SMBL).

### Morphological Identification

Morphological identification was based on original species descriptions and related literature (Milne-Edwards and Haime, 1851; Bedot, 1907; Vaughan, 1907; Veron and Pichon, 1982; Terraneo et al., 2016). Each five mature corallites per colony were measured to determine the range of calice diameter using a vernier caliper. Seven skeletal characteristics were also examined (calice depth, width of calice wall, morphology of columella, columella divided to six parts or not, tips of columellar threads, existence of pali or paliform lobes, and septa under binocular stereomicroscope to classify the species. If specimens had morphological characteristics typical of both *G. lobata* and *G. djiboutiensis* in different categories, they were classified as “intermediate.”

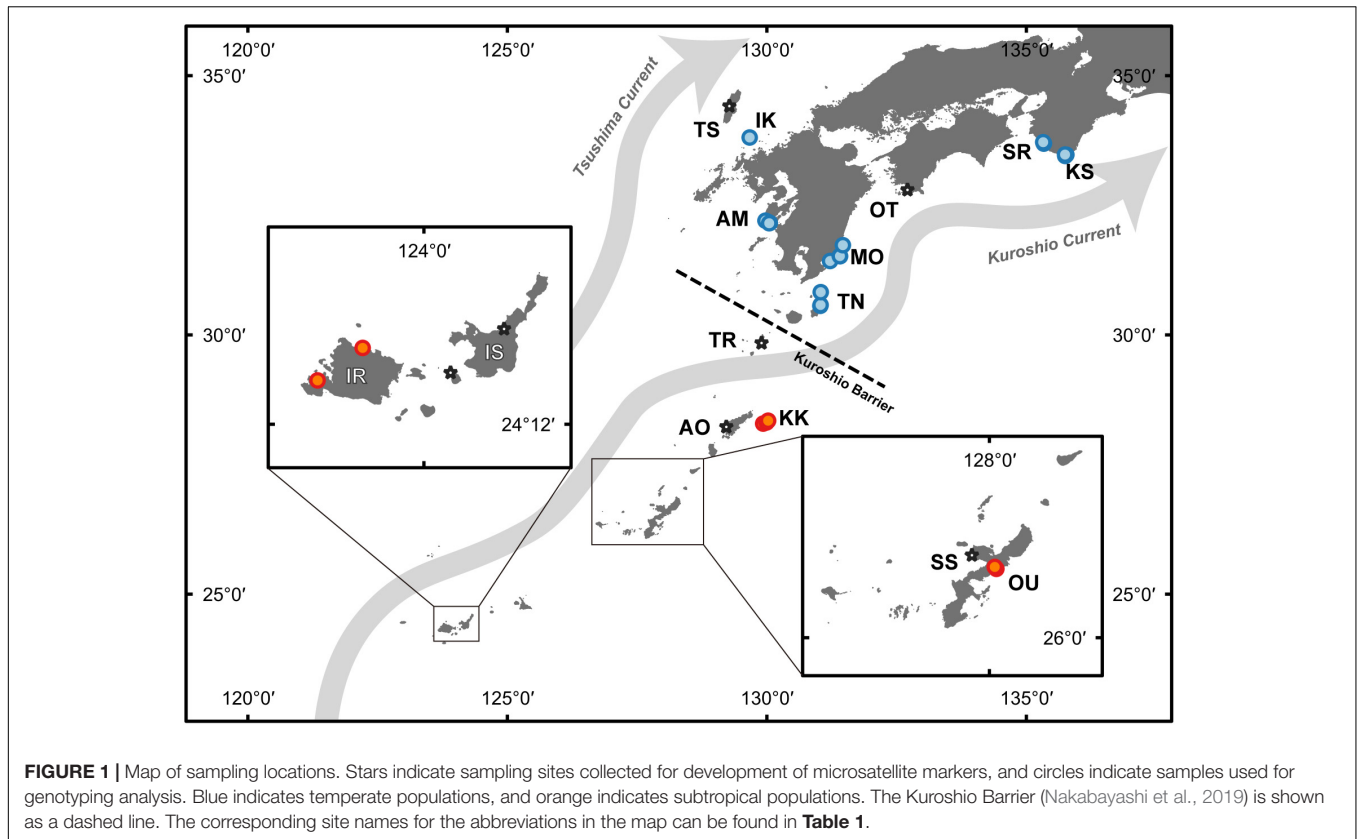
### ITS Analysis

In order to compare the microsatellite results of the present study with those obtained in previous studies, the ITS region (including partial 18S, ITS-1, 5.8S, ITS-2, and partial 28S) was sequenced and compared with the sequences reported by Terraneo et al. (2016). Polymerase chain reaction (PCR) and sequencing conditions were exactly the same as in protocol (Kitano et al., 2013). Previously published sequences (*G. lobata*

**TABLE 1** | The list of *G. lobata*-like and *G. djiboutiensis*-like samples used in this study.

Locality	Abbreviation	Latitude (N)	Longitude (E)	For isolating microsatellite regions using NGS	Number of STRUCTUTRE analysis	ITS	mtDNA	Number of <i>G. lobata</i> morphotypes	Number of non-typical morphs (neither typical <i>G. lobata</i> nor <i>G. djiboutiensis</i> )	Number of <i>G. djiboutiensis</i> morphotypes
Shirahama	SH	33.718	135.325	1	14	16	6	1	13	
Kushimoto	KS	33.453	135.749	3	6	8	2	1	5	
Otsuki	OT	32.797	132.709	1					1	
Tsushima Island	TS	34.414	129.277	3					3	
Iki Island	IK	33.809	129.669	1	5	7	1	1	4	
Amakusa	AM	32.171	130.034	3	20	21	2	3	17	
Miyazaki	MO	31.519	131.410	1	10	12	2	1	9	
Tanegashima Island	TN	30.579	131.035	1	8	11	4		8	
Tokara Islands	TR	29.844	129.897	2					2	
Kikaijima Island	KK	28.313	129.995	1	3	3			2	1
Amami-Oshima Island	AO	28.226	129.219	1					1	
Sesoko Island	SS	26.636	127.866	1					1	
Oura bay	OU	26.545	128.041	1	5	5	1		4	1
Ishigakijima island	IS	24.463	124.221	2					2	
Iriomotejima Island	IR	24.321	123.707	2	5	7	3		2	4
Total				24	76	90	21	7	74	6





and *G. djiboutiensis* in the Red Sea; **Supplementary Table 2**) were also included in the following analysis to identify the conformity of the resultant genetic clades with those reported by Terraneo et al. (2016). The ITS sequences with a maximum length of 926 bp were aligned using MAFFT online (Katoh et al., 2017), and all gap regions were trimmed using the “-nogaps” option in trimAl v. 1.4 (Capella-Gutiérrez et al., 2009), which removes all gap sites in the alignment, resulting in 899 bp in length for analysis. To identify the genetic clades defined by Terraneo et al. (2016), a phylogenetic tree was constructed using two different algorithms: maximum likelihood (ML) using IQ-TREE2 v.2.0.6 (Minh et al., 2020) and Neighbor-Joining (NJ) using MEGA X (Kumar et al., 2018). In total, 135 sequences across 11 *Goniopora* spp. were used for the analysis, including 44 reference sequences reported by Terraneo et al. (2016).

For the ML tree, the best-fitting nucleotide substitution model (K2P + R2) was estimated based on the Bayesian information criterion (BIC), using the “-m MFP” option, which performs extended model selection followed by tree inference. Confidence values for the trees were inferred using the ultrafast bootstrap method (Hoang et al., 2018) with 1,000 replicates. For the NJ tree, the Kimura two-parameter (Kimura, 1980) model with a gamma distribution was selected by a model test implemented in MEGA X, with bootstrap values calculated from 1,000 replicates. Unrooted phylogeny was reconstructed using FigTree v.1.4.4<sup>1</sup>.

<sup>1</sup><http://tree.bio.ed.ac.uk/software/figtree/>

Confidence values for the trees were inferred using 1,000 bootstrap replicates.

## Microsatellite Marker Development Using High-Throughput Sequencing

The total genomic DNA for microsatellite marker isolation was obtained from the samples listed in **Table 1**. The 24 genomic DNA isolates from CHAOS solution samples were mixed and were further purified using the DNeasy Blood and Tissue kits (Qiagen, Hilden, Germany) according to the manufacturer's instructions. The purified genomic DNA was fragmented into c.a. 300–800 bp, and the adapter sequences were ligated to each end of the fragments. The resulting DNA library was subjected to shotgun sequencing on GS FLX Titanium picotiter plates using the Roche GS FLX 454 system. A total of 603,951 sequences were obtained with a total of 306 Mb. These sequencing reads were assembled using Newbler Assembler software ver. 2.6 (Roche Applied Sciences, Indianapolis, IN, United States) with default settings. Subsequent contigs and singletons were screened using a Perl pipeline coupled with Tandem Repeats Finder ver. 4.0.4 (Benson, 1999) and PRIMER 3 ver. 2.2.2 beta (Rozen and Skaletsky, 2000), which were eventually used to design primers for the potential microsatellite loci (Nakamura et al., 2013). A total of 1,136 pairs of primers with di-, tri-, and tetra-nucleotide motif loci were designed, from which 240 primer sets were selected for initial amplification trials. After removing the primers that did not amplify correctly (multiple bands or no amplification), coral

microsatellite markers were further discriminated from those of their symbiont algae (family: Symbiodiniaceae) using the same primers. Owing to the fact that *Goniopora* spp. is known to host Symbiodiniaceae species of *Cladocodium goreau* (formerly clade C type C1) in Taiwan (Chen et al., 2005) and Hong Kong (Wong et al., 2016) and *Durusdinium trenchii* (formerly clade D type D1–4) in Indian Ocean (LaJeunesse et al., 2010), the following four Symbiodiniaceae culture strains were tested: AJIS2-C2 (reported by Yamashita and Koike, 2013, *Symbiodinium microadriaticum* former clade A type A1), CCMP2466 (*C. goreau*), CCMP2556 (*D. trenchii*), and AJIS5-A10 (*D. trenchii*, previously isolated by one of the authors H. Yamashita). The culture strains CCMP2466 and CCMP2556 were purchased from the Provasoli–Guillard National Center for Culture of Marine Algae and Microbiota (ME, United States). As a result, total 39 primer pairs of potential microsatellite markers including trinucleotide motif loci for *Goniopora* spp. were selected. To examine the effectiveness of PCR amplification of the 39 fluorescent-labeled primer pairs that were successfully identified as *Goniopora* microsatellite regions, we performed PCR in a thermal cycler (PC-808, ASTEC) in a reaction mixture (10  $\mu$ L) containing 1  $\mu$ L (ca. 10 ng) template DNA, 5  $\mu$ L of 2 $\times$  Go Taq Colorless Master mix (Promega Corporation, United States, containing Taq DNA polymerase, dNTPs, MgCl<sub>2</sub>, and reaction buffers at optimal concentrations), 0.35  $\mu$ M of each designed primer pair, with one fluorescently labeled primer, and 3.76  $\mu$ L of ultra-pure quality water. The PCR cycling conditions were as follows: 2 min at 95°C, 30 cycles at 95°C for 30 s, 50°C–55°C (primer-specific annealing temperature, **Table 3**) for 30 s, 72°C for 30 s, and a final elongation at 72°C for 5 min.

## Genetic Structure of the *G. lobata* and *G. djiboutiensis* Species Complex

To examine the species boundaries and spatial genetic structure of the *G. lobata* and *G. djiboutiensis* complex, 76 samples were genotyped (**Table 1** and **Figure 1**). One microliter of the 80-times diluted PCR product was added to 10  $\mu$ L Hi-Di formamide containing 0.15  $\mu$ L GeneScan 600 LIZ size standard (Applied Biosystems), followed by denaturation at 95°C for 3 min. The samples were run on an ABI 3130 xl genetic analyzer (Applied Biosystems) and were analyzed using GeneMapper ver. 5.0 software (Applied Biosystems). Using Amakusa, Shirahama, and Miyazaki samples from which more than 10 samples could be collected (**Table 1**), the observed and expected heterozygosity and the Hardy–Weinberg equilibrium (HWE) were calculated using GenAlEx ver. 6.5 (Peakall and Smouse, 2012). Linkage disequilibria between the loci were tested in Genepop ver.4.0 (Raymond and Rousset, 1995) with 5,000 dememorizations, 500 batches, and 5,000 iterations per batch. Micro-Checker version 2.2.3 (Van Oosterhout, 2004) was used to check the presence of scoring error due to stuttering, large allele dropout, and null alleles for each locus.

A total of 10 independent runs of Structure ver. 2.3.4 (Pritchard et al., 2000) were calculated assuming  $K = 1$ –6 with 500,000 Markov chain Monte Carlo (MCMC) iterations after a 500,000 burn-in using admixture and an allele frequency

correlated model to examine genetic structure. To examine the genetic structure assuming different hypotheses, three different priors were used as follows: (1) no prior, (2) morphological prior (two categories: typical *G. lobata*-morph and typical *G. djiboutiensis*-morph) using LOCPRIOR (Hubisz et al., 2009), and (3) oceanographic regions prior (two categories: temperate and subtropical regions). While it was assumed that the largest mean LnP(K) with a biologically meaningful low number of  $K$  was the optimal number of clusters [as suggested by Pritchard et al., 2000], delta  $K$  (Evanno et al., 2005) was also estimated using STRUCTURE HARVESTER (Earl and von Holdt, 2012). Then, CLUMPAK (Kopelman et al., 2015) was used to visualize the STRUCTURE results.

Additionally, the population-based genetic structure was visualized by principal coordinate analysis (PCoA) using GenAlEx ver. 6.5 (Peakall and Smouse, 2012). Furthermore, Arlequin ver. 3.5 (Excoffier and Lischer, 2010) was used to examine the genetic structure ( $F_{CT}$ ) between temperate (Ooura and Iriomote) and subtropical (the others) regions and the calculated global  $F_{ST}$ . With regard to these population-based analyses, the Kikai population was excluded due to an extremely small ( $n = 3$ ) sample size.

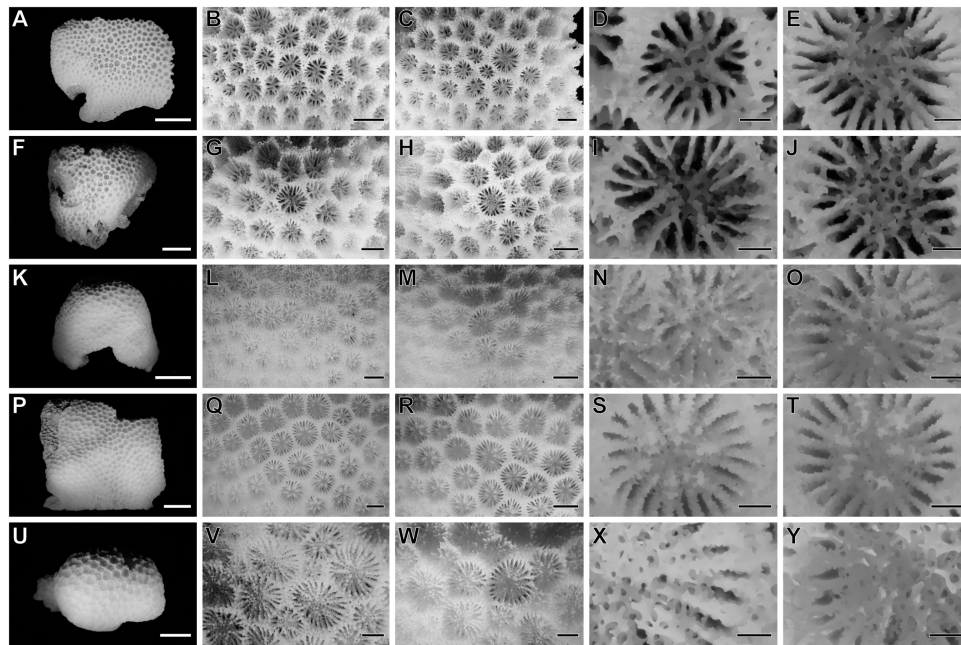
## RESULTS

As mentioned by Kitano et al. (2013), most of the collected samples (64 out of 76) had intermediate morphologies, thereby indicating that it was impossible to distinguish between the two species groups using the current morphological criteria (**Figure 2** and **Supplementary Table 1**). None of the eight morphological features previously used were effectively able to discriminate between *G. lobata* and *G. djiboutiensis* (**Supplementary Table 1**).

The ML and NJ trees using the ITS region were consistent; therefore, only the ML tree has been shown in **Figure 3** (raw data available in **Supplementary Data 1**). The reconstructed ITS tree suggested that all the samples used in this study belonged to clade II in Terraneo et al. (2016), which was previously found to be a *G. lobata* and *G. djiboutiensis* complex clade (**Figure 3**). Consistent with the findings reported by Terraneo et al. (2016), there was no subclade corresponding to geographic areas or specific morphological features within clade II.

After PCR testing, six primer pairs of *Goniopora* spp. that could amplify microsatellite regions were identified, including the tri-nucleotide motif (**Table 2**). No significant linkage disequilibria were detected among the loci after Bonferroni correction ( $\alpha > 0.05$ ). Only the G329 locus in the Miyazaki population was found to be significantly deviated from the HWE locus ( $P = 0.001$ , **Table 3**). Additionally, Micro-Checker analysis detected that the G329 locus might include null alleles. Although analysis was completed with and without G329 and it was confirmed that there was no discrepancy in the results, only the results excluding G329 have been presented this paper. All the used genotyping data is available in **Supplementary Table 2**.

STRUCTURE analysis with a uniform prior showed admixed patterns, and the maximum mean LnP(K) was observed at  $K = 1$ , thereby indicating that only one cluster was estimated (**Figure 4**



**FIGURE 2 |** Morphological variations in the *Goniopora lobata* complex. (A–E) *Goniopora lobata* (KS53), (F–T) Three different “intermediate” types of the two morphological species (F–J): TN79, (K–O): AM26, (P–T): KK16, (U–Y): *Goniopora djiboutiensis* (IR68). Corallum of each sample [(A,F,K,P,U), scale bar = 20 mm], major examples of calices in the corallum [(B,C,G,H,L,M,Q,R,V,W), for (A,F,K,P,U), respectively, scale bar = 3 mm], close-up photography of calices [(D,E,I,J,N,M,S,T,X,Y), scale bar = 1 mm].

and **Supplementary Table 3**). A similar result was obtained using a morphological prior, and while  $K = 2$  was selected as the optimal number of clusters based on the largest Mean LnP(K) value, no genetic structuring between the typical *G. djiboutiensis*-morph and *G. lobata*-morph was found (**Figure 4**). On the other hand, STRUCTURE analysis using oceanographic regions suggested that  $K = 2$  was the best model based on Mean LnP(K) as well as delta  $K$  estimation (**Supplementary Table 3**), and a clear genetic break between subtropical and temperate regions was detected with a low mean  $r$  value (0.365), thereby indicating that the geographic prior was able to detect a genetic structure within the data (**Figure 4** and **Supplementary Table 4**).

Principle coordinate analysis indicated that the subtropical populations (Oura and Iriomote) were separated from the six temperate populations by coordinate 1, which explained 65.12% of the variation in the data (**Figure 5**). A significant genetic structure was observed according to the global  $F_{ST}$  value ( $F_{ST} = 0.033$ ,  $P = 0.027$ ). Genetic structuring among predefined oceanographic groups (subtropical vs. temperate) was also significant ( $F_{CT} = 0.095$ ,  $P = 0.037$ ).

## DISCUSSION

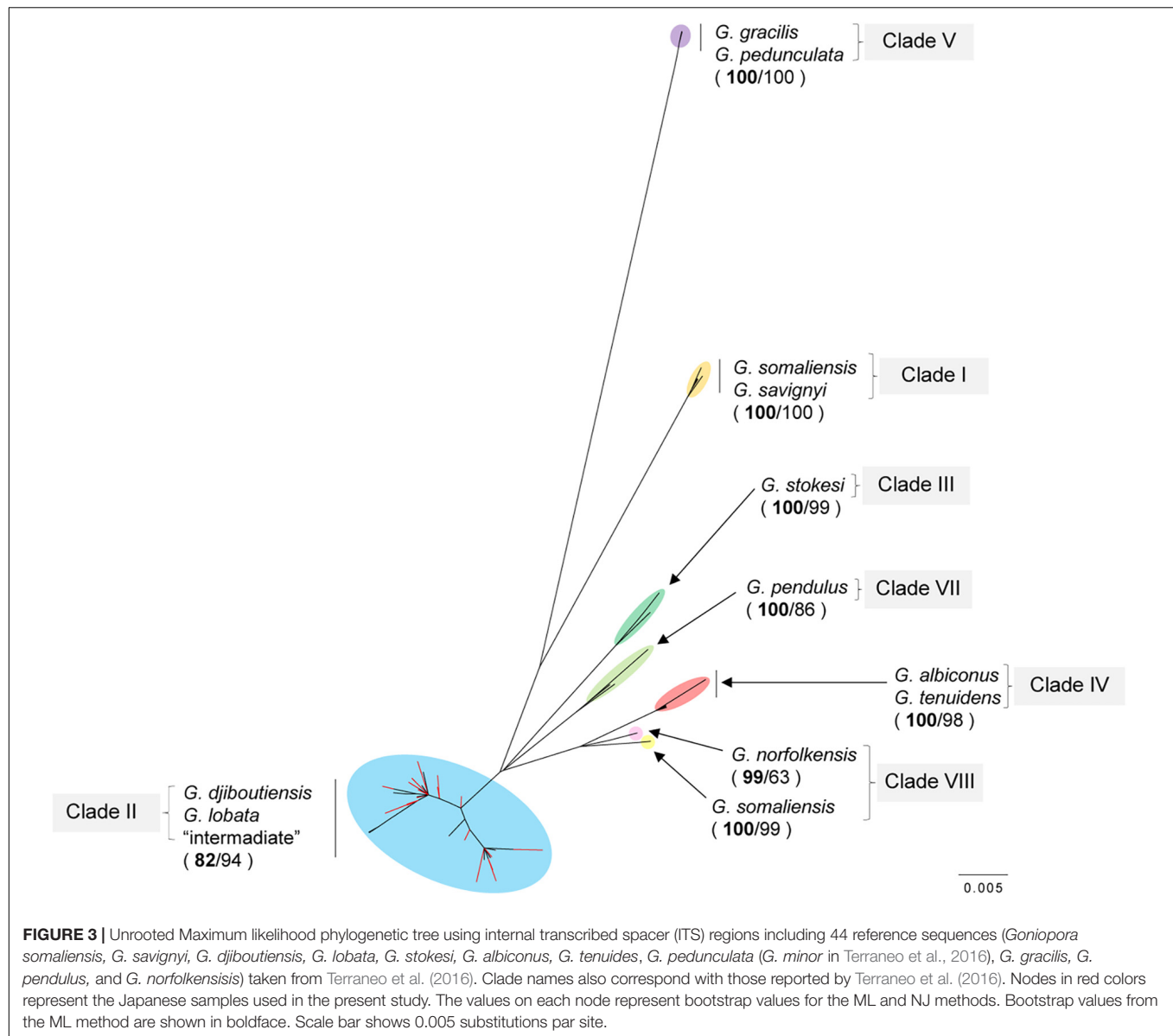
### Microsatellite Markers as a Tool to Examine Species Boundaries

Recent advances in high-throughput sequencing technology have made microsatellite markers rather outdated. In general, a higher number of loci can resolve finer scale genetic structures

(Jeffries et al., 2016). However, in some circumstances, using microsatellite markers can be advantageous compared to newly emerged genomic methods such as RAD-seq (Wagner et al., 2013). Hodel et al. (2016) reviewed and compared microsatellite markers with more recently developed genomic methods and concluded that microsatellite markers remained useful in terms of both effectiveness and cost-efficiency (Hodel et al., 2016).

Microsatellite markers are useful in many molecular ecological applications, including parentage analysis, conservation genetics, phylogeography, and population genetics (Hodel et al., 2016). Among the many molecular markers, microsatellite markers are more useful in detection of species boundaries between closely related coral species. Previous population genetic studies using microsatellite markers in corals with appropriate sampling design including geographical contexts have revealed underestimated species diversity even when phylogenetic trees cannot detect recent speciation owing to incomplete lineage sorting (Bongaerts et al., 2011; Nakajima et al., 2012; Yasuda et al., 2015).

Microsatellite analyses using sufficient sample sizes and including a geographic context enable us to detect species boundaries by accounting for incomplete lineage sorting and/or introgression (Nakajima et al., 2012; Nakabayashi et al., 2019). However, caution is required when planning the sampling design in terms of both the number of samples and the sampling strategy itself because individual-based Bayesian clustering methods, including STRUCTURE, are known to be sensitive to sampling design (Schwartz and McKelvey, 2008). In addition, because the molecular evolutionary patterns of microsatellite regions are not as well-known and the “phylo-” part of the analysis

**TABLE 2 |** Microsatellite markers of *Goniopora* spp. developed in this study.

Marker name	motif	Primer sequence	Length of PCR fragment	Annealing temperature	Accession number entry ID
G113	(TCA)9	attctcatcaccgtccttcact aatgcgaggttcaaagcttaat	107–122	55	LC377512
G205	(TTA)8	gctcaggtagctttccttcaa ttgtggatcaaacgacgactac	186–245	55	LC377513
G217	(TTG)9	tgaagagttgaaggacagcaaa ttattcatctaattggtgcgtgc	191–218	55	LC377514
G328	(AAC)9	atcaccacacctcaatcataccc atttgtcatagcaggcgacttt	286–334	55	LC377515
G329	(GAT)8	ttaggaaagcaaaatctctggc ctttcccagggttaactgacagg	281–331	55	LC377516
G392	(TAT)9	gagtgcttaatcccctaccctt agtgaggctgccaggtagatag	384–405	55	LC377517



**TABLE 3 |** Summary for the basic population genetic parameters using microsatellite loci.

Pop	Locus	N	Na	Ne	I	Ho	He	uHe	F	P
Amakusa	G113	20	4	1.956	0.900	0.500	0.489	0.501	-0.023	0.943
	G205	19	14	7.763	2.305	0.789	0.871	0.895	0.094	0.439
	G217	20	3	1.436	0.583	0.350	0.304	0.312	-0.152	0.825
	G328	20	4	1.778	0.825	0.500	0.438	0.449	-0.143	0.943
	G329	20	6	1.533	0.778	0.200	0.348	0.356	0.424	0.160
Miyazaki	G392	19	6	3.267	1.402	0.737	0.694	0.713	-0.062	0.297
	G113	10	3	1.942	0.791	0.300	0.485	0.511	0.381	0.403
	G205	10	9	6.452	2.013	0.700	0.845	0.889	0.172	0.718
	G217	10	3	1.504	0.613	0.400	0.335	0.353	-0.194	0.891
	G328	10	2	1.724	0.611	0.200	0.420	0.442	0.524	0.098
Shirahama	G329	10	4	1.695	0.800	0.200	0.410	0.432	0.512	<b>0.001</b>
	G392	10	7	4.545	1.704	0.600	0.780	0.821	0.231	0.060
	G113	14	2	1.600	0.562	0.214	0.375	0.389	0.429	0.109
	G205	14	12	8.522	2.283	0.714	0.883	0.915	0.191	0.255
	G217	13	4	1.742	0.797	0.462	0.426	0.443	-0.083	0.543
	G328	12	4	1.419	0.624	0.333	0.295	0.308	-0.129	0.998
	G329	14	4	2.010	0.969	0.286	0.503	0.521	0.431	0.080
	G392	13	5	3.073	1.278	0.538	0.675	0.702	0.202	0.584

Sample size (N), no. of alleles (Na), no. of effective Alleles (Ne), information index (I), observed heterozygosity (Ho), expected and unbiased expected heterozygosity (He, uHe), fixation index (F), and p-value for Hardy-Weinberg equilibrium (HWE), < P are shown in boldface.

will be lost in population-based analysis, integrated approaches taking phylogenetics, morphology, and ecology into account are nonetheless important.

This study confirms the absence of species boundaries between *G. lobata* and *G. djiboutiensis* morphologies using microsatellite markers. Such a multi-locus population genetic approach, including a geographic context, would be also useful for delineating the species boundaries of other closely related species including corals.

## Species Status of *G. lobata* and *G. djiboutiensis*

Although the concept of “species” is a fundamental unit for biodiversity conservation, the species delimitation of closely related coral species has been morphologically and genetically challenging due to high phenotypic plasticity and the paucity of suitable molecular markers. There are many proposed and widely used species concepts, including morphological species concepts that require morphological differentiation, the genealogical species concept that requires allelic coalescence (Baum and Donoghue, 1995), and the biological species concept that requires reproductive isolation (Mayr, 1942). However, whichever species concept is used, a species represents an independent metapopulation lineage through time (de Queiroz, 2005).

In this study, the species boundary between *G. lobata* and *G. djiboutiensis* was examined based on previously used morphological characteristics as well as newly developed microsatellite markers, including a geographic context for testing the hypothesis of “independent metapopulation lineages through time” for each species. The majority (84.2%) of the samples

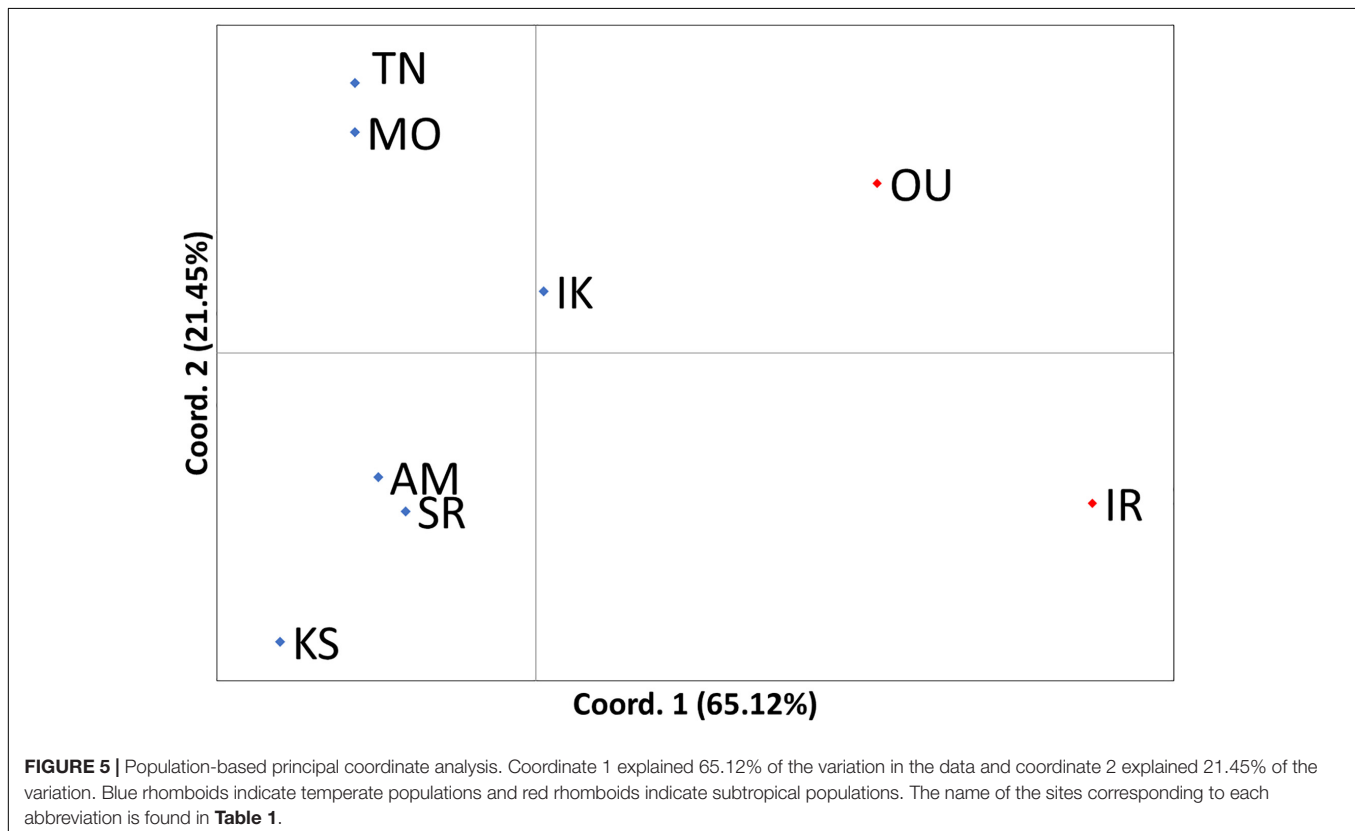
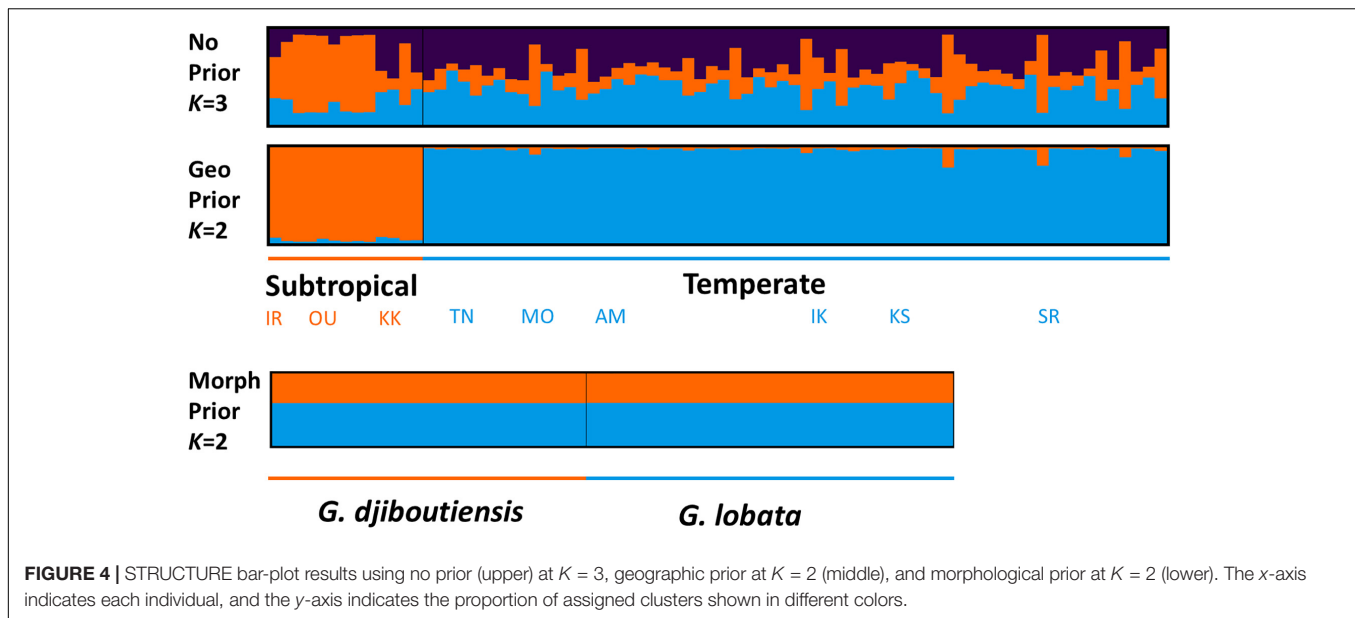
collected in Japan had intermediate forms, suggesting that the eight morphological characteristics used in the present study could not distinguish *G. lobata* from *G. djiboutiensis*. This fact corresponds with a previous study that reported an abundance of morphotypes in *Goniopora* spp. including *G. lobata* and *G. djiboutiensis* in the region (Kitano et al., 2013) and Veron (1993) who noted that *G. lobata* in Japan are “always difficult to identify with certainty in higher latitudes, where skeletal variations occur that are primarily correlated with non-reefal environments.” Additionally, microsatellite STRUCTURE analysis using either uniform prior or morphological prior indicated genetic homogeneity and could not detect any genetic boundaries between typical *G. lobata* and *G. djiboutiensis* morphologies, which was consistent with previous studies using other molecular markers (Kitano et al., 2013). Lastly, a genetic break (0.030 of allele frequency divergence between pops,  $F_{CT}$ -like value estimated by STRUCTURE) was discovered using a geographic prior, which could be explained by the presence of population isolation caused by oceanographic conditions rather than by morphological characteristics. This suggests that the current morphological characteristics defining *G. lobata* and *G. djiboutiensis* do not represent independent metapopulation lineages over time. *Goniopora lobata* and *G. djiboutiensis* could not be morphologically and genetically delimited as species. It is likely that the high morphological diversity in the *G. lobata* species complex may lead to overestimation of morphological species. The present study underlines the usefulness of a population genetics approach including a geographic context in examining the boundaries between closely related species. Given that the nomenclature of *Goniopora lobata* Milne-Edwards and Haime, 1851, has been used more than that of *Goniopora djiboutiensis* Vaughan, 1907, it would be appropriate to use “*G. lobata* species complex” rather than “*G. djiboutiensis* species complex” to describe the samples in clade II.

## The Kuroshio-Associated Oceanographic Barrier

Remarkably, a clear genetic break was discovered between subtropical and temperate regions, irrespective of morphological characteristics, suggesting that genetic exchange via larval dispersal was somewhat limited between subtropical and temperate regions in the *G. lobata* species complex. This genetic break corresponds not only to climatic regions (subtropical vs. temperate) but also to the Kuroshio-associated larval dispersal barrier reported by Nakabayashi et al. (2019). Thus, it is possible that this genetic barrier could be caused by oceanographic barriers and/or local adaptation owing to environmental factors, such as water temperature.

According to larval dispersal oceanographic simulations, larval transport between subtropical and temperate regions in Japan via the Kuroshio Current and its associated currents is limited to a few generations, and this phenomenon is referred to as the Kuroshio-associated barrier (Nakabayashi et al., 2019). *Goniopora* spp. are known to be gonochoric and are broadcast spawners (Richmond and Hunter, 1990) with at least 5 days of pelagic larval duration (Babcock and Heyward, 1986). Although the dispersal potential of the *G. lobata* species complex is not





precisely known, considering the markedly lower population density of the *G. lobata* species complex than that of *Acropora* spp. especially in subtropical areas, the number of larvae that can cross the Kuroshio-associated barrier would be fewer than that of *Acropora* spp., which have similar genetic breaks.

Alternatively, it is possible that this genetic break is caused by environmental factors. Among the environmental factors that we summarized for each sampling region [the mean surface

water temperature of the coldest month, yearly average of mean surface water temperature, chlorophyll-*a* concentration, and particulate inorganic carbon (PIC) concentration], (Yara et al., 2012; NASA, 2018) the range of chlorophyll-*a* and PIC concentration overlapped between temperate and subtropical regions (**Supplementary Table 4**). The ranges of water temperature between the two regions did not overlap, although the difference between the two regions was minor

(**Supplementary Table 4**). In addition, the following gradual changes along latitude were observed: 20.82–22.87°C (coldest month average) and 24.63–26.17°C (year average) in the subtropical region and 14.23–19.57°C (coldest month) and 20.27–24.22°C (year average) in the temperate region (Yara et al., 2012; **Supplementary Table 4**). If there were no clear physical barrier between the temperate and subtropical regions, one would expect a gradual change in different genotypes along the Kuroshio Current. The clear genetic break between temperate and subtropical regions is, therefore, impossible to explain only by the differences in environmental factors (i.e., water temperature, PIC concentration, and chlorophyll-*a* concentration) alone, although we cannot deny the possibility that these differences in environmental factors further facilitate local adaptation and genetic divergence.

In the present study, we used putatively neutral microsatellite markers. Thus, further genomic studies that can detect loci under natural selection, such as restriction site-associated DNA sequencing (RAD-seq, Wagner et al., 2013), as well as physiological studies of larval and adult corals between temperate and subtropical regions are needed to test this hypothesis. Similar genetic evidence of peripheral temperate isolation has been reported in other coral species, such as *Acropora hyacinthus* (Nakabayashi et al., 2019), and other marine species, including sea slugs (Hoang et al., 2018) and groupers. Further genetic connectivity studies of coral and other marine species with different dispersal potential would provide insights into the formation of genetic breaks associated with the Kuroshio-associated barrier.

## Limitations of This Study

While this study indicated a clear genetic break between temperate and subtropical regions irrespective of morphological features, there are some limitations in this study. The number of microsatellite loci analyzed in this study is limited. We only succeeded in isolating six independent microsatellite loci, which may be insufficient to accurately identify asexually produced clones within some populations. Fortunately, to our knowledge there is no report on asexually produced clones in the *G. lobata* species complex. We have also confirmed that there are no possible clones (having exactly the same genotype based on six loci) within our data, indicating all the samples used in this study were sexually reproduced genetically unique individuals.

A second limitation is the number of samples we analyzed in this study. Although this is characteristic of our target region, 84.2% of studied specimens had intermediate morphologies, and only 13 specimens could be identified as morphotypes of *G. lobata* ( $n = 7$ ) or *G. djiboutiensis* ( $n = 6$ ). While Terraneo et al. (2016) found major discordance between morphology and molecular data between *G. lobata* and *G. djiboutiensis* morphotypes, concordant with our study, they could at least identify *G. lobata* and *G. djiboutiensis* morphotypes in the Red Sea (a type locality of *G. lobata*). Thus, genetic analysis using more *G. lobata* and *G. djiboutiensis* morphotypes from other regions including type localities would be necessary to clarify the species boundaries of the *G. lobata* species complex.

Lastly, this study lacks a morphometric analysis, and individual-based environmental data. Further study, providing more detailed morphometric analysis, together with environmental data for each specimen would offer insights into the morphological variations and phenotypic plasticity of this group.

Using the present data as a baseline, genome-wide genetic analyses such as RAD-seq or MIG-seq using a larger number of collected morphotype specimens, including geographic context, would be useful to further clarify species boundaries and possible ecological speciation in relation to morphological features and evolutionary history of *G. lobata* species complex.

## DATA AVAILABILITY STATEMENT

The datasets presented in this study can be found in online repositories. The names of the repository/repositories and accession number(s) can be found below: DNA Data Bank of Japan (accession numbers listed in **Supplementary Table 4**). All the supplementary data is available in Figshare doi: 10.6084/m9.figshare.1479.

## AUTHOR CONTRIBUTIONS

NY and YK conceived the study. YK, TM, and HY collected the samples. YK conducted the morphological identification and Sanger sequencing. NY, SN, HY, and HT developed microsatellite markers. NY conducted the genetic analysis and drafted the manuscript. All the authors have checked and agreed to the final manuscript.

## FUNDING

This study was funded by the Environment Research and Technology Development Fund (grant no. 4RF-1501), Ministry of the Environment, Japan, Japan Society for the Promotion of Science, Grant-in-Aid for Young Scientists (A) (grant no. 17H04996), Grant-in-Aid for Scientific Research (B) (grant no. 21H02274), Grant-in-Aid for Research Fellows: 201921342, and the Program to Disseminate Tenure Tracking System from the Ministry of Education, Culture, Sports, Science and Technology (MEXT).

## ACKNOWLEDGMENTS

We are grateful to the members of the Japanese Society for Coral Taxonomy, particularly Mr. Kenji Iwao, Mr. Keiichi Nomura, Dr. Hiroyuki Yokochi, and Dr. Satoshi Nojima, for providing the coral specimens. We also appreciate Dr. Kazuhiko Sakai's assistance during sampling. We are grateful to Ms. Yumi Yamamoto and Mr. Ryo Shimbo for helping with the genetic experiments. Sampling was conducted under the Okinawa Prefectural Government permit (Nos. 27–81, 27–29, 26–10, 25–44, 24–36) and the Kochi Prefectural Government permit (No. 530). For other samplings, we submitted notifications to the local

governments and worked in agreement with local fishing corporations. We would like to thank Editage ([www.editage.com](http://www.editage.com)) for English language editing. We appreciate the reviewers and editors who assisted in improving this manuscript.

## SUPPLEMENTARY MATERIAL

The Supplementary Material for this article can be found online at: <https://www.frontiersin.org/articles/10.3389/fmars.2021.592608/full#supplementary-material>

## REFERENCES

- Babcock, R. C., and Heyward, A. J. (1986). Larval development of certain gamete-spawning scleractinian corals. *Coral Reefs* 5, 111–116. doi: 10.1007/BF00298178
- Baum, D. A., and Donoghue, M. J. (1995). Choosing among alternative “phylogenetic” species concepts. *Syst. Bot.* 20, 560–573. doi: 10.2307/2419810
- Bedot, M. (1907). Madréporaires d’Amboine. *Rev. Suisse. Zool.* 15, 143–292.
- Benson, G. (1999). Tandem repeats finder: a program to analyze DNA sequences. *Nucleic Acids Res.* 27, 573–580. doi: 10.1093/nar/27.2.573
- Bongaerts, P., Riginos, C., Hay, K., van Oppen, M., Hoegh-Guldberg, O., and Dove, S. (2011). Adaptive divergence in a scleractinian coral: physiological adaptation of *Seriatopora hystrix* to shallow and deep reef habitats. *BMC Evol. Biol.* 11:303. doi: 10.1186/1471-2148-11-303
- Capella-Gutiérrez, S., Silla-Martínez, J. M., and Gabaldón, T. (2009). trimAl: a tool for automated alignment trimming in large-scale phylogenetic analyses. *Bioinformatics* 25, 1972–1973. doi: 10.1093/bioinformatics/btp348
- Carpenter, K. E., Abrar, M., Aeby, G., Aronson, R. B., Banks, S., Bruckner, A., et al. (2008). One-third of reef-building corals face elevated extinction risk from climate change and local impacts. *Science* 321, 560–563. doi: 10.1126/science.1159196
- Chen, C. A., Yang, Y. W., Wei, N. V., Tsai, W. S., and Fang, L. S. (2005). Symbiont diversity in scleractinian corals from tropical reefs and subtropical non-reef communities in Taiwan. *Coral Reefs* 24, 11–22. doi: 10.1007/s00338-004-0389-7
- de Queiroz, K. (2005). A unified concept of species and its consequences for the future of taxonomy. *Proc. Calif. Acad. Sci.* 56, 196–215.
- Earl, D. A., and von Holdt, B. M. (2012). STRUCTURE HARVESTER: a website and program for visualizing STRUCTURE output and implementing the Evanno method. *Conserv. Genet. Res.* 4, 359–361. doi: 10.1007/s12686-011-9548-7
- Evanno, G., Regnaut, S., and Goudet, J. (2005). Detecting the number of clusters of individuals using the software STRUCTURE: a simulation study. *Mol. Ecol.* 14, 2611–2620. doi: 10.1111/j.1365-294X.2005.02553.x
- Excoffier, L., and Lischer, H. E. (2010). Arlequin suite ver 3.5: a new series of programs to perform population genetics analyses under Linux and Windows. *Mol. Ecol. Resour.* 10, 564–567. doi: 10.1111/j.1755-0998.2010.02847.x
- Fukami, H., Budd, A., Levitan, D., Jara, J., Kersanach, R., and Knowlton, N. (2004). Geographic differences in species boundaries among members of the *Montastrea annularis* complex based on molecular and morphological markers. *Evolution* 58, 324–337. doi: 10.1111/j.0014-3820.2004.tb01648.x
- Hoang, D. T., Chernomor, O., von Haeseler, A., Minh, B. Q., and Vinh, L. S. (2018). UFBoot2: improving the ultrafast bootstrap approximation. *Mol. Biol. Evol.* 35, 518–522. doi: 10.1093/molbev/msx281
- Hodel, R. G. J., Segovia-Salcedo, M. C., Landis, J. B., Crowl, A. A., Sun, M., Liu, X., et al. (2016). The report of my death was an exaggeration: a review for researchers using microsatellites in the 21st century. *Appl. Plant. Sci.* 4:1600025. doi: 10.3732/apps.1600025
- Hubisz, M. J., Falush, D., Stephens, M., and Pritchard, J. K. (2009). Inferring weak population structure with the assistance of sample group information. *Mol. Ecol. Resour.* 9, 1322–1332. doi: 10.1111/j.1755-0998.2009.02591.x
- Jeffries, D. L., Copp, G. H., Lawson Handley, L., Olsén, K. H., Sayer, C. D., and Hänfling, B. (2016). Comparing RAD seq and microsatellites to infer complex phylogeographic patterns, an empirical perspective in the Crucian carp, *Carassius carassius*, L. *Mol. Ecol.* 25, 2997–3018. doi: 10.1111/mec.13613
- Katoh, K., Rozewicki, J., and Yamada, K. D. (2017). MAFFT online service: multiple sequence alignment, interactive sequence choice and visualization. *Brief. Bioinform.* 20, 1160–1166. doi: 10.1093/bib/bbx108
- Kimura, M. (1980). A simple method for estimating evolutionary rates of base substitutions through comparative studies of nucleotide sequences. *J. Mol. Evol.* 16, 111–120. doi: 10.1007/BF01731581
- Kitano, Y. F., Obuchi, M., Uyeno, D., Miyazaki, K., and Fukami, H. (2013). Phylogenetic and taxonomic status of the coral *Goniopora stokesi* and related species (Scleractinia: Poritidae) in Japan based on molecular and morphological data. *Zool. Stud.* 52:25. doi: 10.1186/1810-522X-52-25
- Kopelman, N. M., Mayzel, J., Jakobsson, M., Rosenberg, N. A., and Mayrose, I. (2015). Clumpak: a program for identifying clustering modes and packaging population structure inferences across K. *Mol. Ecol. Resour.* 15, 1179–1191. doi: 10.1111/1755-0998.12387
- Kumar, S., Stecher, G., Li, M., Knyaz, C., and Tamura, K. (2018). MEGA X: molecular evolutionary genetics analysis across computing platforms. *Mol. Biol. Evol.* 35, 1547–1549. doi: 10.1093/molbev/msy096
- LaJeunesse, T. C., Pettay, D. T., Sampayo, E. M., Phongsuwan, N., Brown, B., Obura, D. O., et al. (2010). Long-standing environmental conditions, geographic isolation and host-symbiont specificity influence the relative ecological dominance and genetic diversification of coral endosymbionts in the genus *Symbiodinium*. *J. Biogeogr.* 37, 785–800. doi: 10.1111/j.1365-2699.2010.02273.x
- Mayr, E. (1942). *Systematics and the Origin of Species*. New York, NY: Columbia University Press.
- Medrano, M., López-Perea, E., and Herrera, C. M. (2014). Population genetics methods applied to a species delimitation problem: endemic trumpet daffodils (*Narcissus Section Pseudonarcissi*) from the Southern Iberian Peninsula. *Int. J. Planci. Sci.* 175, 501–517. doi: 10.1086/675977
- Milne-Edwards, H., and Haime, J. (1851). A monograph of the British fossil corals. 2. Corals from the oolitic formations. *Monogr. Palaeontogr. Soc.* 5, 73–145. doi: 10.1080/02693445.1851.12113202
- Minh, B. Q., Schmidt, H. A., Chernomor, O., Schrempf, D., Woodhams, M. D., von Haeseler, A., et al. (2020). IQ-TREE 2: new models and efficient methods for phylogenetic inference in the genomic era. *Mol. Biol. Evol.* 37, 1530–1534. doi: 10.1093/molbev/msaa015
- Nakabayashi, A., Yamakita, T., Nakamura, T., Aizawa, H., Kitano, Y. F., Iguchi, A., et al. (2019). The potential role of temperate Japanese regions as refugia for the coral *Acropora hyacinthus* in the face of climate change. *Sci. Rep.* 9:1892. doi: 10.1038/s41598-018-38333-5
- Nakajima, Y., Nishikawa, A., Iguchi, A., and Sakai, K. (2012). The population genetic approach delineates the species boundary of reproductively isolated corymbose *Acropora* corals. *Mol. Phylogenet. Evol.* 63, 527–531. doi: 10.1016/j.ympev.2012.01.006
- Nakamura, Y., Shigenobu, Y., Sugaya, T., Kurokawa, T., and Saitoh, K. (2013). Automated screening and primer design of fish microsatellite DNA loci on pyrosequencing data. *Ichthyol. Res.* 60, 184–187. doi: 10.1007/s10228-012-0317-8
- NASA (2018). *Goddard Space Flight Center, Ocean Ecology Laboratory, Ocean Biology Processing Group MODIS-Aqua Level-2 Ocean Color Data Version*,

- NASA OB.DAAC. doi: 10.5067/AQUA/MODIS/L2/OC/2018 (accessed January 1, 2018).
- Nishihira, M., and Veron, J. E. N. (1995). *Hermatypic Corals of Japan*. Tokyo: Kaiyusha Publishers. (In Japanese).
- Peakall, R., and Smouse, P. (2012). GenA1Ex 6.5: genetic analysis in excel. Population genetic software for teaching and research – an update. *Bioinformatics* 28, 2537–2539. doi: 10.1093/bioinformatics/bts460
- Pritchard, J. K., Stephens, M., and Donnelly, P. (2000). Inference of population structure using multilocus genotype data. *Genetics* 155, 945–959. doi: 10.1093/genetics/155.2.945
- Raymond, M., and Rousset, F. (1995). GENEPOP: population genetics software for exact tests and ecumenicism. *J. Hered.* 86, 248–249. doi: 10.1093/oxfordjournals.jhered.a111573
- Richmond, R. H., and Hunter, C. L. (1990). Reproduction and recruitment of corals: comparisons among the Caribbean, the tropical Pacific, and the Red Sea. *Mar. Ecol. Prog. Ser.* 60, 185–203. doi: 10.3354/meps060185
- Rozen, S., and Skaletsky, H. (2000). Primer3 on the WWW for general users and for biologist programmers. *Methods Mol. Biol.* 132, 365–386. doi: 10.1385/1-59259-192-2:365
- Schwartz, M. K., and McKelvey, K. S. (2008). Why sampling scheme matters: the effect of sampling scheme on landscape genetic results. *Conserv. Genet.* 10:441. doi: 10.1007/s10592-008-9622-1
- Terraneo, T. I., Benzoni, F., Arrigoni, R., and Berumen, M. L. (2016). Species delimitation in the coral genus *Goniopora* (Scleractinia, Poritidae) from the Saudi Arabian Red Sea. *Mol. Phylogenet. Evol.* 102, 278–294. doi: 10.1016/j.ympev.2016.06.003
- Todd, P. (2008). Morphological plasticity in scleractinian corals. *Biol. Rev. Camb. Philos. Soc.* 83, 315–337. doi: 10.1111/j.1469-185x.2008.00045.x
- Van Oosterhout, C. (2004). Micro-checker: software for identifying and correcting genotyping errors in microsatellite data. *Mol. Ecol. Notes* 4, 535–538. doi: 10.1111/j.1471-8286.2004.00684.x
- Vaughan, T. W. (1907). Some madreporarian corals from French Smaliland, East Africa, collected by Dr. Charles Gravier. *Proc. U. S. Natl. Mus.* 32, 249–266. doi: 10.5479/si.00963801.32-1526.249
- Veron, J. E. N. (1993). A biogeographic database of hermatypic corals. Species of the Central Indo-Pacific, genera of the world. *Aust. Inst. Mar. Sci. Monogr. Ser.* 10, 1–433.
- Veron, J. E. N., and Pichon, M. (1982). Scleractinia of eastern Australia. Part 4. *Aust. Inst. Mar. Sci. Monogr. Ser.* 5, 1–159.
- Wagner, C. E., Keller, I., Wittwer, S., Selz, O. M., Mwaiko, S., Greuter, L., et al. (2013). Genome-wide RAD sequence data provide unprecedented resolution of species boundaries and relationships in the Lake Victoria cichlid adaptive radiation. *Mol. Ecol.* 22, 787–798. doi: 10.1111/mec.12023
- Wong, J. C., Thompson, P., Xie, J. Y., Qiu, J. W., and Baker, D. M. (2016). Symbiodinium clade C generality among common scleractinian corals in subtropical Hong Kong. *Reg. Stud. Mar. Sci.* 8, 439–444. doi: 10.1016/j.rsma.2016.02.005
- Yamano, H., Sugihara, K., and Nomura, K. (2011). Rapid poleward range expansion of tropical reef corals in response to rising sea surface temperatures. *Geophys. Res. Lett.* 38:L04601. doi: 10.1029/2010GL046474
- Yamashita, H., and Koike, K. (2013). Genetic identity of free-living Symbiodinium obtained over a broad latitudinal range in the Japanese coast. *Psychol. Res.* 61, 68–80. doi: 10.1111/pre.12004
- Yara, Y., Vogt, M., Fujii, M., Yamano, H., Hauri, C., Steinacher, M., et al. (2012). Ocean acidification limits temperature-induced poleward expansion of coral habitats around Japan. *Biogeosciences* 9, 4955–4968. doi: 10.5194/bg-9-4955-2012
- Yasuda, N., Taquet, C., Nagai, S., Fortes, M., Fan, T.-Y., Harii, S., et al. (2015). Genetic diversity, paraphyly and incomplete lineage sorting of mtDNA, ITS2 and microsatellite flanking region in closely related *Heliopora* species (Octocorallia). *Mol. Phylogenet. Evol.* 93, 161–171. doi: 10.1016/j.ympev.2015.07.009

**Conflict of Interest:** The authors declare that the research was conducted in the absence of any commercial or financial relationships that could be construed as a potential conflict of interest.

Copyright © 2021 Yasuda, Kitano, Taninaka, Nagai, Mezaki and Yamashita. This is an open-access article distributed under the terms of the Creative Commons Attribution License (CC BY). The use, distribution or reproduction in other forums is permitted, provided the original author(s) and the copyright owner(s) are credited and that the original publication in this journal is cited, in accordance with accepted academic practice. No use, distribution or reproduction is permitted which does not comply with these terms.



# *In vitro* Symbiosis of Reef-Building Coral Cells With Photosynthetic Dinoflagellates

## OPEN ACCESS

### Edited by:

James Davis Reimer,  
University of the Ryukyus, Japan

### Reviewed by:

Virginia M. Weis,  
Oregon State University,  
United States  
Daniel Aagren Nielsen,  
University of Technology Sydney,  
Australia  
Ikuko Yuyama,  
Yamaguchi University, Japan

### \*Correspondence:

Kaz Kawamura  
kazuk@kochi-u.ac.jp  
Noriyuki Satoh  
norisky@oist.jp

### †ORCID:

Kaz Kawamura  
orcid.org/0000-0003-2118-9511  
Koki Nishitsuji  
orcid.org/0000-0002-4015-7139  
Eiichi Shoguchi  
orcid.org/0000-0003-3136-5558  
Shigeki Fujiwara  
orcid.org/0000-0001-9464-180X  
Noriyuki Satoh  
orcid.org/0000-0002-4480-3572

‡These authors have contributed  
equally to this work

### Specialty section:

This article was submitted to  
Coral Reef Research,  
a section of the journal  
Frontiers in Marine Science

**Received:** 07 May 2021

**Accepted:** 21 June 2021

**Published:** 14 July 2021

### Citation:

Kawamura K, Sekida S,  
Nishitsuji K, Shoguchi E, Hisata K,  
Fujiwara S and Satoh N (2021) *In vitro*  
Symbiosis of Reef-Building Coral Cells  
With Photosynthetic Dinoflagellates.  
Front. Mar. Sci. 8:706308.  
doi: 10.3389/fmars.2021.706308

Kaz Kawamura<sup>1\*†</sup>, Satoko Sekida<sup>2†</sup>, Koki Nishitsuji<sup>3†</sup>, Eiichi Shoguchi<sup>3†</sup>, Kanako Hisata<sup>3</sup>,  
Shigeki Fujiwara<sup>1†</sup> and Noriyuki Satoh<sup>3\*†</sup>

<sup>1</sup> Department of Applied Science, Kochi University, Kochi, Japan, <sup>2</sup> Kuroshio Science Program, Graduate School  
of Integrated Arts and Sciences, Kochi University, Kochi, Japan, <sup>3</sup> Marine Genomics Unit, Okinawa Institute of Science  
and Technology Graduate University, Okinawa, Japan

Coral reefs are the biodiversity hot spots of the oceans, but they have suffered from increasing environmental stresses caused principally by anthropogenic global warming. The keystone species of coral reefs are scleractinian corals, which maintain obligatory symbiotic relationships with photosynthetic dinoflagellates. Understanding cellular and molecular mechanisms of symbiosis is therefore essential for future preservation of coral reefs. To date, however, almost no *in vitro* experimental systems have been devised to illuminate such mechanisms. To this end, our previous study established stable *in vitro* cell culture lines, including IVB5, originating from planula larvae of the scleractinian coral, *Acropora tenuis*. Here, we show that soon after mixture with the dinoflagellate, *Breviolum minutum*, flattened amorphous coral cells with endodermal properties exhibited elevated locomotor activity using filopodia and lamellipodia and interacted with dinoflagellates. Several minutes thereafter, coral cells began to incorporate *B. minutum*, and *in vitro* symbiosis appeared to have been accomplished within 30 min. Nearly a half of the coral cells had incorporated algal cells within 24 h in a reproducible manner. Coral cells that harbored algal cells gradually became round and less mobile, and the algal cells sometimes settled in vacuole-like structures in coral cell cytoplasm. This symbiosis state was maintained for at least a month. The IVB5 line of *A. tenuis* therefore provides an experimental system to explore cellular and molecular mechanisms involved in coral-dinoflagellate symbiosis at the single-cell level, results of which may be useful for future preservation of coral reefs.

**Keywords:** *in vitro* symbiosis, corals, dinoflagellates, *Acropora*, endoderm, phagocytosis

## INTRODUCTION

During evolution of cnidarians, the lineage leading to scleractinian corals or stony, reef-building corals acquired the capacity to establish obligatory symbiosis with photosynthetic dinoflagellates. In this endosymbiosis, corals provide shelter for their algal symbionts, which supply most of their photosynthetic products to the host corals (Yellowlees et al., 2008). This alga-animal symbiosis resulted in extraordinary prosperity of scleractinian corals, which produce stony reefs by depositing calcium carbonate skeletons. Although coral reefs cover only 0.2~0.3% of the marine surface, they harbor an estimated one-third of all described marine species (Reaka-Kudla, 2001; Wilkinson, 2008). Coral reefs therefore support the most biodiverse ecosystems in the oceans. These ecosystems



also support human life in tropical and subtropical countries by virtue of fisheries, tourism, and culture (Spalding et al., 2017). Coral reefs, however, are in crisis due to environmental changes, including increased seawater temperatures, acidification, and pollution, mainly caused by human activities (Hughes et al., 2017; Sully et al., 2019). These stresses cause collapse of coral-dinoflagellate symbioses, resulting in white, dead reefs, a process known as coral bleaching, leading to loss of coral reefs and all the species they support (Hoegh-Guldberg et al., 2007; Hughes et al., 2017; Sully et al., 2019). Conservation of coral reefs is therefore one of the most urgent environmental crises facing humanity.

Most scleractinian corals incorporate photosynthetic dinoflagellates of the family Symbiodiniaceae through the digestive tract into the gastrodermis (Coffroth and Santos, 2005), although some species inherit symbionts vertically (Loh et al., 2001). Modulation of coral host inert immunity allows symbiosis of given species of algae in their cytoplasm (Davy et al., 2012). Although many studies have attempted to explore cellular and molecular mechanisms of coral-dinoflagellate endosymbiosis (Dove, 2004; Davy et al., 2012; Yuyama et al., 2018; Weis, 2019; Rosset et al., 2021; Yoshioka et al., 2021), many questions remain, especially regarding recognition mechanisms involved in the initial contact of animal and algal cells, cellular mechanisms allowing dinoflagellate endocytosis and maintenance of endosymbiosis, especially at the single-cell level (Davy et al., 2012). Recently, our knowledge of mechanisms involved in cnidaria-dinoflagellate symbiosis has been advanced by studies using the sea anemone, *Exaiptasia diaphana* (Weis, 2019), and the soft coral, *Xenia* sp. (Hu et al., 2020). Simultaneously, we need to understand symbiosis mechanisms of reef-building corals. Thus, many studies have attempted to culture *in vitro* lines of stony coral cells, by which mechanisms of coral-dinoflagellate symbiosis might be tackled. However, most attempts have failed to establish stable *in vitro* cultures, although primary cultures of cells or cell aggregates have been accomplished (Rinkevich, 2011; Domart-Coulon and Ostrander, 2016).

In a previous study, we developed *in vitro* coral cell lines originating from planula larvae of the scleractinian coral, *Acropora tenuis*. After several trials to improve culture media, we succeeded in producing various stable *in vitro* lines of coral cells, twenty of which have been cryo-preserved (Kawamura et al., 2021). Most cells of several lines are dark, flattened, amorphous cells with lamellipodia and locomotor activity. Judging from their morphology, behavior, and higher expression of endoderm-related genes, they likely originated from larval endoderm. Then we examined whether these cells could interact *in vitro* with dinoflagellates when mixed in culture media or seawater. We report here the occurrence of *in vitro* symbiosis between coral cells and dinoflagellates in culture dishes.

## MATERIALS AND METHODS

### *Acropora tenuis* IVB5 Line

Detailed methods for production of stable *in vitro* culture lines of coral cells are described in Kawamura et al. (2021). Although the IVB5 line was not described in that report,

the essence of establishment of this line was same as those reported there. Briefly, basic seawater medium consisted of natural seawater, one-fifth volume of H<sub>2</sub>O, 10 mM HEPES (final pH 6.8), and the antibiotics penicillin (100 U/mL), streptomycin (100 µg/mL), and amphotericin B (0.25 µg/mL). Immediately before use, the basic medium was mixed with Dulbecco's modified Eagle's medium (DMEM) containing 15% fetal bovine serum, penicillin (100 U/mL), and streptomycin (100 µg/mL) at a ratio of 9:1. In the secondary cell culture, plasmin (166-24231, FUJIFILM Wako Pure Chemical Corp., Osaka, Japan) was added to the growth medium at a final concentration of 2 µg/mL. Dissociated cells were centrifuged at 300 x g for 5 min and resuspended in growth medium at a density of 2–5 x 10<sup>7</sup> cells/mL. Aliquots (0.5 mL each) were dispensed to a 24-well multiplate and maintained at 20°C by adding 0.2 mL of fresh growth medium to the old medium twice a week. Proliferating cells were replated in new multiplates every month.

### The Dinoflagellate, *Breviolum minutum*

A culturable dinoflagellate, *Breviolum minutum* (LaJeunesse et al., 2018), was used in this study. *B. minutum* was previously named *Symbiodinium minutum* (LaJeunesse et al., 2012). The *B. minutum* strain used was originally harbored by the Caribbean coral, *Orbicella faveolata* (previously *Montastraea faveolata*), maintained in the laboratory of Dr. Mary Alice Coffroth, at State University at New York, Buffalo, United States and then in the laboratories of Okinawa Institute of Science and Technology Graduate University and Kochi University. The culture ID of this strain is Mf1.05b (McIlroy and Coffroth, 2017), which is currently provided through National Institute of Environmental Science, Tsukuba, Japan under <https://mcc.nies.go.jp/strainList.do?strainId=3806> upon request. For symbiosis experiments with the *A. tenuis* IVB5 line, the *B. minutum* strain was precultured at 20°C with standard IMK medium using an incubator (SANYO MIR-554) under 12 h:12 h dark and light conditions for more than 10 months. A fluorescent lamp producing 20 µmol/m<sup>2</sup>/s was used for the algae culture.

### Mixture of Coral Cells and Dinoflagellate, and Observation

A 200–250-µL drop of culture medium containing *B. minutum* was added to each well of a 24-well multiplate, which contained approximately 1 mL of medium for culturing cells of the IVB5 line. A 24-well multiplate that contained cultured coral cells and algae was put in a translucent, moist container and exposed to natural lighting at 20–22°C throughout culture and observation. Immediately after addition, interactions between the coral cells and the dinoflagellates were observed using an inverted microscope (Olympus CKX41) equipped with a color digital camera (WRAYMER SR300). Photos obtained by consecutive observation with time-lapse video (2–3-s interval) was converted to a time-lapse video using iPhoto. Pictures and videos were also taken with an ordinary microscope (Nikon

Eclipse 80i) equipped with a differential interference contrast (DIC) apparatus.

## Immunocytochemistry with Antibodies Specific to *Acropora tenuis*

In a previous study, we made two rabbit antibodies against synthetic oligopeptides, one corresponding to a part of *A. tenuis* Snail protein (a zinc finger transcriptional repressor) and the other to a part of *A. tenuis* Fat1 protein (a Fat-like cadherin-related tumor suppressor homolog) (for details, see Kawamura et al., 2021). To confirm that cells of the IVB5 line that engulfed algae are of *A. tenuis*, we carried out immunocytochemistry using the antibodies. Cultured cells suspended in the culture medium were centrifuged at 300 × g for 5 min and resuspended in phosphate-buffered salt solution (PBS). Cells were fixed with 4% paraformaldehyde in PBS for 15 min in an ice bath. After quenching with 200 mM glycine for 2 min and permeabilizing with 0.1% Triton X-100 for 10 min, cells were incubated in a mixture of 0.25% blocking reagent (Roche, Mannheim, Germany) and 5% skim milk in PBS for 30 min. Then, they were reacted with the rabbit primary antibody diluted 400-fold with PBS for 1 h and with goat anti-rabbit secondary antibody labeled with fluorescein isothiocyanate (FITC) (Vector Laboratory, Burlingame, CA, USA) diluted 200-fold with PBS for 30 min. After washing by centrifugation for 5 min twice with PBS, cells were counterstained with 4',6-diamidino-2-phenylindole (DAPI). They were observed by means of a confocal microscopy system (ECLIPSE C1si, Nikon Co. LTD., Tokyo, Japan).

## Semi-Thin Sectioning

Seven hours after mixing coral cells and dinoflagellates, cells were fixed for semi-thin sectioning for light microscopy. Cells were fixed in 3% glutaraldehyde in 0.1 M phosphate buffer (pH 7.2) containing 0.2 M sucrose and 1% tannic acid for 2 h at 4°C. Samples were rinsed with the buffer containing 0.2 M sucrose and post-fixed in buffer containing 1% osmium tetroxide and 0.2 M sucrose for 2 h at 4°C. Post-fixed specimens were dehydrated in an acetone series and embedded in Spurr's resin. Semi-thin sections (0.5–1.5 µm) were cut with a diamond knife using a Leica Ultracut UCT ultra-microtome (Leica Microsystems, Germany), stained with 0.5% toluidine blue O and observed through a light microscope (Nikon Eclipse 80i).

## RESULTS

### *Acropora tenuis* IVB5-Line Cells

IVB5 is one of 20 cryo-reserved cell lines established from *A. tenuis* planula larvae in 2020 (Figure 1A). After replating the culture line several times, cells were frozen in 2-mL serum tubes in liquid nitrogen for permanent preservation. A few months later, cells in a tube were melted back into culture medium to proliferate as the original line of cells did (Figure 1A). Although the IVB5 line is polyclonal and contains several types of cells with different morphologies, the majority are dark, flattened, amorphous cells, 20–30 µm in length (Figure 1A). The line also

contains a few brilliant cells (Figure 1A) and small elongated cells (Figure 1A). A large vacuole (Figures 1B1,B3) and several small vesicles (Figures 1B1,B2) are found in the cytoplasm of flattened amorphous cells. They extend lamellipodia and sometimes filopodia as well (Figures 1B2,B3) and show moderate locomotor activity (Supplementary Movie 1).

Using immunocytochemistry, we examined dark, flattened, amorphous cells that did not engulf symbiotic dinoflagellates (Supplementary Figure 1A) and cells that did (Supplementary Figures 1B,1C). Although the former maintained their flattened, amorphous morphology, the latter became spherical (described later). Both showed distinct fluorescent signals in response to *A. tenuis*-specific antibodies (Supplementary Figures 1A–1C). In the case of anti-AtSnail, signals were restricted to the nucleus (Supplementary Figure 1C), while in the case of anti-AtFat1, fluorescent signals appeared throughout the entire cell bodies (Supplementary Figures 1A,1B). In contrast, negative control cells that were stained with non-immunized rabbit serum did not exhibit FITC signals, but confirmed DAPI signals (Supplementary Figure 1D). These results indicate that cells of the IVB5 line that engulfed symbiotic algae are of *Acropora tenuis*.

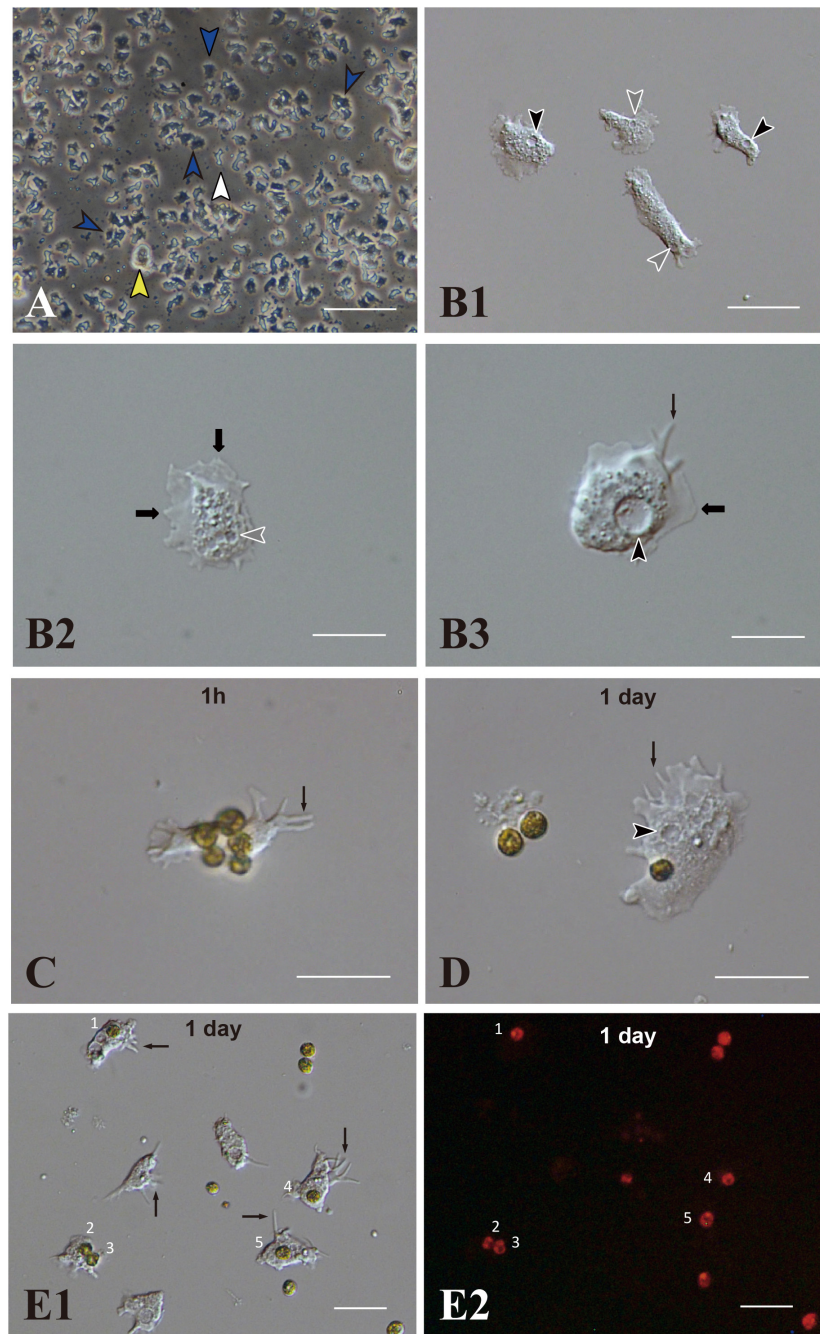
### The Dinoflagellate, *Breviolum minutum*

*Breviolum minutum* (Figures 1C,D) has been maintained in our laboratories for 8 years. During the proliferation stage, brown cells appear globular, approximately 8 µm in diameter, do not extend flagella, and show no locomotor activity. On the other hand, during steady state, some algal cells extend flagellae and swim in the culture medium. The *B. minutum* genome has been sequenced (Shoguchi et al., 2013). The identity of *B. minutum* used in this study was identified by partial genome sequence to be strain ITS2-type B1 (Supplementary Figure 2)."

### Occurrence of *in vitro* Symbiosis of Coral Cells With Dinoflagellates

A 200–250-µL drop of culture medium containing *B. minutum* was added to each well of a 24-well multiplate that contained subconfluent coral cells in approximately 1 mL of growth medium. Most immobilized *B. minutum* gradually settled at the bottom of the culture plate wells after 5 or 6 min. The first change detected after mixing animal and algal cells was increased locomotor activity of flattened amorphous cells. Immediately after mixing, coral cells developed filopodia and actively extended and retracted pseudopodia (Figures 1C,D,E1, arrows). They crept faster than those in plates that lacked dinoflagellates (Supplementary Movie 1). Interactions between cells of the two taxa occurred shortly after mixing (Figure 1C), followed by coral cell phagocytosis of dinoflagellates (Figure 1D). Coral cells incorporated coccoid cells, but not thecate motile cells. One day after mixing, one or two and sometimes three dinoflagellates were found in the cytoplasm of individual cultured coral cells (Figures 1E1,E2). We repeated experiments more than five times and obtained the same results, indicating that this *in vitro* symbiosis is reproducible.

We examined whether the culture medium affects the interaction between coral and dinoflagellate cells. Three media,



**FIGURE 1** | *Acropora tenuis* cells of the IVB5 line and symbiosis with the photosynthetic dinoflagellate, *Breviolum minutum*. **(A)** A vertical microscope image of IVB5 line. Most cells are dark, flattened, amorphous cells (blue arrowheads), while a few brilliant cells (yellow arrowhead) and small cells of different morphology (white arrowhead) are present as well. **(B–D)** Differential interference microscopy images showing morphological features of flattened, amorphous cells. **(B1)** Lower and **(B2,B3)** higher magnification. Flattened amorphous cells contain a large vacuole (black arrowheads) and several small vesicles (white arrowheads) in the cytoplasm. They extend lamellipodia (bold black arrows) and/or filopodia (thin black arrows) and show locomotor activity. **(C–E)** Coral cell engulfment of dinoflagellates, **(C)** 1 h (1 h) and **(D,E)** 1 day after mixing cells of the two taxa. **(E2)** is a dark-field image of **(E1)**, showing red auto-fluorescence of dinoflagellates. Cells endocytosed dinoflagellates numbered 1–5. Filopodia are indicated by arrows and vacuoles by black arrowheads. Scale bars, 100  $\mu\text{m}$  in **(A)**, 50  $\mu\text{m}$  in **(B1)**, 20  $\mu\text{m}$  in **(B2,B3,C,D)**, and 50  $\mu\text{m}$  in **(E1,E2)**.

the conditioned cell growth medium that had been used for cell culture for 2 weeks or more, newly prepared cell growth medium, and basic seawater medium, were examined. One day after

inoculation in the conditioned medium,  $50.2 \pm 30.2\%$  (number of observation fields,  $n = 12$ , which contained approximately 20 cells) of cultured host cells incorporated algae (**Supplementary**



**Figure 3A**). In newly prepared growth medium, algal uptake was observed in  $45.7 \pm 28.8\%$  ( $n = 14$ ) of all cells (**Supplementary Figure 3B**), and in seawater medium,  $45.5 \pm 30.3\%$  ( $n = 7$ ) (**Supplementary Figure 3C**). These results indicate that 1 day after inoculation, coral cell symbiosis with algal cells occurred similarly in each of the three media in approximately 50% of the cultured coral cells. Several days after mixing, coral cells did not show further incorporation of dinoflagellates. Even when dinoflagellates were present near or attached to coral cells, they appeared to show no interest in dinoflagellates.

## Realtime Observations of *in vitro* Interactions Between Coral Cells and Dinoflagellates

Two examples of *in vitro* symbiosis are described below. In the first case (**Supplementary Movie 2**), three coral cells and four dinoflagellates are present in the frames (**Figure 2A**). At 0:00:00 (starting time of observation, **Figure 2A**), coral cell b extended a filopodium further and further (**Figure 2B**), and after approximately 20 sec, the filopodium contacted dinoflagellate x (**Figure 2C**). Maintaining contact with dinoflagellate x, the filopodium of cell b became thicker and thicker (**Figures 2C–E**), and ~2 min after contact, dinoflagellate x was phagocytosed by the thickened filopodium or a part of the cytoplasm of cell b (**Figure 2F**). Dinoflagellate x was moved to the center of cell b (from **Figures 2F–J**). Cell b still extended lamellipodia

and showed active locomotion. The accomplishment of *in vitro* symbiosis between b and x, from contact of the two cells until the settlement of x in the cytoplasm of b, took only five min. In addition, during this time, cell c contacted dinoflagellate y with its cell membrane or a thin lamellipodium (**Figure 2A**). Cell c actively shifted the membrane around y (**Figures 2A–C**) and quickly incorporated y into the cytoplasm (**Figure 2D**). With symbiotic dinoflagellate y in the cytoplasm, cell c exhibited locomotion using pseudopodia (**Figures 2E–J**). Cell c also promptly engulfed dinoflagellate y within a few min after their first encounter.

In the second case (**Supplementary Movie 3**), at the start of observations, coral cell b contacted the cell wall of dinoflagellate x with its lamellipodium (**Figure 3A**). Although cell b showed extensive lamellipodial activity, the interaction between b and x appeared not to proceed further (**Figures 3A–C**). In the interim, neighboring cell c that had already engulfed dinoflagellate y, extended lamellipodia toward x (**Figures 3B,C**). Within 30 s thereafter, dinoflagellate x was engulfed by cell c (**Figure 3D**). While actively shuffling its membrane, an interaction between cells b and c continued for a while (**Figures 3E–H**). Finally, cell c departed from b, with two dinoflagellates, x and y, in its cytoplasm (**Figures 3I,J**). This *in vitro* symbiosis between coral cells and dinoflagellates was accomplished within ~5 min (**Figure 3**).

As described above, flattened amorphous coral cells repeatedly extended and retracted filopodia and lamellipodia around algal cells. Many coral cells had engulfed dinoflagellates within ~5 min after mixing.

No cell types other than the flattened amorphous cells showed this behavior. Coral cell membranes around the region that attached to algal cells showed extensive shuffling activity, which may be necessary for the cells to endocytose algal cells. Sometimes coral cells endocytosed dinoflagellates and then exocytosed them (**Supplementary Movie 4**). Some cells repeated this process. In addition, single coral cells sometimes incorporated multiple symbionts (**Figures 1E, 3**). The number of coral cells that incorporated dinoflagellates increased throughout the day of mixing (see next section).

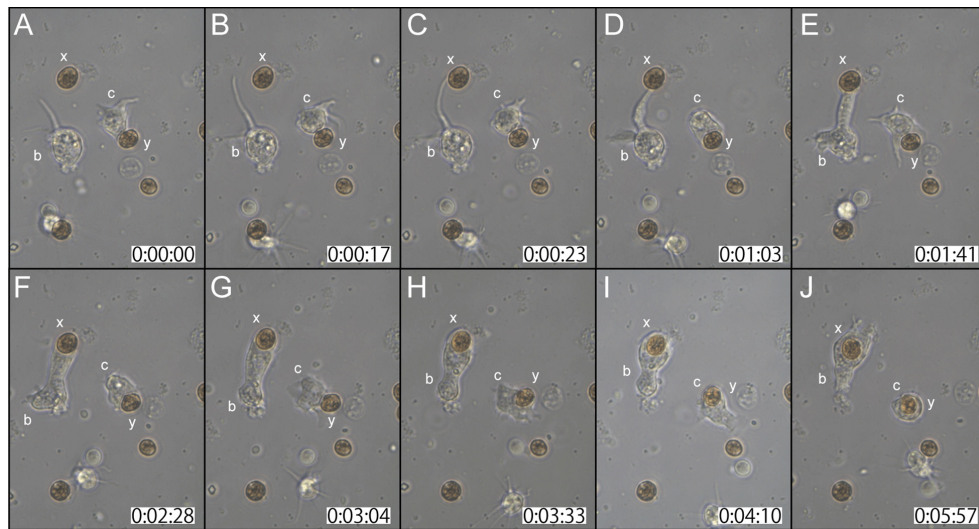
## Observations of Semi-Thin Sections of Coral Cell-Alga Interactions

We examined and confirmed the interaction of coral cells with algal cells by observation of semi-thin sections of the cells, 7 h after mixture of the two types of cells (**Figure 4**). **Figure 4A** shows a micrograph in which a coral cell filopodium extended over an algal cell. In the next step, more than a half of the alga body was covered by coral cell membrane (**Figure 4B**). Then, another section revealed complete engulfment of an algal cell in host coral-cell cytoplasm (**Figure 4C**). **Figures 4D,E** show the relationship between engulfed algal cells and a large vacuole of host cell cytoplasm. In **Figure 4D**, an engulfed algal cell was close to the vacuole, but the two were separated by membranes. In **Figure 4E**, however, the cytoplasmic membrane enclosing an alga and the membrane of a vacuole appeared fused into a continuous structure. **Figure 4F** shows that an engulfed algal cell

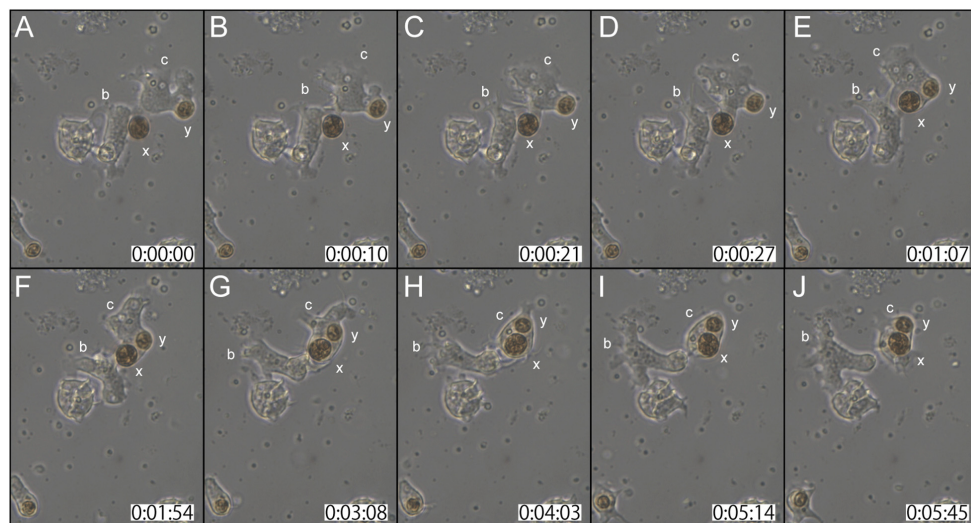
**TABLE 1 |** Representative *Acropora tenuis* genes highly expressed in the IVB5 cell line.

GeneID	TMM	Blast annotation
<b>Usual physiological function</b>		
aten_s0009.g61	246187	60S ribosomal protein L40
aten_s0244.g12	196019	Polyubiquitin-C
aten_s0027.g69	193466	40S ribosomal protein S25-like
aten_s0013.g132	75176	Actin, cytoplasmic-like
aten_s0094.g60	34872	Elongation factor 1 -alpha
<b>Proliferation</b>		
aten_s0092.g59	968	Transcriptional regulator Myc-B-like isoform X2
aten_s0035.g57	1082	Late histone H1-like
<b>Gastroderm</b>		
aten_s0139.g34	19574	Collagen alpha-1 (XVII) chain-like
aten_s0075.g93	134	Soma ferritin-like
<b>Glandular/secretory</b>		
aten_s0009.g9	21339	A disintegrin and metalloproteinase with thrombospondin motifs 6-like isoform X4
aten_s0282.g5	18605	Mucin-2-like isoform XI
aten_s0007.g144	1128	Chymotrypsin-like protease CTRL-1
<b>Epidermis</b>		
aten_s0062.g70	4512	CUB and zona pellucida-like domain-containing protein 1
<b>Neuron</b>		
aten_s0002.g29	3015	Synaptotagmin-like protein 2





**FIGURE 2** | A time-lapse video of symbiotic interactions of coral cells (b and c) and dinoflagellates (x and y). The starting point of observations is shown at 0 h: 00 min: 00 s. (A–J) Serial pictures are taken at time intervals indicated at the bottom. Coral cell b engulfs symbiont x, whereas coral cell c endocytoses symbiont y. See the detailed description in the text.



**FIGURE 3** | Another time-lapse video of symbiotic interactions of coral cells (b and c) and dinoflagellates (x and y). The starting point of observations is shown at 0 h: 00 min: 00 s. (A–J) Serial pictures are taken at time intervals indicated at the bottom. Coral cell b interacted with symbiont x, but did not incorporate it, whereas coral cell c endocytosed both x and y. See the detailed description in the text.

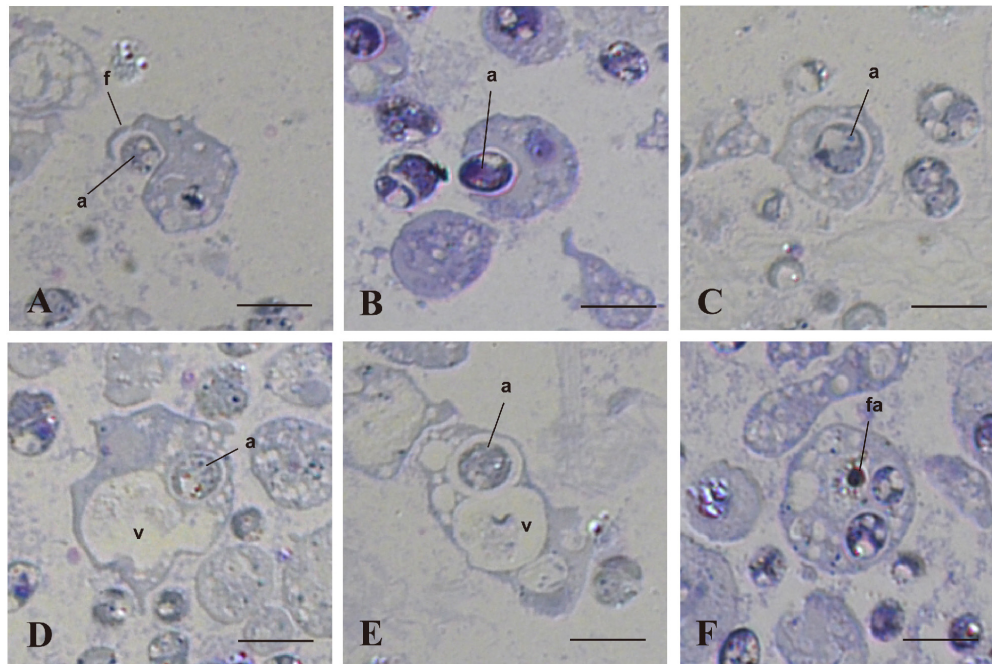
became fragmented in the host coral cell cytoplasm. The semi-thin section undoubtedly demonstrates coral cell engulfment of dinoflagellates.

### Subsequent Fates of Symbiotic Algal Cells and Host Coral Cells

One half to 1 day after inoculation, some engulfed algal cells remained in the cytoplasm of host coral cells (Figure 5A). On the other hand, some other algal cells were present within large vacuoles in the cytoplasm (Figure 5B). Algal cells in the cytoplasm (not in vacuoles) were approximately 12  $\mu\text{m}$  in

diameter (Figure 5A), which was somewhat larger than those in vacuoles (Figure 5B) and non-engulfed algal cells, which were usually 8–10  $\mu\text{m}$  in diameter (Figures 5C,D, arrows). This may indicate swelling of dinoflagellates in host coral cell cytoplasm. In addition, some algal cells began to exhibit fragmentation (Figure 5C), and debris remained in the cytoplasm (Figure 5D; Supplementary Movie 5). These changes were consistent with the observation of semi-thin sections (Figure 4).

After 2 days of culture, cells with unfragmented algae survived in the culture dish (Figure 6A, broken circles). They withdrew pseudopods, stopped moving, and assumed a spherical form



**FIGURE 4 |** *In vitro* interactions between coral cells and algae, 7 h after coral cell-algae mixture. Semi-thin sections were stained with toluidine blue. **(A)** Coral cell extending filopodium over an alga. **(B)** Coral cell engulfing an alga. **(C)** Alga incorporated into coral cell cytoplasm. **(D)** Algal phagosome in association with a coral cell vacuole. **(E)** Algal phagosome fused with a host vacuole. **(F)** Fragmented alga in a coral cell. a, algae; f, filopodium; fa, fragmented alga; v, vacuole. Bars, 10  $\mu$ m.

(Figure 5B). Spherical cells with algal cells increased in number until about a week of cell culture (Figures 6A,B,C1). In many cases of 7-day-old cell culture, algae were in the cytoplasm of host cells. Approximately 80% of spherical cells contained 1–3 unfragmented algae in their cell bodies (Figure 6C3). In some cases, algal cells were observed within endogenous large vacuoles in host cells (Figure 6C2), indicating translocation of engulfed algae from cytoplasmic vesicles to vacuoles. However, it is uncertain at present which phagosome-like vesicles or vacuolar organelles become genuine, long-sustainable symbiosomes, because it became more and more difficult to discriminate between vacuolar membranes and phagosomal membranes. In 22-day-old symbionts, algal cells were still found in cultured host cells, although host cells possessing algae had significantly decreased in number (Figures 6D1,D2). At present, we failed in subculturing coral cells with symbionts, because the symbionts die after replating.

## DISCUSSION

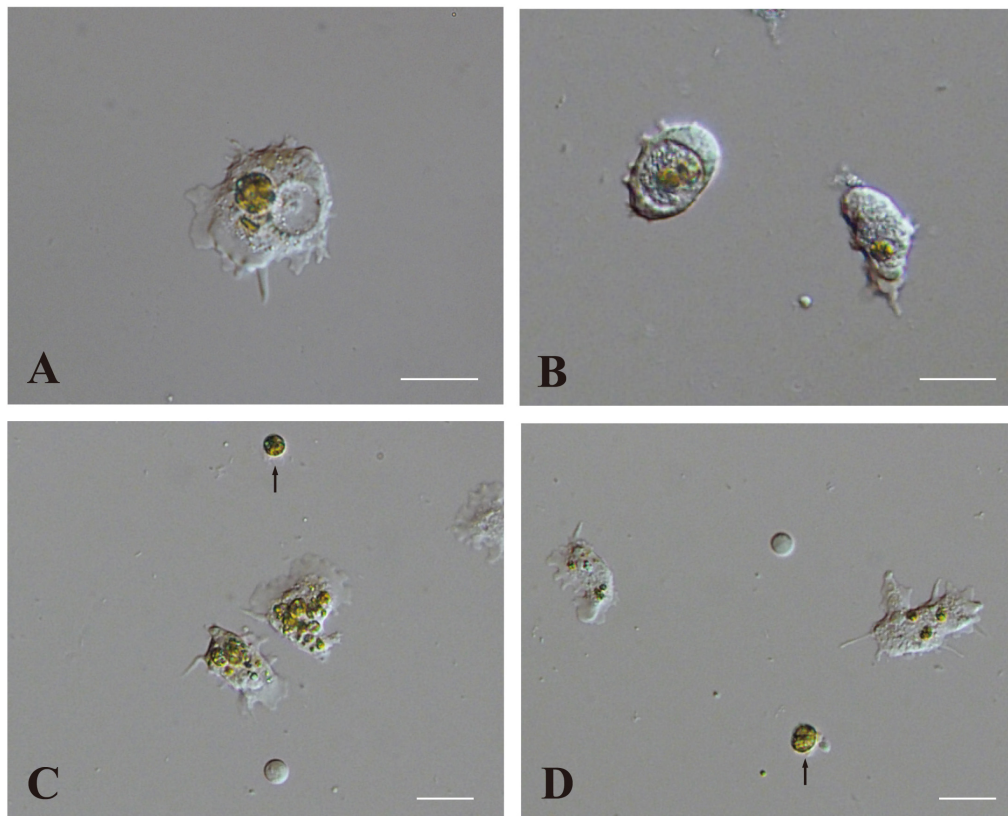
We reported here the occurrence of *in vitro* symbiosis of cells of the reef-building coral, *Acropora tenuis*, with ITS2-type B1 dinoflagellates (*Breviolum minutum*). Dark flattened amorphous cells of the IVB5 line have properties of endoderm and engulfed algal cells by actively shuffling cell membranes and by extending filopodia and lamellipodia. Phagocytosis itself was completed within 5 min after contact of coral cells with algal cells. Approximately half of flattened amorphous coral cells achieved symbiosis in the first day of the mixture, irrespective of the type

of culture medium. This *in vitro* symbiosis is highly reproducible; thus, this *in vitro* system will facilitate exploration of cellular and molecular mechanisms involved in coral-dinoflagellate symbiosis at the single-cell level. Knowledge obtained in future studies using this system may advance our understanding of coral biology associated with bleaching, thereby providing cues for methodological improvements of coral reef preservation.

The phagocytotic behavior of flattened amorphous coral cells is very dynamic, and phagocytosis occurs very quickly (Figures 2, 3). It is uncertain whether *in vivo* phagocytosis of planula larva endoderm cells is like that of this *in vitro* system. However, such dynamic and prompt symbiosis tempts us to speculate that the first evolutionary step of coral-dinoflagellate interactions was active coral cell phagocytosis of dinoflagellates, moving through the gastric cavity into coral gastroderm cells. It is likely that corals have maintained this high potential for phagocytosis throughout evolution so that when they are cultured *in vitro*, they show high ancestral phagocytotic activity.

One of the questions raised by this *in vitro* system is whether symbiosis is accomplished by flattened amorphous cells alone (without mixture or indirect help of other types of cells) or only in a mixture containing other types of cells (Figure 1A). The IVB5 line is polyclonal and contains other types of cells beside flattened amorphous cells. The cellular composition of the IVB5 line therefore resembles that of planula larvae, which consist of outer ectoderm and inner endoderm. Such a complex, harmonious mixture of cells may be required for flattened amorphous cells of endodermal origin to initiate symbiosis with algal cells. This should be examined in the future using monoclonal, flattened,





**FIGURE 5 |** Two modes of interaction between coral cells and dinoflagellates. **(A,B)** Settlement of dinoflagellates in coral cell cytoplasm, **(A)** outside and **(B)** inside a vacuole. **(C,D)** Fragmentation followed by collapse of dinoflagellates in coral cell cytoplasm. Fragmentation appears more severe in **(C)** than **(D)**. Dinoflagellates not engulfed by coral cells are indicated with arrows. Scale bar, 20  $\mu\text{m}$ .

amorphous cells. Nevertheless, the IVB5 line serves as an *in vitro* system for studying coral cell symbiosis with photosynthetic dinoflagellates at the single-cell level.

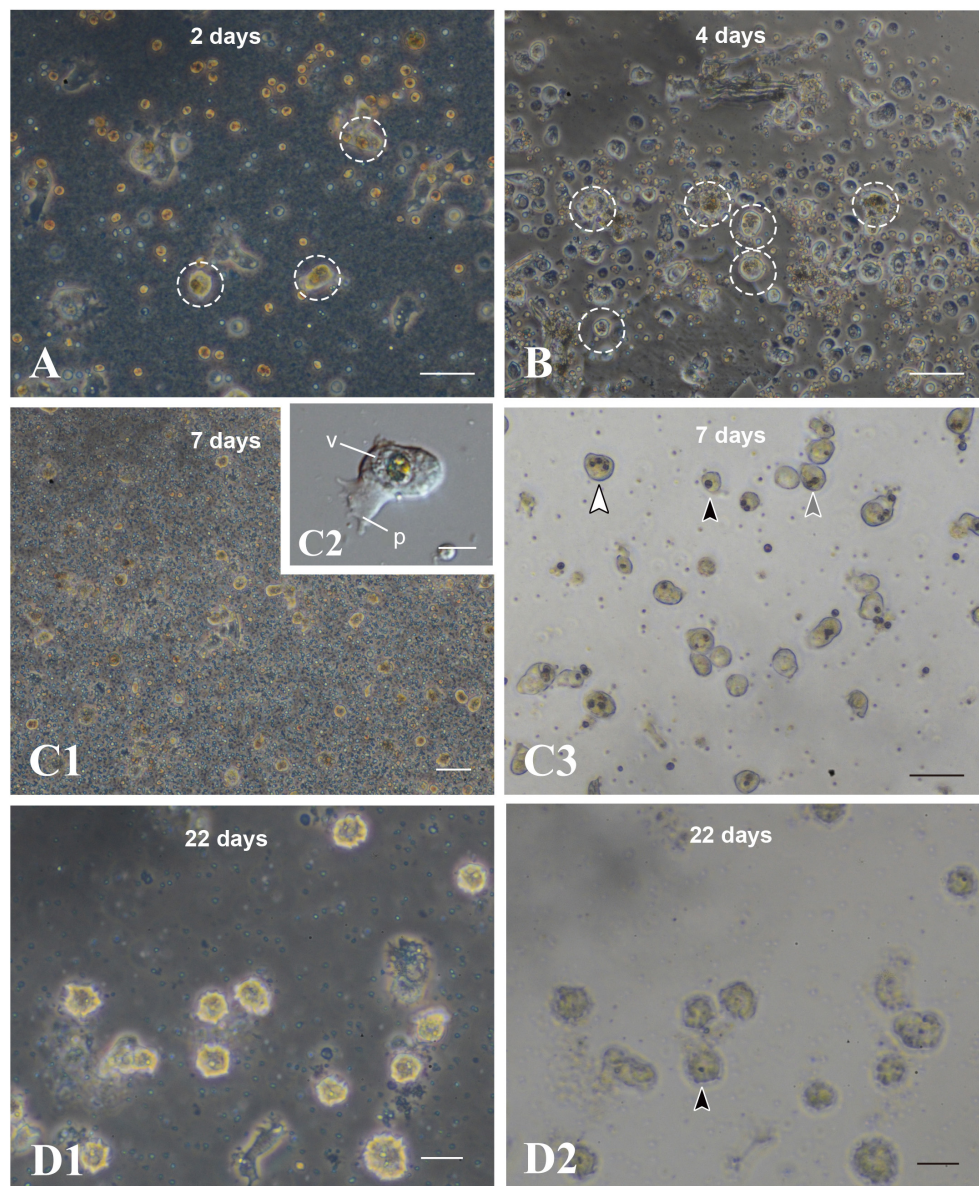
### Future Studies Using This *in vitro* System

There are many questions regarding cellular and molecular mechanisms involved in coral-dinoflagellate symbiosis. Three major overlapping, interrelated processes involved in this symbiosis are (1) the onset of symbiosis and mechanisms of partner recognition, (2) maintenance and dynamic homeostasis, and (3) dysbiosis that leads to bleaching (reviewed by Davy et al., 2012; Weis, 2019).

In relation to the first process of coral-dinoflagellate symbiosis, classification of symbiotic species of the family Symbiodiniaceae has recently been revised and these taxa are classified into *Symbiodinium* (previously Clade A *Symbiodinium*), *Breviolum* (Clade B), *Cladocopium* (Clade C), *Durisdinium* (Clade D), *Effrenium* (Clade E), and others (LaJeunesse et al., 2018). Of these, *Symbiodinium*, *Breviolum*, *Cladocopium*, and *Durisdinium* comprise major coral symbionts. Extensive studies have been carried out to examine specificity, preferences, or exchange of dinoflagellates of different genera hosted by different species of corals (in case of *A. tenuis*, e.g., Yamashita et al., 2013, 2014, 2018). In our laboratory conditions, *Acropora tenuis* larvae harbor

*Symbiodinium*, *Breviolum*, and *Cladocopium*, although ratios of symbiosis differ depending on the algal species (Shoguchi et al., unpublished data). Future studies should examine whether dinoflagellates other than *Breviolum* are engulfed by the IVB5 line. If the IVB5 line shows different acceptance ratios, we might address the question of symbiont recognition and specificity using the IVB5 line and different species of dinoflagellates.

As to the second issue of maintenance and dynamic homeostasis, algal cells need to be enclosed by an endomembrane to form “symbiosome,” which is a critical component of coral-dinoflagellate symbiosis (Wakefield and Kempf, 2001; Davy et al., 2012; Rosset et al., 2021). How does its composition and/or structures differ from the plasma membrane in function, and what is the role of membrane trafficking in its regulation and maintenance (Weis, 2019)? In the IVB5-line system, algae engulfed by cultured cells likely have two destinations: fragmentation or settlement in vacuoles (Figures 4, 5). Fragmentation of *Breviolum minutum* does not occur during the culture process, as far as our experience goes. On the other hand, fragmentation of engulfed algae occurred in cells of the IVB5 line. It is natural to assume that in the cytoplasm, a phagosomal membrane encircling the algal cell fuses with lysosomal membranes to make secondary lysosomes as part of the normal pathway for degradation of foreign material (Davy et al.,



**FIGURE 6 |** Maintenance of coral cells with symbiotic dinoflagellates. **(A)** 2 days, **(B)** 4 days, **(C)** 7 days, and **(D)** 22 days after mixture of the two types of cells. Coral cells with symbiotic dinoflagellates (broken circles) became spherical, without pseudopodial extensions, and exhibit less and less locomotor activity. Those cells became globular, bright cells. **(C3,D2)** are bright field images of **(C1,D1)**, showing one (black arrowhead), two (gray arrowhead), and three algae (white arrowhead) in single cells. p, pseudopodium; v, vacuole. Scale bars, 50  $\mu\text{m}$  in **(A,B,C3)**, 100  $\mu\text{m}$  in **(C1)**, 10  $\mu\text{m}$  in **(C2)**, and 20  $\mu\text{m}$  in **(D1,D2)**.

2012). Therefore, the escape of engulfed algae from the lysosomal digestion by host cells is essential to establish symbiosis. If algal cells are transferred from the phagosome to a vacuole, they may escape lysosomal digestion. However, at present, it is uncertain whether fragmentation always occurs in algae that were not engulfed by vacuoles. Future studies should explore the role of organelles as well as intracellular membranes in the establishment of symbiosis *in vitro*.

The IVB5 line also provides a system to explore molecular mechanisms involved in coral-dinoflagellate symbiosis. Studies should strive to duplicate results of previous transcriptomic

studies (Yuyama et al., 2018; Yoshioka et al., 2021) and of single-cell RNA-seq analyses (Hu et al., 2020). If genes that play pivotal roles in the symbiosis are found in future studies, an introduction of CRISPR/Cas9-mediated genome editing method seems challenging (Cleves et al., 2018). Since genomes of both *Acropora tenuis* (Shinzato et al., 2021) and *Breviolum minutum* (Shoguchi et al., 2013) have been decoded, molecular biological studies may be facilitated using genomic information. Transcriptome analyses of gene expression changes in the IVB5-line cells after interaction and phagocytosis of algal cells are now in progress.



## AUTHOR CONTRIBUTIONS

KK and NS conceived and designed the study and prepared the manuscript. ES and SS cultured dinoflagellates. KK, SS, KN, KH, SF, and NS carried out analyses. All authors commented on it.

## FUNDING

This work was supported by an OIST fund for collaboration with Kochi University, and also funded in part by the Mrs. Sumiko Imano Memorial Foundation. Sachiko McAlinn and Miki McAlinn were acknowledged for their funding support.

## ACKNOWLEDGMENTS

We would like to thank all members of the Marine Genomics Unit at OIST for their support. Steven D. Aird (<https://www.sda-technical-editor.org>) is acknowledged for editing the manuscript. Professor Virginia Weis, one of the reviewers of this manuscript, kindly noted the mistake in our transcriptome presentation.

## REFERENCES

- Cleves, P. A., Strader, M. E., Bay, L. K., Pringle, J. R., and Matz, M. V. (2018). CRISPR/Cas9-mediated genome editing in a reef-building coral. *Proc. Natl. Acad. Sci. U.S.A.* 115, 5235–5240. doi: 10.1073/pnas.1722151115
- Coffroth, M. A., and Santos, S. R. (2005). Genetic diversity of symbiotic dinoflagellates in the genus *Symbiodinium*. *Protist* 156, 19–34. doi: 10.1016/j.protis.2005.02.004
- Davy, S. K., Allemand, D., and Weis, V. M. (2012). Cell biology of cnidarian-dinoflagellate symbiosis. *Microbiol. Mol. Biol. Rev.* 76, 229–261. doi: 10.1128/mmb.05014-11
- Domart-Coulon, I., and Ostrander, G. K. (2016). “Coral cell and tissue methods,” in *Diseases of Coral*, eds C. M. Woodley, C. A. Downs, A. W. Bruckner, J. W. Porter, and S. B. Galloway (Hoboken, NJ: Wiley), 489–505. doi: 10.1002/9781118828502.ch37
- Dove, S. G. (2004). Scleractinian corals with photoprotective host pigments are hypersensitive to thermal bleaching. *Mar. Ecol. Prog. Ser.* 272, 99–116. doi: 10.3354/meps272099
- Hoegh-Guldberg, O., Mumby, P. J., Hooten, A. J., Steneck, R. S., Greenfield, P., Gomez, E., Harvell, C. D., et al. (2007). Coral reefs under rapid climate changes and ocean acidification. *Science* 318, 1737–1742.
- Hu, M., Zheng, X., Fan, C.-H., and Zheng, Y. (2020). Lineage dynamics of the endosymbiotic cell type in the soft coral *Xenia*. *Nature* 582, 534–538. doi: 10.1038/s41586-020-2385-7
- Hughes, T. P., Kerry, J. T., Alvarez-Noriega, M., Alvarez-Romero, J. G., Anderson, K. D., Baird, A. H., et al. (2017). Global warming and recurrent mass bleaching of corals. *Nature* 543, 373–377.
- Kawamura, K., Nishitsuji, K., Shoguchi, E., Fujiwara, S., and Satoh, N. (2021). Establishing sustainable cell lines of a coral, *Acropora tenuis*. *Mar. Biotechnol.* 23, 373–388. doi: 10.1007/s10126-021-10031-w
- LaJeunesse, T. C., Parkinson, J. E., and Reimer, J. D. (2012). A genetics-based description of *Symbiodinium minutum* sp. nov. and *S. psygmophilum* sp. nov. (Dinophyceae), two dinoflagellates symbiotic with cnidaria. *J. Phycol.* 48, 1380–1391. doi: 10.1111/j.1529-8817.2012.01217.x
- LaJeunesse, T. C., Parkinson, J. E., Gabrielson, P. W., Jeong, H. J., Reimer, J. D., Woolstra, C. R., and Santos, S. R. (2018). Systematic revision of symbiodiniaceae

## SUPPLEMENTARY MATERIAL

The Supplementary Material for this article can be found online at: <https://www.frontiersin.org/articles/10.3389/fmars.2021.706308/full#supplementary-material>

**Supplementary Movie 1** | A time-lapse video showing locomotor activity of flattened amorphous cells. Soon after replating, the cells extend lamellipodia and filopodia and show moderate locomotor activity. Frames were taken 20 sec intervals.

**Supplementary Movie 2** | A time-lapse video showing that coral cells engulf dinoflagellates into the cytoplasm using filopodia and lamellipodia. For more detailed, see **Figure 2** and the main text. Frames were taken 2–3 sec intervals.

**Supplementary Movie 3** | A time-lapse video showing another case in which coral cells engulf dinoflagellates into the cytoplasm using filopodia and lamellipodia. For more detailed, see **Figure 3** and the main text. Frames were taken 2–3 sec intervals.

**Supplementary Movie 4** | A time-lapse video showing extensive shuffling activity of coral cell membranes around the region that attached to algal cells, by which coral cells endocytose algal cells and then exocytose them. Some coral cells repeat this process. Frames were taken 2–3 sec intervals.

**Supplementary Movie 5** | A time-lapse video showing coral cells that incorporated dinoflagellates in host coral-cell cytoplasm, and fragmentation of dinoflagellates in the coral-cell cytoplasm. Frames were taken 20 sec intervals.

- high- lights the antiquity and diversity of coral endosymbionts. *Curr. Biol.* 28, 2570–2580. doi: 10.1016/j.cub.2018.07.008
- Loh, W. K. W., Loi, T., Carter, D., and Hoegh-Guldberg, O. (2001). Genetic variability of the symbiotic dinoflagellates from the wide ranging coral species *Seriatopora hystrix* and *Acropora longicyathus* in the Indo-West Pacific. *Mar. Ecol. Prog. Ser.* 222, 97–107. doi: 10.3354/meps222097
- McIlroy, S. E., and Coffroth, M. A. (2017). Coral ontogeny affects early symbiont acquisition in laboratory-reared recruits. *Coral Reefs* 36, 927–932. doi: 10.1007/s00338-017-1584-7
- Reaka-Kudla, M. L. (2001). “Coral reefs: biodiversity and conservation,” in *Contemporary Approaches to the Study of Biodiversity*, eds H. M. Hernandez, A. N. Garcia Aldrete, F. Alvarez, and M. Ulloa (Laramie, WY: Instituto de Biodiversity), 221–243.
- Rinkevich, B. (2011). Cell cultures from marine invertebrates: insights for capturing endless stemness. *Mar. Biotechnol.* 13, 345–354. doi: 10.1007/s10126-010-9354-3
- Rosset, S.L., Oakley, C. A., Ferrier-Page's, C., Suggett, D.J., Weis, V. M., and Davy, S. K. (2021). The molecular language of the cnidarian-dinoflagellate symbiosis. *Trends Microbiol.* 29, 320–333. doi: 10.1016/j.tim.2020.08.005
- Sebe-Pedros, A., Saudemont, B., Chomsky, E., Plessier, F., Mailhé, M. P., Renno, J., Loe-Mie, Y., et al. (2018). Cnidarian cell types diversity and regulation revealed by whole-organism single-cell RNA-seq. *Cell* 173, 1520–1534.e20.
- Shinzato, C., Khalturin, K., Inoue, J., Zayasu, Y., Kanda, K., Kawamitsu, M., Yoshioka, Y., Yamashita, H., Suzuki, G., and Satoh, N. (2021). Eighteen coral genomes reveal the evolutionary origin of *Acropora* strategies to accommodate environmental changes. *Mol. Biol. Evol.* 38, 16–30. doi: 10.1093/molbev/msaa216
- Shoguchi, E., Shinzato, C., Kawashima, T., Gyoja, F., Mungpakdee, S., Koyanagi, R., Takeuchi, T., Hisata, K., Tanaka, M., Fujiwara, M., et al. (2013). Draft assembly of the *Symbiodinium minutum* nuclear genome reveals dinoflagellate gene structure. *Curr. Biol.* 23, 1399–1408. doi: 10.1016/j.cub.2013.05.062
- Spalding, M., Burke, L., Wood, S. A., Ashpole, J., Hutchison, J., and zu Ermgassene, P. (2017). Mapping the global value and distribution of coral reef tourism. *Mar. Policy* 82, 104–113. doi: 10.1016/j.marpol.2017.05.014



- Sully, S., Burkepille, D. E., Donovan, M. K., Hodgson, G., and van Woesik, R. (2019). A global analysis of coral bleaching over the past two decades. *Nat. Commun.* 10:1264.
- Wakefield, T. S., and Kempf, S. C. (2001). Development of host- and symbiont-specific monoclonal antibodies and confirmation of the origin of the symbiosome membrane in a cnidarian–dinoflagellate symbiosis. *Biol. Bull.* 200, 127–143. doi: 10.2307/1543306
- Weis, Y. M. (2019). Cell biology of coral symbiosis: foundational study can inform solution to the coral reef crisis. *Integr. Comp. Biol.* 59, 845–855. doi: 10.1093/icb/icz067
- Wilkinson, C. (2008). *Status of Coral Reefs of the World: 2008*. Townsville, AU: Global Coral Reef Monitoring Network.
- Yamashita, H., Suzuki, G., Hayashibara, T., and Koike, K. (2013). *Acropora* recruits harbor “rare” *Symbiodinium* in the environmental pool. *Coral Reefs* 32, 355–366. doi: 10.1007/s00338-012-0980-2
- Yamashita, H., Suzuki, G., Kai, S., Hayashibara, T., and Koike, K. (2014). Establishment of coral–algal symbiosis requires attraction and selection. *PLoS One* 9:e97003. doi: 10.1371/journal.pone.0097003
- Yamashita, H., Suzuki, G., Shinzato, C., Jimbo, M., and Koike, K. (2018). Symbiosis process between *Acropora* larvae and *Symbiodinium* differs even among closely related *Symbiodinium* types. *Mar. Ecol. Prog. Ser.* 592, 119–128. doi: 10.3354/meps12474
- Yellowlees, D., Rees, T. A., and Leggat, W. (2008). Metabolic interactions between algal symbionts and invertebrate hosts. *Plant Cell Environ.* 31, 679–694. doi: 10.1111/j.1365-3040.2008.01802.x
- Yoshioka, Y., Yamashita, H., Suzuki, G., Zayaus, Y., Tada, I., Kanda, M., et al. (2021). Whole-genome transcriptome analyses of native symbionts reveal host coral genomic novelties for establishing coral–algae symbioses. *Genome Biol. Evol.* 13:evaa240. doi: 10.1093/gbe/evaa240
- Yuyama, I., Ishikawa, M., Nozawa, M., Yoshida, M. A., and Ikeo, K. (2018). Transcriptomic changes with increasing algal symbiont reveal the detailed process underlying establishment of coral–algal symbiosis. *Sci. Rep.* 8:16802.
- Zardoya, R., Costas, E., López-Rodas, V., Garrido-Pertierra, A., and Bautista, J. M. (1995). Revised dinoflagellate phylogeny inferred from molecular analysis of large-subunit ribosomal RNA gene sequences. *J. Mol. Evol.* 41, 637–645. doi: 10.1007/BF00175822

**Conflict of Interest:** The handling editor declared a shared committee with one of the authors, NS, at time of review.

The authors declare that the research was conducted in the absence of any commercial or financial relationships that could be construed as a potential conflict of interest.

Copyright © 2021 Kawamura, Sekida, Nishitsuji, Shoguchi, Hisata, Fujiwara and Satoh. This is an open-access article distributed under the terms of the Creative Commons Attribution License (CC BY). The use, distribution or reproduction in other forums is permitted, provided the original author(s) and the copyright owner(s) are credited and that the original publication in this journal is cited, in accordance with accepted academic practice. No use, distribution or reproduction is permitted which does not comply with these terms.



## OPEN ACCESS

### Edited by:

James Davis Reimer,  
University of the Ryukyus, Japan

### Reviewed by:

Virginia M. Weis,  
Oregon State University, United States

### \*Correspondence:

Kaz Kawamura  
kazuk@kochi-u.ac.jp  
Noriyuki Satoh  
norisky@oist.jp

### †ORCID:

Kaz Kawamura  
orcid.org/0000-0003-2118-9511  
Koki Nishitsuji  
orcid.org/0000-0002-4015-7139  
Eiichi Shoguchi  
orcid.org/0000-0003-3136-5558  
Noriyuki Satoh  
orcid.org/0000-0002-4480-3572  
Shigeki Fujiwara  
orcid.org/0000-0001-9464-180X

‡These authors have contributed  
equally to this work

### Specialty section:

This article was submitted to  
Coral Reef Research,  
a section of the journal  
Frontiers in Marine Science

**Received:** 23 October 2021

**Accepted:** 19 November 2021

**Published:** 10 December 2021

### Citation:

Kawamura K, Sekida S, Nishitsuji K,  
Shoguchi E, Hisata K, Fujiwara S and  
Satoh N (2021) Corrigendum: *In vitro*  
Symbiosis of Reef-Building Coral Cells  
With Photosynthetic Dinoflagellates.  
Front. Mar. Sci. 8:800737.  
doi: 10.3389/fmars.2021.800737

# Corrigendum: *In vitro* Symbiosis of Reef-Building Coral Cells With Photosynthetic Dinoflagellates

Kaz Kawamura<sup>1\*†‡</sup>, Satoko Sekida<sup>2†</sup>, Koki Nishitsuji<sup>3†</sup>, Eiichi Shoguchi<sup>3†</sup>, Kanako Hisata<sup>3</sup>, Shigeki Fujiwara<sup>1†</sup> and Noriyuki Satoh<sup>3\*†</sup>

<sup>1</sup> Department of Applied Science, Kochi University, Kochi, Japan, <sup>2</sup> Kuroshio Science Program, Graduate School of Integrated Arts and Sciences, Kochi University, Kochi, Japan, <sup>3</sup> Marine Genomics Unit, Okinawa Institute of Science and Technology Graduate University, Okinawa, Japan

**Keywords:** *In vitro* symbiosis, corals, dinoflagellates, *Acropora*, endoderm, phagocytosis

## A Corrigendum on

### *In vitro* Symbiosis of Reef-Building Coral Cells With Photosynthetic Dinoflagellates

by Kawamura, K., Sekida, S., Nishitsuji, K., Shoguchi, E., Hisata, K., Fujiwara, S., and Satoh, N. (2021). Front. Mar. Sci. 8:706308. doi: 10.3389/fmars.2021.706308

In the original article, in order to show that cells of the IVB5 line are derived from planula larvae of the coral *Acropora tenuis*, the authors presented transcriptome data from the IVB5 line cells in **Table 1**, **Supplementary Table 1**, and **BioProjectID**, PRJDB11647 (BioSampleID, SAMD00325495; and RawReadsID, DRA012135) as published. However, we later discovered that the medium of our culture system contains not only coral cells, but also other contaminating organisms. The RNA-seq data therefore included sequences of organisms other than *Acropora tenuis*. As a consequence, the data did not always support the coral origin of IVB5 line cells. Therefore, we have withdrawn these transcriptome-related data. Instead, we present experimental results of immunocytochemistry to show *in vitro* symbiosis of reef-building coral cells with photosynthetic dinoflagellates more clearly. The following corrections have been made:

1. **Materials and Methods, Immunocytochemistry with Antibodies Specific to *Acropora tenuis***, paragraph one has been replaced with:

“In a previous study, we made two rabbit antibodies against synthetic oligopeptides, one corresponding to a part of *A. tenuis* Snail protein (a zinc finger transcriptional repressor) and the other to a part of *A. tenuis* Fat1 protein (a Fat-like cadherin-related tumor suppressor homolog) (for details, see Kawamura et al., 2021). To confirm that cells of the IVB5 line that engulfed algae are of *A. tenuis*, we carried out immunocytochemistry using the antibodies. Cultured cells suspended in the culture medium were centrifuged at 300 x g for 5 min and resuspended in phosphate-buffered salt solution (PBS). Cells were fixed with 4% paraformaldehyde in PBS for 15 min in an ice bath. After quenching with 200 mM glycine for 2 min and permeabilizing with 0.1% Triton X-100 for 10 min, cells were incubated in a mixture of 0.25% blocking reagent (Roche, Mannheim, Germany) and 5% skim milk in PBS for 30 min. Then, they were reacted with the rabbit primary

antibody diluted 400-fold with PBS for 1 h and with goat anti-rabbit secondary antibody labeled with fluorescein isothiocyanate (FITC) (Vector Laboratory, Burlingame, CA, USA) diluted 200-fold with PBS for 30 min. After washing by centrifugation for 5 min twice with PBS, cells were counterstained with 4',6-diamidino-2-phenylindole (DAPI). They were observed by means of a confocal microscopy system (ECLIPSE C1si, Nikon Co. LTD., Tokyo, Japan)."

**2. Results, *Acropora tenuis* IVB5-Line Cells**, paragraphs 1–3 have been replaced with:

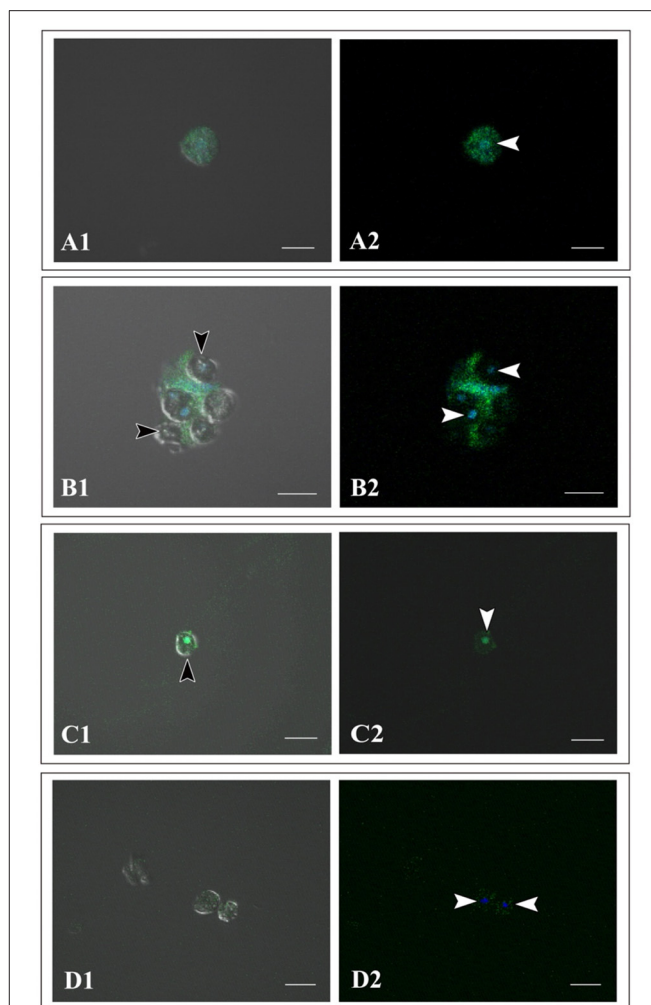
"IVB5 is one of 20 cryo-reserved cell lines established from *A. tenuis* planula larvae in 2020 (Figure 1A). After replating the culture line several times, cells were frozen in 2-mL serum tubes in liquid nitrogen for permanent preservation. A few months later, cells in a tube were melted back into culture medium to proliferate as the original line of cells did (Figure 1A). Although the IVB5 line is polyclonal and contains several types of cells with different morphologies, the majority are dark, flattened, amorphous cells, 20–30  $\mu\text{m}$  in length (Figure 1A). The line also contains a few brilliant cells (Figure 1A) and small elongated cells (Figure 1A). A large vacuole (Figure 1B1, B3) and several small vesicles (Figure 1B1, B2) are found in the cytoplasm of flattened amorphous cells. They extend lamellipodia and sometimes filopodia as well (Figure 1B2, B3) and show moderate locomotor activity (Supplementary Movie 1).

Using immunocytochemistry, we examined dark, flattened, amorphous cells that did not engulf symbiotic dinoflagellates (Supplementary Figure 1A) and cells that did (Supplementary Figures 1B, 1C). Although the former maintained their flattened, amorphous morphology, the latter became spherical (described later). Both showed distinct fluorescent signals in response to *A. tenuis*-specific antibodies (Supplementary Figures 1A–1C). In the case of anti-AtSnail, signals were restricted to the nucleus (Supplementary Figure 1C), while in the case of anti-AtFat1, fluorescent signals appeared throughout the entire cell bodies (Supplementary Figures 1A, 1B). In contrast, negative control cells that were stained with non-immunized rabbit serum did not exhibit FITC signals, but confirmed DAPI signals (Supplementary Figure 1D). These results indicate that cells of the IVB5 line that engulfed symbiotic algae are of *Acropora tenuis*."

**3. Results, The Dinoflagellate, *Breviolum minutum***, paragraph one have been replaced with:

*Breviolum minutum* "(Figures 1C,D) has been maintained in our laboratories for 8 years. During the proliferation stage, brown cells appear globular, approximately 8  $\mu\text{m}$  in diameter, do not extend flagella, and show no locomotor activity. On the other hand, during steady state, some algal cells extend flagellae and swim in the culture medium. The *B. minutum* genome has been sequenced (Shoguchi et al., 2013). The identity of *B. minutum* used in this study was identified by partial genome sequence to be strain ITS2-type B1 (Supplementary Figure 2)."

**4. Results, Occurrence of *in vitro* Symbiosis of Coral Cells With Dinoflagellates**, paragraphs 1–2 have been replaced with:



**Supplementary Figure 1 |** Immunocytochemistry of cells of *Acropora tenuis* IVB5 line with specific antibodies, anti-AtFat (A,B) and anti-AtSnail (C). (D) A negative control stained with non-immunized rabbit serum. (A1–D1) Bright field images and (A2–D2) dark field images. (A) A flattened, amorphous cell that does not contain symbiotic algae. (B–D) Spherical cells that have engulfed symbiotic algae for two weeks or more. Black arrowheads indicate engulfed symbiotic algae and white arrowheads indicate nuclei of coral cells. DAPI stains the nucleus blue. Distinct staining with *A. tenuis*-specific antibodies indicates that the IVB5 line cells that have engulfed symbiotic algae are coral cells. Scale bar, 20  $\mu\text{m}$ .

"A 200–250- $\mu\text{L}$  drop of culture medium containing *B. minutum* was added to each well of a 24-well multiplate that contained subconfluent coral cells in approximately 1 mL of growth medium. Most immobilized *B. minutum* gradually settled at the bottom of the culture plate wells after 5 or 6 min. The first change detected after mixing animal and algal cells was increased locomotor activity of flattened amorphous cells. Immediately after mixing, coral cells developed filopodia and actively extended and retracted pseudopodia (Figures 1C,D,E1, arrows). They crept faster than those in plates that lacked

Primer pairs (Zardoya et al. 1995)  
 28S-F-1:CCCGCTGAATTTAAGCATATAAGTAAGCGG  
 28S-R-1:GTTAGACTCCTTGGTCCGTGTTTCAAGA

>PCR amplified 28S rDNA (Query)

ACACCTGTCTGAGTCCCACACCGCACAGAGGAACACTAACAAGTGTACCATGTGAGCTGAAGGCCATCCTCAAACAAATGTGGCTAATGACTC  
 GCATGCTGAGAAACACTGCGGGTAAATGCTCACACATAAGCAGTCAGCTTGCCTTACATGCTCAAGGCTCACAAAGACCCACAGCAATCTCA  
 GCACGACATGTGGCTCCGTTTCGCTTCTCAGCAATTTCAAACACTTTTAACTCTCTTTCCAAAGTCCTTTTCATCTTTCCCTCATGGTAC  
 TTGTTTGTCTATTGGTCTCGAGCTTCTATTAGCTTTGGATGAAACTTACCACCTGATTTACGCTCCAATTCGAGGAGCGTGACTCTCAGGAC  
 AAGCACTGTGGACAGCGGACATCGAGCGAAATGCAGGATTCTCACCCGGGCACACGCTCTATTCCAAGAGGCTTGCCTCGAGCCGCCGATAG  
 CGCTATGCCTGCAGGCTACAGCCCGACACAGATGTATCGGTTTCAGCCTGAGCTCATCCTGTTTCATTCGCCATTACTGAGGGAATCCTATT  
 TAGTTCCTTTT

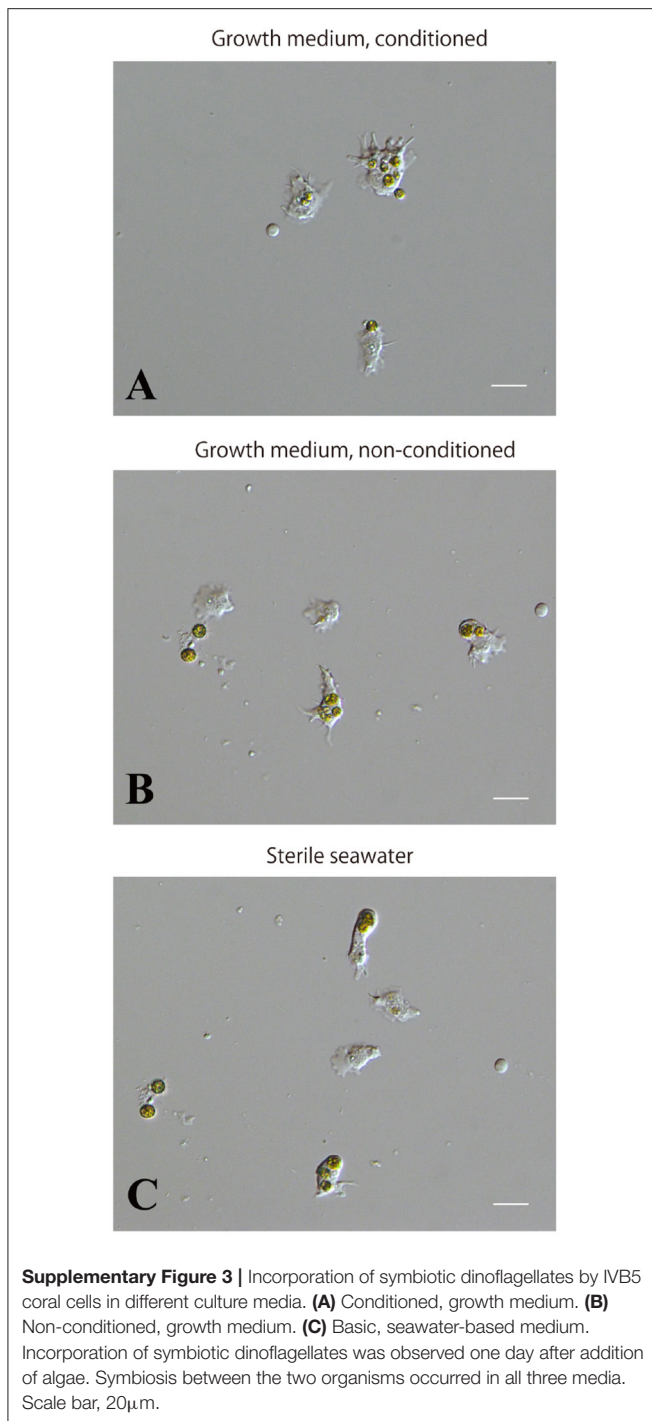
> scaffold5386.1 of *Breviolum minutum* (Sbjct)  
 ([https://marinegenomics.oist.jp/symb/viewer/info?project\\_id=21](https://marinegenomics.oist.jp/symb/viewer/info?project_id=21))

Score = 1046 bits (566), Expect = 0.0  
 Identities = 568/569 (99%), Gaps = 0/569 (0%)  
 Strand=Plus/Plus

Query	1	ACACCTGTCTGAGTCCCACACCGCACAGAGGAACACTAACAAGTGTACCATGTGAGCTGA	60
Sbjct	20148	ACACCTGTCTGAGTCCCACACCGCACAGAGGAACACTAACAAGTGTACCATGTGAGCTGA	20207
Query	61	AGGCCATCCTCAAACAAATGTGGCTAATGACTCGCATGCTGAGAAACACTGCGGGTAAAT	120
Sbjct	20208	AGGCCATCCTCAAACAAATGTGGCTAATGACTCGCATGCTGAGAAACACTGCGGGCAAT	20267
Query	121	GCTCACACATAAGCAGTCAGCTTGCCTTACATGCTCAAGGCTCACAAAGACCCACAGCA	180
Sbjct	20268	GCTCACACATAAGCAGTCAGCTTGCCTTACATGCTCAAGGCTCACAAAGACCCACAGCA	20327
Query	181	ATCTCAGCAGCAGATGTGGCTCCGTTTCGCTTCTCAGCAATTTCAAACACTTTTAAAC	240
Sbjct	20328	ATCTCAGCAGCAGATGTGGCTCCGTTTCGCTTCTCAGCAATTTCAAACACTTTTAAAC	20387
Query	241	TCTCTTTCCAAAGTCCTTTTCATCTTTCCCTCATGGTACTTGTGCTATTGGTCTCGAG	300
Sbjct	20388	TCTCTTTCCAAAGTCCTTTTCATCTTTCCCTCATGGTACTTGTGCTATTGGTCTCGAG	20447
Query	301	CTTCTATTTAGCTTTGGATGAAACTTACCACCTGATTTACGCTCCAATTCGAGGAGCGT	360
Sbjct	20448	CTTCTATTTAGCTTTGGATGAAACTTACCACCTGATTTACGCTCCAATTCGAGGAGCGT	20507
Query	361	GACTCTCAGGACAAGCACTGTGGACAGCGGACATCGAGCGAAATGCAGGATTCTCACCCG	420
Sbjct	20508	GACTCTCAGGACAAGCACTGTGGACAGCGGACATCGAGCGAAATGCAGGATTCTCACCCG	20567
Query	421	GGCACACGCTCTATTCCAAGAGGCTTGCCTCGAGCCGCCGATAGCGCTATGCCTGCAGG	480
Sbjct	20568	GGCACACGCTCTATTCCAAGAGGCTTGCCTCGAGCCGCCGATAGCGCTATGCCTGCAGG	20627
Query	481	CTACAGCCCGACACAGATGTATCGGTTTCCAGCCTGAGCTCATCCCTGTTTCATTGCCAT	540
Sbjct	20628	CTACAGCCCGACACAGATGTATCGGTTTCCAGCCTGAGCTCATCCCTGTTTCATTGCCAT	20687
Query	541	TACTGAGGGAATCCTATTAGTTCCTTTT	569
Sbjct	20688	TACTGAGGGAATCCTATTAGTTCCTTTT	20716

**Supplementary Figure 2** | Confirmation of the used Symbiodiniaceae strain by PCR amplified 28S rDNAs sequences (Zardoya et al., 1995). The alignment shows that the 28S rDNAs sequences from PCR amplification corresponded to scaffold 5386 in the draft genome of *Breviolum minutum* (Shoguchi et al., 2013), confirming that the strain is the *B. minutum*. The single nucleotide difference between two sequences is due to a variation among 28S rDNAs copies of the clone.





dinoflagellates (Supplementary Movie 1). Interactions between cells of the two taxa occurred shortly after mixing (Figure 1C), followed by coral cell phagocytosis of dinoflagellates (Figure 1D). Coral cells incorporated coccoid cells, but not thecate motile cells. One day after mixing, one or two and sometimes three dinoflagellates were found in the cytoplasm of individual cultured coral cells (Figure 1E1, E2). We repeated experiments more than five times and obtained the same results, indicating that this *in vitro* symbiosis is reproducible.

We examined whether the culture medium affects the interaction between coral and dinoflagellate cells. Three media, the conditioned cell growth medium that had been used for cell culture for 2 weeks or more, newly prepared cell growth medium, and basic seawater medium, were examined. One day after inoculation in the conditioned medium,  $50.2 \pm 30.2\%$  (number of observation fields,  $n = 12$ , which contained approximately 20 cells) of cultured host cells incorporated algae (**Supplementary Figure 3A**). In newly prepared growth medium, algal uptake was observed in  $45.7 \pm 28.8\%$  ( $n = 14$ ) of all cells (**Supplementary Figure 3B**), and in seawater medium,  $45.5 \pm 30.3\%$  ( $n = 7$ ) (**Supplementary Figure 3C**). These results indicate that 1 day after inoculation, coral cell symbiosis with algal cells occurred similarly in each of the three media in approximately 50% of the cultured coral cells. Several days after mixing, coral cells did not show further incorporation of dinoflagellates. Even when dinoflagellates were present near or attached to coral cells, they appeared to show no interest in dinoflagellates.”

5. The **Data Availability Statement** should have been removed.

6. The **Author Contributions** statement should have read “KK and NS conceived and designed the study and prepared the manuscript. ES and SS cultured dinoflagellates. KK, SS, KN, KH, SF, and NS carried out analyses. All authors commented on it.”

7. The **Acknowledgments** should have read “We would like to thank all members of the Marine Genomics Unit at OIST for their support. Steven D. Aird (<https://www.sda-technical-editor.org>) is acknowledged for editing the manuscript. Professor Virginia Weis, one of the reviewers of this manuscript, kindly noted the mistake in our transcriptome presentation.”

The corrected **Supplementary Material** is shown at this article and is available online.

The authors apologize for these errors and state that they do not change the scientific conclusions of the article in any way. The original article has been updated.

## REFERENCES

Kawamura, K., Nishitsuji, K., Shoguchi, E., Fujiwara, S., and Satoh, N. (2021). Establishing sustainable cell lines of a coral, *Acropora tenuis*. *Mar. Biotechnol.* 23, 373–388. doi: 10.1007/s10126-021-10031-w

Shoguchi, E., Shinzato, C., Kawashima, T., Gyoja, F., Mungpakdee, S., Koyanagi, R., Takeuchi, T., Hisata, K., Tanaka, M., Fujiwara, M., et al. (2013). Draft assembly of the *Symbiodinium minutum* nuclear genome reveals dinoflagellate gene structure. *Curr. Biol.* 23, 1399–1408. doi: 10.1016/j.cub.2013.05.062

Zardoya, R., Costas, E., López-Rodas, V., Garrido-Pertierra, A., and Bautista, J. M. (1995). Revised dinoflagellate phylogeny inferred from molecular analysis

of large-subunit ribosomal RNA gene sequences. *J. Mol. Evol.* 41, 637–645. doi: 10.1007/BF00175822

**Publisher's Note:** All claims expressed in this article are solely those of the authors and do not necessarily represent those of their affiliated organizations, or those of the publisher, the editors and the reviewers. Any product that may be evaluated in this article, or claim that may be made by its manufacturer, is not guaranteed or endorsed by the publisher.

Copyright © 2021 Kawamura, Sekida, Nishitsuji, Shoguchi, Hisata, Fujiwara and Satoh. This is an open-access article distributed under the terms of the Creative Commons Attribution License (CC BY). The use, distribution or reproduction in other forums is permitted, provided the original author(s) and the copyright owner(s) are credited and that the original publication in this journal is cited, in accordance with accepted academic practice. No use, distribution or reproduction is permitted which does not comply with these terms.



# Spatial Autocorrelation Analysis Using MIG-seq Data Indirectly Estimated the Gamete and Larval Dispersal Range of the Blue Coral, *Heliopora coerulea*, Within Reefs

Daniel Frikli Mokodongan<sup>1†</sup>, Hiroki Taninaka<sup>2†</sup>, La Sara<sup>3</sup>, Taisei Kikuchi<sup>4</sup>, Hideaki Yuasa<sup>5</sup>, Yoshihisa Suyama<sup>6</sup> and Nina Yasuda<sup>7\*</sup>

<sup>1</sup> Museum Zoology Bogoriense (MZB), Zoology Division of Research Center for Biology, Indonesia Institute of Science (LIPI), Cibinong, Indonesia, <sup>2</sup> Interdisciplinary Graduate School of Agriculture and Engineering, University of Miyazaki, Miyazaki, Japan, <sup>3</sup> Faculty of Fisheries and Marine Sciences, Halu Oleo University, Kendari, Indonesia, <sup>4</sup> Division of Parasitology, Faculty of Medicine, University of Miyazaki, Miyazaki, Japan, <sup>5</sup> School of Life Sciences and Technology, Department of Life Science and Technology, Tokyo Institute of Technology, Tokyo, Japan, <sup>6</sup> Field Science Center, Graduate School of Agricultural Science, Tohoku University, Miyagi, Japan, <sup>7</sup> Faculty of Agriculture, Department of Marine Biology and Environmental Science, University of Miyazaki, Miyazaki, Japan

## OPEN ACCESS

### Edited by:

Wei Jiang,  
Guangxi University, China

### Reviewed by:

Rafael A. Cabral-Tena,  
Center for Scientific Research  
and Higher Education in Ensenada  
(CICESE), Mexico  
Cecilia Conaco,  
University of the Philippines Diliman,  
Philippines

### \*Correspondence:

Nina Yasuda  
nina27@cc.miyazaki-u.ac.jp

<sup>†</sup>These authors share first authorship

### Specialty section:

This article was submitted to  
Coral Reef Research,  
a section of the journal  
Frontiers in Marine Science

**Received:** 30 April 2021

**Accepted:** 28 June 2021

**Published:** 20 July 2021

### Citation:

Mokodongan DF, Taninaka H,  
Sara L, Kikuchi T, Yuasa H, Suyama Y  
and Yasuda N (2021) Spatial  
Autocorrelation Analysis Using  
MIG-seq Data Indirectly Estimated  
the Gamete and Larval Dispersal  
Range of the Blue Coral, *Heliopora*  
*coerulea*, Within Reefs.  
Front. Mar. Sci. 8:702977.  
doi: 10.3389/fmars.2021.702977

Spatial autocorrelation analysis is a well-established technique for detecting spatial structures and patterns in ecology. However, compared to inter-population genetic structure, much less studies examined spatial genetic structure (SGS) within a population by means of spatial autocorrelation analysis. More SGS analysis that compares the robustness of genome-wide single nucleotide polymorphisms (SNPs) and traditional population genetic markers in detecting SGS, and direct comparison between the estimated dispersal range based on SGS and the larval dispersal range of corals directly surveyed in the field would be important. In this study, we examined the SGS of a reef-building coral species, *Heliopora coerulea*, in two different reefs (Shiraho and Akaishi) using genome-wide SNPs derived from Multiplexed inter-simple sequence repeat (ISSR) genotyping by sequencing (MIG-seq) analysis and nine microsatellite loci for comparison. Microsatellite data failed to reveal significant spatial patterns when using the same number of samples as MIG-seq, whereas MIG-seq analysis revealed significant spatial autocorrelation patterns up to 750 m in both Shiraho and Akaishi reefs based on the maximum significant distance method. However, detailed spatial genetic analysis using fine-scale distance classes (25–200 m) found an x-intercept of 255–392 m in Shiraho and that of 258–330 m in Akaishi reef. The latter results agreed well with a previously reported direct field observation of larval dispersal, indicating that the larvae of *H. coerulea* settled within a 350 m range in Shiraho reef within one generation. Overall, our results empirically demonstrate that the x-intercept of the spatial correlogram agrees well with the larval dispersal distance that is most frequently found in field observations, and they would be useful for deciding effective conservation management units for maintenance and/or recovery within an ecological time scale.

**Keywords:** spatial autocorrelation analysis, MIG-seq, coral reefs, reef-building coral, larval dispersal

## INTRODUCTION

Coral reefs are highly diverse marine ecosystems, although they are now facing threats such as degradation due to climate change, ocean acidification, frequent outbreaks of corallivore, and other anthropogenic stressors (Wilkinson, 2006). Reef-building corals are the foundation species of coral reef ecosystems that require effective conservation efforts (Carpenter et al., 2008). Although the adults are sessile, reef-building corals release gametes and/or larvae that disperse from their native habitats (Fisk and Harriott, 1990). Because such gamete and larval dispersal results in genetic connectivity among population forming metapopulation structure, estimating the range of gamete and larval dispersal is essential for conservation management (Connolly and Baird, 2010).

Spatial autocorrelation analysis is a well-established technique for assessing spatial dispersal patterns (Epperson, 2005; Schwartz and McKelvey, 2009), but has been overlooked in the field of molecular ecology, especially for benthic marine invertebrates (Billingham and Ayre, 1996; McFadden and Aydin, 1996; Adjeroud and Tsuchiya, 1999; Yund and O'Neil, 2000; Calderón et al., 2007). Compared to intensively studied inter-population genetic structure, much less studies have examined the spatial genetic structure (SGS) of reef-building coral species within a population. Such individual-based SGS within a population have provided important insights into the micro-evolutionary processes and sampling strategies of coral populations (Underwood et al., 2007, 2020; Gorospe and Karl, 2013; Chan et al., 2019; Dubé et al., 2020). However, most of the studies were based on traditional microsatellite loci and to our knowledge no study has used genome-wide single nucleotide polymorphisms (SNPs) and compared the results with the dispersal range directly measured in the field. Theoretically, the detailed genotype information for each sample using genome-wide SNPs would improve the efficiency of detecting significant SGSs, as stochastic error in genotype is one of the challenges in spatial autocorrelation analysis (Slatkin and Arter, 1991).

Owing to the advent of next-generation sequencing (NGS) technology, genome-wide analysis has also become available for non-model organisms. Multiplexed inter-simple sequence repeat (ISSR) genotyping by sequencing (MIG-seq) (Suyama and Matsuki, 2015) is an easy and cost-effective method to obtain a moderate amount of genome-wide SNP data. MIG-seq amplifies putatively neutral ISSR regions, and has proven useful for delimitating species boundaries (Richards et al., 2018; Takata et al., 2019) and for population genetic analysis (Takahashi et al., 2016).

In this study, we used an exhaustive sampling strategy and conducted spatial autocorrelation analysis of two populations of a reef-building coral species, *Heliopora coerulea*, using both traditional microsatellite loci and MIG-seq. *H. coerulea* is a gorgonian coral (Anthozoa, Octocorallia) characterized by an exceptionally hard skeleton. Similar to the primary reef-building corals (Anthozoa, Hexacorallia), this species provides complex habitats for other reef species and thus contributes to sustain high biodiversity in coral reef ecosystems (Zann and Bolton, 1985). In some Indo-Pacific reefs, large populations of *H. coerulea*

are found, and is a dominant coral species (Zann and Bolton, 1985; Takino et al., 2010; Yasuda et al., 2012; Atrigenio et al., 2017). However, the International Union for Conservation of Nature now lists this species as a threatened species because its habitats are degrading, similar to other reef-building coral species (Obura et al., 2008). In this context, identifying the spatial scale of an operational conservation unit – the spatial range of larval and gamete dispersal that occurs in ecological time scales – for *H. coerulea*, is important. *Heliopora coerulea* is a brooding species whose internal fertilization occurs inside female polyps, and almost-competent larvae are released once a year during the summer (Babcock, 1990; Harii et al., 2002; Taninaka et al., 2018). Consistent with the short dispersal duration (Harii et al., 2002), Harii and Kayanne (2003) used settlement tiles in Shiraho reef and directly demonstrated that *H. coerulea* larvae settle within a range of 350 m. Previous population genetic studies performed using microsatellite markers and numerical simulation analyses indicated that larval dispersal among different reef habitats is quite limited (Taninaka et al., 2019); however, one population genetic analysis study reported infrequent long-distance larval dispersal in multiple generations (Yasuda et al., 2014). Strong population genetic differentiation has been observed within a 20 m × 40 km area (Taninaka et al., 2019), indicating that *H. coerulea* may have a finer SGS even within a continuous large population. Individual-based SGS analysis is more useful to detect such a finer scale genetic structure than other population-based genetic methods, and thus would provide more practical larval dispersal estimates for species conservation. Thus, applying SGS analysis for large *H. coerulea* populations would be feasible and beneficial for the conservation of *H. coerulea*. SGS analysis often involves two complementary methods to estimate dispersal range (Peakall et al., 2003; Underwood et al., 2007); one is a conservative estimation that uses the  $x$ -intercept of the spatial correlogram and the other is a more progressive estimation to find the maximum first distance class that is significant. However, no study has ever compared the dispersal distances estimated by alternative SGS methods with direct larval dispersal measurements in the field.

Therefore, this study aimed (i) to examine the SGS of a reef building coral, *H. coerulea*, using traditional microsatellite and genome-wide SNP data for evaluating the effectiveness of using genome-wide SNPs for SGS analysis and then (ii) to compare the dispersal distances estimated by SGS with the direct larval dispersal measurement in the field reported in a previous study (Harii and Kayanne, 2003) to reveal which dispersal estimation method of SGS best matches the direct larval dispersal measurement in the field within ecological time scales.

## MATERIALS AND METHODS

### Sample Collection and Study Sites

All samples from Shiraho reef were collected in 2007 for microsatellite analysis, and the genotyping data were re-used in this study (Yasuda et al., 2010). Samples from Akaishi reef were collected in August 2008 by snorkeling and were preserved in



99.5% ethanol. Genomic DNA samples for microsatellite and MIG-seq analysis were extracted using DNeasy Blood and Tissue kit (Qiagen) from ethanol-preserved tissue samples and were then genotyped as described by Yasuda et al. (2008, 2010). In brief, nine highly polymorphic microsatellite loci were amplified on a PCR thermal cycler, and electrophoresed on 6% Long Ranger sequencing gel (EMC Bioproducts) using SQ-5500E sequencer (Hitachi). Allele sizes were determined using FRAGLYS ver. 3 (Hitachi). First, we used 87 samples from the Shiraho population and 22 samples from the Akaishi population for both MIG-seq and microsatellite analyses (**Figure 1**). Additional microsatellite analysis was performed by increasing the number of samples (271 for Shiraho and 48 for Akaishi reef). In both the reefs, the maximum depth of the sampling sites during high tide was approximately 3 m and the morphologies of the colonies were either lobate growth form or thick-branching growth form that belongs to *H. coerulea* group in Taninaka et al. (2021).

Both the Shiraho and Akaishi populations are developed within fringing reefs forming micro-atoll structures (most of the colony tops reach the sea level during low tide) located on the southeast (Shiraho) and northeast (Akaishi) coast of Ishigaki Island, southwest Japan. The Shiraho population is one of the largest *Heliopora* populations in the Northern Hemisphere (Harii and Kayanne, 2003). *Heliopora coerulea* in Shiraho is densely, but unevenly distributed on the reef, forming a massive reef pavement behind the crest. Its abundance is high at the center of its distribution in the south (approximately 400 m NS in length with 200 m EW in width and the maximum distance between a pair of samples was found to be 1,288 m). However, the density decreased sharply, forming small patches with colonies spanning several meters to several decimeters in the further north and south of the reef (**Figure 1**). The Akaishi population is also a large, dense population that was discovered in 2008 (Takino et al., 2010). The Akaishi reef population is 400 m in length (NE–SW) and 30 m in width (NW–SE), and the maximum distance between a pair of samples was 1,948 m (**Figure 1**). There is a channel crossing the fringing reef crest that exchanges seawater via tidal currents approximately 400 m NE, away from the aggregated population, where we could find a few *H. coerulea* colonies. The Akaishi population is developed near the beach that is 60–80 m away, different from the Shiraho population, which is developed near the reef crest (Takino et al., 2010). The dense colonies of *H. coerulea* in each reef look continuous.

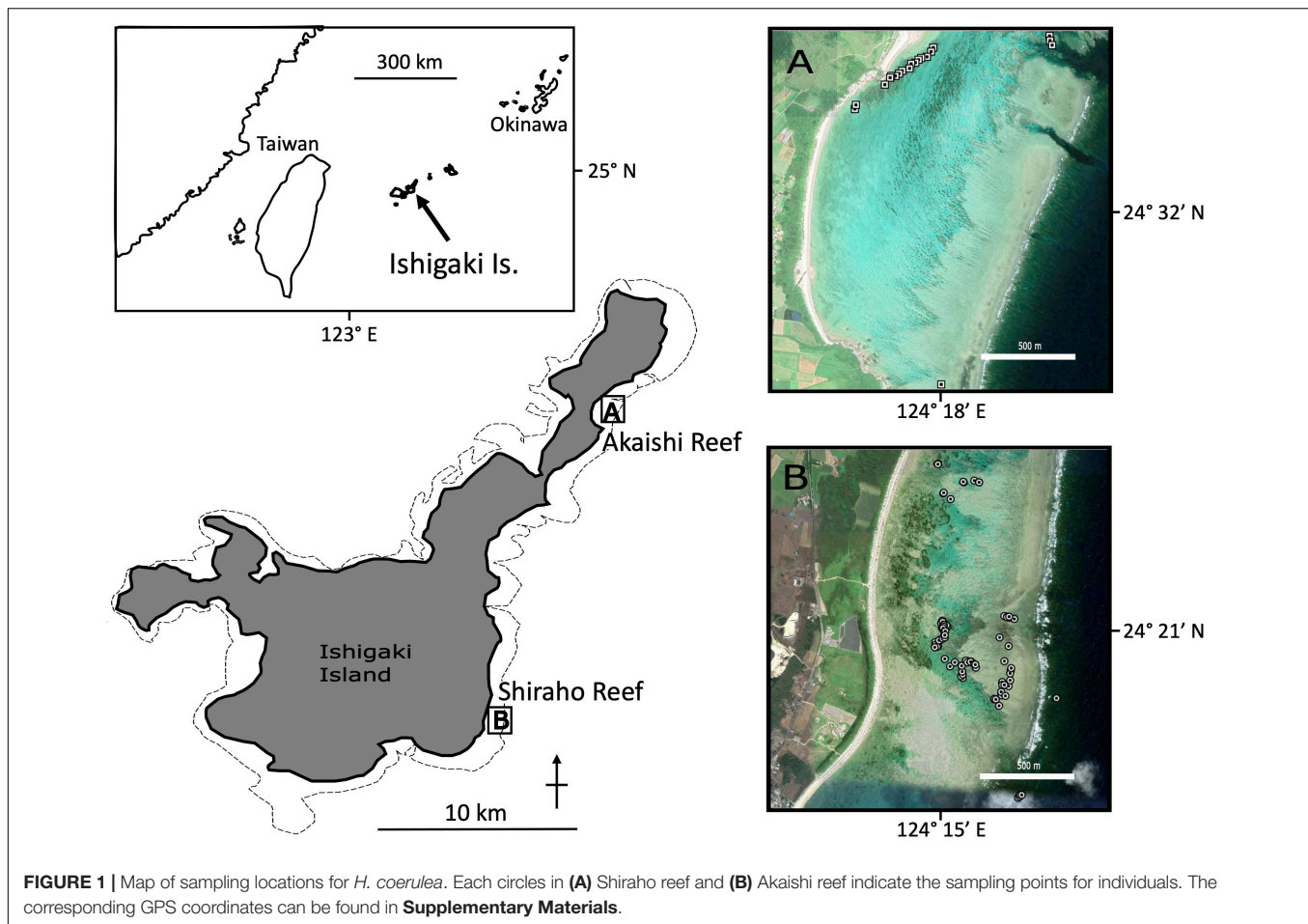
We tried the following two different sampling strategies: random sampling, covering the dense population as evenly as possible, and transect-like linear sampling with relatively regular sampling. In Shiraho reef, we randomly collected samples by covering the whole main dense populations in the south as well as patchily distributed samples in the north. In Akaishi reef, we linearly collected samples from the main population at regular intervals as much as possible, and also collected the patchily-distributed samples near the channel of the reef crest. The raw data for pair-wised geographic distances across samples and microsatellite data sets for Shiraho and Akaishi populations are available in **Supplementary Data 1–3**.

## Single Nucleotide Polymorphisms Detection of MIG-seq

We performed MIG-seq analysis to obtain a relatively large number of SNPs, following the protocol described by Suyama and Matsuki (2015). We used eight pairs of multiplex ISSR primers (MIG-seq primer set 1 in Suyama and Matsuki, 2015). The DNA libraries from each sample with a different index were pooled and sequenced using MiSeq (Sequencing Control Software v2.0.12, Illumina) and MiSeq Reagent v3 150 cycle kit (Illumina). Image analysis and base calling were performed using the real-time analysis software v1.17.21 (Illumina). We then eliminated the low-quality reads and primer sequences from the raw data using FASTX-toolkit (version 0.0.14; fastq\_quality\_filter) (Gordon and Hannon, 2012) with a fastq-quality-filter setting of  $-Q\ 33 -q\ 30 -p\ 40$ . We removed the adapter sequences for the Illumina MiSeq run from both the 5' end (GTCAGATCGGAAGAGCACACGTCTGAACTCCAGTCAC) and the 3' end (CAGAGATCGGAAGAGCGTCGTGTAGGGAAAGAC) using Cutadapt version 2.10 (Martin, 2011) with the  $-e\ 0.05$  option, and we then excluded the short reads less than 80 bp. The quality-filtered sequence data were demultiplexed using Stacks v2.2 (Catchen et al., 2011, 2013). We used the GSTACKS program in Stacks v. 2.2 (Catchen et al., 2013; Rochette and Catchen, 2017) to genotype the individuals using the reference sequence of *H. coerulea* obtained from symbiont-free larvae (Richards et al., 2018). GSTACKS reads all input files simultaneously from the external alignment program, Burrows-WheelerAligner (BWA) version 0.0.17-r118 (Li and Durbin, 2009), and scans the genome for MIG-seq loci using a sliding window method. We used the GSTACKS option ( $-rm\ pcr\ duplicates$ ) to remove PCR duplicates by randomly discarding all but one pair of each set of reads. We used the POPULATIONS program in Stacks v. 2.2 (Catchen et al., 2011) to exclude loci with more than 40% missing data ( $-r\ 0.6$ ). We also changed the  $r$  values (0.9, 0.8, and 0.7) and confirmed that the results did not change for MIG-seq analysis (data not shown here). BayeScan v 2.1 (Narum and Hess, 2011) was used to detect the possible SNPs under natural selection, assuming different species or populations with a default setting for each data set. The SNPs data in the GenAlEx format are available in **Supplementary Data 4**.

## Spatial Autocorrelation Analysis

Multilocus genotypes (MLGs) were determined using the microsatellite dataset. We assumed that the same MLGs found within each population by microsatellite analysis were possible asexually fragmented clones. GenAlEx ver. 6.5 (Peakall and Smouse, 2012) was used to calculate the probability of identity (PI) and spatial autocorrelation analysis. We used two different methods to estimate dispersal range (Peakall et al., 2003; Underwood et al., 2007). One method involved estimation of the dispersal range using the  $x$ -intercept of spatial autocorrelation correlograms, in which the correlation  $r$  is plotted for a given range of distance classes. If larval dispersal is limited and thus gene flow is restricted, the  $r$  value will be significantly positive in the short distance class and will then cross the  $x$ -axis and



become negative (Peakall et al., 2003). The  $x$ -intercept indicates the point at which the random effect of genetic drift can be used to estimate the extent of the positive genetic structure. However, estimation of the  $x$ -intercept is strongly affected by the chosen distance class size and the number of samples within the distance class. In this study, because the dense sampling was within 400 m apart at both sites, we used a distance class size of up to 200 m to estimate the  $x$ -intercept value (so that if any, negative significance could be also detected using a sufficient number of sample pairs). We tested five different distance classes: 25, 50, 100, 150, and 200 m. Another method to estimate dispersal range involves finding the maximum first distant class using multiple distance class plots. Compared to the rather conservative permutation test of the  $x$ -intercept method, this method uses a more powerful permutation, but the range includes weak correlations (low  $r$  value). We used the *Multiple Dclass* option and a 50 m base distance class size for testing 16 distance class sizes.

The analysis superimposes the 95% confidence interval for the null hypothesis of random SGS on the correlogram. The number of permutation tests was set to 9,999 for each analysis. Although we conducted MIG-seq and microsatellite analysis using the same number of samples, we also performed extra spatial autocorrelation analyses using more samples collected

only for the microsatellite data set to test whether the increased number of samples led to significant SGS detection in the microsatellite data (271 Shiraho and 48 Akaishi samples). All data are available in the **Supplementary Material 1–4**.

## RESULTS

Using nine microsatellite markers, we identified possible clone-mates as sample pairs that have exactly the same genotype. Based on the genotyping data using nine microsatellite markers, the PIs were  $5.3 \times 10^{-5}$  for Shiraho and  $4.6 \times 10^{-5}$  for Akaishi reef. In this study, to estimate the range of larval dispersal rather than fragmentation (asexual clonal propagation), we excluded possible clones and used a total of 87 Shiraho samples and 21 Akaishi samples for both MIG-seq and microsatellite analysis. In the microsatellite analysis samples, we used 266 Shiraho samples and 47 Akaishi samples after excluding the possible clones for subsequent analysis.

For MIG-seq analysis, 46,541,760 raw reads with an average of 426,989 reads per sample were obtained from 109 individuals. Low-quality reads were filtered, and 45,269,554 reads with an average of 415,317 reads per sample were obtained. We further excluded index, adapter, and short reads less than

80 bp, and obtained 13,245,206 reads with an average of 121,515 reads. In total, 6,535,144 reads were mapped onto the reference genome, with an average of 59,955 reads per sample. Finally, 2,012 SNPs were obtained from the MIG-seq analysis. BayeScan analysis indicated that no loci were under natural selection ( $q$  values  $>0.05$ ); thus, we used all the loci for the subsequent analysis.

Spatial autocorrelation analysis using a moderate number of loci (2,012 SNPs) based on MIG-seq analysis indicated a significant SGS in both the Shiraho and Akaishi reefs; however, microsatellite analysis using the same number of samples as MIG-seq (87 Shiraho and 21 Akaishi samples) could not reveal a significant SGS in both reefs (**Figure 2** and **Table 1**). By increasing the number of samples, spatial autocorrelation analysis using the microsatellite data (266 samples) in Shiraho reef indicated a significant genetic structure similar to MIG-seq analysis, whereas microsatellite analysis (47 samples, excluding one possible clone) in Akaishi reef could not reveal any significant genetic structure (**Figure 2** and **Table 1**), indicating that MIG-seq analysis is more robust than microsatellite analysis for detecting SGS. Hereafter, we used the SGS data based on MIG-seq analysis.

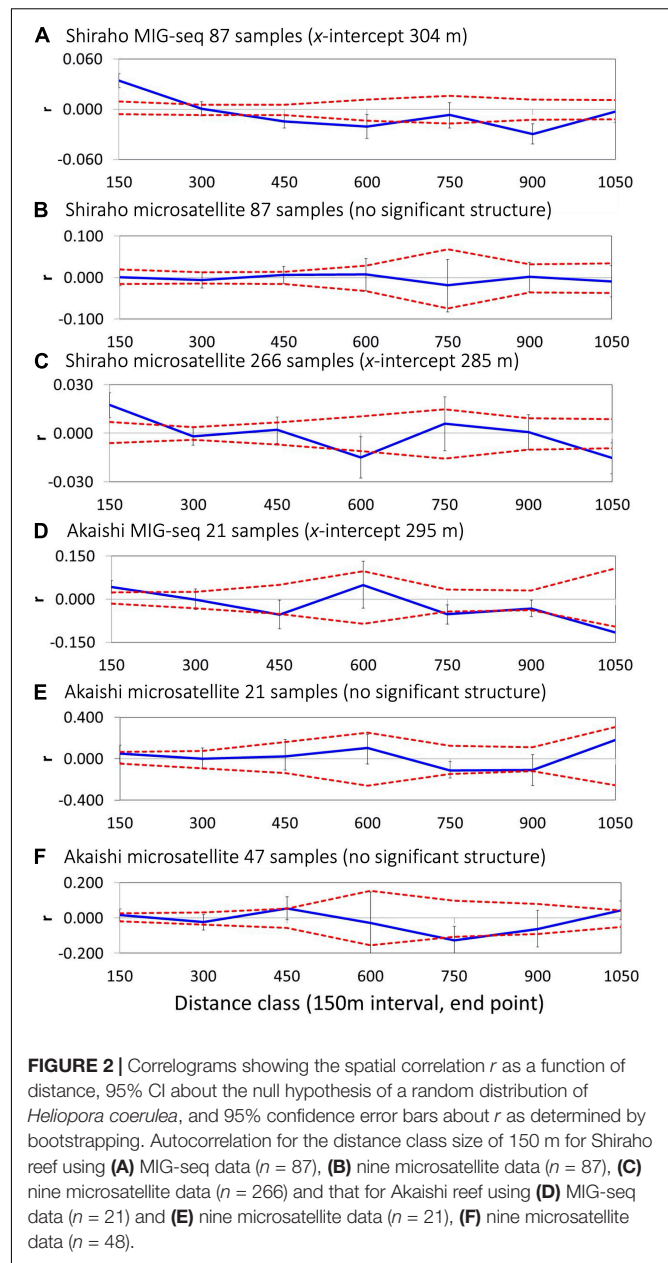
As mentioned above, the estimation of  $x$ -intercept was strongly affected by the selected distance class size and the number of samples within the distance class; using five different distance classes, the  $x$ -intercept values ranged from 255 to 392 m in Shiraho reef and from 241 to 330 m in Akaishi reef for MIG-seq analysis and from 199 to 394 m in Shiraho reef for microsatellite analysis (using 266 samples) (**Table 1**). The  $x$ -intercept increased as we used a larger distance class, whereas the correlation value  $r$  for the first distance class became smaller as we used a larger distance class (**Table 1**), indicating a stronger correlation within a smaller geographic range. On the contrary, a finer scale of isolation by distance patterns was detected using a smaller distance class; the shortest first negative significance was detected at 400 m (using 25 and 50 m of distance class) in Shiraho reef and at 275 m (using 25 m of distance class) in Akaishi reef (**Table 1**).

The maximum first distant class results indicated that the maximum significant distance was up to 750 m in both the Shiraho and Akaishi reefs (**Figure 3**).

## DISCUSSION

### MIG-seq Data for Spatial Autocorrelation Analysis

Using a moderate number of MIG-seq loci (2,012 SNPs and 87 Shiraho, 21 Akaishi samples), we successfully detected the significant SGS of *H. coerulea* populations both in Shiraho and Akaishi reef. Thus, proximate *H. coerulea* colonies were found to be genetically more alike than more distant colonies. Although spatial autocorrelation analysis is affected by several variances caused by population genetics, stochastic processes, and spatial processes (Slatkin and Arter, 1991), similar patterns of SGS were observed for the two different populations (Shiraho and Akaishi) with different microhabitat environments. This suggests that the positive spatial autocorrelation observed at short



distance classes in MIG-seq analyses supports the small-scale isolation-by-distance patterns due to the limitation of gamete and larval dispersal in *H. coerulea*, as theoretically predicted for species with limited dispersal in the absence of natural selection (Smouse and Peakall, 1999).

In this study, we could directly compare the robustness of microsatellite markers and genome-wide SNP data to detect SGS in sessile shallow-water marine invertebrate species. Microsatellite data using a small number of samples failed to reveal significant structure whereas MIG-seq could successfully reveal significant SGS even when using the same number of samples, thus indicating the robustness of the moderate number of SNPs (2,012 SNPs) in MIG-seq for SGS analysis. It is possible that the resolution of detecting different genetic distances among

**TABLE 1** | The results of spatial autocorrelation of *Heliopora coerulea* and for the analysis with distance class sizes of 25, 50, 100, 150, and 200 m.

Population	Shiraho	Shiraho	Shiraho	Akaishi	Akaishi	Akaishi
Data used	MIG-seq	Microsatellite	Microsatellite	MIG-seq	Microsatellite	Microsatellite
Number of samples used	<b>87</b>	<b>87</b>	<b>266</b>	<b>21</b>	<b>21</b>	<b>47</b>
<b>Distance class size = 25 m</b>						
<i>n</i>	165	169	1083	11	11	83
<i>r</i>	<b>0.045</b>	0.000	<b>0.011</b>	<b>0.073</b>	0.000	0.000
U	0.020	0.046	0.017	0.063	0.212	0.076
L	-0.015	-0.040	-0.016	-0.060	-0.196	-0.062
<i>P</i> ( <i>r</i> -rand $\geq r$ -data)	<b>0.001</b>	0.168	0.091	<b>0.012</b>	0.689	0.160
Ur	0.065	0.066	0.030	0.115	0.101	0.108
Lr	0.026	-0.024	-0.007	0.029	-0.197	-0.038
<i>x</i> -Intercept (m)	<b>0</b>		<b>0</b>	<b>0</b>	0	
First significant negative (m)	<b>400</b>			<b>275</b>		
<b>Distance class size = 50 m</b>						
<i>n</i>	310	312	2252	26	27	158
<i>r</i>	<b>0.039</b>	0.000	<b>0.012</b>	<b>0.079</b>	0.000	0.000
U	0.015	0.033	0.012	0.043	0.131	0.051
L	-0.011	-0.029	-0.010	-0.035	-0.117	-0.042
<i>P</i> ( <i>r</i> -rand $\geq r$ -data)	<b>&lt; 0.001</b>	0.368	<b>0.026</b>	<b>0.001</b>	0.147	0.084
Ur	0.052	0.038	0.025	0.103	0.174	0.085
Lr	0.026	-0.030	0.000	0.056	-0.040	-0.017
<i>x</i> -Intercept (m)	<b>263</b>		<b>199</b>	<b>258</b>		
First significant negative (m)	<b>400</b>			<b>300</b>		
<b>Distance class size = 100 m</b>						
<i>n</i>	583	588	3718	47	49	279
<i>r</i>	<b>0.039</b>	0.000	<b>0.021</b>	<b>0.052</b>	0	<b>0.029</b>
U	0.010	0.023	0.009	0.031	0.088	0.035
L	-0.007	-0.019	-0.008	-0.022	-0.074	-0.028
<i>P</i> ( <i>r</i> -rand $\geq r$ -data)	<b>&lt; 0.001</b>	0.139	<b>&lt; 0.001</b>	<b>0.002</b>	0.193	<b>0.040</b>
Ur	0.049	0.036	0.031	0.076	0.127	0.068
Lr	0.030	-0.012	0.012	0.028	-0.061	-0.010
<i>x</i> -Intercept (m)	<b>280</b>		<b>266</b>	<b>262</b>	279	<b>166</b>
First significant negative (m)	<b>800</b>			<b>500</b>		
<b>Distance class size = 150 m</b>						
<i>n</i>	741	803	6127	67	71	400
<i>r</i>	0.034	0	0.017	0.043	0	0
U	0.009	0.020	0.007	0.023	0.062	0.025
L	-0.006	-0.016	-0.006	-0.015	-0.050	-0.020
<i>P</i> ( <i>r</i> -rand $\geq r$ -data)	<b>&lt; 0.001</b>	0.421	<b>&lt; 0.001</b>	<b>0.002</b>	0.057	0.071
Ur	0.043	0.022	0.025	0.065	0.132	0.051
Lr	0.026	-0.020	0.010	0.021	-0.032	-0.016
<i>x</i> -Intercept (m)	<b>304</b>	172	<b>285</b>	<b>295</b>	297	
First significant negative (m)	<b>450</b>			<b>450</b>		
<b>Distance class size = 200 m</b>						
<i>n</i>	936	1046	9451	82	88	513
<i>r</i>	<b>0.028</b>	0.000	<b>0.012</b>	<b>0.039</b>	<b>0.042</b>	0.000
U	0.008	0.016	0.006	0.018	0.046	0.019
L	-0.005	-0.013	-0.004	-0.012	-0.038	-0.014
<i>P</i> ( <i>r</i> -rand $\geq r$ -data)	<b>&lt; 0.001</b>	0.555	<b>0.001</b>	<b>0.001</b>	<b>0.032</b>	0.128
Ur	0.036	0.017	0.018	0.060	0.116	0.039

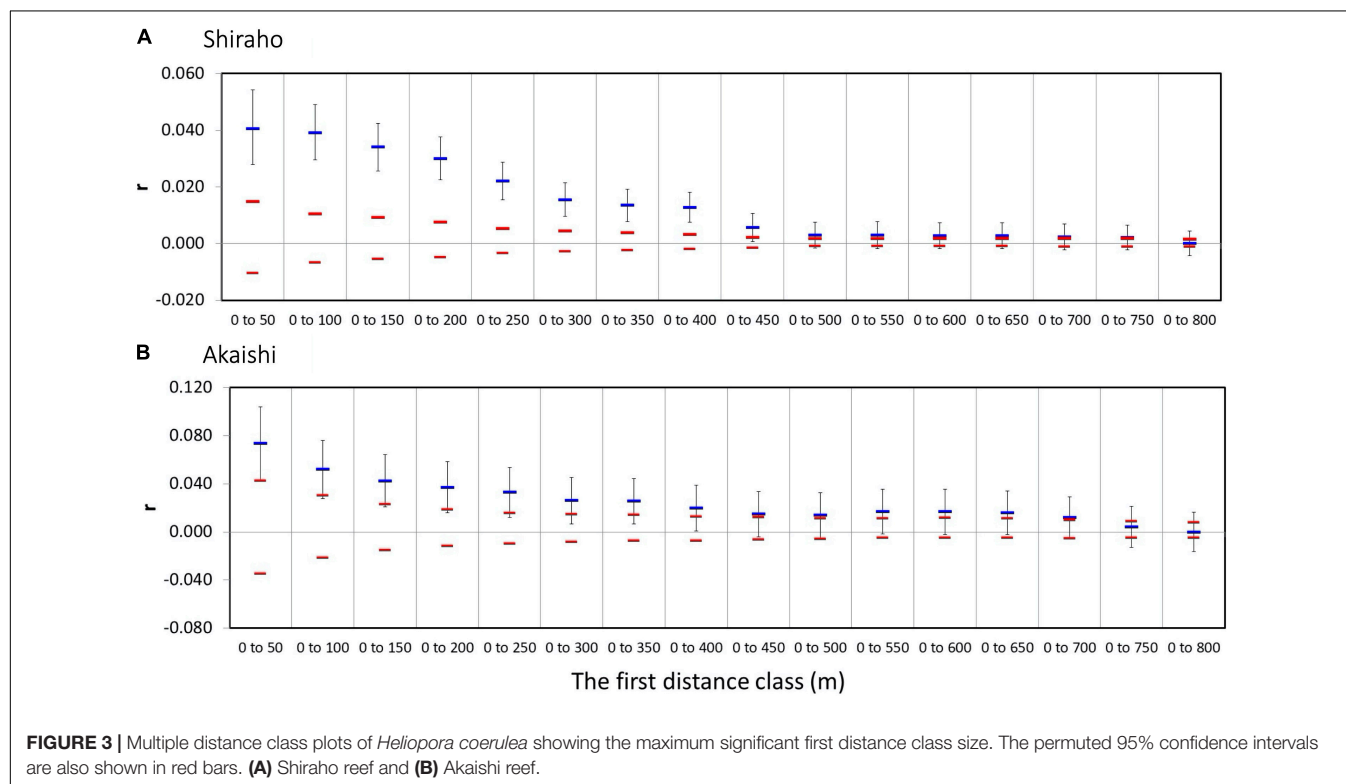
(Continued)



TABLE 1 | Continued

Population	Shiraho	Shiraho	Shiraho	Akaishi	Akaishi	Akaishi
Data used	MIG-seq	Microsatellite	Microsatellite	MIG-seq	Microsatellite	Microsatellite
Lr	0.021	−0.020	0.006	0.017	−0.034	−0.019
x-Intercept (m)	<b>392</b>	682	<b>394</b>	<b>330</b>	<b>628</b>	343
First significant negative (m)	<b>800</b>			<b>600</b>		

The correlation  $r$  is shown for the first distance class in each analysis.  $n$  is the number of pairwise comparisons for the calculation of  $r$ , upper  $U$  and lower  $L$  bounds for the 95% confidence interval about the null hypothesis of random spatial structure ( $r = 0$ ) and the upper  $U$  and lower  $L$  about  $r$  as determined by bootstrapping. The probability  $P$  of a one-tailed test for positive autocorrelation, and the estimated  $x$ -intercept of spatial correlogram.  $r$  was converted to zero when  $r$  was not significantly different from zero. First significant negative distances are only shown for MIG-seq data. Significant values are shown in bold face.



individuals was improved by increasing the number of loci (from nine microsatellite loci to 2,012 SNPs). Notably, we could detect significant SGS similar to MIG-seq analysis when using a larger number of samples (266) in the microsatellite analysis. The increased number of samples might have compensated for the small number of loci, and therefore increased the power of SGS detection in the microsatellite analysis. This study demonstrated the robustness of MIG-seq analysis in detecting SGS, which can easily reveal a sufficient number of loci to detect SGS even with a limited number of samples.

## Comparison of SGS Results and Larval Dispersal Based on Direct Field Observation

Estimating the larval dispersal of benthic marine species with pelagic larval duration that occurs on an ecological time scale (within a few generations) is often difficult to extract from

genetic analysis, such as using  $F$ -statistics that include historical gene flow and assume genetic equilibrium (Benzie, 1999). The assignment test is a potential alternative method to estimate dispersal occurring within a few generations if the overall  $F_{ST}$  values are large, such as in terrestrial animals (Berry et al., 2004). Spatial autocorrelation analysis has been proven as a robust method for estimating dispersal range (e.g., Epperson and Li, 1996) and is often applied to plant species (e.g., Smouse and Peakall, 1999), but compared to plant, much less been applied to marine organisms, especially reef-building corals [although there are increasing number of recent references such as Underwood et al. (2007); Thomas et al. (2014), Chan et al. (2019); Dubé et al. (2020), and Underwood et al. (2020)]. This is partly because for marine species, the geographic positions of each individual are relatively laborious to record. In addition, this may also occur because interpretation of resultant distances using SGS ( $x$ -intercept and the maximum significant distance) is rather difficult, and is fundamentally related to the nature of larval

dispersal itself. Even within the same population within a marine species, larval dispersal distance is highly variable and cannot be uniquely determined because of highly fluctuating ocean conditions as well as different dispersal potential among different individuals. In the case of *H. coerulea*, 74% of laboratory-cultured larvae settle within a day, but their competency lasts for up to 30 days (Harii et al., 2002), indicating that *H. coerulea* larvae have infrequent long-distance dispersal potential. The results of SGS in this study could also reflect this nature. The maximum significant (but with weak correlation value) distance found was 750 m for both Shiraho and Akaishi reefs, whereas the  $x$ -intercept using different distance classes ranged from 255 to 392 m in Shiraho reef and from 241 to 330 m in Akaishi reef. By testing five different distance classes (25–200 m), we found the minimum significantly negative spatial range to be 400 m (using the 25 and 50 m distance classes) in Shiraho and 275 m (using the 25 m distance class) in Akaishi reef, implying that most larvae and gametes do not disperse more than 400 m and 275 m in Shiraho and Akaishi reef, respectively. The estimated dispersal range based on the  $x$ -intercept corresponded well with the field observation that larval dispersal in Shiraho reef occurred within a range of 350 m (Harii and Kayanne, 2003), indicating that the  $x$ -intercept of the correlograms agrees well with the ecological larval dispersal range. Such larval dispersal range is essential for maintaining and/or recovering coral populations within an ecological time scale. This empirical demonstration also agreed well with the proposal by Diniz-Filho and De Campos Telles (2002) that the  $x$ -intercept of the spatial correlogram is useful for deciding the management unit for establishing conservation and sampling strategies.

It is also possible that larvae infrequently disperse up to 750 m in Shiraho and Akaishi, as small correlation values imply a maximum significant distance. A previous population genetic study also suggested an infrequent longer larval dispersal of *H. coerulea* (Yasuda et al., 2014). To our knowledge, this is the first study to compare larval dispersal distance measured in the field with the results of SGS analysis in a marine benthic species.

## Larval and Gamete Dispersal of *Heliopora coerulea*

This study demonstrated that the larval and gamete dispersal of *H. coerulea* within well-developed fringing Shiraho and Akaishi reefs occurs at a maximum of 750 m, and the most of the dispersal occurs within 400 m. This indicates that if we are to collect samples from “one population” of *H. coerulea* from Shiraho and Akaishi populations, collection should be within the range of 750 m in diameter. In addition, to determine the conservation unit, a sustainable population within which a sufficient number of larvae can disperse and maintain or replenish the population within an ecological time scale would be less than 400 m in size. The maximum diameter of 750 m indicates that patchily-distributed colonies and dense colonies can be collected within 750 m as one meta-population. Less than 400 m diameter almost corresponded to the size of the dense populations of each studied reef, indicating that gene flow between the dense population and

distant patchy colonies even within the same fringing reef should be conserved separately.

Spatial genetic structure analysis could not distinguish between gamete and larval dispersal. Although the gamete (sperm) dispersal range of *H. coerulea* is still unknown, our data suggest that gamete dispersal may not exceed larval dispersal within a fringing reef, indicating that the dispersal potential of *H. coerulea* sperm is also limited. This provides important insights for the conservation of *H. coerulea*. As *H. coerulea* is typically gonochoristic (only one exception was found by Taninaka and Yasuda, 2018), there would be a very low chance of fertilization if the male and female colonies are separated by more than 750 m in Shiraho and Akaishi reefs. Future studies on the spatial distribution of male and female colonies of *H. coerulea* in each population would be important for conservation, as such information is not available currently. The physical environment within well-developed fringing reefs, as in this study, is relatively calmer than that outside the reef crest, where corals are subject to stronger currents as described below. The larval and gamete dispersal distance of *H. coerulea* in a more open environment might thus be larger.

Although we obtained similar results from Shiraho and Akaishi reefs, we cannot generalize these dispersal distance results to other *H. coerulea* populations if each population is subject to different hydrodynamic and environmental conditions. Hydrodynamic surveys have been previously performed on Shiraho reef (e.g., Nakamori et al., 1992; Nadaoka et al., 2001) but not on Akaishi reef. Because of the shallow complex reef topologies associated with several coral microatoll and patches and emergence of well-developed reef crest during low tide, detailed measurement of the current system in Shiraho reef with acceptable accuracy is difficult (Tamura et al., 2007). Field measurement and numerical simulation in Shiraho reef during summer period showed that the current velocity and direction are highly variable depending on tidal cycle; the wave set-up effect and big channels play important role in the current system in Shiraho (Tamura et al., 2007). The study indicated that the overall weak southward tidal-driven current predominates around the dense population of *H. coerulea*. Harii and Kayanne (2003) found no larval disperse and settle in the northern patches in the field. They also found most *H. coerulea* larvae in Shiraho reef dispersed in mid to lower water column where the current velocity is weak (ranging from 1 cm s<sup>-1</sup> during low tide and 3 cm s<sup>-1</sup> during high tide). Given that the larvae of *H. coerulea* can only settle in slower flow velocity in the laboratory experiment (Harii and Kayanne, 2003), it is possible that *H. coerulea* larvae release only when the current velocity is weak regardless of the reef and tend to settle near their parent colonies, similar to our SGS analysis in Shiraho and Akaishi reefs.

Larval dispersal and subsequent SGS might be affected by other environmental factors. Based on the field measurement of the thermal characteristics in Shiraho reef, the distributions of different coral species well agreed with the thermal conditions among different reef micro-habitats (north and south of the moat, reef-flat, and reef-crest) during summer time (Kumagai et al., 2004). The distribution of the dense population of *H. coerulea* corresponded to relatively warm environment in Shiraho reef in

the south (Kumagai et al., 2004). Such study implies the success of larval recruitment and survival, and subsequent SGS depends on the thermal condition of micro-habitats within a fringing reef as well as spatial competition with other coral species. It is also possible that the abundance and distribution of larval predators including butterfly fish (Villanueva and Edwards, 2010) affect dispersal and settlement within the reef.

This study also indicated that if the number of samples are sufficient, the estimated larval and gamete dispersal range found by microsatellite analysis and MIG-seq analysis are comparable and do not depend on the method used for analysis. Other reef-building shallow water brooder coral species whose dispersal range were estimated based on the microsatellite loci had a shorter SGS than that of *H. coerulea*; for instance, a brooding coral *Pocillopora damicornis* (Fan et al., 2006) with a maximum 100 days of competent larvae (Harri et al., 2002) shows only 16 m of dispersal distance based on the  $x$ -intercept of the correlogram (Tioho et al., 2001; Gorospe and Karl, 2013), whereas another brooding coral, *Seriatopora hystrix* (Fan et al., 2006) with at least 10 days of larval survival period in laboratory experiments (Isomura and Nishihira, 2001), shows a distance of 100 m (based on  $x$ -intercept) and up to 220 m (based on the multiple distance plots) (Underwood et al., 2007). These species are different from *H. coerulea* in that they are hermaphroditic brooder whose larvae have zooxanthellae (Atoda, 1947, 1951). It is unclear that why such brooding coral species that may have longer larval dispersal potential than *H. coerulea* have shorter dispersal range. It is possible other ecological factors such as abundance of predator of larvae and the environmental factors of the studied areas as discussed above constrain larval dispersal. Further research is needed to determine if and why *H. coerulea* has a relatively longer dispersal range as compared with the two brooding reef-building coral species. On the other hand, broadcast spawner coral species with longer dispersal potential, which does not release competent larvae like brooder corals and in more open environment than fringing reef, had longer dispersal range <12 km (Takata et al., 2021) than *H. coerulea* as revealed by SGS analysis based on genome-wide SNPs like in this study.

## REFERENCES

- Adjeroud, M., and Tsuchiya, M. (1999). Genetic variation and clonal structure in the scleractinian coral *Pocillopora damicornis* in the Ryukyu Archipelago, Southern Japan. *Mar. Biol.* 134, 753–759. doi: 10.1007/s002270050592
- Atoda, K. (1947). The larva and postlarval development of some reef-building corals. I. *Pocillopora damicornis* cespitosa (Dana). *Sci. Rep. Tohoku Univ.* 18, 24–47.
- Atoda, K. (1951). The larva and postlarval development of some reef-building corals. V. *Seriatopora hystrix* Dana. *Sci. Rep. Tohoku Univ.* 19, 33–39.
- Atrigenio, M., Aliño, P., and Conaco, C. (2017). Influence of the Blue coral *Heliopora coerulea* on scleractinian coral larval recruitment. *J. Mar. Sci.* 2017:6015143. doi: 10.1155/2017/6015143
- Babcock, R. (1990). Reproduction and development of the blue coral *Heliopora coerulea* (Alcyonaria: Coenothecalia). *Mar. Biol.* 104, 475–481. doi: 10.1007/BF01314352

## DATA AVAILABILITY STATEMENT

The datasets presented in this study can be found in online repositories. The names of the repository/repositories and accession number(s) can be found below: DDBJ (accession: DRA011718), FigShare (doi: 10.6084/m9.figshare.14910546).

## AUTHOR CONTRIBUTIONS

NY conceived the study and collected the samples. HT, TK, HY, and YS performed the MIG-seq analyses (including bioinformatics). DFM, HT, LS, and NY analyzed all the data. DFM and NY drafted and revised the manuscript. All authors have checked and agreed to the final manuscript.

## FUNDING

This study was funded by the Japan Society for the Promotion of Science (grant numbers 17H04996, 19H03212, Grant-in-Aid for Research Fellows: 19J21342) and JSPS Bilateral Joint Research (JPJSBP120209929).

## ACKNOWLEDGMENTS

Sampling was conducted under the Okinawa Prefectural Government permit (No. 18-34, 19-60).

## SUPPLEMENTARY MATERIAL

The Supplementary Material for this article can be found online at: <https://www.frontiersin.org/articles/10.3389/fmars.2021.702977/full#supplementary-material>

**Supplementary Data 1** | Pair-wised geographic distances of the samples.

**Supplementary Data 2** | Microsatellite data of Shiraho reef.

**Supplementary Data 3** | Microsatellite data of Akaishi reef.

**Supplementary Data 4** | MIG-seq data in the GenAIEX format.

- Benzie, J. A. H. (1999). Genetic structure of coral reef organisms: ghosts of dispersal past. *Am. Zool.* 39, 131–145. doi: 10.1093/icb/39.1.131
- Berry, O., Tocher, M. D., and Sarre, S. D. (2004). Can assignment tests measure dispersal? *Mol. Ecol.* 13, 551–561. doi: 10.1046/j.1365-294X.2004.2081.x
- Billingham, M., and Ayre, D. J. (1996). Genetic subdivision in the subtidal, clonal sea anemone *Anethothoe albocincta*. *Mar. Biol.* 125, 153–163. doi: 10.1007/BF00350769
- Calderón, I., Ortega, N., Duran, S., Becerro, M., Pascual, M., and Turon, X. (2007). Finding the relevant scale: clonality and genetic structure in a marine invertebrate (*Crambe crambe*, Porifera). *Mol. Ecol.* 16, 1799–1810. doi: 10.1111/j.1365-294X.2007.03276.x
- Carpenter, K. E., Abrar, M., Aeby, G., Aronson, R. B., Banks, S., Bruckner, A., et al. (2008). One-third of reef-building corals face elevated extinction risk from climate change and local impacts. *Science* 321, 560–563. doi: 10.1126/science.1159196

- Catchen, J. M., Amores, A., Hohenlohe, P., Cresko, W., and Postlethwait, J. H. (2011). Stacks: building and genotyping loci de novo from short-read sequences. *G3* 1, 171–182. doi: 10.1534/g3.111.000240
- Catchen, J., Hohenlohe, P. A., Bassham, S., Amores, A., and Cresko, W. A. (2013). Stacks: an analysis tool set for population genomics. *Mol. Ecol.* 22, 3124–3140. doi: 10.1111/mec.12354
- Chan, A. N., Lewis, C. L., Neely, K. L., and Baums, I. B. (2019). Fallen pillars: the past, present, and future population dynamics of a rare, specialist coral–algal symbiosis. *Front. Mar. Sci.* 6:218. doi: 10.3389/fmars.2019.00218
- Connolly, S. R., and Baird, A. H. (2010). Estimating dispersal potential for marine larvae: dynamic models applied to scleractinian corals. *Ecology* 91, 3572–3583. doi: 10.1890/10-0143.1
- Diniz-Filho, J. A. F., and De Campos Telles, M. P. (2002). Spatial autocorrelation analysis and the identification of operational units for conservation in continuous populations. *Conserv. Biol.* 16, 924–935. doi: 10.1046/j.1523-1739.2002.00295.x
- Dubé, C. E., Boissin, E., Mercière, A., and Planes, S. (2020). Parentage analyses identify local dispersal events and sibling aggregations in a natural population of *Millepora* hydrocorals, a free-spawning marine invertebrate. *Mol. Ecol.* 29, 1508–1522. doi: 10.1111/mec.15418
- Epperson, B. K. (2005). Estimating dispersal from short distance spatial autocorrelation. *Heredity* 95, 7–15. doi: 10.1038/sj.hdy.6800680
- Epperson, B. K., and Li, T. (1996). Measurement of genetic structure within populations using Moran's spatial autocorrelation statistics. *Proc. Natl. Acad. Sci. U.S.A.* 93, 10528–10532. doi: 10.1073/pnas.93.19.10528
- Fan, T. Y., Lin, K. H., Kuo, F. W., Soong, K., Liu, L. L., and Fang, L. S. (2006). Diel patterns of larval release by five brooding scleractinian corals. *Mar. Ecol. Prog. Ser.* 321, 133–142.
- Fisk, D. A., and Harriott, V. J. (1990). Spatial and temporal variation in coral recruitment on the great barrier reef: implications for dispersal hypotheses. *Mar. Biol.* 107, 485–490. doi: 10.1007/BF01313433
- Gordon, A., and Hannon, G. J. (2012). *FASTX-Toolkit. FASTQ/A Short-Reads Pre-Processing Tools*. Available online at: [http://hannonlab.cshl.edu/fastx\\_toolkit/](http://hannonlab.cshl.edu/fastx_toolkit/)
- Gorospe, K. D., and Karl, S. A. (2013). Genetic relatedness does not retain spatial pattern across multiple spatial scales: dispersal and colonization in the coral, *Pocillopora damicornis*. *Mol. Ecol.* 22, 3721–3736. doi: 10.1111/mec.12335
- Harii, S., and Kayanne, H. (2003). Larval dispersal, recruitment, and adult distribution of the brooding stony octocoral *Heliopora coerulea* on Ishigaki Island, Southwest Japan. *Coral Reefs* 22, 188–196. doi: 10.1007/s00338-003-0302-9
- Harii, S., Kayanne, H., Takigawa, H., Hayashibara, T., and Yamamoto, M. (2002). Larval survivorship, competency periods and settlement of two brooding corals, *Heliopora coerulea* and *Pocillopora damicornis*. *Mar. Biol.* 141, 39–46. doi: 10.1007/s00227-002-0812-y
- Isomura, N., and Nishihira, M. (2001). Size variation of planulae and its effect on the lifetime of planulae in three pocilloporid corals. *Coral Reefs* 20, 309–315. doi: 10.1007/s003380100180
- Kumagai, W., Tamura, H., Nadaoka, K., Harii, S., Mitsui, J., Suzuki, Y., et al. (2004). Characteristics of thermal environment and distribution of reef-building coral communities in Shiraho reef, Ishigaki Island. *J. JSCE* 51, 1066–1070. doi: 10.2208/proce1989.51.1066
- Li, H., and Durbin, R. (2009). Fast and accurate short read alignment with Burrows-Wheeler transform. *Bioinformatics* 25, 1754–1760. doi: 10.1093/bioinformatics/btp324
- Martin, M. (2011). Cutadapt removes adapter sequences from high-throughput sequencing reads. *EMBnet J.* 17, 10–12. doi: 10.14806/ej.17.1.200
- McFadden, C. S., and Aydin, K. Y. (1996). Spatial autocorrelation analysis of small-scale genetic structure in a clonal soft coral with limited larval dispersal. *Mar. Biol.* 126, 215–224. doi: 10.1007/BF00347446
- Nadaoka, K., Nihei, Y., Kumano, R., Yokobori, T., Omija, T., and Wakaki, K. (2001). A field observation on hydrodynamic and thermal environments of a fringing reef at Ishigaki Island under typhoon and normal atmospheric conditions. *Coral Reefs* 20, 387–398. doi: 10.1007/s00338-001-0188-3
- Nakamori, T., Suzuki, A., and Iryu, Y. (1992). Water circulation and carbon flux on Shiraho coral reef of the Ryukyu Islands, Japan. *Cont. Shelf Res.* 12, 951–970. doi: 10.1016/0278-4343(92)90054-N
- Narum, S. R., and Hess, J. E. (2011). Comparison of  $F_{ST}$  outlier tests for SNP loci under selection. *Mol. Ecol. Resour.* 11(Suppl. 1), 184–194. doi: 10.1111/j.1755-0998.2011.02987.x
- Obura, D., Fenner, D., Hoeksema, B., Devantier, L., and Sheppard, C. (2008). *Heliopora coerulea*. The IUCN Red List of Threatened Species 2008: e.T133193A3624060. Available online at: <https://dx.doi.org/10.2305/IUCN.UK.2008.RLTS.T133193A3624060.en>
- Peakall, R., Ruibal, M., and Lindenmayer, D. B. (2003). Spatial autocorrelation analysis offers new insights into gene flow in the Australian Bush Rat, *Rattus fuscipes*. *Evolution* 57, 1182–1195. doi: 10.1554/0014-3820(2003)057[1182: SAAONI]2.0.CO;2
- Peakall, R., and Smouse, P. E. (2012). GenAlEx 6.5: genetic analysis in excel. population genetic software for teaching and research—an update. *Bioinformatics* 28, 2537–2539. doi: 10.1093/bioinformatics/bts460
- Richards, Z. T., Yasuda, N., Kikuchi, T., Foster, T., Mitsuyuki, C., Stat, M., et al. (2018). Integrated evidence reveals a new species in the ancient blue coral genus *Heliopora* (Octocorallia). *Sci. Rep.* 8:15875. doi: 10.1038/s41598-018-32969-z
- Rochette, N. C., and Catchen, J. M. (2017). Deriving genotypes from RAD-seq short-read data using Stacks. *Nat. Protoc.* 12, 2640–2659. doi: 10.1038/nprot.2017.123
- Schwartz, M. K., and McKelvey, K. S. (2009). Why sampling scheme matters: the effect of sampling scheme on landscape genetic results. *Conserv. Genet.* 10, 441–452. doi: 10.1007/s10592-008-9622-1
- Slatkin, M., and Arter, H. E. (1991). Spatial autocorrelation methods in population genetics. *Am. Nat.* 138, 499–517. doi: 10.1086/285228
- Smouse, P. E., and Peakall, R. (1999). Spatial autocorrelation analysis of individual multiallele and multilocus genetic structure. *Heredity* 82, 561–573. doi: 10.1038/sj.hdy.6885180
- Suyama, Y., and Matsuki, Y. (2015). MIG-seq: an effective PCR-based method for genome-wide single-nucleotide polymorphism genotyping using the next-generation sequencing platform. *Sci. Rep.* 5:16963. doi: 10.1038/srep16963
- Takahashi, Y., Suyama, Y., Matsuki, Y., Funayama, R., Nakayama, K., and Kawata, M. (2016). Lack of genetic variation prevents adaptation at the geographic range margin in a damselfly. *Mol. Ecol.* 25, 4450–4460. doi: 10.1111/mec.13782
- Takata, K., Iwase, F., Iguchi, A., Yuasa, H., Taninaka, H., Iwasaki, N., et al. (2021). Genome-wide SNPs data revealed significant spatial genetic structure in the deep-sea precious coral *Corallium japonicum*. *Front. Mar. Sci.* 8:667481. doi: 10.3389/fmars.2021.667481
- Takata, K., Taninaka, H., Nonaka, M., Iwase, F., Kikuchi, T., Suyama, Y., et al. (2019). Multiplexed ISSR genotyping by sequencing distinguishes two precious coral species (Anthozoa: Octocorallia: Coralliidae) that share a mitochondrial haplotype. *PeerJ* 7:e7769. doi: 10.7717/peerj.7769
- Takino, T., Watanabe, A., Motooka, S., Nadaoka, K., Yasuda, N., and Taira, M. (2010). Discovery of a large population of *Heliopora coerulea* at Akaishi Reef, Ishigaki Island, Southwest Japan. *Galaxea J. Coral Reef Stud.* 12, 85–86.
- Tamura, H., Nadaoka, K., and Paringit, E. C. (2007). Hydrodynamic characteristics of a fringing coral reef on the east coast of Ishigaki Island, southwest Japan. *Coral Reefs* 26, 17–34. doi: 10.1007/s00338-006-0164-z
- Taninaka, H., and Yasuda, N. (2018). Occurrence of simultaneous hermaphrodite in the “gonochoric” octocoral *Heliopora coerulea* (Pallas, 1766). *Galaxea J. Coral Reef Stud.* 20, 29–30.
- Taninaka, H., Bernardo, L. P. C., Saito, Y., Nagai, S., Ueno, M., Kitano, Y. F., et al. (2019). Limited fine-scale larval dispersal of the threatened brooding corals *Heliopora* spp. as evidenced by population genetics and numerical simulation. *Conserv. Genet.* 20, 1449–1463. doi: 10.1007/s10592-019-01228-7
- Taninaka, H., Harii, S., Kagawa, H., Ueno, M., Kitano, F. Y., Saito, Y., et al. (2018). Estimation of the reproductive timing of two genetically different lineages of the blue coral *Heliopora coerulea* (Pallas, 1766) around Sekisei Lagoon. *J. Jpn. Coral Reef Soc.* 20, 39–51. doi: 10.3755/jcrs.20.39
- Taninaka, H., Maggioni, D., Seveso, D., Huang, D., Townsend, A., Richards, Z., et al. (2021). Phylogeography of blue corals (genus *Heliopora*) across the Indo-West Pacific. *Front. Mar. Sci.* 8:714662. doi: 10.3389/fmars.2021.714662
- Thomas, L., Kendrick, G. A., Stat, M., Travaille, K. L., Shedrawi, G., and Kennington, W. J. (2014). Population genetic structure of the *Pocillopora damicornis* morphospecies along Ningaloo Reef, Western Australia. *Mar. Ecol. Prog. Ser.* 513, 111–119. doi: 10.3354/meps10893



- Tioho, H., Tokeshi, M., and Nojima, S. (2001). Experimental analysis of recruitment in a scleractinian coral at high latitude. *Mar. Ecol. Prog. Ser.* 213, 79–86. doi: 10.3354/meps213079
- Underwood, J. N., Richards, Z., Berry, O., Oades, D., Howard, A., and Gilmour, J. P. (2020). Extreme seascape drives local recruitment and genetic divergence in brooding and spawning corals in remote north-west Australia. *Evol. Appl.* 13, 2404–2421. doi: 10.1111/eva.13033
- Underwood, J. N., Smith, L. D., Van Oppen, M. J. H., and Gilmour, J. P. (2007). Multiple scales of genetic connectivity in a brooding coral on isolated reefs following catastrophic bleaching. *Mol. Ecol.* 16, 771–784. doi: 10.1111/j.1365-294X.2006.03187.x
- Villanueva, R. D., and Edwards, A. J. (2010). Butterflyfishes feed on externally brooded larvae of the blue coral, *Heliopora coerulea*. *Coral reefs*. 29, 105–105. doi: 10.1007/s00338-009-0553-1
- Wilkinson, C. (2006). Status of coral reefs of the world: summary of threats and remedial action. *Coral Reef Conserv.* 13, 3–39.
- Yasuda, N., Abe, M., Takino, T., Kimura, M., Lian, C., Nagai, S., et al. (2012). Large-scale mono-clonal structure in the north peripheral population of blue coral, *Heliopora coerulea*. *Mar. Genomics*. 7, 33–35. doi: 10.1016/j.margen.2012.02.001
- Yasuda, N., Nagai, S., Lian, C., Hamaguchi, M., Hayashibara, T., and Nadaoka, K. (2008). Identification and characterization of microsatellite loci in the blue coral *Heliopora coerulea* (Alcyonaria: Coenothecalia). *Conserv. Genet.* 9, 1011–1013. doi: 10.1007/s10592-007-9436-6
- Yasuda, N., Takino, T., Kimura, M., Lian, C., Nagai, S., and Nadaoka, K. (2010). “Genetic structuring across the reef crest in the threatened blue coral *Heliopora coerulea* (Helioporidae, Octacorallia) in Shiraho reef, Southwest Japan,” in *Advances in Genetics Research*, ed. V. K. Urbano (New York, NY: Nova Science Publishers), 315–324.
- Yasuda, N., Taquet, C., Nagai, S., Fortes, M., Fan, T. Y., Phongsuwan, N., et al. (2014). Genetic structure and cryptic speciation in the threatened reef-building coral *Heliopora coerulea* along Kuroshio Current. *Bull. Mar. Sci.* 90, 233–255. doi: 10.5343/bms.2012.1105
- Yund, P. O., and O’Neil, P. G. (2000). Microgeographic genetic differentiation in a colonial ascidian (*Botryllus schlosseri*) population. *Mar. Biol.* 137, 583–588. doi: 10.1007/s002270000378
- Zann, L. P., and Bolton, L. (1985). The distribution, abundance and ecology of the blue coral *Heliopora coerulea* (Pallas) in the Pacific. *Coral Reefs* 4, 125–134. doi: 10.1007/BF00300871

**Conflict of Interest:** The authors declare that the research was conducted in the absence of any commercial or financial relationships that could be construed as a potential conflict of interest.

Copyright © 2021 Mokodongan, Taninaka, Sara, Kikuchi, Yuasa, Suyama and Yasuda. This is an open-access article distributed under the terms of the Creative Commons Attribution License (CC BY). The use, distribution or reproduction in other forums is permitted, provided the original author(s) and the copyright owner(s) are credited and that the original publication in this journal is cited, in accordance with accepted academic practice. No use, distribution or reproduction is permitted which does not comply with these terms.



# *In situ* Estimation of Coral Recruitment Patterns From Shallow to Mesophotic Reefs Using an Optimized Fluorescence Imaging System

## OPEN ACCESS

### Edited by:

James Davis Reimer,  
University of the Ryukyus, Japan

### Reviewed by:

Tyler Burton Smith,  
University of the Virgin Islands,  
US Virgin Islands  
Chuki Hongo,  
Nanki Kumano Geopark Center,  
Japan

### \*Correspondence:

Gretchen Goodbody-Gringley  
ggoodbody@reefresearch.org  
Tali Mass  
tmass@univ.haifa.ac.il

### †Present address:

Stephane Martinez,  
Centre Scientifique de Monaco, Coral  
Ecophysiology Team,  
Monaco, Monaco

### Specialty section:

This article was submitted to  
Coral Reef Research,  
a section of the journal  
Frontiers in Marine Science

**Received:** 13 May 2021

**Accepted:** 12 July 2021

**Published:** 30 July 2021

### Citation:

Nativ H, Scucchia F, Martinez S,  
Einbinder S, Chequer A,  
Goodbody-Gringley G and Mass T  
(2021) *In situ* Estimation of Coral  
Recruitment Patterns From Shallow to  
Mesophotic Reefs Using an  
Optimized Fluorescence Imaging  
System. *Front. Mar. Sci.* 8:709175.  
doi: 10.3389/fmars.2021.709175

**Hagai Nativ<sup>1,2</sup>, Federica Scucchia<sup>1,3</sup>, Stephane Martinez<sup>1,2†</sup>, Shai Einbinder<sup>1,2</sup>, Alex Chequer<sup>4</sup>, Gretchen Goodbody-Gringley<sup>4\*</sup> and Tali Mass<sup>1,2\*</sup>**

<sup>1</sup> Department of Marine Biology, Leon H. Charney School of Marine Sciences, University of Haifa, Haifa, Israel, <sup>2</sup> Morris Kahn Marine Research Station, The Leon H. Charney School of Marine Sciences, University of Haifa, Haifa, Israel, <sup>3</sup> The Interuniversity Institute of Marine Sciences, Eilat, Israel, <sup>4</sup> Central Caribbean Marine Institute, Little Cayman, Cayman Islands

Coral recruitment represents a key element for coral reef persistence and resilience in the face of environmental disturbances. Studying coral recruitment patterns is fundamental for assessing reef health and implementing appropriate management strategies in an era of climate change. The FluorIS system has been developed to acquire high resolution, wide field-of-view (FOV) *in situ* images of coral recruits fluorescence and has proven successful in shallow reef environments. However, up to now, its applicability to mesophotic coral ecosystems remains unknown due to the complexity of the system and the limited time available when working at mesophotic depth. In this study we optimized the FluorIS system by utilizing a single infrared-converted camera instead of the bulkier regular dual-camera system, substantially reducing the system complexity and significantly decreasing the acquisition time to an average of 10 s for a set of 3 images. Moreover, the speed-FluorIS system is much more economical, decreasing the cost of the full set-up by roughly 40% compared to the original dual-camera system. We tested the utility of the speed-FluorIS by surveying coral recruits across shallow and mesophotic reefs of the Red Sea (Gulf of Eilat) and Bermuda, two of the most northerly reefs in the world with markedly different substrate and topography, and demonstrate that the modified system enables fast imaging of fluorescence to study coral recruitment patterns over a broader range of depths and reef topographies than previous fluorescence methods. Our single-camera system represents a valuable, non-invasive and rapid underwater tool which will help standardize surveys and long-term monitoring of coral recruits, contributing to our understanding of these vital and delicate early life stages of corals.

**Keywords:** coral recruitment, ecological monitoring, fluorescence, underwater imaging, underwater survey tool

## INTRODUCTION

Over the last three decades, coral reef ecosystems have been suffering massive declines due to both local (e.g., pollution, nutrient enrichment, overfishing, and sedimentation) and global stressors (global warming, ocean acidification, and sea level rise) (Dustan and Halas, 1987; Hoegh-Guldberg and Bruno, 2010; D'Angelo and Wiedenmann, 2014). The resilience of these ecosystems under the pressure of rapid environmental change heavily relies on successful recruitment of juvenile corals. The presence of new coral recruits is a strong indicator of the health of the reef (Glassom et al., 2004; Baird et al., 2006). Thus, knowledge and monitoring of recruitment processes assist the implementation of conservation and management actions to preserve coral reef ecosystems (Glassom et al., 2004; Martinez and Abelson, 2013).

Coral recruitment patterns are commonly quantified by examination of artificial settlement tiles that are deployed on the reef and subsequently inspected in the lab using microscopes under UV light. This method, however, does not allow continuous monitoring of recruitment dynamics, as the tiles need to be taken out for inspection (Mundy, 2000; Soong et al., 2003; Field et al., 2007). As an alternative, *in situ* visual surveys are also conducted (Miller et al., 2000; Soong et al., 2003; Martinez and Abelson, 2013), but they can be very time-consuming. Coral recruits in fact are very small and often cryptic at settlement, which makes them very difficult to detect via normal census techniques (Baird et al., 2006). Fluorescence census techniques instead have increasingly been used as they make coral recruits much easier and faster to detect than under standard white light census (Piniak et al., 2005). Fluorescence techniques depend on the high abundance of fluorescent pigments in many coral species (Papina et al., 2002). Most scleractinian corals contain two primary groups of fluorophores in their tissues. The first major group is comprised of photosynthetic pigments, mainly chlorophyll-a, from the coral endosymbiotic dinoflagellate algae (Symbiodiniaceae family) (Warner et al., 2010; LaJeunesse et al., 2018), and the second group includes GFP-like fluorescent proteins (FPs) found in the coral host tissue (Alieva et al., 2008). Recently, the FluorIS system was developed to acquire high resolution, wide field-of-view (FOV) *in situ* images of coral recruits fluorescence during daytime (Zweifler et al., 2017), enabling simultaneous imaging of GFP and chlorophyll-a with a single excitation source. Such a system has been shown to be successful in shallow reef environments (Zweifler et al., 2017), however, its application to mesophotic ecosystems is highly challenging, due to the time limits and technical constraints imposed by non-recreational deep diving.

Ranging from 30 m to approximately 150 m depth, mesophotic coral ecosystems (MCEs) comprise a diverse abundance of habitat-building taxa including corals, crustose coralline algae, macroalgae, and sponges (Kahng et al., 2016). In view of the large-scale degradation affecting shallow reef systems, MCEs have gained substantial interest as they appear to be protected from many of the local and global impacts affecting shallow-water coral reefs (Hoegh-Guldberg et al., 2007;

Lesser et al., 2009; Bongaerts et al., 2010; Kahng et al., 2010). Even though MCEs are not immune to the impacts of disturbance (Bongaerts et al., 2013; Appeldoorn et al., 2016; Smith et al., 2016), they have not experienced the same degree of decline as their shallow-water counterparts (Bak et al., 2005). Therefore, it is hypothesized that coral populations at depths greater than 30 m may serve as a refuge for coral reef species and provide a source for recruits, genetic diversity, and repopulation of shallow regions via larval exchange (termed the Deep Reef Refuges Hypothesis “DRRH”; Bongaerts et al., 2010; Lesser et al., 2018). Despite their inferred importance, data on recruitment patterns of MCEs are sparse, mainly due to the difficulties in accessing these habitats that lie beyond recreational SCUBA diving limits (Pyle, 2019), which poses increased logistical challenges. MCEs have been studied in only few areas around the world, making it difficult to obtain generalizable knowledge of the processes regulating their structure and dynamics, such as recruitment (Turner et al., 2017). If MCEs are in fact an important life-boat for coral survival, it is critical to develop and adopt broad, ecosystem-wide approaches that allow to have better understanding of recruitment dynamics in these deeper reefs worldwide. Some technological advances have enabled access to study MCEs, such as technical SCUBA diving, but pose significant challenges in terms of the amount of time that can be spent underwater.

To overcome these challenges and facilitate the assessment of coral recruitment dynamics at mesophotic depths, we optimized the FluorIS system by utilizing a single infrared-converted camera instead of the bulkier regular dual-camera system (Treibitz et al., 2015). We thus significantly reduced the system complexity and the time consumed for completing the underwater survey, while also broadening the types of terrain shapes and slopes that can be surveyed. With this faster, more flexible and easier to handle system we surveyed coral recruits across shallow and mesophotic reefs of the Red Sea (Gulf of Eilat) and Bermuda, two of the northern-most coral reefs in the world. These two locations are characterized by different substrate topographies and reef structures (Kahng et al., 2010; Murdoch and Murdoch, 2016). In Bermuda, cover of reef-building scleractinian corals declines with depth, although both shallow and mesophotic reefs maintain similar topographic complexity (Murdoch and Murdoch, 2016). In Eilat, branching structures in shallow waters become encrusting or plate-like at mesophotic depths, and this flattening creates a relatively low complexity and low rugosity of reef structure on MCEs (Kahng et al., 2010). The existence of such variations in reef structure across depths, and in general between reefs located in different geographical areas, represents a potential challenge for the development of an underwater survey system capable of efficiently detecting coral recruits with a standardized methodology.

With our improved system we provide a valuable, non-invasive and rapid underwater tool to investigate coral reproductive ecology *in situ* across wide depth ranges and different terrain shapes, significantly increasing the speed of coral recruit counts underwater. This new system ultimately allows us to obtain a deeper understanding of coral recruitment patterns across depths, which is of utmost importance for developing suitable reef conservation and management strategies

aiming at protecting these ecosystems in the face of increasing local and global stressors.

## MATERIALS AND METHODS

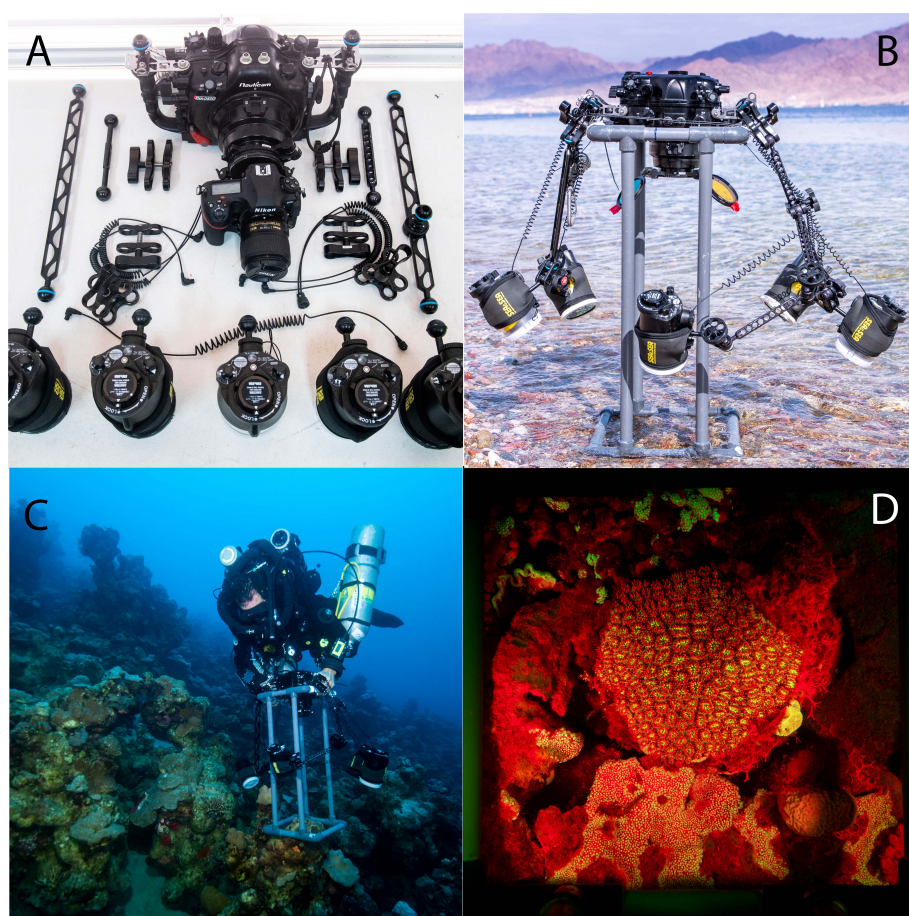
### Imaging System

We modified the two cameras FluorIS system (Zweifler et al., 2017) to enable a wider spectrum capability and faster working volume in a one camera system, that we named speed-FluorIS (Figure 1). Specifically, similar to Treibitz et al. (2015), we removed the Infrared Cut filter (ICF), which is regularly located on top of the camera sensor, by applying an infrared conversion to the camera (Life Pixel, United States). The converted camera (we used Nikon D850) can capture a spectrum of 200–1200 nm, which improves the ability to record red fluorescence of chlorophyll-*a*, while giving the surveyor another layer of information that can be used for identification purposes, compared to a non-converted camera that can record only 200–700 nm. However, we replaced the use of a dome port with a flat port which allowed us to place the barrier filter out of the housing, this modification allowed us

to attach or detach the different filters rapidly underwater and to use a single camera system. A barrier filter is needed to block the blue UV light from the strobes and to let only the emission of fluorescence light to be seen by the sensor. When the barrier filter is removed, the camera acts as a wide spectrum camera, and can record ambient or white light (reflectance, or strobe light).

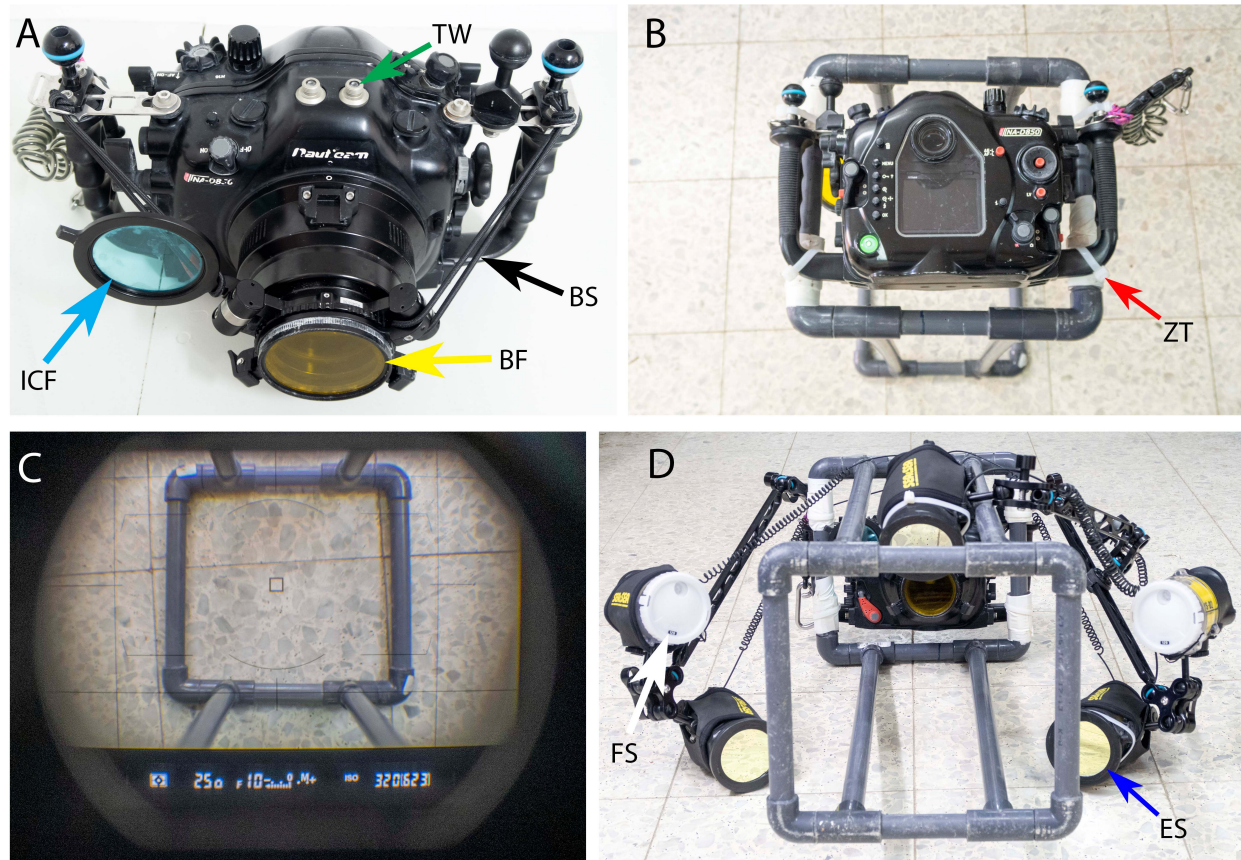
The camera was fitted with a Nikon 35 mm 1.8 lens and housed within a Nauticam NAD850 housing with a set of five Sea & Sea YS-D2 underwater strobes with a guide number of 32 (Figure 2). The original FluorIS used the same type of lens, as it is considered to be a very sharp prime lens with wide FOV and relatively no aberrations or optical distortion. In addition, this is the widest FOV lens that is suitable to use with a flat port, which is necessary for the ability to change filters underwater and is the fundamental condition of using a one camera system.

Three of the strobes were covered with excitation filters (Schott-BG39 and Night-Sea filters on top of each other) to give an excitation light of 385–500 nm, and the other two strobes, with 120° diffusers on, were unfiltered for white light (full spectrum). When shooting a fluorescence and reflectance image, the Full Spectrum (FS) set is disabled (turned off) and the barrier filter



**FIGURE 1 | (A)** Complete gear set of Nauticam housing, Nikon D850 camera with 35 mm lens, strobes and arms before assembly. **(B)** The complete set assembled on the quadrat before diving. **(C)** A diver equipped with closed circuit rebreather and the speed-FluorIS at 45 m in Bermuda. **(D)** An example of stony coral's image taken in Bermuda at daytime at 45 m with the fluorescence excitation strobe without subtraction.





**FIGURE 2 | (A)** The Nauticam NAD850 camera housing with Nauticam double filter holder for a Barrier Filter (BF-yellow arrow) and Infrared Cut Filter (ICF-blue arrow). See the Bungee Straps (BS-black arrow) added to the setup that helps to retract the filter from the port in one finger touch and the Trigger Window (TW-green arrow) on the upper side of the housing. **(B)** The housing is mounted on the quadrat frame with Zip-Ties (ZT-red arrow). **(C)** A look via the camera viewfinder to verify if the camera is centered with the quadrat and the shooting parameters are correct. **(D)** The speed-FluorIS is mounted and ready to use with five strobes, 3 Excitation Strobes (ES-blue arrow) and 2 Full Spectrum (FS-white arrow) strobes.

is on, and when shooting a FS image, the excitation strobes are off, and the barrier filter is removed from the camera port. The camera triggers the strobes through two sets of dual fiber optic cables (Nauticam, United States). One set is triggering the excitation strobes, and the other set is triggering the FS strobes. To trigger the 3rd excitation strobe, we connect it with a single fiber optic cable to one of the excitation strobes triggered directly by the camera. By alternating between the two fiber optic cables and holding them in front of the housing synchronization window we can trigger the different strobe sets. Such modification enables the system to record the fluorescence, reflectance and FS image using one camera. The camera housing is equipped with a Nauticam Macro Port 60 in front of the camera lens and with a Nauticam double filter holder. We used two filters: one barrier filter (Tiffen yellow 12) to block the blue excitation light from the filtered strobes (all wavelengths below 510 nm), and a second external ICF filter, replacing the one removed from the camera sensor, for FS reflectance images (see **Table 1** for a full list of the equipment used). The ICF blocks any wavelength above 750 nm. However, we found that the difference between images taken with or without the ICF was minor and, if needed, could be easily

adjusted in a post-processing software with the white balance tool as demonstrated in **Figure 3** and **Supplementary Movie 1**.

## Building the Quadrat and the Support Structure

A custom-made 25 × 25 cm quadrat (standard quadrat size used in ecological monitoring programs) was constructed to enable rapid imaging of the same area (**Figure 1**). In order to find the best working distance to get the highest possible resolution for the 25 × 25 cm quadrat, we performed test shots in a 500 L water tank (80 W × 120 L × 60 H cm): we submerged all the setup and checked on the camera Viewfinder (VF) for a distance that showed all the corners of the quadrat. Once the right distance was found, we measured it from the quadrat plane to the tray handles plane, to later build the spacer rods at a determined length of 65 cm. The structure was built using 25 mm-diameter PVC pipes and its parts glued together to create a strong and solid structure that can hold the camera and strobes on land and underwater in a position that enables the diver to take multiple images at the same camera position, without damaging the reef and with minimal

**TABLE 1** | Full list of the equipment needed for the speed-FluorIS.

Product	Quantity	Cost \$	Total \$	Seller
Converted D850 full spectrum	1	3,350	3,350	Lifepixel.com
Nikon 35 mm 1.8 Lens	1	530	530	Bhphotovideo.com
Memory card	1	30	30	Bhphotovideo.com
Nauticam NA-D850 housing	1	3970	3970	Nauticam.com
Nauticam macro port 60	1	480	480	Nauticam.com
M67 flip filter holder	1	270	270	Nauticam.com
Barrier filter	1	50	50	Backscatter.com
Excitation filter	3	190	570	Backscatter.com
Schott-BG39	3	80	240	Shop.schott.com
400 mm aluminum arm	2	60	120	Nauticam.com
Triple clamp	2	50	100	Nauticam.com
Nauticam clamp	4	45	180	Nauticam.com
200 mm aluminum arm	1	55	55	Nauticam.com
Standard 1" ball mount	1	40	40	Nauticam.com
YS-D2 strobe	5	690	3450	Seaandsea.jp
Nauticam to Sea & Sea dual fiber optic cable	2	230	460	Housingcamera.com
Eneloop AA rechargeable	5	20	100	Bhphotovideo.com
Ni-MH batteries (pack of 4)				
Subtotal			13,995	

Cells in green correspond to pieces of equipment that need to be doubled in quantity to build the original two-camera FluorIS system.

addition to its weight ( $\sim 1$  pound) and drag. The quadrat frame was attached to the camera housing using zip-ties (**Figure 2B**), facing down at a distance of  $\sim 65$  cm measured from the quadrat plane to the sensor plane.

## Study Sites

Both the Gulf of Eilat and Bermuda are situated at  $\sim 30^\circ\text{N}$ , however, environmental conditions differ significantly, as Eilat is within an enclosed oligotrophic bay, whereas Bermuda is an oceanic island situated in the oligotrophic Sargasso Sea.

In Bermuda, two study sites in the Bermuda platform that varied in environmental conditions were selected (**Figure 4**): a shallow reef ( $\sim 5$  m depth;  $32.45733^\circ\text{N}$ ,  $64.83475^\circ\text{W}$ ) and a mesophotic reef ( $\sim 45$  m depth;  $32.49145^\circ\text{N}$ ,  $64.85449^\circ\text{W}$ ), located at 4.3 km from each other. Temperatures at shallow reefs sites in Bermuda vary from  $22.8$  to  $29.5^\circ\text{C}$ , and from  $22.2$  to  $27.8^\circ\text{C}$  at the mesophotic reef (Goodbody-Gringley et al., 2015). The clarity of oceanic water surrounding Bermuda greatly extends the euphotic zone, where the 10% photosynthetically active radiation (PAR) depth varies seasonally from  $\sim 30$  to  $\sim 60$  m (Siegel et al., 1995). Macroalgal cover up to 45 m depth is low mainly because of the slope and storm wave action. Fish richness, abundance and biomass increase with depth from the shallow to the mesophotic zone, with community structure strongly changing across depths (Pinheiro et al., 2016).

In Eilat, the survey was conducted in the shallow ( $\sim 5$  m depth) and mesophotic ( $\sim 45$  m depth) reefs adjacent to the Interuniversity Institute (IUI) for Marine Sciences ( $29.50221^\circ\text{N}$ ,  $34.91660^\circ\text{E}$ ) (**Figure 4**), located at a distance of around 100 m from each other. Annual monitoring at these reefs sites records temperatures that range from  $20.7$  to  $29.8^\circ\text{C}$  in the shallow reef

and  $20.9$ – $27.8^\circ\text{C}$  at 40 m depth (National Monitoring Program, Eilat). Light attenuation varies significantly with the annual cycle, with the depths of 6% PAR varying between 30–60 m depth (Dishon et al., 2012). Fleshy algae flourish at mesophotic depths and are sometimes present on top of reef structures at a higher coverage than in shallower environments. Reef fish assemblages reveal a change along the depth gradient of the Red Sea due to the steep bathymetry of the region. The abundance, biomass, and density of the most common herbivorous fish decreased along the depth gradient in the Gulf, potentially leading to reduced grazing pressure on MCEs (Brokovich et al., 2010).

## Testing the Imaging Method in the Field

In order to find the right camera settings, test shots with the system were made on the reef adjacent to the Interuniversity Institute (IUI) of Eilat. Repetitive co-located images with and without filters of different stony corals and algae were captured during daytime at depths of approximately 6 m and 40 m. To capture two sequential shots with the shortest interval possible, the camera was set to shoot in continuous mode of 7 Frames Per Second (FPS), which is the highest frame rate possible for this camera model. During image post-processing, the Image Calculator function of the FIJI software (Schindelin et al., 2012) was used for subtracting the fluorescence effect in daylight, in order to assess the quality of the shots.

## Survey of Coral Recruits Using the Speed-FluorIS

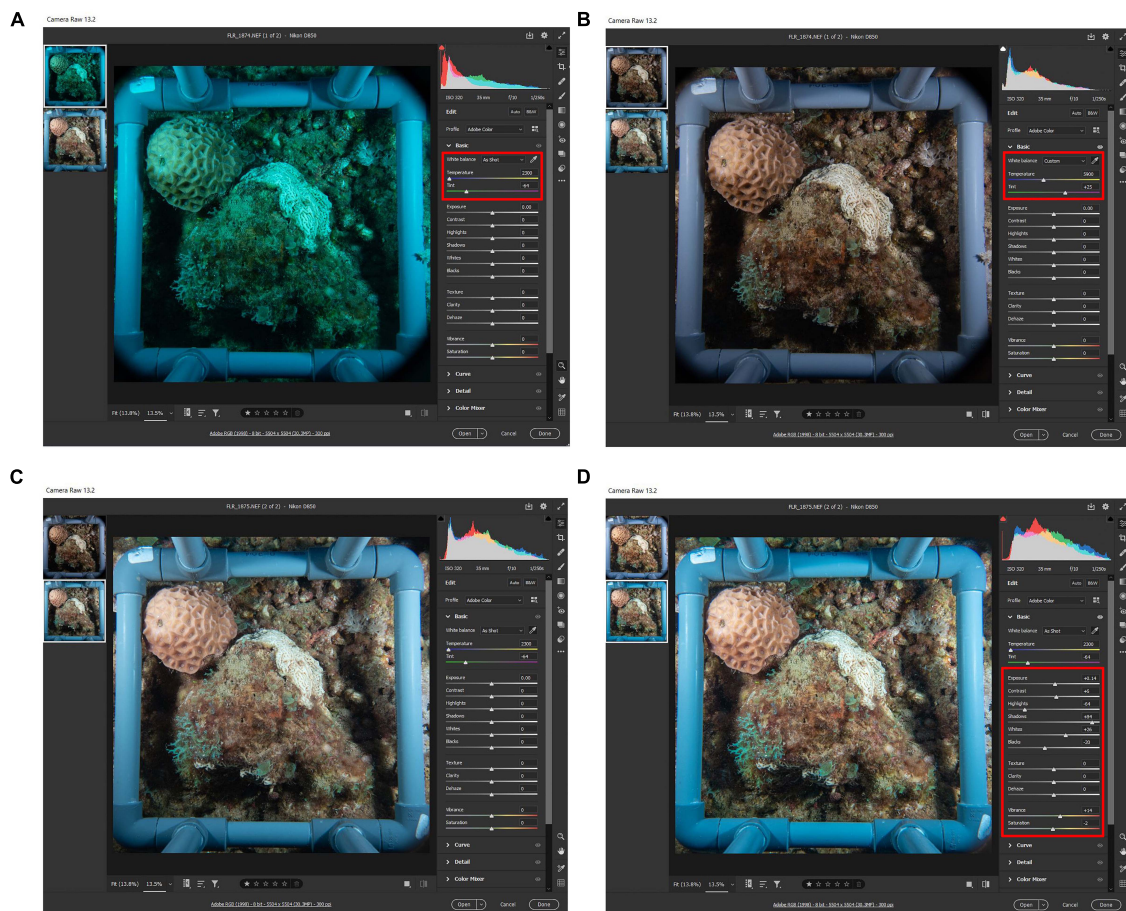
Once found the optimal camera settings with the test shots, co-located reflectance and fluorescence image-pairs were captured during daytime to survey coral recruits among the shallow and mesophotic reefs of Eilat (April 2019) and Bermuda (July 2019). Image locations were chosen randomly at each depth (5 and 45 m) in both sites. In Eilat, 46 random locations were selected for the shots at 5 m and 36 were selected at 45 m. In Bermuda, 17 random locations were selected at 5 m and 21 were selected at 45 m.

During image post-processing, the FIJI software was employed to subtract the strobes-off images from the strobes-on images, using the Image Calculator function. Coral recruits between 1 mm and 2 cm of diameter expressing FP fluorescence were counted using the Cell Counter plugin in FIJI. Reflectance FS images under white light illumination were used to verify that the fluorescent organisms detected in the fluorescence images corresponded to coral recruits by shape.

## Statistical Analysis

Recruit count data were tested for normality (Shapiro-Wilk test) and homogeneity of variance (Brown-Forsythe test). As the assumption of normality was violated, a non-parametric Mann-Whitney test was used to compare recruit numbers between depths at the same location. Significant groups have a value of  $P \leq 0.05$ . The GraphPad Prism software version 8.0.2 (GraphPad Inc.) was used to perform the statistical tests. Results are presented as mean  $\pm$  standard error.





**FIGURE 3 |** Demonstrating the irrelevance of the Infrared Cut Filter. **(A)** Raw image taken with ICF on the camera port. **(B)** The same image from A after white balance (WB) correction in post processing using adobe camera raw (Adobe, United States). **(C)** Raw image taken without ICF shows the correct colors without the need of WB correction. **(D)** The same image from C after automatic editing tool using adobe camera raw (Adobe, United States). Red box indicates the command setting.

All raw data used in this study are accessible through the electronic notebook<sup>1</sup>.

## RESULTS

### Camera Settings Optimization

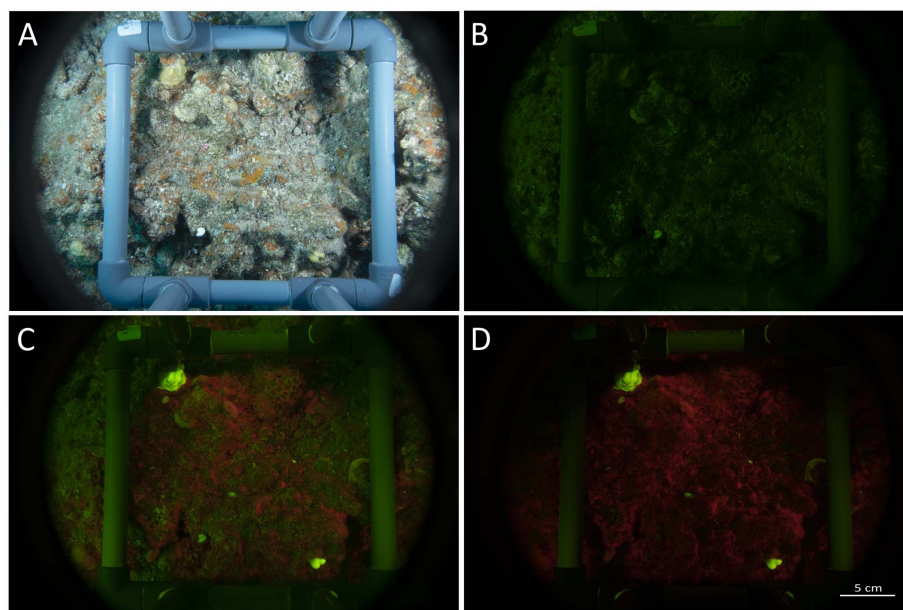
Setting the camera to shoot at the highest frame rate (i.e., 7 FPS) does not provide enough recharging time to the excitation strobes, that with the highest output (GN32) can fire at less than 1.5 s between shots. As a result, the first image of each set is full power fluorescent shoot, and the subsequent shoot is reflectance (ambient) light (**Figure 5**). If ambient light is absent or weak, for example at depth or at sunrise and sunset, we found that there is no need to make a reflectance image for subtraction, since the fluorescence is strong enough (**Figure 1D**). However, at shallow depth and with strong light during the day, there is an advantage in using the software developed with the FluorIS (Zweifler et al., 2017) or with FIJI software for subtracting and

emphasizing the fluorescence effect in daylight (**Figure 5**). The result of the subtraction is a fluorescence image excited solely by the blue strobes (**Figure 5D**). Alternatively, the system can be used without the need for subtracting by eliminating as much ambient light as possible with few basic adjustments and considerations before and during the dive. First, the exposure value of the camera should be set to a value that minimizes ambient light, allowing at the same time as much strobe light as the sensor can record. To accomplish that, we found that the shutter needs to be set to the highest synchronization speed allowed by the camera. With the Nikon D850 this corresponds to 1/250th of a second (note that each camera model can present a different value for synchronization speed). The aperture of the lens has to be set to a value that allows a good depth of field and sharpness but gives enough strobe light to penetrate to the sensor. We found that such aperture value corresponds to f10. The sensor sensitivity was set to a final value of ISO320, so to summarize, the ultimate exposure parameters were set to 1/250th, f10, ISO320. Using these settings, we reduced the acquisition time to an average of 10 s for a set of 3 images produced on each quadrat.

<sup>1</sup>[https://github.com/Mass-Lab/Fluorescence\\_imaging\\_of\\_coral\\_recruits](https://github.com/Mass-Lab/Fluorescence_imaging_of_coral_recruits)



**FIGURE 4 |** Satellite images of the study sites. Images of Eilat (left) and Bermuda (right) showing the sampling locations. Red locators in the bottom images indicate the shallow reefs, blue locators indicate the mesophotic reefs. Image source: Earthexplorer.usgs.gov.



**FIGURE 5 |** Images set taken with the speed-FluorS. (A) Reflectance image taken under white illumination, (B) ambient image (blue strobes off), (C) fluorescence image (blue strobes on), and (D) fluorescence image after subtracting image (B) from image (C) using Fiji software (Schindelin et al., 2012).

Another two points that are recommended when removing the ICF and using a barrier filter is to set the camera White Balance (WB) to 2300K or less and to

set the tint to green. This setting can be done in the camera WB menu, or by adjusting a preset WB, or in post processing if the images file format is set to RAW.



We found that these two points allow complete control on the final picture.

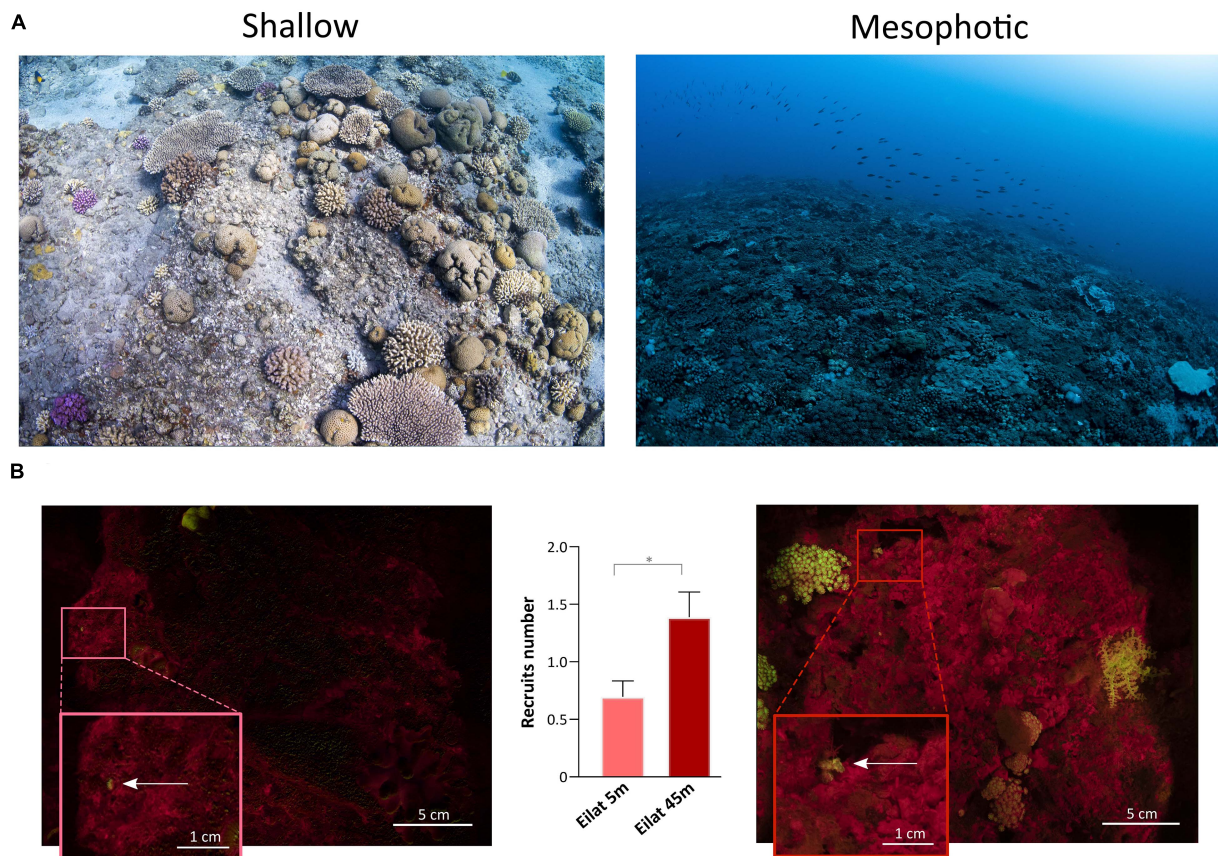
Because light underwater fades rapidly with increasing distance from the source, it is crucial to position the strobes as close as possible to the subject without the strobe body appearing in the image. To achieve this, we used 40 cm Nauticam light mounting arms that can hold the strobes to the housing handles and give the flexibility to move and lock the strobes in the desired position (**Figure 2D**). However, we observed that the use of the excitation filters significantly reduces the strobes power, therefore it is crucial to set them on full output and to place the strobe approximately 20 cm from the target. The two FS strobes can instead be placed in a larger distance or set on lower output, as their power is not affected by filters. Finally, the surveyor's body can be used to block the ambient light on the subject. Even with the exposure value mentioned above and maximal excitation strobe output, the intensity of direct sunlight at noon in tropic areas is strong enough to overcome the fluorescence emission and to be undetected by the camera. To avoid this, the surveyor should plan the dives to early morning or afternoon, but if diving at noon time, the surveyor can hover right above the quadrat and shade it with the diving gear and body, so that the intensity of

the ambient light in the image drops dramatically and a good reflectance image can be easily captured.

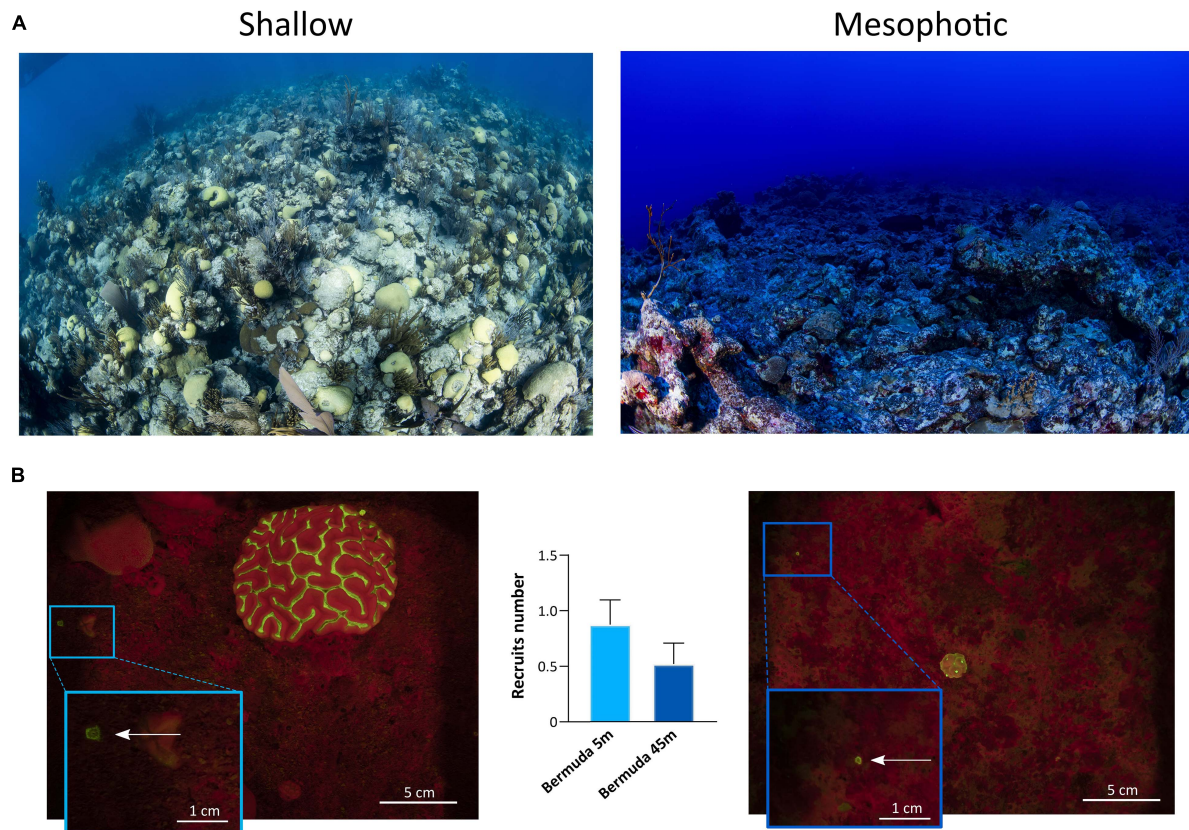
## Changes in Reef Structure With Depth and Coral Recruits Survey

The topography of the sampling sites differed significantly across depths in each geographic location (**Figures 6, 7**). In Eilat, scattered stony coral colonies with mainly branching morphology in the shallow reef are replaced by encrusting or plate-like colonies in the mesophotic reef, which leads to a flattening of the reef structure with increasing depth (**Figure 6A**). Differently in Bermuda, the high density of stony and soft corals substantially declines at mesophotic depths, where a non-coral dominated reef with a high topographic complexity is predominant (**Figure 7A**).

In Eilat and Bermuda, the total distance that we sampled corresponded to around 100 m in both shallow and mesophotic reefs. Considering the total time needed to complete each dive, we estimated that we employed a maximum of 1 min to sample each single quadrat. Using the speed-FluorIS system we recorded wide FOV fluorescence images of coral recruits from 1 mm to 2 cm in diameter (**Figures 6B, 7B**). In Eilat, we found



**FIGURE 6 |** Shallow and mesophotic reefs in Eilat and detection of coral recruits. **(A)** Images of the sampling sites at the shallow (left) and mesophotic (right) reefs in Eilat. **(B)** Fluorescence images of the quadrat deployed in the shallow (left) and mesophotic (right) reefs of Eilat. The arrows within the insets point to coral recruits. The central graph shows the number of recruits identified in the shallow ( $n = 46$  quadrats) and mesophotic ( $n = 36$  quadrats) reefs of Eilat. Values are shown as means  $\pm$  SEM. Asterisk indicates statistical difference (Mann-Whitney test,  $P < 0.05$ ).



**FIGURE 7 |** Shallow and mesophotic reefs in Bermuda and detection of coral recruits. **(A)** Images of the sampling sites at the shallow (left) and mesophotic (right) reefs in Bermuda. **(B)** Fluorescence images of the quadrat deployed in the shallow (left) and mesophotic (right) reefs of Bermuda. The arrows within the insets point to coral recruits. The central graph shows the number of recruits identified in the shallow ( $n = 17$  quadrats) and mesophotic ( $n = 21$  quadrats) reefs of Bermuda. Values are shown as means  $\pm$  SEM.

significantly higher numbers of recruits in the randomly placed  $25 \times 25$  cm quadrat at 45 m compared to 5 m (Mann-Whitney,  $P = 0.009$ ) (**Figure 6B**). In Bermuda instead, we found no significant difference between the shallow and mesophotic reefs (Mann-Whitney,  $P > 0.05$ ) (**Figure 7B**).

## DISCUSSION

The development of the FluorIS system has demonstrated the biases of *in situ* visual surveys of coral recruits, by providing a higher precision and standardized method to accurately assess coral recruitment (Zweifler et al., 2017). Such a system eases and speeds up the detection of small and highly cryptic coral recruits (**Figures 6B, 7B**), overcoming the limitations of non-standardized and labor-intensive visual recruit counts. Here we show that the speed-FluorIS system greatly facilitates high sensitivity *in situ* fluorescence imaging of coral ecosystems, especially by eliminating the excess weight and encumbrance of a double-camera system and by reducing the time needed to acquire all sets of images. In fact, the use of speed-FluorIS significantly reduces the acquisition time to an average of 10 s for a set of 3 images, reducing the overall time employed to

sample a single quadrat to 1 min. This time frame is significantly shorter compared to the sampling time of the original FluorIS system, which corresponds to  $\sim 6$  min per quadrat (Zweifler et al., 2017; data not shown). As survey depth increases, the dive complexity increases as well. For example, technical dives are needed to go beyond recreational dive limits, which require heavier and bulkier equipment and are strictly limited in time. Therefore, conducting underwater surveys with speed-FluorIS brings several advantages for the diver, including safety, ease of navigation, reducing fatigue, and simplifying the logistics of conducting fluorescent surveys in the field. Moreover, the speed-FluorIS system is much more economical compared to the original dual-camera system, reducing the cost of the full set-up of about 40% (**Table 1**).

In this study, we demonstrate that speed-FluorIS enables a fast imaging of fluorescence to study coral recruitment patterns over a broader range of depths and reef topographies than previous fluorescence methods (**Figures 6, 7**; Schmidt-Roach et al., 2008; Roth and Knowlton, 2009; Hsu et al., 2014; Zweifler et al., 2017; Ramesh et al., 2019), providing a standardized survey methodology that can be applied in different sites across the world. Solely based on the results of our survey (**Figures 6B, 7B**), it is difficult to estimate recruitment



dynamics in the shallow and mesophotic reefs of Eilat and Bermuda, considering that coral recruitment greatly varies between seasons and years (Jouval et al., 2019, and references therein). Further long-term surveys would significantly improve the resolution and accuracy of temporal and spatial data, revealing the full picture of coral recruitment patterns and assessing the true status of the reef. Moreover, environmental data such as light, temperature, nutrients, algae and fish abundance of the sampling sites also need to be assessed, as they have a strong influence on coral recruitment patterns (Brokovich et al., 2010; Kramer et al., 2019; Loya et al., 2019; Stefanoudis et al., 2019).

In mesophotic reefs, *in situ* surveys of recruitment patterns have mostly been limited to the northern Red Sea and Western Australia, where artificial settlement tiles have been employed to count new coral recruits (Turner et al., 2018; Kramer et al., 2019; Shlesinger and Loya, 2021). Several studies have evaluated *in situ* coral recruitment patterns in the shallow reefs of Eilat and Bermuda through visual underwater identification of coral recruits on settlement tiles or on the natural substrate (Smith, 1992; Glassom et al., 2004; Abelson et al., 2005; Glassom and Chadwick, 2006; Martinez and Abelson, 2013; Shlesinger and Loya, 2016; Guerrini et al., 2020). Although being performed on the same site, these surveys revealed high variation in coral recruit numbers. Inconsistent findings in recruitment studies using different methods have been attributed to the differences in substrate, method of attachment, and duration and depth of tile deployment (Harriott and Fisk, 1988; Mumby, 1999; Glassom et al., 2004; Abelson et al., 2005). In addition, the use of settlement tiles of different sizes may also affect abundances of coral recruits, which in turn will affect the number of individuals per unit area (Birkeland et al., 1981). Thus, studies on coral recruitment based on this methodology can be difficult to compare, especially since the type and preparation of recruitment tiles greatly affect which organisms will settle on them (Brandt et al., 2019). Such lack of a standardized methodology hinders the comparison of recruitment patterns between reef sites worldwide (Glassom et al., 2004; Zweifler et al., 2017). Moreover, the labor-intensive demands of executing visual surveys and direct counts of recruits in the field make it difficult to generalize findings to broader geographic extents and across wide depth distributions (Shlesinger and Loya, 2016).

Fluorescent proteins fluorescence has been widely used for better detection of coral recruits by divers and in images (Piniak et al., 2005; Baird et al., 2006; Schmidt-Roach et al., 2008; Roth and Knowlton, 2009). However, FPs fluorescence alone might not be enough to identify young corals, since FPs fluorescence intensity greatly varies among species (Eyal et al., 2015), with some corals showing very weak or no FPs signal (Baird et al., 2006; Roth et al., 2010). Moreover, there are other organisms besides corals that contain fluorescent pigments, such as algae, sponges, and worms. Therefore, accurate identification is only possible by comparing each coral recruit identified in the fluorescence image to a high-resolution FS image, as we did in this study, which can also facilitate taxonomic identification (Baird et al., 2006).

The speed-FluorIS that we propose here represents an easy-to-use and non-invasive method that will help standardize surveys and long-term monitoring of coral recruits. In the future, speed-FluorIS can be applied via underwater vehicles for rapid and automated surveys. The recorded data could be uploaded to create universal and easily accessible databases that contribute to our understanding of the vital and delicate early life stages of corals. Importantly, if MCEs are in fact important lifeboats for coral survival as increasingly advocated (Bongaerts et al., 2010; Lesser et al., 2018), it is imperative to accurately investigate coral recruitment dynamics of these deeper reefs. Coral recruitment has been long identified as a key process in the ability of reefs to recover from disturbances (Hughes et al., 2007, 2010; Ritson-Williams et al., 2009). Therefore, understanding the recruitment process is essential for developing suitable reef conservation and management strategies to protect these vital ecosystems.

## DATA AVAILABILITY STATEMENT

The original contributions presented in the study are included in the article/**Supplementary Material**, further inquiries can be directed to the corresponding authors.

## AUTHOR CONTRIBUTIONS

HN, GG-G, and TM designed the research. HN, GG-G, SM, SE, AC, and TM performed the underwater surveys. FS and HN carried out the image analysis and recruit counts. HN, FS, GG-G, and TM wrote the manuscript. All authors contributed to improving, revision and approval of the manuscript.

## FUNDING

This project has received funding from the joint United States National Science Foundation and United States – Israel Binational Science Foundation (NSF #1937770 to GG-G; BSF #2019653 to TM) the ASSEMBLE Plus consortium for an access grant (ref. SR16022018108e1) to the Interuniversity Institute for Marine Sciences in Eilat and a Grant-in-Aid from the Bermuda Institute of Ocean Sciences (BIOS).

## ACKNOWLEDGMENTS

We would like to thank T. Triebitz, A. Avni, and A. Meri-Esh for technical support. Additional thank go to Eran Rozen, diving safety officer of the Morris Kahn Research Station, and the IUI staff.

## SUPPLEMENTARY MATERIAL

The Supplementary Material for this article can be found online at: <https://www.frontiersin.org/articles/10.3389/fmars.2021.709175/full#supplementary-material>

## REFERENCES

- Abelson, A., Olinky, R., and Gaines, S. (2005). Coral recruitment to the reefs of Eilat, Red Sea: temporal and spatial variation, and possible effects of anthropogenic disturbances. *Mar. Pollut. Bull.* 50, 576–582. doi: 10.1016/j.marpolbul.2005.02.021
- Alieva, N. O., Konzen, K. A., Field, S. F., Meleshkevitch, E. A., Hunt, M. E., Beltran-Ramirez, V., et al. (2008). Diversity and evolution of coral fluorescent proteins. *PLoS One* 3:e2680. doi: 10.1371/journal.pone.0002680
- Appeldoorn, R., Ballantine, D., Bejarano, I., Carlo, M., Nemeth, M., Otero, E., et al. (2016). Mesophotic coral ecosystems under anthropogenic stress: a case study at Ponce, Puerto Rico. *Coral Reefs* 35, 63–75. doi: 10.1007/s00338-015-1360-5
- Baird, A. H., Salih, A., and Trevor-Jones, A. (2006). Fluorescence census techniques for the early detection of coral recruits. *Coral Reefs* 25, 73–76. doi: 10.1007/s00338-005-0072-7
- Bak, R. P. M., Nieuwland, G., and Meesters, E. H. (2005). Coral reef crisis in deep and shallow reefs: 30 years of constancy and change in reefs of Curacao and Bonaire. *Coral Reefs* 24, 475–479. doi: 10.1007/s00338-005-0009-1
- Birkeland, C., Rowley, D., and Randall, R. H. (1981). Coral recruitment patterns at Guam. *Proc. 4th Int. Coral Reef Symp.* 2, 339–344.
- Bongaerts, P., Muir, P., Englebert, N., Bridge, T. C. L., and Hoegh-Guldberg, O. (2013). Cyclone damage at mesophotic depths on Myrmidon Reef (GBR). *Coral Reefs* 32, 935–935. doi: 10.1007/s00338-013-1052-y
- Bongaerts, P., Ridgway, T., Sampayo, E. M., and Hoegh-Guldberg, O. (2010). Assessing the ‘deep reef refugia’ hypothesis: focus on Caribbean reefs. *Coral Reefs* 29, 309–327. doi: 10.1007/s00338-009-0581-x
- Brandt, M. E., Olinger, L. K., Chaves-Fonnegra, A., Olson, J. B., and Gochfeld, D. J. (2019). Coral recruitment is impacted by the presence of a sponge community. *Mar. Biol.* 166:49. doi: 10.1007/s00227-019-3493-5
- Brokovich, E., Ayalon, I., Einbinder, S., Segev, N., Shaked, Y., Genin, A., et al. (2010). Grazing pressure on coral reefs decreases across a wide depth gradient in the Gulf of Aqaba, Red Sea. *Mar. Ecol. Prog. Ser.* 399, 69–80. doi: 10.3354/meps08354
- D’Angelo, C., and Wiedenmann, J. (2014). Impacts of nutrient enrichment on coral reefs: new perspectives and implications for coastal management and reef survival. *Curr. Opin. Environ. Sustain.* 7, 82–93. doi: 10.1016/j.custos.2013.11.029
- Dishon, G., Dubinsky, Z., Fine, M., and Iluz, D. (2012). Underwater light field patterns in subtropical coastal waters: a case study from the Gulf of Eilat (Aqaba). *Isr. J. Plant Sci.* 60, 265–275. doi: 10.1560/IJPS.60.1-2.265
- Dustan, P., and Halas, J. C. (1987). Changes in the reef-coral community of Carysfort reef, Key Largo, Florida: 1974 to 1982. *Coral Reefs* 6, 91–106. doi: 10.1007/BF00301378
- Eyal, G., Wiedenmann, J., Grinblat, M., D’Angelo, C., Kramarsky-Winter, E., Treibitz, T., et al. (2015). Spectral diversity and regulation of coral fluorescence in a mesophotic reef habitat in the Red Sea. *PLoS One* 10:e0128697. doi: 10.1371/journal.pone.0128697
- Field, S. N., Glassom, D., and Bythell, J. (2007). Effects of artificial settlement plate materials and methods of deployment on the sessile epibenthic community development in a tropical environment. *Coral Reefs* 26, 279–289. doi: 10.1007/s00338-006-0191-9
- Glassom, D., and Chadwick, N. (2006). Recruitment, growth and mortality of juvenile corals at Eilat, northern Red Sea. *Mar. Ecol. Prog. Ser.* 318, 111–122. doi: 10.3354/meps318111
- Glassom, D., Zakai, D., and Chadwick-Furman, N. E. (2004). Coral recruitment: a spatio-temporal analysis along the coastline of Eilat, northern Red Sea. *Mar. Biol.* 144, 641–651. doi: 10.1007/s00227-003-1243-0
- Goodbody-Gringley, G., Marchini, C., Chequer, A. D., and Goffredo, S. (2015). Population structure of *Montastraea cavernosa* on Shallow versus Mesophotic Reefs in Bermuda. *PLoS One* 10:e0142427. doi: 10.1371/journal.pone.0142427
- Guerrini, G., Yerushalmy, M., Shefy, D., Shashar, N., and Rinkevich, B. (2020). Apparent recruitment failure for the vast majority of coral species at Eilat, Red Sea. *Coral Reefs* 39, 1715–1726. doi: 10.1007/s00338-020-01998-4
- Harriott, V., and Fisk, D. (1988). Recruitment patterns of scleractinian corals: a study of three reefs. *Mar. Freshw. Res.* 39, 409–416. doi: 10.1071/MF9880409
- Hoegh-Guldberg, O., and Bruno, J. F. (2010). The impact of climate change on the world’s marine ecosystems. *Science* 328, 1523–1528. doi: 10.1126/science.1189930
- Hoegh-Guldberg, O., Mumby, P. J., Hooten, A. J., Steneck, R. S., Greenfield, P., Gomez, E., et al. (2007). Coral reefs under rapid climate change and ocean acidification. *Science* 318, 1737–1742. doi: 10.1126/science.1152509
- Hsu, C. M., de Palmas, S., Kuo, C. Y., Denis, V., and Chen, C. A. (2014). Identification of scleractinian coral recruits using fluorescent censusing and DNA barcoding techniques. *PLoS One* 9:e017366. doi: 10.1371/journal.pone.0107366
- Hughes, T. P., Graham, N. A. J., Jackson, J. B. C., Mumby, P. J., and Steneck, R. S. (2010). Rising to the challenge of sustaining coral reef resilience. *Trends Ecol. Evol.* 25, 633–642. doi: 10.1016/j.tree.2010.07.011
- Hughes, T. P., Rodrigues, M. J., Bellwood, D. R., Ceccarelli, D., Hoegh-Guldberg, O., McCook, L., et al. (2007). Phase shifts, herbivory, and the resilience of coral reefs to climate change. *Curr. Biol.* 17, 360–365. doi: 10.1016/j.cub.2006.12.049
- Jouval, F., Latreille, A. C., Bureau, S., Adjeroud, M., and Penin, L. (2019). Multiscale variability in coral recruitment in the mascarene islands: from centimetric to geographical scale. *PLoS One* 14:e0214163. doi: 10.1371/journal.pone.0214163
- Kahng, S., Copus, J. M., and Wagner, D. (2016). “Mesophotic coral ecosystems,” in *Marine Animal Forests*, eds S. Rossi, L. Bramanti, A. Gori, and C. Orejas (Cham: Springer), 1–22. doi: 10.1007/978-3-319-17001-5\_4-1
- Kahng, S. E., Garcia-Sais, J. R., Spalding, H. L., Brokovich, E., Wagner, D., Weil, E., et al. (2010). Community ecology of mesophotic coral reef ecosystems. *Coral Reefs* 29, 255–275. doi: 10.1007/s00338-010-0593-6
- Kramer, N., Eyal, G., Tamir, R., and Loya, Y. (2019). Upper mesophotic depths in the coral reefs of Eilat, Red Sea, offer suitable refuge grounds for coral settlement. *Sci. Rep.* 9:2263. doi: 10.1038/s41598-019-38795-1
- LaJeunesse, T. C., Parkinson, J. E., Gabrielson, P. W., Jeong, H. J., Reimer, J. D., Voolstra, C. R., et al. (2018). Systematic revision of symbiodiniaceae highlights the antiquity and diversity of coral endosymbionts. *Curr. Biol.* 28, 2570–2580.e6. doi: 10.1016/j.cub.2018.07.008
- Lesser, M. P., Slattery, M., and Leichter, J. J. (2009). Ecology of mesophotic coral reefs. *J. Exp. Mar. Biol. Ecol.* 375, 1–8. doi: 10.1016/j.jembe.2009.05.009
- Lesser, M. P., Slattery, M., and Mobley, C. D. (2018). Biodiversity and functional ecology of mesophotic coral reefs. *Annu. Rev. Ecol. Syst.* 49, 49–71. doi: 10.1146/annurev-ecolsys-110617-062423
- Loya, Y., Puglise, K. A., and Bridge, T. C. L. (eds) (2019). *Mesophotic Coral Ecosystems*, Vol. 12. New York, NY: Springer. doi: 10.1007/978-3-319-92735-0
- Martinez, S., and Abelson, A. (2013). Coral recruitment: the critical role of early post-settlement survival. *ICES J. Mar. Sci.* 70, 1294–1298. doi: 10.1093/icesjms/fst035
- Miller, M. W., Weil, E., and Szmant, A. M. (2000). Coral recruitment and juvenile mortality as structuring factors for reef benthic communities in Biscayne National Park, USA. *Coral Reefs* 19, 115–123. doi: 10.1007/s003380000079
- Mumby, P. (1999). Can Caribbean coral populations be modelled at metapopulation scales? *Mar. Ecol. Prog. Ser.* 180, 275–288. doi: 10.3354/meps180275
- Mundy, C. N. (2000). An appraisal of methods used in coral recruitment studies. *Coral Reefs* 19, 124–131. doi: 10.1007/s003380000081
- Murdoch, T. J. T., and Murdoch, J. M. H. (2016). *Murdoch TJT, Murdoch JMH (2016) Baseline Condition of the Coral Reefs and Fishes Across Three Depth Zones of the Forereef of Bermuda. BREAM: Bermuda Reef Ecosystem Analysis and Monitoring Programme Report, Bermuda Zoological Society, Flatts Bermuda. BBP-2016-237. Flatts: Bermuda Aquarium, Museum and Zoo. doi: 10.13140/RG.2.2.22260.35204*
- Papina, M., Sakihama, Y., Bena, C., van Woessik, R., and Yamasaki, H. (2002). Separation of highly fluorescent proteins by SDS-PAGE in Acroporidae corals. *Comp. Biochem. Physiol. Part B Biochem. Mol. Biol.* 131, 767–774. doi: 10.1016/S1096-4959(02)00025-8
- Pinheiro, H. T., Goodbody-Gringley, G., Jessup, M. E., Shepherd, B., Chequer, A. D., and Rocha, L. A. (2016). Upper and lower mesophotic coral reef fish communities evaluated by underwater visual censuses in two Caribbean locations. *Coral Reefs* 35, 139–151. doi: 10.1007/s00338-015-1381-0
- Piniak, G. A., Fogarty, N. D., Addison, C. M., and Kenworthy, W. J. (2005). Fluorescence census techniques for coral recruits. *Coral Reefs* 24, 496–500. doi: 10.1007/s00338-005-0495-1
- Pyle, R. L. (2019). “Advanced technical diving,” in *Mesophotic Coral Ecosystems*, Vol. 12, eds Y. Loya, K. A. Puglise, and T. C. L. Bridge (Cham: Springer), 959–972. doi: 10.1007/978-3-319-92735-0\_50



- Ramesh, C. H., Koushik, S., Shunmugaraj, T., and Murthy, M. R. (2019). A rapid in situ fluorescence census for coral reef monitoring. *Reg. Stud. Mar. Sci.* 28:100575. doi: 10.1016/j.rsma.2019.100575
- Ritson-Williams, R., Arnold, S., Fogarty, N., Steneck, R. S., Vermeij, M., and Paul, V. J. (2009). New perspectives on ecological mechanisms affecting coral recruitment on reefs. *Smithson. Contrib. Mar. Sci.* 38, 437–457. doi: 10.5479/si.01960768.38.437
- Roth, M., and Knowlton, N. (2009). Distribution, abundance, and microhabitat characterization of small juvenile corals at Palmyra Atoll. *Mar. Ecol. Prog. Ser.* 376, 133–142. doi: 10.3354/meps07787
- Roth, M. S., Latz, M. I., Goericke, R., and Deheyn, D. D. (2010). Green fluorescent protein regulation in the coral *Acropora yongei* during photoacclimation. *J. Exp. Biol.* 213, 3644–3655. doi: 10.1242/jeb.040881
- Schindelin, J., Arganda-Carreras, I., Frise, E., Kaynig, V., Longair, M., Pietzsch, T., et al. (2012). Fiji: an open-source platform for biological-image analysis. *Nat. Methods* 9, 676–682. doi: 10.1038/nmeth.2019
- Schmidt-Roach, S., Kunzmann, A., and Martinez Arbizu, P. (2008). In situ observation of coral recruitment using fluorescence census techniques. *J. Exp. Mar. Biol. Ecol.* 367, 37–40. doi: 10.1016/j.jembe.2008.08.012
- Shlesinger, T., and Loya, Y. (2016). Recruitment, mortality, and resilience potential of scleractinian corals at Eilat, Red Sea. *Coral Reefs* 35, 1357–1368. doi: 10.1007/s00338-016-1468-2
- Shlesinger, T., and Loya, Y. (2021). Depth-dependent parental effects create invisible barriers to coral dispersal. *Commun. Biol.* 4:202. doi: 10.1038/s42003-021-01727-9
- Siegel, D. A., Michaels, A. F., Sorensen, J. C., O'Brien, M. C., and Hammer, M. A. (1995). Seasonal variability of light availability and utilization in the Sargasso Sea. *J. Geophys. Res.* 100, 8695–8713. doi: 10.1029/95JC00447
- Smith, S. R. (1992). Patterns of coral recruitment and post-settlement mortality on Bermuda's reefs: comparisons to Caribbean and pacific reefs. *Am. Zool.* 32, 663–673. doi: 10.1093/icb/32.6.663
- Smith, T. B., Gyory, J., Brandt, M. E., Miller, W. J., Jossart, J., and Nemeth, R. S. (2016). Caribbean mesophotic coral ecosystems are unlikely climate change refugia. *Glob. Change Biol.* 22, 2756–2765. doi: 10.1111/gcb.13175
- Soong, K., Chen, M., Chen, C., Dai, C., Fan, T., Li, J., et al. (2003). Spatial and temporal variation of coral recruitment in Taiwan. *Coral Reefs* 22, 224–228. doi: 10.1007/s00338-003-0311-8
- Stefanoudis, P. V., Rivers, M., Smith, S. R., Schneider, C. W., Wagner, D., Ford, H., et al. (2019). Low connectivity between shallow, mesophotic and rariphotic zone benthos. *R. Soc. Open Sci.* 6:190958. doi: 10.1098/rsos.190958
- Treibitz, T., Neal, B. P., Kline, D. I., Beijbom, O., Roberts, P. L. D., Mitchell, B. G., et al. (2015). Wide Field-of-view fluorescence imaging of coral reefs. *Sci. Rep.* 5:7694. doi: 10.1038/srep07694
- Turner, J. A., Babcock, R. C., Hovey, R., and Kendrick, G. A. (2017). Deep thinking: a systematic review of mesophotic coral ecosystems. *ICES J. Mar. Sci.* 74, 2309–2320. doi: 10.1093/icesjms/fsx085
- Turner, J. A., Thomson, D. P., Cresswell, A. K., Trapon, M., and Babcock, R. C. (2018). Depth-related patterns in coral recruitment across a shallow to mesophotic gradient. *Coral Reefs* 37, 711–722. doi: 10.1007/s00338-018-1696-8
- Warner, M. E., Lesser, M. P., and Ralph, P. J. (2010). "Chlorophyll fluorescence in reef building corals," in *Chlorophyll a Fluorescence in Aquatic Sciences: Methods and Applications*, eds D. J. Suggett, O. Prášil, and M. A. Borowitzka (Dordrecht: Springer), 209–222. doi: 10.1007/978-90-481-9268-7\_10
- Zweifel, A., Akkaynak, D., Mass, T., and Treibitz, T. (2017). In situ analysis of coral recruits using fluorescence imaging. *Front. Mar. Sci.* 4:273. doi: 10.3389/fmars.2017.00273

**Conflict of Interest:** The authors declare that the research was conducted in the absence of any commercial or financial relationships that could be construed as a potential conflict of interest.

**Publisher's Note:** All claims expressed in this article are solely those of the authors and do not necessarily represent those of their affiliated organizations, or those of the publisher, the editors and the reviewers. Any product that may be evaluated in this article, or claim that may be made by its manufacturer, is not guaranteed or endorsed by the publisher.

Copyright © 2021 Nativ, Scucchia, Martinez, Einbinder, Chequer, Goodbody-Gringley and Mass. This is an open-access article distributed under the terms of the Creative Commons Attribution License (CC BY). The use, distribution or reproduction in other forums is permitted, provided the original author(s) and the copyright owner(s) are credited and that the original publication in this journal is cited, in accordance with accepted academic practice. No use, distribution or reproduction is permitted which does not comply with these terms.



# Application of RNA Interference Technology to Acroporid Juvenile Corals

Ikuko Yuyama<sup>1\*</sup>, Tomihiko Higuchi<sup>2</sup> and Michio Hidaka<sup>3</sup>

<sup>1</sup> Graduate School of Science and Technology for Innovation, Yamaguchi University, Yamaguchi, Japan, <sup>2</sup> Atmosphere and Ocean Research Institute, The University of Tokyo, Kashiwa, Japan, <sup>3</sup> Faculty of Science, The University of the Ryukyus, Nishihara, Japan

## OPEN ACCESS

### Edited by:

James Davis Reimer,  
University of the Ryukyus, Japan

### Reviewed by:

Isabelle Domart-Coulon,  
Muséum National d'Histoire Naturelle,  
France

Kátia Cristina Cruz Capel,  
University of São Paulo, Brazil

### \*Correspondence:

Ikuko Yuyama  
yuyamai@gmail.com

### Specialty section:

This article was submitted to  
Coral Reef Research,  
a section of the journal  
Frontiers in Marine Science

**Received:** 31 March 2021

**Accepted:** 21 June 2021

**Published:** 09 August 2021

### Citation:

Yuyama I, Higuchi T and Hidaka M  
(2021) Application of RNA  
Interference Technology to Acroporid  
Juvenile Corals.  
Front. Mar. Sci. 8:688876.  
doi: 10.3389/fmars.2021.688876

Numerous genes involved in calcification, algal endosymbiosis, and the stress response have been identified in corals by large-scale gene expression analysis, but functional analysis of those genes is lacking. There are few experimental examples of gene expression manipulation in corals, such as gene knockdown by RNA interference (RNAi). The purpose of this study is to establish an RNAi method for coral juveniles. As a first trial, the genes encoding green fluorescent protein (GFP, an endogenous fluorophore expressed by corals) and thioredoxin (TRX, a stress response gene) were selected for knockdown. Synthesized double-stranded RNAs (dsRNAs) corresponding to GFP and TRX were transformed into planula larvae by lipofection method to attempt RNAi. Real-time PCR analysis to verify knockdown showed that GFP and TRX expression levels tended to decrease with each dsRNA treatment (not significant). In addition, stress exposure experiments following RNAi treatment revealed that planulae with TRX knockdown exhibited increased mortality at elevated temperatures. In GFP-knockdown corals, decreased GFP fluorescence was observed. However, the effect of GFP-knockdown was confirmed only in the coral at the initial stages of larval metamorphosis into polyps, but not in planulae and 1 month-old budding polyps. This study showed that lipofection RNAi can be applied to coral planulae and polyps after settlement, and that this method provides a useful tool to modify expression of genes involved in stress tolerance and fluorescence emission of the corals.

**Keywords:** scleractinian coral, RNAi, stress response, thioredoxin, GFP

## INTRODUCTION

RNA interference (RNAi) is a sequence-specific gene silencing phenomenon in which double-stranded RNA (dsRNA) causes a reduction of the complementary RNA (Fjose et al., 2001). The RNAi method has been widely used in model organisms and cell cultures for functional genomic study (Buckingham et al., 2004; Perrimon and Mathey-Prevot, 2007). Recently, large-scale sequencing analyses and metabolome analyses have been increasingly used in coral-algae symbiosis, and studies of the identification of symbiosis-, stress-, and skeletogenesis-related genes are increasing (Hillyer et al., 2016; Thomas and Palumbi, 2017; Hou et al., 2018; Yuyama et al., 2018; Ying et al., 2019; Zhang et al., 2019; Shinzato et al., 2021). Following identification, the functions of these genes need to be determined by genetic manipulation and examination of their expression localization. However, there have been only a few attempts to manipulate the expression of coral

genetic material by molecular approaches, such as RNAi (Yasuoka et al., 2016; Cleves et al., 2018). Meanwhile, there are some reports of RNAi in other members of the phylum Cnidarian, such as hydra and sea anemone. RNAi experiments in hydra have revealed the genes involved in cephalic and foot development, budding, and axis determination (Lohmann et al., 1999; Amimoto et al., 2006; Galliot et al., 2007; Jakob and Schierwater, 2007; Chera et al., 2009). These findings have helped clarify how body plans evolved in metazoan organisms. In addition, a recent gene expression silencing experiment using a marine hydrozoan model (*Hydractinia symbiolongicarpus*) has shown that knockdown of an exogenous green fluorescent protein (GFP) was successful by electroporation of shRNAs (Quiroga-Artigas et al., 2020). Knockdown of actin (ACT) and caspases in sea anemones (*Aiptasia pallida*) has been reported to reduce their gene expression levels (Dunn et al., 2007). Although sea anemones have been used as models of coral–algae symbiosis (Gabay et al., 2018; Jones et al., 2018; Li et al., 2018), the symbiotic relationship between coral–algae and sea anemones has different aspects: algal in corals contribute significantly to host skeletogenesis (Yuyama and Higuchi, 2014). Establishing RNAi technology for corals will enable further analysis of coral-specific phenomena, while morpholino oligo injection and CRISPR/Cas9-mediated genome editing are also an promising approach for gene knockdown in corals (Yasuoka et al., 2016; Cleves et al., 2018).

The objective of this study was to establish an RNAi method for use in coral. Although coral larvae and eggs are easy to manipulate genetically, their spawning period is limited to once or twice a year. A series of experiments using juvenile polyps and planula larvae of *Acropora tenuis* showed that the larvae could be used for fluorescence observation and stress experiments (Yuyama et al., 2005, 2012b, 2016). Given that they can be maintained in a small container, and the incubation conditions are similar to *Aiptasia*, it is possible that the RNAi method (lipofection method) performed in sea anemones could be performed in young *A. tenuis* (Dunn et al., 2007). Therefore, we performed RNAi by lipofection in *A. tenuis*, referring to the method performed in *Aiptasia*.

In this study, thioredoxin (TRX) and GFP were targeted by RNAi. TRX is a redox-regulating protein that functions as an indicator of oxidative stress in an organism (Arnér and Holmgren, 2000; Yoshida et al., 2003). TRX expression is up-regulated in corals in high temperature environments (Edge et al., 2005); we confirmed this in planula larvae by real-time PCR as well in preliminary experiments. GFP is a fluorescent protein naturally present in coral, and thus its expression in planula larvae and juvenile polyps is easily monitored using fluorescence stereomicroscopy (Strader et al., 2015; Yuyama et al., 2018). GFP is expressed throughout tissues in the planula, and is especially abundant in the endoderm (Haryanti and Hidaka, 2019). The GFP intensity of juvenile polyps was reportedly changed due to the algal symbiosis and stress exposure (Yuyama et al., 2012a). We synthesized dsRNA probes containing sequences complementary to TRX and GFP, transfected them into coral, and verified RNAi-mediated knockdown using real-time PCR. The effectiveness of TRX knockdown was

assessed by calculating the survival rate of TRX-dsRNA-treated corals exposed to high temperature. GFP-dsRNA silencing was confirmed by fluorescence stereomicroscopy. In these experiments, ACT dsRNA transfection was used to confirm the specificity of each knockdown.

## MATERIALS AND METHODS

### Coral Samples

Collection of *A. tenuis* larvae was performed as described previously (Iwao et al., 2002) at the Akajima Marine Science Laboratory (Okinawa, Japan). In 2013, the annual mean seawater temperature in the coastal area in Okinawa was 24.5°C, and the highest temperature of 31.2°C was recorded in early August (Higuchi et al., 2015). More than five parental colonies were used to produce larvae. A portion of the larvae were induced to undergo metamorphosis by exposure to 22 µM Hym 248 in filtered sea water (Iwao et al., 2002) in glass Petri dishes (55 mm in diameter) at 24°C under a 12-h light (20 µE/m<sup>2</sup>/s):12-h dark cycle. No significant change in the growth rate of larvae was observed within the same peptide stimulation batch. Seawater was filtered using a 0.22-µm filter (Millipore, Billerica, MA, United States).

### Preparation of RNAi Target Genes

The coral TRX sequence used for RNAi was identified from *A. tenuis* as follows. Total RNA was isolated from *A. tenuis* aposymbiotic juvenile polyps using an Absolutely RNA reverse transcription (RT)-PCR Miniprep Kit (Stratagene, La Jolla, CA, United States) and TRX cDNA was prepared using a SMART rapid amplification of cDNA ends (RACE) cDNA amplification kit (Takara Bio, CA, United States). Using the cDNA, fragments of approximately 200 bp containing TRX coding sequences were amplified by RT-PCR with degenerate primers (5'-TTRCANGGNCCRCACCA-3' and 5'-YTTRCANGGNCCRCACCA-3'). Then, 5' and 3' RACE was carried out to identify cDNA sequences that were 5' and 3' of the fragments, using the cDNA described above. In 3' RACE, RT was performed with gene-specific primers (5'-GGATCCGAGAAAGAATAATGAA-3'), whose sequences were designed from isolated fragments, and subsequent nested PCR was performed with specific primers (5'-CTATCCTGACAAGCTGTTGG-3'). For 5' RACE, the primers 5'-CCAACAGCTTGTCAGGATAG-3' were used as forward primers. The RACE PCR products were cloned into the pGEM-T Easy vector and sequenced on both strands by MacroGen<sup>1</sup>. A homology search in the “Protein-All” database was conducted on the DNA Data Bank of Japan (DDBJ) website<sup>2</sup>. A search of the Pfam database was performed using the “Motif Search” program on the Genome Net website (<http://www.genome.jp/ja/>; Bioinformatics Center, Institute for Chemical Research, Kyoto University, Japan). The TRX sequences identified here been registered in DDBJ (accession

<sup>1</sup><https://www.macrogen-japan.co.jp/>

<sup>2</sup><https://www.ddbj.nig.ac.jp/index-e.html>

no. LC532156). The gene encoding GFP, identified by Yuyama et al. (2012a; accession no. AY646066; Yuyama et al., 2012a), was used for RNAi. In addition, the ACT gene of *A. tenuis* (accession no. BJ999688), identified by Kii et al. (2007), was used in these experiments.

## Preparation of dsRNA for RNAi

An RNAi experiment was performed in accordance with the previously published method of Dunn et al., 2007. The dsRNAs were synthesized using the MEGAscript RNAi kit (Ambion, Austin, TX, United States). dsRNAs specific for TRX (311 bp), GFP (607 bp), and ACT (499 bp) were generated. The fragments were amplified from *A. tenuis* cDNA using specific primers flanked with the T7 RNA polymerase promoter sequence (Table 1). After amplifying the target sequence by PCR using each primer, sequences of PCR product were confirmed with sanger-sequencing by MACROGEN JAPAN (Tokyo, Japan). Fifty planula larvae or five polyps were placed in each well of a 24-well plate with 1 mL of filtered seawater (0.22-μm filter) with 0.2 μg/mL ampicillin and 0.5 μg/mL kanamycin. The liposomal compound (DMRIE-C, Invitrogen/Gibco, Co Dublin, Ireland) was used as an RNA transfection agent. Then, 1 mL of filtered seawater with 0.5 μg/mL or 1 μg/mL dsRNA and DMRIE-C was further added to the coral. For control treatments of TRX- or GFP-targeting RNAi, filtered seawater containing only DMRIE-C or ACT- dsRNA + DMRIE-C was prepared. After incubation for 3 days, corals were fixed in RNAlater for real-time PCR analysis, or the following assay (Verification of knockdown by stress exposure and fluorescence observation) was performed.

## Real-Time PCR

RNA was extracted from 50 planula larvae in each well. Samples were fixed in RNAlater (Ambion) after 72 h of incubation with dsRNA. Since planulae had better RNA extraction efficiency than primary polyps, we performed real-time PCR using planulae. Total RNA was extracted using the PureLink RNA Mini Kit (Thermo Fisher Scientific, Tokyo, Japan). Then, first strand cDNAs were synthesized from 20 ng of total RNA using the Superscript VILO Master Mix (Invitrogen, Carlsbad, CA, United States) for the PCR template. For real-time PCR, the expression levels of TRX and GFP were determined in triplicate using SYBR PreMix ExTaq II (Sigma, Tokyo, Japan). Primers for real-time PCR analyses were designed using Primer Express 3.0

software (Applied Biosystems, Foster City, CA, United States; Table 2). It has been confirmed that PCR using each primer set and cDNA of *A. tenuis* yields the desired PCR product by electrophoresis. Genome analysis of *A. tenuis* has revealed that there are multiple isoforms of GFP (Satoh et al., 2021). Here, we used primers that detect only the GFP of accession no. AY646066, that showed high expression levels in planulae and polyps (Yuyama et al., 2012a). This is the only sequence isolated from the cDNA library of the similar origin *A. tenuis*. Each PCR reaction contained 10 μL of PCR master mix of SYBR PreMix ExTaq II (Sigma), 1.5 mM forward primer, 1.5 mM reverse primer, and 2.0 μL of cDNA template. The PCR conditions were as follows: denaturation at 95°C for 20 s, followed by 40 cycles of denaturation at 95°C for 30 s and annealing at 58°C for 30 s, and extension at 72°C for 30 s. The mean values were calculated using the Thermal Cycler Dice Real-time System (TAKARA, Sigma). The data were normalized to the expression levels of tubulin and elongation factor of *A. tenuis*. As candidates for expression normalization, the tubulin, elongation factor, and ribosomal protein L5 genes, which have been used previously for normalization in real-time PCR (Yuyama et al., 2012b), were selected and their expression levels tested using NormFinder (Andersen et al., 2004). Elongation factor and tubulin were found to be relatively stable, and the average expression levels of these genes were used for normalization. As a control group, corals of ACT -targeting RNAi were used.

## Verification of Knockdown by Stress Exposure and Fluorescence Observation

To investigate the effect of GFP-targeting RNAi, the GFP expression of planula larvae and juvenile polyps was observed by fluorescence microscope (Olympus SZX16, Olympus, Tokyo, Japan). In this experiment, three types of corals at different stages of growth were used: planula larvae, early-stage morphogenetic polyps 2 days after metamorphosis induction, and polyps 1 month after metamorphosis. At day 3 after dsRNA treatment, corals were tested to confirm the effect of each treatment on GFP expression. Epifluorescence photomicrographs of Juvenile polyps were taken under Olympus SZX16 (Olympus, Tokyo, Japan) using a digital camera (Tucsen Photonics, Fuzhou, China). Images were analyzed using imageJ software (Wayne Rasband,

**TABLE 1** | The primer sets used for dsRNA synthesis.

Gene	Primer (5'-3')
GFP	(F)TAATACGACTCACTATAGGGCAGTGTCAATGGCCATGAA (R)TAATACGACTCACTATAGGGGCAGCATGTTCTTCCAGCTT
TRX	(F)TAATACGACTCACTATAGGGGAGGGATCCGAGAAAGAATA (R)TAATACGACTCACTATAGGGTTATCGTTAAGGAACCTTG
ACT	(F)TAATACGACTCACTATAGGGGATCCGGTATGTGCAAAGCT (R)TAATACGACTCACTATAGGGTCCAGACGTAAGATGGCATG

Each gene has a T7 promoter sequence (TAATACGACTCACTATAGGG) at the 5' end of the gene specific sequence.

**TABLE 2** | Forward (F) and reverse (R) primer sets used in the quantitative real-time PCR.

Gene	Primer (5'-3')
GFP	(F)TTGGCCAAAGTGCAAAGG (R)ATGAGCCGAGCATGTTCT
TRX	(F)GAGGGATCCGAGAAAGAATA (R)TTATCGTTAAGGAACCTTTG
Ribosomal protein L5	(F)CCATTGTAATCTCATGCAGATTCA (R)TCCTTGACCTTCAACAGAACAT
Elongation factor	(F)TTTGCGCTGCAATGCT (R)CAGACTTTCATGGTGCATTCAA
β-Tublin	(F)TCAGCGTTGTACCATCTCCAA (R)AACTGATGGACGGACAGTGT



National Institutes of Health, Bethesda, MD, United States) to estimate fluorescence intensity in each polyp ( $n = 3$ ). The amount of GFP in the polyp was estimated using the RawIntDen function of imageJ. Photographs of polyps before and after RNAi treatment were stacked and compared their fluorescent intensity and the rate of change in the amount of GFP (after-RNAi/pre-RNAi) was calculated. One image per polyp was used for imageJ analyses. To investigate the effect of TRX-targeting RNAi, planula larvae were incubated at high temperature ( $31.5^{\circ}\text{C}$ ); these experiments were performed in triplicate containing 90 planula larvae. 3 days after dsRNA ( $0.5 \mu\text{g/mL}$ ) treatment in a 24-well plate as described above, thirty treated larvae were picked up and added to 50 mL of filtered seawater in a Falcon centrifuge tubes (Fisher scientific) and incubated at  $31.5^{\circ}\text{C}$  for 1 day. The survival rate after 1 day was confirmed. A coral exposed to DMRIE-C alone and corals treated with ACT-dsRNA for 3 days was used as a control. We prepared three 50 mL experimental sets for each treatment group.

## Statistical Analyses

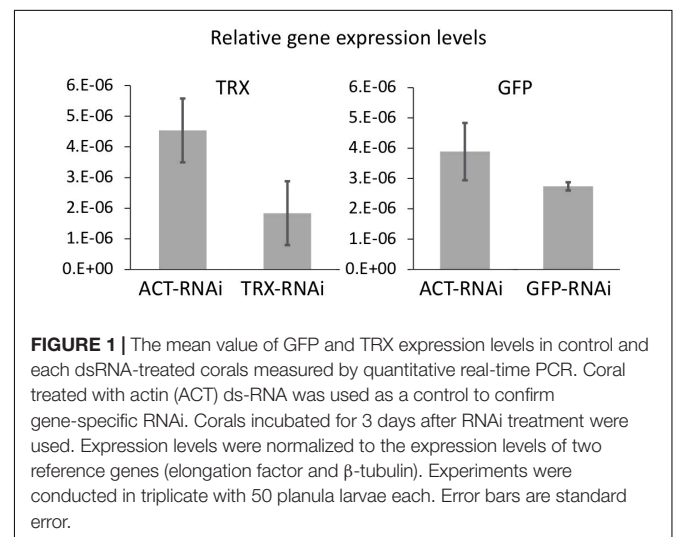
Statistical analyses were performed using Python (Python 3.8.5 version, Anaconda 3, Continuum Analytics, Inc., United States). The survival rates were analyzed for treatment using a Turkey-Kramer HSD (honestly significant difference) test. To confirm whether the response was specific to GFP or TRX dsRNA, the same assay was performed with corals treated with ACT dsRNA. Student's *t*-test was used for comparing the relative gene expression levels and fluorescence levels after RNAi treatment.

## RESULTS AND DISCUSSION

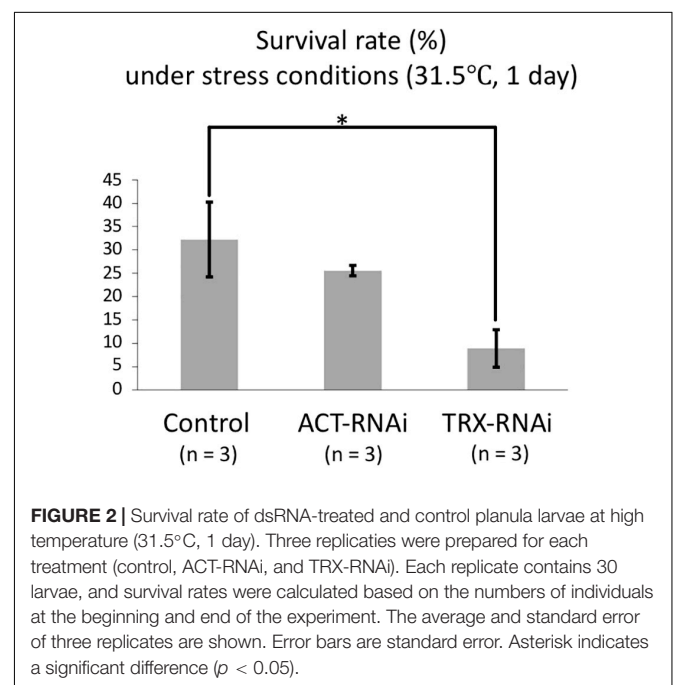
As the initial knockdown trial in corals, TRX and GFP were used for RNAi targets. From *A. tenuis* planula larvae, cDNA clones that comprised a full-length open reading frame of GFP and TRX, respectively, were isolated, and dsRNA were synthesized from these clones. We introduced these TRX and GFP dsRNA into planula larvae at two concentrations ( $0.5$  and  $1 \mu\text{g/mL}$ ) by lipofection (Dunn et al., 2007). Larvae incubated in  $1 \mu\text{g/mL}$  each dsRNA, melted during the 3 days incubation period. Larvae treated with  $0.5 \mu\text{g/mL}$  dsRNA showed no phenotypic changes, and all 50 planula larvae in the well of a multi-well plate survived. Based on these results,  $0.5 \mu\text{g/mL}$  dsRNA was used in subsequent experiments.

The effect of RNAi on the expression levels of each gene was examined by real-time PCR (Figure 1). Gene expression levels of GFP and TRX tended to decrease in the GFP-ds RNA treated and TRX-ds RNA treated groups, respectively, compared to the control group (ACT dsRNA treated larvae) on day 3. GFP-RNAi had lower knockdown efficiency than TRX-RNAi. This may be due to the presence of complex gene regulatory networks that control GFP expression, such as the involvement of multiple isoforms in GFP expression. Since the expression levels of each gene varied greatly and the number of replicates was small ( $n = 3$ ), there was no significant decrease in gene expression compared to the control treatment group.

Coral TRX expression was previously reported to respond to high temperature stress (Edge et al., 2005; Maor-Landaw and Levy, 2016); therefore, we confirmed the TRX knockdown using high-temperature incubation experiments. Coral planula larvae are vulnerable to environmental changes; the effects of stress exposure on planula larvae can be assessed by survival rates. To assess the TRX dsRNA-specific response to temperature stress, control larvae treated with ACT dsRNA were also assessed. As shown in Figure 2, the survival rate was 8.9% in TRX dsRNA-treated planula larvae, while the survival rates of ACT dsRNA-treated population and the control population (treated with DMRIE-C reagent) were 25.6 and 32.2%, respectively. The survival rate of TRX-treated larvae under non-stress conditions was 100%.



**FIGURE 1 |** The mean value of GFP and TRX expression levels in control and each dsRNA-treated corals measured by quantitative real-time PCR. Coral treated with actin (ACT) ds-RNA was used as a control to confirm gene-specific RNAi. Corals incubated for 3 days after RNAi treatment were used. Expression levels were normalized to the expression levels of two reference genes (elongation factor and  $\beta$ -tubulin). Experiments were conducted in triplicate with 50 planula larvae each. Error bars are standard error.

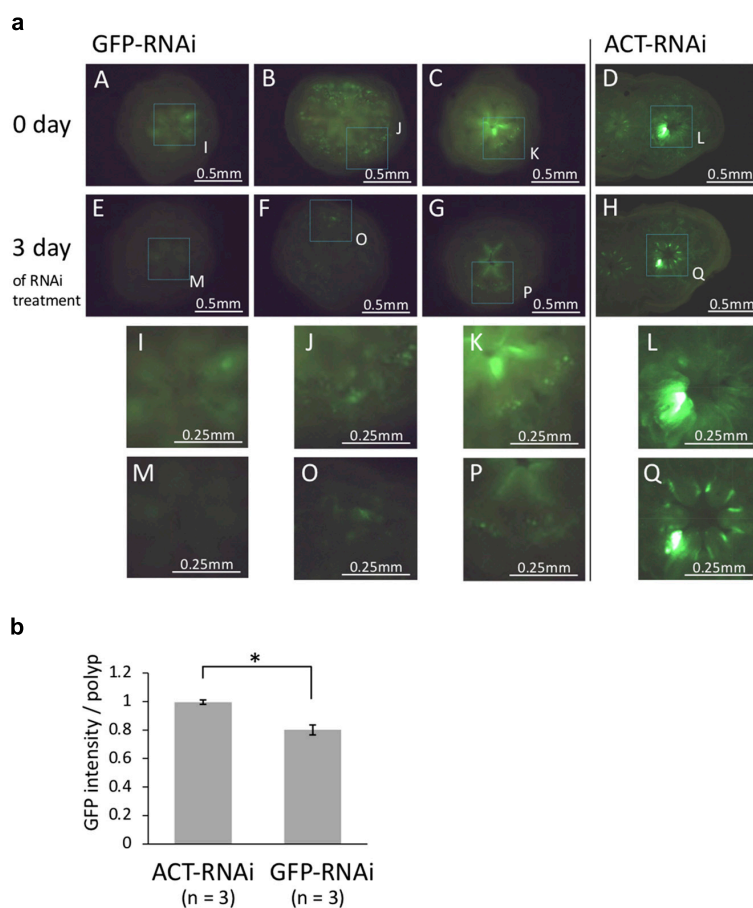


**FIGURE 2 |** Survival rate of dsRNA-treated and control planula larvae at high temperature ( $31.5^{\circ}\text{C}$ , 1 day). Three replicates were prepared for each treatment (control, ACT-RNAi, and TRX-RNAi). Each replicate contains 30 larvae, and survival rates were calculated based on the numbers of individuals at the beginning and end of the experiment. The average and standard error of three replicates are shown. Error bars are standard error. Asterisk indicates a significant difference ( $p < 0.05$ ).

TRX-knockdown corals exhibited a significantly reduced survival rate ( $p < 0.05$ , HSD test) compared with the other treatment groups under high temperature conditions. It is suggested that TRX knockdown reduces the ability of coral to relieve oxidative stress, making the coral vulnerable to temperature stress. However, the survival rate of the control group was low, suggesting that acute stress responses other than TRX knockdown are also significantly involved in the death of planula larvae treated with TRX-dsRNA. TRX has two thiol residues, and their redox reaction might be involved in defense against oxidative stress either directly removing active oxygen or regulating the activity of target enzymes as signal transducer of intracellular oxidative stress (Cunningham et al., 2015). Use of the redox state of TRX as indicator of intracellular oxidative stress has been suggested (Hidaka, 2016). Considering our results, further analyses of TRX functions via gene knockdown

experiment are necessary to reveal the role of TRX in coral stress response.

To determine whether GFP dsRNA suppress GFP expression, coral polyps were observed under fluorescence microscope. The coral at different growth stages were used to observe the effect of RNAi treatment: juvenile polyps immediately after metamorphosis (day 3 after Hym treatment), polyps 1 month after metamorphosis, and planula larvae. A decrease in GFP fluorescence was observed only in polyps immediately after metamorphosis (**Figure 3a**). The quantification of the GFP fluorescence in the photo image showed that the GFP fluorescence decreased significantly after application of GFP-targeting RNAi (**Figure 3b**,  $P < 0.05$ ,  $t$ -test). In planula larvae, GFP fluorescence was strong, and only one of four individuals showed a large difference before and after treatment (data not shown). Haryanti and Hidaka (2019) showed that acroporid planula larvae exhibited strong green fluorescence, and



**FIGURE 3 | (a)** Fluorescence microscopy images of juvenile polyps (day 6 after metamorphosis) treated with GFP-dsRNA and ACT-dsRNA. Corals treated with ACT-dsRNA were prepared as a control group to confirm the response was specific to GFP-dsRNA. GFP-dsRNA-treated corals showed a tendency toward decreased green auto-fluorescence. (A–E, B–F, C–G, and D–H) Show the same colonies before-after treatment with each dsRNA. (I–Q) show higher magnification of dashed box region in A–H. The same part in the photos before-after dsRNA treatment is surrounded by dotted lines. The same area of the two figures (before-after treatment) is surrounded by dotted lines and enlarged. **(b)** The rate of change in GFP content (after-RNAi/pre-RNAi). The GFP contents were estimated from juvenile polyps ( $n = 3$ ) treated with GFP-dsRNA or ACT-dsRNA using the RawIntDen function of imageJ. The green fluorescence intensity was decreased in corals treated with GFP-dsRNA. Bars represent the mean GFP fluorescence intensity of corals treated with ds-GFP or ds-ACT. Error bars are standard error. Asterisk indicate significant differences ( $p < 0.05$ ).

the fluorescence was decreased after metamorphosis. The inherently high expression level of GFP in planula larvae might be a reason for the lower RNAi effect on GFP intensity. It was possible that the larvae had a fast GFP turnover and that resulted in a weak knockdown efficiency. Polyps at 1 month after metamorphosis appeared to be minimally affected by RNAi targeting of GFP. At 1 month after metamorphosis, corals are covered with mesh-like calcareous skeleton; these corals might be less receptive to the application of dsRNA. Thus, polyps immediately after metamorphosis were optimal for observing the effects of GFP dsRNA. As mentioned above, there are multiple isoforms of GFP in *A. tenuis* (Satoh et al., 2021). The GFP-dsRNA and its four isoforms have 253–579 bp homologous regions, and it is possible that multiple GFP isoforms were knocked down during RNAi processing, resulting in increased efficacy. Our results suggest that RNAi may not be successful in corals in which the body wall is covered with mesh-like calcareous skeleton, even when targeting multiple isoforms.

In summary, RNAi using juvenile corals resulted in a reduction in target gene expression although there was statistically no significant difference from the control group. Moreover, RNAi targeting TRX and GFP confirmed the involvement of each gene in coral stress tolerance in the planula stage or GFP intensity 3 days after settlement, significantly. However, the effect of RNAi on GFP was confirmed only in the corals at the initial stages after metamorphosis, and no effect on GFP color development was observed in planulae and 1 month-old budding juveniles. There are still improvements to be made in this method for corals. We used dsRNA based on previous studies, but the use of other interfering RNAs, such as morpholino antisense oligonucleotides and small interfering RNAs (siRNAs), could also be useful. The use of siRNAs and morpholino antisense oligonucleotides is likely to produce a more pronounced effect than RNAi (Layden et al., 2013; Guo et al., 2018). In future studies, it might be desirable to make sure that dsRNA is actually incorporated by all or certain cell types using fluorescent dye-conjugated dsRNA, and to use suitable positive and negative control dsRNAs in addition to the controls used in the present study. In addition, the results of this study suggest the effects of RNAi are reduced in skeletonized corals, and planula larvae and polyps are appropriate for genetic manipulation. However, as planula larvae can only be obtained once or twice a year, the number of RNAi experiments that can

be performed is limited. Furthermore, the genetic diversity of planula larvae may have affected RNAi efficiency. In the future, coral cell clumps could be useful for advancement the RNAi method (Nesa and Hidaka, 2008). Alternatively, the use of sea anemones and hydra as models to elucidate common symbiotic relationships may be informative. Here, we showed that RNAi by lipofection can be applied to juvenile corals, and the effect on gene expression, coral stress tolerance and fluorescence intensity were tested. It is expected that such RNAi experiments will be utilized for functional identification of coral-specific genes.

## DATA AVAILABILITY STATEMENT

The datasets presented in this study can be found in online repositories. The names of the repository/repositories and accession number(s) can be found in the article.

## AUTHOR CONTRIBUTIONS

IY: study conception and design, data collection, and draft manuscript preparation. TH: statistic analysis, drafting, and writing. MH: drafting and writing. All authors contributed to the article and approved the submitted version.

## FUNDING

This work was supported by a research grant by the Japan Society for the Promotion of Science (IY, #14J40135 and #19H03026), the Environment Research and Technology Development Fund (No. 4-1806) from the Ministry of the Environment in Japan, and the Kurita Water and Environment Foundation (18B083).

## ACKNOWLEDGMENTS

We thank the members of Laboratory for DNA data analysis in NIG (National Institute of Genetics), especially Hisako Tashiro and Chie Iwamoto for supporting our incubation experiments, and also thank the member of Laboratory of Molecular Evolution of Microbes in University of Tsukuba.

## REFERENCES

- Amimoto, Y., Kodama, R., and Kobayakawa, Y. (2006). Foot formation in Hydra: a novel gene, anklet, is involved in basal disk formation. *Mech. Dev.* 123, 352–361. doi: 10.1016/j.mod.2006.03.002
- Andersen, C. L., Jensen, J. L., and Ørntoft, T. F. (2004). Normalization of real-time quantitative reverse transcription-PCR data: a model-based variance estimation approach to identify genes suited for normalization, applied to bladder and colon cancer data sets. *Cancer Res.* 64, 5245–5250. doi: 10.1158/0008-5472.CAN-04-0496
- Arnér, E. S., and Holmgren, A. (2000). Physiological functions of thioredoxin and thioredoxin reductase. *Eur. J. Biochem.* 267, 6102–6109. doi: 10.1046/j.1432-1327.2000.01701.x
- Buckingham, S. D., Esmaeili, B., Wood, M., and Sattelle, D. B. (2004). RNA interference: from model organisms towards therapy for neural and neuromuscular disorders. *Hum. Mol. Genet.* 13, 275–288. doi: 10.1093/hmg/ddh224
- Chera, S., Buzgariu, W., Ghila, L., and Galliot, B. (2009). Autophagy in *Hydra*: a response to starvation and stress in early animal evolution. *Biochim. Biophys. Acta* 1793, 1432–1443. doi: 10.1016/j.bbamcr.2009.03.010
- Cleves, P. A., Strader, M. E., Bay, L. K., Pringle, J. R., and Matz, M. V. (2018). CRISPR/Cas9-mediated genome editing in a reef-building coral. *Proc. Natl. Acad. Sci.* 115, 5235–5240. doi: 10.1073/pnas.1722151115
- Cunningham, G. M., Roman, M. G., Flores, L. C., Hubbard, G. B., Salmon, A. B., Zhang, Y., et al. (2015). The paradoxical role of thioredoxin on oxidative stress and aging. *Arch. Biochem. Biophys.* 576, 32–38. doi: 10.1016/j.abb.2015.02.025

- Dunn, S. R., Phillips, W. S., Green, D. R., and Weis, V. M. (2007). Knockdown of actin and caspase gene expression by RNA interference in the symbiotic anemone *Aiptasia pallida*. *Biol. Bull.* 212, 250–258. doi: 10.2307/25066607
- Edge, S. E., Morgan, M. B., Gleason, D. F., and Snell, T. W. (2005). Development of a coral cDNA array to examine gene expression profiles in *Montastraea faveolata* exposed to environmental stress. *Mar. Pollut. Bull.* 51, 507–523. doi: 10.1016/j.marpolbul.2005.07.007
- Fjose, A., Ellingsen, S., Wargelius, A., and Seo, H. C. (2001). RNA interference: mechanisms and applications. *Biotechnol. Annu. Rev.* 7, 31–57. doi: 10.1016/s1387-2656(01)07032-6
- Gabay, Y., Weis, V. M., and Davy, S. K. (2018). Symbiont identity influences patterns of symbiosis establishment, host growth, and asexual reproduction in a model cnidarian-dinoflagellate symbiosis. *Biol. Bull.* 234, 1–10. doi: 10.1086/696365
- Galliot, B., Miljkovic-Licina, M., Ghila, L., and Chera, S. (2007). RNAi gene silencing affects cell and developmental plasticity in hydra. *C. R. Biol.* 330, 491–497. doi: 10.1016/j.crv.2007.01.008
- Guo, X., Wang, Y., Sinakevitch, I., Lei, H., and Smith, B. H. (2018). Comparison of RNAi knockdown effect of tyramine receptor 1 induced by dsRNA and siRNA in brains of the honey bee, *Apis mellifera*. *J. Insect Physiol.* 111, 47–52. doi: 10.1016/j.jinsphys.2018.10.005
- Haryanti, D., and Hidaka, M. (2019). Developmental changes in the intensity and distribution pattern of green fluorescence in coral larvae and juveniles. *Galaxea J. Coral Reef Stud.* 21, 13–25. doi: 10.3755/galaxea.21.1\_13
- Hidaka, M. (2016). “Life History and Stress Response of Scleractinian Corals” in *Coral Reef Science: Strategy for Ecosystem Symbiosis and Coexistence With Humans Under Multiple Stresses Coral Reefs of the World*, ed. H. Kayanne (Tokyo: Springer). 1–24. doi: 10.1007/978-4-431-54364-0\_1
- Higuchi, T., Agostini, S., Casareto, B. E., Suzuki, Y., and Yuyama, I. (2015). Northern limit of corals of the genus *Acropora* in temperate zones is determined by their resilience to cold bleaching. *Sci. Rep.* 5:18467. doi: 10.1038/srep18467
- Hillyer, K. E., Tumanov, S., Villas-Bôas, S., and Davy, S. K. (2016). Metabolite profiling of symbiont and host during thermal stress and bleaching in a model cnidarian-dinoflagellate symbiosis. *J. Exp. Biol.* 219, 516–527. doi: 10.1242/jeb.128660
- Hou, J., Xu, T., Su, D., Wu, Y., Cheng, L., Wang, J., et al. (2018). RNA-Seq reveals extensive transcriptional response to heat stress in the stony coral *Galaxea fascicularis*. *Front. Genet.* 9:37. doi: 10.3389/fgene.2018.00037
- Iwao, K., Fujisawa, T., and Hatta, M. (2002). A cnidarian neuropeptide of the GLWamide family induces metamorphosis of reef-building corals in the genus *Acropora*. *Coral Reefs* 21, 127–129. doi: 10.1007/s00338-002-0219-8
- Jakob, W., and Schierwater, B. (2007). Changing hydrozoan bauplans by silencing Hox-like genes. *PLoS One* 2:e694. doi: 10.1371/journal.pone.0000694
- Jones, V. A. S., Bucher, M., Hambleton, E. A., and Guse, A. (2018). Microinjection to deliver protein, mRNA, and DNA into zygotes of the cnidarian endosymbiosis model *Aiptasia* sp. *Sci. Rep.* 8:16437. doi: 10.1038/s41598-018-34773-1
- Kii, S.-I., Tanaka, J., and Watanabe, T. (2007). Guanine-cytosine contents of the host and symbiont cDNA in a symbiotic coral. *Fish. Sci.* 73, 1362–1372. doi: 10.1111/j.1444-2906.2007.01479.x
- Layden, M. J., Röttinger, E., Wolenski, F. S., Gilmore, T. D., and Martindale, M. Q. (2013). Microinjection of mRNA or morpholinos for reverse genetic analysis in the starlet sea anemone. *Nematostella vectensis*. *Nat. Protoc.* 8, 924–934. doi: 10.1038/nprot.2013.009
- Li, Y., Liew, Y. J., Cui, G., Czesielski, M. J., Zahran, N., Michell, C. T., et al. (2018). DNA methylation regulates transcriptional homeostasis of algal endosymbiosis in the coral model *Aiptasia*. *Sci. Adv.* 4:eat2142. doi: 10.1126/sciadv.aat2142
- Lohmann, J. U., Endl, I., and Bosch, T. C. G. (1999). Silencing of developmental genes in *Hydra*. *Dev. Biol.* 214, 211–214. doi: 10.1006/dbio.1999.9407
- Maor-Landaw, K., and Levy, O. (2016). Gene expression profiles during short-term heat stress; branching vs. massive Scleractinian corals of the Red Sea. *PeerJ*. 4:e1814. doi: 10.7717/peerj.1814
- Nesa, B., and Hidaka, M. (2008). “Thermal stress increases oxidative DNA damage in coral cell aggregates,” in *Proceedings of the 11th International Coral Reef Symposium*, Vol. 5, Fort Lauderdale, FL. 144–148.
- Perrimon, N., and Mathey-Prevot, B. (2007). Applications of high-throughput RNA interference screens to problems in cell and developmental biology. *Genetics* 175, 7–16. doi: 10.1534/genetics.106.069963
- Quiroga-Artigas, G., Duscher, A., Lundquist, K., Waletich, J., and Schnitzler, C. E. (2020). Gene knockdown via electroporation of short hairpin RNAs in embryos of the marine hydroid *Hydractinia symbiolongicarpus*. *Sci. Rep.* 30:12806. doi: 10.1038/s41598-020-69489-8
- Satoh, N., Kinjo, K., Shintaku, K., Kezuka, D., Ishimori, H., Yokokura, A., et al. (2021). Color morphs of the coral, *Acropora tenuis*, show different responses to environmental stress and different expression profiles of fluorescent-protein genes. *G3* 11:jkab018. doi: 10.1093/g3journal/jkab018
- Shinzato, C., Khalturin, K., Inoue, J., Zayasu, Y., Kanda, M., Kawamitsu, M., et al. (2021). Eighteen coral genomes reveal the evolutionary frigin of *Acropora* strategies to accommodate environmental changes. *Mol. Biol. Evol.* 38, 16–30. doi: 10.1093/molbev/msaa216
- Strader, M. E., Davies, S. W., and Matz, M. V. (2015). Differential responses of coral larvae to the colour of ambient light guide them to suitable settlement microhabitat. *R. Soc. Open Sci.* 2:150358. doi: 10.1098/rsos.150358
- Thomas, L., and Palumbi, S. R. (2017). The genomics of recovery from coral bleaching. *Proc. R. Soc. B Biol. Sci.* 284:20171790. doi: 10.1098/rspb.2017.1790
- Yasuoka, Y., Shinzato, C., and Satoh, N. (2016). The mesoderm-forming gene brachyury regulates ectoderm-endoderm demarcation in the coral *Acropora digitifera*. *Curr. Biol.* 26, 2885–2892. doi: 10.1016/j.cub.2016.08.011
- Ying, H., Hayward, D. C., Cooke, I., Wang, W., Moya, A., Siemering, K. R., et al. (2019). The whole-genome sequence of the coral *Acropora millepora*. *Genom. Biol. Evol.* 11, 1374–1379. doi: 10.1093/gbe/evz077
- Yoshida, T., Oka, S., Masutani, H., Nakamura, H., and Yodoi, J. (2003). The role of thioredoxin in the aging process: involvement of oxidative stress. *Antioxid. Redox Signal.* 5, 563–570. doi: 10.1089/152308603770310211
- Yuyama, I., Harii, S., and Hidaka, M. (2012a). Algal symbiont type affects gene expression in juveniles of the coral *Acropora tenuis* exposed to thermal stress. *Mar. Environ. Res.* 76, 41–47. doi: 10.1016/j.marenvres.2011.09.004
- Yuyama, I., Ito, Y., Watanabe, T., Hidaka, M., Suzuki, Y., and Nishida, M. (2012b). Differential gene expression in juvenile polyps of the coral *Acropora tenuis* exposed to thermal and chemical stresses. *J. Exp. Mar. Biol. Ecol.* 43, 17–24. doi: 10.1016/j.jembe.2012.06.020
- Yuyama, I., Hayakawa, H., Endo, H., Iwao, K., Takeyama, H., Maruyama, T., et al. (2005). Identification of symbiotically expressed coral mRNAs using a model infection system. *Biochem. Biophys. Res. Commun.* 336, 793–798. doi: 10.1016/j.bbrc.2005.08.174
- Yuyama, I., and Higuchi, T. (2014). Comparing the effects of symbiotic algae (Symbiodinium) clades C1 and D on early growth stages of *Acropora tenuis*. *PLoS One* 9:e98999. doi: 10.1371/journal.pone.0098999
- Yuyama, I., Ishikawa, M., Nozawa, M., Yoshida, M., and Ikeo, K. (2018). Transcriptomic changes with increasing algal symbiont reveal the detailed process underlying establishment of coral-algal symbiosis. *Sci. Rep.* 8:16802. doi: 10.1038/s41598-018-34575-5
- Yuyama, I., Nakamura, T., Higuchi, T., and Hidaka, M. (2016). Different stress tolerances of juveniles of the coral *Acropora tenuis* associated with clades C1 and D *Symbiodinium*. *Zool. Stud.* 55:9.
- Zhang, Y., Chen, Q., Xie, J. Y., Yeung, Y. H., Xiao, B., Liao, B., et al. (2019). Development of a transcriptomic database for 14 species of scleractinian corals. *BMC Genom.* 20:387. doi: 10.1186/s12864-019-5744-8

**Conflict of Interest:** The authors declare that the research was conducted in the absence of any commercial or financial relationships that could be construed as a potential conflict of interest.

**Publisher's Note:** All claims expressed in this article are solely those of the authors and do not necessarily represent those of their affiliated organizations, or those of the publisher, the editors and the reviewers. Any product that may be evaluated in this article, or claim that may be made by its manufacturer, is not guaranteed or endorsed by the publisher.

Copyright © 2021 Yuyama, Higuchi and Hidaka. This is an open-access article distributed under the terms of the Creative Commons Attribution License (CC BY). The use, distribution or reproduction in other forums is permitted, provided the original author(s) and the copyright owner(s) are credited and that the original publication in this journal is cited, in accordance with accepted academic practice. No use, distribution or reproduction is permitted which does not comply with these terms.





# Phylogeography of Blue Corals (Genus *Heliopora*) Across the Indo-West Pacific

Hiroki Taninaka<sup>1</sup>, Davide Maggioni<sup>2,3</sup>, Davide Seveso<sup>2,3</sup>, Danwei Huang<sup>4,5,6</sup>, Abram Townsend<sup>7</sup>, Zoe T. Richards<sup>8,9</sup>, Sen-Lin Tang<sup>10</sup>, Naohisa Wada<sup>10</sup>, Taisei Kikuchi<sup>11</sup>, Hideaki Yuasa<sup>12</sup>, Megumi Kanai<sup>13</sup>, Stéphane De Palmas<sup>10,14,15</sup>, Nipphon Phongsuwan<sup>16</sup> and Nina Yasuda<sup>17\*</sup>

<sup>1</sup> Interdisciplinary Graduate School of Agriculture and Engineering, University of Miyazaki, Miyazaki, Japan, <sup>2</sup> Department of Earth and Environmental Sciences (DISAT), University of Milano-Bicocca, Milan, Italy, <sup>3</sup> Marine Research and High Education Center (MaRHE Center), Faafu Magoodhoo, Maldives, <sup>4</sup> Department of Biological Sciences, National University of Singapore, Singapore, Singapore, <sup>5</sup> Tropical Marine Science Institute, National University of Singapore, Singapore, Singapore, <sup>6</sup> Centre for Nature-based Climate Solutions, National University of Singapore, Singapore, Singapore, <sup>7</sup> Division of Natural Sciences, University of Guam, Mangilao, GU, United States, <sup>8</sup> Coral Conservation and Research Group, Trace and Environmental DNA Laboratory, School of Molecular and Life Sciences, Curtin University, Bentley, WA, Australia, <sup>9</sup> Collections and Research, Western Australian Museum, Welshpool, WA, Australia, <sup>10</sup> Biodiversity Research Center, Academia Sinica, Taipei, Taiwan, <sup>11</sup> Parasitology, Faculty of Medicine, University of Miyazaki, Miyazaki, Japan, <sup>12</sup> Department of Life Science and Technology, School of Life Sciences and Technology, Tokyo Institute of Technology, Tokyo, Japan, <sup>13</sup> Okinawa Environment Science Center, Urasoe, Japan, <sup>14</sup> Biodiversity Program, Taiwan International Graduate Program, Academia Sinica and National Taiwan Normal University, Taipei, Taiwan, <sup>15</sup> Institute of Oceanography, National Taiwan University, Taipei, Taiwan, <sup>16</sup> Phuket Marine Biological Center, Muang, Thailand, <sup>17</sup> Faculty of Agriculture, University of Miyazaki, Miyazaki, Japan

## OPEN ACCESS

### Edited by:

Wei Jiang,  
Guangxi University, China

### Reviewed by:

Snaebjörn Pálsson,  
University of Iceland, Iceland  
Nicole De Voogd,  
Naturalis Biodiversity Center,  
Netherlands

### \*Correspondence:

Nina Yasuda  
nina27@cc.miyazaki-u.ac.jp

### Specialty section:

This article was submitted to  
Coral Reef Research,  
a section of the journal  
Frontiers in Marine Science

**Received:** 25 May 2021

**Accepted:** 23 June 2021

**Published:** 13 August 2021

### Citation:

Taninaka H, Maggioni D, Seveso D, Huang D, Townsend A, Richards ZT, Tang S-L, Wada N, Kikuchi T, Yuasa H, Kanai M, De Palmas S, Phongsuwan N and Yasuda N (2021) Phylogeography of Blue Corals (Genus *Heliopora*) Across the Indo-West Pacific. *Front. Mar. Sci.* 8:714662. doi: 10.3389/fmars.2021.714662

Species delimitation of corals is one of the most challenging issues in coral reef ecology and conservation. Morphology can obscure evolutionary relationships, and molecular datasets are consistently revealing greater within-species diversity than currently understood. Most phylogenetic studies, however, have examined narrow geographic areas and phylogeographic expansion is required to obtain more robust interpretations of within- and among- species relationships. In the case of the blue coral *Heliopora*, there are currently two valid species (*H. coerulea* and *H. hiberniana*) as evidenced by integrated genetic and morphological analyses in northwestern Australia. There are also two distinct genetic lineages of *H. coerulea* in the Kuroshio Current region that are morphologically and reproductively different from each other. Sampling from all *Heliopora* spp. across the Indo-Pacific is essential to obtain a more complete picture of phylogeographic patterns. To examine phylogenetic relationships within the genus *Heliopora*, we applied Multiplexed inter simple sequence repeat (ISSR) Genotyping by sequencing (MIG-seq) on > 1287 colonies across the Indo-West Pacific. Maximum likelihood phylogenetic trees indicated the examined *Heliopora* samples comprise three genetically distinct groups: *H. coerulea* group, *H. hiberniana* group, and a new undescribed *Heliopora* sp. group with further subdivisions within each group. Geographic structuring is evident among the three species with *H. hiberniana* group found in the Indo-Malay Archipelago and biased toward the Indian Ocean whilst *Heliopora* sp. was only found in the Kuroshio Current region and Singapore, indicating that this taxon is distributed in the western Pacific and the Indo-Malay Archipelago.

*Heliopora coerulea* has a wider distribution, being across the Indian Ocean and western Pacific. This study highlights the effectiveness of phylogenetic analysis using genome-wide markers and the importance of examining populations across their distribution range to understand localized genetic structure and speciation patterns of corals.

**Keywords:** MIG-seq, single nucleotide polymorphism, *Helioporadae*, octocoral, species delimitation, coral reef, evolutionary relationships, species diversity

## INTRODUCTION

Coral reef ecosystems have the highest biodiversity of all marine ecosystems (Fisher et al., 2015) and are important in terms of their scientific, economic, and social value (Moberg and Folke, 1999; Spalding et al., 2001; Cesar et al., 2003). However, reef-building corals, the foundation organisms in coral reefs, have been rapidly deteriorating (Hughes et al., 2003; Altieri et al., 2017; Eyre et al., 2018) due to coral mass bleaching and other threats associated with the on-going climate change (e.g., global warming and ocean acidification) (Hoegh-Guldberg et al., 2007; Hoegh-Guldberg and Bruno, 2010; Hoegh-Guldberg, 2011; Hughes et al., 2018); local anthropogenic impacts (e.g., red-soil runoff, nutrient enrichment, and marine plastic pollution) (Halpern et al., 2008; Omori, 2011; Huang et al., 2020; de Oliveira Soares et al., 2020); outbreaks of corallivorous animals (Birkeland and Lucas, 1990; Yasuda, 2018; Montalbetti et al., 2019) and coral disease (Bruno et al., 2003, 2007; Burge et al., 2014). Approximately one-third of the world's reef-building corals are facing an elevated risk of extinction (Carpenter et al., 2008; Wilkinson, 2008), but many more cryptic species may be undescribed (Bickford et al., 2007) and if the natural range of species is misunderstood, their threatened status may be under-estimated (Richards et al., 2016).

The classification of reef-building coral species has traditionally been based mainly on morphological characteristics (Veron, 2000; Fabricius and Alderslade, 2001). In some cases, however, morphological classification has been difficult due to a high level of phenotypic plasticity across geographic and depth gradients, and in some genera, there is a lack of discrete morphological features that can be used to underpin species identifications (e.g., Forsman et al., 2009; Marti-Puig et al., 2014; McFadden et al., 2017). More recently, genetic information based on several molecular markers has shown morphology can conceal cryptic evolutionary relationships (Richards et al., 2013) and it is increasingly common for genetically distinct cryptic species or lineages to be found within widespread coral species (e.g., Nakajima et al., 2012; Pinzón et al., 2013; Warner et al., 2015). Such discordance between morphology and genetics has led to confusion regarding the species boundaries in many groups (e.g., *Acropora*, van Oppen et al., 2001; Marquez et al., 2002, *Pocillopora*, Flot et al., 2008; Souter, 2010; Schmidt-Roach et al., 2013). Such ambiguity threatens to undermine effective biodiversity conservation efforts and prevents the true complexity of coral reef ecosystems from being properly understood.

Molecular data is not, however, always able to provide a definitive answer about species boundaries within reef-building corals. Molecular systematic studies have been partly hindered by

the lack of appropriate genetic markers and the traditionally used mitochondrial markers have suffered from inadequate analytical resolution (Shearer et al., 2002; Ridgway and Gates, 2006; Bilewitch and Degnan, 2011). The ability to interpret nuclear datasets is also hampered by the multi-copy nature of genes (Vollmer and Palumbi, 2004) even those that were originally thought to be single copy (e.g., Pax-C, Rosser et al., 2017), introgressive hybridization events (Veron, 1995; Richards et al., 2013) and/or incomplete lineage sorting (e.g., van Oppen et al., 2001; Souter, 2010; Yasuda et al., 2015). Recent advances in High-Throughput Sequencing (HTS) have enabled the use of genome-wide polymorphisms such as restriction site associated DNA sequencing (RAD-seq, Miller et al., 2007; Baird et al., 2008; Rowe et al., 2011; and Dart-seq, Rosser et al., 2017) and Multiplexed inter simple sequence repeat (ISSR) genotyping by sequencing (MIG-seq, Suyama and Matsuki, 2015) to infer phylogenetic relationships. Such techniques often successfully delimit species of non-model organisms including corals with higher resolution than traditional genetic markers (RAD-seq, e.g., Pante et al., 2015; Herrera and Shank, 2016; Quattrini et al., 2019 and MIG-seq, e.g., Tamaki et al., 2017; Park et al., 2019; Hirai, 2019).

MIG-seq is an easy, cost-effective, novel method to obtain a moderate number of single nucleotide polymorphisms (SNPs) of non-model organisms with polymerase chain reaction (PCR) and HTS technology. The number of SNPs from MIG-seq analysis is generally less than those obtained using other techniques such as RAD-seq. However, MIG-seq has several advantages, since the method can be performed with small amounts and/or low-quality DNA and is relatively easy and cheap. Indeed, MIG-seq successfully revealed species boundaries of octocoral species that could be undetectable by traditional genetic markers (Richards et al., 2018; Takata et al., 2019). While some studies examined genetic relationships of closely related reef-building corals using HTS techniques in geographically restricted regions (e.g., Forsman et al., 2017; Johnston et al., 2017), only a few studies have analyzed speciation and/or genetic divergence patterns covering the Indo-Pacific scale (but see Warner et al., 2015; Nakajima et al., 2017; Arrigoni et al., 2020; Wepfer et al., 2020). For a more comprehensive picture of the phylogeographic structure of coral species in the Indo-Pacific, and to understand the species diversity of corals, it is necessary to obtain more extensive representation of species across their geographic range.

Increasingly recognized is the importance of integrating information about reproductive timing and physiology with genetic and morphological data to obtain more robust estimates of coral species (see Ohki et al., 2015; Rosser, 2015; Villanueva, 2016; Luzon et al., 2017; Richards et al., 2018). Timing of reproduction in broadcast spawning species is particularly

important because gametes are viable for only a few hours, so individuals that spawn more than a few hours apart are unlikely to cross-fertilize (Leviton et al., 2011) and in this regard, reproductive timing heavily influences evolutionary patterns. Whilst integrated datasets that include reproductive data and cover a wide geographic area are emerging as the gold standard in phylogenetic studies, practical and logistical constraints often mean it is not possible to obtain complete sampling coverage in every region (Keyse et al., 2014; Wepfer et al., 2021). Nevertheless, examining the species boundaries, ecological preferences, and distribution of reef-building corals is fundamental for promoting effective conservation and management strategies.

The blue corals (genus *Heliopora*) are members of octocorals, though it has a well-developed aragonite skeleton like those of scleractinians (Quattrini et al., 2020). Owing to their hard skeleton, *Heliopora* spp. play an important role in coral reef accretion in various Indo-West Pacific reefs (e.g., Zann and Bolton, 1985; Planck et al., 1988; Abe et al., 2008; Takino et al., 2010), and therefore is an important reef-building coral taxon. *Heliopora coerulea* (Pallas, 1766) has mainly three growth forms, namely lobate, columnar, and encrusting (Dana, 1846), but with high morphological plasticity and continuous variations among growth forms (Eguchi, 1948; Colgan, 1984; H. Taninaka pers. obs.). *Heliopora coerulea* has long been regarded as a living fossil, being the sole extant member of the family Helioporidae (Colgan, 1984) until the recent description of *Heliopora hiberniana* Richards et al., 2018, a morphologically, genetically and reproductively distinct species from northwestern Australia in the Indian Ocean (Richards et al., 2018). To date, *H. coerulea* is known to be distributed throughout the Indo-Pacific realm (Wells, 1954; Bouillon and Houvenaghel-Crévecoeur, 1970; Zann and Bolton, 1985), whereas *H. hiberniana* is known from the north-west shelf of Western Australia, the Maldives, and the Wakatobi and Gili Islands in Indonesia (Richards et al., 2018, 2020).

*Heliopora* spp. are gonochoric, brooding corals (Babcock, 1990) with short larval dispersal durations (Harii et al., 2002; Harii and Kayanne, 2003). Due to such a low larval dispersal ability, genetic connectivity among geographically separate populations may be limited, a pattern that was evident within the scale of several hundred square kilometers (Taninaka et al., 2019). Therefore, it is possible that *Heliopora* includes further genetically distinct lineages in the Indo-Pacific. Previous genetic studies have indicated that additional cryptic species may indeed be present within *H. coerulea* along the Kuroshio Current region of the Philippines, Taiwan and Japan (Yasuda et al., 2014). Study from Yasuda et al., 2014 hypothesized that there are at least two genetically distinct lineages (HC-A and HC-B) of *H. coerulea* in the Kuroshio Current region that can also be distinguished by different gross morphologies (small branch for HC-A and flat shapes for HC-B, Yasuda et al., 2014, 2015; Iguchi et al., 2019). Subsequent observations (Saito et al., 2015; Villanueva, 2016) and histological examination (Taninaka et al., 2018) revealed that the reproductive timing of the two lineages is different by almost one month even under similar environmental conditions. However, the phylogeographical relationships among HC-A and B in the Kuroshio Current regions, and with *H. hiberniana* and

*H. coerulea* in northwestern Australia are still unknown. The aim of this study was to clarify the phylogenetic relationships and distributions of the genus *Heliopora* across the Indo-West Pacific to gain insights on the speciation patterns of Indo-Pacific coral species. To achieve this goal, we collected *Heliopora* samples widely from the Indo-West Pacific region and applied genome-wide phylogenetic, phylogeographic, and population genetic analyses using the MIG-seq method.

## MATERIALS AND METHODS

### Sample Collection and DNA Extraction

A total of 1287 *Heliopora* samples from a total of 73 sites across three western Pacific regions (Japan, Taiwan and Guam) and Singapore, and three Indian Ocean regions (northwestern Australia, Thailand, and the Maldives) were collected using SCUBA from 2008 to 2019 (Supplementary Table 1). Additionally, we used previously collected samples from Japan and northwestern Australia (Supplementary Table 1). The samples include those from the northernmost distribution site (Yaku Island in Japan; Nakabayashi et al., 2017), and the known deepest depth (from 50 m depth from Green Island, Taiwan). All coral fragments were preserved in 99.5% EtOH and kept at  $-20^{\circ}\text{C}$  until DNA extraction. During sampling, colonies were photographed, and GPS information was acquired wherever possible. All overseas sample collection was conducted through legal procedures and collection cooperation with the support of local research collaborating institutions; Academia Sinica in Taiwan, University of Guam in Guam, National University of Singapore in Singapore, Western Australian Museum and Curtin University in Western Australia, Phuket Marine Biological Center in Thailand, University of Milano-Bicocca and Marine Research and High Education Center in Maldives (see also FIELD STUDY PERMISSION). Genomic DNA was extracted from the preserved samples using the hot alkaline solution method (Meeker et al., 2007) or QIAGEN DNeasy Blood & Tissue kit (QIAGEN, Hilden, Germany) on site. The first PCR procedure of MIG-seq analysis was carried out at each overseas laboratory except for Thailand samples from which ethanol preserved coral fragments were imported in 2011 (CITES number: AC.0510.2/407). We used them in this study under an additional permit from the Department of Marine and Coastal Resources in Thailand.

### MIG-seq Library Preparation and Sequencing

All the DNA extraction and first PCR procedure except for domestic samples were carried out locally, and the first PCR products were transported to Miyazaki, Japan. The first PCR step was performed by using 8 pairs of multiplex ISSR primers of Suyama and Matsuki (2015). The fragments were amplified with the Multiplex PCR Assay Kit Ver.2 using a total volume of 7  $\mu\text{L}$  reaction in a thermal cycler with the following modified profile:  $94^{\circ}\text{C}$  for 1 min followed by 29 cycles at  $94^{\circ}\text{C}$  for 30 s,  $38^{\circ}\text{C}$  for 1 min,  $72^{\circ}\text{C}$  for 1 min, and a final extension at  $72^{\circ}\text{C}$  for 10 min. The 50-fold diluted first PCR product was used as the template



DNA for the second, tailed-PCR to add the individual index and the Illumina adapter sequence to each sample. PrimeSTAR GXL DNA polymerase (TaKaRa Bio Inc., Otsu, Shiga, Japan) was used for second PCR with a total volume of 12  $\mu$ L reaction in a thermal cycler with a following profile: 20 cycles at 98°C for 10 s, 54°C for 15 s, 68°C for 1 min. The second PCR products were pooled as a single mixture library by using 1  $\mu$ L of each product. The mixed sample was electrophoresed on 0.1% agarose gel to verify amplification. The size ranged from 350 to 800 bp and DNA was manually extracted from the gel on a transilluminator. After extracting genomic DNA from the gel using FastGene Gel/PCR Extraction Kit (Nippon Genetics, Tokyo, Japan), library concentration was measured with a Qubit fluorometer (Thermo Fisher Scientific, Waltham, MA, United States). Finally, the DNA library was sequenced on a MiSeq Sequencer (sequencing control software v2.0.12, Illumina, San Diego, CA, United States) using a MiSeq Reagent Kit v3 (150 cycles; Illumina). Image analysis and base calling were performed using real-time analysis software v1.17.21 (Illumina). DarkCycle option was changed “Amplicon-dark 17-3” to “Amplicon-dark 17-17” on the “Chemistry” line (see also Suyama and Matsuki, 2015).

## Sequence Processing and SNP Genotyping

The FASTX-toolkit version 0.0.14 (Gordon and Hannon, 2012), with a fastq-quality-filter setting of  $-Q\ 33\ -q\ 30\ -p\ 40$ , was used to eliminate low-quality reads and primer sequences from the MIG-seq raw data. Adapter sequences for Illumina MiSeq were removed from both 5' end and 3' end using Cutadapt version 2.10 (Martin, 2011). Short reads less than 80 bp were excluded using an in-house python script. To further exclude contamination from Symbiodiniaceae-DNA, and to obtain larger numbers of loci (Shafer et al., 2017), the filtered raw reads were mapped onto the reference genome of *Heliopora coerulea* obtained from Symbiodiniaceae-free larvae (10.6084/m9.figshare.14356418) using Stacks version 2.2.0 (Catchen et al., 2011; Rochette et al., 2019) with the reference-aligned pipeline for single nucleotide polymorphism (SNP) discovery and genotyping. As a first step, the unpaired reads were removed using the repair.sh software tool within BBtools software package (Bushnell, 2017). Next, the retained reads were aligned to the reference genome using Burrows-Wheeler Aligner (BWA) version 0.0.17-r118 (bwa index and mem with default parameters) (Li and Durbin, 2009). Alignments were then compressed, sorted, and indexed with SAMtools version 1.10 (Li et al., 2009). Finally, SNP genotyping for each individual was carried out using the *gstacks* program in Stacks with default setting. SNP calling for each genetic analysis was carried out using the *populations* program in Stacks with the option *-r* to obtain different minimum proportions of genotyped individuals per locus (0.1 for phylogenetic analyses, 0.9 for assigning clones and population genetic analyses), and the option *-ordered\_export* to ensure that only one of the overlapping SNPs is output from reference aligned data. All the output files from Stacks were converted to the appropriate formats for each genetic analysis using PGDSpider version 2.1.1.5 (Lischer and Excoffier, 2012).

## Assign Clones

We used the software GenoDive version 3.04 (Meirmans, 2020) to assign possible clones within each population based on the infinite allele model (IAM) omitting all missing data. Less than 12 differences of multi-locus genotype within the same population were identified as possible clone mates (estimated by inspection of the pairwise distance histogram in GenoDive). All clone mates except for one individual with the least missing data were removed from this study. After removing possible clones, we selected up to three least missing data samples per sampling site. In case multiple different gross morphologies and/or genetically different lineages were found within the same site, up to three samples per morphology were selected. Finally, we rerun Stacks using this selected dataset excluding possible clones to obtain new SNPs for phylogenetic and population genetic analyses.

## Phylogenetic Analysis

We estimated phylogenetic trees based on the Maximum likelihood (ML) method. The program IQ-TREE2 version 2.0.6 (Minh et al., 2020), using the TVM + F + R5 model selected based on the Bayesian Information Criterion (BIC), was used to reconstruct a phylogenetic hypothesis for *Heliopora* spp. The bootstrap analysis was performed with 1000 replicates using UFBoot, Ultrafast Bootstrap Approximation (Minh et al., 2013). The final tree was drawn using FigTree version 1.4.4 (Rambaut, 2012).

## Population Genetic Analysis

We conducted Principal Coordinates Analysis (PCoA) to examine genetic relationships among *Heliopora* individuals using GenAlEx version 6.502 (Peakall and Smouse, 2012). In addition, Discriminant Analysis of Principal Components (DAPC) (ade4 package version 2.1.3 in R version 4.0.2) (Jombart, 2008; Jombart et al., 2010; Jombart and Ahmed, 2011) was performed to visualize the genetic structure. The lowest BIC was used to detect the optimal number of *K* clusters.

## RESULTS

### Number of Reads and SNPs From MIG-seq Analysis

In total 339,818,358 raw reads with an average of 264,039 reads per sample were obtained for 1,287 individuals. After filtering low-quality reads, 335,164,915 reads with an average of 260,423 reads per sample were obtained. After excluding index, adapter, and short reads less than 80 bp, 139,837,592 reads with an average of 108,654 reads were obtained. In total 67,119,478 reads were mapped onto the reference-genome with an average of 52,152 reads per sample. We used 795 SNPs across 1,287 individuals (*r* = 0.9) to find possible clones, and then excluded 576 individuals from the subsequently genetic analyses. We finally selected 245 individuals from 73 sampling sites from 7 regions (DRA Accession No. DRA012077) for phylogenetic (ML tree; 24,741 SNPs, *r* = 0.1) and population genetic analyses

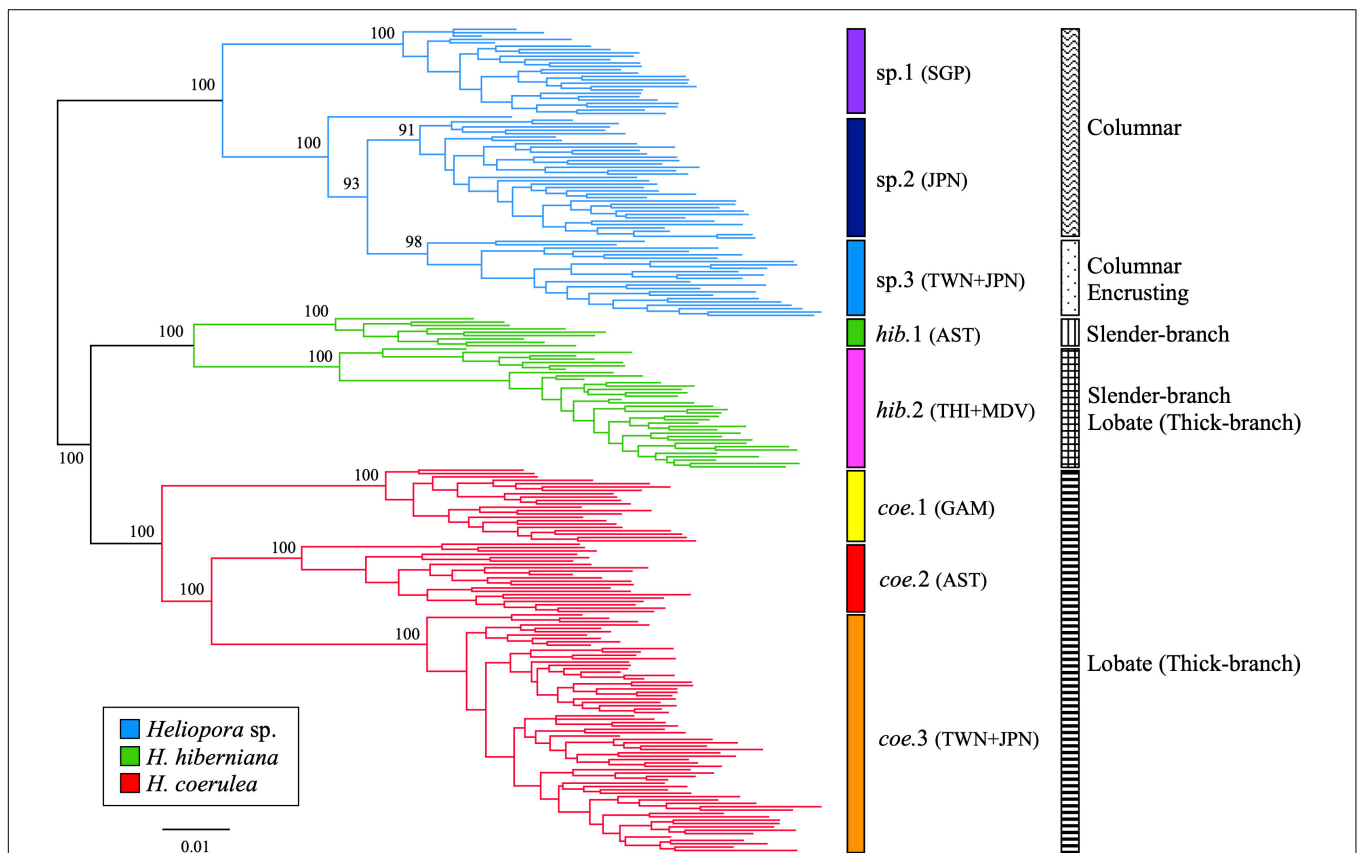


(PCoA and DAPC; 1,092 SNPs,  $r = 0.9$ ). For the latter, we selected 238 individuals from the final dataset after excluding seven individuals with a missing rate of more than 50% per 1,092 SNPs.

## Phylogenetic Relationships

ML phylogenetic analysis revealed three major groups of *Heliopora* spp. in the Indo-West Pacific with 100% bootstrap values (Figure 1). The phylogenetic hypothesis presented here indicated that there is one new undescribed group (hereafter *Heliopora* sp. group) genetically different from the other two groups, each of which includes typical morphologies of the previously described species (slender-branching growth form *H. hiberniana* whose type locality is in the northwestern Australia; lobate growth form *H. coerulea* whose type locality is in the Indian Ocean). The “*Heliopora* sp.” group (shown in blue in Figure 1) comprises the HC-A lineage found in Kuroshio Current regions including Japan and Taiwan (Yasuda et al., 2010, 2014, 2015; Taninaka et al., 2019), and Singapore. The “*H. hiberniana*” group (shown in green in Figure 1) includes the holotype of *H. hiberniana* found in northwestern Australia (Richards et al., 2018) and the eastern Indian Ocean samples from Thailand and the Maldives. The “*H. coerulea*” group (shown in

red in Figure 1) comprises mainly lobate growth morphs HC-B lineage found in Kuroshio Current regions including Japan and Taiwan (Yasuda et al., 2010, 2014, 2015; Taninaka et al., 2019), Guam, and *H. coerulea* found in northwestern Australia (Richards et al., 2018). In addition, there were genetically isolated subclades within each group that clustered together by different growth forms or geographic regions (Figure 1; sp.1–3, *hib*.1–2, and *coe*.1–3). The *Heliopora* sp. group was divided into three subclades: Singapore subclade (sp.1), HC-A with only columnar growth form subclade of Japan (sp.2), and HC-A with both encrusting and columnar growth forms subclade found in both Japan and Taiwan (sp.3). *Heliopora* sp.3 also included a sample collected from 50m depth in Green Island, Taiwan. A sample collected from Yaku Island in Japan, the northernmost distribution site, looks like an outgroup of sp.2 and sp.3 in the phylogeny, possibly because it had a hybrid genotype between *Heliopora* sp.2 and sp.3 based on STRUCTURE analysis (data shown in Supplementary Figure 1). The group “*H. hiberniana*” was divided into two subclades: northwestern Australia *H. hiberniana* subclade (*hib*.1) and a subclade consisting of Thailand and the Maldives samples (*hib*.2). The group “*H. coerulea*” was divided into three subclades; a



**FIGURE 1 |** Maximum likelihood phylogeny of *Heliopora* spp. Node supports are provided if bootstrap values  $\geq 90\%$ . Blue *Heliopora* sp. group composed of three subclades; Singapore subclade (sp.1), a subclade of HC-A with columnar growth form found in Japan (sp.2), and a subclade of HC-A with both encrusting and columnar growth forms found in Japan and Taiwan (sp.3). Green *H. hiberniana* group composed of two subclades; a subclade including the holotype of *H. hiberniana* found in northwestern Australia (*hib*.1) and a Thailand and the Maldives subclade (*hib*.2). Red *H. coerulea* group composed of three subclades; Guam subclade (*coe*.1), a subclade of *H. coerulea* in northwestern Australia (*coe*.2), and a subclade of HC-B found in Japan and Taiwan (*coe*.3).

Guam subclade (*coe.1*), *H. coerulea* in northwestern Australia subclade (*coe.2*), and a subclade consisting of HC-B found in Japan and Taiwan samples (*coe.3*).

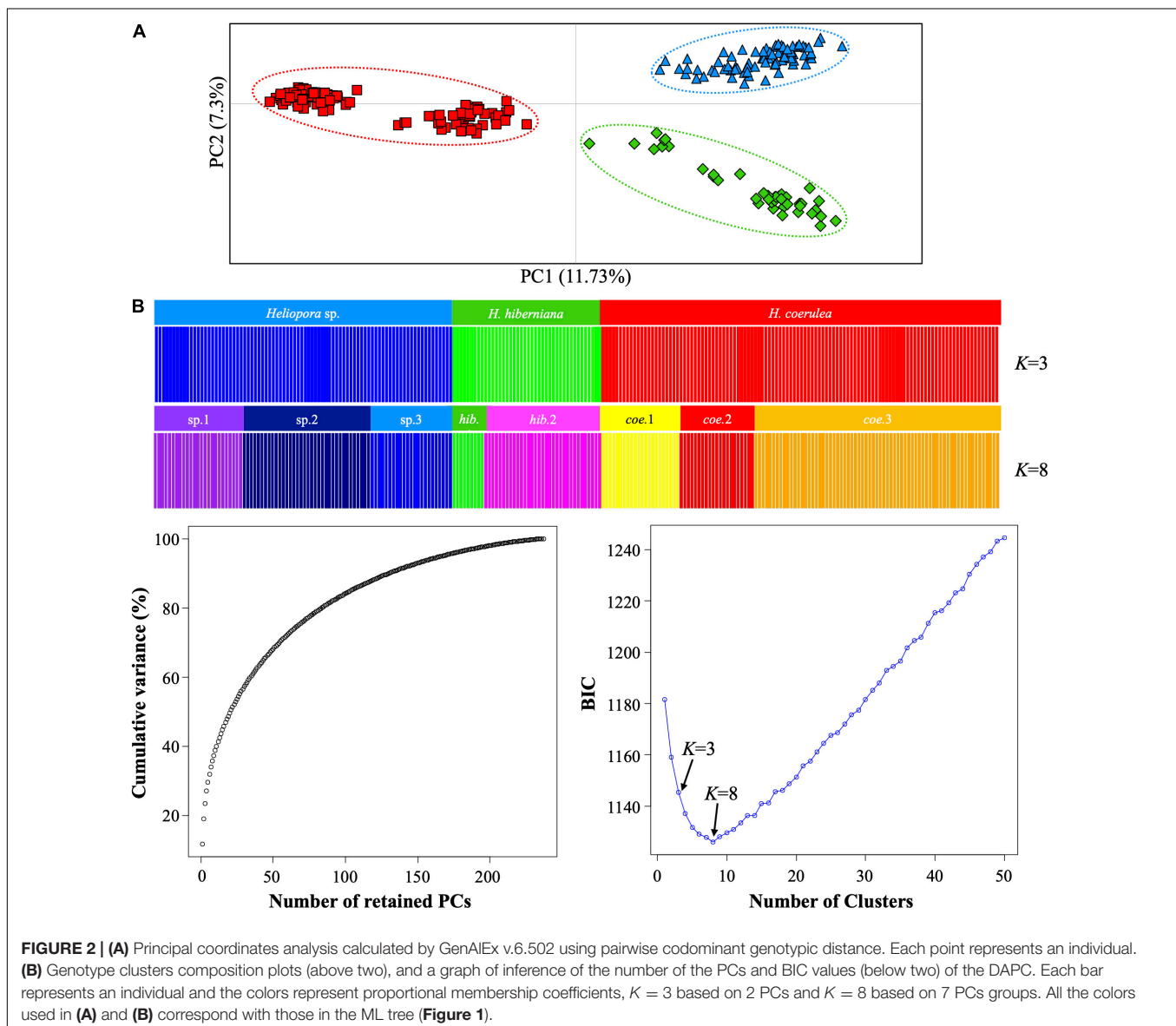
### Individual-Based Genetic Differentiation

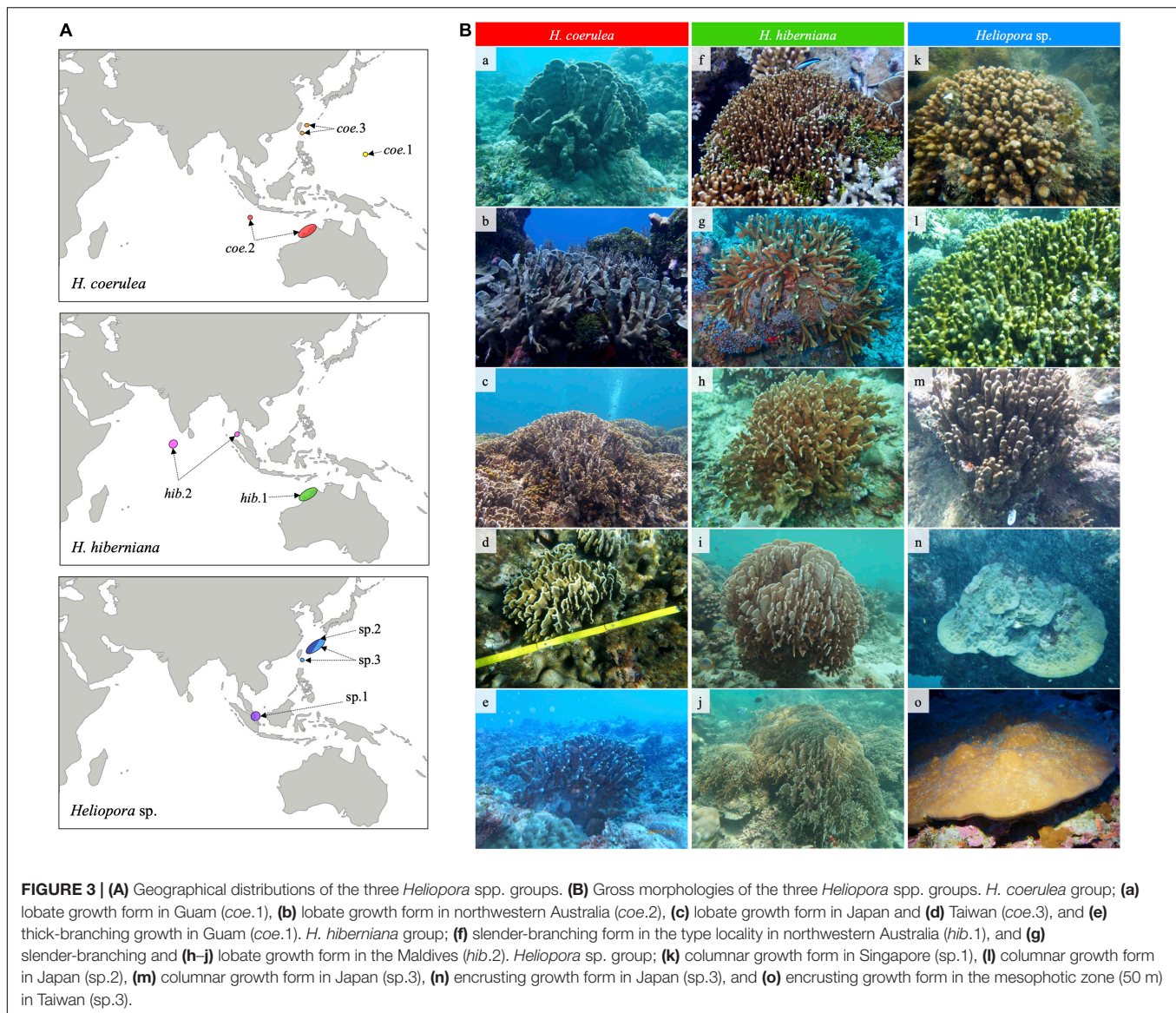
Consistent with the phylogenetic analysis result, population genetic analyses revealed three genetic isolated groups of *Heliopora* with eight subclades in the Indo-West Pacific (Figures 2A,B). The PCoA showed three clusters based on 11.73% (PC1) and 7.3% (PC2) of the total variability (Figure 2A). The DAPC also showed clear genetic separation of the three clusters and eight subclades (Figure 2B).  $K = 3$  was selected supporting the ML phylogeny result, while  $K = 8$  was determined as the optimal number of clusters by calculating the first 200 PCs for the maximum of 50 clusters based on BIC. The posterior DAPC assignments of both  $K = 3$  and 8 were

consistent with the prior clusters (all blue crosses were on red rectangles).

### Geographical Distribution

The three groups of *Heliopora* indicated uneven geographical distribution (Figure 3A). The distribution of *Heliopora* sp. group was biased to western Pacific Ocean side including Kuroshio Current region (Japan and Taiwan) and the South China Sea (Singapore). On the contrary, the distribution of *H. hiberniana* group was mainly in the Indian Ocean side such as Kimberley region and Christmas Island in northwestern Australia, the Andaman Sea (Thailand), and the Maldives. The *H. coerulea* group was distributed both in the Indian Ocean and western Pacific ranging from the Guam and the Kuroshio Current region (Japan and Taiwan) to Kimberley and Christmas Island in northwestern Australia. The distribution of *H. coerulea* group





was partly overlapping with the other two species groups in Japan, Taiwan, and northwestern Australia (Figure 3A, coe.2 and hib.1; coe.3 and sp.2–3).

## Gross Morphology

The gross morphologies of the three groups of *Heliopora* were highly variable (Figure 3B). *H. coerulea* group included two typical morphs; lobate growth form (Figure 3B, a–d) and thick-branching growth form (Figure 3B, e). *H. hiberniana* group included two typical morphs; slender-branching growth form (Figure 3B, f,g) and lobate growth form (Figure 3B, h–j). *Heliopora* sp. group included two typical morphs; columnar growth form (Figure 3B, k–m) and encrusting growth form (Figure 3B, n,o). The typical growth forms of *Heliopora* sp. group were relatively distinct from other two species, while the morphologies of *H. hiberniana* group and *H. coerulea*

group partly overlapped and were difficult to identify by gross morphology.

## DISCUSSION

In the present study, we examined the phylogenetic relationships, gross morphological variations, and the geographical distributions of *Heliopora* spp. collected from the Indo-West Pacific region. Our phylogenetic reconstruction indicates that there are three genetically isolated species groups in the genus *Heliopora* and we provide evidence that there is substantial subcladal genetic structuring within each group.

We do not describe the newly found *Heliopora* sp. group or its subclades as new species of the genus *Heliopora* in this study. Cladistic analysis and formal species description are being undertaken separately.



## Phylogeography and Speciation Patterns of *Heliopora*

Phylogenetic and population genetic analyses using genome-wide SNPs by MIG-seq showed that the Indo-West Pacific *Heliopora* was divided into three groups: *H. coerulea* group, distributed in the Indo-West Pacific and including HC-B in the Kuroshio Current region; *H. hiberniana* group distributed mainly in the Indian Ocean including the type locality of *H. hiberniana* in northwestern Australia; and a new undescribed *Heliopora* sp. group distributed mainly in the Western Pacific Ocean, including HC-A in the Kuroshio Current region (Figures 1, 2 and 3A; Supplementary Table 1).

The new undescribed *Heliopora* sp. group was distributed mainly in the Western Pacific (Japan and Taiwan) and Singapore in this study, while *H. hiberniana* group was distributed mainly in the Indian Ocean (northwestern Australia, the Andaman Sea in Thailand, and the Maldives in this study; distributed also in Indonesia, Richards et al., 2020). Such uneven geographical distributions imply the origin of *Heliopora* sp. group could be in the Pacific Ocean and that of *H. hiberniana* could be in the Indian Ocean, but this remains to be tested with a dated phylogeny. Cenozoic tectonic events (Hall and Holloway, 1998) and sea-level fluctuations associated with climate change (Pillans et al., 1998) in the area between the Indian and Pacific Oceans are thought to have promoted allopatric speciation in many coral reef organisms (Carpenter et al., 2011) including starfish (Benzie, 1999; Vogler et al., 2008) and reef fishes (Gaither et al., 2011; Bowen et al., 2013). It is, therefore, possible that the genus *Heliopora* has also allopatrically speciated into the two groups, *Heliopora* sp. and *H. hiberniana*, due to the physical division between the Indian and Pacific Oceans caused by past tectonic and climatic changes. Morphological and molecular analyses on other Indo-Pacific reef-building coral species also found sibling species between the Indian and Pacific Oceans (Veron, 1995; van Oppen et al., 2001; Pinzón et al., 2013; Huang et al., 2014; Arrigoni et al., 2020; Wepfer et al., 2020).

The *H. coerulea* group is distributed in both the Indian and Western Pacific Oceans. The distribution of *H. coerulea* group partially overlaps with the *Heliopora* sp. group in the western Pacific and with the *H. hiberniana* group in northwestern Australia. Previous studies revealed sympatrically distributed *Heliopora* spp. have different reproductive timing: the reproductive timing of *Heliopora* sp. group (HC-A) and *H. coerulea* group (HC-B) in Japan (Saito et al., 2015; Taninaka et al., 2018) and the Philippines (Villanueva, 2016) differ by almost one month. *Heliopora hiberniana* and *H. coerulea* colonies in northwestern Australia also have been found to have different reproductive timings even when found in sympatry (Richards et al., 2018). These patterns suggest that endogenetic regulation may contribute to differences in reproductive timing. A previous study revealed that there are fixed species-specific substitutions in the dopamine receptor 2-like gene (Isomura et al., 2013) and cryptochrome-1 (Oldach et al., 2017), both of which were

identified as the genes that regulate reproductive timing in *Acropora* species (Iguchi et al., 2019). It is possible that allochronic speciation have occurred between these sympatrically distributed *Heliopora* spp. groups, or at least allochronism in reproductive timing plays a central role to keep their species boundaries after speciation. The difference in reproductive timing is an important mechanism as a prezygotic isolation for marine species that release gametes into the water column (Knowlton, 1993; Palumbi, 1994). Indeed, many of the sympatrically distributed broadcast spawning coral species have different reproductive timing in the same genus (e.g., *Orbicella*, Knowlton et al., 1997; Szmant et al., 1997; *Acropora*, Fukami et al., 2003; Nakajima et al., 2012; Ohki et al., 2015). Generally, the reproductive timing of corals is also strongly associated with environmental factors (e.g., moon phases, moonlight, solar radiation, water temperature) in addition to genetic factors (e.g., circadian clock genes, photoreceptor proteins) that correlate with the environmental factors (e.g., Levy et al., 2007; Brady et al., 2009; Crowder et al., 2017; Oldach et al., 2017). Thus, future studies on reproductive timing of *Heliopora* spp. that include both environmental and genetic factors may provide further insights into speciation of sympatrically distributed *Heliopora* spp.

The *Heliopora* sp. group was found both in Yaku Island in Japan (N 30°16'21.45", Nakabayashi et al., 2017), the northernmost site and at a depth of 50 m on Green Island in Taiwan, the deepest habitat records of the genus *Heliopora*. Therefore, contrary to previous knowledge on the ecological traits of *H. coerulea* that it prefers warm shallow water habitats (Zann and Bolton, 1985), *Heliopora* sp. group could be found in colder and deeper habitat; the northernmost known habitat of *H. coerulea* group (HC-B) is Miyako Island (N 24°51'52.10", Yasuda et al., 2014) and that of *Heliopora* sp. group (HC-A) is Yaku Island (N 30°16'21.45", Nakabayashi et al., 2017). In the field, contrasting ecological differences have been previously observed for *Heliopora* sp. group (HC-A) and *H. coerulea* group (HC-B). Colonies of *Heliopora* sp. group (HC-A) are relatively small and more abundant outside the well-developed fringing reef, where water temperature is lower, while colonies of *H. coerulea* group (HC-B) can be larger, forming micro-atolls, and dominating inner reef habitats where water temperature is higher (Yasuda et al., 2010; Taninaka et al., 2018), providing evidence of niche differentiation which further support the hypothesis of ecological speciation between these two groups.

## Gross Morphological Diversity of *Heliopora*

There are some specific growth forms within each *Heliopora* group. Columnar and encrusting growth forms are relatively distinct from other morphologies and specific to *Heliopora* sp. group (Figure 3B, k-o). Slender-branching growth form with whitish skeleton (Figure 3B, f-g) is also specific to *H. hiberniana* group. However, lobate growth form (Figure 3B, a-d and h-j) can be found in both *H. coerulea* and *H. hiberniana* groups. Like



other reef-building coral species, young and/or juvenile stages are hard to distinguish among closely related species (Babcock, 1992; Babcock et al., 2003). Previous studies have also reported intermediate growth forms sometimes rendering it difficult to distinguish even between HC-A (*Heliopora* sp. group) and HC-B (*H. coerulea* group) possibly due to infrequent hybridization and phenotypic plasticity in the field (Yasuda et al., 2014; Taninaka et al., 2018). Therefore, not all colonies can be clearly classified into the *Heliopora* groups based on field observation alone.

Phenotypic plasticity and continuous morphological variation among closely related coral species are a common phenomenon and have hindered accurate morphological species identification (e.g., Forsman et al., 2009; Marti-Puig et al., 2014; McFadden et al., 2017). Light intensity and water movement are the most influential environmental factors responsible for coral phenotypic plasticity (Todd, 2008), while other physical environmental factors (e.g., dredging, sediment disturbances, turbidity, competition) are also correlated with morphological diversity, leading to continuous morphological variation of different species under similar environmental conditions (e.g., Darling et al., 2012; Erftemeijer et al., 2012; Swierts and Vermeij, 2016). However, it is still unclear what environmental factors influence gross morphological diversity in *Heliopora* spp.

Richards et al. (2018) previously reported the key morphological characteristics to distinguish *H. coerulea* from *H. hiberniana*, including gross morphology, the intensity of bluish skeletal color, and skeletal microstructure (e.g., highly elaborated coenenchymal echinulations and smaller and more numerous autopores), indicating skeletal color can be a key morphological characteristic. In the western Pacific, a few colonies with whitish skeletons have been found in the *Heliopora* sp. group in Japan (H. Taninaka and N. Yasuda pers. obs.). Contrary to the case in the northwestern Australian region, there was no genetic difference between the whitish and other bluish skeleton colonies, indicating skeletal color cannot be a universal key morphological character to distinguish *Heliopora* sp. from the other species.

Based on these findings, it is necessary to clarify the relationship between morphological diversity including fine skeletal structure and environmental and/or genetic factors among *Heliopora* spp. in more detail in the future.

## Subclades Within Each *Heliopora* Group

Our phylogenetic tree showed substantial phylogenetic structure and multiple genetically isolated subclades exist within each *Heliopora* species group. These subclades partially correspond to typical growth forms and geographical distributions (Figures 1, 2 and 3A). In the *Heliopora* sp. group for example, the geographically distant Singapore subclade (sp.1) first diverged from Japan-Taiwan clades (sp.2 and 3). Then, the Japan-Taiwan clades were split into only columnar growth form subclade (sp.2) found only in Japan and encrusting and columnar growth forms subclade (sp.3) found in both Japan and Taiwan. These two subclades were genetically distinct despite being sympatric. In the field, some ecological differences can be observed between the two subclades: *Heliopora* sp.2 tends to be found in shallow inner reef areas with strong

sunlight and relatively weak waves. *Heliopora* sp.3 tends to be found in relatively deep darker areas such as outer reef slope with fast water currents and turbidity (H. Taninaka pers. obs.). Further ecological and physiological differences between *Heliopora* sp.2 and *Heliopora* sp.3 would clarify the species status of the two subclades. The *Heliopora* sp.2 and *Heliopora* sp.3 subclades could not be distinguished in the previous studies using traditional genetic markers (e.g., mitochondrial DNA, ITS2, microsatellite and microsatellite flanking region sequences) (Yasuda et al., 2014, 2015; Taninaka et al., 2019), while this study corroborated the effectiveness of using genome-wide SNPs to elucidate detailed genetic boundaries between closely related lineages/species as in the case of other octocorals (Herrera and Shank, 2016; Quattrini et al., 2019; Takata et al., 2019).

In the *H. hiberniana* group, two subclades (*hib.1-2*) showed deep genetic divergence corresponding to geographical distance, namely the northwestern Australian subclade (*hib.1*) and the Maldives-Thailand subclade (*hib.2*). This genetic isolation could be the result of long-term restriction of gene flow between the two subclades. The current circulation system in the Indian Ocean mainly consists of currents that move from east to west that does not directly connect northern (Maldives and Thailand) and southern (northwestern Australia) sides of the mid-east Indian Ocean (Schott and McCreary, 2001; Schott et al., 2009). Due to such current patterns, previous studies on other marine organisms with pelagic larval phase also showed similar genetic isolation in the Indian Ocean (Benzie et al., 2002; Bay et al., 2004; Hui et al., 2016). On the other hand, geological research (Schettino and Turco, 2011; Keith et al., 2013; Obura, 2016), fossils, and phylogenetic data (Obura, 2012, 2016; Veron et al., 2015) propose a hypothesis that tectonic changes occurred during the Paleogene and the Neogene and may have promoted genetic isolation and speciation events in the Indian Ocean. Such historical geographic events might have promoted genetic divergence of *Heliopora* spp. in the Indian Ocean, but this requires further testing within a calibrated phylogenetic framework.

In the *H. coerulea* group, three subclades (*coe.1-3*) corresponding to geographically distinct regions were found, namely Guam subclade (*coe.1*), the northwestern Australia subclade (*coe.2*), and Japan-Taiwan subclade (*coe.3*). The most genetically isolated subclade that first split from the others is the Guam subclade (*coe.1*). It is notable that Japan-Taiwan subclade (*coe.3*) is genetically more closely related to the northwestern Australia subclade (*coe.2*) in the Indian Ocean than to the geographically closer Guam subclade (*coe.1*). It is likely that genetic connectivity has been restricted between Guam and Japan-Taiwan since the Guam subclade (*coe.1*) diverged from the other two subclades early in the history of *H. coerulea*. This is unusual because genetic connectivity between Mariana Islands region including Guam and the Kuroshio Current region is often strong in most of the marine invertebrate species with larval dispersal period (e.g., Palumbi et al., 1997; Williams and Benzie, 1998; Lessios et al., 2001; Pinzón et al., 2013; Arrigoni et al., 2020; Wepfer et al., 2020; but see exception

in Wörheide et al., 2008). Although the reasons for the genetic break between Guam and Kuroshio Current region in *Heliopora* spp. are unclear, it could be caused by limited larval dispersal capability of *Heliopora* spp. (Taninaka et al., 2019) and/or local adaptation of each subclade. On the other hand, northwestern Australian populations of other marine species are genetically more similar to west Pacific populations than other Indian Ocean populations (e.g., Williams and Benzie, 1998; Lessios et al., 2001; Pinzón et al., 2013; Arrigoni et al., 2020; Wepfer et al., 2020) but contrary examples also exist where Indian and Pacific Ocean coral populations are divergent (e.g., Richards et al., 2016). Williams and Benzie (1998) discussed that this might be due to Western Australia being recently colonized by recruits from the Western Pacific lineage after the end of the last ice age. Recent genome-wide phylogeographic analysis of reef-building corals have also found such large discrepancies between geographic and genetic distances (Arrigoni et al., 2020; Wepfer et al., 2020), which need to be examined in closer detail in the future.

## CONCLUSION

The present study provides a comprehensive picture of phylogenetic relationships, distribution, and growth form patterns among closely related *Heliopora* species that gives new insights into speciation patterns of *Heliopora* spp. in the Indo-West Pacific. Our genome-wide genetic data of *Heliopora* spp. revealed three major groups with eight subclades. *Heliopora* sp. group was genetically distinct from the other two groups (*H. coerulea* group and *H. hiberniana* group) containing the samples from type localities of the previously described species. Genetic diversification in the genus *Heliopora* could be attributed to allopatry, allochrony, and local and/or ecological adaptation. Further studies incorporating more genome-wide markers for phylogeographic analysis, geohistorical information, physiological and ecological data would more precisely delineate the boundaries of *Heliopora* species.

Our study also demonstrates the effectiveness of the MIG-seq method for clarifying the species boundaries of octocoral species that were indistinguishable using traditional genetic markers such as *mtDNA* and ITS2. In addition, we highlight the importance of wide geographic sampling to generate a more complete picture of the phylogeographic relationships and speciation patterns among closely related octocoral species and how they diversified across the Indo-Pacific. It is expected that the MIG-seq method can be applied to other coral species and non-model organisms to resolve longstanding questions in marine evolution.

## FIELD STUDY PERMISSION

Domestic sampling except for Amami Oshima was conducted under each prefectural government permits; Yaku Island (Kagoshima Prefectural Government permit, No. 2–56), Okinawa including Okinawa Mainland, Kume Island, Ishigaki

Island, Sekisei Lagoon, and Iriomote Island (Okinawa Prefectural Government permits, Nos. 18–34, 19–39, 19–60, 21–18, 22–15, 25–44, 26–10, 27–29, 27–81, 28–78, 30–42, and 31–18), and Amami Oshima was conducted under personal permit by Mr. Katsuki Oki. Foreign sampling was conducted under each local government permits; Taiwan (samples collected from Dabaisha and Gongguan, the Taitung County Government, No. 1074150258; a 50 m specimen collected in Chaiko, Taitung County Government, No. 1040000285, and that is registered at the Zoological collection of the Biodiversity Research Museum in Academia Sinica AZIC0001313), Guam (SC-19-006 (occ), University of Guam Marine Laboratory), Singapore (National Parks Board Permit NP/RP16-156), Australia (samples in Western Australia were collected under permit number AU-COM2013-203 and Australian Government approval number 006-RRRW-130723-01), Thailand (the permission for collecting and sending the specimens is granted by the Department of Fisheries), Maldives (Permit No. (OTHR)30-D/INDIV/2017/123 released by the Maldivian Ministry of Fisheries and Agriculture). All the 1st PCR except for those from Thailand were conducted on site and only 1st PCR products were brought or sent to Japan. Ethanol-preserved coral fragment samples from Thailand were imported to Japan in 2011 (CITES number: AC.0510.2/407), and we used them in this study under an additional permit from the Department of Marine and Coastal Resources in Thailand.

## DATA AVAILABILITY STATEMENT

The datasets presented in this study can be found in online repositories. The names of the repository/repositories and accession number(s) can be found below: DDBJ (accession: DRA012077), FigShare (doi: 10.6084/m9.figshare.14356418 and doi: 10.6084/m9.figshare.14814231).

## AUTHOR CONTRIBUTIONS

HT and NY conceived the study and drafted the manuscript. All authors except for TK and HY collected samples and conducted molecular genetic experiment. HT, TK, and HY conducted genetic analysis. All authors edited the draft and approved it for publication.

## FUNDING

Funding of this study was provided by the Environmental Research and Technology Development Fund (4RF-1501 and 4-1304) of the Ministry of the Environment, Japan; a Grant-in-Aid for Young Scientists (A) (17H04996); a Grant-in-Aid for Research Fellows (19J21342) by The Japan Society for the Promotion of Science (JSPS); and the Marine Science R&D Programme (MSRDP-P03) supported by the National Research Foundation, Prime Minister's Office, Singapore. ZR was supported by a JSPS short-term visiting Fellowship to the University of Miyazaki and samples from Western Australia were

collected with the support of Woodside Energy on the Woodside Kimberley Collection Project.

## ACKNOWLEDGMENTS

We are grateful to Eriko Nagahiro for her assistance for genetic analysis. DM would like to thank Marco Casartelli and Julian Sitemba for their help in laboratory activities.

## SUPPLEMENTARY MATERIAL

The Supplementary Material for this article can be found online at: <https://www.frontiersin.org/articles/10.3389/fmars.2021.714662/full#supplementary-material>

## REFERENCES

- Abe, M., Ohno, M., Kurozumi, T., Goto, T., Suzuki, R., Hasegawa, H., et al. (2008). *Report of the Survey of Heliopora coerulea Communities in Oura Bay, Okinawa* (in Japanese).
- Altieri, A. H., Harrison, S. B., Seemann, J., Collin, R., Diaz, R. J., and Knowlton, N. (2017). Tropical dead zones and mass mortalities on coral reefs. *Proc. Natl. Acad. Sci. U.S.A.* 114, 3660–3665. doi: 10.1073/pnas.1621517114
- Arrigoni, R., Berumen, M. L., Mariappan, K. G., Beck, P. S. A., Hulver, A. M., Montano, S., et al. (2020). Towards a rigorous species delimitation framework for scleractinian corals based on RAD sequencing: the case study of *Leptastrea* from the Indo-Pacific. *Coral Reefs* 39, 1001–1025. doi: 10.1007/s00338-020-01924-8
- Babcock, R. (1990). Reproduction and development of the blue coral *Heliopora coerulea* (Alcyonaria: Coenothecalia). *Mar. Biol.* 104, 475–481. doi: 10.1007/bf01314352
- Babcock, R. C. (1992). *Workshop on Coral and Fish Recruitment*. Manila, PH: University of the Philippines.
- Babcock, R. C., Baird, A. H., Piromvaragorn, S., Thomson, D. P., and Willis, B. L. (2003). Identification of scleractinian coral recruits from Indo-Pacific reefs. *Zool. Stud.* 42, 211–226.
- Baird, N. A., Etter, P. D., Atwood, T. S., Currey, M. C., Shiver, A. L., Lewis, Z. A., et al. (2008). Rapid SNP discovery and genetic mapping using sequenced RAD markers. *PLoS One* 3:e3376. doi: 10.1371/journal.pone.0003376
- Bay, L., Choat, J. H., Herwerden, L., and Robertson, D. R. (2004). High genetic diversities and complex genetic structure in an Indo Pacific tropical reef fish (*Chlorurus sordidus*): evidence of an unstable evolutionary past? *Mar. Biol.* 144, 757–767. doi: 10.1007/s00227-003-1224-3
- Benzie, J. A. H. (1999). Genetic structure of coral reef organisms: ghosts of dispersal past. *Am. Zool.* 39, 131–145. doi: 10.1093/icb/39.1.131
- Benzie, J. A. H., Ballment, E., Forbes, A. T., Demetriades, N. T., Sugama, K., and Haryanti, M. S. (2002). Mitochondrial DNA variation in Indo-Pacific populations of the giant tiger prawn, *Penaeus monodon*. *Mol. Ecol.* 11, 2553–2569. doi: 10.1046/j.1365-294x.2002.01638.x
- Bickford, D. P., Lohman, D. J., Sodhi, N. S., Ng, P. K. L., Meier, R., Winker, K., et al. (2007). Cryptic species as a window on diversity and conservation. *Trends Ecol. Evol.* 22, 148–155. doi: 10.1016/j.tree.2006.11.004
- Bilewicz, J. P., and Degnan, S. M. (2011). A unique horizontal gene transfer event has provided the octocoral mitochondrial genome with an active mismatch repair gene that has potential for an unusual self-contained function. *BMC Evol. Biol.* 11:228. doi: 10.1186/1471-2148-11-228
- Birkeland, C., and Lucas, J. S. (1990). *Acanthaster planci: Major Management Problem of Coral Reefs*. West Palm Beach: CRC Press.
- Bouillon, J., and Houvenaghel-Grévecoeur, N. (1970). Etude monographique du genre *Heliopora* de Blainville (Cenothecalia - Alcyonaria - Coelenterata). *Ann. Mus. Roy. Afr. Centr. Sci. Zool.* 178, 1–83.
- Supplementary Figure 1** | A bar plot of *Heliopora* sp. estimated by STRUCTURE ver. 2.3.4 assuming the number of cluster  $K = 3$  using 225 SNPs obtained from the Stacks ( $r = 0.9$  with the option `-write_single_snp`). Ten independent runs based on 200,000 burn-in followed by 200,000 Markov chain Monte Carlo (MCMC) replications were conducted using admixture models assuming correlated allele frequencies among 84 samples with uniform prior. The x-axis indicates each individual for *Heliopora* sp. that were classified into three subclades (sp.1–sp.3) in the phylogenetic tree (**Figure 1**). Different colors of the y-axis indicate the probability of assignment to different clusters. Red allows indicate possible hybrid individuals.
- Supplementary Table 1** | Summary of sample information in this study: name of sampling country “Country,” name of sampling region “Region,” name of sampling site “Location,” longitude and latitude “Coordinates,” number of collected samples “Ns” and analyzed samples “Na,” ratio of assigned possible clones within each population “Rc,” name of *Heliopora* species group “Spp. group” and subclade “Subclade,” observed growth forms within each subclade “Major form (minor form),” and sampling years with published references “Year (References).”
- Bowen, B. W., Rocha, L. A., Toonen, R. J., and Karl, S. A. (2013). The origins of tropical marine biodiversity. *Trends Ecol. Evol.* 28, 359–366. doi: 10.1016/j.tree.2013.01.018
- Brady, A. K., Hilton, J. D., and Vize, P. D. (2009). Coral spawn timing is a direct response to solar light cycles and is not an entrained circadian response. *Coral Reefs* 28, 677–680. doi: 10.1007/s00338-009-0498-4
- Bruno, J. F., Petes, L. E., Harvell, C. D., and Hettinger, A. (2003). Nutrient enrichment can increase the severity of coral diseases. *Ecol. Lett.* 6, 1056–1061. doi: 10.1046/j.1461-0248.2003.00544.x
- Bruno, J. F., Selig, E. R., Casey, K. S., Page, C. A., Willis, B. L., Harvell, C. D., et al. (2007). Thermal stress and coral cover as drivers of coral disease outbreaks. *PLoS Biol.* 5:e124. doi: 10.1371/journal.pbio.0050124
- Burge, C. A., Mark Eakin, C., Friedman, C. S., Froelich, B., Hershberger, P. K., Hofmann, E. E., et al. (2014). Climate change influences on marine infectious diseases: implications for management and society. *Ann. Rev. Mar. Sci.* 6, 249–277. doi: 10.1146/annurev-marine-010213-135029
- Bushnell, B. (2017). *BBTools Software Package*. Available online at: <http://sourceforge.net/projects/bbmap> (accessed November 13, 2019).
- Carpenter, K. E., Abrar, M., Aeby, G., Aronson, R. B., Banks, S., Bruckner, A., et al. (2008). One-third of reef-building corals face elevated extinction risk from climate change and local impacts. *Science* 321, 560–563.
- Carpenter, K. E., Barber, P. H., Crandall, E. D., Ablan-Lagman, M. C. A., Ambaryanto, M., Mahardika, G. N., et al. (2011). Comparative phylogeography of the coral triangle and implications for marine management. *J. Mar. Biol.* 2011, 1–14. doi: 10.1155/2011/396982
- Catchen, J. M., Amores, A., Hohenlohe, P., Cresko, W., and Postlethwait, J. H. (2011). Stacks: building and genotyping loci de novo from short-read sequences. *G3 Genes Genom. Genet.* 1, 171–182. doi: 10.1534/g3.111.000240
- Cesar, H., Burke, L., and Pet-Soede, L. (2003). *The Economics of Worldwide Coral Reef Degradation*. Arnhem: Cesar Environmental Economics Consulting.
- Colgan, M. W. (1984). “The cretaceous coral *Heliopora* (Octocorallia, Coenothecalia)-a common indo-pacific reef builder,” in *Living Fossils*, eds N. Eldredge and S. M. Stanley (Berlin: Springer).
- Crowder, C. M., Meyer, E., Fan, T. Y., and Weis, V. M. (2017). Impacts of temperature and lunar day on gene expression profiles during a monthly reproductive cycle in the brooding coral *Pocillopora damicornis*. *Mol. Ecol.* 26, 3913–3925. doi: 10.1111/mec.14162
- Dana, J. D. (1846). *Zoophytes. United States Exploring Expedition V.7*. Washington: Smithsonian libraries, 740.
- Darling, E. S., Alvarez-Filip, L., Oliver, T. A., McClanahan, T. R., and Côté, I. M. (2012). Evaluating life-history strategies of reef corals from species traits. *Ecol. Lett.* 15, 1378–1386. doi: 10.1111/j.1461-0248.2012.01861.x
- de Oliveira Soares, M., Matos, E., Lucas, C., Rizzo, L., Allcock, L., and Rossi, S. (2020). Microplastics in corals: an emergent threat. *Mar. Pollut. Bull.* 161:111810. doi: 10.1016/j.marpolbul.2020.111810
- Eguchi, M. (1948). Fossil Helioporidae from Japan and the South Sea Islands. *J. Paleont.* 22, 362–364.



- Erfteimeijer, P. L. A., Riegl, B., Hoeksema, B. W., and Todd, P. A. (2012). Environmental impacts of dredging and other sediment disturbances on corals: a review. *Mar. Pollut. Bull.* 64, 1737–1765. doi: 10.1016/j.marpolbul.2012.05.008
- Eyre, B. D., Cyronak, T., Drupp, P., De Carlo, E. H., Sachs, J. P., and Andersson, A. J. (2018). Coral reefs will transition to net dissolving before end of century. *Science* 359, 908–911. doi: 10.1126/science.aao1118
- Fabricius, K., and Alderslade, P. (2001). *Soft Corals and Sea Fans: a Comprehensive Guide to the Tropical Shallow-Water Genera of the Central-West Pacific, the Indian Ocean and the Red Sea*. Townsville, AU: Australian Institute of Marine Science.
- Fisher, R., O'Leary, R. A., Low-Choy, S., Mengersen, K., Knowlton, N., Brainard, R. E., et al. (2015). Species richness on coral reefs and the pursuit of convergent global estimates. *Curr. Biol.* 25, 500–505. doi: 10.1016/j.cub.2014.12.022
- Flot, J. F., Magalon, H., Cruaud, C., Couloux, A., and Tillier, S. (2008). Patterns of genetic structure among Hawaiian corals of the genus *Pocillopora* yield clusters of individuals that are compatible with morphology. *C. R. Biol.* 331, 239–247. doi: 10.1016/j.crvi.2007.12.003
- Forsman, Z. H., Barshis, D. J., Hunter, C. L., and Toonen, R. J. (2009). Shape-shifting corals: molecular markers show morphology is evolutionarily plastic in *Porites*. *BMC Evol. Biol.* 9:45. doi: 10.1186/1471-2148-9-45
- Forsman, Z. H., Knapp, I. S. S., Tisthammer, K., Eaton, D. A. R., Belcaid, M., and Toonen, R. J. (2017). Coral hybridization or phenotypic variation? Genomic data reveal gene flow between *Porites lobata* and *P. compressa*. *Mol. Phylogenet. Evol.* 111, 132–148. doi: 10.1016/j.ympev.2017.03.023
- Fukami, H., Omori, M., Shimoike, K., Hayashibara, T., and Hatta, M. (2003). Ecological and genetic aspects of reproductive isolation by different spawning times in *Acropora* corals. *Mar. Biol.* 142, 679–684. doi: 10.1007/s00227-002-1001-8
- Gaither, M. R., Bowen, B. W., Bordenave, T. R., Rocha, L. A., Newman, S. J., Gomez, J. A., et al. (2011). Phylogeography of the reef fish *Cephalopholis argus* (Epinephelidae) indicates Pleistocene isolation across the Indo-Pacific Barrier with contemporary overlap in the Coral Triangle. *BMC Evol. Biol.* 11:189. doi: 10.1186/1471-2148-11-189
- Gordon, A., and Hannon, G. J. (2012). *FASTX-Toolkit. FASTQ/A Short-Reads Pre-Processing Tools*. Available online at: [http://hannonlab.cshl.edu/fastx\\_toolkit/](http://hannonlab.cshl.edu/fastx_toolkit/) (accessed November 13, 2019).
- Hall, R., and Holloway, J. D. (1998). *Biogeography and Geological Evolution of SE Asia*. Palo Alto, CA: Backhuys.
- Halpern, B. S., Walbridge, S., Selkoe, K. A., Kappel, C. V., Micheli, F., D'Agrosa, C., et al. (2008). A global map of human impact on marine ecosystems. *Science* 319, 948–952.
- Harii, S., and Kayanne, H. (2003). Larval dispersal, recruitment, and adult distribution of the brooding stony octocoral *Heliopora coerulea* on Ishigaki Island, southwest Japan. *Coral Reefs* 22, 188–196. doi: 10.1007/s00338-003-0302-9
- Harii, S., Kayanne, H., Takigawa, H., Hayashibara, T., and Yamamoto, M. (2002). Larval survivorship, competency periods and settlement of two brooding corals, *Heliopora coerulea* and *Pocillopora damicornis*. *Mar. Biol.* 141, 39–46. doi: 10.1007/s00227-002-0812-y
- Herrera, S., and Shank, T. M. (2016). RAD sequencing enables unprecedented phylogenetic resolution and objective species delimitation in recalcitrant divergent taxa. *Mol. Phylogenet. Evol.* 100, 70–79. doi: 10.1016/j.ympev.2016.03.010
- Hirai, J. (2019). Insights into reproductive isolation within the pelagic copepod *Pleuromamma abdominalis* with high genetic diversity using genome-wide SNP data. *Mar. Biol.* 167:1. doi: 10.1007/s00227-019-3618-x
- Hoegh-Guldberg, O. (2011). Coral reef ecosystems and anthropogenic climate change. *Reg. Environ. Chang.* 11, S215–S227.
- Hoegh-Guldberg, O., and Bruno, J. F. (2010). The impact of climate change on the world's marine ecosystems. *Science* 328, 1523–1528. doi: 10.1126/science.1189930
- Hoegh-Guldberg, O., Mumby, P. J., Hooten, A. J., Steneck, R. S., Greenfield, P., Gomez, E., et al. (2007). Coral reefs under rapid climate change and ocean acidification. *Science* 318, 1737–1742. doi: 10.1126/science.1152509
- Huang, D., Benzoni, F., Arrigoni, R., Baird, A. H., Berumen, M. L., Bouwmeester, J., et al. (2014). Towards a phylogenetic classification of reef corals: the Indo-Pacific genera *Merulina*, *Goniastrea* and *Scapophyllia* (Scleractinia, Merulinidae). *Zool. Scripta* 43, 531–548. doi: 10.1111/zsc.12061
- Huang, W., Chen, M., Song, B., Deng, J., Shen, M., Chen, Q., et al. (2020). Microplastics in the coral reefs and their potential impacts on corals: a mini-review. *Sci. Total Environ.* 762:143112. doi: 10.1016/j.scitotenv.2020.143112
- Hughes, T. P., Anderson, K. D., Connolly, S. R., Heron, S. F., Kerry, J. T., Lough, J. M., et al. (2018). Spatial and temporal patterns of mass bleaching of corals in the Anthropocene. *Science* 359, 80–83. doi: 10.1126/science.aan8048
- Hughes, T. P., Baird, A. H., Bellwood, D. R., Card, M., Connolly, S. R., Folke, C., et al. (2003). Climate change, human impacts, and the resilience of coral reefs. *Science* 301, 929–933. doi: 10.1126/science.1085046
- Hui, M., Kraemer, W. E., Seidel, C., Nuryanto, A., Joshi, A., and Kochzius, M. (2016). Comparative genetic population structure of three endangered giant clams (Cardiidae: *Tridacna* species) throughout the Indo-West Pacific: implications for divergence, connectivity and conservation. *J. Mollusc. Stud.* 82, 403–414. doi: 10.1093/mollus/eyw001
- Iguchi, A., Yoshioka, Y., Forsman, Z. H., Knapp, I. S., Toonen, R. J., Hongo, Y., et al. (2019). RADseq population genomics confirms divergence across closely related species in blue coral (*Heliopora coerulea*). *BMC Evol. Biol.* 19:187. doi: 10.1186/s12862-019-1522-0
- Isomura, N., Yamauchi, C., Takeuchi, Y., and Takemura, A. (2013). Does dopamine block the spawning of the acroporid coral *Acropora tenuis*? *Sci. Rep.* 3:2649.
- Johnston, E. C., Forsman, Z. H., Flot, J. F., Schmidt-Roach, S., Pinzón, J. H., Knapp, I. S. S., et al. (2017). A genomic glance through the fog of plasticity and diversification in *Pocillopora*. *Sci. Rep.* 7:5991. doi: 10.1038/s41598-017-06085-3
- Jombart, T. (2008). adegenet: a R package for the multivariate analysis of genetic markers. *Bioinformatics* 24, 1403–1405. doi: 10.1093/bioinformatics/btn129
- Jombart, T., and Ahmed, I. (2011). adegenet 1.3-1: new tools for the analysis of genome-wide SNP data. *Bioinformatics* 27, 3070–3071. doi: 10.1093/bioinformatics/btr521
- Jombart, T., Devillard, S., and Balloux, F. (2010). Discriminant analysis of principal components: a new method for the analysis of genetically structured populations. *BMC Genet.* 11:94. doi: 10.1186/1471-2156-11-94
- Keith, S. A., Baird, A. H., Hughes, T. P., Madin, J. S., and Connolly, S. R. (2013). Faunal breaks and species composition of Indo-Pacific corals: the role of plate tectonics, environment and habitat distribution. *Proc. R. Soc. Lond.* 280:20130818. doi: 10.1098/rspb.2013.0818
- Keyse, J., Crandall, E. D., Toonen, R. J., and Trembl, E. A. (2014). The scope of published population genetic data for Indo-Pacific marine fauna and future research opportunities in the region. *Bull. Mar. Sci.* 90, 47–78. doi: 10.5343/bms.2012.1107
- Knowlton, N. (1993). Sibling species in the sea. *Annu. Rev. Ecol. Syst.* 24, 189–216. doi: 10.1146/annurev.es.24.110193.001201
- Knowlton, N., Mate, J. L., Guzman, H. M., Rowan, R., and Jara, J. (1997). Direct evidence for reproductive isolation among the three species of the *Montastraea annularis* complex in Central America (Panama and Honduras). *Mar. Biol.* 127, 705–711. doi: 10.1007/s002270050061
- Lessios, H. A., Kessing, B. D., and Pearse, J. S. (2001). Population structure and speciation in tropical seas: global phylogeography of the sea urchin *Diadema*. *Evolution* 55, 955–975. doi: 10.1554/0014-3820(2001)055[0955:psait]2.0.co;2
- Levitani, D. R., Fogarty, N. D., Jara, J., Lotterhos, K. E., and Knowlton, N. (2011). Genetic, spatial, and temporal components of precise spawning synchrony in reef building corals of the *Montastraea annularis* species complex. *Evolution* 65, 1254–1270. doi: 10.1111/j.1558-5646.2011.01235.x
- Levy, O., Appelbaum, L., Leggat, W., Gothliff, Y., Hayward, D. C., Miller, D. J., et al. (2007). Light-responsive cryptochromes from a simple multicellular animal, the coral *Acropora millepora*. *Science* 318, 467–470. doi: 10.1126/science.1145432
- Li, H., and Durbin, R. (2009). Fast and accurate short read alignment with Burrows - Wheeler transform. *Bioinformatics* 25, 1754–1760. doi: 10.1093/bioinformatics/btp324
- Li, H., Handsaker, B., Wysoker, A., Fennell, T., Ruan, J., Homer, N., et al. (2009). The Sequence Alignment/Map format and SAMtools. *Bioinformatics* 25, 2078–2079. doi: 10.1093/bioinformatics/btp352
- Lischer, H. E. L., and Excoffier, L. (2012). PGDSpider: an automated data conversion tool for connecting population genetics and genomics programs. *Bioinformatics* 28, 298–299. doi: 10.1093/bioinformatics/btr642
- Luzon, K. S., Lin, M. F., Lagman, M. C. A. A., Licuanan, W. R. Y., and Chen, C. A. (2017). Resurrecting a subgenus to genus: molecular phylogeny of *Euphyllia* and *Fimbriaphyllia* (order Scleractinia; family Euphyllidae; clade V). *PeerJ* 5:e4074. doi: 10.7717/peerj.4074



- Marquez, L. M., van Oppen, M. J. H., Willis, B. L., and Yan, M. (2002). Sympatric populations of the highly cross-fertile coral species, *Acropora hyacinthus* and *Acropora cytherea*, are genetically distinct. *Proc. R. Soc. B* 269, 1289–1294. doi: 10.1098/rspb.2002.2014
- Martin, M. (2011). Cutadapt removes adapter sequences from high-throughput sequencing reads. *EMBnet J.* 17, 10–12. doi: 10.14806/ej.17.1.200
- Marti-Puig, P., Forsman, Z. H., Haverkort-Yeh, R. D., Knapp, I. S., Maragos, J. E., and Toonen, R. J. (2014). Extreme phenotypic polymorphism in the coral genus *Pocillopora*: micro-morphology corresponds to mitochondrial groups, while colony morphology does not. *Bull. Mar. Sci.* 90, 211–231. doi: 10.5343/bms.2012.1080
- McFadden, C. S., Haverkort-Yeh, R., Reynolds, A. M., Halász, A., Quattrini, A. M., Forsman, Z. H., et al. (2017). Species boundaries in the absence of morphological, ecological or geographical differentiation in the Red Sea *Octocoral* genus *Ovabunda* (Alcyonacea: Xenidiidae). *Mol. Phylogenet. Evol.* 112, 174–184. doi: 10.1016/j.ympev.2017.04.025
- Meeker, N. D., Hutchinson, S. A., Ho, L., and Trede, N. S. (2007). Method for isolation of PCR-ready genomic DNA from zebrafish tissues. *Biotechniques* 43, 610–614. doi: 10.2144/000112619
- Meirmans, P. G. (2020). GENODIVE version 3.0: easy-to-use software for the analysis of genetic data of diploids and polyploids. *Mol. Ecol. Resour.* 20, 1126–1131. doi: 10.1111/1755-0998.13145
- Miller, M. R., Dunham, J. P., Amores, A., Cresko, W. A., and Johnson, E. A. (2007). Rapid and cost-effective polymorphism identification and genotyping using restriction site associated DNA (RAD) markers. *Genome Res.* 17, 240–248. doi: 10.1101/gr.5681207
- Minh, B. Q., Nguyen, M. A., and von Haeseler, A. (2013). Ultrafast approximation for phylogenetic bootstrap. *Mol. Biol. Evol.* 30, 1188–1195. doi: 10.1093/molbev/mst024
- Minh, B. Q., Schmidt, H. A., Chernomor, O., Schrempf, D., Woodhams, M. D., von Haeseler, A., et al. (2020). IQ-TREE 2: new models and efficient methods for phylogenetic inference in the genomic era. *Mol. Biol. Evol.* 37, 1530–1534. doi: 10.1093/molbev/msaa015
- Moberg, F., and Folke, C. (1999). Ecological goods and services of coral reef ecosystems. *Ecol. Econ.* 29, 215–233. doi: 10.1016/s0921-8009(99)00009-9
- Montalbetti, E., Saponari, L., Montano, S., Maggioni, D., Dehnert, I., Galli, P., et al. (2019). New insights into the ecology and corallivory of *Culcita* sp. (Echinodermata: Asteroidea) in the Republic of Maldives. *Hydrobiologia* 827, 353–365. doi: 10.1007/s10750-018-3786-6
- Nakabayashi, A., Matsumoto, T., Kitano, Y. F., Nagai, S., and Yasuda, N. (2017). Discovery of the northernmost habitat of the blue coral *Heliopora coerulea*: possible range expansion due to climate change? *Galaxea J. Coral Reef Stud.* 18, 1–2. doi: 10.3755/galaxea.19.1\_1
- Nakajima, Y., Nishikawa, A., Iguchi, A., Nagata, T., Uyeno, D., Sakai, K., et al. (2017). Elucidating the multiple genetic lineages and population genetic structure of the brooding coral *Seriatopora* (Scleractinia: Pocilloporidae) in the Ryukyu Archipelago. *Coral Reefs* 36, 415–426. doi: 10.1007/s00338-017-1557-x
- Nakajima, Y., Nishikawa, A., Iguchi, A., and Sakai, K. (2012). The population genetic approach delineates the species boundary of reproductively isolated corymbose acroporid corals. *Mol. Phylogenet. Evol.* 63, 527–531. doi: 10.1016/j.ympev.2012.01.006
- Obura, D. O. (2012). The diversity and biogeography of Western Indian Ocean reef-building corals. *PLoS One* 7:e45013. doi: 10.1371/journal.pone.0045013
- Obura, D. O. (2016). An Indian Ocean centre of origin revisited: palaeogene and neogene influences defining a biogeographic realm. *J. Biogeogr.* 43, 229–242. doi: 10.1111/jbi.12656
- Ohki, S., Kowalski, R. K., Kitanobo, S., and Morita, M. (2015). Changes in spawning time led to the speciation of the broadcast spawning corals *Acropora digitifera* and the cryptic species *Acropora* sp. 1 with similar gamete recognition systems. *Coral Reefs* 34, 1189–1198. doi: 10.1007/s00338-015-1337-4
- Oldham, M. J., Workentine, M., Matz, M. V., Fan, T. Y., and Vize, P. D. (2017). Transcriptome dynamics over a lunar month in a broadcast spawning acroporid coral. *Mol. Ecol.* 26, 2514–2526. doi: 10.1111/mec.14043
- Omori, M. (2011). Degradation and restoration of coral reefs: experience in Okinawa. *Jpn. Mar. Biol. Res.* 7, 3–12. doi: 10.1080/17451001003642317
- Pallas, P. S. (1766). *Elenchus Zoophytorum Sistens Generum Adumbrationes Generationes et Speciarum Cognitarum Succintas Descriptiones cum Selectis Auctoribus Synonymis*. Hagae-Comitum: Petrus van Cleef, 1–451.
- Palumbi, S. R. (1994). Genetic divergence, reproductive isolation, and marine speciation. *Annu. Rev. Ecol. Syst.* 25, 547–572. doi: 10.1146/annurev.es.25.110194.002555
- Palumbi, S. R., Grabowsky, G., Duda, T., Geyer, L., and Tachino, N. (1997). Speciation and population genetic structure in tropical Pacific sea urchins. *Evolution* 51, 1506–1517. doi: 10.1111/j.1558-5646.1997.tb01474.x
- Pante, E., Abdelkrim, J., Viricel, A., Gey, D., France, S. C., Boisselier, M. C., et al. (2015). Use of RAD sequencing for delimiting species. *Heredity* 114, 450–459. doi: 10.1038/hdy.2014.105
- Park, J. S., Takayama, K., Suyama, Y., and Choi, B. H. (2019). Distinct phylogeographic structure of the halophyte *Suaeda malacosperma* (Chenopodiaceae/Amaranthaceae), endemic to Korea-Japan region, influenced by historical range shift dynamics. *Plant Syst. Evol.* 305, 193–203. doi: 10.1007/s00606-018-1562-8
- Peakall, R., and Smouse, P. E. (2012). GenAlEx 6.5: genetic analysis in Excel. Population genetic software for teaching and research—an update. *Bioinformatics* 28, 2537–2539. doi: 10.1093/bioinformatics/bts460
- Pillans, B., Chappell, J., and Naish, T. R. (1998). A review of the Milankovitch climatic beat: template for Plio-Pleistocene sea-level changes and sequence stratigraphy. *Sediment. Geol.* 122, 5–21. doi: 10.1016/S0037-0738(98)00095-5
- Pinzón, J. H., Sampayo, E., Cox, E., Chauka, L. J., Chen, C. A., Voolstra, C. R., et al. (2013). Blind to morphology: genetics identifies several widespread ecologically common species and few endemics among Indo-Pacific cauliflower corals (*Pocillopora*, Scleractinia). *J. Biogeogr.* 40, 1595–1608. doi: 10.1111/jbi.12110
- Planck, R. J., McAllister, D. E., and McAllister, A. T. (1988). *Shiraho Coral Reef and The Proposed New Ishigaki Island Airport, Japan*. Gland: IUCN.
- Quattrini, A. M., Rodriguez, E., Faircloth, B. C., Cowman, P. F., Brugler, M. R., Farfan, G. A., et al. (2020). Paleoclimate ocean conditions shaped the evolution of corals and their skeletons through deep time. *Nat. Ecol. Evol.* 4, 1531–1538. doi: 10.1038/s41559-020-01291-1
- Quattrini, A. M., Wu, T., Soong, K., Jeng, M. S., Benayahu, Y., and McFadden, C. S. (2019). A next generation approach to species delimitation reveals the role of hybridization in a cryptic species complex of corals. *BMC Evol. Biol.* 19:116. doi: 10.1186/s12862-019-1427-y
- Rambaut, A. (2012). *FigTree: Tree Figure Drawing Tool Version 1.4.4*. Available online at: <http://tree.bio.ed.ac.uk/software/figtree> (accessed November 13, 2019).
- Richards, Z. T., Berry, O., and van Oppen, M. J. (2016). Cryptic genetic divergence within threatened species of *Acropora* coral from the Indian and Pacific Oceans. *Conserv. Genet.* 17, 577–591. doi: 10.1007/s10592-015-0807-0
- Richards, Z. T., Haines, L., Scaps, P., and Ader, D. (2020). New records of *Heliopora hiberniana* from SE Asia and the Central Indian Ocean. *Diversity* 12:328. doi: 10.3390/d12090328
- Richards, Z. T., Miller, D. J., and Wallace, C. C. (2013). Molecular phylogenetics of geographically restricted *Acropora* species: implications for threatened species conservation. *Mol. Phylogenet. Evol.* 69, 837–851. doi: 10.1016/j.ympev.2013.06.020
- Richards, Z. T., Yasuda, N., Kikuchi, T., Foster, T., Mitsuyuki, C., Stat, M., et al. (2018). Integrated evidence reveals a new species in the ancient blue coral genus *Heliopora* (Octocorallia). *Sci. Rep.* 8:15875.
- Ridgway, T., and Gates, D. (2006). Why are there so few genetic markers available for coral population analyses? *Symbiosis* 41, 1–7. doi: 10.1093/oso/9780190907976.003.0001
- Rochette, N. C., Rivera-Colon, A. G., and Catchen, J. M. (2019). Stacks 2: analytical methods for paired end sequencing improve RADseq-based population genomics. *Mol. Ecol.* 28, 4737–4754. doi: 10.1111/mec.15253
- Rosser, N. L. (2015). Asynchronous spawning in sympatric populations of a hard coral reveals cryptic species and ancient genetic lineages. *Mol. Ecol.* 24, 5006–5019. doi: 10.1111/mec.13372
- Rosser, N. L., Thomas, L., Stankowski, S., Richards, Z. T., Kennington, W. J., and Johnson, M. S. (2017). Phylogenomics provides new insight into evolutionary relationships and genealogical discordance in the reef-building coral genus *Acropora*. *Proc. R. Soc. B Biol. Sci.* 284:20162182. doi: 10.1098/rspb.2016.2182
- Rowe, H. C., Renaut, S., and Guggisberg, A. (2011). RAD in the realm of next-generation sequencing technologies. *Mol. Ecol.* 20, 3499–3502.
- Saito, Y., Ueno, M., Kiatano, Y. F., and Yasuda, N. (2015). Potential of different reproductive timing between sympatric *Heliopora coerulea* lineages southeast of Iriomote Island, Japan. *Bul. Mar. Sci.* 91, 397–398. doi: 10.5343/bms.2015.1024

- Schettino, A., and Turco, E. (2011). Tectonic history of the western Tethys since the Late Triassic. *Geol. Soc. Am. Bull.* 123, 89–105. doi: 10.1130/b30064.1
- Schmidt-Roach, S., Lundgren, P., Miller, K. J., Gerlach, G., Noreen, A. M. E., and Andreakis, N. (2013). Assessing hidden species diversity in the coral *Pocillopora damicornis* from Eastern Australia. *Coral Reefs* 32, 161–172. doi: 10.1007/s00338-012-0959-z
- Schott, F. A., and McCreary, J. P. (2001). The monsoon circulation of the Indian Ocean. *Prog. Oceanogr.* 51, 11–23.
- Schott, F. A., Xie, S. P., and McCreary, J. P. Jr. (2009). Indian Ocean circulation and climate variability. *Rev. Geophys.* 47:RG1002. doi: 10.1029/2007RG000245
- Shafer, A. B. A., Peart, C. R., Tusso, S., Maayan, I., Brelsford, A., Wheat, C. W., et al. (2017). Bioinformatic processing of RAD-seq data dramatically impacts downstream population genetic inference. *Methods Ecol. Evol.* 8, 907–917. doi: 10.1111/2041-210x.12700
- Shearer, T. L., van Oppen, M. J. H., Romano, S. L., and Worheide, G. (2002). Slow mitochondrial DNA sequence evolution in the Anthozoa (Cnidaria). *Mol. Ecol.* 11, 2475–2487. doi: 10.1046/j.1365-294x.2002.01652.x
- Souter, P. (2010). Hidden genetic diversity in a key model species of coral. *Mar. Biol.* 157, 875–885. doi: 10.1007/s00227-009-1370-3
- Spalding, M. D., Ravilious, C., and Green, E. P. (2001). *World Atlas of Coral Reefs. Prepared at the UNEP World Conservation Monitoring Centre.* Berkeley, CA: University of California Press.
- Suyama, Y., and Matsuki, Y. (2015). MIG-seq: an effective PCR-based method for genome-wide single-nucleotide polymorphism genotyping using the next-generation sequencing platform. *Sci. Rep.* 5:16963. doi: 10.1038/srep16963
- Swierts, T., and Vermeij, M. J. (2016). Competitive interactions between corals and turf algae depend on coral colony form. *PeerJ* 4:e1984.
- Szmant, A. M., Weil, E., Miller, M., and Colon, D. E. (1997). Hybridization within the species complex of the scleractinian coral *Montastraea annularis*. *Mar. Biol.* 129, 561–572. doi: 10.1007/s002270050197
- Takata, K., Taninaka, H., Nonaka, M., Iwase, F., Kikuchi, T., Suyama, Y., et al. (2019). Multiplexed ISSR genotyping by sequencing distinguishes two precious coral species (Anthozoa: Octocorallia: Coralliidae) that share a mitochondrial haplotype. *PeerJ* 7:e7769. doi: 10.7717/peerj.7769
- Takino, T., Watanabe, A., Motooka, S., Nadaoka, K., Yasuda, N., and Taira, M. (2010). Discovery of a large population of *Heliopora coerulea* at akaishi reef, Ishigaki Island, southwest Japan. *Galaxea J. Coral Reef Stud.* 12, 85–86. doi: 10.3755/galaxea.12.85
- Tamaki, I., Yoichi, W., Matsuki, Y., Suyama, Y., and Mizuno, M. (2017). Inconsistency between morphological traits and ancestry of individuals in the hybrid zone between two *Rhododendron japonheptamerum* varieties revealed by a genotyping-by-sequencing approach. *Tree Genet. Genom.* 13:4.
- Taninaka, H., Bernardo, L. P. C., Saito, Y., Nagai, S., Ueno, M., Kitano, Y. F., et al. (2019). Limited fine-scale larval dispersal of the threatened brooding corals *Heliopora* spp. as evidenced by population genetics and numerical simulation. *Conserv. Genet.* 20, 1449–1463. doi: 10.1007/s10592-019-01228-7
- Taninaka, H., Harii, S., Kagawa, H., Ueno, M., Kitano, Y. F., Saito, Y., et al. (2018). Estimation of the reproductive timing of two genetically different lineages of the blue coral *Heliopora coerulea* (Pallas, 1766) around Sekisei Lagoon. *J. Jpn. Coral Reef Soc.* 20, 39–51. doi: 10.3755/jcrs.20.39
- Todd, P. A. (2008). Morphological plasticity in scleractinian corals. *Biol. Rev.* 83, 315–337. doi: 10.1111/j.1469-185x.2008.00045.x
- van Oppen, M. J. H., McDonald, B. J., Willis, B., and Miller, D. J. (2001). The evolutionary history of the coral genus *Acropora* (Scleractinia, Cnidaria) based on a mitochondrial and a nuclear marker: reticulation, incomplete lineage sorting, or morphological convergence? *Mol. Biol. Evol.* 18, 1315–1329. doi: 10.1093/oxfordjournals.molbev.a003916
- Veron, J. E. (1995). *Corals in Space and Time: The Biogeography and Evolution of the Scleractinia.* Sydney: UNSW Press.
- Veron, J. E. N. (2000). *Corals of the World*, Vol. 1–3. Townsville, AU: Australian Institute of Marine Science and CRR.
- Veron, J. E. N., Stafford-Smith, M., De Vantier, L., and Turak, E. (2015). Overview of distribution patterns of zooxanthellate Scleractinia. *Front. Mar. Sci.* 1:81. doi: 10.3389/fmars.2014.00081
- Villanueva, R. D. (2016). Cryptic speciation in the stony octocoral *Heliopora coerulea*: temporal reproductive isolation between two growth forms. *Mar. Biodivers.* 46, 503–507. doi: 10.1007/s12526-015-0376-y
- Vogler, C., Benzie, J., Lessios, H., Barber, P., and Worheide, G. (2008). A threat to coral reefs multiplied? Four species of crown-of-thorns starfish. *Biol. Lett.* 4, 696–699. doi: 10.1098/rsbl.2008.0454
- Vollmer, S. V., and Palumbi, S. R. (2004). Testing the utility of internally transcribed spacer sequences in coral phylogenetics. *Mol. Ecol.* 13, 2763–2772. doi: 10.1111/j.1365-294x.2004.02265.x
- Warner, P. A., van Oppen, M. J., and Willis, B. L. (2015). Unexpected cryptic species diversity in the widespread coral *Seriatopora hystrix* masks spatial-genetic patterns of connectivity. *Mol. Ecol.* 24, 2993–3008. doi: 10.1111/mec.13225
- Wells, J. W. (1954). Recent corals of the Marshall Islands. *U.S. Geol. Surv. Prof. Pap.* 260, 285–486.
- Wepfer, P. H., Nakajima, Y., Sutthacheep, M., Radice, V. Z., Richards, Z., Ang, P., et al. (2020). Evolutionary biogeography of the reef-building coral genus *Galaxea* across the Indo-Pacific ocean. *Mol. Phylogenet. Evol.* 151:106905. doi: 10.1016/j.ympev.2020.106905
- Wepfer, P. H., Nakajima, Y., Sutthacheep, M., Radice, V. Z., Richards, Z., Ang, P., et al. (2021). Inclusivity is key to progressing coral biodiversity research: reply to comment by Bonito et al. 2021. *Mol. Phylogenet. Evol.* 6:107135. doi: 10.1016/j.ympev.2021.107135
- Wilkinson, C. (2008). *Status of Coral Reefs of the World.* Townsville: Global Coral Reef Monitoring Network and Reef and Rain forest Research Centre, 296.
- Williams, S. T., and Benzie, J. A. H. (1998). Evidence of a biogeographic break between populations of a high dispersal starfish: congruent regions within the Indo-West Pacific defined by color morphs, mtDNA and allozyme data. *Evolution* 52, 87–99. doi: 10.2307/2410923
- Wörheide, G., Epp, L. S., and Macis, L. (2008). Deep genetic divergences among Indo-Pacific populations of the coral reef sponge *Leucetta chagosensis* (Leucettidae): founder effects, vicariance, or both? *BMC Evol. Biol.* 8:24. doi: 10.1186/1471-2148-8-24
- Yasuda, N. (2018). “Distribution expansion and historical population outbreak patterns of crown-of-thorns starfish, *Acanthaster planci* sensu lato,” in *Coral Reef Studies of Japan. Coral Reefs of the World, Japan From 1912 to 2015*, Vol. 13, eds A. Iguchi and C. Hongo (Singapore: Springer), 125–148. doi: 10.1007/978-981-10-6473-9\_9
- Yasuda, N., Takino, T., Kimura, M., Lian, C., Nagai, S., and Nadaoka, K. (2010). “Genetic structuring across the reef crest in the threatened blue coral *Heliopora coerulea* (Helioporidae, Octacorallia) in Shiraho reef, Southwest Japan,” in *Advances in Genetics Research*, ed. K. V. Urbano (New York, NY: Nova Science Publishers, Inc), 315–324.
- Yasuda, N., Taquet, C., Nagai, S., Fortes, M., Fan, T. Y., Harii, S., et al. (2015). Genetic diversity, paraphyly & incomplete lineage sorting of mtDNA, ITS2 and microsatellite flanking region in closely related *Heliopora* species (Octacorallia). *Mol. Phylogenet. Evol.* 93, 161–171.
- Yasuda, N., Taquet, C., Nagai, S., Fortes, M., Fan, T. Y., Phongsuwan, N., et al. (2014). Genetic structure and cryptic speciation in the threatened reef-building coral *Heliopora coerulea* along Kuroshio Current. *Bull. Mar. Sci.* 90, 233–255. doi: 10.5343/bms.2012.1105
- Zann, L. P., and Bolton, L. (1985). The distribution, abundance and ecology of the blue coral *Heliopora coerulea* (Pallas) in the Pacific. *Coral reefs* 4, 125–134. doi: 10.1007/bf00300871

**Conflict of Interest:** The authors declare that the research was conducted in the absence of any commercial or financial relationships that could be construed as a potential conflict of interest.

**Publisher's Note:** All claims expressed in this article are solely those of the authors and do not necessarily represent those of their affiliated organizations, or those of the publisher, the editors and the reviewers. Any product that may be evaluated in this article, or claim that may be made by its manufacturer, is not guaranteed or endorsed by the publisher.

Copyright © 2021 Taninaka, Maggioni, Seveso, Huang, Townsend, Richards, Tang, Wada, Kikuchi, Yuasa, Kanai, De Palmas, Phongsuwan and Yasuda. This is an open-access article distributed under the terms of the Creative Commons Attribution License (CC BY). The use, distribution or reproduction in other forums is permitted, provided the original author(s) and the copyright owner(s) are credited and that the original publication in this journal is cited, in accordance with accepted academic practice. No use, distribution or reproduction is permitted which does not comply with these terms.



# Its What's on the Inside That Counts: An Effective, Efficient, and Streamlined Method for Quantification of Octocoral Symbiodiniaceae and Chlorophyll

Rosemary Kate Steinberg<sup>1,2\*</sup>, Emma L. Johnston<sup>1</sup>, Teresa Bednarek<sup>1,3</sup>, Katherine A. Dafforn<sup>2,4</sup> and Tracy D. Ainsworth<sup>1</sup>

<sup>1</sup> Faculty of Science, School of Biological, Earth, and Environmental Sciences, Evolution and Ecology Research Centre and Centre for Marine Science and Innovation, University of New South Wales, Sydney, NSW, Australia, <sup>2</sup> Sydney Institute of Marine Science, Mosman, NSW, Australia, <sup>3</sup> RUHR Univstadt Bochum, Bochum, Germany, <sup>4</sup> Department of Earth and Environmental Sciences, Macquarie University, North Ryde, NSW, Australia

## OPEN ACCESS

### Edited by:

James Davis Reimer,  
University of the Ryukyus, Japan

### Reviewed by:

Christopher Bennett Wall,  
University of Hawai'i at Mānoa,  
United States  
Andrea Oliveira Ribeiro Junqueira,  
Federal University of Rio de Janeiro,  
Brazil

### \*Correspondence:

Rosemary Kate Steinberg  
rosiekstein@gmail.com  
orcid.org/0000-0002-6153-2743

### Specialty section:

This article was submitted to  
Coral Reef Research,  
a section of the journal  
Frontiers in Marine Science

**Received:** 17 May 2021

**Accepted:** 09 August 2021

**Published:** 09 September 2021

### Citation:

Steinberg RK, Johnston EL,  
Bednarek T, Dafforn KA and  
Ainsworth TD (2021) Its What's on  
the Inside That Counts: An Effective,  
Efficient, and Streamlined Method  
for Quantification of Octocoral  
Symbiodiniaceae and Chlorophyll.  
Front. Mar. Sci. 8:710730.  
doi: 10.3389/fmars.2021.710730

Ocean warming driven bleaching is one of the greatest threats to zooxanthellate cnidarians in the Anthropocene. Bleaching is the loss of Symbiodiniaceae, chlorophyll, or both from zooxanthellate animals. To quantify bleaching and recovery, standardised methods for quantification of Symbiodiniaceae and chlorophyll concentrations have been developed for reef-building scleractinian corals, but no such standard method has been developed for octocorals. For stony corals, quantification of Symbiodiniaceae and chlorophyll concentrations often relies on normalisation to skeletal surface area or unit of biomass [i.e., protein, ash-free dry weight (AFDW)]. Stiff octocorals do not change their volume, as such studies have used volume and surface area to standardise densities, but soft-bodied octocorals can alter their size using water movement within the animal; therefore, Symbiodiniaceae and chlorophyll cannot accurately be measured per unit of surface area and are instead measured in units of Symbiodiniaceae and chlorophyll per  $\mu\text{g}$  of host protein or AFDW. Though AFDW is more representative of the full biomass composition than host protein, AFDW is more time and resource intensive. Here, we provide a streamlined methodology to quantify Symbiodiniaceae density, chlorophyll concentration, and protein content in soft-bodied octocorals. This technique uses minimal equipment, does not require freeze-drying or burning samples to obtain ash weight, and is effective for down to 0.2 g wet tissue. Bulk samples can be centrifuged, the Symbiodiniaceae pellet washed, and the supernatant saved for protein analysis. This efficient technique allows for clean, easy to count samples of Symbiodiniaceae with minimal animal protein contamination. Chlorophyll *a* and *c*<sub>2</sub> extractions occurs at different rates, with chlorophyll *a* taking 24 h to extract completely at 4°C and chlorophyll *c*<sub>2</sub> taking 48 h. Finally, we found that where necessary, wet weight may be used as a proxy for protein content, but the correlation of protein and wet weight varies by species and protein should be used when possible. Overall, we have created a rapid and accurate method for quantification of bleaching markers in octocorals.

**Keywords:** bleaching, coral bleaching, soft coral, alcyonacea, zooxanthellae, anemone, soft coral bleaching, Symbiodiniaceae density



## INTRODUCTION

Coral bleaching is increasing in frequency and severity across tropical and subtropical reefs, and is estimated to become a yearly occurrence by the year 2050 if greenhouse gas emissions remain unchecked (Van Hooidonk et al., 2014). Bleaching is caused by the breakdown of the symbiotic relationship between the animal host and their photosynthetic endosymbionts, Symbiodiniaceae (Hughes et al., 2003). Not all zooxanthellate animals on reefs are affected equally though. For example, in Japan, Loya et al. (2001) found that massive stony corals were the “winners” and branching stony and octocorals were the “losers” in a coral bleaching event. Bleaching impacts are often assessed and compared between species and reef locations, by quantifying the Symbiodiniaceae and chlorophyll concentrations in photosynthetic animals during, before, and/or after marine heat waves or other stress inducing events (Jones, 1997a,b). In fact, coral bleaching is defined as the significant reduction in symbiont and/or photosynthetic pigments from the coral host (Hoegh-Guldberg, 1999). Thermal thresholds at which coral photosystems begin to break down can be determined using 50% effective dose ( $ED_{50}$ ), or the temperature at which Symbiodiniaceae lose 50% of their thermal efficiency, as developed by Evensen et al. (2021). Standardised methods for quantification of symbiont densities and chlorophyll concentrations have been in use for years to quantify Symbiodiniaceae and chlorophyll concentrations in stony corals (Johannes and Wiebe, 1970), however, there is no such rapid standardised method for fleshy soft-bodied photosynthetic animals such as octocorals, with many homogenisation and standardisation methods used in the literature, many which are time intensive (Riegl, 1995; Ferrier-Pagès et al., 2009; Hannes et al., 2009; Pupier et al., 2018; Rossi et al., 2018). Developing standardised methods for different photosynthetic animals is therefore crucial to understand which species on reefs are either sensitive or resilient to bleaching, and how each of these species is impacted to help inform conservation initiatives.

Photosynthetic octocorals can be the second most abundant benthic group in coral reefs after hard corals and can be just, if not more, susceptible to bleaching (Loya et al., 2001; Prada et al., 2010; Dias and Gondim, 2016). Though octocorals do not build calcified reef structure they are still critically important parts of coral reef benthic communities by providing food and habitat for many reef dwelling fishes and invertebrates (Griffith, 1994; Pratchett, 2007; Pratchett et al., 2016). In fact, fish richness in the Great Barrier Reef has been shown to increase relative to octocoral, but not stony coral, cover at some locations (Epstein and Kingsford, 2019). As such, loss of octocorals from reefs has potential implications to reef ecosystem structure and function, and it is imperative that we can accurately quantify and understand the impacts of bleaching on octocorals.

Octocorals are structurally very different from stony corals and as such require different methods for quantification of bleaching impacts. Methods for quantifying Symbiodiniaceae and chlorophyll concentrations usually rely on the ease of removing tissue from the coral skeletons, and using skeletal

surface area or unit biomass (protein, AFDW) to standardise concentrations (Johannes and Wiebe, 1970; Grotto et al., 2006; McCowan et al., 2011). Surface area and/or volume work well for standardisation of Symbiodiniaceae and chlorophyll for stiff octocorals such as gorgonians and *Briarium* spp. (Ferrier-Pagès et al., 2009; Hannes et al., 2009), but because soft-bodied cnidarians do not have solid skeletal structures, surface area and/or volume are inappropriate standardisations for the vast majority of soft-bodied zooxanthellate cnidarians. Instead, these groups have either calcified spicules (octocorals) or no skeletal structure (anemones) (Koehl, 1982; Sethmann and Wörheide, 2008). Many octocorals also quickly change the water content of their tissues, which can make both weight and surface area inappropriate standards (e.g., Davis et al., 2015). In studies of both stony corals and octocorals, chlorophyll concentrations are usually reported as  $\mu\text{g}$  chlorophyll per Symbiodiniaceae cell, AFDW (grams), protein ( $\mu\text{g}$ ), or surface area ( $\text{cm}^2$ ), though occasionally wet weight (grams) or volume ( $\text{cm}^3$ ) are also used (Falkowski and Dubinsky, 1981; Riegl, 1995; Jones, 1997b; Hueerkamp et al., 2001; Pupier et al., 2018; Rossi et al., 2018). For further discussion on normalisation approaches, see Edmunds and Gates (2002). Existing methods for extracting chlorophyll use different solvents, solvent concentrations, incubation times, and temperatures, all of which may impact chlorophyll measurements, though 90–100% acetone at 4 or  $-20^\circ\text{C}$  is most common (Falkowski and Dubinsky, 1981; Riegl, 1995; Jones, 1997b; Hueerkamp et al., 2001; Pupier et al., 2018). Unfortunately, these disparate standardisation measures, and perhaps differences in extraction protocols, can make direct comparisons between studies difficult, and as such a standardised method would greatly enhance comparability between studies. A standardised method has been proposed for separation of Symbiodiniaceae from octocoral tissue that maximises chlorophyll yield and is useful for studies focusing on this parameter (Pupier et al., 2018), however, the method of sample processing is time consuming. Here, we propose a combined protocol for extracting and quantifying Symbiodiniaceae, chlorophyll, and protein concentrations from wet frozen samples of soft-bodied cnidarians. We aim to provide an efficient and effective standardised protocol for separating Symbiodiniaceae from animal tissue in octocorals and test if wet weight can be used as a proxy for protein concentration.

## MATERIALS AND EQUIPMENT

Tissue homogeniser, such as the OMNI TH tissue homogeniser with 10 mm stainless steel bit Plate spectrophotometer, such as the Bio-Rad iMark<sup>TM</sup> Microplate Absorbance Reader Single spectrophotometer, such as the VWR UV-6300PC, Double Beam Spectrophotometer, Centrifuge with 50 and 10 ml tube adaptors, Vortex, Freezer,  $-20$  to  $-30^\circ\text{C}$  Refrigerator, 4C Surgical scissors, 10 and 50 ml falcon tubes Repeater pipettes (10–1,000  $\mu\text{l}$ ), Pasteur pipettes, 96 well plates, Optical glass cuvettes, Bradford's assay kit, such as the Thermo Scientific Coomassie Plus (Bradford) kit, RO water, Phosphate buffered saline tablets or filtered sea water (100  $\mu\text{m}$  minimum), and 100% acetone.



## METHODS

### Sample Collection

Soft-bodied coral samples were collected on snorkel from the world heritage listed Lord Howe Island Marine Park Lagoon. Three species were sampled – *Xenia cf crassa*, *Cladiella* sp. 1, and *Cladiella* sp. 2. These species were chosen because they represent two genera and three growth forms, and were common at the sampling sites. Collections were conducted March 15–25, April 28–May 1, and October 22–28, 2019 at three reefs within the lagoon (Coral Gardens, North Bay, and Sylph's Hole). Ninety approximately five-by-three-centimetre samples per species were collected using surgical scissors. For *Xenia cf crassa*, a stalk with 1–3 stems and all attached polyps were collected, depending on the size of the stems. For both *Cladiella* sp. 1 and *Cladiella* sp. 2, one stalk with all attached lobes and polyps was collected. Samples were stored at  $-4^{\circ}\text{C}$  in the field and during transport before transfer to  $-20^{\circ}\text{C}$  for storage in the laboratory until processing.

### Separation of Coral Symbiodiniaceae From Tissue

To investigate the appropriate quantity of octocoral tissue needed for accurate Symbiodiniaceae quantification, subsamples were taken from 0.2 to 0.7 g and defrosted on paper towels for  $\sim 15$  min before being placed in 50 ml tubes. These sizes were chosen as the pieces were small enough to fit in the homogenisation mechanism, but not so small as to be difficult to handle. Because the species have very different anatomical features, only tentacles were taken from *X. cf crassa* and only lobe tips were taken from *Cladiella* sp. 1 and *Cladiella* sp. 2. Thus, *X. cf crassa* were placed in tubes without further handling, while *Cladiella* sp. 1 and *Cladiella* sp. 2 were cut into small ( $\sim 1\text{ mm}^3$ ) pieces with scissors before placing into tubes. Tubes were then filled to the 20 ml mark with RO water. RO water was used as it is recommended by Pupier et al. (2018) to maximise protein content. Samples were homogenised for 30 s using an OMNI TH tissue homogeniser with a 10 mm stainless steel bit, checking halfway to ensure that no pieces had become stuck in the mechanism. Samples were vortexed to remove any air bubbles that could trap Symbiodiniaceae cells at the surface and then centrifuged at 160 RCF for 2 min. The supernatant was removed with a pipette and saved. It is important to note that the pellet is not very stable, and supernatant must be pipetted instead of poured off. The tube containing the Symbiodiniaceae pellet was then refilled to the 20 ml mark with RO water and resuspended with a vortex. Centrifugation was repeated at 130 RCF for 2 min. Supernatant was once again removed and added to the previously removed supernatant for a total of  $\sim 40$  ml. The separated Symbiodiniaceae were topped up with 1 ml of  $3\times$  PBS. Symbiodiniaceae and supernatant from both separations were then frozen until ready to use.

### Coral Protein Quantification

To quantify protein, supernatant was defrosted and topped up with RO water to the 40 ml mark to standardise volume between

samples. Protein was then quantified against a bovine albumin standard using the Thermo Scientific Coomassie Plus (Bradford) kit and protocol. The standard microplate protocol using  $15\text{ }\mu\text{l}$  of sample was followed for both *Cladiella* sp. 1 and *Cladiella* sp. 2, while the micro microplate procedure was followed for *X. cf crassa*. The standard microplate protocol has a working range of 100–1,500  $\mu\text{g/ml}$ , while the micro microplate protocol has a working range of 1–25  $\mu\text{g/ml}$  (Thermo Scientific, 2018). All spectrophotometer measurements were taken on a Bio-Rad iMark<sup>TM</sup> Microplate Absorbance Reader at 595 nm. Results were reported in units of  $\mu\text{g/ml}$ .

### Symbiodiniaceae Quantification

To count Symbiodiniaceae, the Symbiodiniaceae pellet was topped up to the 5 ml mark using  $3\times$  PBS and resuspended using a vortex. A 200  $\mu\text{l}$  subsample was placed on a Neubauer Improved haemocytometer and counted. For ease and speed of counting, if there were more than 30 cells per square in the test sample, the entire treatment was diluted in separate Eppendorf tubes by either mixing 500  $\mu\text{l}$  Symbiodiniaceae with 500  $\mu\text{l}$   $3\times$  PBS ( $2\times$  dilution) or 250  $\mu\text{l}$  Symbiodiniaceae with 750  $\mu\text{l}$  of  $3\times$  PBS ( $4\times$  dilution). All *X. cf crassa* samples were  $4\times$  diluted, all *Cladiella* sp. 2 samples were  $2\times$  diluted, and *Cladiella* sp. 1 samples were either  $2\times$  diluted or not diluted at all. The final count was then multiplied by the dilution to attain correct counts. Each haemocytometer fill was considered a technical replicate, while the squares counted within the grid were considered a sub-replicate. Six technical replicates and 5 sub-replicates per technical replicate were performed, for a total of 30 replicates. Replicate numbers were chosen based on previous work in stony and octocorals and anemones (Brown et al., 1995; Hueerkamp et al., 2001; Hill and Scott, 2012; Hill et al., 2014; Pupier et al., 2018; Gierz et al., 2020).

The number of Symbiodiniaceae cells was standardised to the total protein concentration of the supernatant. The dilution factor (DF) of the supernatant compared to the resuspended Symbiodiniaceae pellet must be considered when calculating Symbiodiniaceae concentrations. In this study, the supernatant had a volume of 40 ml and the resuspended Symbiodiniaceae had a volume of 5 ml, and as such the DF was 8. Symbiodiniaceae per ml was calculated using the following formula:  $\frac{\text{count} \times \text{dilution}}{6.25 \times 10^{-6}}$ , where  $6.25 \times 10^{-6}$  is the volume of one haemocytometer grid square. Symbiodiniaceae per  $\mu\text{g}$  protein was calculated using the following formula:  $\frac{\frac{\text{Symbiodiniaceae}}{\text{ml}}}{\text{DF} \times \text{protein}(\frac{\mu\text{g}}{\text{ml}})}$  or  $\frac{\frac{\text{count} \times \text{dilution}}{6.25 \times 10^{-6}}}{\text{DF} \times \text{protein}(\frac{\mu\text{g}}{\text{ml}})}$ .

### Chlorophyll Extraction

To test incubation time for Symbiodiniaceae chlorophyll extraction, a subset of two individuals of each species were used to test two incubation times, 24 and 48 h. For both, chlorophyll concentrations were quantified by removing two replicate 1 ml subsamples of resuspended Symbiodiniaceae and placing them in the centrifuge for 10 min at 805 RCF. Supernatant was removed and discarded. Samples were then resuspended in 5 ml of 100% acetone and incubated in the dark at  $4^{\circ}\text{C}$  for either 24 or 48 h. All acetone was removed and measured using Pasteur pipettes

as acetone damages repeater pipettes. 24 h was chosen based on Lesser (1989), and 48 h was also tested when high concentrations of chlorophyll  $c_2$  were found to remain in Symbiodiniaceae after initial extraction.

After the allotted time, extracts were centrifuged for 10 min at 805 RCF and 2 ml of extracted chlorophyll in acetone was aliquoted into two optical glass cuvettes. Absorbance was measured at 630, 663, and 750 nm using a VWR UV-6300PC Double Beam Spectrophotometer. Concentrations of chlorophyll  $a$  and  $c_2$  in  $\mu\text{g/ml}$  were calculated using the following equations from Jeffrey and Humphrey (1975) for dinoflagellates:

$$\text{Chlorophyll } a = 11.43E_{663} - 0.64E_{630}$$

$$\text{Chlorophyll } c_2 = 27.09E_{630} - 3.63E_{663}$$

As 1 ml of resuspended Symbiodiniaceae pellet was extracted in 5 ml of acetone, chlorophyll concentrations were multiplied by five. To calculate chlorophyll per  $\mu\text{g}$  protein, the following equation was used:  $\frac{5 \times \text{chlorophyll } (\frac{\mu\text{g}}{\text{ml}})}{8 \times \text{protein } (\frac{\mu\text{g}}{\text{ml}})}$ .

To test how much chlorophyll was left in the Symbiodiniaceae after initial extraction and ensure all possible chlorophyll was extracted from Symbiodiniaceae, all remaining acetone was removed and discarded, and the samples were resuspended in 5 ml fresh acetone and allowed to incubate at 4°C for 24 h. Samples were then centrifuged and absorbances measured as above. After testing, the 48 h time point was chosen to obtain further data. Replicates were excluded if spicules were present in the acetone during reading. All laboratory work was completed at the Sydney Institute of Marine Science.

## Statistical Analysis

All graphing and statistical analyses were performed in R version 3.6.1. Differences in protein content between species were tested using the lme4 glmer function with a Gamma distribution. Correlations between weight and log of protein concentration was tested using a linear model with interactions. Differences in Symbiodiniaceae per protein concentrations between species were tested using the glmer function in the package lme4 with a nonbinomial distribution (Bates et al., 2015). Differences in chlorophyll incubation time were tested using the glmer function with Gaussian distribution, with chlorophyll  $a$  concentrations square root transformed to meet assumptions of homoscedasticity. Differences in chlorophyll per  $\mu\text{g}$  of protein between species was tested using the lme4 lmer function with log transformed data. Random effects for all mixed-effects models were individual colony and date and location collected. All pairwise comparisons were made using emmeans and all distributions were chosen by comparing residual plots (Lenth et al., 2018).

To examine precision of methods, coefficients of variation (CV) for counts within each sample were calculated by calculating the mean and standard deviation (SD) of sub-replicates within each technical replicate, and then taking the mean of these per sample. CV was then calculated using the following equation:  $\frac{\text{SD of mean}}{\text{Mean of mean}} \times 100$ . To calculate the CV between samples within each sampling site and sampling period,

the mean and SD of each sample was taken and CV calculated using the follow equation:  $\frac{\text{SD}}{\text{Mean}} \times 100$ . The mean of this number for each sampling site within each sampling period was then calculated. The mean  $\pm$  SE of all sample CVs is reported.

Coefficients of variation of measurements for chlorophyll  $a$  and  $c_2$  within each sample are calculated similarly. Because there are no sub-replicates (all samples were taken from different colonies), the mean and SD of the two replicate measures taken are calculated and CV calculated using the following equation:  $\frac{\text{SD}}{\text{Mean}} \times 100$ . CV between samples within each sampling site during each sampling period was calculated as above. The mean  $\pm$  SE of all sample CVs is reported.

## RESULTS

### Separation of Coral Symbiodiniaceae From Tissues

Weights of all samples were recorded, with a median weight of 0.46 g, a mean of 0.47 g, a minimum of 0.17 g, and a maximum of 0.75 g. Homogenising time was standardised to 30 s for all species and samples. The homogeniser mechanism was checked for remaining tissue after 15 s, pieces were removed with tweezers and placed back into the homogenate, and then homogenisation resumed for 15 more seconds, after which visual homogenisation (no visible tissue) was achieved. Symbiodiniaceae and animal tissue were successfully separated in all but one sample. Successful separation was determined visually by presence of a distinct algal pellet at the bottom of the test tube after centrifugation.

### Coral Protein Quantification

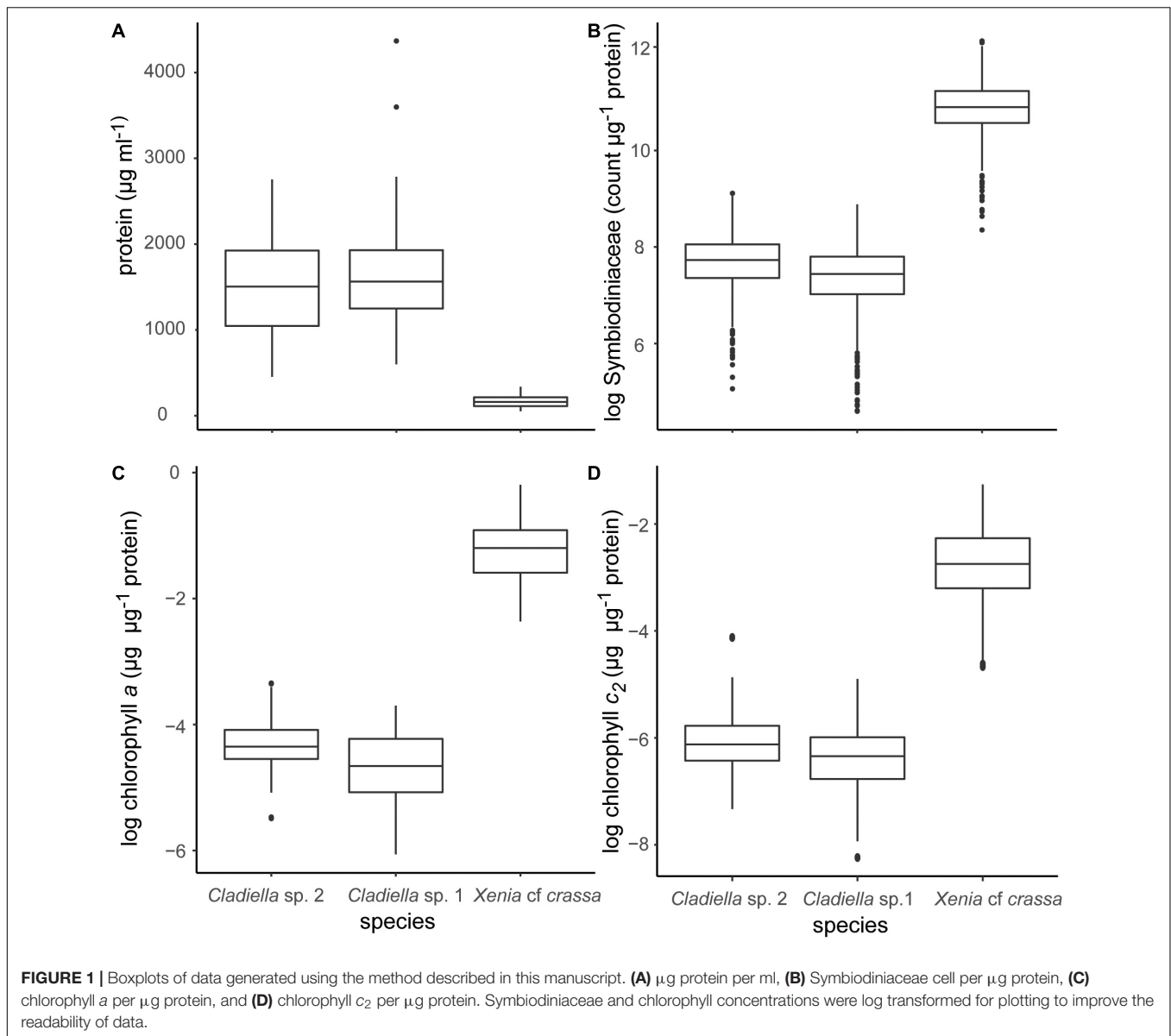
Here, we found that although both *Cladiella* sp. 1 and *Cladiella* sp. 2 had high enough protein concentrations to use the standard microplate procedure (range: 75.8–231.8 and 56.6–344.1  $\mu\text{g/ml}$ , respectively), *Xenia cf. crassa* had very low protein concentrations and the micro microplate procedure was required (range: 6.4–42.1  $\mu\text{g/ml}$ ).

After multiplication by eight to keep protein and Symbiodiniaceae concentrations consistent, protein content of *Cladiella* sp. 1, *Cladiella* sp. 2, and *Xenia cf. crassa* were  $1,667.9 \pm 12.8$  SE,  $1,500.4 \pm 10.96$  SE, and  $167.4 \pm 1.4$  SE  $\mu\text{g/ml}$ , respectively (Figure 1A).

Overall, wet weight was highly correlated with log protein concentration ( $R^2 = 0.95$ ,  $p < 0.0005$ , Figure 2). This pattern was consistent across species (*Xenia cf. crassa*:  $R^2 = 0.37$ ,  $p < 0.0005$ ; *Cladiella* sp. 1:  $R^2 = 0.68$ ,  $p < 0.0005$ ; *Cladiella* sp. 2:  $R^2 = 0.69$ ,  $p < 0.0005$ ; Figure 2).

### Symbiodiniaceae Quantification

The method described above successfully quantified Symbiodiniaceae concentration per  $\mu\text{g}$  protein. Symbiodiniaceae concentration of *Cladiella* sp. 1, *Cladiella* sp. 2, and *Xenia cf. crassa* were  $1,720.6 \pm 19.1$  SE,  $2,273.9 \pm 21.2$  SE, and  $52,143.3 \pm 481.4$  SE cells per  $\mu\text{g}$  protein, respectively (Figure 1B). Coefficient of variance (CV) of Symbiodiniaceae per  $\mu\text{g}$  protein



within samples was  $17.2 \pm 0.5$  SE. CV of Symbiodiniaceae per  $\mu\text{g}$  protein between samples within site and trip was  $34.6 \pm 1.3$  SE.

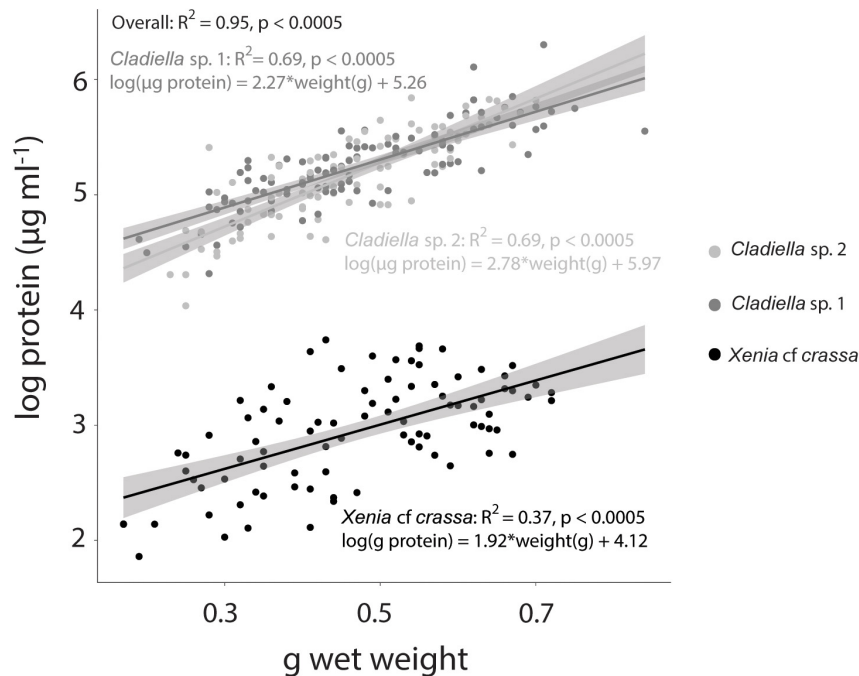
## Chlorophyll Extraction

Because Symbiodiniaceae contain both chlorophyll *a* and *c*<sub>2</sub>, extraction time was tested for both types. Extraction time was tested by allowing the Symbiodiniaceae pellet to extract for either 24 or 48 h, removing all acetone, and resuspending the previously extracted pellet. This allowed us to test if the amount of chlorophyll extracted was higher at 48 than 24 h, and to test how much chlorophyll was still in the Symbiodiniaceae after extraction. For extraction of chlorophyll *a*, there was no significant difference between acetone incubation time of 24 or 48 h, suggesting that 24 h was sufficient to extract all chlorophyll from the pellet. Additionally, there was no significant difference in the amount of chlorophyll found in the second round of

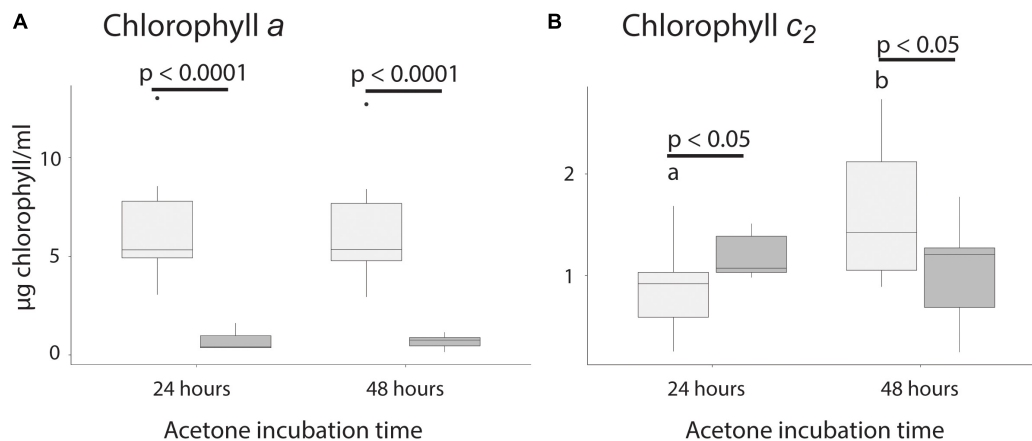
incubation between samples incubated 24 or 48 h, confirming that 24 h was sufficient for full extraction ( $p > 0.05$ , **Figure 3A** and **Table 1**). There was significantly less chlorophyll extracted in the second round of extraction than the first, suggesting that very little chlorophyll was left after initial incubation ( $p > 0.05$ , **Figure 3A** and **Table 1**).

For chlorophyll *c*<sub>2</sub>, there was significantly more chlorophyll extracted after 48 than 24 h and after 48 h there was significantly less chlorophyll in the second extraction ( $p < 0.05$ , **Figure 3B** and **Table 1**), suggesting that 24 h of incubation is not long enough to extract all chlorophyll. The amount of chlorophyll left over after the initial round of incubation was not significantly different between 24 and 48 h ( $p > 0.05$ , **Figure 3B**).

Chlorophyll *a* concentrations of *Cladiella* sp. 1, *Cladiella* sp. 2, and *Xenia cf crassa* were  $0.008 \pm 0.0004$  SE,  $0.01 \pm 0.0004$ , and  $0.3 \pm 0.08$  SE  $\mu\text{g}$  chlorophyll *a* per  $\mu\text{g}$  protein, respectively



**FIGURE 2 |** Tissue wet weight vs. log protein concentration in three species of octocoral. Linear model lines of best fit with 95% confidence intervals are represented for each species in the same colour as the scatter points.



**FIGURE 3 |** Chlorophyll extraction time for chlorophyll a and c<sub>2</sub>. **(A)** Extraction of chlorophyll a between initial and secondary extraction after 24 and 48 h. **(B)** Extraction of chlorophyll c<sub>2</sub> between original and refilled vials after 24 and 48 h. Significant differences between fills are indicated by a bar and the associated  $p$ -value, while significant differences between time points are indicated using different letters.

(Figure 1C). Chlorophyll c<sub>2</sub> concentrations of *Cladiella* sp. 1, *Cladiella* sp. 2, and *Xenia cf crassa* were  $0.002 \pm 0.00009$  SE,  $0.003 \pm 0.0001$  SE, and  $0.08 \pm 0.004$  SE  $\mu\text{g chlorophyll c}_2$  per  $\mu\text{g protein}$ , respectively (Figure 1D). CV of chlorophyll a per  $\mu\text{g protein}$  within samples was  $4.5 \pm 0.3$  SE. CV of chlorophyll a per  $\mu\text{g protein}$  between samples within site and collection interval was  $4.5 \pm 0.4$  SE. CV of chlorophyll c<sub>2</sub> per  $\mu\text{g protein}$  within samples was  $14.8 \pm 0.9$  SE. CV of chlorophyll c<sub>2</sub> per  $\mu\text{g protein}$  between samples within site and collection interval was  $14.8 \pm 1.3$  SE.

## DISCUSSION

Here, we provide an efficient and effective method for quantifying Symbiodiniaceae and chlorophyll concentrations in octocorals, which may also be useful for other thick-fleshed zooxanthellate animals (Figure 4). The homogenisation method described here takes only 30 s per sample and is effective in separating Symbiodiniaceae from coral tissue for quantification of Symbiodiniaceae, chlorophyll, and protein. Although methods have been long established for stony corals, soft zooxanthellate



**TABLE 1 |** Generalised linear mixed model results of extraction time of chlorophylls *a* and *c*<sub>2</sub>.

Chlorophyll <i>a</i> extraction time			
	Chisq	Df	Pr (>Chisq)
Time	0.02	1	0.9
Fill	184.5	1	<b>&lt;0.0001</b>
Time × fill	0.004	1	0.95
Chlorophyll <i>c</i> <sub>2</sub> extraction time			
Time	2.6	1	0.1
Fill	0.6	1	0.4
Time × fill	6.0	1	<b>0.01</b>
Chlorophyll <i>c</i> <sub>2</sub> pairwise comparisons of interaction term			
	t-ratio	Df	p-value
Original fill 24–48 h	−2.9	18	<b>0.01</b>
Refill 24–48 h	0.6	18	0.6
24 h original fill–refill	−1.2	18	0.3
48 h original fill–refill	2.3	18	<b>0.04</b>

Significant values are indicated in boldface.

cnidarians have posed a challenge due to their unique anatomy. Standardised methods for quantifying bleaching markers such as Symbiodiniaceae and chlorophyll concentrations are imperative for studies of colony health and reactions to stressors. We found that using a tissue homogeniser instead of a tissue grinder reduced wet sample processing time to ~30 s per sample instead of 30 min, though samples did need to be defrosted before homogenisation which may have affected chlorophyll concentrations. Other studies have also used tissue homogenisers, though homogenisation time varied greatly or was not reported, with some studies homogenised for up to 2 min for whole colonies (e.g., Kirk et al., 2005; Studivan et al., 2015; Rossi et al., 2018). Previous reductions in chlorophyll concentrations using frozen and defrosted specimens were possibly attributed to the long processing time and heat produced during grinding as increased handling can reduce pigment concentrations (Metaxatos and Ignatiades, 2002; Hannides et al., 2014; Pupier et al., 2018). In addition, the method developed here requires very small sample sizes but can be used successfully for a range of weights (0.17–0.75 g wet weight). Here, we discuss the optimisation and application of our proposed methods for use with soft-bodied cnidarians and outline the caveats and considerations with using this approach.

## Separation of Coral Symbiodiniaceae From Tissues

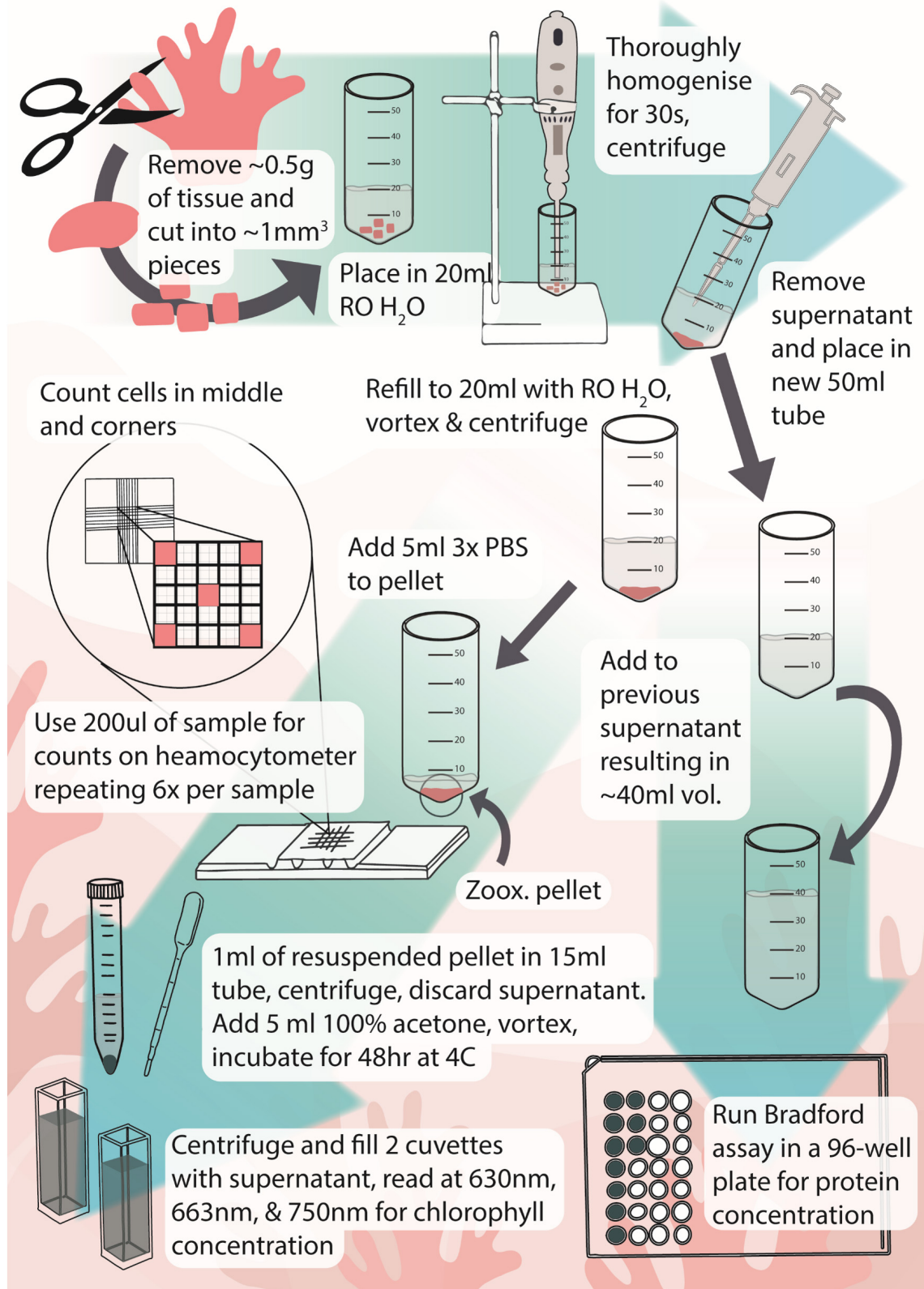
Though a method has previously been published for separating Symbiodiniaceae from coral tissue in freeze dried samples, this method is ineffective for wet samples (Pupier et al., 2018). This method takes 5 min per freeze-dried sample or 30 min per wet frozen sample, which can be prohibitive in experiments with many treatments and/or replicates. The Pupier method was specifically developed to optimise chlorophyll yield and

as such is not appropriate for all samples and situations. Though Pupier found that freeze drying significantly increased chlorophyll yields, they found no effect on Symbiodiniaceae concentrations, suggesting that while this method may be superior for quantification of chlorophyll, it is inefficient for quantification of Symbiodiniaceae. We found that using a tissue homogeniser instead of a tissue grinder reduced wet sample processing time to ~30 s per sample instead of 30 min. A caveat to this method is that we tested it only on three species and it may not apply to all octocorals or other soft zooxanthellate cnidarians. On the other hand, a similar method has previously been used to separate Symbiodiniaceae from tissue in anemones and octocorals with varying tissue characteristics (Hannes et al., 2009; Hill and Scott, 2012; Hill et al., 2014; Studivan et al., 2015; Rossi et al., 2018), and as such may be able to be applied to other groups of zooxanthellate animals that are difficult to quantify by weight or surface area such as sponges, jellies, and thick-fleshed stony corals (e.g., *Heliofungia* spp.), though this still requires verification. Some studies that homogenised tissues do not report on the type of homogeniser used, or homogenise for different purposes, such as genetic extraction, and use methods that do not preserve the integrity of the Symbiodiniaceae cells (e.g., Kirk et al., 2005; Wessels et al., 2017), which makes finding an appropriate homogenisation method in the literature difficult. Overall, separation with a tissue homogeniser works well for creating Symbiodiniaceae samples that are relatively free of contamination by coral tissue which can clog the haemocytometer and make counting difficult.

During homogenisation, we observed that spicule-rich tissue easily became stuck in the homogenisation mechanism, and that centrifugation could create a layer of coral tissue on top of the Symbiodiniaceae pellet which could interfere with counting. For lobed colonies or colonies with many spicules it is important to cut the sample into smaller pieces (~1 mm<sup>3</sup>) before homogenisation, as large pieces are likely to get caught in the homogeniser mechanism. This can be achieved quickly and easily by placing the sample in a 50 ml tube and making a few cuts with scissors against the side of the tube. To separate Symbiodiniaceae from coral tissue in a centrifuge, we found that the ideal method was to use relatively low RPMs for a short time, as high RPMs or long times would cause protein to be pulled onto the Symbiodiniaceae pellet and would interfere with counting, as reported in the methods.

## Coral Protein Quantification

The most commonly used normalisation metrics for octocoral Symbiodiniaceae and chlorophyll measurements are surface area or volume, ash-free dry weight (AFDW), or protein content (e.g., Ferrier-Pagès et al., 2009; Hannes et al., 2009; Studivan et al., 2015; Pupier et al., 2018; Rossi et al., 2018). For a full list of all the normalisation metrics used in previous octocoral literature, see Pupier et al. (2018). Surface area and volume are only appropriate for stiff octocorals, such as gorgonians, which do not change their volume over time. The most comprehensive measure is AFDW, as it considers total tissue composition, but involves using a muffle furnace over the course of many hours. Protein



**FIGURE 4 |** Infographic of protocol for extraction and measurement of Symbiodiniaceae and chlorophyll from octocorals. Icons and infographic by Melissa Pappas, EmergingCreativesOfScience.com.

content is relatively simple to measure from wet homogenised samples, as protein kits simply require a small amount of coral supernatant to be added to a pre-mixed reagent solution and read in a spectrophotometer (Thermo Scientific, 2018). Previously, Pupier et al. (2018) found that total DW and AFDW are not well correlated and suggested use of AFDW as a normalisation parameter. As determination of protein content does not require drying or burning of samples, and takes only 10 min of incubation time after mixing with reagent solution, the authors suggest normalising Symbiodiniaceae and chlorophyll concentrations to protein content for efficiency, or to AFDW for comparison to total tissue composition. If protein or AFDW cannot be obtained, wet weight could be used as a proxy. The degree of correlation varied between species, with an  $R^2$  of only 0.37 for *Xenia cf. crassa*, suggesting that wet weight is not appropriate as a substitute for protein for all species. Overall, the authors recommend using protein concentration whenever possible to maintain consistency among studies.

## Symbiodiniaceae and Chlorophyll Quantification

Counting Symbiodiniaceae cells by microscopy was not particularly precise, with mean CV between sites and trips nearly 35, suggesting that there is a large amount of variability in the data, but not enough to be indicative of problems, especially given these are natural samples (Brown, 1998). On the other hand, CV of Symbiodiniaceae within a single sample was much lower at only 17.2, showing that the variation found in counts is due to treatment and not found within individual colonies. Extraction of chlorophyll using the method described above was extremely precise, with mean CV of both types of chlorophyll well below the ~30% that Brown (1998) has suggested could be indicative of problems in the data, though more leniency is given for natural samples. Chlorophyll *a* and *c*<sub>2</sub> did not extract at the same rate, as such if chlorophyll *a* is the only pigment of interest, then 24 h of incubation is sufficient. If chlorophyll *c*<sub>2</sub> concentrations are also being investigated, then 48 h incubation time is necessary. Freeze drying samples previously resulted in a twofold increase in chlorophyll concentration (Pupier et al., 2018), results using the method described here likely will not be directly comparable with results from freeze dried samples. While we extracted chlorophyll in a 4°C refrigerator, other studies have successfully extracted in -20°C freezer (e.g., Jones, 1997a), but may not be directly comparable so care should be taken when comparing between studies that extract using different methods or at different temperatures.

## CONCLUSION

Here, we have developed an effective, efficient, and streamlined process for quantifying Symbiodiniaceae and chlorophyll concentrations of octocorals which may also be useful in studies of other fleshy zooxanthellate animals (Figure 4). Though freeze-drying yields higher chlorophyll concentrations and may be more appropriate for studies focusing on this parameter, it

takes significantly longer to process samples. The speed with which samples can be processed makes this method ideal for studies that involve large numbers of samples, for example, when examining the effects of natural bleaching events. While the method has been demonstrated for three quite different octocorals, testing on species with a wider range of spicules and protein concentrations is now warranted.

This method is a synthesis of disparate methods from the literature, and as such comparisons made using this method against others in the literature should be done carefully. Many factors may affect reported concentrations, including chlorophyll extraction time, medium, and temperature; and whether weight, dry weight, or protein content were used to standardise measurements. Because of this, the authors believe it is important to have a standardised, comparable method of extraction and quantification of Symbiodiniaceae cells, protein, and chlorophylls for future work in this field. It is the recommendation of the authors that chlorophyll should be extracted in 100% acetone at 4°C for 24 h if only chlorophyll *a* will be examined, or 48 h if chlorophyll *c*<sub>2</sub> is also of interest, and that all concentrations should be standardised to protein content when possible. Octocorals are an important part of reef ecosystems and are becoming the focus of many studies. This rapid method may therefore represent a timely addition to the suite of tools of any octocoral researcher.

## DATA AVAILABILITY STATEMENT

The datasets presented in this study can be found in Steinberg (2021).

## AUTHOR CONTRIBUTIONS

RS developed the method in collaboration with TB and wrote the initial manuscript. EJ and KD supervised laboratory work and edited the manuscript. TB collaborated on method development. TA supervised laboratory and field work, and edited the manuscript. All authors contributed to the article and approved the submitted version.

## FUNDING

This study was supported by the University of New South Wales and a Scientia Fellowship awarded to TA in 2018. RS was supported by a Research Training Program Scholarship provided by the Australian Government.

## ACKNOWLEDGMENTS

We would like to extend our respects to the Borogegal and Bedegal people, who are the traditional owners of the land on which this research was conducted. We would like to



send our deepest thanks to Sallyann Gudge, Britt Anderson, and Caitlin Woods from the Lord Howe Island Marine Parks Service, Dean Hiscox from Lord Howe Island Environmental Tours, Aaron and Lisa Ralph from ProDive Lord Howe Island, Tess Moriarty from the University of Newcastle, and Charlotte Page and Jesse Bergman from the University of New South Wales for their assistance with field logistics and field work. We thank the Thompson Family at Blue Lagoon Lodge for field accommodations and field laboratory provisioning. We thank

Tom Bridge at James Cook University, Catherine McFadden at Harvey Mudd College, and Yehuda Benayahu at Tel Aviv University for their invaluable help with species identification. We thank Andrew Niccum, Amanda Scholes, and Nigel Coombs at the Sydney Institute of Marine Science for provision of laboratory facilities and help with laboratory work. Finally, we also thank Eve Slavich and Ben Maslen from Stats Central at the University of New South Wales for invaluable input into statistical analyses.

## REFERENCES

- Bates, D., Maechler, M., Bolker, B., Walker, S., Christensen, R. H. B., Singmann, H., et al. (2015). *Package 'lme4.' Version 1.1-27.1*.
- Brown, B. E., Le Tissier, M. D. A., and Bythell, J. C. (1995). Mechanisms of bleaching deduced from histological studies of reef corals sampled during a natural bleaching event. *Mar. Biol.* 122, 655–663. doi: 10.1007/BF00350687
- Brown, C. E. (1998). *Coefficient of Variation. Applied Multivariate Statistics in Geohydrology and Related Sciences*. Berlin: Springer, 155–157.
- Davis, T. R., Harasti, D., and Smith, S. D. A. (2015). Extension of dendronephthya australis soft corals in tidal current flows. *Mar. Biol.* 162, 2155–2159. doi: 10.1007/s00227-015-2732-7
- Dias, T. L. P., and Gondim, A. I. (2016). Bleaching in scleractinians, hydrocorals, and octocorals during thermal stress in a northeastern Brazilian reef. *Mar. Biodivers* 46, 303–307. doi: 10.1007/s12526-015-0342-8
- Edmunds, P. J., and Gates, R. D. (2002). Normalizing physiological data for scleractinian corals. *Coral. Reefs* 21, 193–197. doi: 10.1007/s00338-002-0214-0
- Epstein, H. E., and Kingsford, M. J. (2019). Are soft coral habitats unfavourable? A closer look at the association between reef fishes and their habitat. *Environ. Biol. Fishes* 102, 479–497. doi: 10.1007/s10641-019-0845-4
- Evensen, N. R., Fine, M., Perna, G., Voolstra, C. R., and Barshis, D. J. (2021). Remarkably high and consistent tolerance of a Red Sea coral to acute and chronic thermal stress exposures. *Limnol. Oceanogr.* 9999, 1–12. doi: 10.1002/lno.11715
- Falkowski, P. G., and Dubinsky, Z. (1981). Light-shade adaptation of *Stylophora pistillata*, a hermatypic coral from the Gulf of Eilat. *Nature* 289, 172–174. doi: 10.1038/289172a0
- Ferrier-Pagès, C., Tambutté, E., Zamoum, T., Segonds, N., Merle, P. L., Bensoussan, N., et al. (2009). Physiological response of the symbiotic gorgonian *Eunicella singularis* to a longterm temperature increase. *J. Exp. Biol.* 212, 3007–3015. doi: 10.1242/jeb.031823
- Gierz, S., Ainsworth, T. D., and Leggat, W. (2020). Diverse symbiont bleaching responses are evident from 2-degree heating week bleaching conditions as thermal stress intensifies in coral. *Mar. Freshw Res.* 71, 1149–1160. doi: 10.1071/MF19220
- Griffith, J. K. (1994). Predation on soft corals (Octocorallia: Alcyonacea) on the great barrier reef. *Aust. Mar. Freshw Res.* 45, 1281–1284.
- Grottoli, A. G., Rodrigues, L. J., and Palardy, J. E. (2006). Heterotrophic plasticity and resilience in bleached corals. *Nature* 440, 1186–1189. doi: 10.1038/nature04565
- Hannes, A. R., Barbeitos, M., and Coffroth, M. A. (2009). Stability of symbiotic dinoflagellate type in the octocoral *briareum asbestinum*. *Mar. Ecol. Prog. Ser.* 391, 65–72. doi: 10.3354/meps07990
- Hannides, A. K., Glazer, B. T., and Sansone, F. J. (2014). Extraction and quantification of microphytobenthic Chl a within calcareous reef sands. *Limnol. Oceanogr. Methods* 12, 126–138. doi: 10.4319/lom.2014.12.126
- Hill, R., and Scott, A. (2012). The influence of irradiance on the severity of thermal bleaching in sea anemones that host anemonefish. *Coral. Reefs* 31, 273–284. doi: 10.1007/s00338-011-0848-x
- Hill, R., Fernance, C., Wilkinson, S. P., Davy, S. K., and Scott, A. (2014). Symbiont shuffling during thermal bleaching and recovery in the sea anemone *Entacmaea quadricolor*. *Mar. Biol.* 161, 2931–2937. doi: 10.1007/s00227-014-2557-9
- Hoegh-Guldberg, O. (1999). Climate change, coral bleaching and the future of the world's coral reefs. *Mar. Freshw Res.* 50, 839–866. doi: 10.1071/MF99078
- Hueerkamp, C., Glynn, P. W., D'Croz, L., Maté, J. L., and Colley, S. B. (2001). Bleaching and recovery of five eastern pacific corals in an El Niño-related temperature experiment. *Bull. Mar. Sci.* 69, 215–236.
- Hughes, T. P., Baird, A. H., Bellwood, D. R., Card, M., Connolly, S. R., Folke, C., et al. (2003). Climate change, human impacts, and the resilience of coral reefs. *Science* 301, 929–933. doi: 10.1126/science.112850389
- Jeffrey, S. W., and Humphrey, G. F. (1975). New spectrophotometric equations for determining chlorophylls a, b, c1, and c2 in higher plants, algae and natural phytoplankton. *Biochem. Physiol. Pflanz* 167, 191–194. doi: 10.1016/0022-2860(75)85046-0
- Johannes, R. E., and Wiebe, W. J. (1970). Method for determination of coral tissue biomass and composition. *Limnol. Oceanogr.* 15, 822–824. doi: 10.4319/lo.1970.15.5.0822
- Jones, R. J. (1997a). Changes in zooxanthellar densities and chlorophyll concentrations in corals during and after a bleaching event. *Mar. Ecol. Prog. Ser.* 158, 51–59. doi: 10.3354/meps158051
- Jones, R. J. (1997b). Zooxanthellae loss as a bioassay for assessing stress in corals. *Mar. Ecol. Prog. Ser.* 149, 163–171. doi: 10.3354/meps149163
- Kirk, N. L., Ward, J. R., and Coffroth, M. A. (2005). Stable *Symbiodinium* composition in the sea fan *Gorgonia ventalina* during temperature and disease stress. *Biol. Bull.* 209, 227–234. doi: 10.2307/3593112
- Koehl, M. A. R. (1982). Mechanical design of spicule-reinforced connective tissue: stiffness. *J. Exp. Biol.* 98, 239–267.
- Lenth, R., Singmann, H., and Love, J. (2018). *Emmeans: Estimated Marginal Means, Aka Least-Squares Means. R Package Version 1.1.3*.
- Lesser, M. P. (1989). Photobiology of natural populations of zooxanthellae. *Cytometry* 10, 653–658.
- Loya, Y., Sakai, K., Yamazato, K., Nakano, Y., Sambali, H., and van Woesik, R. (2001). Coral bleaching: the winners and the losers. *Ecol. Lett.* 4, 122–131.
- McCowan, D. M., Pratchett, M. S., Paley, A. S., Seeley, M., and Baird, A. H. (2011). A comparison of two methods of obtaining densities of zooxanthellae in *Acropora millepora*. *Galaxea. J. Coral. Reef Stud.* 13, 29–34. doi: 10.3755/galaxea.13.29
- Metaxatos, A., and Ignatiades, L. (2002). Seasonality of algal pigments in the sea water and interstitial water / sediment system of an eastern mediterranean coastal area. *Estuarine. Coastal Shelf Sci.* 55, 415–426. doi: 10.1006/ecss.2001.0915
- Prada, C., Weil, E., and Yoshioka, P. M. (2010). Octocoral bleaching during unusual thermal stress. *Coral. Reefs* 29, 41–45. doi: 10.1007/s00338-009-0547-z
- Pratchett, M. S. (2007). Dietary selection by coral-Feeding butterflyfishes (chaetodontidae) on the great barrier reef, Australia. *Raffles Bull. Zool* 2014, 171–176.
- Pratchett, M. S., Hoey, A. S., and Wilson, S. K. (2016). "Habitat-use and Specialisation among coral reef damselfishes," in *Biology of Damselfishes*, eds B. Frédérick and E. Parmentier (CRC Press), 102–139.
- Pupier, C. A., Bednarz, V. N., and Ferrier-Pagès, C. (2018). Studies with soft corals recommendations on sample processing and normalization metrics. *Front. Mar. Sci.* 5:1–9. doi: 10.3389/fmars.2018.00348
- Riegl, B. (1995). Effects of sand deposition on scleractinian and alcyonacean corals. *Mar. Biol.* 121, 517–526. doi: 10.1007/BF00349461
- Rossi, S., Schubert, N., Brown, D., Soares, M., de, O., Grosso, V., et al. (2018). Linking host morphology and symbiont performance in octocorals. *Sci. Rep.* 8, 1–14. doi: 10.1038/s41598-018-31262-3
- Sethmann, I., and Wörheide, G. (2008). Structure and composition of calcareous sponge spicules: a review and comparison to structurally



- related biominerals. *Micron* 39, 209–228. doi: 10.1016/j.micron.2007.01.006
- Steinberg, R. K. (2021). Octocoral methods – Symbiodiniaceae, chlorophyll, and protein content. *Mend. Data* V1. doi: 10.17632/3hpnr5c3gg.1
- Studivan, M. S., Hatch, W. I., and Mitchelmore, C. L. (2015). Responses of the soft coral *Xenia elongata* following acute exposure to a chemical dispersant. *Springerplus* 4:80. doi: 10.1186/s40064-015-0844-7
- Thermo Scientific (2018). *Coomassie Plus (Bradford) Assay Kit Instructions*. Rockford, Illinois: Pierce Biotechnology.
- Van Hooidek, R., Maynard, J. A., Manzello, D., and Planes, S. (2014). Opposite latitudinal gradients in projected ocean acidification and bleaching impacts on coral reefs. *Glob Chang. Biol.* 20, 103–112. doi: 10.1111/gcb.12394
- Wessels, W., Sprungala, S., Watson, S. A., Miller, D. J., and Bourne, D. G. (2017). The microbiome of the octocoral *Lobophytum pauciflorum*: minor differences between sexes and resilience to short-term stress. *FEMS Microbiol. Ecol.* 93, 1–13. doi: 10.1093/femsec/fix013

**Conflict of Interest:** The authors declare that the research was conducted in the absence of any commercial or financial relationships that could be construed as a potential conflict of interest.

**Publisher's Note:** All claims expressed in this article are solely those of the authors and do not necessarily represent those of their affiliated organizations, or those of the publisher, the editors and the reviewers. Any product that may be evaluated in this article, or claim that may be made by its manufacturer, is not guaranteed or endorsed by the publisher.

Copyright © 2021 Steinberg, Johnston, Bednarek, Dafforn and Ainsworth. This is an open-access article distributed under the terms of the Creative Commons Attribution License (CC BY). The use, distribution or reproduction in other forums is permitted, provided the original author(s) and the copyright owner(s) are credited and that the original publication in this journal is cited, in accordance with accepted academic practice. No use, distribution or reproduction is permitted which does not comply with these terms.



# Comparison of Standard Caribbean Coral Reef Monitoring Protocols and Underwater Digital Photogrammetry to Characterize Hard Coral Species Composition, Abundance and Cover

Erick Barrera-Falcon<sup>1,2</sup>, Rodolfo Rioja-Nieto<sup>2,3\*</sup>, Roberto C. Hernández-Landa<sup>2</sup> and Edgar Torres-Irineo<sup>3</sup>

<sup>1</sup> Posgrado en Ciencias del Mar y Limnología, Universidad Nacional Autónoma de México, Mérida, Mexico, <sup>2</sup> Laboratorio de Análisis Espacial de Zonas Costeras (COSTALAB), Unidad Multidisciplinaria de Docencia e Investigación-Sisal, Facultad de Ciencias, Universidad Nacional Autónoma de México, Mérida, Mexico, <sup>3</sup> Escuela Nacional de Estudios Superiores, Unidad Mérida, Universidad Nacional Autónoma de México, Mérida, Mexico

## OPEN ACCESS

### Edited by:

James Davis Reimer,  
University of the Ryukyus, Japan

### Reviewed by:

Ruy Kenji Papa De Kikuchi,  
Federal University of Bahia, Brazil  
Andrew G. Bauman,  
National University of Singapore,  
Singapore

### \*Correspondence:

Rodolfo Rioja-Nieto  
rioja@ciencias.unam.mx

### Specialty section:

This article was submitted to  
Coral Reef Research,  
a section of the journal  
Frontiers in Marine Science

**Received:** 09 June 2021

**Accepted:** 06 September 2021

**Published:** 14 October 2021

### Citation:

Barrera-Falcon E, Rioja-Nieto R, Hernández-Landa RC and Torres-Irineo E (2021) Comparison of Standard Caribbean Coral Reef Monitoring Protocols and Underwater Digital Photogrammetry to Characterize Hard Coral Species Composition, Abundance and Cover. *Front. Mar. Sci.* 8:722569. doi: 10.3389/fmars.2021.722569

The precise assessing and monitoring of coral reefs are necessary to address and understand the threats and changes in coral communities. With the development of new technologies and algorithms for image processing, new protocols like underwater photogrammetry are implemented to study these ecosystems. This study compares the main ecological metrics for reef condition assessment, obtained with an underwater digital photogrammetry protocol (UWP) and traditional sampling design simulations in coral reefs of the Cozumel Reefs National Park. Three orthomosaics (380 m<sup>2</sup>) per reef on six fringing reefs were constructed, and the hard coral community characterized using a Geographic Information System (GIS). The orthomosaics were also used as a basis to simulate transect lines and obtain data on the hard coral community according to the video transect (VT) protocol, point intercept (PIT) protocol, and the Atlantic and Gulf Rapid Reef Assessment (AGGRA) protocol. Higher colony abundance, species richness, and lower coral cover estimates ( $p < 0.05$ ) were obtained with the UWP. This protocol was also sensitive to small sized species. All the sampling designs showed similar capability to identify dominant species in terms of colony abundance and coral cover. The VT, PIT, and AGGRA showed similar coral cover values ( $p > 0.05$ ), which seems to indicate that these sampling designs overestimate this important metric. Our results will help to understand and integrate the observations obtained with UWP with long-term data obtained with commonly used monitoring protocols in the Caribbean region.

**Keywords:** underwater photogrammetry, coral reef monitoring, standard monitoring protocols, ecological metrics, coral cover

## 1. INTRODUCTION

The depletion of coral reefs and the rapid loss of living coral tissue are a consequence of a synergy of disturbances of human and natural origin, and effects related to climate change (Jackson et al., 2001; Hughes et al., 2003, 2018; Pandolfi et al., 2003; Steffen et al., 2011). Since the early 1990s, several systematic visual surveys have been used throughout the Caribbean and other regions, for

the evaluation and monitoring of coral reef ecosystems (English S, 1997; Hill and Wilkinson, 2004). Widely used protocols in the Caribbean include the line intercept transect protocol (LIT), point intercept transect (PIT) protocol, Caribbean coastal marine productivity (CARICOMP) protocol, and Atlantic and Gulf Reef Rapid Reef Assessment (AGRRA) protocol (<http://www.agrra.org/>), Reef Check (<http://www.reefcheck.org/>), among others (for details see English S, 1997; Kjerfve, 1998; Hill and Wilkinson, 2004; Lang et al., 2010; Jokiel et al., 2015). These protocols are based on the counting of points having as sampling unit line-transects, which were previously established by Loya (1972) and Porter (1972). Quadrants and images obtained by means of underwater photography or video were later incorporated, and are also commonly used to estimate relative percentages of cover of reef benthic organisms and other key ecological attributes such as species richness and colony abundance (Aronson et al., 1994; English S, 1997; Kjerfve, 1998; Hill and Wilkinson, 2004; Lang et al., 2010; Jokiel et al., 2015).

The choice of monitoring protocol depends on different characteristics. Main drivers might be related to the socialization of the protocol (training availability and experience of surveyors), needs for data standardization between regions, and objectives of the monitoring program and availability of financial resources. The time required for acquisition and data processing may also influence which protocol is most appropriate (Wilkinson et al., 2003; Brown et al., 2004). Therefore, coral reef researchers and managers are often faced with the challenge of obtaining data while maintaining a compromise between high accuracy, reproducibility, and statistical power, with low cost and time for analysis (Aronson et al., 1994).

Comparisons between PIT, AGRRA, and videotransect (VT) have been previously performed to assess their efficiency (Leujak and Ormond, 2007; Jokiel et al., 2015). The main findings indicate that the protocols based on visual surveys like, AGRRA and PIT, have low repeatability and high variability on benthic cover estimates, when compared to image-based protocols (Carleton and Done, 1995; Brown et al., 2004; Lam et al., 2006; Leujak and Ormond, 2007; Montilla et al., 2020). The use of VT has also shown to provide more accurate estimates on the benthic cover of organisms (Aronson et al., 1994; Leujak and Ormond, 2007; Jokiel et al., 2015). Image-based protocols also produce a permanent record, where species identification and other metrics are obtained under laboratory conditions (Page et al., 2016).

Underwater digital photogrammetry protocols (UWP) with different approaches have recently been used to address changes in the 3D structure associated with natural disturbances (Burns et al., 2015; Peck et al., 2021), assess patterns in the spatial distribution of reef-building corals (Edwards et al., 2017) and reef structural complexity (Burns et al., 2016; Price et al., 2019), and characterize the ecological structure and demographic characteristics of coral colonies (Capra et al., 2017; Edwards et al., 2017; Young et al., 2017; Bianchi, 2019; Lechene et al., 2019; Neyer et al., 2019; Bayley and Mogg, 2020; Burns et al., 2020; Hernández-Landa et al., 2020; Nocerino et al., 2020; Rossi et al., 2020). Results on comparisons between UWP and monitoring protocols to assess reefs characteristics obtained from sites in the Indian and Pacific ocean have been varied.

Urbina-Barreto et al. (2021) showed that the LIT overestimates coral cover in comparison to UWP. However, Couch et al. (2021) observed a high consistency of data between UWP and field visual surveys. Considering the advantages and recent integration of underwater photogrammetry to monitor coral reefs, there is a clear need to compare its performance with commonly used protocols. For the Caribbean region, where several standard monitoring protocols are used to assess coral reefs, this has not yet been performed. In this study, we compare the difference in terms of community structure, coral cover, abundance, and species richness estimates, between UWP and simulations of the VT, PIT, and AGRRA sampling designs, using the insular reefs of Cozumel as a case study. These reefs have differences in terms of depth, coral cover, community structure, and structural complexity and can be considered as representative of coral reefs in the region.

## 2. MATERIALS AND METHODS

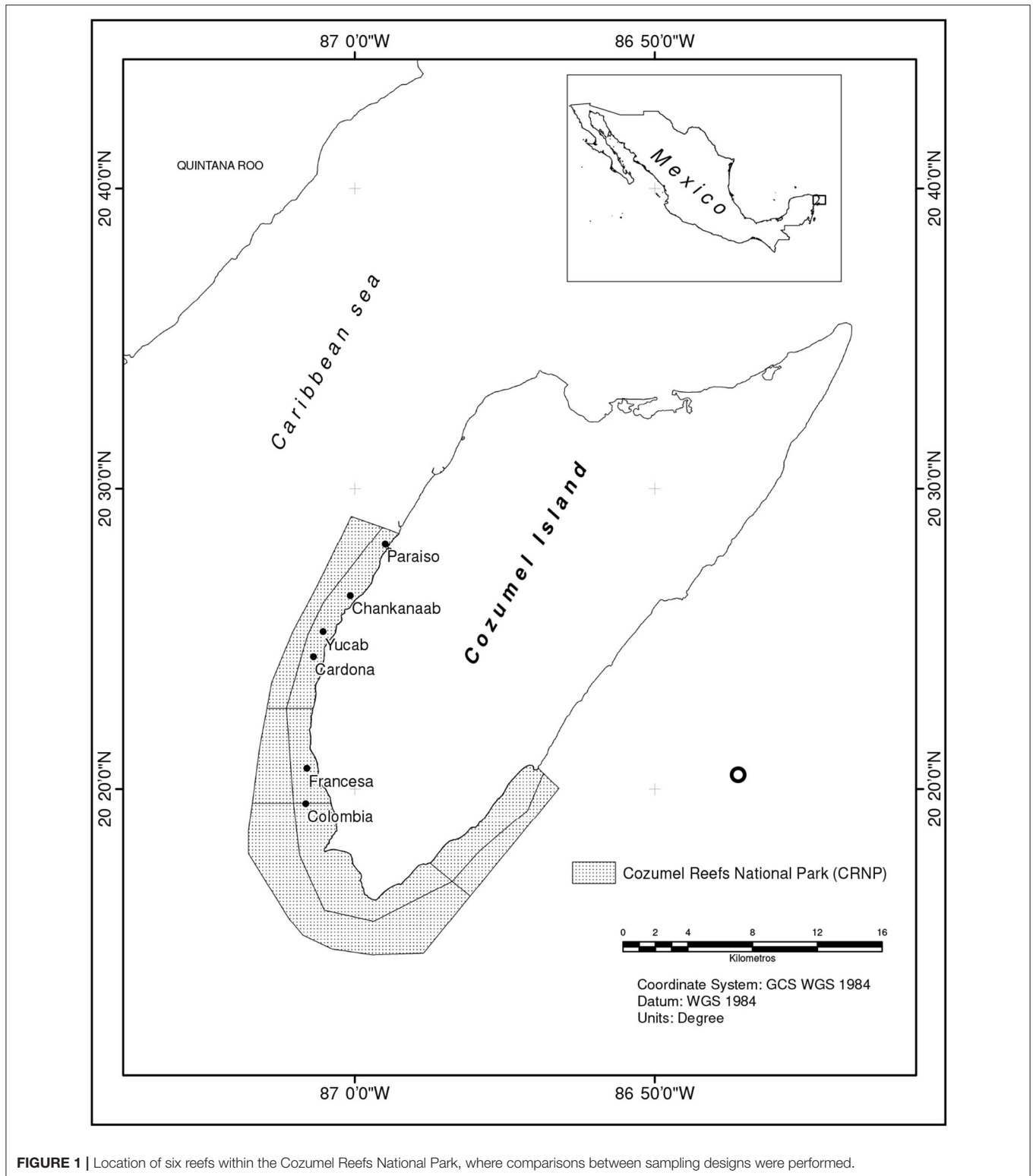
The Cozumel Reefs National Park (CRNP) is located 16 km from the coast of Quintana Roo, México (**Figure 1**). The characteristic seascape of the CRNP is a mixture of fringing reefs, patch reefs, and mixed corals on hard calcareous substrate, with algal and seagrass beds, and mangrove areas (Rioja-Nieto et al., 2019). The shallow sublittoral slope tends to be narrow, with the most developed reefs found along the edge of the southwestern insular shelf (Muckelbauer, 1990).

Six fringing reefs (6–14 m depth), distributed in a north to south gradient in terms of increasing reef structural complexity (Fenner, 1988; Muckelbauer, 1990), and abundance and live coral cover of dominant species (Hernández-Landa et al., 2020), were characterized using a UWP (**Figure 1**).

On each reef, photographs were obtained by divers along transects that followed the development of the reef (**Table 1**).

The divers swam at a constant speed 2 m above the average depth of the reef, taking photographs with the self-timer setting of the camera to ensure a high overlap (>80%) across and along images. The obtained images were processed with Agisoft metashape (v. 1.5) to construct orthomosaics and obtain Digital Surface Models. Custom made quadrants of vinyl polychloride (PVC), measuring 0.6 m, were used as a scale constraint in order to get accurate measurements from coral colonies. Vector files based on the orthomosaics were constructed with ArcMap v.10.5 by digitizing all coral colonies with a size >5 cm [for further details, see Hernández-Landa et al. (2020)]. The coral species were identified using the Humann and DeLoach (2002) and Lang et al. (2010), identification guides.

The orthomosaics (three per reef measuring c.a 150 m<sup>2</sup> each) were used as a basis for a surface analysis (UWP) and to simulate transects to obtain data on the hard coral community according to the VT, PIT, and AGRRA monitoring protocols (**Table 1**). For the UWP, a surface area of 380 m<sup>2</sup> was delimited from the orthomosaics in each reef. This area of analysis is considered to be representative of >90% of the hard coral species richness in these same reefs (Hernández-Landa et al., 2020). The percentage of cover of each species, based on the digitized vector files described



**FIGURE 1** | Location of six reefs within the Cozumel Reefs National Park, where comparisons between sampling designs were performed.

above, was estimated as the percentage of the total area surveyed that was covered by a hard coral species (**Figure 2**).

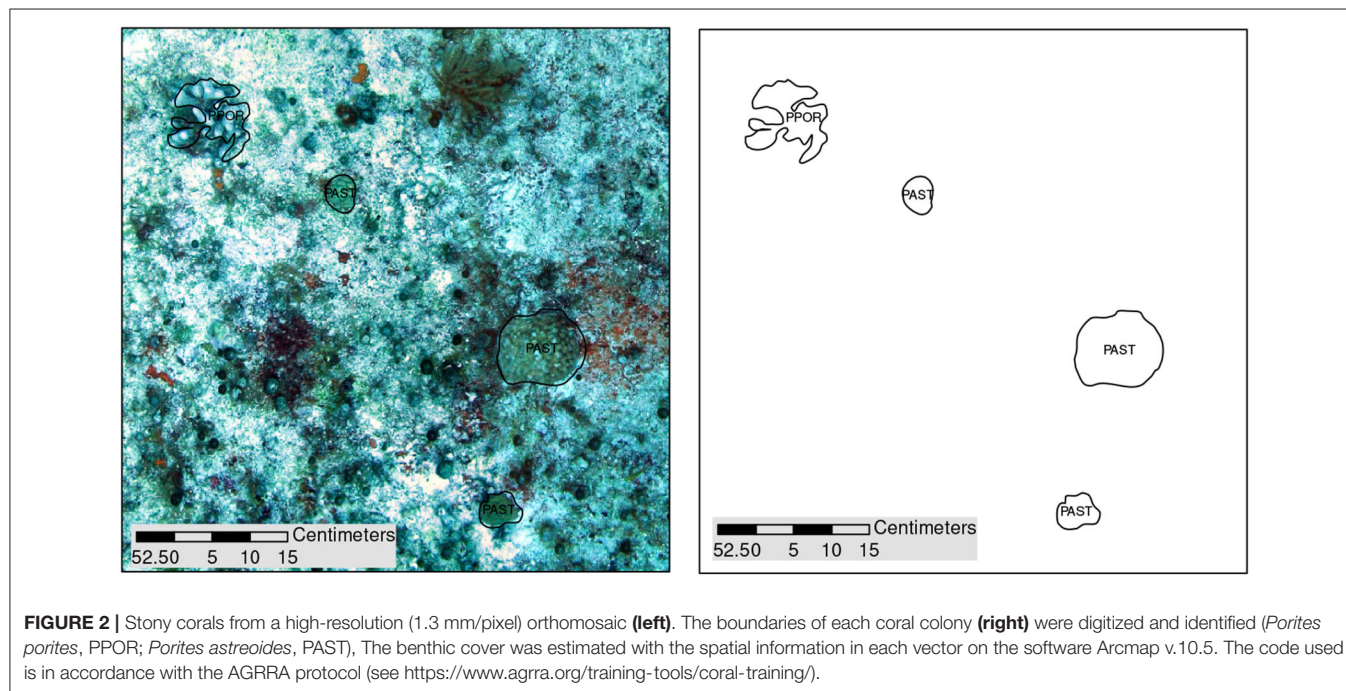
For the VT, two transects (six per reef) on each orthomosaic ( $0.6 \times 29.6$  m) were randomly simulated. In order to sample 100

m<sup>2</sup> (Aronson et al., 1994; Leujak and Ormond, 2007), frames were extracted every 0.63 m at a scale that ensured an area covering  $60 \times 60$  cm per frame (**Figure 3**). Thirteen randomly distributed points were selected on each frame, and a spatial



**TABLE 1** | Sampling protocols used for benthic communities, underwater digital photogrammetry (UWP), videotransect (VT), point intercept transect (PIT), and Atlantic and Gulf Rapid Reef Assessment (AGRRA).

Protocol	Sampling replicates per reef	Sampling area m <sup>2</sup>	Details	References
UWP	3	380	Three plots of 5 × 25.4 m for a total of 380 m <sup>2</sup>	Bayley and Mogg, 2020; Hernández-Landa et al., 2020
Video transect (VT)	10	100	Transects of 25 m × 60 cm and evaluation of 13 random points per frame.	Aronson et al., 1994; Leujak and Ormond, 2007
Point intercept protocol (PIT)	1	NA	A 50 m transect over the reef structure with evaluations every 10 cm.	Hill and Wilkinson, 2004
AGRRA	6	NA	Six 10 m transects over the reef structure with evaluations every 10 cm.	Lang et al., 2010



intersection function with the vector files was used to select coral colonies. The number of points analyzed per frame was chosen considering the average between the analyzed points reported by Aronson et al. (1994) and Leujak and Ormond (2007). The coral cover for each reef was estimated as the percentage of points that intersected with a coral species.

In the PIT, three transects, 16.7 m long (one per orthomosaic), were randomly simulated to survey c.a. 50 m (Hill and Wilkinson, 2004) on each reef. The identity of the substrate intersected by the transect was recorded every 10 cm (Figure 4), and coral cover estimated as the percentage of points where a hard coral species was detected.

In the case of AGRRA, six transects per reef (two per orthomosaic), with a 10 m length, were randomly simulated. Coral cover was estimated following the same procedure described for the PIT sampling design.

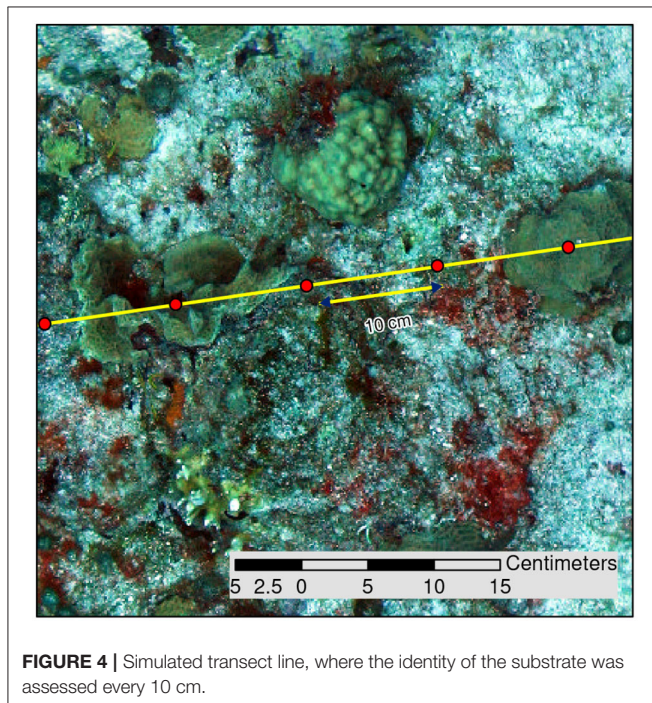
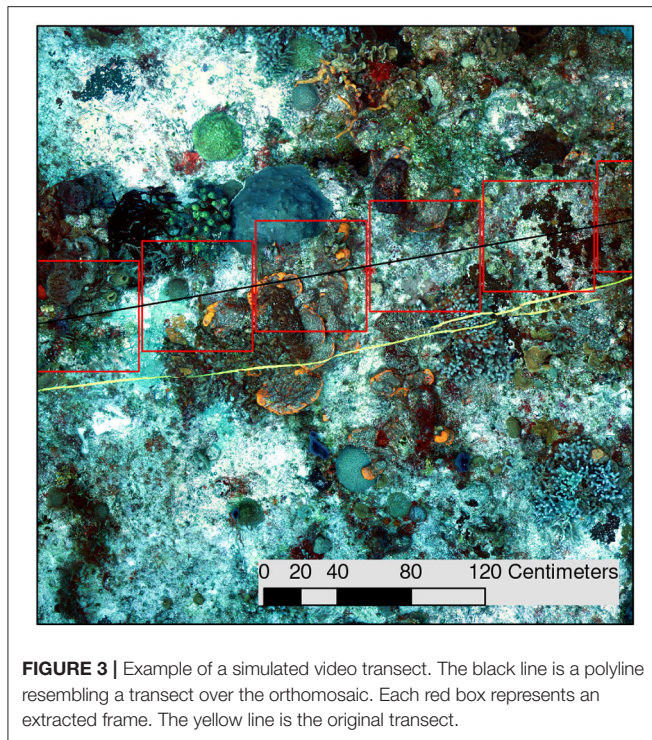
For all sampling designs, species richness and colony abundance were estimated as the number of species detected or colonies counted in the area (380 m<sup>2</sup> for UWP) or points

analyzed (3601 for VT, 500 for PIT, and 600 for AGRRA), considering the representative sample size published in the literature (Table 1). For the definition of colony, we followed Loya (1972), where a coral colony was considered a detached set of polyps interconnected by live tissue, regardless of neighboring colonies.

## 2.1. Data Analysis

The sampling techniques simulations were compared in terms of percentage of cover, species richness, and species abundance. Given the different characteristics in the coral community structure between reefs (Hernández-Landa et al., 2020), each reef was considered as a replica for the analysis.

Generalized linear models (GLM) were used to assess differences on percentage of cover and species richness among monitoring sampling designs. A Gamma and Poisson error distributions for coral cover and species richness, respectively, were assumed (Zuur et al., 2009). The species richness presented overdispersion; thus, SE were corrected using a quasi-GLM



model (Zeileis and Hothorn, 2002; Hothorn et al., 2008; Zuur et al., 2009). The models were validated using standard residual diagnostics. A plot of residuals vs. fitted values was used for the assumption of homoscedasticity, and q-q plots of residuals were used to test the residual normality assumption. Species

abundance estimates did not accomplish GLM assumptions. Therefore, a generalized estimating equation (GEE) approach was used to compare species abundance among monitoring sampling designs. GEE is similar to GLM but allows for the use of a correlation matrix structure that takes into account the lack of independence of each cluster (Yan, 2002; Yan and Fine, 2004; Halekoh et al., 2006; Zuur et al., 2009). The abundance estimates for each species from the monitoring sampling designs can violate the independence assumption, increasing the risk of type I error. Thus, they were compared among correlation structures (i.e., independence, exchangeable, and ar1) to consider correlation between abundance measures for the same cluster (i.e., each species). The correlation structure with the lowest value of correlation information criterion was the ar1. In all cases, a log link function, and a one-factor ANOVA (Zuur et al., 2009) were used. Community structure characteristics were considered as dependent variables, and the sampling designs were defined as factors. When a significant difference ( $p < 0.05$ ) was observed, a Tukey HSD *post-hoc* multiple comparison test was used to identify differences among sampling techniques simulations (Bauer, 2000). All data were analyzed in R v3.6.1 (R Core Team, 2019).

To identify the species that contributed to 90% of the abundance and cover (dominant species) according to each sampling design, a SIMPER analysis (Clarke and Warwick, 2001), was performed with PRIMER v.7.

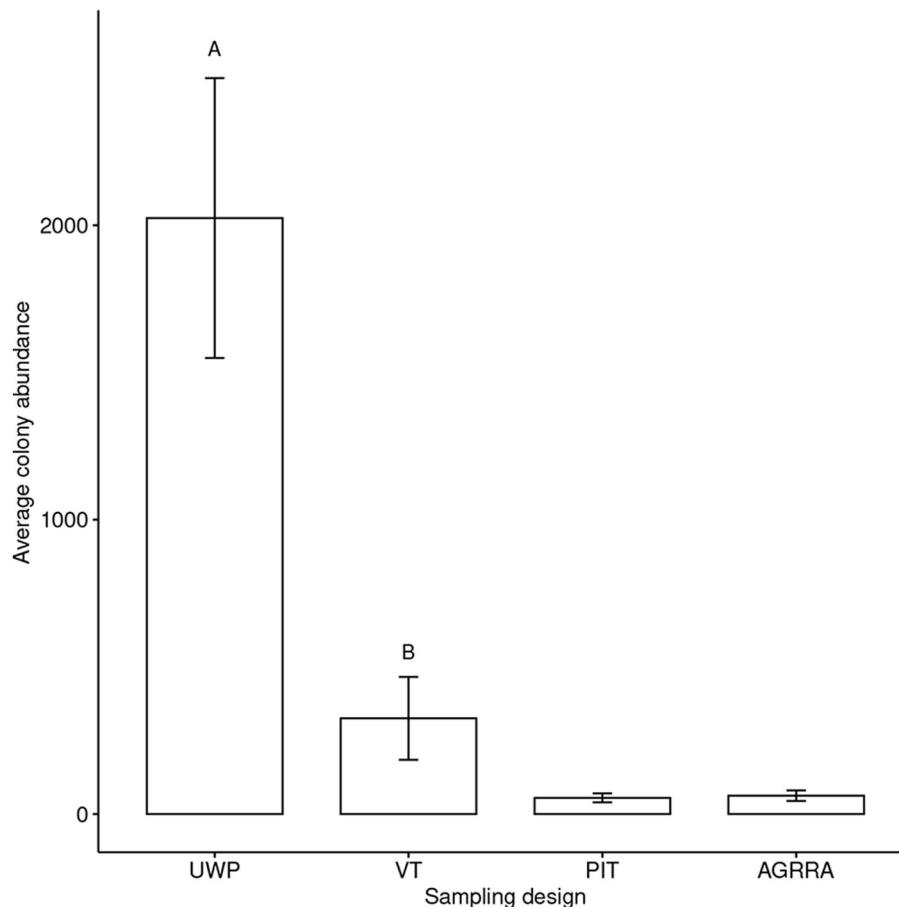
### 3. RESULTS

#### 3.1. Coral Colony Abundance

The average number of colonies observed was 2024 (UWP), 325 (VT), 62 (AGRRA), and 54 (PIT). The values obtained with each sampling design per reef are presented in **Supplementary Table 1**. The UWP recorded a significantly higher mean colony abundance than the other sampling designs ( $p < 0.001$ ) (see **Supplementary Table 2**). VT recorded a higher mean colony abundance than AGRRA and PIT ( $p < 0.001$ ). No significant differences ( $p > 0.05$ ) were observed between AGRRA and PIT (**Figure 5**). The species *Agaricia agaricites*, *Porites porites*, and *Siderastrea siderea* were identified as those with the highest percentage of contribution to abundance in all the sampling designs (**Table 2**). However, important differences on the percentage of contribution between sampling designs can be observed. *Porites astreoides* was not detected as dominant by the VT but was identified in the other survey designs. *Orbicella annularis* was only identified by PIT, AGRRA, and VT. The UWP was the only protocol where the *Eusmilia fastigiata* was identified as a dominant species.

#### 3.2. Coral Cover

The average percent of coral cover obtained was 6.02 (UWP), 8.86 (VT), 10.96 (PIT), and 10.38 (AGRRA). The values obtained with each sampling design per reef are presented in **Supplementary Table 3**. The UWP estimated a lower coral cover ( $p < 0.03$ ) than the other sampling designs (**Figure 6**). No other significant differences were observed ( $p > 0.05$ ; see **Supplementary Table 4**). *Agaricia agaricities* and *Siderastrea*



**FIGURE 5 |** Average colony abundance ( $\pm$ SD) obtained with each sampling design. Underwater digital photogrammetry (UWP), videotranssect (VT), point intercept transect (PIT), and Atlantic and Gulf Rapid Reef Assessment (AGRRA). Letters indicate the sampling designs where the average colony abundance had a significant difference ( $p < 0.001$ ).

*siderea* accounted for the majority of coral cover recorded across methods (Table 3). Differences in the species contribution are observed. *Porites astreoides* was considered dominant according to the UWP, PIT, and AGRRA. The species *Agaricia tenuifolia* is dominant for the UWP, VT, and AGRRA. UWP and AGRRA listed the same dominant species *P. porites*, *S. siderea*, and *P. astreoides* (Table 3).

### 3.3. Species Richness

Considering all sampling designs, a total of 31 species were recorded (Table 4). The UWP detected more species ( $p < 0.001$ , Supplementary Table 5) than VT, PIT, and AGRRA (Figure 7). The species *Dichocoenia stokessi*, *Solenastrea Bournoni*, *Scolymia* sp., *Isophyllia rigida*, *Colpophyllia natans*, and *Manicina areolata*, were only detected by UWP (Table 4). With the exception of *O. franksi* and *M. lamarckiana* for species abundance, and *A. tenuifolia*, *P. furcata*, *M. cavernosa*, *O. faveolata*, and *P. clivosa* for coral cover, the observations obtained with UWP showed higher values for the species abundance and lower values for coral cover than the other sampling designs.

## 4. DISCUSSION

Higher colony abundance, species richness, and lower coral cover estimates were obtained with the UWP. However, all the sampling designs showed a similar capability to identify dominant species in terms of colony abundance and coral cover. The VT, PIT, and AGRRA showed similar coral cover values, which seems to indicate that these commonly used protocols overestimate this metric. The reefs used for the analyses are distributed at different depths and have differences in structural complexity and community structure, representing reef characteristics observed in other regions of the Caribbean.

### 4.1. Coral Cover, Colony Abundance, and Species Richness

In terms of coral cover, our results are similar to the study of Urbina-Barreto et al. (2021), where underwater photogrammetry provided significantly lower estimates on coral cover than the line intercept protocol. The average percentage of coral cover obtained by the UWP (c.a. 6), is lower than those reported from



**TABLE 2 |** Dominant species in terms of abundance, identified with a SIMPER analysis by each sampling design.

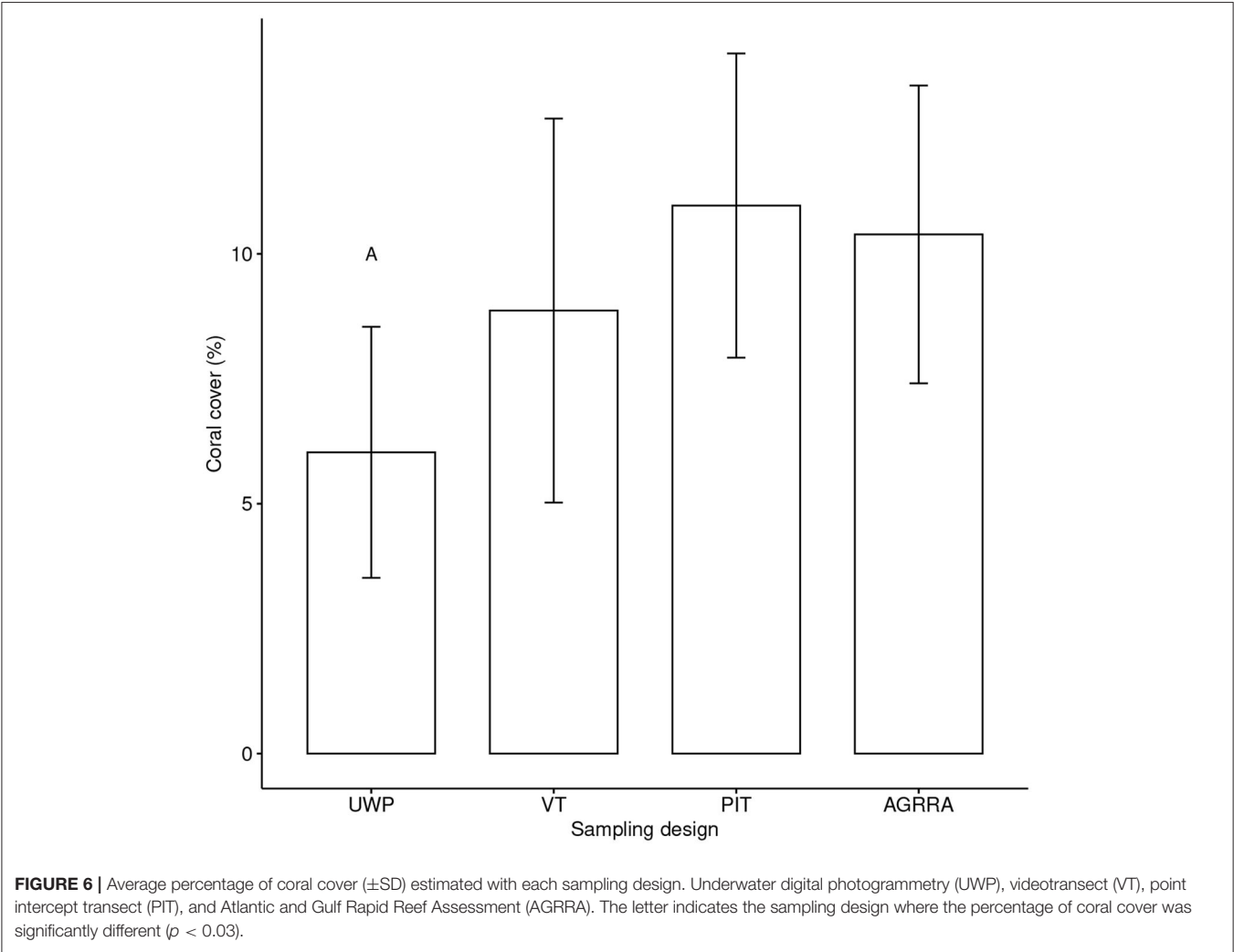
Protocol	Spp	%					Protocol	Spp	%				
UWP	AAGA PAST SSID PPOR EFAS	39.1	22.49	17.45	10.01	2.69	VT	ATEN AAGA PPOR OANN SSID	34.62	28.02	18.41	7.21	6.01
PIT	AAGA PPOR SSID PAST OANN	44.23	18.35	10.92	10.39	7.92	AGRRA	AAGA PPOR PAST OANN SSID	51.71	17.98	9.37	8.06	6.85

*Agaricia agaricites* (AAGA), *A. tenuifolia* (ATEN), *Eusmilia fastigiata* (EFAS), *Orbicella annularis* (OANN), *Porites astreoides* (PAST), *P. porites* (PPOR), and *Siderastrea siderea* (SSID). Underwater digital photogrammetry (UWP), point intercept transect (PIT), videotransect (VT), and Atlantic and Gulf Rapid Reef Assessment (AGRRA).

**TABLE 3 |** Dominant species in terms of cover, identified with a SIMPER analysis by each sampling design, the order of appearance indicates the contribution to the total cover.

Protocol	Spp	%					Protocol	Spp	%				
UWP	AAGA PAST SSID PPOR ATEN	41.3	17.58	16.20	13.71	4.58	VT	ATEN AAGA PPOR OANN SSID	34.62	28.02	18.41	7.21	6.01
PIT	AAGA SSID PPOR PAST	51.27	20.31	10.76	7.78		AGRRA	AAGA PPOR PAST SSID ATEN	35.82	22.24	20.74	9.99	5.08

*Agaricia agaricites* (AAGA), *Agaricia tenuifolia* (ATEN), *Orbicella annularis* (OANN), *Porites astreoides* (PAST), *Porites porites* (PPOR), and *Siderastrea siderea* (SSID). Underwater digital photogrammetry (UWP), point intercept transect (PIT), videotransect (VT), and Atlantic and Gulf Rapid Reef Assessment (AGRRA).



visual surveys for reefs in Cozumel. Reyes-Bonilla et al. (2014), Barranco et al. (2016), and McField et al. (2018) have reported coral cover values of c.a. 11, 29, and 17%, respectively.

The standardization of underwater photogrammetry protocols needs to be considered. In a recent study, Couch et al. (2021) detected no differences on the estimation of coral



**TABLE 4 |** Colony abundance for each of the species recorded by the sampling designs.

Spp	UWP	AGRRA	PIT	VT	Cover
<i>Agaricia agaricites</i> , AAGA	3898	101	85	386	
<i>Agaricia Humilis</i> , AHUM	298	7	4	22	
<i>Agaricia tenuifolia</i> , ATEN	686	30	35	405	
<i>Agaricia fragilis</i> , AFRA	34	1		8	
<i>Agaricia lamarcki</i> , ALAM	15			6	
<i>Porites porites</i> , PPOR	1,885	58	53	348	
<i>Madracis decactis</i> , MDEC	55	1	1		
<i>Porites furcata</i> , PFUR	103	7	2	8	
<i>Siderastrea siderea</i> , SSID	1,241	45	41	186	
<i>Montastraea cavemosa</i> , MCAV	343	11	9	68	










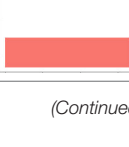
(Continued)

**TABLE 4 |** Continued

Spp	UWP	AGRRA	PIT	VT	Cover
<i>Orbicella annularis</i> , OANN	660	31	30	202	
<i>Orbicella faveolata</i> , OFAV	62	4	5	52	
<i>Porites astreoides</i> , PAST	1,797	44	40	165	
<i>Orbicella franksi</i> , OFRA	10			10	
<i>Favia fragum</i> , FFRA	79	3		2	
<i>Stephanocoenia intersepta</i> , SINT	2	1	1		
<i>Dichocoenia stokesii</i> , DSTO	7				
<i>Solenastrea bourmoni</i> , SBOU	7				
<i>Mycetophyllia</i> sp., MYCE	8			2	
<i>Meandrina jacksoni</i> , MJAC	4	1	1		


(Continued)

TABLE 4 | Continued

Spp	UWP	AGRRA	PIT	VT	Cover
<i>Meandrina meandrites</i> , MMEA	40	2	2	13	
<i>Dendrogyra cylindrus</i> , DCYL	8	1	1	6	
<i>Isophyllia rigida</i> , IRIG	14				
<i>Manicina areolata</i> , MARE	4				
<i>Mycetophyllia lamarckiana</i> , MLAM	1		1		
<i>Pseudodiploria clivosa</i> , PCLI	15			2	
<i>Diploria labyrinthiformis</i> , DLAB	33	3	1	4	
<i>Eusmilia fastigiata</i> , EFAS	445	10	5	19	
<i>Siderastrea radians</i> , SRAD	329	6	6	17	
<i>Colpophyllia natans</i> , CNAT	1				

(Continued)

TABLE 4 | Continued

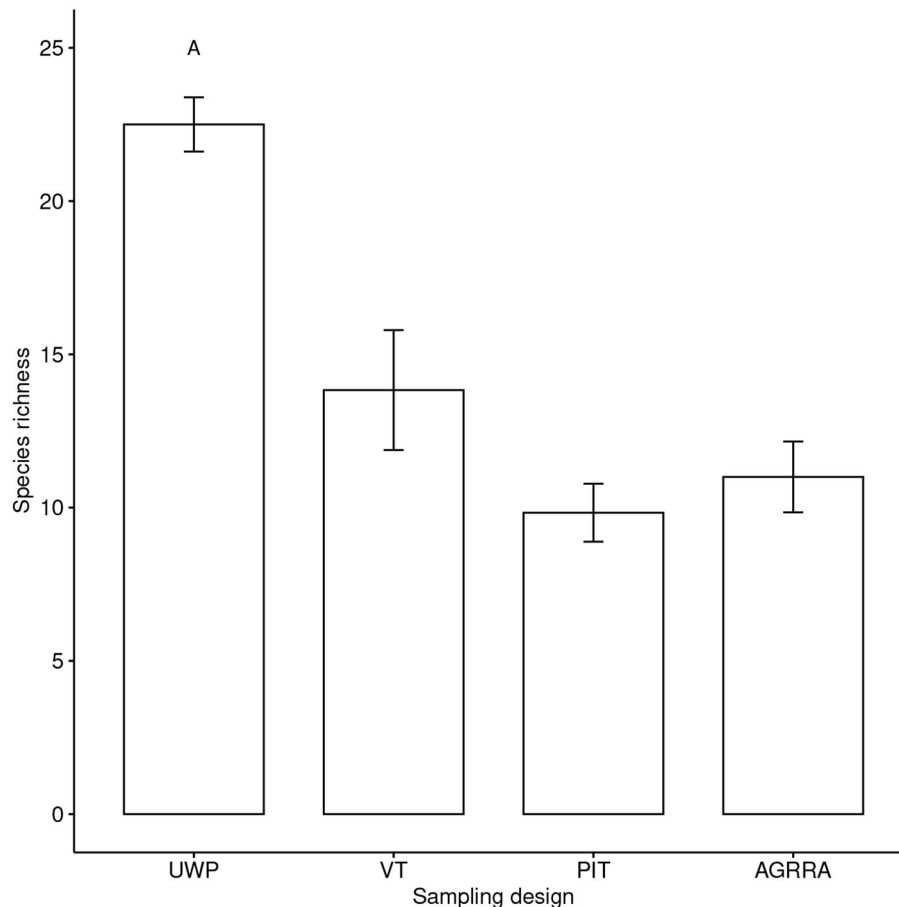
Spp	UWP	AGRRA	PIT	VT	Cover
<i>Scolymia</i> sp., SCOL	1				

Relative coral cover range in the graphs is between 0 and 2.83. The colors represent each protocol. Underwater digital photogrammetry (UWP), point intercept transect (PIT), videotranssect (VT), and Atlantic and Gulf Rapid Reef Assessment (AGRRA).

cover and other metrics (e.g., species richness, adult colony density, and average colony diameter) between an underwater photogrammetry protocol and in water visual surveys. This seems to be related to the area of analysis used in that study (60 m<sup>2</sup>). It has been reported that this same surveyed area with photogrammetry only represents 55% of all benthic features (Lechene et al., 2019). Furthermore, Hernández-Landa et al. (2020), determined that for the CRNP reefs an area of c.a. 380 m<sup>2</sup> is needed to obtain representative species richness data.

The species *A. agaricites*, *P. porites*, and *S. siderea* were identified in all cases as dominant and have been reported as typical of the Caribbean region (Reyes-Bonilla et al., 2014; Barranco et al., 2016; González-Barrios and Álvarez Filip, 2018). Other species such as *P. astreoides* and *A. tenuifolia* were also considered important in most of the sampling designs. For UWP, the species *E. fastigiata* was identified as dominant. This is an uncommon and small sized species (colonies about 20 cm in adult phase) (Veron J.E.N. and L.M., 2016; Horton et al., 2021), which suggests this sampling design to be sensitive to detect species with similar morphological characteristics and colony size. AGRRA, PIT, and VT are known to underestimate colonies that are too small or rare (Leujak and Ormond, 2007; Jokiel et al., 2015; Facon et al., 2016). VT was the only protocol that identified the massive species *O. annularis* as dominant in terms of cover. With big sized massive species, the area of the colonies can exceed the size of the evaluated frame. In this case, all the points distributed on the frame detect the same colony, but are assumed to belong to different ones (Bennett et al., 2016; Page et al., 2016). If these types of colonies are recurrent in the transect band, the proportions are prone to generate estimates that differ from the true values (Hill and Wilkinson, 2004). This can also occur with AGRRA and PIT when the diameter of the colonies exceeds c.a. 20 cm (Leujak and Ormond, 2007). For the UWP, it is important to consider local ecological characteristics, and maintain an homogeneous definition of a colony. The latter is particularly important, as an increase in the number of colonies could be related to partial colony mortality and the fission and fragmentation of colonies as a result of disturbance (Hughes and Jackson, 1980; Jaramillo González and Acosta, 2016).

The UWP recorded six uncommon species that were not detected by the other sampling designs. Five of these, *D. stokesii*, *S. bournoni*, *M. areolata*, *Scolymia* sp., and *I. rigida*, are small sized with adult colonies measuring c.a. 20 cm (Veron J.E.N. and



**FIGURE 7 |** Average number of species ( $\pm$ SD) obtained with each sampling design. Underwater digital photogrammetry (UWP), videotranssect (VT), point intercept transect (PIT), and Atlantic and Gulf Rapid Reef Assessment (AGRRA). UWP recorded the highest number of species. The letter indicates a significant difference ( $p < 0.001$ ).

L.M., 2016; Horton et al., 2021) *C. natans* is a massive species (Torruco et al., 2021). Considering the large area of analysis and the detailed colony digitization on the orthomosaics, the species richness based on the UWP is not affected by species traits such as colony size or abundance.

## 4.2. Comparisons Between Monitoring Protocols

Point Intercept Transect and AGRRA are suitable for coral reef characterization due to their ease of use and fast data availability (Carleton and Done, 1995; Hill and Wilkinson, 2004; Leujak and Ormond, 2007; Facon et al., 2016). Also, in sites with a high structural complexity (i.e., spurs and grooves), PIT performs better given the orthographic projection to a 2D that is needed for image-based protocols (Nadon and Stirling, 2006). However, these protocols need well-trained experienced divers for *in situ* species identification and data collection. The ecological characteristics of the sampling sites (e.g., sites with low coral coverage or high structural complexity) can also have an effect on the estimates based on the data obtained from these sampling designs. In sites with low coral cover, such as most of

the sites sampled in here (and arguably in the Caribbean region), the obtained data tend to have low representativeness and be less accurate (Molloy et al., 2013). Furthermore, the contour effect of the colonies, where transect lines follow the edge of large coral colonies, can also affect data collection (Lam et al., 2006).

Video Transect is a cost-effective protocol that can reduce the economic costs of data acquisition for large areas vs. PIT and AGRRA (Aronson et al., 1994). This monitoring protocol has the necessary inputs to adopt a photogrammetric approach by applying small adjustments, and should be explored. Like UWP, VT generates a permanent record that can be later verified. However, the taxonomic identification on some benthic groups (e.g., macroalgae and sponges) can be limited by the images resolution (Aronson et al., 1994; Carleton and Done, 1995).

Underwater digital photogrammetry is a rapid survey protocol for large areas without the need for trained personnel in species identification (Chirayath and Instrella, 2019; Lechene et al., 2019; Price et al., 2019; Bayley and Mogg, 2020; Hernández-Landa et al., 2020). This protocol allows extracting not only cover and community metrics but also important demographic information

on the size of the colonies and the spatial relationships in the benthic community (Edwards et al., 2017; Hernández-Landa et al., 2020). With the use of UWP, accurate 3D, and digital elevation models can also be produced. Furthermore, establishing permanent markers on the substrate can allow precise long-term monitoring of coral common (e.g., coral cover and species richness), and marginally explored characteristics (e.g., colony size variation and spatial distribution, changes in 3D metrics over depth, or disturbance gradients) of the reef community at large spatial scales. This will increase our understanding of the processes that shape coral reef communities. The image processing in UWP and subsequent data analysis can be time-consuming (2–3 months for a full time experienced person) or expensive to implement considering the need of specialized hardware and software. However, there are several options for the adoption of free or proprietary software (Leon et al., 2015; Lechene et al., 2019) and the use of affordable devices such as the Jetson Nano GPU NVIDIA (Barba-Guaman et al., 2020). For the data analysis, automated species identification and artificial intelligence are being developed (Chirayath and Instrella, 2019; Pavoni et al., 2020; Yuval et al., 2021) and may reduce the time needed to obtain valuable information.

Underwater photogrammetry protocols are increasingly being used to assess coral reefs. To our knowledge, at least six studies using underwater photogrammetry for coral reef monitoring have been published. The protocols mainly differ in the area sampled for analysis, ranging from 60 to 1,655 m<sup>2</sup>, but are similar in image acquisition procedure, cameras utilized, image processing algorithms, fieldwork environmental conditions during data collection (clear water, shallow sites), use of internal control points, and the colony data processing (Palma et al., 2017, 2019; Lechene et al., 2019; Hernández-Landa et al., 2020; Couch et al., 2021; Urbina-Barreto et al., 2021). UWP relies on the surface analysis of the benthic substrate, and obtained metrics seem to be biased by the area considered. More studies are needed to determine the representative sampling area for photogrammetric analysis in the different regions where coral reefs distribute. This will ensure that direct comparisons in different regions, can be made between long-term monitoring programs. Our results also suggest that commonly used monitoring protocols in the Caribbean are overestimating coral cover, and underestimating species richness and colony abundance with the “standardized” sampling effort,

and this needs to be further explored. Finally, it is important to consider that the data obtained for the VT, PIT, and AGGRA protocols presented in here were not obtained under field conditions. Therefore, circumstances that can have an impact on the quality of the data acquired with these sampling designs such as current effects, availability of time to conduct the surveys, and *in situ* species identification, among others, are not considered.

## DATA AVAILABILITY STATEMENT

The original contributions presented in the study are included in the article/Supplementary Material, further inquiries can be directed to the corresponding author.

## AUTHOR CONTRIBUTIONS

EB-F, RR-N, and RH-L: conceptualization, methodology, validation, writing—review and editing, and writing—original draft preparation. EB-F, RR-N, and ET-I: formal analysis. EB-F: investigation, visualization, and software. RR-N: supervision, project administration, resources, and funding acquisition. All authors have read and agreed to the published version of the manuscript.

## FUNDING

This research was funded by the PAPIIT grant (IN218219) from the National Autonomous University of Mexico supported this work. EB-F was supported by a CONACYT postgraduate scholarship. RH-L was funded by a postdoctoral scholarship awarded by the Programa de Becas Posdoctorales Convocatoria 2017, UNAM-DGAPA.

## ACKNOWLEDGMENTS

The authors would like to thank M. C. Carlos Cruz Vázquez and the CRNP staff for field work assistance.

## SUPPLEMENTARY MATERIAL

The Supplementary Material for this article can be found online at: <https://www.frontiersin.org/articles/10.3389/fmars.2021.722569/full#supplementary-material>

## REFERENCES

- Aronson, R. B., Edmunds, J. P., Precht, F. W., Swanson, W. D., and Levitan, R. D. (1994). Large-scale, long-term monitoring of caribbean coral reefs: simple, quick, inexpensive techniques. *Atoll Res. Bull.* 421, 1–19. doi: 10.5479/si.00775630.421.1
- Barba-Guaman, L., Eugenio Naranjo, J., and Ortiz, A. (2020). Deep learning framework for vehicle and pedestrian detection in rural roads on an embedded GPU. *Electronics* 9:589. doi: 10.3390/electronics9040589
- Barranco, L., Carriquiry, J., Rodriguez Zaragoza, F., Cupul-Magaña, A., Villascusa, J., and Calderon-Aguilera, L. (2016). Spatiotemporal variations of live coral cover in the northern Mesoamerican reef system, Yucatan peninsula, Mexico. *Sci. Mar.* 80, 143–150. doi: 10.3989/scimar.04294.23A
- Bauer, P. (2000). Multiple comparisons- theory and methods. *Stat. Med.* 19:1951. doi: 10.1002/1097-0258(20000730)19:14<1951::AID-SIM471>3.0.CO;2-W
- Bayley, D. T. I., and Mogg, A. O. M. (2020). A protocol for the large-scale analysis of reefs using structure from motion photogrammetry. *Methods Ecol. Evol.* 11, 1410–1420. doi: 10.1111/2041-210X.13476
- Bennett, K., Wilson, S. K., Shedrawi, G., McLean, D. L., and Langlois, T. J. (2016). Can diver operated stereo-video surveys for fish be used to collect meaningful data on benthic coral reef communities? *Limnol. Oceanogr.* 14, 874–885. doi: 10.1002/lom3.10141
- Bianchi, C. N. (2019). “2019 IWMS 2D photogrammetry Maldives,” in *Conference: 2019 IMEKO TC-19 International Workshop on Metrology for the Sea Genoa* (Genova).



- Brown, E., Cox, E., Jokiel, P., Rodgers, K., Smith, W., Tissot, B., et al. (2004). Development of benthic sampling methods for the coral reef assessment and monitoring program (cramp) in Hawai'i. *Pac. Sci.* 58, 145–158. doi: 10.1353/psc.2004.0013
- Burns, J. H. R., Delparte, D., Gates, R. D., and Takabayashi, M. (2015). Integrating structure-from-motion photogrammetry with geospatial software as a novel technique for quantifying 3d ecological characteristics of coral reefs. *PeerJ* 3:e1077. doi: 10.7717/peerj.1077
- Burns, J. H. R., Delparte, D., Kapon, L., Belt, M., Gates, R. D., and Takabayashi, M. (2016). Assessing the impact of acute disturbances on the structure and composition of a coral community using innovative 3d reconstruction techniques. *Methods Oceanogr.* 15–16, 49–59. doi: 10.1016/j.mio.2016.04.001
- Burns, J. H. R., Weyenberg, G., Mandel, T., Ferreira, S. B., Gotshalk, D., Kinoshita, C. K., et al. (2020). A comparison of the diagnostic accuracy of *in-situ* and digital image-based assessments of coral health and disease. *Front. Mar. Sci.* 7:304. doi: 10.3389/fmars.2020.00304
- Capra, A., Castagnetti, C., Dubbini, M., Gruen, A., Guo, T., Mancini, F. T., et al. (2017). "High accuracy underwater photogrammetric surveying," in *3rd IMEKO International Conference on Metrology for Archeology and Cultural Heritage* (Lecce).
- Carleton, J. H., and Done, T. J. (1995). Quantitative video sampling of coral reef benthos: large-scale application. *Coral Reefs* 14, 35–46. doi: 10.1007/BF00304070
- Chirayath, V., and Instrella, R. (2019). Fluid lensing and machine learning for centimeter-resolution airborne assessment of coral reefs in American Samoa. *Remote Sens. Environ.* 235:111475. doi: 10.1016/j.rse.2019.111475
- Clarke, K., and Warwick, R. (2001). *Clarke KR, Warwick RM. Change in Marine Communities: An Approach to Statistical Analysis and Interpretation*. Plymouth: Primer-E Ltd.
- Couch, C. S., Oliver, T. A., Suka, R., Lamirand, M., Asbury, M., Amir, C., et al. (2021). Comparing coral colony surveys from in-water observations and structure-from-motion imagery shows low methodological bias. *Front. Mar. Sci.* 8:622. doi: 10.3389/fmars.2021.647943
- Edwards, C. B., Eynaud, Y., Williams, G. J., Pedersen, N. E., Zgliczynski, B. J., Gleason, A. C. R., et al. (2017). Large-area imaging reveals biologically driven non-random spatial patterns of corals at a remote reef. *Coral Reefs* 36, 1291–1305. doi: 10.1007/s00338-017-1624-3
- English, S., Wilkinson, C., and Baker, V. (1997). *Survey Manual for Tropical Marine Resources*. Townsville, QLD: Australian Institute of Marine Science.
- Facon, M., Pinault, M., Obura, D., Pioch, S., Pothin, K., Bigot, L., et al. (2016). A comparative study of the accuracy and effectiveness of line and point intercept transect methods for coral reef monitoring in the southwestern Indian ocean islands. *Ecol. Indic.* 60, 1045–1055. doi: 10.1016/j.ecolind.2015.09.005
- Fenner, D. P. (1988). Some leeward reefs and corals of Cozumel, Mexico. *Bull. Mar. Sci.* 42, 133–144.
- González-Barrios, F. J., and Álvarez Filip, L. (2018). A framework for measuring coral species-specific contribution to reef functioning in the Caribbean. *Ecol. Indic.* 95, 877–886. doi: 10.1016/j.ecolind.2018.08.038
- Halekoh, U., Højsgaard, S., and Yan, J. (2006). The R package geepack for generalized estimating equations. *J. Stat. Softw.* 15/2, 1–11. doi: 10.18637/jss.v015.i02
- Hernández-Landa, R. C., Barrera-Falcon, E., and Rioja-Nieto, R. (2020). Size-frequency distribution of coral assemblages in insular shallow reefs of the Mexican Caribbean using underwater photogrammetry. *PeerJ* 8:e8957. doi: 10.7717/peerj.8957
- Hill, J., and Wilkinson, C. (2004). *Methods for Ecological Monitoring of Coral Reefs*. Townsville, QLD: Australian Institute of Marine Science.
- Horton, T., Kroh, A., Ahyong, S., Bailly, N., Boyko, C., Brandão, S., et al. (2021). *World Register of Marine Species (WoRMS)*. Available online at: <https://www.marinespecies.org> (accessed August 13, 2021).
- Hothorn, T., Bretz, F., and Westfall, P. (2008). Simultaneous inference in general parametric models. *Biometr.* J. 50, 346–363. doi: 10.1002/bimj.200810425
- Hughes, T. P., Anderson, K. D., Connolly, S. R., Heron, S. F., Kerry, J. T., Lough, J. M., et al. (2018). Spatial and temporal patterns of mass bleaching of corals in the anthropocene. *Science* 359:80. doi: 10.1126/science.aan8048
- Hughes, T. P., Baird, A. H., Bellwood, D. R., Card, M., Connolly, S. R., Folke, C., et al. (2003). Climate change, human impacts, and the resilience of coral reefs. *Science* 301:929. doi: 10.1126/science.1085046
- Hughes, T. P., and Jackson, J. B. C. (1980). Do corals lie about their age? Some demographic consequences of partial mortality, fission, and fusion. *Science* 209:713. doi: 10.1126/science.209.4457.713
- Humann, P., and DeLoach, N. (2002). *Reef Creature Identification: Florida, Caribbean, Bahamas*. Jacksonville, FL: New World Publications.
- Jackson, J. B. C., Kirby, M. X., Berger, W. H., Bjorndal, K. A., Botsford, L. W., Bourque, B. J., et al. (2001). Historical overfishing and the recent collapse of coastal ecosystems. *Science* 293:629. doi: 10.1126/science.1059199
- Jaramillo González, J., and Acosta, A. (2016). Comparación temporal en la estructura de una comunidad coralina en primeros estados de sucesión, isla de san andrés, Colombia. *Boletín de Invest. Mar. Costeras* 38, 29–53. doi: 10.25268/bimc.invemar.2009.38.2.170
- Jokiel, P. L., Rodgers, K. S., Brown, E. K., Kenyon, J. C., Aeby, G., Smith, W. R., et al. (2015). Comparison of methods used to estimate coral cover in the Hawaiian Islands. *PeerJ* 3:e954. doi: 10.7717/peerj.954
- Kjerfve, B. E. (1998). *CARICOMP - Caribbean Coral Reef, Seagrass and Mangrove Sites*. Paris: UNESCO.
- Lam, K., Shin, P. K. S., Bradbeer, R., Randall, D., Ku, K. K. K., Hodgson, P., et al. (2006). A comparison of video and point intercept transect methods for monitoring subtropical coral communities. *J. Exp. Mar. Biol. Ecol.* 333, 115–128. doi: 10.1016/j.jembe.2005.12.009
- Lang, J., Marks, K., Kramer, P., Kramer, P., and Ginsburg, R. (2010). *Agrra protocols version 5.4. ReVision* (Miami, FL).
- Lechene, M. A., Haberstroh, A. J., Byrne, M., Figueira, W., and Ferrari, R. (2019). Optimising sampling strategies in coral reefs using large-area mosaics. *Remote Sens.* 11:2907. doi: 10.3390/rs11242907
- Leon, J. X., Roelfsema, C. M., Saunders, M. I., and Phinn, S. R. (2015). Measuring coral reef terrain roughness using "structure-from-motion" close-range photogrammetry. *Geomorphology* 242, 21–28. doi: 10.1016/j.geomorph.2015.01.030
- Leujak, W., and Ormond, R. F. G. (2007). Comparative accuracy and efficiency of six coral community survey methods. *J. Exp. Mar. Biol. Ecol.* 351, 168–187. doi: 10.1016/j.jembe.2007.06.028
- Loya, Y. (1972). Community structure and species diversity of hermatypic corals at eilat, red sea. *Mar. Biol.* 13, 100–123. doi: 10.1007/BF00366561
- McField, M., Kramer, P., Alvarez-Filip, L., Drysdale, I., Flores, M., Petersen, A., et al. (2018). *2018 Mesoamerican Reef Report Card* (Washington, DC). doi: 10.13140/RG.2.2.19679.36005
- Molloy, P. P., Evanson, M., Nellis, A. C., Rist, J. L., Marcus, J. E., Koldewey, H. J., et al. (2013). How much sampling does it take to detect trends in coral-reef habitat using photoquadrat surveys? *Aquat. Conserv.* 23, 820–837. doi: 10.1002/aqc.2372
- Montilla, L. M., Miyazawa, E., Ascanio, A., López-Hernández, M., Mariño-Briceño, G., Rebolledo-Sánchez, Z., et al. (2020). The use of pseudo-multivariate standard error to improve the sampling design of coral monitoring programs. *PeerJ* 2020:e8429. doi: 10.7717/peerj.8429
- Muckelbauer, G. (1990). The shelf of cozumel, mexico: topography and organisms. *Facies* 23, 185–200. doi: 10.1007/BF02536713
- Nadon, M.-O., and Stirling, G. (2006). Field and simulation analyses of visual methods for sampling coral cover. *Coral Reefs* 25, 177–185. doi: 10.1007/s00338-005-0074-5
- Neyer, F., Nocerino, E., and Gruen, A. (2019). Image quality improvements in low-cost underwater photogrammetry. *Int. Arch. Photogramm. Remote Sens. Spatial Inf. Sci.* XLII-2/W10, 135–142. doi: 10.5194/isprs-archives-XLII-2-W10-135-2019
- Nocerino, E., Menna, F., Gruen, A., Troyer, M., Capra, A., Castagnetti, C., et al. (2020). Coral reef monitoring by scuba divers using underwater photogrammetry and geodetic surveying. *Remote Sens.* 12:3036. doi: 10.3390/rs12183036
- Page, C. A., Field, S. N., Pollock, F. J., Lamb, J. B., Shedrawi, G., and Wilson, S. K. (2016). Assessing coral health and disease from digital photographs and in situ surveys. *Environ. Monitor. Assess.* 189:18. doi: 10.1007/s10661-016-5743-z
- Palma, M., Magliozzi, C., Rivas Casado, M., Pantaleo, U., Fernandes, J., Coro, G., et al. (2019). Quantifying coral reef composition of recreational diving sites: a structure from motion approach at seascape scale. *Remote Sens.* 11:3027. doi: 10.3390/rs11243027

- Palma, M., Rivas Casado, M., Pantaleo, U., and Cerrano, C. (2017). High resolution orthomosaics of African coral reefs: a tool for wide-scale benthic monitoring. *Remote Sens.* 9:705. doi: 10.3390/rs9070705
- Pandolfi, J. M., Bradbury, R. H., Sala, E., Hughes, T. P., Bjorndal, K. A., Cooke, R. G., et al. (2003). Global trajectories of the long-term decline of coral reef ecosystems. *Science* 301:955. doi: 10.1126/science.1085706
- Pavoni, G., Corsini, M., Callieri, M., Fiameni, G., Edwards, C., and Cignoni, P. (2020). On improving the training of models for the semantic segmentation of benthic communities from orthographic imagery. *Remote Sens.* 12:3106. doi: 10.3390/rs12183106
- Peck, M., Tapilatu, R. F., Kurniati, E., and Rosado, C. (2021). Rapid coral reef assessment using 3d modelling and acoustics: acoustic indices correlate to fish abundance, diversity and environmental indicators in west Papua, Indonesia. *PeerJ* 9:e10761. doi: 10.7717/peerj.10761
- Porter, J. W. (1972). Patterns of species diversity in Caribbean reef corals. *Ecology* 53, 745–748. doi: 10.2307/1934796
- Price, D. M., Robert, K., Callaway, A., Lo Iacono, C., Hall, R. A., and Huvenne, V. A. I. (2019). Using 3d photogrammetry from ROV video to quantify cold-water coral reef structural complexity and investigate its influence on biodiversity and community assemblage. *Coral Reefs* 38, 1007–1021. doi: 10.1007/s00338-019-01827-3
- R Core Team (2019). *R: A Language and Environment for Statistical Computing*. Vienna: R Foundation for Statistical Computing.
- Reyes-Bonilla, H., Millet, E., and Alvarez-Filip, L. (2014). Community structure of scleractinian corals outside protected areas in Cozumel Island, Mexico. *Atoll Res. Bull.* 601, 1–16. doi: 10.5479/si.00775630.601
- Rioja-Nieto, R., Garza-Pérez, R., Álvarez Filip, L., Ismael, M.-T., and Cecilia, E. (2019). “Chapter 27 - The Mexican Caribbean: from Xcalak to holbox,” in *World Seas: An Environmental Evaluation, 2nd Edn.* ed C. Sheppard (London: Academic Press), 637–653. doi: 10.1016/B978-0-12-805068-2.00033-4
- Rossi, P., Castagnetti, C., Capra, A., Brooks, A. J., and Mancini, F. (2020). Detecting change in coral reef 3d structure using underwater photogrammetry: critical issues and performance metrics. *Appl. Geomat.* 12, 3–17. doi: 10.1007/s12518-019-00263-w
- Steffen, W., Persson, A., Deutsch, L., Zalasiewicz, J., Williams, M., Richardson, K., et al. (2011). The anthropocene: from global change to planetary stewardship. *AMBIO* 40:739. doi: 10.1007/s13280-011-0185-x
- Torruco, D., González-Solis, A., and Torruco-González, A. D. (2021). Large-scale and long-term distribution of corals in the Gulf of Mexico and Caribbean sea of Mexico and adjacent areas: corals distribution in Mexico and adjacent areas. *Region. Stud. Mar. Sci.* 44:101764. doi: 10.1016/j.rsma.2021.101764
- Urbina-Barreto, I., Garnier, R., Elise, S., Pinel, R., Dumas, P., Mahamadaly, V., et al. (2021). Which method for which purpose? A comparison of line intercept transect and underwater photogrammetry methods for coral reef surveys. *Front. Mar. Sci.* 8:577. doi: 10.3389/fmars.2021.636902
- Veron J.E.N., Stafford-Smith M.G., T. E. and L.M., D. (2016). *Corals of the World*. Available online at: [http://www.coralsoftheworld.org/species\\_factsheets/](http://www.coralsoftheworld.org/species_factsheets/) (accessed May 1, 2021).
- Wilkinson, C. R., Green, A., Almany, J., and Dionne, S. (2003). *Monitoring Coral Reef Marine Protected Areas: A Practical Guide on How Monitoring Can Support Effective Management of MPAs* (Townsville, AU). Available online at: <https://repository.library.noaa.gov/view/noaa/10859>
- Yan, J. (2002). Geepack: Yet another package for generalized estimating equations. *R-News*. 2/3, 12–14.
- Yan, J., and Fine, J. P. (2004). Estimating equations for association structures. *Stat. Med.* 23, 859–880. doi: 10.1002/sim.1650
- Young, G. C., Dey, S., Rogers, A. D., and Exton, D. (2017). Cost and time-effective method for multi-scale measures of rugosity, fractal dimension, and vector dispersion from coral reef 3d models. *PLoS ONE* 12:e0175341. doi: 10.1371/journal.pone.0175341
- Yuval, M., Alonso, I., Eyal, G., Tchernov, D., Loya, Y., Murillo, A. C., et al. (2021). Repeatable semantic reef-mapping through photogrammetry and label-augmentation. *Remote Sens.* 13:659. doi: 10.3390/rs13040659
- Zeileis, A., and Hothorn, T. (2002). Diagnostic checking in regression relationships. *R News* 2, 7–10. Available online at: [https://www.r-project.org/doc/Rnews/Rnews\\_2002-3.pdf](https://www.r-project.org/doc/Rnews/Rnews_2002-3.pdf)
- Zuur, A., Ieno, E. N., Walker, N., Saveliev, A. A., and Smith, G. M. (2009). *Mixed Effects Models and Extensions in Ecology with R. Statistics for Biology and Health, 1st Edn.* New York, NY: Springer-Verlag. doi: 10.1007/978-0-387-87458-6

**Conflict of Interest:** The authors declare that the research was conducted in the absence of any commercial or financial relationships that could be construed as a potential conflict of interest.

**Publisher's Note:** All claims expressed in this article are solely those of the authors and do not necessarily represent those of their affiliated organizations, or those of the publisher, the editors and the reviewers. Any product that may be evaluated in this article, or claim that may be made by its manufacturer, is not guaranteed or endorsed by the publisher.

Copyright © 2021 Barrera-Falcon, Rioja-Nieto, Hernández-Landa and Torres-Irineo. This is an open-access article distributed under the terms of the Creative Commons Attribution License (CC BY). The use, distribution or reproduction in other forums is permitted, provided the original author(s) and the copyright owner(s) are credited and that the original publication in this journal is cited, in accordance with accepted academic practice. No use, distribution or reproduction is permitted which does not comply with these terms.



# A Comparison of Size, Shape, and Fractal Diversity Between Coral Rubble Sampled From Natural and Artificial Coastlines Around Okinawa Island, Japan

Giovanni D. Masucci<sup>1,2,3\*</sup>, Piera Biondi<sup>1,3</sup> and James D. Reimer<sup>1,4</sup>

<sup>1</sup> Molecular Invertebrate Systematics and Ecology Laboratory, Graduate School of Engineering and Science, University of the Ryukyus, Nishihara, Japan, <sup>2</sup> Physics and Biology Unit, Okinawa Institute of Science and Technology Graduate University (OIST), Onna-son, Japan, <sup>3</sup> The Oceancy MitteTulundusÜhing, Kuusalu Parish, Estonia, <sup>4</sup> Tropical Biosphere Research Center, University of the Ryukyus, Nishihara, Japan

## OPEN ACCESS

### Edited by:

Charles Alan Jacoby,  
St. Johns River Water Management  
District, United States

### Reviewed by:

Kennedy Wolfe,  
The University of Queensland,  
Australia  
Kátia Cristina Cruz Capel,  
University of São Paulo, Brazil

### \*Correspondence:

Giovanni D. Masucci  
giovanni.masucci@oist.jp

### Specialty section:

This article was submitted to  
Coral Reef Research,  
a section of the journal  
Frontiers in Marine Science

**Received:** 30 April 2021

**Accepted:** 18 October 2021

**Published:** 08 November 2021

### Citation:

Masucci GD, Biondi P and  
Reimer JD (2021) A Comparison  
of Size, Shape, and Fractal Diversity  
Between Coral Rubble Sampled From  
Natural and Artificial Coastlines  
Around Okinawa Island, Japan.  
*Front. Mar. Sci.* 8:703698.  
doi: 10.3389/fmars.2021.703698

Substrate surface area and fractal complexity have been reported to influence the abundance and diversity of mobile cryptic animal communities. Surfaces with higher fractal dimensions not only offer additional space for colonization, but bias space availability toward smaller size ranges, increasing the number of available niches. Conversely, smaller surface areas tend to be associated with a decrease in abundances while reduced fractal complexities may support less diversity in the benthic community. In this study, we compared morphological parameters between rubble sampled from rubble mounds accumulated at the seaward side of artificial breakwaters and rubble sampled from a nearby location with no breakwaters (=control site). The purpose of this work was to establish a methodology for comparing the surface area and fractal complexity of coral rubble fragments using easily available equipment that could be efficiently utilized during field work. Rubble fragments were individually weighed and photographed in controlled light conditions. Each photograph was then analyzed using ImageJ software. Rubble pieces from each photograph went through segmentation, the separation of sample outlines from the picture background, before being measured and analyzed for surface area, width, and length (size estimators), and circularity, aspect ratio, roundness, solidity, and Feret properties (shape estimators). Surface fractal complexity was also measured, using the box counting method on segmented rubble surfaces. We observed lowered surface areas, weight, and fractal complexity for rubble fragments sampled at the breakwater. We demonstrate how this method could be used to compare coral rubble from a variety of environmental conditions, thus becoming a useful aid in environmental monitoring, in addition to adding important information to the collection and analyses of biological data.

**Keywords:** spatial complexity, fractals, breakwaters, coastal development, Okinawa, Japan

## INTRODUCTION

Substrate surface area and fractal complexity have been reported to influence the abundance and diversity of living organisms, both marine and terrestrial (McClanahan, 1994; Kostylev et al., 2005; Soares et al., 2021). In general, more spatially complex substrates can host a higher number of organisms (Fraser and Sedberry, 2008). Habitat complexity can be expressed by the fractal dimension (D) (Mandelbrot, 1967), which Tokeshi and Arakaki (2012) summarized as “the density of a projected profile of solid geometry in a chosen plane.” The same authors pointed out how the fractal dimension of a surface alone might not be adequate to assess the overall habitat complexity. The fractal dimension of a surface represents the complexity of its geometry (Mandelbrot, 1983). Fractal dimension is a good indicator of environment heterogeneity and has been used in previous studies, including at tropical latitudes (Kostylev et al., 2005).

Besides offering additional space for colonization, substrates with higher fractal dimensions seem to provide additional opportunities for colonization of organisms of different size ranges and functional traits, increasing the number of available niches. While the total surface area seems to be more strongly associated with abundance, fractal complexity is more strongly connected with diversity (Kostylev et al., 2005).

The complex three-dimensional skeletal structures of scleractinian corals host a variety of sessile and mobile animals of variable size called cryptofauna (Enochs, 2012). Organisms from the reef cryptofauna are essential for the functionality of coral reef ecosystems, both in terms of biomass (they constitute the largest part of reef's diversity; Richter et al., 2001) and functionality, since they contribute to the aggregation and recycling of nutrients, providing biomass upwards in the trophic net (Richter et al., 2001; Kramer et al., 2013; Wolfe et al., 2020). Even coral rubble, dead coral skeletal frameworks detached from the substrate, has been shown to host a rich and diverse community and, for this reason, has been used as an indicator of reef diversity and environmental impact (Takada et al., 2014; Wee et al., 2019). When analyzing different reef substrates, Enoch and Manzanillo (2012b) observed that the highest richness in cryptofauna was surprisingly found within coral rubble, which hosted significantly higher cryptic diversity than healthy corals. Moreover, previous research has suggested that cryptofaunal abundance and diversity are linked with habitat type (Wolfe et al., 2020), and influenced by rubble shapes and complexity (Biondi et al., 2020). Branching rubble fragments appear to support more biodiversity and animal abundance than massive rubble (Biondi et al., 2020).

A variety of human activities (such as coastal armoring, dredging, and land reclamation) have the potential to alter the structure of the benthic substrate components and coastal armoring in particular can lead to the formation of rubble mounds at the seaward side of breakwaters (Masucci et al., 2020). Following our observations in Okinawa Island (southwest Japan) of differences in rubble cryptofauna abundance and diversity between samples from a breakwater and others from nearby control sites (with rubble from control sites characterized by higher abundances and diversity levels, Masucci et al., 2021),

and of differences in abundance and diversity based on rubble shape (Biondi et al., 2020), we decided to further investigate the nature of the rubble mounds facing breakwaters. This was done by sampling coral rubble from these mounds and comparing their morphological parameters with those of rubble sampled at natural mounds from a nearby location with no breakwaters (=control site). As no uniform metric exists to measure or quantify rubble, the main purpose of this work was to establish a methodology for comparing the surface area and fractal complexity of coral rubble fragments using easily available equipment that could be efficiently utilized during field work. Because rubble plays a fundamental role in coral reef diversity, but a standardized procedure for measuring rubble is currently missing, this method could be a useful operative tool for practical applications such as impact assessments, habitat restorations, and monitoring.

## MATERIALS AND METHODS

### Study Location and Survey Design

An ideal location to analyze the effects of coastal armoring should combine the presence of artificial barriers with low levels of population density and urban development. The north-west coast of Okinawa Main Island (North Kunigami Area, **Figure 1**) was chosen to conduct fieldwork. Data were collected from the Hentona breakwater (**Figure 1C**; GPS: 26°45'25.6"N 128°11'15.8"E), which was built in the 1980s, and a neighboring, non-armored region on the shore of Hentona village (**Figure 1D**; GPS: 26°45'05.4"N 128°11'04.5"E).

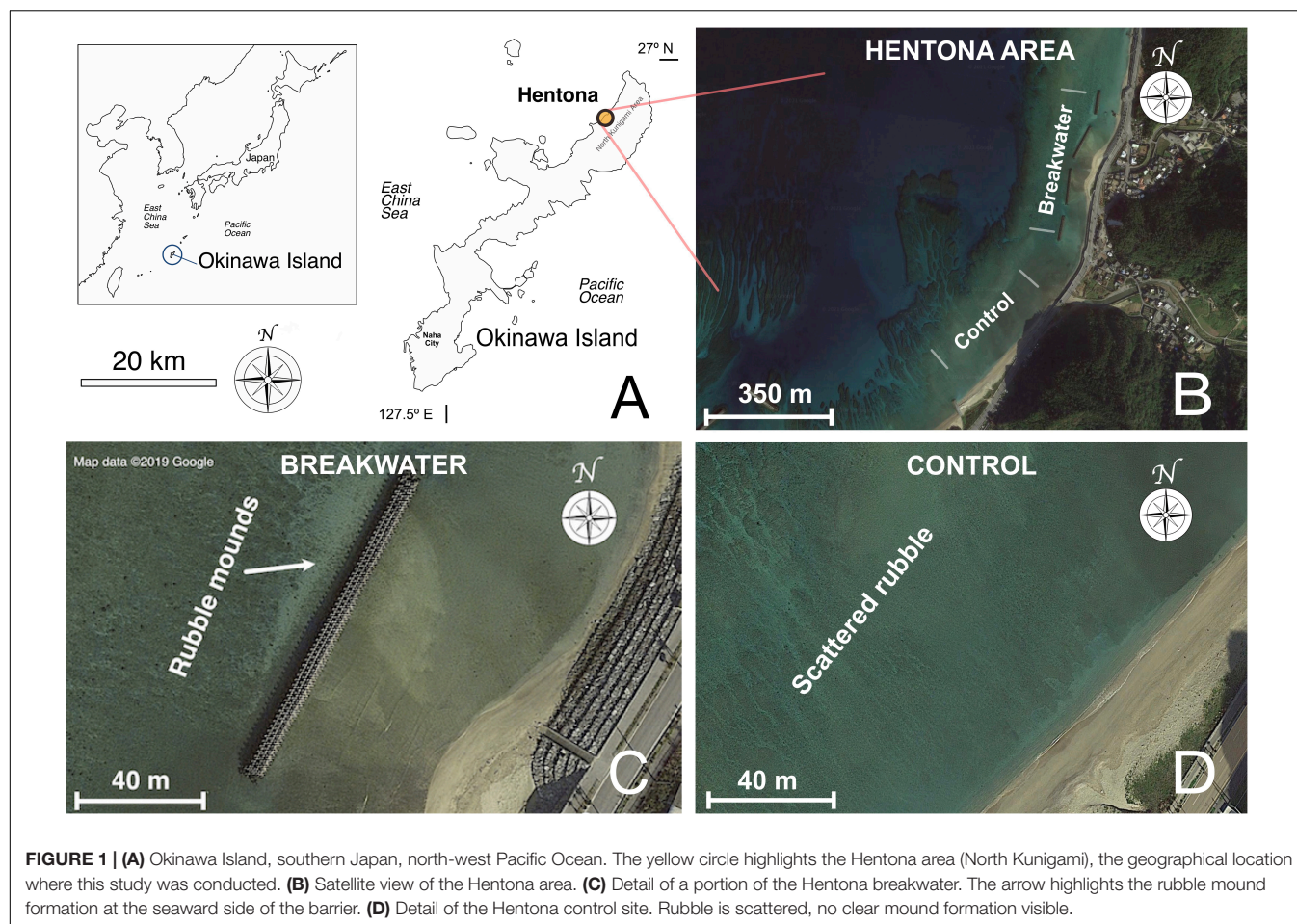
### Rubble Size, Shape, and Fractal Complexity

Rubble was sampled by hand over 10 m transect lines (1 piece of rubble randomly taken every 3 m, swimming parallel to the coastline; for each site  $n = 20$ ) and transported back to the shore using hermetically sealed buckets. Sampling was conducted at the surface of the rubble layer, at a depth of about 1.5 m for both sites, at the lowest astronomic tide. Tide normalization was performed using the WXTIDE software (ver. 32.4.7; Flater, 2007), set to the nearby Hentona tide station.

Rubble was transported to the laboratory and dried using an oven at 60°C for 48 h. Each rubble piece was individually measured with a ruler (width × length), weighted, and photographed under artificial light, with controlled and consistent light conditions, using a Sony a6300 24.2 MP APS-C camera and Sony E 30 mm f/3.5 macro lens (shutter speed = 1/160 s, aperture = f/10, ISO 250, manual white balance at 4750k, light provided by a strobe of guide number of 32 m, set at power level = 1/16, camera sensor positioned at a constant distance of 1 m from rubble samples, black background, scale included in each picture).

Rubble photographs (total  $N = 40$ ) were then analyzed using the software ImageJ (version 1.52p; Schneider et al., 2012). After setting the scale, rubble from each photograph went through segmentation (the separation of sample outlines from picture background). In order to minimize bias from



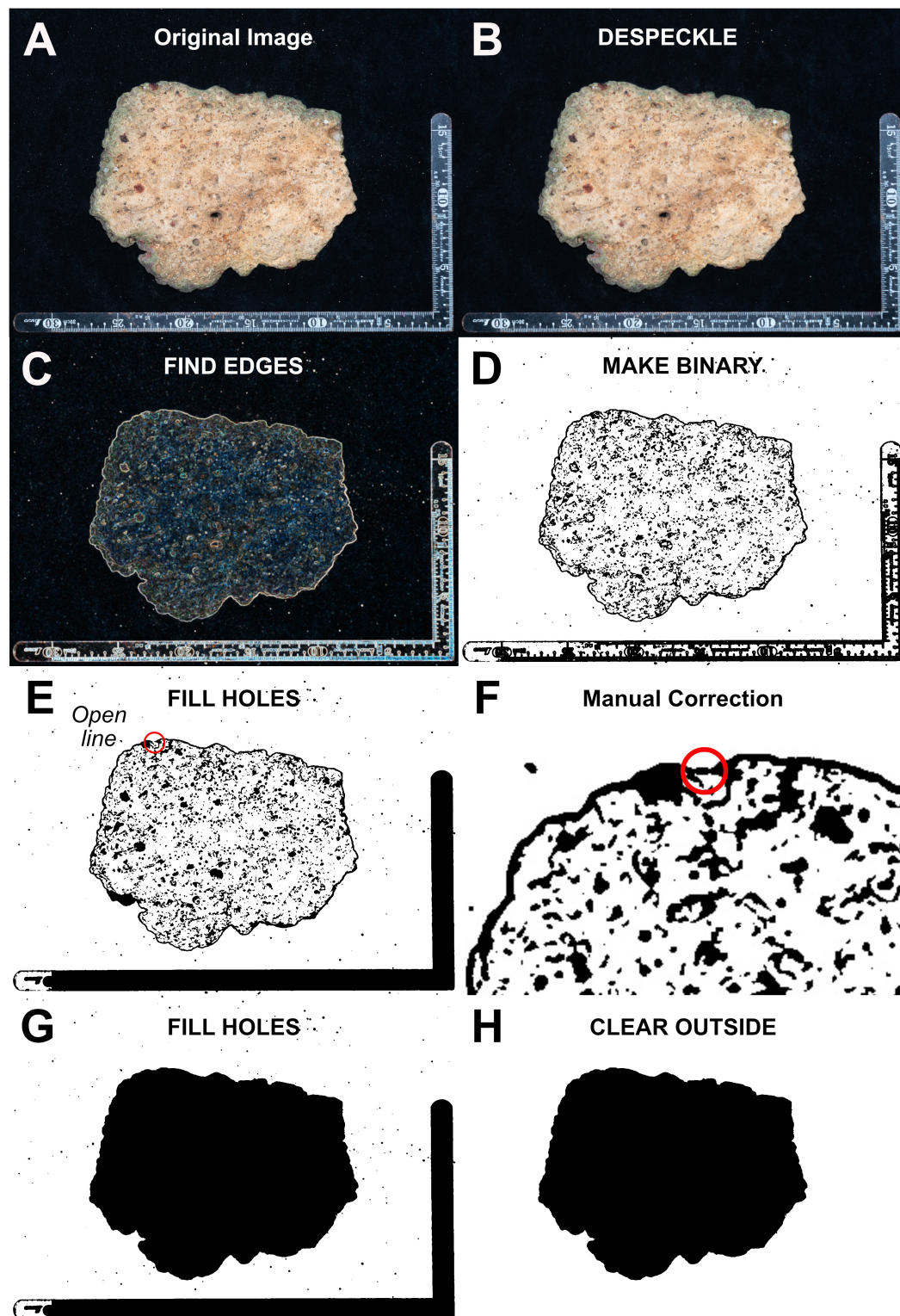


human operators, the segmentation workflow (**Figure 2**) was standardized, automatized and kept constant for the whole analysis, using the following ImageJ functions, in the reported order: “Process → Noise → DESPECKLE” (reduces digital noise and particles such as sand to avoid false positives in the automatic segmentation process); “Process → FIND EDGES” (automatic tracing or rubble outlines); “Process → Binary → MAKE BINARY” (produces a black and white outline); Finally, a visual check for unclosed lines (with the aid of the “Process → Binary → FILL HOLES” function), and manual fixing if needed. The resulting outlines were selected, saved as ROI files, and overlapped to the original image for measurements. Analyzed parameters (Schneider et al., 2012) included surface area, width, and length as size estimators, and as shape estimators: (a) Circularity, defined as the ratio between the inscribed and the circumscribed circumferences; (b) Roundness, the ratio between the minor and major axes of the object, (c) Aspect Ratio, the ratio between the major and minor axes of the object; (d) Solidity, the area of a particle divided by its convex hull area; (e) Feret properties, which describe the diameter of an elliptical fit for the object. Width and length measurements taken from pictures using ImageJ were compared with measurements of the same parameters taken from each rubble piece using a ruler, to compare the two approaches.

Surface fractal complexity (Mandelbrot, 1967) was measured, using the box counting method (Liebovitch and Toth, 1989), by selecting segmented rubble surfaces, removing backgrounds with the function “Edit → CLEAR OUTSIDE,” converting the resulting files into binary images, and finally calling the ImageJ function “Analyze → Tools → FRACTAL BOX COUNT,” to calculate the fractal dimension (D) of the surface of each sampled rubble. **Supplementary Figure 1** graphically summarizes the aforementioned sampling workflow.

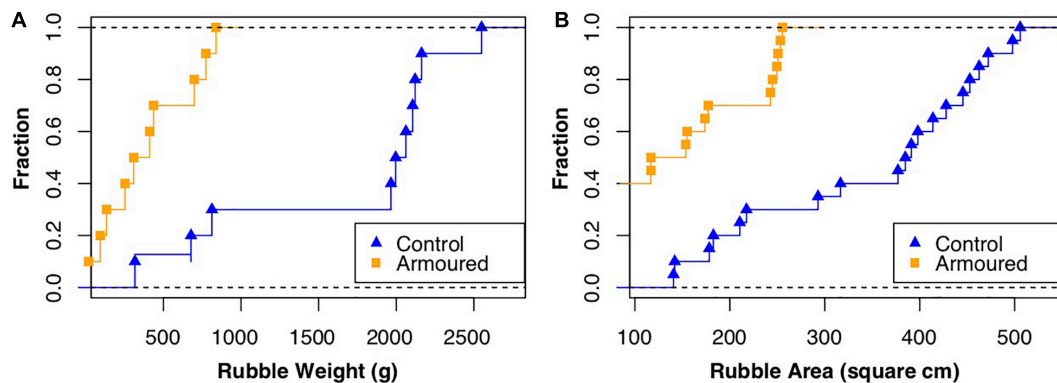
## Statistics

Statistical analyses were conducted by using R, v 3.6 (R Development Core Team, 2019). The level of significance for all tests was set at 95%. Normality and Homoscedasticity of variables were verified, respectively, with the Shapiro-Wilk test (Royston, 1982 and with the Bartlett’s test (Bartlett, 1937). Since most variables representing rubble size, shape, and fractal complexity variables were not normally distributed, they were analyzed using the non-parametric Wilcoxon rank-sum test (also known as Mann-Whitney test; Hollander and Wolfe, 1973). For the same reason, medians were used in place of means as descriptive statistics. The two methods for measuring weight and length (ruler measurements vs. photo analyses) were compared using a *t*-test. The dataset was then log-transformed and the effects of



**FIGURE 2 |** Rubble segmentation workflow from the original image to the final outline. ImageJ function names are written fully capitalized. **(A)** Original image. **(B)** DESPECKLE. The presence of digital noise, filaments, and sand particles has been reduced. **(C)** FIND EDGES. The outline of the rubble piece has been highlighted. **(D)** MAKE BINARY. Pixels have been converted to black or white values. **(E)** FILL HOLES. In this example, the outline was not closing perfectly (a red circle is added to this figure to highlight the problematic area). **(F)** Manual correction. The open spot within the red circle has now been manually fixed (traced). **(G)** FILL HOLES. The function confirmed that the outline was properly closed. **(H)** Final outline. If not needed, background elements can optionally be removed using the CLEAR OUTSIDE function.





**FIGURE 3** | Cumulative curves of rubble (A) weight and (B) surface area for rubble sampled at breakwater and control site.

armoring on the overall shape of rubble were tested using 1-way PERMANOVA (Anderson, 2014), by using the “Adonis” function from the *Vegan* package for R (version 2.5-5; Oksanen et al., 2019), Bray-Curtis distance, and 999 permutations. Correlation patterns between variables were graphically displayed with a Principal Component Analysis (PCA), using the “rda” function from the *Vegan* package for R. Results were displayed as a biplot (scaling 2; Gabriel, 1971) with shape parameters expressed as labels and observations from different sites as triangular shapes.

## RESULTS

Overall, the automated segmentation process worked properly for all the analyzed rubble fragments pictures and was able to generate detailed outlines which required minimal or no manual correction. The manual correction of unclosed spaces between lines, when needed, only required the tracing of a small number of pixels. The “FILL HOLES” function of ImageJ was useful in terms of time savings, allowing to either highlight problematic instances in which automatically traced lines did not meet perfectly (Figure 2E) or providing confirmation of the proper closure of an outline (Figure 2G). In terms of time, the whole procedure could be performed in <5 min per picture.

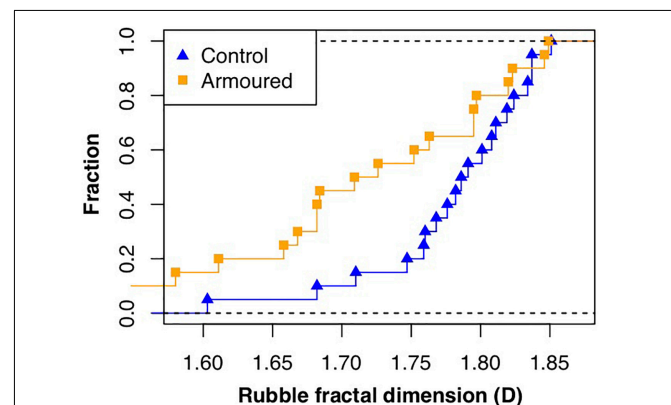
### Rubble Size, Shape, and Fractal Complexity

For the armored site, rubble weight (median) = 360.5 g, area (median) = 135.3 cm<sup>2</sup>, width (median) = 14.9 cm, and length (median) = 12.9 cm were smaller than those from the control; weight (median) = 2029.0 g, area (median) = 388.0 cm<sup>2</sup>, width (median) = 26.8 cm, and length (median) = 20.32 cm. Differences in medians were statistically significant for weight (Wilcoxon rank-sum test,  $W = 36$ ,  $p < 0.001$ ), area (Wilcoxon rank-sum test,  $W = 44$ ,  $p < 0.001$ ), width (Wilcoxon rank-sum test,  $W = 39$ ,  $p = 2.4e06$ ), and length (Wilcoxon rank-sum test,  $W = 71$ ,  $p = 0.0003$ ) (see Figure 3 for cumulative distributions of rubble weight and area). Width and length, when measured directly on rubble using a ruler, also showed significant results, but with higher  $p$ -values than when measuring the same parameters

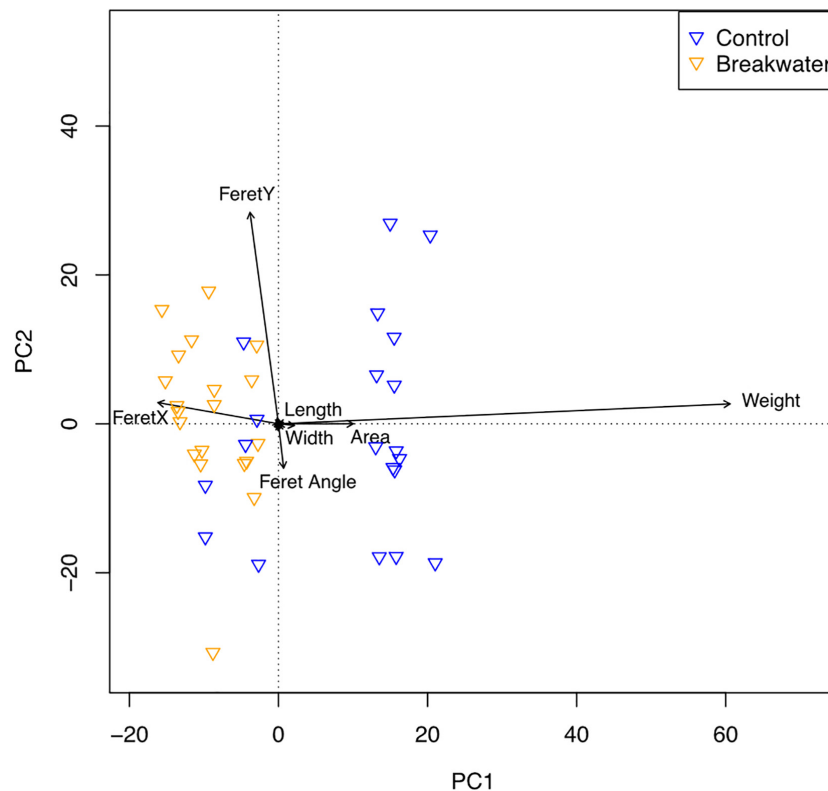
from pictures using ImageJ (width: Wilcoxon rank-sum test,  $W = 9$ ,  $p = 0.002$ ; length: Wilcoxon rank-sum test,  $W = 14.5$ ,  $p = 0.001$ ). When compared directly, the two methods did not show significant differences (width:  $t = 0.362$ ,  $df = 41.438$ ,  $p = 0.719$ ; length:  $t = 0.693$ ,  $df = 41.428$ ,  $p = 0.492$ ). The Minimum Feret diameters was significantly longer in rubble pieces from the control group (Wilcoxon rank-sum test,  $W = 68$ ,  $p < 0.001$ ) and so was the Maximum Feret diameter (Wilcoxon rank-sum test,  $W = 34$ ,  $p < 0.001$ ).

Although rubble sampled at breakwaters appeared to be slightly less elongated (higher circularity, median = 0.51 at the armored site, 0.40 at the control site), this was not supported by the statistics (Wilcoxon rank-sum test,  $W = 263$ ,  $p = 0.081$ ). For all the other variables related to shape, no significant differences were recorded ( $p > 0.05$ ). Overall, rubble shape appeared to be similar between the armored site and the natural coastline.

However, rubble sampled at breakwaters showed a lower fractal complexity in their surfaces, reflected by lower fractal dimensions [armored,  $D$  (median) = 1.7; control,  $D$  (median) = 1.8; Figure 4]. Differences in surface fractal complexity were statistically significant (Wilcoxon rank-sum test,  $W = 124$ ,  $p = 0.019$ ).



**FIGURE 4** | Cumulative curves of rubble fractal dimension (D) at breakwater and control site.



**FIGURE 5 |** Principal Component Analysis (PCA) biplot of coral rubble spatial complexity at the breakwater and control sites. Arrow directions points toward stronger associations.

The PCA (**Figure 5**) revealed differences between the two sites, confirmed to be significant by PERMANOVA ( $R^2 = 0.533$ ,  $p < 0.001$ ), mainly driven by area, weight, and Feret parameters, with rubble pieces from the armored site not only being characterized by a smaller area, but also by tighter clustering, indicating a narrower range of variation.

Among all variables, weight was the main driver of differences between the two groups.

## DISCUSSION

The method described here may provide the first uniform approach to characterizing coral rubble morphometrics. We demonstrate that photo analyses of rubble pieces using ImageJ software are effective in detecting differences among rubble pieces, even at low sample sizes. Rubble morphometrics differed between our control rubble bed ( $n = 20$ ) and an armored breakwall ( $n = 20$ ) in Hentona, driven primarily by differences in rubble area, weight and Feret properties. Analyses through ImageJ may provide a more useful indicator of rubble size and complexity than simple length and weight measurements alone, particularly given the importance of rubble complexity and microtopography in coral reefs (Brandl and Bellwood, 2007), meaning that this method shows promise as a uniform approach for broader incorporation in future rubble-based

research. Moreover, compared to manual tracing of outlines, the process allows to save time and overcoming operator bias.

In our previous assessment of coral rubble in Hentona (Masucci et al., 2021), rubble cryptofauna was more abundant in locations away from artificial breakwaters (i.e., in control sites). In addition, the seaward side of the armored barrier appeared to be characterized by rubble mound formations, due to the accumulation of small rubble at the base of the blocks.

Control rubble (=natural coastline) was both larger in size and more complex in their surfaces compared to those sampled at breakwaters rubble mounds. Previous research has clarified how, at different scales, diversity, and habitat complexity feature positive relations (Johnson et al., 2003). Kostylev et al. (2005) verified that both surface size and fractal complexity are directly related to abundances and diversity of cryptic animals on rocky shores. Specifically, smaller surface areas were mainly associated with a decrease in total and relative abundances while less fractal complexity, also supporting lower abundances, was strongly associated with reduced taxonomic richness (Kostylev et al., 2005). Surfaces with higher fractal dimensions do not just offer additional spaces for colonization, but bias space availability toward smaller size ranges, increasing the number of available niches (Morse et al., 1985).

Unlike on rocky shores, which present as 2D surfaces, coral rubble pieces together make complex 3D networks. As a result, species diversity in rubble may be influenced from the level



of an individual piece through to the entire rubble bed. However, little is known about the influence of fractal and bed complexity in coral rubble communities. Several factors appear to be involved in determining community abundance and composition (Takada et al., 2007), but different studies have clarified that coral and rubble skeletal erosion levels can drive the richness and abundances of their respective communities (Enochs, 2012; Enoch and Manzello, 2012b; Troyer et al., 2018), with dead coral rubble fragments of intermediate degradation levels seemingly able to sustain richer communities (Enochs et al., 2011; Enoch, 2012; Enoch and Manzello, 2012a,b).

The proposed method has limitations that need to be acknowledged: a manual correction, albeit limited to a small number of pixels, can still be needed when the automatic segmentation presents imperfections. In our experience this did not introduce problems in terms of bias and data accuracy. Secondly, light conditions can significantly affect the output of the automatic segmentation procedure. It is therefore important to take pictures in controlled light conditions (artificial light in a dark room). The importance of controlling light can limit the usefulness of this method in situations where light conditions cannot be controlled, which can be the case when working in the field. This can be an issue from a logistical point of view, especially when working with high numbers of replicates. Finally, using this method, the quality of the camera determines the quality and resolution of the final tracing, which by itself presents a potential risk of introducing biases when comparing data from different studies. In the current study, simple measurements of width, length, and weight were enough to reveal significant differences between breakwater and controls. Yet, other parameters would be arduous, time-consuming, or impossible (e.g., fractal complexity) to measure using this approach. We believe that the choice between a simpler field measurement of width and length and more detailed image analyses will depend on the parameters of interest, research questions, sample size, and desired accuracy.

In terms of future research opportunities, one issue that remains to be addressed is the relative amount of outlining of rubble that is needed to generate useful data. It may be that partial outlines (especially if acquired at higher resolutions and thus more accurate) can generate data of comparable quality, allowing researchers to work with incomplete photographs. We hope to explore this issue and the automatized generation of partial outlines in subsequent studies, potentially allowing for greater applicability of the methods described here.

While armoring can exert disturbances on native assemblages through a variety of mechanisms, we believe that a direct reduction in habitat size and spatial complexity constitutes an important link between reductions in abundance and diversity of rubble mobile cryptofauna and the presence of artificial hard

blocks in their proximities. Following appropriate replication, this method could be used to compare coral rubble from a variety of environmental conditions or locations, thus becoming a useful aid in environmental monitoring, in addition to adding important information to the collection and analyses of biological data. This line of research is particularly urgent when considering the extension of artificially altered coastlines already present around Okinawa Island (>60%; Masucci and Reimer, 2019).

## DATA AVAILABILITY STATEMENT

The raw data supporting the conclusions of this article will be made available by the authors, without undue reservation.

## AUTHOR CONTRIBUTIONS

GM, PB, and JR: conceptualization and first submission and revisions. GM and PB: fieldwork and figures. GM: software workflow and data analysis. GM and JR: first draft preparation. JR: English proofing. All authors listed have made a substantial, direct and intellectual contribution to the work, and approved it for publication.

## FUNDING

This work was supported by the Physics and Biology Unit of the Okinawa Institute of Science and Technology Graduate University (OIST).

## ACKNOWLEDGMENTS

We would like to thank Hin Boo Wee, Giun Yee Soong, Hiroki Kise, and Yee Wah Lau for their support and advice during the creation and implementation of this study. We thank Maika Reimer and Seira Reimer for their assistance in taking rubble measurements. Comments and suggestions from two reviewers greatly improved the quality of the final manuscript.

## SUPPLEMENTARY MATERIAL

The Supplementary Material for this article can be found online at: <https://www.frontiersin.org/articles/10.3389/fmars.2021.703698/full#supplementary-material>

**Supplementary Figure 1** | Flow-chart summarizing the methodology proposed in this research.

## REFERENCES

- Anderson, M. J. (2014). *Permutational multivariate analysis of variance (PERMANOVA)*. Wiley StatsRef: Statistics Reference Online. Hoboken: Wiley, 1–15. doi: 10.1002/9781118445112.stat07841
- Bartlett, M. S. (1937). Properties of sufficiency and statistical tests. *Proc. R. Soc. Lond. Ser. A* 160, 268–282. doi: 10.1098/rspa.1937.0109
- Biondi, P., Masucci, G. D., and Reimer, J. D. (2020). Coral cover and rubble cryptofauna abundance and diversity at outplanted reefs in Okinawa, Japan. *PeerJ* 8:e9185. doi: 10.7717/peerj.9185
- Brandl, S. J., and Bellwood, D. R. (2007). Microtopographic refuges shape consumer-producer dynamics by mediating consumer functional diversity. *Oecologia* 182, 203–217. doi: 10.1007/s00442-016-3643-0

- Enochs, I. C. (2012). Motile cryptofauna associated with live and dead coral substrates: implications for coral mortality and framework erosion. *Mar. Biol.* 159, 709–722. doi: 10.1007/s00227-011-1848-7
- Enochs, I. C., and Manzello, D. P. (2012a). Responses of cryptofaunal species richness and trophic potential to coral reef habitat degradation. *Diversity* 4, 94–104. doi: 10.3390/d4010094
- Enochs, I. C., and Manzello, D. P. (2012b). Species richness of motile cryptofauna across a gradient of reef framework erosion. *Coral Reefs* 31, 653–661. doi: 10.1007/s00338-012-0886-z
- Enochs, I. C., Toth, L. T., Brandtneris, V. W., Afflerbach, J. C., and Manzello, D. P. (2011). Environmental determinants of motile cryptofauna on an eastern Pacific coral reef. *Mar. Ecol. Prog. Ser.* 438, 105–118. doi: 10.3354/meps09259
- Flater, D. (2007). *WXTide32—a Free Windows Tide and Current Prediction Program*. Tampa. Available online at: <http://www.wx Tide32.com/>
- Fraser, S. B., and Sedberry, G. R. (2008). Reef morphology and invertebrate distribution at continental shelf edge reefs in the South Atlantic Bight. *Southeast. Nat.* 7, 191–206. doi: 10.1656/1528-7092(2008)7[191:RMAIDA]2.0.CO;2
- Gabriel, K. R. (1971). The biplot graphical display of matrices with application to principal component analysis. *Biometrika* 58, 453–467. doi: 10.1093/biomet/58.3.453
- Hollander, M., and Wolfe, D. A. (1973). *Nonparametric Statistical Methods*. New York: Wiley.
- Johnson, M. P., Frost, N. J., Mosley, M. W., Roberts, M. F., and Hawkins, S. J. (2003). The area-independent effects of habitat complexity on biodiversity vary between regions. *Ecol. Lett.* 6, 126–132. doi: 10.1046/j.1461-0248.2003.00404.x
- Kostylev, V. E., Erlandsson, J., Mak, Y. M., and Williams, G. A. (2005). The relative importance of habitat complexity and surface area in assessing biodiversity: fractal application on rocky shores. *Ecol. Complex.* 2, 272–286. doi: 10.1016/j.ecocom.2005.04.002
- Kramer, M. J., Bellwood, O., and Bellwood, D. R. (2013). The trophic importance of algal turfs for coral reef fishes: the crustacean link. *Coral Reefs* 32, 575–583. doi: 10.1007/s00338-013-1009-1
- Liebovitch, L. S., and Toth, T. (1989). A fast algorithm to determine fractal dimensions by box counting. *Phys. Lett. A* 141, 386–390. doi: 10.1016/0375-9601(89)90854-2
- Mandelbrot, B. B. (1967). How long is the coast of Britain? Statistical self-similarity and fractional dimension. *Science* 156, 636–638. doi: 10.1126/science.156.3775.636
- Mandelbrot, B. B. (1983). *The Fractal Geometry of Nature (Vol. 173)*. New York: WH freeman.
- Masucci, G. D., Acierno, A., and Reimer, J. D. (2020). Eroding diversity away: impacts of a tetrapod breakwater on a subtropical coral reef. *Aquat. Conserv.* 30, 290–302. doi: 10.1002/aqc.3249
- Masucci, G. D., Biondi, P., and Reimer, J. D. (2021). Impacts of coastal armouring on rubble mobile cryptofauna at shallow coral reefs in Okinawa, Japan. *Plankton Benthos Res.* (in press)
- Masucci, G. D., and Reimer, J. D. (2019). Expanding walls and shrinking beaches: loss of natural coastline in Okinawa Island, Japan. *PeerJ* 7:e7520. doi: 10.7717/peerj.7520
- McClanahan, T. R. (1994). Kenyan coral reef lagoon fish: effects of fishing, substrate complexity, and sea urchins. *Coral Reefs* 13, 231–241. doi: 10.1007/BF00303637
- Morse, D. R., Lawton, J. H., Dodson, M. M., and Williamson, M. H. (1985). Fractal dimension of vegetation and the distribution of arthropod body lengths. *Nature* 314:731. doi: 10.1038/314731a0
- Oksanen, J., Blanchet, F. G., Friendly, M., Kindt, R., Legendre, P., McGlinn, D., et al. (2019). *Vegan: Community Ecology Package*. Available online at: <https://CRAN.R-project.org/package=vegan>
- R Development Core Team. (2019). *R: A Language and Environment for Statistical Computing*. Vienna: R Foundation for Statistical Computing. Available online at: <https://www.r-project.org/>
- Richter, C., Wunsch, M., Rasheed, M., Kötter, I., and Badran, M. I. (2001). Endoscopic exploration of Red Sea coral reefs reveals dense populations of cavity-dwelling sponges. *Nature* 413, 726–730. doi: 10.1038/35099547
- Royston, J. P. (1982). Algorithm AS 181: the W test for normality. *J. R. Stat. Soc. Ser. C Appl. Stat.* 31, 176–180. doi: 10.2307/2347986
- Schneider, C. A., Rasband, W. S., and Eliceiri, K. W. (2012). NIH Image to ImageJ: 25 years of image analysis. *Nat. Methods* 9:671. doi: 10.1038/nmeth.2089
- Soares, D. M., Borges, L. R., da Silva, M. F. F., and Dalle Luche, L. (2021). Effect of substrates of native and exotic plant species on the initial period of colonization of benthic macroinvertebrates in the Cerrado biome. *Community Ecol.* 22, 127–134. doi: 10.1007/s42974-020-00032-5
- Takada, Y., Abe, O., and Shibuno, T. (2007). Colonization patterns of mobile cryptic animals into interstices of coral rubble. *Mar. Ecol. Prog. Ser.* 343, 35–44. doi: 10.3354/meps06935
- Takada, Y., Ikeda, H., Hirano, Y., Saigusa, M., Hashimoto, K., Abe, O., et al. (2014). Assemblages of cryptic animals in coral rubble along an estuarine gradient spanning mangrove, seagrass, and coral reef habitats. *Bull. Mar. Sci.* 90, 723–740. doi: 10.5343/bms.2013.1085
- Tokeshi, M., and Arakaki, S. (2012). Habitat complexity in aquatic systems: fractals and beyond. *Hydrobiologia* 685, 27–47. doi: 10.1007/s10750-011-0832-z
- Troyer, E. M., Coker, D. J., and Berumen, M. L. (2018). Comparison of cryptobenthic reef fish communities among microhabitats in the Red Sea. *PeerJ* 6:e5014. doi: 10.7717/peerj.5014
- Wee, S. Y. C., Sam, S. Q., Sim, W. T., Ng, C. S. L., Taira, D., Afiq-Rosli, L., et al. (2019). The role of *in situ* coral nurseries in supporting mobile invertebrate epifauna. *J. Nat. Conserv.* 50:125710. doi: 10.1016/j.jnc.2019.125710
- Wolfe, K., Desbiens, A., Stella, J., and Mumby, P. J. (2020). Length–weight relationships to quantify biomass for motile coral reef cryptofauna. *Coral Reefs* 39, 1649–1660. doi: 10.1007/s00338-020-01993-9

**Conflict of Interest:** The authors declare that the research was conducted in the absence of any commercial or financial relationships that could be construed as a potential conflict of interest.

**Publisher's Note:** All claims expressed in this article are solely those of the authors and do not necessarily represent those of their affiliated organizations, or those of the publisher, the editors and the reviewers. Any product that may be evaluated in this article, or claim that may be made by its manufacturer, is not guaranteed or endorsed by the publisher.

Copyright © 2021 Masucci, Biondi and Reimer. This is an open-access article distributed under the terms of the Creative Commons Attribution License (CC BY). The use, distribution or reproduction in other forums is permitted, provided the original author(s) and the copyright owner(s) are credited and that the original publication in this journal is cited, in accordance with accepted academic practice. No use, distribution or reproduction is permitted which does not comply with these terms.



# Underwater Light Characteristics of Turbid Coral Reefs of the Inner Central Great Barrier Reef

Ross Jones<sup>1\*</sup>, Mari-Carmen Pineda<sup>1</sup>, Heidi M. Luter<sup>1</sup>, Rebecca Fisher<sup>1</sup>, David Francis<sup>2</sup>, Wojciech Klonowski<sup>3</sup> and Matthew Slivkoff<sup>3</sup>

<sup>1</sup> Australian Institute of Marine Science, Perth, WA, Australia, <sup>2</sup> School of Life and Environmental Sciences, Deakin University, Warrnambool, VIC, Australia, <sup>3</sup> In-situ Marine Optics, Perth, WA, Australia

## OPEN ACCESS

### Edited by:

Shashank Keshavmurthy,  
Biodiversity Research Center,  
Academia Sinica, Taiwan

### Reviewed by:

Nicola Browne,  
Curtin University, Australia  
Kyle Morgan,  
Nanyang Technological  
University, Singapore

### \*Correspondence:

Ross Jones  
r.jones@aims.gov.au

### Specialty section:

This article was submitted to  
Coral Reef Research,  
a section of the journal  
Frontiers in Marine Science

**Received:** 18 June 2021

**Accepted:** 31 August 2021

**Published:** 18 November 2021

### Citation:

Jones R, Pineda M-C, Luter HM, Fisher R, Francis D, Klonowski W and Slivkoff M (2021) Underwater Light Characteristics of Turbid Coral Reefs of the Inner Central Great Barrier Reef. *Front. Mar. Sci.* 8:727206. doi: 10.3389/fmars.2021.727206

Hyper-spectral and multi-spectral light sensors were used to examine the effects of elevated suspended sediment concentration (SSC) on the quantity and quality (spectral changes) of underwater downwelling irradiance in the turbid-zone coral reef communities of the inner, central Great Barrier Reef (GBR). Under elevated SSCs the shorter blue wavelengths were preferentially attenuated which together with attenuation of longer red wavelengths by pure water shifted the peak in the underwater irradiance spectrum ~100 nm to the less photosynthetically useful green-yellow waveband (peaking at ~575 nm). The spectral changes were attributed to mineral and detrital content of the terrestrially-derived coastal sediments as opposed to chromophoric (coloured) dissolved organic matter (CDOM). A simple blue to green (B/G,  $\lambda_{455:555}$  nm) ratio was shown to be useful in detecting sediment (turbidity) related decreases in underwater light as opposed to those associated with clouds which acted as neutral density filters. From a series of vertical profiles through turbid water, a simple, multiple component empirical optical model was developed that could accurately predict the light reduction and associated spectral changes as a function of SSC and water depth for a turbid-zone coral reef community of the inner GBR. The relationship was used to assess the response of a light sensitive coral, *Pocillopora verrucosa* in a 28-d exposure laboratory-based exposure study to a daily light integral of 1 or 6 mol quanta m<sup>-2</sup>. PAR with either a broad spectrum or a green-yellow shifted spectrum. Light reduction resulted in a loss of the algal symbionts (zooxanthellae) of the corals (bleaching) and significant reduction in growth and lipid content. The 6 mol quanta m<sup>-2</sup> d<sup>-1</sup> PAR treatment with a green-yellow spectrum also resulted in a reduction in the algal density, Chl a content per cm<sup>2</sup>, lipids and growth compared to the same PAR daily light integral under a broad spectrum. Turbid zone coral reef communities are naturally light limited and given the frequency of sediment resuspension events that occur, spectral shifts are a common and previously unrecognised circumstance. Dedicated underwater light monitoring programs and further assessment of the spectral shifts by suspended sediments are essential for contextualising and further understanding the risk of enhanced sediment run-off to the inshore turbid water communities.

**Keywords:** turbidity, coral reef, suspended sediment, downwelling irradiance, spectral changes

## INTRODUCTION

Light is essential for reef-building corals on account of their mutualistic symbiosis with photosynthetic symbiotic dinoflagellates (Falkowski et al., 1990; Muscatine, 1990; Lesser, 2004; Roth, 2014). Although corals are capable of feeding heterotrophically (Houlbrèque and Ferrier-Pagès, 2009), photosynthetic energy conversion provides much more energy influencing many aspects of their physiology and ecology (Falkowski et al., 1990; Yentsch et al., 2002; Gattuso et al., 2006; Dubinsky and Falkowski, 2011; Roth, 2014). The exponential decrease in light with water depth contributes significantly to changes in species composition and abundance and morphology (Goreau, 1959; Goreau and Wells, 1967; Dustan, 1982; Huston, 1985; Schuhmacher and Zibrowius, 1985; Wyman et al., 1987; Kramer et al., 2020). Latitudinal decreases in light availability has also been suggested a possible critical limiting factor for corals (Kleypas et al., 1999; Muir et al., 2015). The attenuation of light from increased water cloudiness (turbidity) from enhanced terrestrial runoff has been suggested as a threat to coastal marine ecosystems (ISRS, 2004; GBRMPA, 2020). Yet despite its significance, Yentsch et al. (2002) and more recently Edmunds et al. (2018) and Hochberg et al. (2020) have questioned why light on reefs has not been critically examined to the same extent as for other environmental factors (e.g., temperature, salinity, disease, etc.).

Solar radiation penetration to the seabed is determined by season, solar elevation, sea state, water depth and especially the optical properties of the water column (Kirk, 2010). Components of the water that can modify the underwater light field fall within three broad categories including phytoplankton, chromophoric (coloured) dissolved organic matter (CDOM) and non-algal particulates (NAP) (Mobley, 1994; Kirk, 2010). Together with the spectral attenuation of the pure seawater itself the relative contributions of the individual components determine the intensity and spectral quality of the light reaching the seabed (Prieur and Sathyendranath, 1981; Babin et al., 2003b; Kirk, 2010).

Over the visible/photosynthetic part of the spectrum (400–700 nm) water absorbs strongly in the longer red wavelengths (Smith and Baker, 1981; Kirk, 2010). Phytoplankton absorb mostly in the shorter blue and blue green wavelengths (Prieur and Sathyendranath, 1981; Van Duin et al., 2001) and CDOM absorbs more strongly in the shorter blue wavelengths and into the ultraviolet (Bricaud et al., 1981; Hansell and Carlson, 2002; Shi et al., 2013). Non-algal particulates consisting of mineral sediments, non-living organic detritus such as faecal matter and degrading phytoplankton cells (Binding et al., 2008), produce a similar spectral signal to CDOM, absorbing in the shorter blue wavelength and decreasing steadily towards the longer red wavelengths (Kirk, 1985, 2010; Babin and Stramski, 2002, 2004; Bowers and Binding, 2006; Binding et al., 2008).

Most studies of light absorption and scattering have focused on Case-1 waters in the bipartite classification scheme of Morel and Prieur (1977). These waters are optically “simple” and include most open water, oceanic environments (Babin et al., 2003a) where the optical properties are largely determined by

phytoplankton (represented by chlorophyll) alone (Smith and Baker, 1978; Morel, 1988; Mobley, 1994; Lee et al., 2007b; Morel et al., 2007). Case-1 waters typify the “traditional” perception of coral reefs as occurring in a “clear-water” or “blue water,” nutrient-poor, oligotrophic environments (Potts and Jacobs, 2000). In Case-1 waters the water column gradually narrows the spectrum with depth to one dominated by blue light. Since the initial work of Dustan (1982), many studies have now described this spectral change and examined and partitioned the bio-optical properties in clear-water reefs (Dunne and Brown, 1996; Maritorena and Guillocheau, 1996; Lesser and Gorbunov, 2001; Lesser, 2004; Blondeau-Patissier et al., 2009; Lesser et al., 2009; Kuwahara et al., 2010; Mass et al., 2010; Dubinsky and Falkowski, 2011; Brandon et al., 2019; Kahng et al., 2019; Hochberg et al., 2020).

Case-2 waters are more optically complex because light absorption and scattering is influenced by suspended sediments (mineral NAPs) as well as CDOM and phytoplankton (Jerlov, 1976; Mobley, 1994; IOCCG, 2000; Babin et al., 2003a; Kirk, 2010). Case-2 waters are typically in coastal areas influenced by terrestrial run off and wind and wave induced resuspension of the shallow seabed with mineral NAPs often dominating the spectral signal (Duarte et al., 1998; Bowers and Binding, 2006; Binding et al., 2008). Corals reefs are commonly found in such environments (turbid-water reefs) and referred to as “alternative states” to the typical clear-water notion of reefs (Perry and Larcombe, 2003; Zweifler et al., 2021). The turbid-zone coral reef communities of the inner, central Great Barrier Reef (GBR) (Woolfe and Larcombe, 1998, 1999; Larcombe and Woolfe, 1999; Perry and Larcombe, 2003; Browne et al., 2012; Zweifler et al., 2021) are very well-known example of reefs in Case-2 waters, with vertically compressed coral depth distributions (Morgan et al., 2016) as noted in other turbid reef systems such as in Singapore (Morgan et al., 2020).

The GBR turbid-zone coral reef communities have been the focus of considerable attention as land runoff and poor water quality is considered a major threat to the Great Barrier Reef Marine Park particularly the inshore areas (GBRMPA, 2020). Runoff from highly modified catchments can enhance the delivery of sediments, nutrients and other organic particles and could have detrimental effects by reducing the available light for seagrass and corals in the inner GBR (GBRMPA, 2020) and elsewhere in the world (Morgan et al., 2020). Conversely, reduced light availability could have “beneficial” effects and reduced levels of coral bleaching in turbid, coastal coral reef environments during heat waves has now been noted in many studies (Guest et al., 2012, 2016; Van Woesik et al., 2012; Cacciapaglia and Van Woesik, 2016; Fisher et al., 2019; Mies et al., 2020; Sully and Van Woesik, 2020), including the inshore GBR (Morgan et al., 2017). This increased resilience could be related to turbidity reducing light levels and reducing or ameliorating the physiological stress associated with the combined effects of light and elevated water temperatures (Sully and Van Woesik, 2020). To further understand these possible detrimental or “beneficial” effects of turbidity requires a better understanding of light characteristics of turbid-zone reef communities.



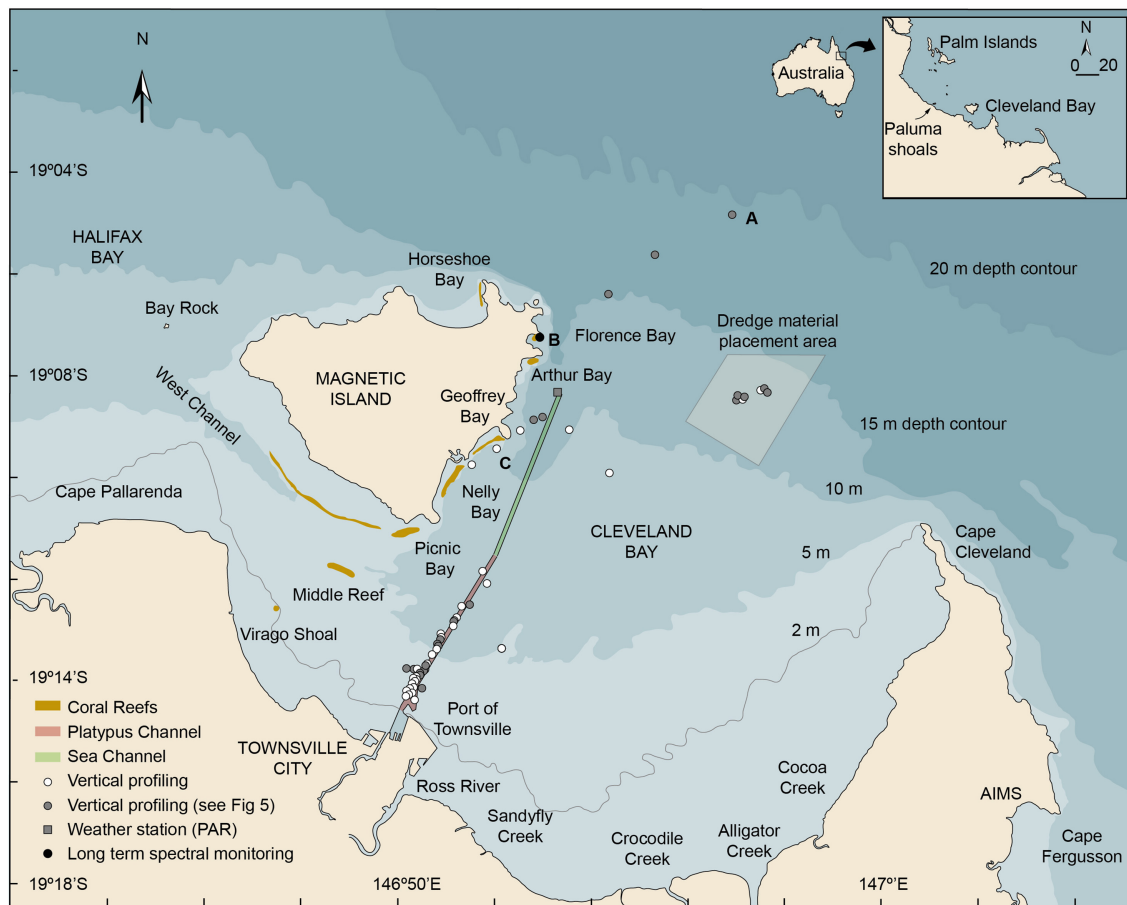
In two recent studies involving vertical profiling of light in very turbid waters (elevated suspended sediment concentrations caused by dredging) preferential attenuation of shorter blue wavelengths was noted in addition to overall loss of light (Jones et al., 2016; Fearn et al., 2019). This resultant shift in underwater colour spectrum to the green/yellow waveband, which is less photosynthetically useful (Gallegos et al., 2009; Falkowski and Raven, 2013), could have implications for benthic photoautotrophs (Jones et al., 2016). In this study, we further examine the effects of NAPs on quantity and quality of underwater light using elevated SSCs caused by dredging to derive wavelength specific light attenuation coefficients by water column profiling using a hyper-spectral radiometer. An empirical spectral solar irradiance model was developed to describe the underwater light spectrum and how it changes with sun-angle, water depth and suspended sediment concentration. Measurements were also made of spectral changes during a wind/wave natural resuspension event using an *in situ* multi-spectral radiometer. The model was used to define the exposure conditions for a laboratory-based

exposure study to investigate sublethal physiological effects of a light sensitive coral incubated under different light quality and quantity scenarios.

## MATERIALS AND METHODS

### Site Description

Fieldwork was conducted in the inner central Great Barrier Reef (GBR) in Cleveland Bay and on the reefs around Magnetic Island (**Figure 1**). The oceanographic and sedimentary setting of the bay has been described by Larcombe et al. (1995) and the turbid-zone reef communities have been the subject of several studies associated with understanding sedimentary processes, transport and fate, and the effects of watershed development on reef growth in “marginal” (cf Perry and Larcombe, 2003) environments (Carter et al., 1993; Larcombe et al., 1995, 2001; Lou and Ridd, 1996; Larcombe and Woolfe, 1999; Orpin et al., 1999, 2004; Anthony et al., 2004; Browne et al., 2010, 2012, 2013; Lambrechts et al., 2010; Bainbridge et al., 2012; Orpin and Ridd,



**FIGURE 1** | Location map showing Cleveland Bay and Magnetic Island off the coastal city of Townsville in the inner central Great Barrier Reef (Australia) showing the locations of (a) the multispectral light logger deployment in Florence Bay ( $19.121917^{\circ}$ ,  $146.883167^{\circ}$ ), (b) the vertical light and turbidity profiling sites conducted beside the shipping channel, the reefs off Magnetic Island, in the dredge material placement area (DMPA), and seaward of the 15 m isobath, (c) the Cleveland Bay weather station ( $-19.140556^{\circ}$   $146.889537^{\circ}$ ) where above water PAR levels were recorded (AIMS, 2020). The inset figure shows the location of Cleveland Bay in the inner central Great Barrier Reef (GBR) region and coral collection sites near the Palm Islands.

2012; Perry et al., 2012; Macdonald et al., 2013; Delandmeter et al., 2015; Whinney et al., 2017).

Briefly, Cleveland Bay is a shallow (15 m at its seaward edge) northward-facing embayment of around 325 km<sup>2</sup> located off the coastal city of Townsville in Northern Queensland, Australia (**Figure 1**). The bay is landlocked around its southern and eastern sides by the mainland and bordered by Magnetic Island, a granitic continental high island on its north-western margin (**Figure 1**). On the SE of the island there are a series of bays with well-developed fringing reefs—Florence Bay, Arthur Bay, Geoffrey Bay, Nelly Bay and Picnic Bay—and on the southern section a large detached reef, Cockle Bay (Hopley, 1982) (**Figure 1**). The reefs are composed of hard and soft corals and algae (Bull, 1982; Mapstone et al., 1992; Kaly et al., 1994) overlying accumulations of non-biogenic sediments (Hopley, 1982).

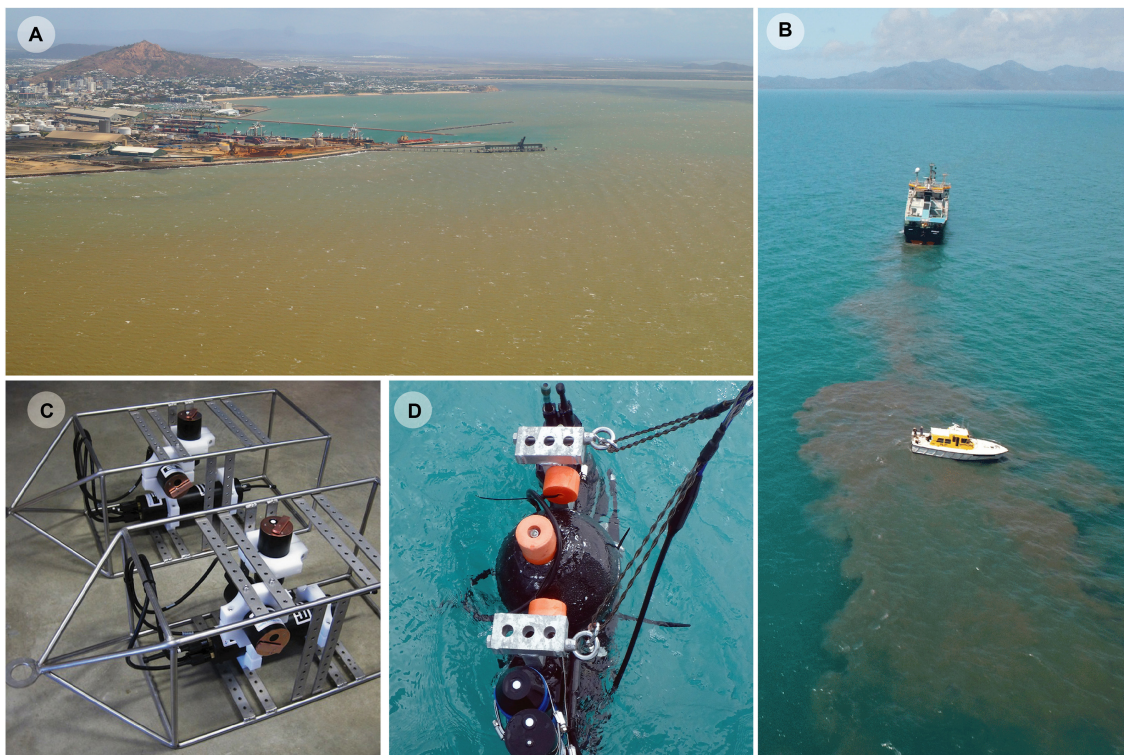
The bay is naturally very turbid and resuspension of bottom sediment by wave action augmented to some extent by tides and currents is the most significant long-term contributor to elevated SSCs (Larcombe et al., 1995, 2001; Lou and Ridd, 1996; Orpin et al., 1999, 2004; Anthony et al., 2004; Orpin and Ridd, 2012; Macdonald et al., 2013; Luter et al., 2021). Background SSCs in Cleveland Bay are typically <5 mg/L<sup>-1</sup> (Larcombe et al., 1995), and 1–2 mg/L<sup>-1</sup> on the reefs around Magnetic

Island (Waterhouse et al., 2021), but winds sufficient to cause resuspension of bottom sediments in the bay at 5 m depth occur on an estimated 220 days per year, and higher energy events sufficient to cause resuspension of bottom sediments at 15 m depth on 40 days per year (**Figure 2A**) (Orpin et al., 1999; Orpin and Ridd, 2012).

The frequent resuspension requires annual or sometimes biannual maintenance dredging of two connected shipping channels to allow safe passage of cargo ships (**Figure 1**). Currently, the majority of the dredging is performed by an 85 m long ocean-going trailing arm suction dredge (TSHD) that has two trailing arm suction heads which are lowered and dragged along the seafloor, dredging the seabed either side of the vessel (**Figures 2B,C**). Turbidity generation is associated with disturbance of the seabed by the drag heads and by propeller wash and by dredge material placement at the 3.7 × 3.7 km dredge material placement area (DMPA) located in the bay itself (**Figures 1, 2B**).

### Turbidity and Light (Spectrum) Time Series

From 28 May 2017 to 27 June 2017 underwater measurements of photosynthetically active radiation (PAR, 400–700 nm), turbidity and depth (m) were measured at 15 min intervals (averaging for



**FIGURE 2 | (A)** Aerial photograph of Cleveland Bay on 9 Sept 2013 during a period of elevated wind speeds. The turbidity is a natural event and not caused by dredging. **(B)** Research vessel with scientists vertically profiling a sediment plume from an 85 m long ocean-going trailing arm suction dredge (TSHD) disposing sediment at the dredge material placement area in Cleveland Bay. **(C)** Two upward facing IMO-MS8 eight wavelength multispectral irradiance sensors and sideways facing IMO-NTU turbidity sensors in stainless steel frames used on the reefs at Florence Bay to measure changes in light quality, quantity and water cloudiness during natural suspension events, **(D)** a combined USSIMO hyper-spectral radiometer and IMO-NTU turbidity sensor which was placed in plumes generated by dredging (or dredge material disposal) and allowed to slowly sink, recording turbidity and underwater irradiance at wavelengths between 400 and 700 nm.

10 s) using sensors attached to a seabed mounted stainless steel instrument platform in Florence Bay (**Figures 1, 2C**). Permitting restrictions prevented deployment of the sensors on the reef itself, so the platform was placed at the very base of the reef slope at 8.5 m on a sandy seabed. Instruments included a vertically mounted IMO-MS8 eight wavelength (425, 455, 485, 515, 555, 615, 660, and 695 nm) multi-spectral irradiance sensor and a horizontally-mounted IMO-NTU turbidity sensor, and were both connected to an IMO-DL3 data logger with built-in depth and temperature sensors [In situ Marine Optics (IMO), Perth, Western Australia] (**Figure 2D**). To prevent biofouling, the MS8 and turbidity sensors have copper-based wiper mechanisms that sweep over the sensors every 15 min and park over the sensors when not sampling.

PAR data was calculated from the 8 wavelengths by interpolating to higher resolution 1 nm spacing using the *approx* function from the *stats* package in R (R Core Team, 2020), and then summing across all estimated values from 400–700 nm to calculate the total interpolated Photosynthetically Available Radiation (hereafter simply PAR) expressed as an instantaneous value ( $\mu\text{mol photons m}^{-2} \text{s}^{-1}$ ) or on a daily basis as a daily light integral (DLI,  $\text{mol photons m}^{-2} \text{d}^{-1}$ ) calculated by summing the per second quantum flux measurements over the day (Fisher et al., 2015; Jones et al., 2015). Simple linear interpolation between the peak wavelength of each of the 8 sensors is a relatively robust means of estimating PAR as there is considerable overlap in the spectral sensitivity of each of the individual sensors for the MS8 multi-spectral loggers. Photosynthetically usable radiation (PUR), which is a product of the light availability (PAR) and absorption efficiency (Morel, 1978) was also calculated using equation 1.

$$PUR = \int_{400}^{700} PAR(\lambda) A \quad (1)$$

based on absorption coefficients (for symbiotic algae of corals) digitised from Figure 2b of Hennige et al. (2009), and as shown in **Figure 5A**.

To compliment the *in situ* measurements, surface measurements of PAR were obtained from an instrument mounted on a channel marker buoy (nominally 10 m above sea level) situated 1.9 km south of Florence Bay (**Figure 1**, 19.140906°, 146.889565°; AIMS, 2020).

## Vertical Water Quality Profiling

Over a 4-d period (12–15 September 2016), 94 light and turbidity vertical profiles were measured in and just outside of Cleveland Bay using a USSIMO hyper-spectral radiometer (In Situ Marine Optics, Perth, Australia) and IMO-NTU turbidity sensor (**Figure 2D**). The USSIMO incorporates a Carl Zeiss UV/VIS miniature monolithic spectrometer module as the internal light recording device providing irradiance measurement values at nanometre spectral spacing with instrument tilt and temperature sensors (Antoine et al., 2017). The instruments were mounted vertically on an aluminium frame, with the radiometer orientated upwards and turbidity sensor downwards. The frame was

designed to sit vertically in the water column using polystyrene floats and was made slightly negatively buoyant using lead weights. Sampling involved holding the instrument frame at 0.5 m depth in plumes created by the dredging activities (**Figure 2B**) and then allowing the instrument frame to drift away from the boat and slowly sink (free-fall) at a rate of 0.5 m/s through the plume recording light and turbidity and depth until it reached the seabed. Sampling rates were up to 5 HZ with 20–250 samples taken per cast depending on depth. A reference USSIMO radiometer was also positioned on the mast of the survey vessel and was used to identify reductions in light during the profile as a result of intermittent clouds (see below). Profiles were conducted in the shipping channel and turning basin and in shallower water either side of the channel ( $n = 76$  sites, depths of up to 12 m) in the spoil ground area ( $n = 12$  sites, depths up to ~11–13 m) beside Geoffrey Bay reef ( $n = 3$  sites depths) and outside of Cleveland Bay ( $n = 3$  sites, depths of 16–21 m) (**Figure 1**).

At the start of each profile a water sample was collected using a Niskin<sup>TM</sup> bottle (General Oceanics, Miami, Florida, US) and triplicate water samples were drawn from the Niskin bottle and subsequently filtered onto Whatman (Cytiva, Marlborough, MA, USA) 47 mm GF/F filters (nominal pore size 0.7  $\mu\text{m}$ ), using 100 mL of distilled water to rinse the container, filter funnel and filter pads of salts. Filters were then dried overnight in a 65°C oven and weighed with a precision balance (capable of weighing to 0.0001 g) and used to generate the relationship between SSC and turbidity (NTU).

## Light Exposure Experiments

Studies examining the effect of light quantity and quality on the branching coral *Pocillopora verrucosa* (Ellis and Solander, 1786) were conducted at the National Sea Simulator (SeaSim) aquarium facilities at the Australian Institute of Marine Science (AIMS, Townsville), using corals collected from 3–5 m depth from the Palm Islands, central GBR (**Figure 1**). Fragments from four colonies were collected using a mallet and chisel and transported to the SeaSim where they were further fragmented (~5–9 cm length) and glued onto numbered aragonite plugs. Fragments were left to recover for 1 month in 1,200 L holding tanks with flow-through seawater maintained at 27°C, 36 PSU salinity, and under a 12-h light: dark (L:D) cycle of ascending and decreasing light levels, equivalent to a DLI of 6  $\text{mol photons m}^{-2} \text{d}^{-1}$ . Throughout the holding and experimental periods, an enriched *Artemia* spp. (targeted concentration in tanks of 0.5 nauplii  $\text{mL}^{-1}$ ) and a mix of microscopic algae (2,000 cells  $\text{mL}^{-1}$ ) were fed daily.

Utilising the same tank system, control mechanisms and custom-made LED light fittings as recently described in Luter et al. (2021), corals were exposed to four different experimental light scenarios for 28-d. Experiments were conducted at 27°C and the individual 1200 L tanks received fresh seawater at a rate of 2,500  $\text{mL min}^{-1}$  resulting in 3 complete turnovers per day. Each scenario consisted of either a high or low light level in combination with a “normal” or “green-yellow shifted” spectrum (see Results section, **Figure 9**). There were two replicate tanks for each scenario, with a total of eight fragments per treatment ( $n=4$  per tank, representing each genotype). Unlike Luter et al.



(2021), no suspended sediments were added to the tanks during the exposure period.

All corals were photographed and weighed, using the buoyant weight method (Spencer Davies, 1989), at the start and end of the experiment. Following the 28-d exposure, coral tissue was removed by air blasting in 30 mL of 0.5  $\mu\text{m}$  filtered seawater. The resulting tissue slurry was homogenised for 60 s, the exact volume recorded, and aliquots taken for symbiotic dinoflagellate density (1 mL, fixed in 10% buffered formalin), pigments (1 mL) and lipid (10 mL) analyses. The surface area of corals was determined using the wax-dip method (Stimson and Kinzie, 1991). To determine symbiotic dinoflagellate density, a volume of 0.4  $\text{mm}^3$  from each aliquot was counted six times using a Neubauer hemocytometer (LO - Laboroptik Ltd, Lancing UK) containing 8  $\mu\text{L}$  of homogenised solution.

To determine pigment concentrations, algal pellets from coral blastate samples were weighed and ground with a small amount of 100% acetone using a glass mortar and pestle, settled in ice. The ground blastate was transferred to a 10 mL centrifuge tube, vortexed for 30 s and sonicated in an ice-water bath for 20 min in the dark, followed by an overnight incubation ( $\sim 15$  h) at 4°C in the dark. Extracts were then centrifuged at 2,500 rpm for 5 min at  $-2^\circ\text{C}$  and transferred to 10 mL volumetric flasks using Pasteur pipettes. Three mL of 100% acetone was added to each sample before repeating the vortex and sonication steps. The second extract was left for 2 h before centrifugation, and then both extracts were combined. One mL of water was added to each flask and then made up to 10 mL with 100% acetone to render a final extract of 90% acetone:water. Sample extracts required dilution with 90% acetone:water to have a concentration within the linear range of the standard calibration for all pigments. The final extract was filtered through a 0.2  $\mu\text{m}$  membrane filter (Whatman, anatope) prior to analysis by HPLC (high performance liquid chromatography) using a Waters Alliance HPLC system (Waters, USA), comprising a 2695XE separations module with column heater and refrigerated autosampler and a 2996 photo-diode array detector. A detailed description of the HPLC method can be found in Clementson (2013). Pigments were identified by retention time and absorption spectrum from a photo-diode array (PDA) detector and concentrations of pigments were determined from commercial and international standards (Sigma; DHI, Denmark). Total lipids and lipid classes were identified by extracting freeze-dried blastate samples following the procedures outlined in Luter et al. (2021), with lipid classes determined using the Iatroscan MK 6s thin layer chromatography flame ionisation detector (Mitsubishi Chemical Medience, Tokyo, Japan). Detailed methods of lipid extraction and quantification procedures can be found in Conlan et al. (2017).

Generalised linear mixed models (GLMM) were used to examine the strengths of treatment effects and assess the differences between individual light scenario treatments. Individual GLMMs were fit for each of the response variables assessed. Since corals can both grow and shrink, a Gaussian distribution was used for growth (buoyant weight expressed as % of initial weight) as this variable can theoretically take positive and negative values and was normally distributed, whereas a

Gamma distribution was used for zooxanthella density (symbiont density), pigment concentration ( $\mu\text{g Chl a cm}^{-2}$ ), total lipids and the ratio of storage to structural lipids, as these variables were continuous on the scale of  $>0$ . The glmer function in the R package lme4 (Bates et al., 2015) was used to fit the models using tank as a random effect. Relative model weights (Burnham and Anderson, 2002) were calculated using AICc values for the model including the treatment effect and a null model including only the random tank effect. To compare individual treatment effects a Bayesian approach based on posterior contrasts was used. Integrated nested Laplace approximation (INLA) for approximating posterior distributions (see Rue et al., 2009) was used to fit Bayesian models of the equivalent GLMM design. A posterior probability similarity of 0.95% or greater was used to identify statistically similar groupings.

## RESULTS

### Turbidity and Light (Spectrum) Time Series

Over the 31-d deployment, which included the austral winter solstice on 21 June, the maximum instantaneous above water (surface) light levels varied more than 2-fold, from 750  $\mu\text{mol quanta m}^{-2} \text{ s}^{-1}$  during an overcast day on June 11 to  $\sim 1,600 \mu\text{mol quanta m}^{-2} \text{ s}^{-1}$  during a series of cloud-free days (Figure 3A). The maximum daily instantaneous underwater PAR varied over an order of magnitude from  $<10 \mu\text{mol quanta m}^{-2} \text{ s}^{-1}$  on 19 June to  $>150 \mu\text{mol quanta m}^{-2} \text{ s}^{-1}$  on 11 days of the deployment 17–21 June (Figure 3A).

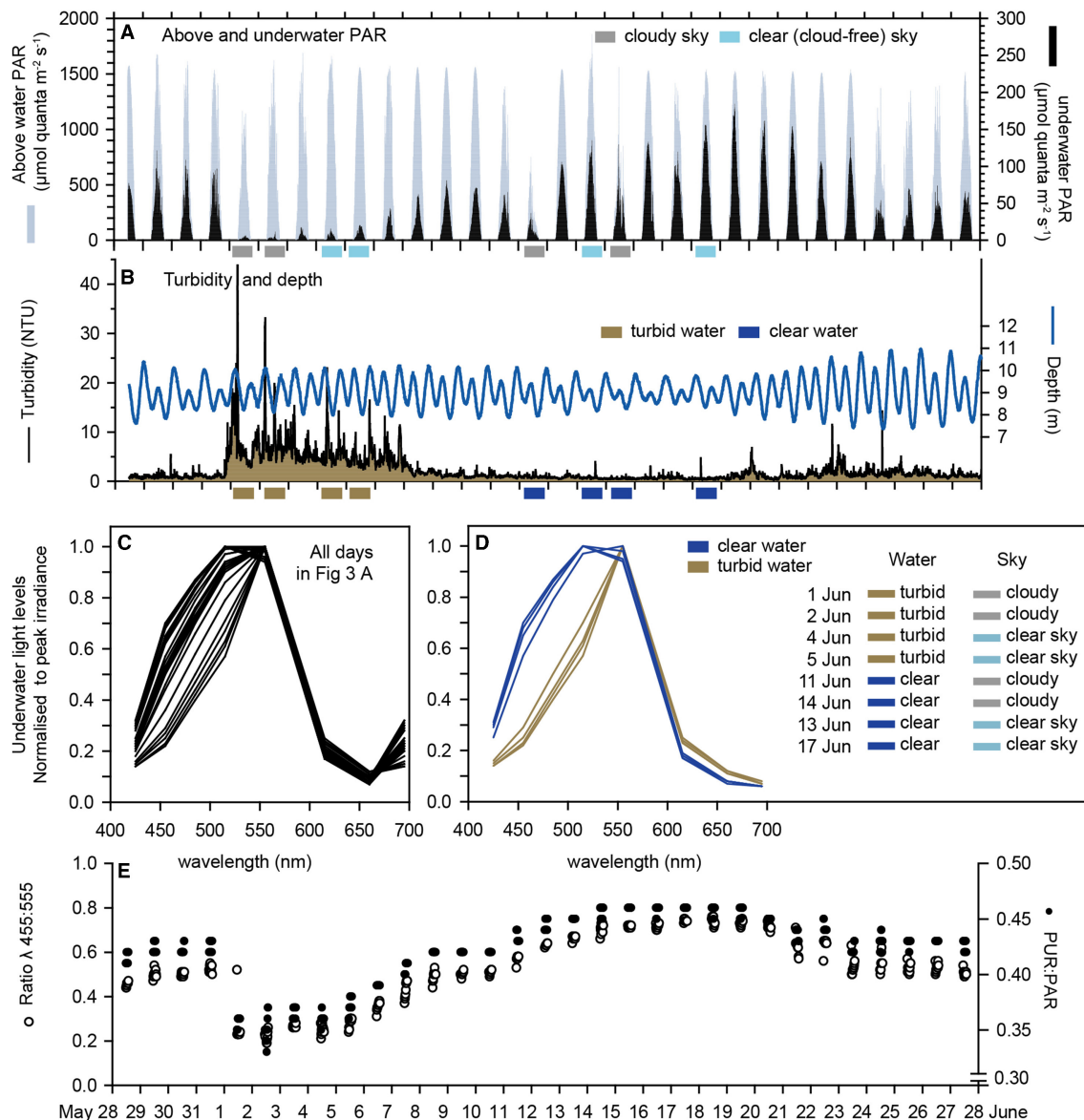
In the first week of June a 7-d natural turbidity event occurred caused by a period of increased wind speeds (data not shown), and average daily nephelometry-derived SSCs (based on a NTU to SSC conversion in Figure 6C) reached  $\sim 10 \text{ mg L}^{-1}$  (including an SSC of  $55 \text{ mg L}^{-1}$  at 05:30 h on 1 June) (Figure 3B) compared to normal background SSCs of 1–2 mg (Waterhouse et al., 2021).

To examine the effects of elevated water turbidity and clouds on the underwater spectral distributions, wavelength specific underwater irradiance values were averaged over a 2 h period centred on solar culmination each day and standardised to a mean of zero and standard deviation of 1. The standardised profiles showed considerable variability but mostly in the shorter blue and blue/green wavelengths (415, 455, 485, and 515 nm) (Figure 3C).

Inspection of Figures 3A,B shows the deployment occurred for several days where there was either (1) high or (2) low turbidity in combination with either (3) high or (4) low surface light (caused by the absence or presence of clouds). Figure 3D shows the normalised spectral response of 2 days in each of these 4 combinations, revealing preferential loss of the blue light wavelengths invariably occurred during periods of high turbidity, or expressed another way, notable spectral changes did not occur when absolute underwater light levels were reduced by clouds alone.

Since the spectral changes were associated with a reduction in blue light an index was calculated based on the ratio of blue light (455 nm) to green light (555 nm). This blue/green ration value fell sharply to  $<0.4$  during the week-long turbidity event





**FIGURE 3 |** Multispectral sensor data: **(A)** Underwater PAR at 8 m depth at Florence Bay and above water PAR at the weather station beside Florence Bay (Figure 1) from 28 May to 28 June (2017) which encompassed the austral winter solstice (21 June). **(B)** Turbidity (NTU) at the seabed (8 m) at Florence Bay and depth (m). **(C)** The ratio of  $\lambda_{455}$  nm to  $\lambda_{555}$  nm light and PUR:PAR. **(D,E)** Normalised irradiance spectra from the underwater multispectral light sensor at Florence Bay over a 2 h period centred on midday for all days and 8 days showing the effects of high and low turbidity with and without cloud cover (see text).

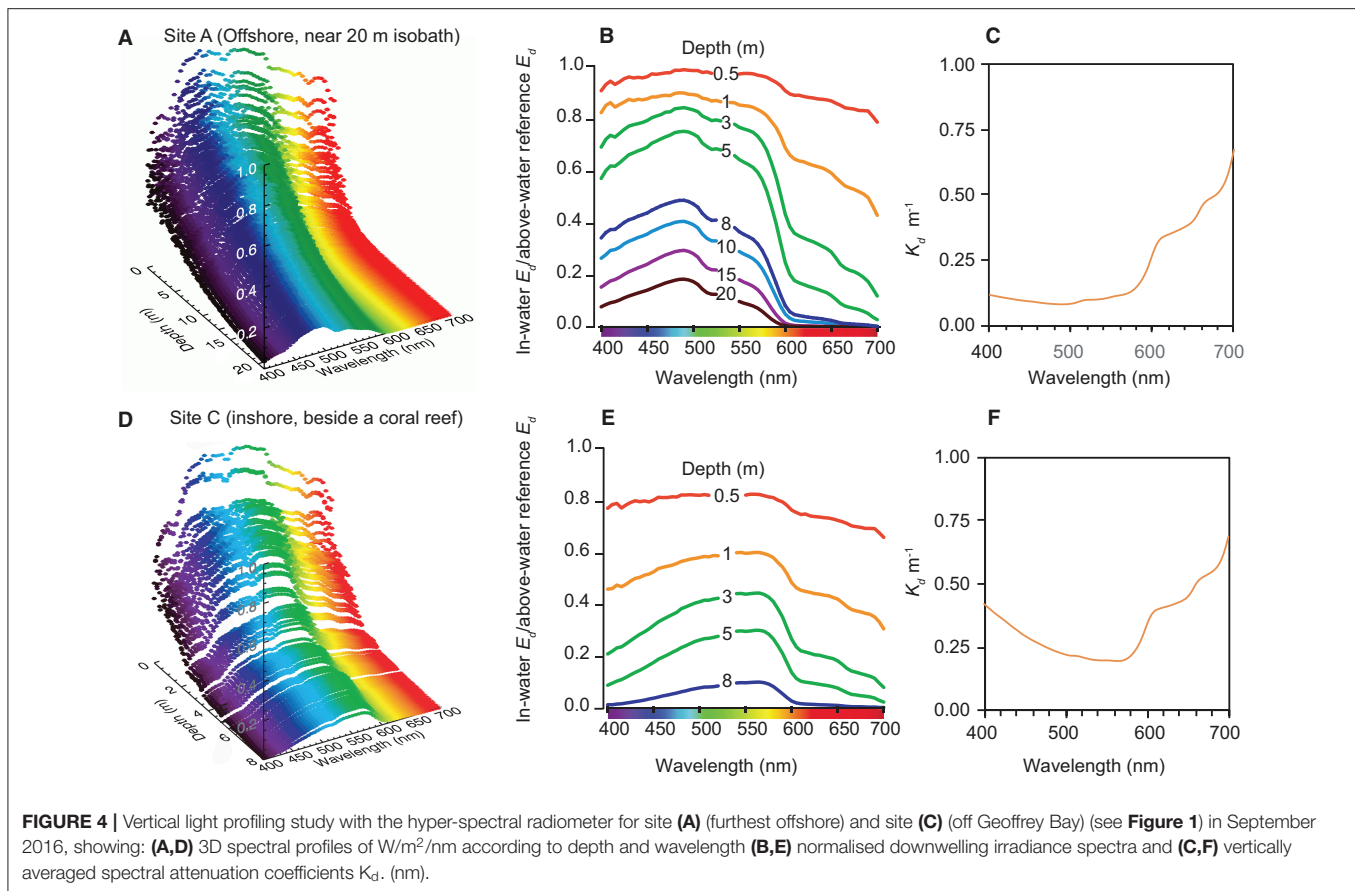
returning to values  $>0.6$  when SSC levels fell back to  $1 \text{ mg L}^{-1}$  (Figure 3E). The PUR:PAR ratio showed similar changes and a 25% reduction during the turbidity peak (Figure 3E) on account of the spectral changes.

## Vertical Water Quality Profiling

Representative vertical spectral light profiles using the hyperspectral radiometer are shown in Figure 4 for a deeper water site (20 m depth) outside Cleveland Bay (Site A in Figure 1), and a shallower site (8 m depth) beside the coral reef at Geoffrey Bay (Site B in Figure 1). Both sites had very low SSCs ( $\sim 1 \text{ mg L}^{-1}$ ) at the time of sampling.

In the offshore site, the upper 0.5 m had a relatively even distribution of blue, green and red wavelengths and there was rapid loss of red light with increasing depth to very low values by 8–10 m (Figures 4A,B). Blue light (450–500 nm) was also attenuated but at a lower rate as indicated by the vertically averaged water column attenuation coefficient (Figure 4C). At the seabed at 20 m the peak wavelength was 475 nm in the blue part of the spectrum (Figures 4A,B).

Beside the reef there was also an even distribution of blue, green and red wavelengths in the upper 0.5 m and also a loss of red light with depth (Figures 4E,F). However, as indicated by the increase in the vertically averaged water column attenuation



coefficient (**Figure 4F**) there was also much greater attenuation of blue wavelengths with depth. Near the seabed (8 m depth), the peak wavelength was 575 nm in the green-yellow part of the spectrum (**Figures 4A,B**).

**Figure 5A** shows the normalised (in-water  $E_d$  divided by above-water reference  $E_d$ ) spectral profiles and **Figure 5B** the vertically average attenuation coefficient at single depth of 3 m for 23 vertical profiles where light was detectable at all wavelengths, including profiles collected outside the bay beyond the 15 m depth contour, in the dredge material placement area (DMPA), in or within 50 m of the Platypus channel, and sites off the reef slope of Geoffrey Bay. A colour-coding scheme based on the mean turbidity (at  $3 \pm 0.1$  m depth) per profile is used to indicate turbidity which ranged from 1 to 11.1 NTU. At increasingly higher turbidity there was loss of light, and also proportionally higher  $K_d$  in the shorter blue wavelengths, resulting in an increase in the peak wavelengths from  $<500$  nm to 575 nm. Also shown in **Figure 5A** is the absorption spectra of the symbiotic dinoflagellates of corals (digitised from Figure 2b in Hennige et al., 2009), indicating light is comparatively poorly absorbed in this part of the spectrum.

**Figure 5C** shows a principal coordinate analysis (PCO) of the 23 sites based on the hyper-spectral data. Analyses were performed in PRIMER 6 (Plymouth, UK) using Euclidean distances and Spearman Rank correlations to identify

wavelengths that contribute most to the differences observed (**Figure 5C**). The shapes correspond to sampling locations and colour of the shape corresponds to the turbidity, which decreased from the highest values (red; left of the ordination) to the lowest values (green; right of the ordination). The wavelengths contributing most to the shift of samples to the right of the ordination include 490, 510, and 525 nm (blue/green), whereas the wavelengths contributing least include 690, 695, and 700 nm (red wavelengths) (**Figure 5C**).

## Empirical Spectral Solar Irradiance Model

From the vertical profiles a simple, multiple component empirical optical model was developed to estimate the spectral reduction of underwater light as a function of solar angle, suspended solid concentration and water depth. The first part of the model represented the input solar irradiance based on a number of clear sky, full-day time-resolved above water irradiance measurements from a dynamic above-water radiance and irradiance collector (DALEC) hyperspectral radiometer (Slivkoff, 2014).

For each wavelength ( $\lambda$ ), a 3rd order polynomial was fitted to the cosine solar zenith angle ( $\theta_z$ ) normalised irradiance data, and then converted to subsurface irradiance using a spectrally-independent conversion factor  $T = 0.965$  (Morel and Antoine, 1994; Morel and Maritorena, 2001). The model was then expressed as an equation to generate estimations of the

subsurface irradiance  $E_d(-0)$ , as a function of solar zenith angle and wavelength (Equation 2).

$$E_d(-0, \lambda, \theta_z) = T[C_0(\lambda) + C_1(\lambda)\theta_z + C_2(\lambda)\theta_z^2 + C_3(\lambda)\theta_z^3] \cos(\theta_z) \quad (2)$$

The next component of the model incorporated the vertical irradiance and NTU profile measurements in Cleveland Bay, alongside the gravimetric total suspended solids measurements (Figure 6A). Each vertical USSIMO Irradiance profile was normalised by the second in-air reference USSIMO radiometer. All radiometer data was then screened to remove measurements where the cosine collector was tilted  $>5^\circ$  from zenith (directly overhead). This typically removed the first 1 m of the vertical profile while the slow-descent instrument frame stabilised. Data from  $<0.03\%$  incident irradiance was also removed from processing, which removed near-seabed data and extremely turbid waters where light reductions could not be quantified as a function of water depth.

The exponential Beer-Lambert equation was fitted to the quality-controlled normalised irradiance data for each

wavelength and sensor depth  $z$  in order to determine the water-column averaged spectral diffuse attenuation coefficients ( $K_d$ ) for each profile.

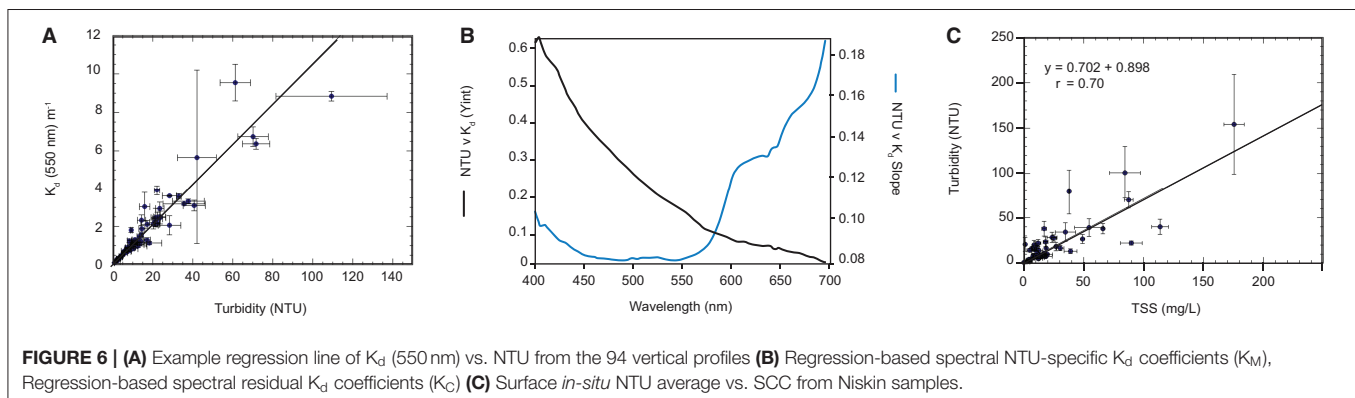
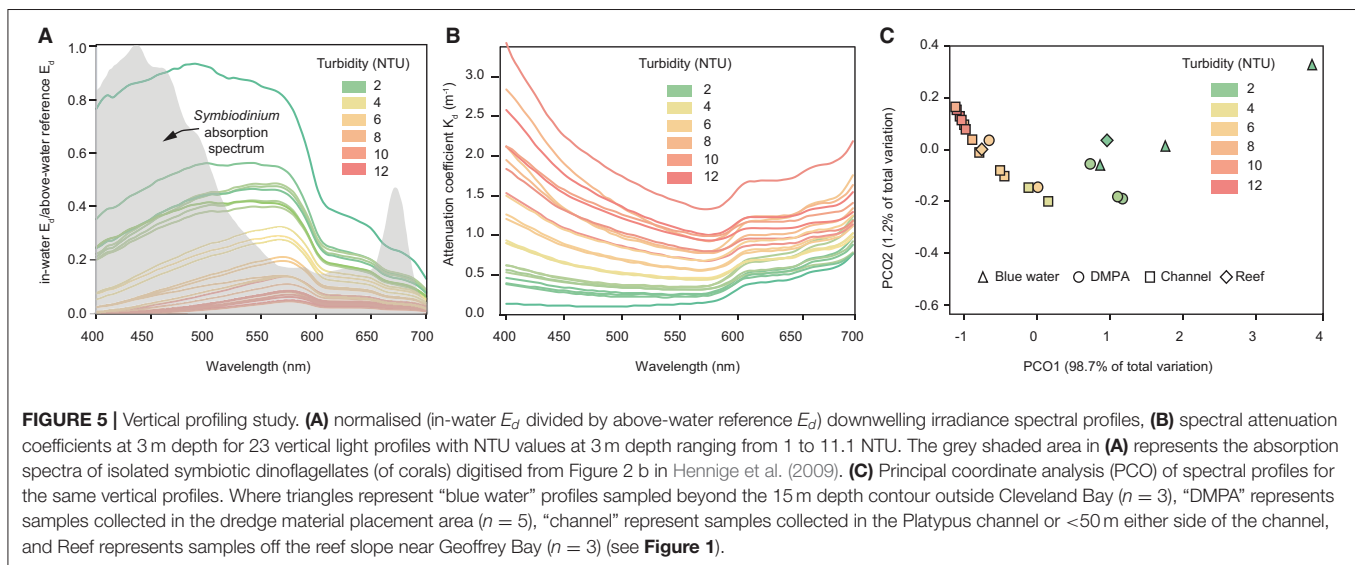
$$K_d(\lambda) = -\frac{\ln\left[\frac{E_d(z, \lambda)}{E_d(+0, \lambda)}\right]}{z} \quad (3)$$

Solar angle normalisation of the  $K_d$  data was not conducted as profiles were typically performed during high sun angles  $<20^\circ$ . To match the water column-averaged  $K_d$  data, full vertical profile NTU data collected simultaneously to the irradiance data was averaged. The spectrally resolved NTU-specific and residual  $K_d$  data was determined using linear regression.

The slope (NTU specific  $K_d$ ) coefficients and the residuals are shown in Figure 6B. The residual spectral shape is strongly influenced by the absorption coefficient of water itself, whereas the spectral shape of the NTU specific coefficients are governed by particulate absorption and scattering (see Slivkoff, 2014).

An estimate of the diffuse attenuation coefficient based on NTU is then expressed as:

$$K_d(\lambda) = K_M(\lambda) [NTU] + K_C(\lambda) \quad (4)$$



As the goal of the modelling study is to relate light attenuation back to SSCs, a regression relating SSCs to NTU was calculated (**Figure 6C**). This relationship is used to express a user input TSS into NTU:

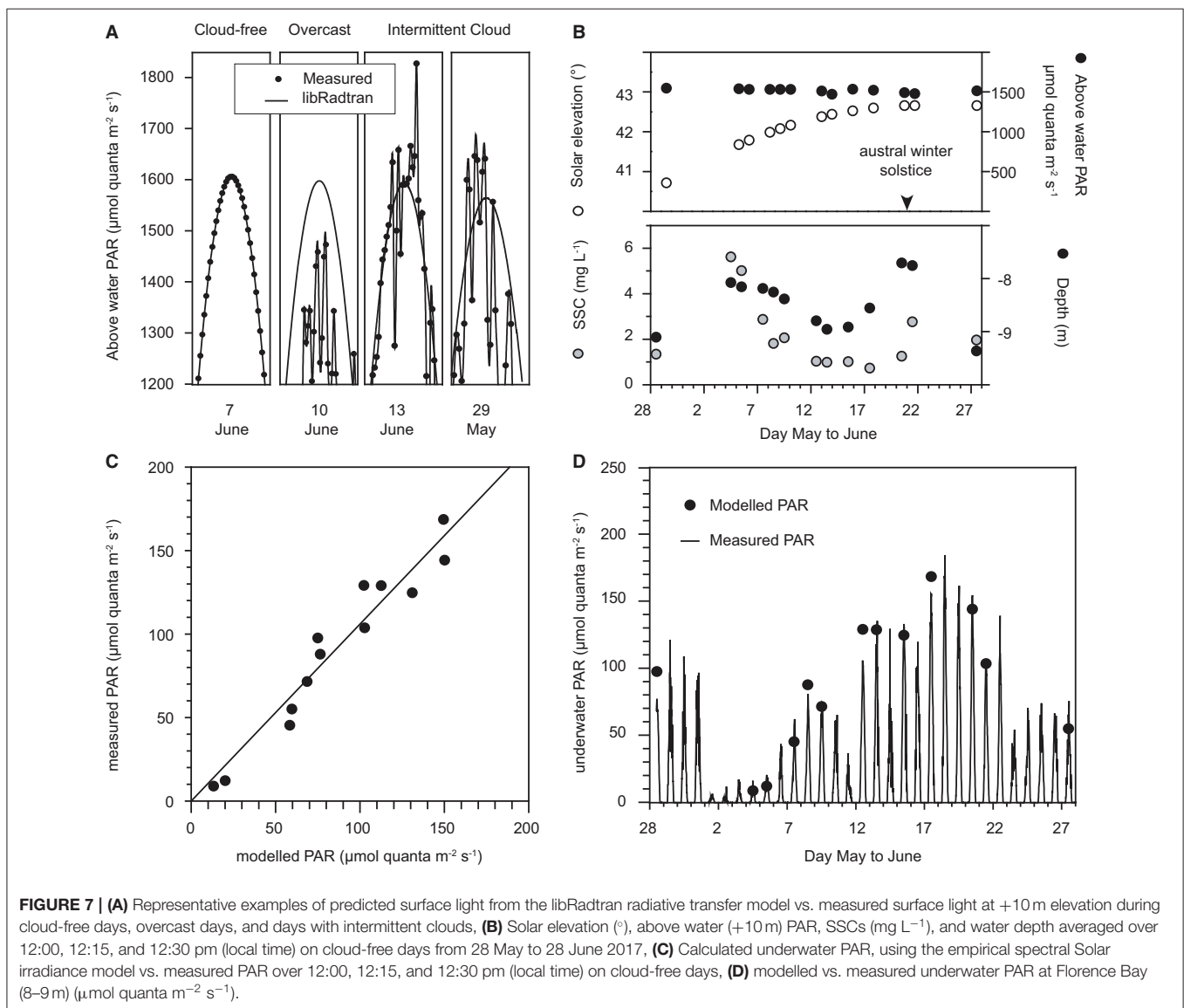
$$NTU = A [TSS] + B \quad (5)$$

Where  $A = 0.702466$  and  $B = 0.898$ .

The final model output is determined by substituting Equation 2, 3, and 4 into the Beer-Lambert law:

$$E_d(z, \lambda, \theta_z) = T [C_0(\lambda) + C_1(\lambda) \theta_z + C_2(\lambda) \theta_z^2 + C_3(\lambda) \theta_z^3] \cos(\theta_z) e^{-[K_M(\lambda)[A(TSS)+B] + K_C(\lambda)]z} \quad (6)$$

The predictive ability of the empirical spectral solar irradiance model developed from the vertical profiling with the hyper-spectral radiometer was assessed against the underwater light measurements collected using the *in situ* multi-spectral radiometer data on the reef at Florence Bay (**Figure 3**). The assessment was made using an average of measurements at 12:00, 12:15, 12:30 pm, which bracketed the solar culmination of 12:10–12:15 pm over the deployment period. The model is based on clear sky irradiance measurements (Slivkoff, 2014) and the multi-spectral radiometer deployment included many days of clear-sky, cloudy and partially cloudy conditions (**Figure 3**), representative examples of which are shown in **Figure 7A** together with predicted surface light from the libRadtran radiative transfer model (Emde et al., 2016). Under a cloud-free (clear-sky) condition the measured surface light levels aligned exactly to the predicted irradiance but was less during a cloudy day (**Figure 7A**). During a partially cloudy day, surface



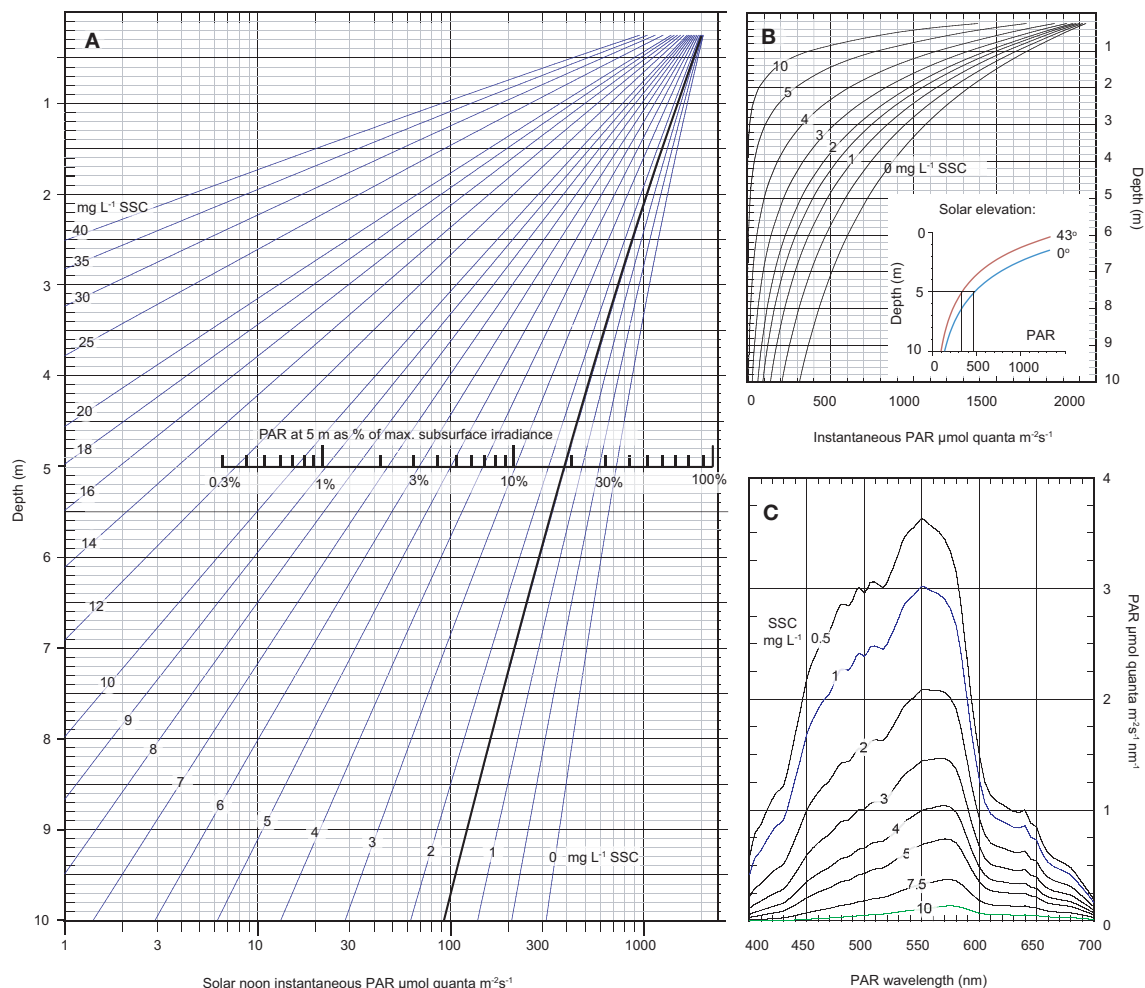


levels were both below and above the light level computed by libRadtran. The higher computed values are *overirradiance* associated with cloud albedo (see Discussion). Only days when the average measured noon-time irradiance was within 3% of the predicted values were used for the model assessment and a total of 14 days met this criterion. The other model inputs included the solar elevation angle (degrees from vertical, from Geoscience Australia: National Mapping Division), SSC ( $\text{mg L}^{-1}$ , converted from turbidity readings using a multiplier of 1.25) and measured water depth (m) which were also averaged over the noon period.

Of the 14 days the surface noon-time irradiance was  $\sim 1,500 \mu\text{mol quanta m}^{-2} \text{s}^{-1}$  (**Figure 7B**) decreasing slightly with increasing solar elevation (from vertical) to the solstice on 21 June (**Figure 7B**). Water depth varied over 1.5 m

(**Figure 7B**) and SSCs varied over an order of magnitude from  $<1$  to  $6 \text{ mg L}^{-1}$  (**Figure 7B**). Underwater light levels varied over an order of magnitude from  $13\text{--}150 \mu\text{mol quanta m}^{-2} \text{s}^{-1}$  (**Figure 7D**). Modelled underwater PAR levels correlated very well with the measured values ( $R^2$  0.90, **Figures 7C,D**).

The empirical spectral solar irradiance model was then used to develop an optical nomograph to graphically represent the underwater PAR levels at depths of 0.5–10 m and at SSC concentrations ranging from 0.5 up to  $40 \text{ mg L}^{-1}$  on a log scale (**Figure 8A**) and linear scale (**Figure 8B**). The solar elevation angle for the analysis was  $0^\circ$  from vertical (i.e., sun directly overhead) and under cloud-free conditions the PAR levels at the depth represent the maximum theoretical instantaneous light levels for



**FIGURE 8 |** Modelled data based on the empirical spectral solar irradiance model derived from the plume profiling exercise showing (A) an optical nomograph of maximum instantaneous PAR (400–700 nm) in  $\mu\text{mol quanta m}^{-2} \text{s}^{-1}$  (x-axis, log scale) and as a % of maximum subsurface irradiance, from 0.25–10 m water depth (y-axis) under a range of SSCs from 0–40  $\text{mg L}^{-1}$  and a solar elevation angle of  $0^\circ$  from vertical (i.e., sun directly overhead), and a cloud-free day, (B) the same data as (A) but without a log scale with the inset figure showing modelled underwater light levels at 1.5  $\text{mg L}^{-1}$  but under a solar elevation of 0 or  $43^\circ$  from vertical (see text), (C) modelled spectral profiles in  $\mu\text{mol quanta m}^{-2} \text{s}^{-1} \text{ nm}$  at 5 m depth under a range of SSCs from 0.5–10  $\text{mg L}^{-1}$  at a solar elevation angle of  $0^\circ$  from vertical and a cloud-free day.

the nominated SSC level (empirically tied to the Florence Bay reef).

At 5 m depth, which is close to the maximum depth distribution of the majority of corals at Magnetic Island and local reefs (Morgan et al., 2016; Ceccarelli et al., 2020), an SSC of 1.5 mg L<sup>-1</sup>, which is the median background SSCs at the study site (Waterhouse et al., 2021), resulted in a maximum instantaneous light levels of 393  $\mu\text{mol quanta m}^{-2} \text{s}^{-1}$  (Figure 8A). At 10 m depth the maximum PAR level was 92  $\mu\text{mol quanta m}^{-2} \text{s}^{-1}$  (Figure 8A).

Considering the effect of SSCs, at 1.5 mg L<sup>-1</sup> maximum instantaneous PAR levels decreased from 393  $\mu\text{mol quanta m}^{-2} \text{s}^{-1}$  to 16  $\mu\text{mol quanta m}^{-2} \text{s}^{-1}$  at 10 mg L<sup>-1</sup> (Figure 8A). The change in the spectral profiles and preferential loss of blue resulting from change in SSCs is shown as a shift of peak irradiance from 550 nm to 575 nm (Figure 8C) (see Figure 4D for empirical measurements of the spectral profile at 1 mg L<sup>-1</sup> at 5 m depth).

Considering the effect of solar elevation, PAR levels at solar noon decreased 30% from 393  $\mu\text{mol quanta m}^{-2} \text{s}^{-1}$  at 0° (the maximum elevation at solar noon in the summer time) to 274  $\mu\text{mol quanta m}^{-2} \text{s}^{-1}$  at 43° (the lowest elevation at solar noon and occurs in the winter time) (inset graph in Figure 8B).

## Light Exposure Experiments

The solar model was used to generate four light scenarios (S) including 6 mol quanta m<sup>2</sup> d<sup>-1</sup> and 1 mol quanta m<sup>2</sup> d<sup>-1</sup> PAR under either a broad spectrum peaking in the blue wavelengths (S1 and S2 in Figure 9A) or under a 'green-yellow-shifted' spectrum (S3 and S4 in Figure 9B). These spectra were then recreated in the aquarium and corals held for 28-d under the 4 different scenarios under a 12 h L:D cycle of ascending and decreasing light level. The scenarios are shown as maximum (noon) instantaneous light and daily light integrals as PAR and also as PUR calculated using equation 1 in Figures 9A,B.

No mortality or partial mortality was observed in *P. verrucosa* over the experiment. Significant treatment effects were identified for growth rate and symbiont density (AICc  $\omega_i$  value of 1 and 0.95, respectively (Table 1) with decreases in the lower light scenarios (S2 and S4) compared to the higher light treatments (S1 and S3). While the higher quantity of light clearly benefited growth, corals exposed to the high light, shifted spectrum scenario (S3) did not grow as much as those in the high light, normal spectra scenario (S1) and had reduced symbiont densities at the end of the exposure period (Figure 9).

Total Chl a concentrations were lowest in the low light treatments (S2 and S4), but also lower in the high light, shifted spectrum (S3) treatment (Figure 9). Conversely, the concentrations of Chl a per cell were highest at the two low light treatments (S2 and S4); however, no significant treatment effect was identified (AICc  $\omega_i$  value 0.077, Table 1).

A significant variation in both the amount of total lipids and the ratio of storage to structural lipids was observed between the four light scenarios (Figure 9) although there was more evidence for a treatment effect with lipid ratios (AICc  $\omega_i$  value of 0.877 vs. 0.667, respectively). Interestingly, both lipid variables showed similar patterns between light treatments and were most

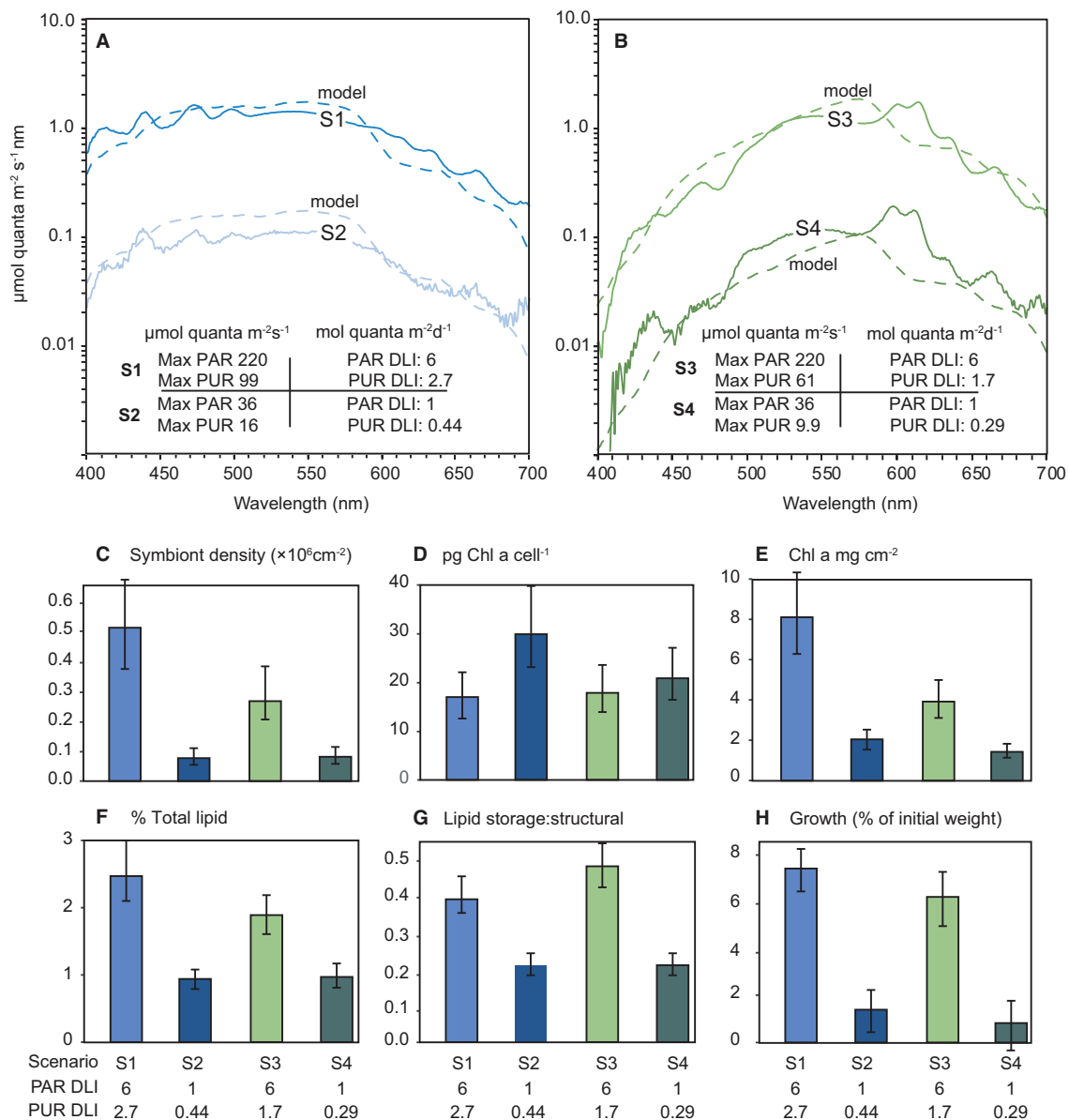
impacted by the low light (S2 and S4) treatments with up to 2-fold decreases observed.

## DISCUSSION AND CONCLUSIONS

Fine sediments in the water column scatter and absorb light reducing light availability for benthic photoautotrophs. The elevated water turbidity (cloudiness) from enhanced sediment runoff from the land is considered a threat to coastal coral reefs and seagrass ecosystem (ISRS, 2004; GBRMPA, 2019, 2020). Despite concerns in the inshore turbid-zone reefs of the inner Great Barrier Reef dating back to the 1980s (Brodie et al., 2012), very few direct measurements of benthic light have been made there (but see Luter et al., 2021). In this study, spectral changes and preferential loss of more photosynthetically useful blue light was identified in the turbid plumes produced by a dredge, supporting earlier observations of Jones et al. (2016). The same changes were also identified during the natural wind-wave induced turbidity event using *in situ* multi-spectral sensor. In the turbid-zone coral reefs communities of the inner GBR sediment resuspension events are frequent (Larcombe et al., 1995, 2001; Orpin et al., 1999; Macdonald et al., 2013; Luter et al., 2021). Light reduction by suspended sediment involving shifts to longer, less photosynthetically useful wavelengths is therefore a common and previously unrecognised occurrence in the inshore turbid-zone reefs.

Light profiling in the blue-water environment outside of the turbid bay near the 20 m isobath showed the well-known depth related attenuation of red light resulting in a spectra peaking at 475 nm wavelength (Smith and Baker, 1981; Kirk, 2010). Inside the bay, profiles beside the reef showed similar attenuation of red light with depth but also attenuation of the shorter (blue) wavelengths with increasing depth. Light profiling through the sediment plumes caused by the dredging showed much more pronounced attenuation of the blue wavelengths proportional to suspended sediment concentration. The net effect of the attenuation at both ends of the PAR spectrum was to monochromate the light with increasing depth, shifting the peak in the underwater spectrum 100 nm to the green-yellow waveband peaking at >575 nm. The shift is a well-known characteristic of turbid water (Van Duin et al., 2001; Mobley et al., 2004; Sundarabalan et al., 2016) and the loss of blue light is significant for corals as green-yellow light is poorly absorbed and hence less useful for photosynthesis (Morel, 1978, 1991). The implications are that sediment resuspension events in the inner GBR can result in a loss of light quantity and quality.

The preferential absorption of red light by pure seawater is well-known (Smith and Baker, 1981), as is the preferential absorption of the blue region which is usually attributed to humic-like and protein-like fluorophores of DOM (i.e., CDOM) produced by the decomposition of plant and animal matter (Bricaud et al., 1981; Jaffé et al., 2008; Hansell and Carlson, 2014; Jerlov, 2014). Known CDOM sources into Cleveland Bay include freshwater input from the many tributaries and creeks entering the bay (Blondeau-Patissier et al., 2009). CDOM sources also include autochthonous production from aquatic primary



**FIGURE 9 | (A,B)** Modelled (dashed lines) and measured (solid lines) irradiance ( $\mu\text{mol quanta m}^{-2}\text{s}^{-1}\text{nm}^{-1}$ ) profiles during the 28-d laboratory experiment with the coral *Pocillopora verrucosa*. The spectral profiles mimic light quantity and spectral quality at 5 m depth (cloud-free days) and a zenith angle of  $19^\circ$  (at solar noon) derived from empirical solar irradiance model and correspond to light levels expected under SSCs of 0.5 and  $10\text{ mg L}^{-1}$ . Numbers in the figures represent the four light treatments used expressed as maximum (12 noon) PAR or PUR as  $\mu\text{mol quanta m}^{-2}\text{s}^{-1}$ , and daily light integral ( $\text{mol quanta m}^{-2}$ ) from the sinusoidal ramping up and down over the 12 h light cycle, **(C–H)** Mean and 95% confidence intervals for each response variable over the 4 light treatments.

producers such as reefs and seagrass beds (Carder et al., 1989; Hansell et al., 2002; Otis et al., 2004), and groundwater and porewater exchange (Webb et al., 2019). Mineral particles are more efficient in scattering light compared with other particulates such as phytoplankton because of their higher refractive indices (Bowers and Binding, 2006). One interpretation of the blue light attenuation signal with elevated SSCs, is that light scattering by mineral NAPs greatly increased the photon pathlength through the water column increasing the probability of absorption of blue

light by CDOM (Kirk, 1976, 1985). Binding et al. (2008) have also suggested that the UV–blue absorption signatures could be due to electrochemical adsorption of CDOM onto the mineral surfaces (Wozniak and Dera, 2007).

A different explanation is that the UV–blue light absorption is related to the detrital material and/or to the sediments themselves and the elemental content of the mineral NAP. Babin et al. (2003b) and Babin and Stramski (2004) examined absorption characteristics of different particles of different mineralogical

**TABLE 1** | Relative model weights for *P. verrucosa* examining effects of 28 days of varied light scenario (S1–S4).

	Symbiont density				Pigments per cell				Pigments per cm <sup>2</sup>			
Tr	0.951				0.077				0.988			
Null	0.049				0.923				0.012			
	Total lipids				Lipid ratio				Buoyant Weight			
Tr	0.667				0.877				1			
Null	0.333				0.123				0			
	Symbiont density				Pigments per cell				Pigment per cm <sup>2</sup>			
	S1	S2	S3	S4	S1	S2	S3	S4	S1	S2	S3	S4
S1	1	0	0	0	1	0	0.39	0.15	1	0	0	0
S2	0	1	0	0.28	0	1	0	0.03	0	1	0	0.04
S3	0	0	1	0	0.39	0	1	0.23	0	0	1	0
S4	0	0.28	0	1	0.15	0.03	0.23	1	0	0.04	0	1
	Total lipids				Lipid ratio				Buoyant weight			
	S1	S2	S3	S4	S1	S2	S3	S4	S1	S2	S3	S4
S1	1	0	0	0.01	1	0	0	0	1	0	0.02	0
S2	0	1	0	0.46	0	1	0	0.39	0	1	0	0.21
S3	0	0	1	0.01	0	0	1	0	0.02	0	1	0
S4	0.01	0.46	0.01	1	0	0.39	0	1	0	0.21	0	1

Model weights are based on AICc comparison between a model with the DLI treatment effect (DLI) and an intercept only "Null" model (Null). Post hoc comparisons were carried out using Bayesian posterior probability contrasts (calculated as the percentage overlap of posterior probabilities densities) between light scenario treatment pairs separately for each response variable.

and elemental composition. Absorption in the visible region was undetectable in pure samples, but blue-green absorption was much higher in sediments with a significant iron content (Babin and Stramski, 2004). The spectral signatures of coastal NAP samples are similar to the absorption spectra of iron oxides or hydroxides (Karickhoff and Bailey, 1973; Sherman and Waite, 1985). It was suggested that Fe<sup>3+</sup> and Fe<sup>2+</sup> cations on the particle surface or within the mineral lattice were responsible (Karickhoff and Bailey, 1973; Babin and Stramski, 2004; Stramski et al., 2007). Light absorption itself resulted from transfer of an electron from oxygen to iron, between iron and an adjacent cation or transfer to a higher energy orbital within the same iron atom (Babin and Stramski, 2004). The interpretation of iron oxide and hydroxide as the inorganic chromophorous agent of mineral NAPs was also supported by the study of Estapa et al. (2012) of mass-specific light absorption by particulate matter from the terrestrially influenced coast of Louisiana (US).

This explanation is consistent with known mineral distribution in sediments on the GBR. The inshore central regions are significantly influenced by terrigenous run off (Hopley et al., 2007), receiving siliciclastic and aluminosilicate clay and silts such as kaolinite, smectite and illite, and silicate sand from point-source fluvial inputs (Belperio, 1983; Belperio and Searle, 1988; Mathews et al., 2007). Al<sub>2</sub>O<sub>3</sub> and Fe<sub>2</sub>O<sub>3</sub> are the major constituents of such terrestrially-derived aluminosilicates or oxyhydroxides (Calvert and Pedersen, 1993) and often used as an indicator of terrigenously-derived sediments on the

GBR (Johns et al., 1994). Cleveland Bay is infilled with fluvial sediments from the Ross and Burdekin rivers (Carter et al., 1993) and total Fe content is high: 0.8–3.3% (Coomans and Brunskill, 2000), 0.8–4.8 % (Reichelt and Jones, 1994) and up to 4–5% (Duckworth et al., 2017), consistent with other measurements of iron in inner GBR sediments (Alongi et al., 1993; Johns et al., 1994). The iron content of these sediments are orders of magnitude higher than the carbonate dominated biogenous mineral particles of the mid and outer shelf reefs (Passlow et al., 2005; Mathews et al., 2007; Duckworth et al., 2017).

The significance of the spectral changes under elevated SSCs is they shift the irradiance from photosynthetically useful to less useful wavelengths. In corals the symbiotic dinoflagellates (family Symbiodiniaceae, Lajeunesse et al., 2018) have two major light harvesting complexes, the water soluble peridinin-chlorophyll a-protein (PCP) complex and the membrane bound chl a chl c<sub>2</sub>-peridinin-protein complex (acpPC) (Prézelin and Haxo, 1976; Song et al., 1976; Iglesias-Prieto et al., 1991, 1993). The absorption peaks for the coral symbionts are in the blue (440–480 nm range) due to chlorophyll a, chlorophyll c<sub>2</sub> and carotenoids, and at 662 nm due to chlorophyll a (Halldal, 1968; Prézelin et al., 1976; Dustan, 1982; Kuhl et al., 1995; Levy et al., 2003; Hennige et al., 2009; Niedzwiedzki et al., 2014; Szabó et al., 2014; Wangpraseurt et al., 2014c). The absorption spectrum of *Symbiodinium* PCP is a broad band between 400–550 nm (Iglesias-Prieto et al., 1991; Iglesias-Prieto and Trench, 1994; Niedzwiedzki et al., 2014). PCP therefore extends the absorption



profile into the blue green (see further below) but the absorption at 550–600 nm is still comparatively weak and this coincides with the peak wavelength of light transmission under elevated SSCs (see **Figure 5A**).

Morel (1978) first suggested weighting PAR according to usability in photosynthesis introducing the term photosynthetically usable radiation (PUR). The weighting is based on a photosynthetic action spectrum. Action and absorption spectra have been derived for *Symbiodiniaceae* from isolated and intact corals (Halldal, 1968; Scott and Jitts, 1977; Dustan, 1982; Schlichter and Fricke, 1991; Kuhl et al., 1995; Hennige et al., 2009; Wangpraseurt et al., 2014c). Action and absorption spectra are usually quite similar (Kirk, 2010) and in this study PUR calculations were based on the absorption spectra of isolated algal symbionts from *in vivo* cultures of multiple different *Symbiodiniaceae* clades (described in Hennige et al., 2009). The data indicates elevated SSCs can result in as much as 25% decrease in the PUR:PAR as the result of the shift away from the main algal symbiont absorption bands. Functionally similar to the PUR:PAR ratio is the simpler blue to green ratio (B/G,  $\lambda_{455:555\text{ nm}}$ ) ratio used in this study. The decrease in underwater light levels caused by elevated SSCs was accompanied by a decrease in the ratio during the week-long turbidity event (**Figure 3E**), returning to background levels as the event decayed. In contrast, decreases in underwater light levels caused by clouds (without elevated SSCs) had no spectral effects indicating clouds tend to act more like neutral density filters (Morel, 1991). The implications are that periods of light reduction by turbidity vs. reduction by clouds can be readily identified by the spectral profile and blue green ratio at a site and depth. Such a diagnostic would be useful for contextualising and further understanding the risk of enhanced sediment run-off to the inshore turbid water communities and alleviate the need for a nearby dedicated above water PAR sensor to identify light reduction by clouds.

The empirical, spectral solar irradiance model developed from the wavelength specific light attenuation (constructed from the hyperspectral plume profiling study, **Figure 5**) accurately predicted benthic PAR measured with the multi-spectral sensor on the reef, using only information on suspended sediment concentration, depth and solar elevation angle (**Figures 7C,D**). Where improved model accuracy is required, the work of Gregg and Carder (1990) or other radiative transfer models such as MODTRAN (Berk et al., 1989) is recommended. The transmittance factor 0.965 (Morel and Antoine, 1994; Morel and Maritorena, 2001) used to correct for loss by reflection at the sea surface is wavelength independent. Although less suitable for low solar elevations and windy conditions as the transmission becomes more dependent on surface roughness (Austin, 1974; Preisendorfer and Mobley, 1986), the testing of modelled vs. measured data was conducted under clear skies and low wind and low zenith angles around solar noon. The measured surface light levels over the testing period aligned to the predicted surface irradiance from libRadtran for cloud free days; however, during partially cloudy noon periods surface levels were both below and above the predicted surface values. The lower values are intuitive and associated with clouds obscuring the path of

the solar beam but the higher than predicted values are less so. We suggest these are examples of cloud enhancement (CE) or overirradiance or irradiance enhancement (Robinson, 1966; Nack and Green, 1974; Pfister et al., 2003; Gueymard, 2017). These cloud enhancement periods are associated with scattering from sides of clouds and strong forward Mie scattering within clouds of low optical depth (Yordanov et al., 2013; Pecenek et al., 2016; Gueymard, 2017). The enhancement periods of elevated light can last for seconds to several minutes and involve up to a 30–60% increases in light (Yordanov et al., 2013, 2015; Almeida et al., 2014). The consequences of these short periods of overirradiance on coral physiology have not been explored. Cloud enhancement at seasonally high light levels could give rise to very high absolute light levels, which in combination with elevated seawater temperatures could result in or at least exacerbate coral bleaching in the photoinhibition model of bleaching (Jones et al., 1998; Hoegh-Guldberg, 1999; Jones and Hoegh-Guldberg, 2001). Interestingly, irrespective of CE effects, cloud seeding and cloud brightening to reduce light levels is currently being tested on the GBR as a local geoengineering solution to decrease solar heating and lower water temperatures to prevent bleaching (McDonald et al., 2019).

Given the success of the empirical, spectral solar irradiance model, the optical nomographs in **Figure 8** was produced to graphically display the light levels corals experience in the turbid-zone reefs of the GBR under a range of SSCs, solar elevation and depth conditions. The reefs around Magnetic Island and at Paluma Shoals (a nearshore turbid-zone reef complex 20 km west of Magnetic Island, **Figure 1** inset) are known to have highly compressed depth distributions (Browne et al., 2010, 2012; Morgan et al., 2016; Ceccarelli et al., 2020) showing virtual loss of branching, tabular and corymbose corals by ~5 m depth. Beyond this depth the corals become sparse and by 7 m are largely limited to isolated foliaceous, encrusting and massive growth forms (typically *Turbinaria* and *Montipora* spp) (Morgan et al., 2016). Using a scenario where the sun is directly overhead i.e., solar culmination and an angle of 0° from vertical, and under an ambient background SSC of 1.5 mg L<sup>-1</sup> (Waterhouse et al., 2021) the maximum instantaneous noon-time PAR at 5 m depth is ~393  $\mu\text{mol quanta m}^{-2} \text{ s}^{-1}$ , or ~18% of light just under the water surface (estimated as 2,200  $\mu\text{mol quanta m}^{-2} \text{ s}^{-1}$ ). At 7 m depth, which is effectively the lower limits for coral presence, the light was 10% of the maximum instantaneous noon-time. This light requirement of the corals in the inshore turbid reef zone communities is the same or slightly higher than minimum light requirement for seagrasses (Duarte, 1991; Dennison et al., 1993; Kenworthy and Fonseca, 1996) which are known to have high light requirements compared to many phytoplankton and macroalgae (1–5% incident light) (Lee et al., 2007a).

The pocilloporid coral *Pocillopora verrucosa* was exposed for 28-d to a 6 or 1 mol quanta m<sup>2</sup> d<sup>-1</sup> light scenario (DLI), each under either a broad spectrum peaking in the blue wavelengths or green-yellow shifted spectrum, mimicking the effect of a 0.5 mg L<sup>-1</sup> or 10 mg L<sup>-1</sup> SSC at a depth of 5 m (from the spectral solar irradiance model). A pocilloporid was chosen for the experiment as they regarded as light sensitive (Ziegler et al., 2014; Poquita-Du et al., 2019) and primarily phototrophic and with nutritional

needs mostly met by photosynthesis (Wellington, 1982). They are one of the families common in high numbers in clear water on the Great Barrier Reef but restricted to less than a 2 m depth in more turbid settings (Thompson et al., 2018). In laboratory experiments Pocilloporids are sensitive to light reduction, losing their algal symbionts and discolouring or bleaching during low light periods (Bessell-Browne et al., 2017b; Jones et al., 2020; Luter et al., 2021). A DLI of 6 mol quanta  $\text{m}^{-2}$  of PAR under a green-yellow shifted spectrum, resulted in a striking 50% loss of algal symbionts compared to the same PAR light level under the broad spectrum. Although PAR levels were the same between treatments (6 mol quanta  $\text{m}^{-2} \text{d}^{-1}$ ), the PUR levels were 40% lower in the green-yellow light scenario. The low light scenario with a broad light spectrum resulted in an increase in the chlorophyll a concentration of the symbionts indicative of photoacclimation, but nevertheless significant decreases in algal symbiont density to <15% of the higher light broad spectrum occurred. Growth, total lipids and the ratio of storage to structural lipids were also much lower. The lower light green spectrum scenario showed similar losses of the algal symbionts although the photoacclimatory increase in Chl a per algal cell in the low light broad spectrum was not observed and Chl a per  $\text{cm}^2$  was significantly different between the two low light treatments.

Similar changes in response to reduced quantity of light from turbidity have been described previously for a range of coral species (Bessell-Browne et al., 2017a,b; Jones et al., 2020; Luter et al., 2021) and the cue for the dissociation of the symbiosis was suggested to be a reduction in translocation of algal-derived photosynthate to the host. The response to the modified quality of light from turbidity has not been described before and emphasises the need to justify and describe the spectrum of artificial light sources used in future laboratory based studies of coral physiology (see also Wangpraseurt et al., 2014c; Luter et al., 2021). These results are preliminary as they are limited to a single species but nevertheless the 50% loss of algal symbionts by the spectral modification and shift from a broad spectrum to greenish light was a strong response. Although the absolute level of light is important, the spectral changes to less photosynthetically useful wavelengths under elevated turbidity also reduces the availability of PAR.

The spectral changes under elevated turbidity are potentially also significant with respect to coral bleaching and the climate change refugia hypothesis of turbid nearshore reefs (Van Woesik et al., 2012). The preliminary experiments of Fitt and Warner (1995) showed that high energy blue light promotes bleaching in cultured algal symbionts. It follows that the preferential attenuation of higher energy blue light by turbidity and elevated SSCs may also ameliorate the physiological stress to the symbiosis associated with light during a marine heatwave (Sully and Van Woesik, 2020 and references therein). For both an underabundance and overabundance of light in turbid water coral communities, both spectral changes as well as total light availability needs to be considered.

The corals dinoflagellate symbionts (family Symbiodiniaceae) containing peridinin as an accessory pigment (Iglesias-Prieto et al., 1991, 1993) which harvests green wavelengths (470–550 nm) where chlorophyll absorbs very poorly (Polívka et al.,

2007). Because of the very high efficiency of Per-Chl-a excitation energy transfer (Song et al., 1976; Carbonera et al., 2014) green wavelengths can still be used for photochemistry albeit much less effectively. This theoretically should lessen the impacts of the spectral changes although clearly not sufficiently enough in the experiment. Further studies of the effects of spectral shifts to yellow-green wavelengths and the use of PUR are recommended, but also need to consider the very different light climate in the intact symbiosis (*in symbio*) which are known to be substantially different from the ambient incident underwater irradiance regime. Light levels in the tissue can be enhanced from multiple scattering of photons and diffuse back scattering by the aragonite skeleton (Kuhl et al., 1995; Enriquez et al., 2005; Brodersen et al., 2014). Host pigments can also scatter, reflect and absorb and remit light (Schlichter et al., 1986; Salih et al., 2000; Dove et al., 2001; Gilmore et al., 2003; D'Angelo et al., 2008; Smith et al., 2017) and so the optical properties of the host tissue strongly effects light use efficiency with rapid attenuation and spectrally dependent changes (Kuhl et al., 1995; Wangpraseurt et al., 2012, 2014a,b; Szabó et al., 2014; Lichtenberg et al., 2016).

The inner GBR turbid zone reef communities routinely experience natural wind and wave induced resuspension events and hence periods of reduced light levels and, as shown in this study, changes in the underwater light spectrum. The potential threat to these reefs by enhanced sediment run off from the land is well-recognised and changes in light availability to benthic photoautotrophs one of the primary cause effect pathways (GBRMPA, 2019, 2020). However, surprisingly few *in situ* irradiance intensity measurements have ever been made there (Luter et al., 2021). This seems an omission and the technology is now available to transition to affordable and calibratable *in situ* multi-spectral light measurements and define the light environment in absolute terms of irradiance intensity—for example DLIs over different periods of time and at different depths (Luter et al., 2021). As shown in the present study, multi-spectral sensors can also allow the partitioning of light reduction by clouds and sediment resuspension providing additional information for a risk assessment of enhanced sediment runoff.

In addition to absorption by CDOM and chlorophyll, the preferential absorption of blue light by NAPS (detrital and mineral) is another potential cause of the green hue of naturally turbid coastal reefs as seen underwater. Similarly, as seen from above, Bowers and Binding (2006) noted moderately turbid seas look green, an effect which is often attributed to algal blooms but could also be attributed to the blue light absorption of low levels of NAPs coupled to red light absorption of water (Claustre et al., 2002). Such an effect may also contribute to the green colouration of river plumes once entering the coastal GBR as seen from ocean colour satellites (Devlin et al., 2012, 2015; Petus et al., 2018).

## DATA AVAILABILITY STATEMENT

The raw data supporting the conclusions of this article will be made available by the authors, without undue reservation.

## AUTHOR CONTRIBUTIONS

RJ: conception and wrote the first draft. M-CP, HL, RF, and RJ: experimental design. M-CP and HL: conducting the experiments. M-CP, HL, RF, RJ, WK, and MS: data processing and analysis and contributed to writing, reviewing, and editing. RF and HL: statistical analyses. DF: lipid analysis. All authors approved the manuscript for submission.

## FUNDING

This project was funded by the Australian Government's National Environmental Science Programme (NESP Project 2.1.9) to RJ and RF, co-investment by the Australian Institute of Marine

Science, In Situ Marine Optics and the Port of Townsville Limited (POTL).

## ACKNOWLEDGMENTS

We thank the Port of Townsville Limited (POTL) for provision of a boat and crew for the field work and permitting close access to the dredge for sampling; Matt Salmon, Craig Humphrey, Andrea Severati, Paul Boyd, and Eduardo Arias for design of the lighting systems; Manuel Nunez for the libRadtran calculations and QA/QC of the surface light measurements; and Leslie Clements for her help with pigment analyses.

## REFERENCES

- AIMS (2020). *Australian Institute of Marine Science. Northern Australia Automated Marine Weather and Oceanographic Stations, Sites: (Cleveland Bay), Parameters: (Light)*. doi: 10.25845/5c09bf93f315d
- Almeida, M. P., Zilles, R., and Lorenzo, E. (2014). Extreme overirradiance events in São Paulo, Brazil. *Solar Energy* 110, 168–173. doi: 10.1016/j.solener.2014.09.012
- Alongi, D. M., Tirendi, F., and Christoffersen, P. (1993). Sedimentary profiles and sediment-water solute exchange of iron and manganese in reef- and river-dominated shelf regions of the Coral Sea. *Cont. Shelf Res.* 13, 287–305. doi: 10.1016/0278-4343(93)90111-A
- Anthony, K., Ridd, P., Orpin, A., Larcombe, P., and Lough, J. (2004). Temporal variation of light availability in coastal benthic habitats: effects of clouds, turbidity, and tides. *Limnol. Oceanogr.* 49, 2201–2211. doi: 10.4319/lo.2004.49.6.2201
- Antoine, D., Schroeder, T., Slivkoff, M., Klonowski, W., Doblin, W., Lovell, J., et al. (2017). *The IMOS Radiometry Task Team. Final Report*. Hobart, TAS: Integrated Marine Observing System (IMOS). Available online at: <http://imos.org.au/facilities/task-teams/radiometry/>
- Austin, R. (1974). "The remote sensing of spectral radiance from below the ocean surface," in *Optical Aspects of Oceanography*, eds N. G. Jerlov and E. S. Nielsen (San Diego, CA: Academic), 317–344.
- Babin, M., Morel, A., Fournier-Sicre, V., Fell, F., and Stramski, D. (2003a). Light scattering properties of marine particles in coastal and open ocean waters as related to the particle mass concentration. *Limnol. Oceanogr.* 48, 843–859. doi: 10.4319/lo.2003.48.2.0843
- Babin, M., and Stramski, D. (2002). Light absorption by aquatic particles in the near-infrared spectral region. *Limnol. Oceanogr.* 47, 911–915. doi: 10.4319/lo.2002.47.3.0911
- Babin, M., and Stramski, D. (2004). Variations in the mass-specific absorption coefficient of mineral particles suspended in water. *Limnol. Oceanogr.* 49, 756–767. doi: 10.4319/lo.2004.49.3.0756
- Babin, M., Stramski, D., Ferrari, G. M., Claustre, H., Bricaud, A., Obolensky, G., et al. (2003b). Variations in the light absorption coefficients of phytoplankton, nonalgal particles, and dissolved organic matter in coastal waters around Europe. *J. Geophys. Res. Oceans* 108:882. doi: 10.1029/2001JC000882
- Bainbridge, Z., Wolanski, E., Alvarez-Romero, J., Lewis, S., and Brodie, J. (2012). Fine sediment and nutrient dynamics related to particle size and floc formation in a Burdekin River flood plume, Australia. *Mar. Pollut. Bull.* 65, 236–248. doi: 10.1016/j.marpolbul.2012.01.043
- Bates, D., Mächler, M., Bolker, B., and Walker, S. (2015). Fitting linear mixed-effects models using lme4. 67:48. doi: 10.18637/jss.v067.i01
- Belperio, A. (1983). Terrigenous sedimentation in the central Great Barrier Reef lagoon: a model from the Burdekin region. *BMR J. Austr. Geol. Geophys.* 8, 179–190.
- Belperio, A., and Searle, D. (1988). "Terrigenous and carbonate sedimentation in the Great Barrier Reef province," in *Carbonate -Clastic Transitions. Developments in Sedimentology*, eds L. J. Doyle and H. H. Roberts (Amsterdam: Elsevier), 42, 143–174.
- Berk, A., Bernstein, L., and Robertson, D. (1989). *MODTRAN: A Moderate Resolution Model for LOWTRAN7*. GL-TR-89-0122, Air Force Geophysics Lab, Hanscom AFB.
- Bessell-Browne, P., Negri, A. P., Fisher, R., Clode, P. L., Duckworth, A., and Jones, R. (2017a). Impacts of turbidity on corals: the relative importance of light limitation and suspended sediments. *Mar. Pollut. Bull.* 117, 161–170. doi: 10.1016/j.marpolbul.2017.01.050
- Bessell-Browne, P., Negri, A. P., Fisher, R., Clode, P. L., and Jones, R. (2017b). Impacts of light limitation on corals and crustose coralline algae. *Sci. Rep.* 7:11553. doi: 10.1038/s41598-017-11783-z
- Binding, C. E., Jerome, J. H., Bukata, R. P., and Booty, W. G. (2008). Spectral absorption properties of dissolved and particulate matter in Lake Erie. *Remote Sens. Environ.* 112, 1702–1711. doi: 10.1016/j.rse.2007.08.017
- Blondeau-Patissier, D., Brando, V. E., Oubelkheir, K., Dekker, A. G., Clementson, L. A., and Daniel, P. (2009). Bio-optical variability of the absorption and scattering properties of the Queensland inshore and reef waters, Australia. *J. Geophys. Res. Oceans* 114:C5. doi: 10.1029/2008JC005039
- Bowers, D. G., and Binding, C. E. (2006). The optical properties of mineral suspended particles: a review and synthesis. *Estuar. Coast. Shelf Sci.* 67, 219–230. doi: 10.1016/j.ecss.2005.11.010
- Brandon, R., Dierssen, H., and Hochberg, E. (2019). Water column optical properties of pacific coral reefs across geomorphic zones and in comparison to offshore waters. *Rem. Sens.* 11:1757. doi: 10.3390/rs11151757
- Bricaud, A., Morel, A., and Prieur, L. (1981). Absorption by dissolved organic matter of the sea (yellow substance) in the UV and visible domains. *Limnol. Oceanogr.* 26, 43–53. doi: 10.4319/lo.1981.26.1.0043
- Broderson, K., Lichtenberg, M., Ralph, P., Kühl, M., and Wangpraseurt, D. (2014). Radiative energy budget reveals high photosynthetic efficiency in symbiont-bearing corals. *J. R. Soc. Interface* 11:20130997. doi: 10.1098/rsif.2013.0997
- Brodie, J., Kroon, F., Schaffelke, B., Wolanski, E., Lewis, S., Devlin, M., et al. (2012). Terrestrial pollutant runoff to the Great Barrier Reef: an update of issues, priorities and management responses. *Mar. Pollut. Bull.* 65, 81–100. doi: 10.1016/j.marpolbul.2011.12.012
- Browne, N. K., Smithers, S. G., and Perry, C. T. (2010). Geomorphology and community structure of Middle Reef, central Great Barrier Reef, Australia: an inner-shelf turbid zone reef subject to episodic mortality events. *Coral Reefs* 29, 683–689. doi: 10.1007/s00338-010-0640-3
- Browne, N. K., Smithers, S. G., and Perry, C. T. (2012). Coral reefs of the turbid inner-shelf of the Great Barrier Reef, Australia: an environmental and geomorphic perspective on their occurrence, composition and growth. *Earth Sci. Rev.* 115, 1–20. doi: 10.1016/j.earscirev.2012.06.006
- Browne, N. K., Smithers, S. G., and Perry, C. T. (2013). Spatial and temporal variations in turbidity on two inshore turbid reefs on the Great Barrier Reef, Australia. *Coral Reefs* 32, 195–210. doi: 10.1007/s00338-012-0965-1



- Bull, G. (1982). Scleractinian coral communities of two inshore high island fringing reefs at Magnetic Island, North Queensland. *Mar. Ecol. Progr. Ser. Oldendorf* 7, 267–277. doi: 10.3354/meps007267
- Burnham, K. P., and Anderson, D. R. (2002). *Model Selection and Multimodel Inference: A Practical Information-Theoretic Approach*. New York, NY: Springer.
- Cacciapaglia, C., and Van Woessik, R. (2016). Climate-Change Refugia: shading reef corals by turbidity. *Glob. Change Biol.* 22, 1145–1154. doi: 10.1111/gcb.13166
- Calvert, S. E., and Pedersen, T. F. (1993). Geochemistry of recent oxic and anoxic marine sediments: implications for the geological record. *Mar. Geol.* 113, 67–88. doi: 10.1016/0025-3227(93)90150-T
- Carbonera, D., Di Valentin, M., Spezia, R., and Mezzetti, A. (2014). The unique photophysical properties of the Peridinin-chlorophyll- $\alpha$ -protein. *Curr. Prot. Pept. Sci.* 15, 332–350. doi: 10.2174/1389203715666140327111139
- Carder, K. L., Steward, R. G., Harvey, G. R., and Ortner, P. B. (1989). Marine humic and fulvic acids: their effects on remote sensing of ocean chlorophyll. *Limnol. Oceanogr.* 34, 68–81. doi: 10.4319/lo.1989.34.1.0068
- Carter, R., Johnson, D., and Hooper, K. (1993). Episodic post-glacial sea-level rise and the sedimentary evolution of a tropical continental embayment (Cleveland Bay, Great Barrier Reef shelf, Australia). *Austr. J. Earth Sci.* 40, 229–255. doi: 10.1080/08120099308728077
- Ceccarelli, D. M., Evans, R. D., Logan, M., Mantel, P., Puotinen, M., Petus, C., et al. (2020). Long-term dynamics and drivers of coral and macroalgal cover on inshore reefs of the Great Barrier Reef Marine Park. *Ecol. Appl.* 30:e02008. doi: 10.1002/eap.2008
- Claustre, H., Morel, A., Hooker, S. B., Babin, M., Antoine, D., Oubelkheir, K., et al. (2002). Is desert dust making oligotrophic waters greener? *Geophys. Res. Lett.* 29, 29–101. doi: 10.1029/2001GL014056
- Clementson, L. (2013). “The CSIRO Method,” in *The Fifth SeaWiFS HPLC Analysis Round-Robin Experiment (SeaHARRE-5) NASA Technical Memorandum 2012-217503*, eds S. Hooker, L. Clementson, C. Thomas, L. Schlüter, M. Allerup, J. Ras, et al. Greenbelt, MD: NASA Goddard Space Flight Center.
- Conlan, J. A., Rocker, M. M., and Francis, D. S. (2017). A comparison of two common sample preparation techniques for lipid and fatty acid analysis in three different coral morphotypes reveals quantitative and qualitative differences. *PeerJ* 5:e3645. doi: 10.7717/peerj.3645
- Coomans, D., and Brunskill, G. J. (2000). Modelling natural and enhanced trace metal concentrations in sediments of Cleveland Bay, Australia. *Mar. Freshw. Res.* 51, 739–747. doi: 10.1071/MF98141
- D’Angelo, C., Denzel, A., Vogt, A., Matz, M. V., Oswald, F., Salih, A., et al. (2008). Blue light regulation of host pigment in reef-building corals. *Mar. Ecol. Progr. Ser.* 364, 97–106. doi: 10.3354/meps07588
- Delandmeter, P., Lewis, S., Lambrechts, J., Deleersnijder, E., Legat, V., and Wolanski, E. (2015). The transport and fate of riverine fine sediment exported to a semi-open system. *Estuar. Coast. Shelf Sci.* 167, 336–346. doi: 10.1016/j.ecss.2015.10.011
- Dennison, W. C., Orth, R. J., Moore, K. A., Stevenson, J. C., Carter, V., Kollar, S., et al. (1993). Assessing water quality with submersed aquatic vegetation. *Bioscience* 43, 86–94. doi: 10.2307/1311969
- Devlin, M. J., Mckinna, L. W., Álvarez-Romero, J. G., Petus, C., Abbott, B., Harkness, P., et al. (2012). Mapping the pollutants in surface riverine flood plume waters in the Great Barrier Reef, Australia. *Mar. Pollut. Bull.* 65, 224–235. doi: 10.1016/j.marpolbul.2012.03.001
- Devlin, M. J., Petus, C., Da Silva, E., Tracey, D., Wolff, N. H., Waterhouse, J., et al. (2015). Water quality and river plume monitoring in the great barrier reef: an overview of methods based on ocean colour satellite data. *Rem. Sens.* 7, 12909–12941. doi: 10.3390/rs71012909
- Dove, S. G., Hoegh-Guldberg, O., and Ranganathan, S. (2001). Major colour patterns of reef-building corals are due to a family of GFP-like proteins. *Coral Reefs* 19, 197–204. doi: 10.1007/PL00006956
- Duarte, C. M. (1991). Seagrass depth limits. *Aquat. Bot.* 40, 363–377. doi: 10.1016/0304-3770(91)90081-F
- Duarte, C. M., August, S., Satta, M. P., and Vaque, D. (1998). Partitioning particulate light absorption: a budget for a Mediterranean Bay. *Limnol. Oceanogr.* 43, 236–244. doi: 10.4319/lo.1998.43.2.0236
- Dubinsky, Z., and Falkowski, P. (2011). “Light as a source of information and energy in zooxanthellate corals,” in *Coral Reefs: An Ecosystem in Transition*, eds Z. Dubinsky and N. Stambler (Dordrecht: Springer Netherlands), 107–118.
- Duckworth, A., Giofre, N., and Jones, R. (2017). Coral morphology and sedimentation. *Mar. Pollut. Bull.* 125, 289–300. doi: 10.1016/j.marpolbul.2017.08.036
- Dunne, R., and Brown, B. (1996). Penetration of solar UVB radiation in shallow tropical waters and its potential biological effects on coral reefs; results from the central Indian Ocean and Andaman Sea. *Mar. Ecol. Progr. Ser.* 144, 109–118. doi: 10.3354/meps144109
- Dustan, P. (1982). Depth-dependent photoadaptation by zooxanthellae of the reef coral *Montastrea annularis*. *Mar. Biol.* 68, 253–264. doi: 10.1007/BF00409592
- Edmunds, P. J., Tsounis, G., Boulon, R., and Bramanti, L. (2018). Long-term variation in light intensity on a coral reef. *Coral Reefs* 37, 955–965. doi: 10.1007/s00338-018-1721-y
- Emde, C., Buras-Schnell, R., Kylling, A., Mayer, B., Gasteiger, J., Hamann, U., et al. (2016). The libRadtran software package for radiative transfer calculations (version 2.0.1). *Geosci. Model Dev.* 9, 1647–1672. doi: 10.5194/gmd-9-1647-2016
- Enriquez, S., Méndez, E. R., and Iglesias-Prieto, R. (2005). Multiple scattering on coral skeletons enhances light absorption by symbiotic algae. *Limnol. Oceanogr.* 50, 1025–1032. doi: 10.4319/lo.2005.50.4.1025
- Estapa, M. L., Boss, E., Mayer, L. M., and Roesler, C. S. (2012). Role of iron and organic carbon in mass-specific light absorption by particulate matter from Louisiana coastal waters. *Limnol. Oceanogr.* 57, 97–112. doi: 10.4319/lo.2012.57.1.0097
- Falkowski, P., Jokiel, P., and Kinzie, R. (1990). “Irradiance and corals,” in *Ecosystems of the World*, ed Z. Dubinsky (Amsterdam: Elsevier), 89–107.
- Falkowski, P. G., and Raven, J. A. (2013). *Aquatic Photosynthesis*. Princeton, NJ: Princeton University Press.
- Fearn, P., Dorji, P., Broomhall, M., Chedzey, H., Symonds, G., Mortimer, N., et al. (2019). *Plume Characterisation—Field Studies. Report of Theme 3—Project 3.2.1, Prepared for the Dredging Science Node*. Perth, WA: Western Australian Marine Science Institution. Available online at: <https://www.wamsi.org.au/dredging-science-node/dsn-reports>
- Fisher, R., Bessell-Browne, P., and Jones, R. (2019). Synergistic and antagonistic impacts of suspended sediments and thermal stress on corals. *Nat. Commun.* 10:2346. doi: 10.1038/s41467-019-10288-9
- Fisher, R., Stark, C., Ridd, P., and Jones, R. (2015). Spatial patterns in water quality changes during dredging in tropical environments. *PLoS ONE* 10:e0143309. doi: 10.1371/journal.pone.0143309
- Fitt, W., and Warner, M. (1995). Bleaching patterns of four species of Caribbean reef corals. *Biol. Bull.* 189, 298–307.
- Gallegos, C. L., Kenworthy, W. J., Biber, P. D., and Wolfe, B. S. (2009). Underwater spectral energy distribution and seagrass depth limits along an optical water quality gradient. *Smithson. Contrib. Mar. Sci.* 38, 359–367.
- Gattuso, J.-P., Gentili, B., Duarte, C. M., Kleypas, J. A., Middelburg, J. J., and Antoine, D. (2006). Light availability in the coastal ocean: impact on the distribution of benthic photosynthetic organisms and their contribution to primary production. *Biogeosciences* 3, 489–513. doi: 10.5194/bg-3-489-2006
- GBRMPA (2019). *Great Barrier Reef Outlook Report 2019*. Great Barrier Reef Marine Park Authority, Townsville, QLD. Available online at: <http://hdl.handle.net/11017/3474>
- GBRMPA (2020). *Great Barrier Reef Marine Park Authority. Position Statement. Water Quality. Document No: 100516 Revision: 0 Date: 27-Oct-2020*.
- Gilmore, A. M., Larkum, A. W. D., Salih, A., Itoh, S., Shibata, Y., Bena, C., et al. (2003). Simultaneous time resolution of the emission spectra of fluorescent proteins and zooxanthellar chlorophyll in reef-building corals. *Photochem. Photobiol.* 77, 515–523. doi: 10.1562/0031-8655(2003)077andlt;0515:STROTEandgt;2.0.CO;2
- Goreau, T. F. (1959). The ecology of Jamaican coral reefs I. Species composition and zonation. *Ecology* 40, 67–90. doi: 10.2307/1929924
- Goreau, T. F., and Wells, J. (1967). The shallow-water Scleractinia of Jamaica: revised list of species and their vertical distribution range. *Bull. Mar. Sci.* 17, 442–453.
- Gregg, W. W., and Carder, K. L. (1990). A simple spectral solar irradiance model for cloudless maritime atmospheres. *Limnol. Oceanogr.* 35, 1657–1675. doi: 10.4319/lo.1990.35.8.1657
- Guest, J. R., Baird, A. H., Maynard, J. A., Muttaqin, E., Edwards, A. J., Campbell, S. J., et al. (2012). Contrasting patterns of coral bleaching susceptibility in



- 2010 suggest an adaptive response to thermal stress. *PLoS ONE* 7:e33353. doi: 10.1371/journal.pone.0033353
- Guest, J. R., Low, J., Tun, K., Wilson, B., Ng, C., Raingeard, D., et al. (2016). Coral community response to bleaching on a highly disturbed reef. *Sci. Rep.* 6:20717. doi: 10.1038/srep20717
- Gueymard, C. A. (2017). Cloud and Albedo enhancement impacts on solar irradiance using high-frequency measurements from thermopile and photodiode radiometers. Part 1: impacts on global horizontal irradiance. *Solar Energy* 153, 755–765. doi: 10.1016/j.solener.2017.05.004
- Halldal, P. (1968). Photosynthetic capacities and photosynthetic action spectra of endozoic algae of the massive coral *Favia*. *Biol. Bull.* 134, 411–424. doi: 10.2307/1539860
- Hansell, D. A., and Carlson, C. A. (2002). *Biogeochemistry of Marine Dissolved Organic Matter*. Cambridge, MA: Academic Press.
- Hansell, D. A., and Carlson, C. A. (2014). *Biogeochemistry of Marine Dissolved Organic Matter*. Cambridge, MA: Academic Press.
- Hansell, D. A., Carlson, C. A., and Carlson, C. A. (2002). *Biogeochemistry of Marine Dissolved Organic Matter*. San Diego, CA: Elsevier Science and Technology.
- Hennige, S. J., Suggett, D. J., Warner, M. E., McDougall, K. E., and Smith, D. J. (2009). Photobiology of *Symbiodinium* revisited: bio-physical and bio-optical signatures. *Coral Reefs* 28, 179–195. doi: 10.1007/s00338-008-0444-x
- Hochberg, E. J., Peltier, S. A., and Maritorena, S. (2020). Trends and variability in spectral diffuse attenuation of coral reef waters. *Coral Reefs* 39, 1377–1389. doi: 10.1007/s00338-020-01971-1
- Hoegh-Guldberg, O. (1999). Climate change, coral bleaching and the future of the world's coral reefs. *Mar. Freshw. Res.* 50, 839–866. doi: 10.1071/MF99078
- Hopley, D. (1982). *The Geomorphology of the Great Barrier Reef*. New York, NY: Wiley.
- Hopley, D., Smithers, S. G., and Parnell, K. (2007). *The Geomorphology of the Great Barrier Reef: Development, Diversity and Change*. Cambridge: Cambridge University Press.
- Houlbrèque, F., and Ferrier-Pagès, C. (2009). Heterotrophy in tropical scleractinian corals. *Biol. Rev. Camb. Philos. Soc.* 84, 1–17. doi: 10.1111/j.1469-185X.2008.00058.x
- Huston, M. (1985). Patterns of species diversity on coral reefs. *Annu. Rev. Ecol. Syst.* 16, 149–177. doi: 10.1146/annurev.es.16.110185.001053
- Iglesias-Prieto, R., Govind, N., and Trench, R. (1993). Isolation and characterization of three membranebound chlorophyll-protein complexes from four dinoflagellate species. *Philosophic. Trans. R. Soc. Lond. Ser. B Biol. Sci.* 340, 381–392. doi: 10.1098/rstb.1993.0080
- Iglesias-Prieto, R., Govind, N. S., and Trench, R. K. (1991). Apoprotein composition and spectroscopic characterization of the water-soluble peridinin-Chlorophyll a-proteins from three symbiotic dinoflagellates. *Proc. R. Soc. Lond. Ser. B Biol. Sci.* 246, 275–283. doi: 10.1098/rspb.1991.0155
- Iglesias-Prieto, R., and Trench, R. K. (1994). Acclimation and adaptation to irradiance in symbiotic dinoflagellates. I. Responses of the photosynthetic unit to change in photon flux density. *Mar. Ecol. Progr. Ser.* 113, 163–175. doi: 10.3354/meps113163
- IOCCG (2000). *Remote Sensing of Ocean Colour in Coastal, and Other Optically-Complex, Waters*. Dartmouth, NS.
- ISRS (2004). “The effects of terrestrial runoff of sediments, nutrients and other pollutants on coral reefs,” in *ISRS Briefing Paper 3* (International Society for Reef Studies).
- Jaffé, R., Mcknight, D., Maie, N., Cory, R., McDowell, W., and Campbell, J. (2008). Spatial and temporal variations in DOM composition in ecosystems: the importance of long-term monitoring of optical properties. *J. Geophys. Res. Biogeosci.* 68:113. doi: 10.1029/2008JG000683
- Jerlov, N. G. (1976). *Marine Optics*. Amsterdam: Elsevier.
- Jerlov, N. G. (2014). *Optical Oceanography*. Amsterdam: Elsevier.
- Johns, R. B., Brady, B. A., Butler, M. S., Dembitsky, V. M., and Smith, J. D. (1994). Organic geochemical and geochemical studies of Inner Great Barrier Reef sediments—IV. identification of terrigenous and marine sourced inputs. *Organ. Geochem.* 21, 1027–1035. doi: 10.1016/0146-6380(94)90066-3
- Jones, R., Bessell-Browne, P., Fisher, R., Klonowski, W., and Slivkoff, M. (2016). Assessing the impacts of sediments from dredging on corals. *Mar. Pollut. Bull.* 102, 9–29. doi: 10.1016/j.marpollbul.2015.10.049
- Jones, R., Fisher, R., Stark, C., and Ridd, P. (2015). Temporal patterns in water quality from dredging in tropical environments. *PLoS ONE* 10:e0137112. doi: 10.1371/journal.pone.0137112
- Jones, R., Giofre, N., Luter, H. M., Neoh, T. L., Fisher, R., and Duckworth, A. (2020). Responses of corals to chronic turbidity. *Sci. Rep.* 10:4762. doi: 10.1038/s41598-020-61712-w
- Jones, R., and Hoegh-Guldberg, O. (2001). Diurnal changes in the photochemical efficiency of the symbiotic dinoflagellates (Dinophyceae) of corals: photoprotection, photoinactivation and the relationship to coral bleaching. *Plant Cell Environ.* 24, 89–99. doi: 10.1046/j.1365-3040.2001.00648.x
- Jones, R., Hoegh-Guldberg, O., Larkum, A., and Schreiber, U. (1998). Temperature-induced bleaching of corals begins with impairment of the CO<sub>2</sub> fixation mechanism in zooxanthellae. *Plant Cell Environ.* 21, 1219–1230. doi: 10.1046/j.1365-3040.1998.00345.x
- Kahng, S. E., Akkaynak, D., Shlesinger, T., Hochberg, E. J., Wiedenmann, J., Tamir, R., et al. (2019). “Light, temperature, photosynthesis, heterotrophy, and the lower depth limits of mesophotic coral ecosystems,” in *Mesophotic Coral Ecosystems*, eds Y. Loya, K. A. Puglise and T. C. L. Bridge (New York, NY: Springer), 801–828.
- Kaly, U. L., Mapstone, B. D., Ayling, A. M., and Choat, J. H. (1994). “Coral Communities,” in *Townsville Port Authority Capital Dredging Works 1993: Environmental Monitoring Program*, eds L. Benson, P. Goldsworthy, I. Butler, and J. Oliver (Townsville, QLD: Townsville Port Authority), 55–87.
- Karickhoff, S. W., and Bailey, G. W. (1973). Optical absorption spectra of clay minerals. *Clays Clay Miner.* 21, 59–70. doi: 10.1346/CCMN.1973.0210109
- Kenworthy, W. J., and Fonseca, M. S. (1996). Light requirements of Seagrasses *Halodule wrightii* and *Syringodium filiforme* derived from the relationship between diffuse light attenuation and maximum depth distribution. *Estuaries* 19, 740–750. doi: 10.2307/1352533
- Kirk, J. (2010). *Light and Photosynthesis in Aquatic Ecosystems*, 3rd Edn. New York, NY: Cambridge University Press. doi: 10.1017/CBO9781139168212
- Kirk, J. T. O. (1976). Yellow substance (gelbstoff) and its contribution to the attenuation of photosynthetically active radiation in some inland and coastal south-eastern Australian waters. *Mar. Freshw. Res.* 27, 61–71. doi: 10.1071/MF9760061
- Kirk, J. T. O. (1985). Effects of suspensoids (turbidity) on penetration of solar radiation in aquatic ecosystems. *Hydrobiologia* 125, 195–208.
- Kleypas, J. A., Mcmanus, J. W., and Meñez, L. A. (1999). Environmental limits to coral reef development: where do we draw the line? *Am. Zool.* 39, 146–159. doi: 10.1093/icb/39.1.146
- Kramer, N., Tamir, R., Eyal, G., and Loya, Y. (2020). Coral morphology portrays the spatial distribution and population size-structure along a 5–100 m depth gradient. *Front. Mar. Sci.* 7:615. doi: 10.3389/fmars.2020.00615
- Kuhl, M., Cohen, Y., Dalsgaard, T., Jorgensen, B. B., and Revsbech, N. P. (1995). Microenvironment and photosynthesis of zooxanthellae in scleractinian corals studied with microensors for O<sub>2</sub>, pH and light. *Mar. Ecol. Progr. Ser.* 117, 159–172. doi: 10.3354/meps117159
- Kuwahara, V., Nakajima, R., Othman, B., Kushairi, M., and Toda, T. (2010). Spatial variability of UVR attenuation and bio-optical factors in shallow coral-reef waters of Malaysia. *Coral Reefs* 29, 693–704. doi: 10.1007/s00338-010-0618-1
- Lajeunesse, T. C., Parkinson, J. E., Gabrielson, P. W., Jeong, H. J., Reimer, J. D., Voolstra, C. R., et al. (2018). Systematic revision of Symbiodiniaceae highlights the antiquity and diversity of coral endosymbionts. *Curr. Biol.* 28, 2570–2580. doi: 10.1016/j.cub.2018.07.008
- Lambrechts, J., Humphrey, C., Mckinna, L., Gorge, O., Fabricius, K. E., Mehta, A. J., et al. (2010). Importance of wave-induced bed liquefaction in the fine sediment budget of Cleveland Bay, Great Barrier Reef. *Estuar. Coast. Shelf Sci.* 89, 154–162. doi: 10.1016/j.ecss.2010.06.009
- Larcombe, P., Costen, A., and Woolfe, K. J. (2001). The hydrodynamic and sedimentary setting of nearshore coral reefs, central Great Barrier Reef shelf, Australia: Paluma Shoals, a case study. *Sedimentology* 48, 811–835. doi: 10.1046/j.1365-3091.2001.00396.x
- Larcombe, P., Ridd, P., Prytz, A., and Wilson, B. (1995). Factors controlling suspended sediment on inner-shelf coral reefs, Townsville, Australia. *Coral Reefs* 14, 163–171. doi: 10.1007/BF00367235
- Larcombe, P., and Woolfe, K. J. (1999). Terrigenous sediments as influences upon Holocene nearshore coral reefs, central Great Barrier Reef, Australia. *Aust. J. Earth Sci.* 46, 141–154.

- Lee, K.-S., Park, S. R., and Kim, Y. K. (2007a). Effects of irradiance, temperature, and nutrients on growth dynamics of seagrasses: a review. *J. Exp. Mar. Biol. Ecol.* 350, 144–175. doi: 10.1016/j.jembe.2007.06.016
- Lee, Z., Weidemann, A., Kindle, J., Arnone, R., Carder, K. L., and Davis, C. (2007b). Euphotic zone depth: its derivation and implication to ocean-color remote sensing. *J. Geophys. Res. Oceans* 112:3802. doi: 10.1029/2006JC003802
- Lesser, M., and Gorbunov, M. (2001). Diurnal and bathymetric changes in chlorophyll fluorescence yields of reef corals measured *in situ* with a fast repetition rate fluorometer. *Mar. Ecol. Prog. Ser.* 212, 69–77. doi: 10.3354/meps212069
- Lesser, M. P. (2004). Experimental biology of coral reef ecosystems. *J. Exp. Mar. Biol. Ecol.* 300, 217–252. doi: 10.1016/j.jembe.2003.12.027
- Lesser, M. P., Slattery, M., and Leichter, J. J. (2009). Ecology of mesophotic coral reefs. *J. Exp. Mar. Biol. Ecol.* 1, 1–8. doi: 10.1016/j.jembe.2009.05.009
- Levy, O., Dubinsky, Z., and Achituv, Y. (2003). Photobehavior of stony corals: responses to light spectra and intensity. *J. Exp. Biol.* 206, 4041–4049. doi: 10.1242/jeb.00622
- Lichtenberg, M., Larkum, A. W. D., and Kühl, M. (2016). Photosynthetic acclimation of *Symbiodinium* in hospite depends on vertical position in the tissue of the Scleractinian coral *Montastrea curta*. *Front. Microbiol.* 7:230. doi: 10.3389/fmicb.2016.00230
- Lou, J., and Ridd, P. V. (1996). Wave-current bottom shear stresses and sediment resuspension in Cleveland Bay, Australia. *Coast. Eng.* 29, 169–186. doi: 10.1016/S0378-3839(96)00023-3
- Luter, H. M., Pineda, M.-C., Ricardo, G., Francis, D. S., Fisher, R., and Jones, R. (2021). Assessing the risk of light reduction from natural sediment resuspension events and dredging activities in an inshore turbid reef environment. *Mar. Pollut. Bull.* 170:112536. doi: 10.1016/j.marpolbul.2021.112536
- Macdonald, R., Ridd, P., Whinney, J., Larcombe, P., and Neil, D. (2013). Towards environmental management of water turbidity within open coastal waters of the Great Barrier Reef. *Mar. Pollut. Bull.* 74, 82–94. doi: 10.1016/j.marpolbul.2013.07.026
- Mapstone, B. D., Choat, J., Cumming, R., and Oxley, W. (1992). *The Fringing Reefs of Magnetic Island: Benthic Biota and Sedimentation-A Baseline Study: A Report to the Great Barrier Reef Marine Park Authority*. Research report No. 13. Great Barrier Reef Marine Park Authority, Townsville, QLD.
- Maritorena, S., and Guillocheau, N. (1996). Optical properties of water and spectral light absorption by living and non-living particles and by yellow substances in coral reef waters of French Polynesia. *Mar. Ecol. Prog. Ser.* 131, 245–255. doi: 10.3354/meps131245
- Mass, T., Kline, D. I., Roopin, M., Veal, C. J., Cohen, S., Iluz, D., et al. (2010). The spectral quality of light is a key driver of photosynthesis and photoadaptation in *Stylophora pistillata* colonies from different depths in the Red Sea. *J. Exp. Biol.* 213, 4084–4091. doi: 10.1242/jeb.039891
- Mathews, E. J., Heap, A. D., and Woods, M. (2007). *Inter-Reefal Seabed Sediments and Geomorphology of the Great Barrier Reef, A Spatial Analysis*. (Geoscience Australia, Record 2007/09).
- McDonald, J., Mcgee, J., Brent, K., and Burns, W. (2019). Governing geoenvironmental research for the Great Barrier Reef. *Clim. Policy* 19, 801–811. doi: 10.1080/14693062.2019.1592742
- Mies, M., Francini-Filho, R. B., Zilberberg, C., Garrido, A. G., Longo, G. O., Laurentino, E., et al. (2020). South atlantic coral reefs are major global warming refugia and less susceptible to bleaching. *Front. Mar. Sci.* 7:514. doi: 10.3389/fmars.2020.00514
- Mobley, C. D. (1994). *Light and Water: Radiative Transfer in Natural Waters*. San Diego, CA: Academic Press.
- Mobley, C. D., Stramski, D., Paul Bissett, W., and Boss, E. (2004). Optical modeling of ocean waters: is the case 1-case 2 classification still useful? *Oceanography* 17:60. doi: 10.5670/oceanog.2004.48
- Morel, A. (1978). Available, usable, and stored radiant energy in relation to marine photosynthesis. *Deep Sea Res.* 25, 673–688. doi: 10.1016/0146-6291(78)90623-9
- Morel, A. (1988). Optical modeling of the upper ocean in relation to its biogenous matter content (case I waters). *J. Geophys. Res. Oceans* 93, 10749–10768. doi: 10.1029/JC093iC09p10749
- Morel, A. (1991). Light and marine photosynthesis: a spectral model with geochemical and climatological implications. *Prog. Oceanogr.* 26, 263–306. doi: 10.1016/0079-6611(91)90004-6
- Morel, A., and Antoine, D. (1994). Heating rate within the upper ocean in relation to its bio-optical state. *J. Phys. Oceanogr.* 24, 1652–1665.
- Morel, A., Claustre, H., Antoine, D., and Gentili, B. (2007). Natural variability of bio-optical properties in Case I waters: attenuation and reflectance within the visible and near-UV spectral domains, as observed in South Pacific and Mediterranean waters. *Biogeosciences* 4, 913–925. doi: 10.5194/bg-4-913-2007
- Morel, A., and Maritorena, S. (2001). Bio-optical properties of oceanic waters: a reappraisal. *J. Geophys. Res. Oceans* 106, 7163–7180. doi: 10.1029/2000JC000319
- Morel, A., and Prieur, L. (1977). Analysis of variations in ocean color 1. *Limnol. Oceanogr.* 22, 709–722. doi: 10.4319/lo.1977.22.4.0709
- Morgan, K. M., Moynihan, M. A., Sanwlani, N., and Switzer, A. D. (2020). Light limitation and depth-variable sedimentation drives vertical reef compression on turbid coral reefs. *Front. Mar. Sci.* 7:931. doi: 10.3389/fmars.2020.571256
- Morgan, K. M., Perry, C. T., Johnson, J. A., and Smithers, S. G. (2017). Nearshore turbid-zone corals exhibit high bleaching tolerance on the great barrier reef following the 2016 ocean warming event. *Front. Mar. Sci.* 4:224. doi: 10.3389/fmars.2017.00224
- Morgan, K. M., Perry, C. T., Smithers, S. G., Johnson, J. A., and Daniell, J. J. (2016). Evidence of extensive reef development and high coral cover in nearshore environments: implications for understanding coral adaptation in turbid settings. *Sci. Rep.* 6:29616. doi: 10.1038/srep29616
- Muir, P. R., Wallace, C. C., Done, T., and Aguirre, J. D. (2015). Limited scope for latitudinal extension of reef corals. *Science* 348, 1135–1138. doi: 10.1126/science.1259911
- Muscantine, L. (1990). The role of symbiotic algae in carbon and energy flux in reef corals. *Ecosyst. World* 25, 75–87.
- Nack, M., and Green, A. (1974). Influence of clouds, haze, and smog on the middle ultraviolet reaching the ground. *Appl. Opt.* 13, 2405–2415. doi: 10.1364/AO.13.002405
- Niedzwiedzki, D. M., Jiang, J., Lo, C. S., and Blankenship, R. E. (2014). Spectroscopic properties of the Chlorophyll a–Chlorophyll c2–Peridinin-Protein-Complex (acpPC) from the coral symbiotic dinoflagellate *Symbiodinium*. *Photosyn. Res.* 120, 125–139. doi: 10.1007/s11120-013-9794-5
- Orpin, A., and Ridd, P. (2012). Exposure of inshore corals to suspended sediments due to wave-resuspension and river plumes in the central Great Barrier Reef: a reappraisal. *Cont. Shelf Res.* 47, 55–67. doi: 10.1016/j.csr.2012.06.013
- Orpin, A., Ridd, P., and Stewart, L. (1999). Assessment of the relative importance of major sediment transport mechanisms in the central Great Barrier Reef lagoon. *Austr. J. Earth Sci.* 46, 883–896. doi: 10.1046/j.1440-0952.1999.00751.x
- Orpin, A., Ridd, P., Thomas, S., Anthony, K., Marshall, P., and Oliver, J. (2004). Natural turbidity variability and weather forecasts in risk management of anthropogenic sediment discharge near sensitive environments. *Mar. Pollut. Bull.* 49, 602–612. doi: 10.1016/j.marpolbul.2004.03.020
- Otis, D. B., Carder, K. L., English, D. C., and Ivey, J. E. (2004). CDOM transport from the Bahamas Banks. *Coral Reefs* 23, 152–160. doi: 10.1007/s00338-003-0356-8
- Passlow, V., Rogis, J., Hancock, A., Hemer, M., Glenn, K., and Habib, A. (2005). *National Marine Sediments Database and Seafloor Characteristics Project*. Final report prepared for the National Oceans Office, Hobart, TAS.
- Pecenak, Z. K., Mejia, F. A., Kurtz, B., Evan, A., and Kleissl, J. (2016). Simulating irradiance enhancement dependence on cloud optical depth and solar zenith angle. *Solar Energy* 136, 675–681. doi: 10.1016/j.solener.2016.07.045
- Perry, C., Smithers, S., Gulliver, P., and Browne, N. (2012). Evidence of very rapid reef accretion and reef growth under high turbidity and terrigenous sedimentation. *Geology* 40, 719–722. doi: 10.1130/G33261.1
- Perry, C. T., and Larcombe, P. (2003). Marginal and non-reef-building coral environments. *Coral Reefs* 22, 427–432. doi: 10.1007/s00338-003-0330-5
- Pettus, C., Devlin, M., Teixeira Da Silva, E., Lewis, S., Waterhouse, J., Wenger, A., et al. (2018). Defining wet season water quality target concentrations for ecosystem conservation using empirical light attenuation models: a case study in the Great Barrier Reef (Australia). *J. Environ. Manage.* 213, 451–466. doi: 10.1016/j.jenvman.2018.02.028
- Pfister, G., McKenzie, R., Liley, J., Thomas, A., Forgan, B., and Long, C. N. (2003). Cloud coverage based on all-sky imaging and its impact on surface solar irradiance. *J. Appl. Meteorol. Climatol.* 42, 1421–1434. doi: 10.1175/1520-0450(2003)042andlt;1421:CCBOAandgt;2.0.CO;2

- Polívka, T., Hiller, R. G., and Frank, H. A. (2007). Spectroscopy of the peridinin-chlorophyll-*a* protein: insight into light-harvesting strategy of marine algae. *Arch. Biochem. Biophys.* 458, 111–120. doi: 10.1016/j.abb.2006.10.006
- Poquita-Du, R. C., Quek, Z. B. R., Jain, S. S., Schmidt-Roach, S., Tun, K., Heery, E. C., et al. (2019). Last species standing: loss of *Pocilloporidae* corals associated with coastal urbanization in a tropical city state. *Mar. Biodivers.* 49, 1727–1741. doi: 10.1007/s12526-019-00939-x
- Potts, D., and Jacobs, J. (2000). “Evolution of reef-building scleractinian corals in turbid environments: a paleo-ecological hypothesis,” in *Proceedings of the Ninth International Coral Reef Symposium* (Bali), 249–254.
- Preisendorfer, R. W., and Mobley, C. D. (1986). Albedos and glitter patterns of a wind-roughened sea surface. *J. Phys. Oceanogr.* 16, 1293–1316. doi: 10.1175/1520-0485(1986)016<1293:AAGPOA>2.0.CO;2
- Prézelin, B., and Haxo, F. (1976). Purification and characterization of peridinin-chlorophyll *a*-proteins from the marine dinoflagellates *Glenodinium* sp. and *Gonyaulax polyedra*. *Planta* 128, 133–141. doi: 10.1007/BF00390314
- Prézelin, B., Ley, A. C., and Haxo, F. (1976). Effects of growth irradiance on the photosynthetic action spectra of the marine dinoflagellate, *Glenodinium* sp. *Planta* 130, 251–256. doi: 10.1007/BF00387829
- Prieur, L., and Sathyendranath, S. (1981). An optical classification of coastal and oceanic waters based on the specific spectral absorption curves of phytoplankton pigments, dissolved organic matter, and other particulate materials 1. *Limnol. Oceanogr.* 26, 671–689.
- R Core Team (2020). *R: A Language and Environment for Statistical Computing*. R Foundation for Statistical Computing, Vienna. Available online at: <https://www.R-project.org/>
- Reichelt, A. J., and Jones, G. B. (1994). Trace metals as tracers of dredging activity in Cleveland Bay—field and laboratory studies. *Mar. Freshw. Res.* 45, 1237–1257. doi: 10.1071/MF9941237
- Robinson, N. (1966). *Solar Radiation*. New York, NY: Elsevier.
- Roth, M. S. (2014). The engine of the reef: photobiology of the coral-algal symbiosis. *Front. Microbiol.* 5:422. doi: 10.3389/fmicb.2014.00422
- Rue, H., Martino, S., and Chopin, N. (2009). Approximate bayesian inference for latent gaussian models by using integrated nested laplace approximations. *J. R. Stat. Soc. Ser. B* 71, 319–392. doi: 10.1111/j.1467-9868.2008.00700.x
- Salih, A., Larkum, A., Cox, G., Kühl, M., and Hoegh-Guldberg, O. (2000). Fluorescent pigments in corals are photoprotective. *Nature* 408, 850–853. doi: 10.1038/35048564
- Schlichter, D., and Fricke, H. W. (1991). Mechanisms of amplification of photosynthetically active radiation in the symbiotic deep-water coral *Leptoseris fragilis*. *Hydrobiologia* 216, 389–394. doi: 10.1007/BF00026491
- Schlichter, D., Fricke, H. W., and Weber, W. (1986). Light harvesting by wavelength transformation in a symbiotic coral of the Red Sea twilight zone. *Mar. Biol.* 91, 403–407. doi: 10.1007/BF00428634
- Schuhmacher, H., and Zibrowius, H. (1985). What is hermatypic? *Coral Reefs* 4, 1–9. doi: 10.1007/BF00302198
- Scott, B. D., and Jitts, H. R. (1977). Photosynthesis of phytoplankton and zooxanthellae on a coral reef. *Mar. Biol.* 41, 307–315. doi: 10.1007/BF00389097
- Sherman, D. M., and Waite, T. D. (1985). Electronic spectra of Fe<sup>3+</sup> oxides and oxide hydroxides in the near IR to near UV. *Am. Mineral.* 70, 1262–1269.
- Shi, K., Li, Y., Li, L., and Lu, H. (2013). Absorption characteristics of optically complex inland waters: implications for water optical classification. *J. Geophys. Res. Biogeosci.* 118, 860–874. doi: 10.1002/jgrg.20071
- Slivkoff, M. (2014). *Ocean Colour Remote Sensing of the Great Barrier Reef Waters* [Ph.D. thesis], School of Science, Department of Imaging & Applied Physics, Bentley, WA: Curtin University.
- Smith, E. G., D’angelo, C., Sharon, Y., Tchernov, D., and Wiedenmann, J. (2017). Acclimatization of symbiotic corals to mesophotic light environments through wavelength transformation by fluorescent protein pigments. *Proc. R. Soc. B Biol. Sci.* 284:20170320. doi: 10.1098/rspb.2017.0320
- Smith, R. C., and Baker, K. S. (1978). Optical classification of natural waters 1. *Limnol. Oceanogr.* 23, 260–267. doi: 10.4319/lo.1978.23.2.0260
- Smith, R. C., and Baker, K. S. (1981). Optical properties of the clearest natural waters (200–800 nm). *Appl. Opt.* 20:177. doi: 10.1364/AO.20.000177
- Song, P.-S., Koka, P., Prézelin, B. B., and Haxo, F. T. (1976). Molecular topology of the photosynthetic light-harvesting pigment complex, peridinin-chlorophyll *a*-protein, from marine dinoflagellates. *Biochemistry* 15, 4422–4427. doi: 10.1021/bi00665a012
- Spencer Davies, P. (1989). Short-term growth measurements of corals using an accurate buoyant weighing technique. *Mar. Biol.* 101, 389–395. doi: 10.1007/BF00428135
- Stimson, J., and Kinzie, R. A. (1991). The temporal release of zooxanthellae from the reef coral *Pocillopora damicornis* (Linnaeus) under nitrogen-enrichment and control conditions. *J. Exp. Mar. Biol. Ecol.* 153, 63–74. doi: 10.1016/S0022-0981(05)80006-1
- Stramski, D., Babin, M., and Wozniak, S. B. (2007). Variations in the optical properties of terrigenous mineral-rich particulate matter suspended in seawater. *Limnol. Oceanogr.* 52, 2418–2433. doi: 10.4319/lo.2007.52.6.2418
- Sully, S., and Van Woesik, R. (2020). Turbid reefs moderate coral bleaching under climate-related temperature stress. *Glob. Change Biol.* 26, 1367–1373. doi: 10.1111/gcb.14948
- Sundarabalan, B., Shanmugam, P., and Ahn, Y.-H. (2016). Modeling the underwater light field fluctuations in coastal oceanic waters: validation with experimental data. *Ocean Sci. J.* 51, 67–86. doi: 10.1007/s12601-016-0007-y
- Szabó, M., Wangpraseurt, D., Tamburic, B., Larkum, A. W., Schreiber, U., Suggett, D. J., et al. (2014). Effective light absorption and absolute electron transport rates in the coral *Pocillopora damicornis*. *Plant Physiol. Biochem.* 83, 159–167. doi: 10.1016/j.plaphy.2014.07.015
- Thompson, A., Costello, P., Davidson, J., Logan, M., Coleman, G., and Gunn, K. (2018). *Marine Monitoring Program: Annual Report for Inshore Coral Reef Monitoring: 2016 – 2017*. Great Barrier Reef Marine Park Authority, Townsville, QLD.
- Van Duin, E. H., Blom, G., Los, F. J., Maffione, R., Zimmerman, R., Cerco, C. F., et al. (2001). Modeling underwater light climate in relation to sedimentation, resuspension, water quality and autotrophic growth. *Hydrobiologia* 444, 25–42. doi: 10.1023/A:1017512614680
- Van Woesik, R., Houk, P., Isechal, A. L., Idechong, J. W., Victor, S., and Golbuu, Y. (2012). Climate-change refugia in the sheltered bays of Palau: analogs of future reefs. *Ecol. Evol.* 2, 2474–2484. doi: 10.1002/ecs3.363
- Wangpraseurt, D., Larkum, A. W., Franklin, J., Szabó, M., Ralph, P. J., and Kühl, M. (2014a). Lateral light transfer ensures efficient resource distribution in symbiont-bearing corals. *J. Exp. Biol.* 217, 489–498. doi: 10.1242/jeb.091116
- Wangpraseurt, D., Larkum, A. W., Ralph, P. J., and Kühl, M. (2012). Light gradients and optical microniches in coral tissues. *Front. Microbiol.* 3:316. doi: 10.3389/fmicb.2012.00316
- Wangpraseurt, D., Polerecky, L., Larkum, A. W., Ralph, P. J., Nielsen, D. A., Pernice, M., et al. (2014b). The *in situ* light microenvironment. *Corals* 59, 917–926. doi: 10.4319/lo.2014.59.3.0917
- Wangpraseurt, D., Tamburic, B., Szabó, M., Suggett, D., Ralph, P. J., and Kühl, M. (2014c). Spectral Effects on *Symbiodinium* photobiology studied with a programmable light engine. *PLoS ONE* 9:e112809. doi: 10.1371/journal.pone.0112809
- Waterhouse, J., Gruber, R., Logan, M., Petus, C., Howley, C., Lewis, S., et al. (2021). *Marine Monitoring Program: Annual Report for Inshore Water Quality Monitoring 2019–20*. Report for the Great Barrier Reef Marine Park Authority, Great Barrier Reef Marine Park Authority, Townsville, QLD.
- Webb, J. R., Santos, I. R., Maher, D. T., Tait, D. R., Cyronak, T., Sadat-Noori, M., et al. (2019). Groundwater as a source of dissolved organic matter to coastal waters: insights from radon and CDOM observations in 12 shallow coastal systems. *Limnol. Oceanogr.* 64, 182–196. doi: 10.1002/lno.11028
- Wellington, G. (1982). An experimental analysis of the effects of light and zooplankton on coral zonation. *Oecologia* 52, 311–320.
- Whinney, K. J., Jones, R., Duckworth, A., and Ridd, P. (2017). Continuous *in situ* monitoring of sediment deposition in shallow benthic environments. *Coral Reefs* 36, 521–533. doi: 10.1007/s00338-016-1536-7
- Woolfe, K., and Larcombe, P. (1998). “Terrigenous sediment accumulation as a regional control on the distribution of reef carbonates,” in *Reefs and Carbonate Platforms in the Pacific and Indian Oceans*, eds G. Camoin and P. Davies (International Association of Sedimentologists (IAS) Special Publication) 25, 295–310. doi: 10.1002/9781444304879.ch16
- Woolfe, K. J., and Larcombe, P. (1999). Terrigenous sedimentation and coral reef growth: a conceptual framework. *Mar. Geol.* 155, 331–345. doi: 10.1016/S0025-3227(98)00131-5

- Wozniak, B., and Dera, J. (2007). *Light Absorption in Sea Water*. New York, NY: Springer.
- Wyman, K., Dubinsky, Z., Porter, J., and Falkowski, P. (1987). Light absorption and utilization among hermatypic corals: a study in Jamaica, West Indies. *Mar. Biol.* 96, 283–292. doi: 10.1007/BF00427028
- Yentsch, C., Yentsch, C., Cullen, J., Lapointe, B., Phinney, D., and Yentsch, S. (2002). Sunlight and water transparency: cornerstones in coral research. *J. Exp. Mar. Biol. Ecol.* 268, 171–183. doi: 10.1016/S0022-0981(01)00379-3
- Yordanov, G. H., Midtgård, O.-M., Sætre, T. O., Nielsen, H. K., and Norum, L. E. (2013). Overirradiance (cloud enhancement) events at high latitudes. *IEEE J. Photovoltaics* 3, 271–277. doi: 10.1109/JPHOTOV.2012.2213581
- Yordanov, G. H., Sætre, T. O., and Midtgård, O.-M. (2015). Extreme overirradiance events in Norway: 1.6 suns measured close to 60 N. *Solar Energy* 115, 68–73. doi: 10.1016/j.solener.2015.02.020
- Ziegler, M., Roder, C. M., Büchel, C., and Voolstra, C. R. (2014). Limits to physiological plasticity of the coral *Pocillopora verrucosa* from the central Red Sea. *Coral Reefs* 33, 1115–1129. doi: 10.1007/s00338-014-1192-8
- Zweifler, A., O'leary, M., Morgan, K., and Browne, N. K. (2021). Turbid coral reefs: past, present and future—a review. *Diversity* 13:251. doi: 10.3390/d13060251

**Conflict of Interest:** WK and MS were employed by company In-situ Marine Optics.

The remaining authors declare that the research was conducted in the absence of any commercial or financial relationships that could be construed as a potential conflict of interest.

**Publisher's Note:** All claims expressed in this article are solely those of the authors and do not necessarily represent those of their affiliated organizations, or those of the publisher, the editors and the reviewers. Any product that may be evaluated in this article, or claim that may be made by its manufacturer, is not guaranteed or endorsed by the publisher.

Copyright © 2021 Jones, Pineda, Luter, Fisher, Francis, Klonowski and Slivkoff. This is an open-access article distributed under the terms of the Creative Commons Attribution License (CC BY). The use, distribution or reproduction in other forums is permitted, provided the original author(s) and the copyright owner(s) are credited and that the original publication in this journal is cited, in accordance with accepted academic practice. No use, distribution or reproduction is permitted which does not comply with these terms.





# Novel Mitochondrial DNA Markers for Scleractinian Corals and Generic-Level Environmental DNA Metabarcoding

Chuya Shinzato<sup>1†</sup>, Haruhi Narisoko<sup>2†</sup>, Koki Nishitsuji<sup>2†</sup>, Tomofumi Nagata<sup>3</sup>, Noriyuki Satoh<sup>2</sup> and Jun Inoue<sup>1</sup>

<sup>1</sup> Atmosphere and Ocean Research Institute, The University of Tokyo, Kashiwa, Japan, <sup>2</sup> Marine Genomics Unit, Okinawa Institute of Science and Technology Graduate University, Okinawa, Japan, <sup>3</sup> Okinawa Environment Science Center, Okinawa, Japan

## OPEN ACCESS

### Edited by:

Maren Ziegler,  
University of Giessen, Germany

### Reviewed by:

Danwei Huang,  
National University of Singapore,  
Singapore  
Eslam O. Osman,  
The Pennsylvania State University  
(PSU), United States

### \*Correspondence:

Chuya Shinzato  
c.shinzato@aori.u-tokyo.ac.jp

<sup>†</sup> These authors have contributed  
equally to this work

### Specialty section:

This article was submitted to  
Coral Reef Research,  
a section of the journal  
Frontiers in Marine Science

**Received:** 13 August 2021

**Accepted:** 09 November 2021

**Published:** 30 November 2021

### Citation:

Shinzato C, Narisoko H,  
Nishitsuji K, Nagata T, Satoh N and  
Inoue J (2021) Novel Mitochondrial  
DNA Markers for Scleractinian Corals  
and Generic-Level Environmental  
DNA Metabarcoding.  
Front. Mar. Sci. 8:758207.  
doi: 10.3389/fmars.2021.758207

Coral reefs, the most biodiverse habitats in the ocean, are formed by anthozoan cnidarians, the scleractinian corals. Recently, however, ongoing climate change has imperiled scleractinian corals and coral reef environments are changing drastically. Thus, convenient, high-density monitoring of scleractinian corals is essential to understand changes in coral reef communities. Environmental DNA (eDNA) metabarcoding is potentially one of the most effective means of achieving it. Using publicly available scleractinian mitochondrial genomes, we developed high-specificity primers to amplify mitochondrial 12S ribosomal RNA (12S) and cytochrome oxidase-1 (CO1) genes of diverse scleractinian corals, which could be used for genus-level metabarcoding analyses, using next-generation sequencing technologies. To confirm the effectiveness of these primers, PCR amplicon sequencing was performed using eDNA isolated along the seashore of Okinawa, Japan. We successfully amplified all eDNA samples using PCR. Approximately 93 and 72% of PCR amplicon sequences of 12S and CO1 primers originated from scleractinian 12S and CO1 genes, respectively, confirming higher specificities for coral mitochondrial genes than primers previously used for coral eDNA metabarcoding. We also found that hierarchical clustering, based on the percentage of mapped reads to each scleractinian genus, discriminates between sampling locations, suggesting that eDNA surveys are sufficiently powerful to reveal differences between coral communities separated by <1 km. We conclude that the method reported here is a powerful tool for conducting efficient eDNA surveys targeting scleractinian corals.

**Keywords:** scleractinia, mitochondrial genome, primer development, metabarcoding analyses, environmental DNA (eDNA)

## INTRODUCTION

Coral reefs in tropical and subtropical waters harbor about 30% of all marine life (Knowlton et al., 2010), making them the most biodiverse habitats on Earth. Scleractinian or stony corals (Anthozoa, Cnidaria) create the structure of coral reefs by depositing massive calcium carbonate skeletons. More than 1,300 scleractinian species belonging to 236 genera and 25 families have been

reported as of August 3, 2021, based on the Integrated Taxonomic Information System (ITIS)<sup>1</sup>. In recent years, however, coral bleaching caused by global warming, severe storms, and predation by crown-of-thorns starfish have degraded coral reef ecosystems (De'ath et al., 2012); thus, coral reef environments are constantly and dramatically changing. Therefore, frequent, high-density coral monitoring is essential to assess changing coral reef communities. DNA originating from various sources, such as mucus and damaged tissues of multicellular organisms, exists in soil, seawater, air, etc., and is called environmental DNA (eDNA; Bohmann et al., 2014; Kelly et al., 2014). Recently, eDNA has been used to monitor marine biodiversity, especially among fishes (Miya et al., 2015; Yamamoto et al., 2017). Several studies have reported detection of eDNA from stony corals (Shinzato et al., 2018; Nichols and Marko, 2019; Alexander et al., 2020; Dugal et al., 2021), and eDNA is expected to become a powerful tool in coral monitoring.

Because mitochondrial (mt) DNA contains many sequence variations, genes from mitochondrial genomes are widely used for species identification (or barcoding) and molecular phylogenetic analyses of metazoans. Furthermore, due to their large copy numbers, primers for mt genes are the most widely used targets for PCR amplification in eDNA metabarcoding (e.g., MiFish, Miya et al., 2015), and mt genes of scleractinian corals have been widely used for phylogenetic analyses (for example, Fukami, 2008; Kitahara et al., 2010, 2016). On the other hand, cnidarian mt genomic variation is extremely low (Shearer et al., 2002), preventing species discrimination. Various universal primers for coral mt genes have been reported (Chen and Yu, 2000; Fukami et al., 2008; Lin et al., 2011), but most of these were designed for phylogenetic purposes, so PCR amplicons exceed 600 bp, making full-length sequence decoding impossible with next-generation sequencing (NGS), especially Illumina platforms, that can read only short DNA lengths (maximum 300 bp paired-end with the Illumina MiSeq).

Recently universal primers for coral metabarcoding using NGS have been reported, including primers amplifying mt genes [16S ribosomal DNA and cytochrome oxidase-1 (CO1)] (Nichols and Marko, 2019) and the internal transcribed spacer 2 (ITS2) region of nuclear ribosomal DNA (Alexander et al., 2020). However, the mt genes targeted for primer development might not be chosen so as to amplify scleractinian species specifically. As a result, almost half the PCR amplicon sequencing reads were from non-scleractinian corals (Nichols and Marko, 2019; Alexander et al., 2020), indicating that the specificities and sensitivities of these primers for scleractinian DNA were not very high. For accurate, efficient eDNA metabarcoding, it is essential to design primers with high specificity for the target taxon. Otherwise, PCR conditions must be greatly relaxed (less stringent), by decreasing the annealing temperature or increasing the number of PCR cycles, which may lead to non-specific PCR amplification and increased contamination. Taking advantage of recent decoding of scleractinian mt genomes, we designed primers that can amplify mitochondrial genes from

as diverse a range of scleractinian corals as possible and that can be used for metabarcoding using NGS. To achieve this, we downloaded currently available scleractinian mt genomes from NCBI and performed alignments to select regions suitable for primer development. Then we checked actual PCR amplification from eDNA using the designed primers.

## MATERIALS AND METHODS

### Primer Design to Amplify Diverse Scleractinian Mitochondrial Genes

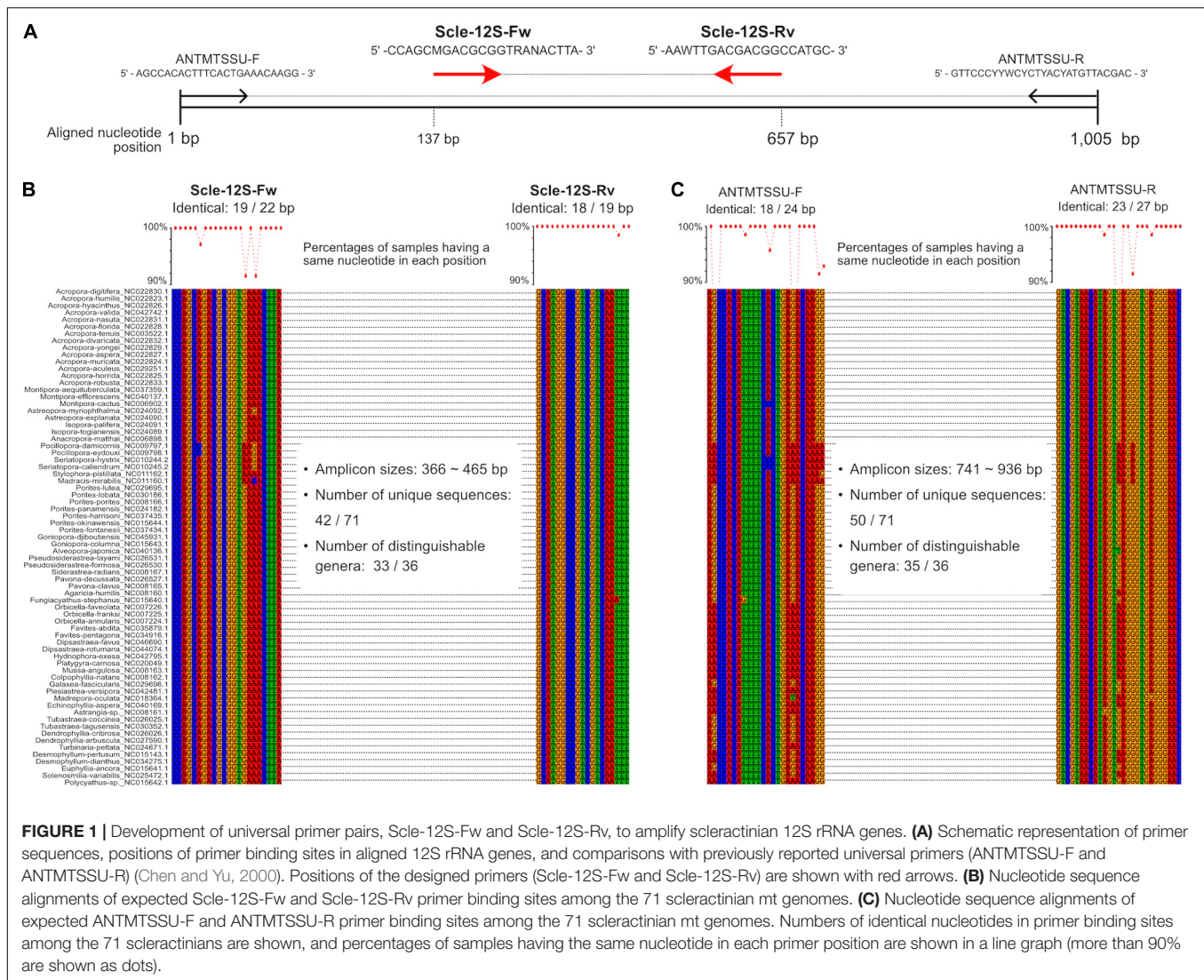
Scleractinian mt genomes representing 71 species, 36 genera, and 15 families were downloaded from the NCBI Genome resource<sup>2</sup> on May 1, 2021 (**Supplementary Table 1**). Downloaded mt genomes were aligned using mafft v7.475 with the --adjustdirection option (Katoh and Standley, 2013). Then, prospective PCR primer regions, highly conserved in all 71 scleractinian species, were visually identified for each mitochondrial gene (13 protein-coding genes and 2 rRNA genes). Primer pairs were designed using Primer3Plus (Untergasser et al., 2007). Primer pairs were selected so that PCR products would be <550 bp for use with the Illumina platform, with a maximum sequencing read length of 300 bp (with paired-end sequencing, and more than 50 bp of overlap length between read 1 and read 2 sequences). After inspection of aligned whole mt genome sequences, we designed a primer pair for the 12S ribosomal RNA gene (12S) and a primer pair for the cytochrome c oxidase subunit I gene (CO1) in sequence regions that are highly conserved among all scleractinians examined. We also examined all other mt genes, but their nucleotide sequences were not conserved, so it was impossible to develop primers for these genes. Only 12S and CO1 are sufficiently conserved to develop universal primers for all scleractinians. Expected PCR-amplified sequences from the 71 mt genomes were extracted using Seqotron version 1.0.1 (Fourment and Holmes, 2016). To check the number of unique sequences in the expected PCR-amplified regions, these sequences were clustered using CD-HIT-EST version 4.6 with 100% nucleotide percent identity (Li and Godzik, 2006). For *in silico* comparison with previously reported universal primers, we used primers for 12S reported in Chen and Yu (2000), primers for CO1 reported in Fukami et al. (2008), and metabarcoding primers for CO1 reported in Nichols and Marko (2019).

### Water Sampling, Environmental DNA Extraction, and PCR Amplicon Sequencing

Five liters of seawater from the surface and from 2–3 m depth were collected at each of three points along a coral reef offshore of Onna Village, Okinawa, Japan, where coral coverage was around 50–90% and the genus *Acropora* was dominant, on 29 April, 2021 (**Figure 3A** and **Supplementary Table 2**). Twenty 50-mL aliquots of seawater were filtered through 0.45-μm Sterivex

<sup>1</sup> www.itis.gov

<sup>2</sup> https://www.ncbi.nlm.nih.gov/genome/browse#/organelles/



filters (Merck), for a total of 1 L from each sample. eDNA in seawater was extracted following the Environmental DNA Sampling and Experiment Manual Version 2.1 (Minamoto et al., 2021; **Supplementary Table 3**).

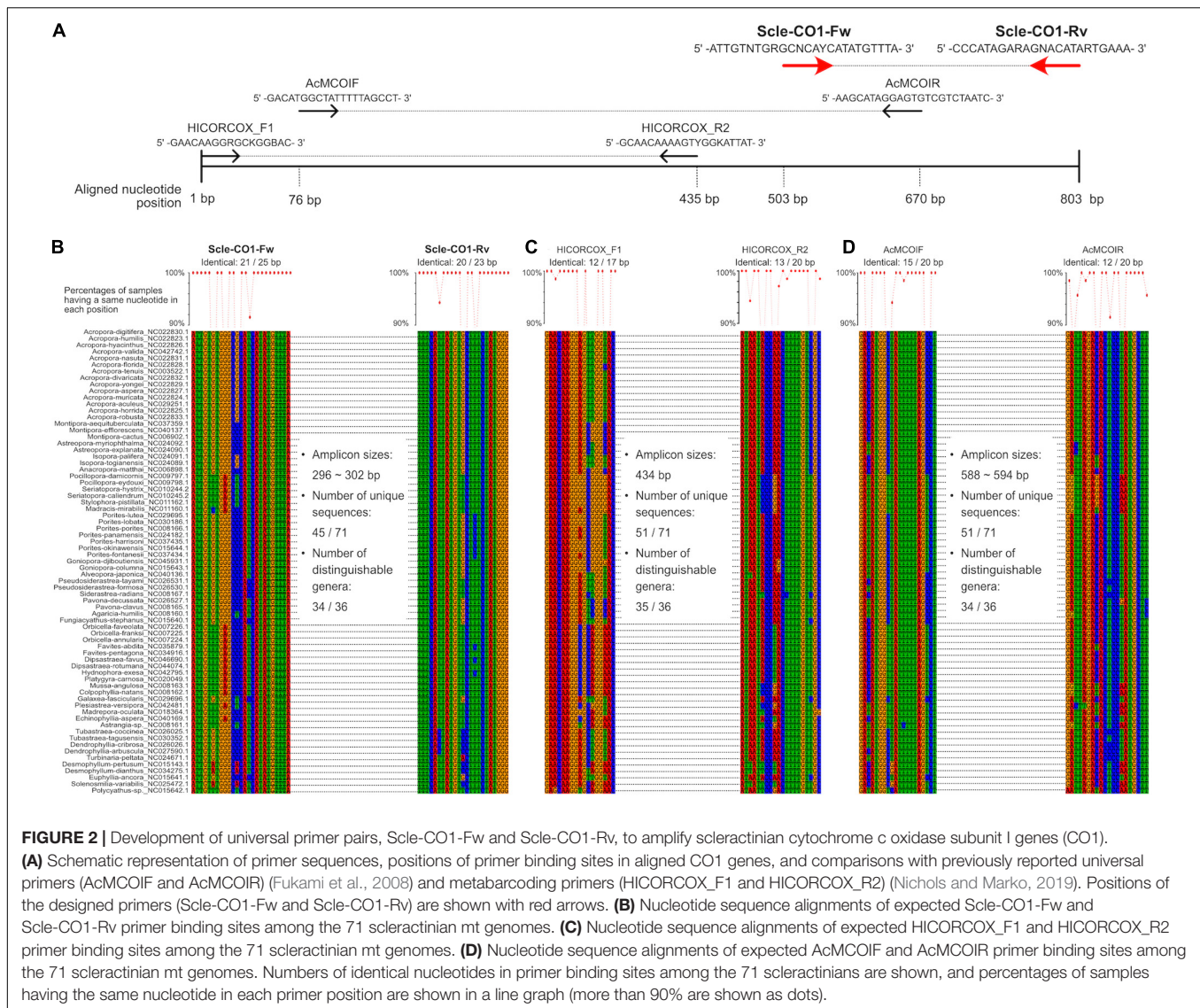
Extracted eDNA samples were PCR-amplified using Scl\_12S\_Fw (5'-CCAGCMGACGCGGTRANACTTA-3') and Scl\_12S\_Rv (5'-AAWTTGACGACGGCCATGC-3') primers to amplify 12S rRNA genes (**Figure 1A**), and Scl\_CO1\_Fw (5'-ATTGTNTGRGCNCAYCATATGTTTA-3') and Scl\_CO1\_Rv (5'-CCCATAGARAGNACATARTGAAA-3') primers for CO1 genes (**Figure 2A**), using genomic DNA isolated from an *Acropora tenuis* colony as a positive PCR control. Tks Gflex<sup>TM</sup> DNA Polymerase (Takara) was used for PCR amplification. PCR cycling conditions were 1 min at 94°C, followed by 35 cycles of 10 s at 94°C, 15 s at 60°C (12S) or 55°C (CO1), and 30 s at 68°C, with an extension of 5 min at 68°C in the final cycle. PCR products were extracted and cleaned with a FastGene Gel/PCR Extraction Kit (NIPPON Genetics). Amplicon sequencing libraries of cleaned PCR products

were prepared using a KAPA Hyper Prep Kit (NIPPON Genetics Co., Ltd.) without fragmentation. Libraries were multiplexed and 300-bp paired-end reads were sequenced on a MiSeq platform (Illumina) using MiSeq Reagent kit v3 (600 cycles).

## Bioinformatic Analysis

First, low-quality bases (Phred quality score <20) and Illumina sequencing adapters were removed from raw sequence reads using cutadapt version 3.4 (Martin, 2011). Sequences ≥200 bp were retained. Merging of paired reads, unique sequence identification, chimera removal, and denoising (error-correction) were performed using USEARCH, version 11.0.667 (Edgar, 2010) as follows. Each pair of quality- and adapter-trimmed read 1 and read 2 sequences were merged (assembled) with the "fastq\_mergepairs" command and the "-fastq\_minovlen 30" option. For each sequencing sample, merged read sequences were dereplicated using the "fastx\_uniques" command with a minimum





abundance of 10 reads (-minuniquesize 10), and denoising and chimera removal were performed using the “unio3” command for each sample with a minimum abundance of 10 reads (-minuniquesize 10). Then, denoised (error-corrected) operational taxonomic units, called ZOTUs (zero-radius operational taxonomic units), were prepared for each sample.

ZOTU sequences from all samples were concatenated and clustered using CD-HIT-EST version 4.6 with 100% nucleotide identity (Li and Godzik, 2006). Clustered unique ZOTU sequences were used for the database for mapping. Merged sequences from each sample were mapped to the clustered ZOTUs and numbers of mapped sequences for each ZOTU were counted using the USEARCH “otutab” command with a percent identity of 99% (-id 0.99).

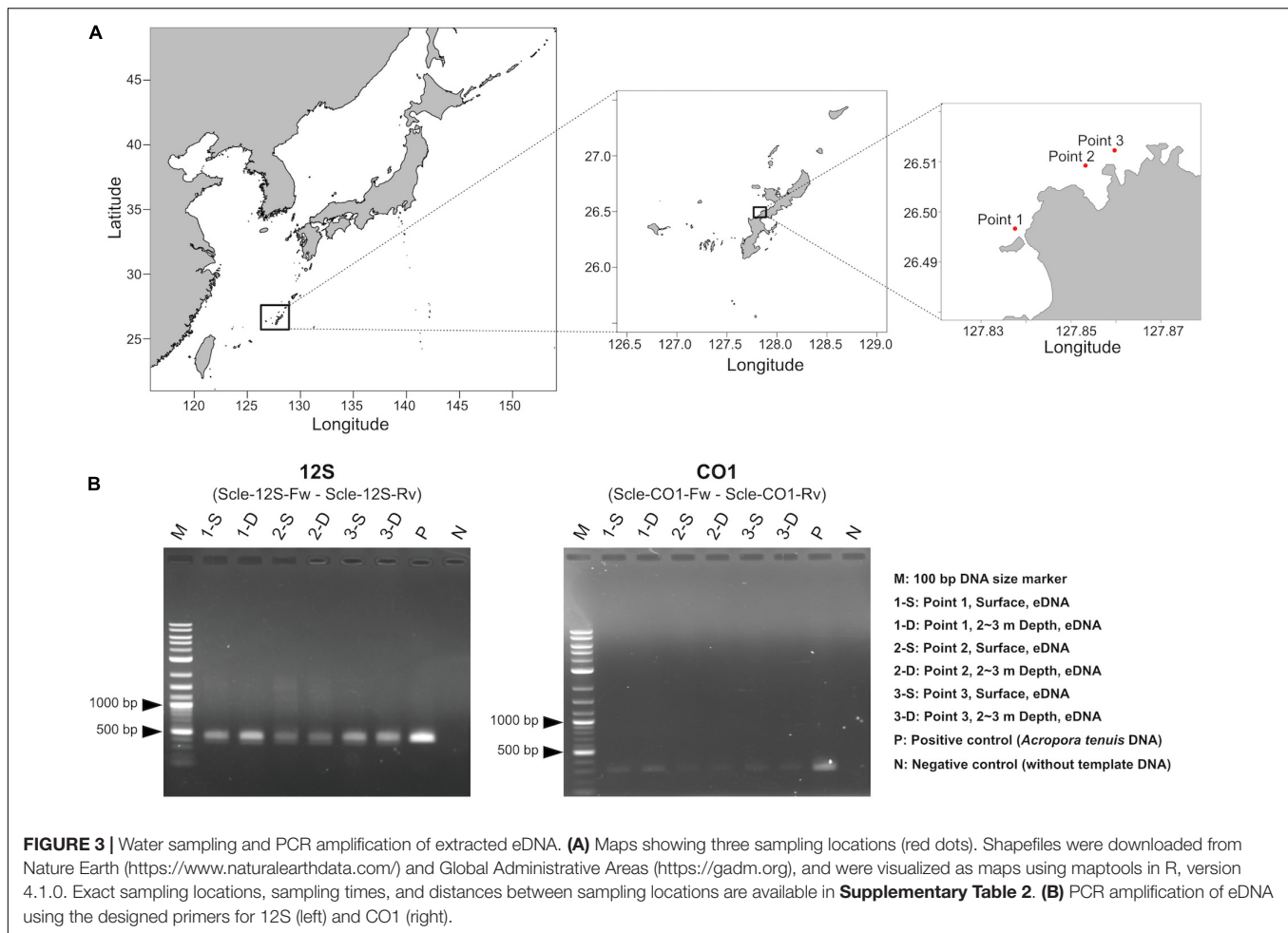
To identify ZOTUs that originated from scleractinians, we selected ZOTUs satisfying the following criteria: (1) taxonomic assignments of ZOTUs using the NCBI NT database

(downloaded on July 9, 2021) were performed using Assign-Taxonomy-with-BLAST<sup>3</sup>, and ZOTUs with the best estimated scleractinian taxonomy were selected. (2) BLASTN searches against expected PCR amplified regions of 12S and CO1 genes from the 71 downloaded scleractinian genomes were performed using BLASTN version 2.12.0 + and ZOTUs with an e-value  $\leq 1e^{-20}$ , percent identity  $\geq 90\%$ , and query coverage  $\geq 95\%$  were selected.

After selecting ZOTUs from Scleractinia, mapped reads to ZOTUs from the same genera were combined. To remove possible errors and contamination, we removed scleractinian genera restricted to the Atlantic Ocean and only genera with more than 0.1% of the total number of mapped reads in a given sample were considered. To infer similarities between samples and sampling locations, hierarchical clustering based on the ward D method was performed using percentages of coral genera

<sup>3</sup><https://github.com/Joseph7e/Assign-Taxonomy-with-BLAST>





detected in each sample using the pheatmap command<sup>4</sup> in R version 4.1.2 (R Core Team, 2015).

## RESULTS

### Novel Primer Design for Amplifying Scleractinian Mitochondrial Genes

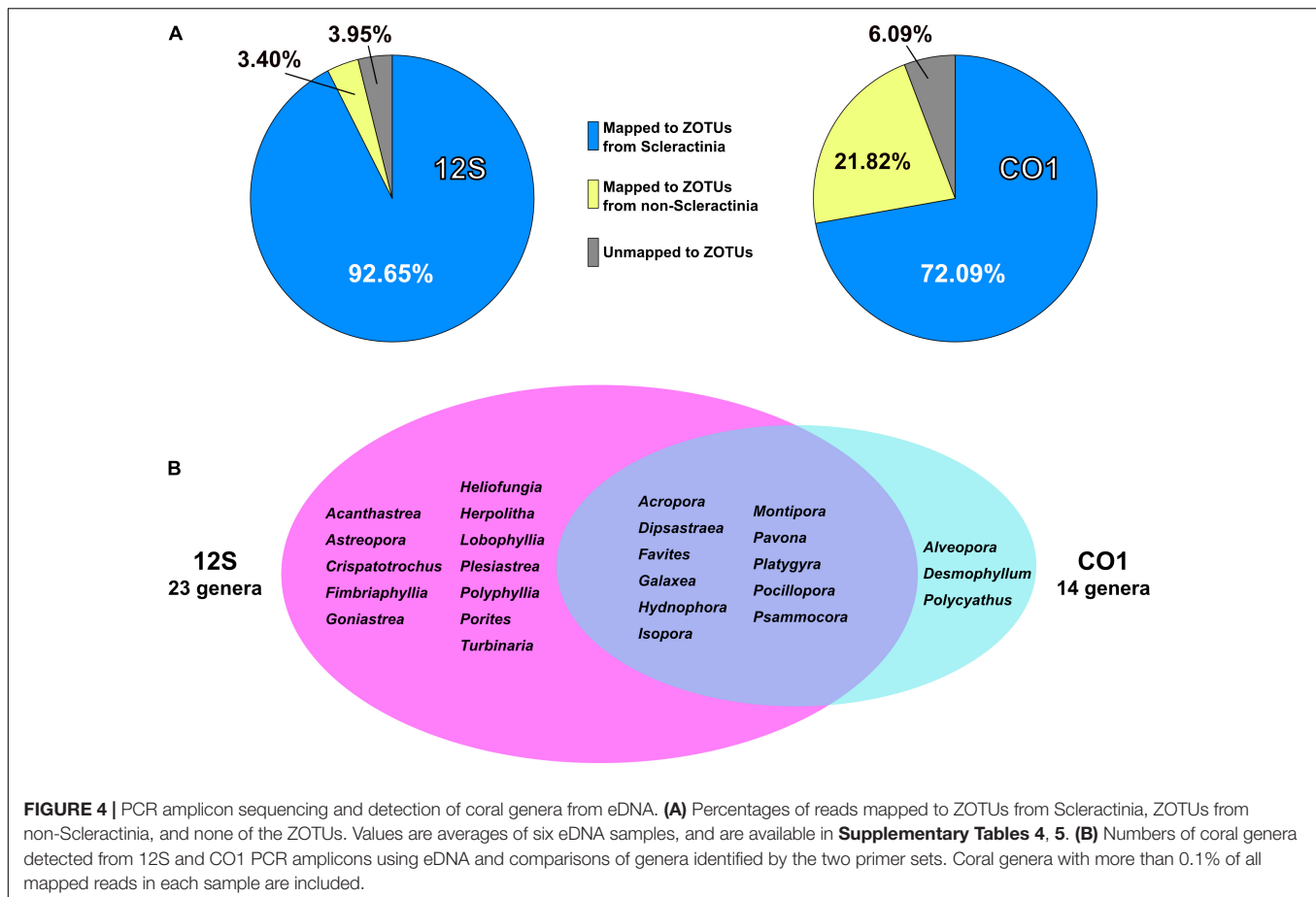
We aligned whole mitochondrial genome sequences of 71 scleractinian species (aligned sequences are available as **Supplementary Figures**). After we checked aligned sequence regions of 13 protein-coding genes and 2 rRNA genes, we designed primer pairs for the 12S gene, which amplified ~366–465 bp (**Figures 1A,B**), and the CO1 gene, which amplified ~296–302 bp (**Figures 2A,B**). Due to the short amplified sequence lengths, fewer unique sequences and distinguishable genera were identified among the expected amplified sequences from 71 scleractinian species than with previously reported universal primers for the 12S and CO1 genes (Chen and Yu, 2000; Fukami et al., 2008; Nichols and Marko, 2019; **Figures 1B,C, 2B–D**). However, conservation of nucleotide

sequences of primer loci among the 71 scleractinians was higher than of previously reported primers (**Figures 1B,C, 2B–D**), indicating that the designed primers for 12S and CO1 have potential to efficiently amplify DNAs of various scleractinians.

### Sequencing of PCR Amplicons From Environmental DNA

We isolated eDNA from three locations (surface and 2~3 m depth), for the six seawater samples (**Figure 3A**). Then we performed PCR amplification to check whether designed primer pairs could amplify scleractinian genes from seawater eDNA. We obtained PCR products of expected sizes from all eDNA samples with 35 PCR cycles (**Figure 3B**). Using cleaned PCR products, we performed amplicon sequencing using an Illumina MiSeq sequencer (300-bp, paired-end reads). We obtained ~345–528 Mbp (570–872 k reads) from 12S amplicons (**Supplementary Table 4**) and ~439–612 Mbp (740–1,031 k reads) from CO1 amplicons (**Supplementary Table 5**). After quality and adapter trimming, each read pair was merged to obtain full length sequences of PCR amplicons. These merged reads were used for clustering and denoising to prepare ZOTUs from each sample. Then, merged and clustered ZOTUs with 100% nucleotide identity were used to create a database

<sup>4</sup><https://cran.r-project.org/web/packages/pheatmap/>



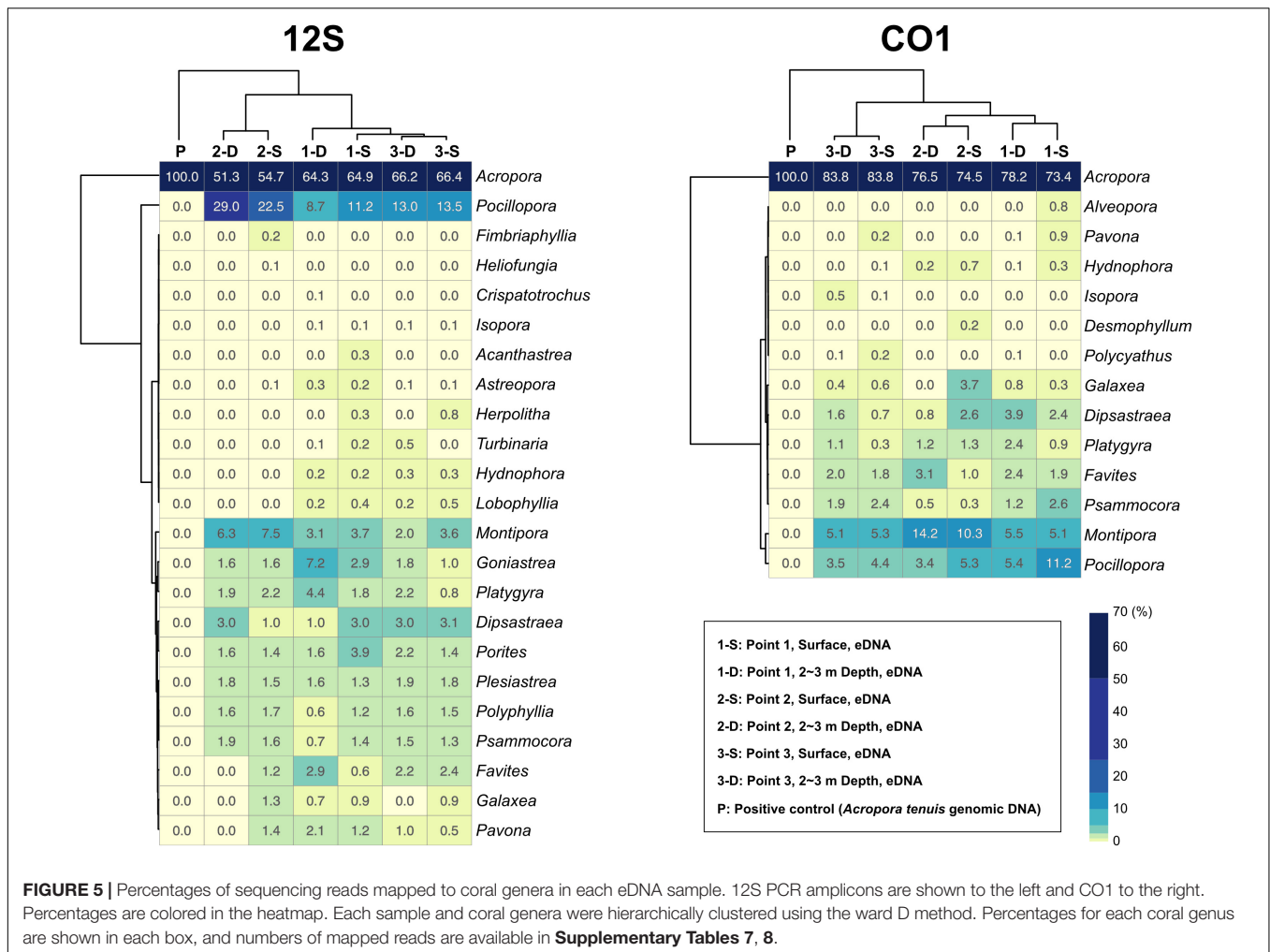
for mapping the merged reads. We obtained 2,193 unique ZOTUs from 12S amplicons and 11,171 unique ZOTUs from CO1 amplicons, which also included sequences from non-scleractinians, respectively. Among those, 1,179 ZOTUs from 12S and 3,366 ZOTUs from CO1 were taxonomically identified as scleractinian (**Supplementary Table 6**). We further selected 1,151 ZOTUs from 12S and 3,356 ZOTUs from CO1 that also showed significant sequence similarities with expected PCR-amplified regions of 12S and CO1 from the 71 scleractinian sequences (BLASTN e-value  $\leq 1e^{-20}$ , percent identity  $\geq 90\%$ , and query coverage  $\geq 95\%$ ). Thus, we concluded that these ZOTUs genuinely originated from scleractinian 12S rRNA and CO1 genes. Numbers of ZOTUs from each eDNA sample are also provided in **Supplementary Tables 4** (12S), **5** (CO1).

92.7% of 12S amplicon reads from eDNA samples were properly mapped to ZOTUs from scleractinians (**Figure 4A** and **Supplementary Table 4**). In contrast, 72% of CO1 amplicon reads from eDNA samples mapped to ZOTUs from scleractinians, whereas 21.8% of reads mapped to ZOTUs from non-scleractinians (**Figure 4A** and **Supplementary Table 5**). Twenty-three genera were detected from 12S amplicons and 14 genera from CO1 amplicons, respectively (**Figure 4B**). Eleven genera were detected from both, and 12 genera were exclusively detected from 12S and three genera from CO1 amplicons (**Figure 4B**). When we used *Acropora tenuis* genomic

DNA as a PCR positive control, almost 100% of reads were mapped to ZOTUs from *Acropora* (**Figure 5**). In all six eDNA samples, almost half of the reads mapped to *Acropora* for both the 12S and CO1 PCR amplicons. The next most abundant genus was *Pocillopora* (12S) and *Montipora* or *Pocillopora* (CO1), respectively (**Figure 5** and **Supplementary Tables 7, 8**). Hierarchical clustering of reads mapped to each genus showed that eDNA samples from both amplicon types were clustered by location, but not by sampling depth (**Figure 5**).

## DISCUSSION

We developed primer pairs that efficiently amplify scleractinian coral DNA (specificity for scleractinian mt genes more than 90% for the 12S ribosomal RNA gene) from eDNA samples. These enabled us to detect eDNA of the most abundant genus *Acropora* at the three sampling points (**Figure 5**). As mentioned above, scleractinian mt genomes are highly conserved between species (Shearer et al., 2002). For example, the 18,479-bp mt genomes of *Acropora digitifera* (NC022830.1) and *A. humilis* (NC022823.1) differ by only 2 bp. Therefore, if mt DNA is used, species-level discrimination of scleractinian corals is almost impossible, even if the whole genome is used. Nevertheless, eDNA analysis targeting mt DNA of scleractinian corals is effective in two regards: easy



PCR amplification from eDNA due to its high copy number, and detection of a wide range of scleractinian genera simultaneously. Mt genes have been widely used for molecular phylogenetic analyses of Scleractinia. As additional mt nucleotide sequence information is registered with NCBI, the accuracy of analyses, especially taxonomic assignments of PCR amplicon sequences from eDNA, will improve. Therefore, we believe that genus-level monitoring of scleractinian corals using eDNA is quite feasible.

### Specificity for Scleractinian Genes and Possible Application to Future Coral Monitoring Using Environmental DNA

Although the distance between sites 2 and 3 is only 730 m (**Figure 3A** and **Supplementary Table 2**), hierarchical clustering based on the percentage of reads mapped to each genus using 12S and CO1 primers was able to separate the three sampling locations, suggesting that this eDNA survey is sufficiently sensitive to differentiate coral communities closer than 1 km. In addition, surface and 2–3-m sample pairs clustered together (**Figure 5**), indicating that eDNA does not vary based on sampling depth at these locations. No differences were observed

in an eDNA survey in western Australia between surface and bottom eDNA samples; thus, sampling from the surface is sufficient (Dugal et al., 2021). In addition, no significant differences in marine metazoan diversity patterns were detected from eDNA samples collected at different depths (Ip et al., 2021). Our results provide additional support for these findings.

Primer pairs that we developed for the 12S and CO1 genes also amplified non-scleractinian genes (**Supplementary Table 6**); however, 92.7% of 12S PCR amplicons and 72% of CO1 amplicons were from scleractinian mt genes (**Figure 4A**). Nichols and Marko (2019) developed a primer pair for CO1 genes (HICORCOX\_F1 and HICORCOX\_R2) and performed eDNA metabarcoding of Hawaiian corals. In our analysis, nucleotide conservation of probable HICORCOX\_F1 and HICORCOX\_R2 binding regions was quite low. 71% of nucleotides for HICORCOX\_F1 and 65% for HICORCOX\_R2 primer positions were identical among the 71 scleractinian species examined here (**Figure 2C**). In contrast, percentages of identical nucleotides in Scl-CO1-Fw and Rv primers were 84 and 87%, respectively (**Figure 2B**), which were also higher than for another universal primer set for the CO1 gene (Fukami et al., 2008), 75% for AcMCOIF and 60% for AcCOIR (**Figure 2D**). The greater

conservation of our Scl-CO1-Fw and Rv primer sequences may be related to the higher percentage of sequencing reads that mapped to scleractinian CO1 genes (72%, **Figure 4A**) than percentages of DNA reads mapped to anthozoan 16S (61%) and CO1 markers (51%) (Nichols and Marko, 2019). Although it may be related to differences of benthic fauna, the percentages of scleractinians among PCR amplicons using primer pairs, CoralITS2 and CoralITS2\_acro, for nuclear ITS-2 genes were around 50% (46.7 and 57.5%, respectively) (Alexander et al., 2020), and those primer pairs sometimes required more PCR cycles (45 cycles), depending on sampling sites (Dugal et al., 2021). Note that percentages of identical nucleotides for Scl-12S-Fw and Rv primers were 86 and 95%, respectively (**Figure 1B**), higher than those of other 12S universal primers, 75% for ANTMTSSU-F and 85% for ANTMTSSU-R (Chen and Yu, 2000; **Figure 1C**) and primers mentioned above for the CO1 gene, indicating high specificity of Scl-12S-Fw and Rv primers for scleractinian mt genes.

With regard to the percentage of PCR amplicon sequences that properly mapped to scleractinian mt genes, our 12S primers (92%) discriminate much more effectively than our CO1 primers (72%) (**Figure 4A**). The number of scleractinian genera detected using 12S primers from eDNA (23 genera) was also larger than for CO1 (14 genera); however, three genera were detected exclusively by our CO1 primers (**Figure 4B**), possibly reflecting differences in numbers and species of sequences deposited in the NCBI database to date. Therefore, to maximize the number of coral genera that can be detected using eDNA, it may be suitable to use both 12S and CO1 primers. If eDNA surveys aim to investigate animals other than stony corals at the same time, previously reported metabarcoding primers would be more useful. However, if eDNA surveys need to target only stony corals, the method reported here would yield the best data. Nonetheless, it will be important to verify the effectiveness of our primers by deploying them in various coral reef environments. We hope that the primer pairs we developed for 12S and CO1 genes will become a powerful tool for coral reef monitoring using eDNA and that they will be applied to coral reefs globally.

## REFERENCES

- Alexander, J. B., Bunce, M., White, N., Wilkinson, S. P., Adam, A. A. S., Berry, T., et al. (2020). Development of a multi-assay approach for monitoring coral diversity using eDNA metabarcoding. *Coral Reefs* 39, 159–171. doi: 10.1007/s00338-019-01875-9
- Bohmann, K., Evans, A., Gilbert, M. T., Carvalho, G. R., Creer, S., Knapp, M., et al. (2014). Environmental DNA for wildlife biology and biodiversity monitoring. *Trends Ecol. Evol.* 29, 358–367. doi: 10.1016/j.tree.2014.04.003
- Chen, C. A., and Yu, J. K. (2000). Universal primers for amplification of mitochondrial small subunit ribosomal RNA-Encoding gene in scleractinian corals. *Mar. Biotechnol. (NY)* 2, 146–153. doi: 10.1007/s101269900018
- De'ath, G., Fabricius, K. E., Sweatman, H., and Puotinen, M. (2012). The 27-year decline of coral cover on the Great Barrier Reef and its causes. *Proc. Natl. Acad. Sci. U. S. A.* 109, 17995–17999. doi: 10.1073/pnas.1208909109
- Dugal, L., Thomas, L., Wilkinson, S. P., Richards, Z. T., Alexander, J. B., Adam, A. A. S., et al. (2021). Coral monitoring in northwest Australia with environmental DNA metabarcoding using a curated reference database for optimized detection. *Environ. DNA*, 1–14. doi: 10.1002/edn3.199
- Edgar, R. C. (2010). Search and clustering orders of magnitude faster than BLAST. *Bioinformatics* 26, 2460–2461. doi: 10.1093/bioinformatics/btq461
- Fourment, M., and Holmes, E. C. (2016). Seqotron: a user-friendly sequence editor for Mac OS X. *BMC Res. Notes* 9:106. doi: 10.1186/s13104-016-1927-4
- Fukami, H. (2008). Short review: molecular phylogenetic analyses of reef corals. *Galaxea* 10, 47–55. doi: 10.3755/galaxea.10.47
- Fukami, H., Chen, C. A., Budd, A. F., Collins, A., Wallace, C., Chuang, Y. Y., et al. (2008). Mitochondrial and nuclear genes suggest that stony corals are monophyletic but most families of stony corals are not (Order Scleractinia, Class Anthozoa, Phylum Cnidaria). *PLoS One* 3:e3222. doi: 10.1371/journal.pone.0003222
- Ip, Y. C. A., Tay, Y. C., Chang, J. J. M., Ang, H. P., Tun, K. P. P., Chou, L. M., et al. (2021). Seeking life in sedimented waters: environmental DNA from diverse habitat types reveals ecologically significant species in a tropical marine environment. *Environ. DNA* 3, 654–668. doi: 10.1002/edn3.162
- Katoh, K., and Standley, D. M. (2013). MAFFT multiple sequence alignment software version 7: improvements in performance and usability. *Mol. Biol. Evol.* 30, 772–780. doi: 10.1093/molbev/mst010

## DATA AVAILABILITY STATEMENT

The datasets presented in this study can be found in online repositories. The names of the repository/repositories and accession number(s) can be found below: BioProject, PRJDB12132.

## AUTHOR CONTRIBUTIONS

JI analyzed mitochondrial genomes of scleractinian corals. CS developed primers, performed bioinformatic analyses, and prepared the manuscript. HN and KN performed molecular biology experiments and PCR amplicon sequencing using the Illumina MiSeq. TN performed water sampling. NS coordinated the project and provided equipment and reagents for experiments. All authors read and commented on the manuscript.

## FUNDING

This study was supported by JSPS KAKENHI grants (20H03235 and 20K21860 for CS and 21H04922 for JI) and FSI project Ocean DNA: Constructing “Bio-map” of Marine Organisms using DNA Sequence Analyses from the University of Tokyo. This study was also supported by OIST research funding to the Marine Genomics Unit (NS).

## ACKNOWLEDGMENTS

We thank Megumi Kanai and Syuichi Mekaru for helping water sampling.

## SUPPLEMENTARY MATERIAL

The Supplementary Material for this article can be found online at: <https://www.frontiersin.org/articles/10.3389/fmars.2021.758207/full#supplementary-material>



- Kelly, R. P., Port, J. A., Yamahara, K. M., Martone, R. G., Lowell, N., Thomsen, P. F., et al. (2014). Environmental monitoring. Harnessing DNA to improve environmental management. *Science* 344, 1455–1456. doi: 10.1126/science.1251156
- Kitahara, M. V., Cairns, S. D., Stolarski, J., Blair, D., and Miller, D. J. (2010). A comprehensive phylogenetic analysis of the Scleractinia (Cnidaria, Anthozoa) based on mitochondrial CO1 sequence data. *PLoS One* 5:e11490. doi: 10.1371/journal.pone.0011490
- Kitahara, M. V., Fukami, H., Benzoni, F., and Huang, D. (2016). “The new systematics of scleractinia: integrating molecular and morphological evidence,” in *The Cnidaria, Past, Present and Future: The World of Medusa and her Sisters*, eds S. Goffredo and Z. Dubinsky (Cham: Springer International Publishing), 41–59.
- Knowlton, N., Brainard, R. E., Fisher, R., Moews, M., Plaisance, L., and Caley, M. J. (2010). “Coral reef biodiversity,” in *Life in the World's Oceans: Diversity, Distribution, and Abundance*, ed. A. D. McIntyre (Chichester: Wiley-Blackwell), 65–79.
- Li, W., and Godzik, A. (2006). Cd-hit: a fast program for clustering and comparing large sets of protein or nucleotide sequences. *Bioinformatics* 22, 1658–1659. doi: 10.1093/bioinformatics/btl158
- Lin, M. F., Luzon, K. S., Licuanan, W. Y., Ablan-Lagman, M. C., and Chen, C. A. (2011). Seventy-four universal primers for characterizing the complete mitochondrial genomes of scleractinian corals (Cnidaria; Anthozoa). *Zool. Stud.* 50, 513–524.
- Martin, M. (2011). Cutadapt removes adapter sequences from high-throughput sequencing reads. *EMBnet J.* 17:10. doi: 10.14806/ej.17.1.200
- Minamoto, T., Miya, M., Sado, T., Seino, S., Doi, H., Kondoh, M., et al. (2021). An illustrated manual for environmental DNA research: water sampling guidelines and experimental protocols. *Environ. DNA* 3, 8–13. doi: 10.1002/edn3.121
- Miya, M., Sato, Y., Fukunaga, T., Sado, T., Poulsen, J. Y., Sato, K., et al. (2015). MiFish, a set of universal PCR primers for metabarcoding environmental DNA from fishes: detection of more than 230 subtropical marine species. *R. Soc. Open Sci.* 2:150088. doi: 10.1098/rsos.150088
- Nichols, P. K., and Marko, P. B. (2019). Rapid assessment of coral cover from environmental DNA in Hawai'i. *Environ. DNA* 1, 40–53. doi: 10.1002/edn3.8
- R Core Team (2015). *R: A Language and Environment for Statistical Computing*. Vienna: R Foundation for Statistical Computing.
- Shearer, T. L., Van Oppen, M. J., Romano, S. L., and Worheide, G. (2002). Slow mitochondrial DNA sequence evolution in the Anthozoa (Cnidaria). *Mol. Ecol.* 11, 2475–2487.
- Shinzato, C., Zayasu, Y., Kanda, S., Kawamitsu, M., Satoh, N., Yamashita, H., et al. (2018). Using seawater to document coral-zoothanthella diversity: a new approach to coral reef monitoring using environmental DNA. *Front. Mar. Sci.* 5:28. doi: 10.3389/fmars.2018.00028
- Untergasser, A., Nijveen, H., Rao, X., Bisseling, T., Geurts, R., and Leunissen, J. A. (2007). Primer3Plus, an enhanced web interface to Primer3. *Nucleic Acids Res.* 35, W71–W74. doi: 10.1093/nar/gkm306
- Yamamoto, S., Masuda, R., Sato, Y., Sado, T., Araki, H., Kondoh, M., et al. (2017). Environmental DNA metabarcoding reveals local fish communities in a species-rich coastal sea. *Sci. Rep.* 7:40368. doi: 10.1038/srep40368

**Conflict of Interest:** The authors declare that the research was conducted in the absence of any commercial or financial relationships that could be construed as a potential conflict of interest.

**Publisher's Note:** All claims expressed in this article are solely those of the authors and do not necessarily represent those of their affiliated organizations, or those of the publisher, the editors and the reviewers. Any product that may be evaluated in this article, or claim that may be made by its manufacturer, is not guaranteed or endorsed by the publisher.

Copyright © 2021 Shinzato, Narisoko, Nishitsuji, Nagata, Satoh and Inoue. This is an open-access article distributed under the terms of the Creative Commons Attribution License (CC BY). The use, distribution or reproduction in other forums is permitted, provided the original author(s) and the copyright owner(s) are credited and that the original publication in this journal is cited, in accordance with accepted academic practice. No use, distribution or reproduction is permitted which does not comply with these terms.



# Endosymbiont Communities in *Pachyseris speciosa* Highlight Geographical and Methodological Variations

Sudhanshi S. Jain<sup>1\*</sup>, Lutfi Afiq-Rosli<sup>1,2</sup>, Bar Feldman<sup>3</sup>, Ismael Kunning<sup>4</sup>, Oren Levy<sup>3</sup>, Ralph R. Mana<sup>4</sup>, Benjamin J. Wainwright<sup>5</sup> and Danwei Huang<sup>1,2,6,7\*</sup>

<sup>1</sup> Department of Biological Sciences, National University of Singapore, Singapore, Singapore, <sup>2</sup> Tropical Marine Science Institute, National University of Singapore, Singapore, Singapore, <sup>3</sup> The Mina and Everard Goodman Faculty of Life Sciences, Bar-Ilan University, Ramat Gan, Israel, <sup>4</sup> School of Natural and Physical Sciences, University of Papua New Guinea, Port Moresby, Papua New Guinea, <sup>5</sup> Yale-NUS College, National University of Singapore, Singapore, Singapore, <sup>6</sup> Centre for Nature-Based Climate Solutions, National University of Singapore, Singapore, Singapore, <sup>7</sup> Lee Kong Chian Natural History Museum, National University of Singapore, Singapore, Singapore

## OPEN ACCESS

### Edited by:

Shashank Keshavmurthy,  
Academia Sinica, Taiwan

### Reviewed by:

Hui Huang,  
South China Sea Institute  
of Oceanology, Chinese Academy  
of Sciences (CAS), China  
Daniel J. Thornhill,  
National Science Foundation (NSF),  
United States

### \*Correspondence:

Sudhanshi S. Jain  
jain.sudhanshi@gmail.com  
Danwei Huang  
huangdanwei@nus.edu.sg

### Specialty section:

This article was submitted to  
Coral Reef Research,  
a section of the journal  
Frontiers in Marine Science

**Received:** 17 August 2021

**Accepted:** 18 November 2021

**Published:** 22 December 2021

### Citation:

Jain SS, Afq-Rosli L, Feldman B,  
Kunning I, Levy O, Mana RR,  
Wainwright BJ and Huang D (2021)  
Endosymbiont Communities  
in *Pachyseris speciosa* Highlight  
Geographical and Methodological  
Variations. *Front. Mar. Sci.* 8:759744.  
doi: 10.3389/fmars.2021.759744

Reef-building corals live in symbiosis with the phototrophic dinoflagellate family Symbiodiniaceae, which comprises diverse genera such as *Cladocopium* and *Durisdinium*. *Pachyseris speciosa*, a widely distributed Indo-Pacific coral found in a variety of reef habitats, is known to be associated with these two Symbiodiniaceae genera, but little is known about the biogeographic variability of the endosymbiont communities across the region. In this study, the diversity and dominance patterns of Symbiodiniaceae at the western and eastern areas of the Central Indo-Pacific region were examined. We sampled *Pachyseris speciosa* colonies at seven and six sites in Singapore and Papua New Guinea, respectively, and genotyped their endosymbionts based on the internal transcribed spacer (ITS) markers using two distinct methods, quantitative polymerase chain reaction (qPCR) and high-throughput sequencing (HTS). Results showed 92% of all colonies in Singapore exhibiting *Cladocopium* dominance. There was a higher abundance of *Durisdinium* compared to *Cladocopium* in certain colonies from one site, Pulau Hantu (mean *Durisdinium* abundance of 90%, compared to 0–14% among all other sites). In contrast, variation in the endosymbiont communities was generally higher among sites in Papua New Guinea. *Cladocopium* expectedly dominated most colonies (75%), although colonies from Kimbe Bay (85%) and Kavieng (65%) showed *Durisdinium* dominance. Between localities, relative genus abundances based on qPCR were not significantly different, but HTS showed that the ratio of *Durisdinium* over *Cladocopium* was significantly higher in Papua New Guinea corals. Notably, 6% of colonies from Singapore and 15% from Papua New Guinea showed endosymbiont dominance patterns that were inconsistent between the two methods, underscoring the need for further validation of symbiotic algal quantification based on HTS. The richness of ITS2 type profiles was clearly lower among colonies from the impacted and turbid reefs of Singapore compared to the less urbanized

reefs of Papua New Guinea. These coral intraspecific variations of Symbiodiniaceae communities within and among localities suggest that local conditions are important drivers of endosymbiosis and may ultimately influence corals' resilience against global stressors such as ocean warming.

**Keywords:** Central Indo-Pacific, high-throughput sequencing, internal transcribed spacer, qPCR, reef corals, Scleractinia, Symbiodiniaceae

## INTRODUCTION

Reef-building stony corals (Cnidaria: Anthozoa: Scleractinia) are associated with the dinoflagellate alga Symbiodiniaceae, forming an ecologically critical symbiotic relationship (Falkowski et al., 1984; Stanley and Fautin, 2001; Baker, 2003). The partnership yields multiple ecological benefits for both the coral host and algal endosymbiont, providing the basis of the tropical coral reef ecosystem and its survival. Symbiotic corals depend on the photosynthetic activities of their mutualistic dinoflagellates (Boilard et al., 2020; LaJeunesse, 2020), or Symbiodiniaceae, to produce the energy required for calcium carbonate skeletal growth of the coral hosts, ultimately driving coral reef development (Al-Horani et al., 2003). In return, *in hospite* Symbiodiniaceae cells are provided with a light-enriched environment and the by-products of host metabolism (Banin et al., 2003).

These extremely diverse microalgae are currently recognized as several phylogenetically distinct genera (LaJeunesse et al., 2018; Boilard et al., 2020). Reef-building stony corals typically host multiple Symbiodiniaceae species and are most commonly associated with four genera (*Symbiodinium*, *Breviolum*, *Cladocopium*, and *Durusdinium*) (Rowan and Knowlton, 1995; Baker, 2003; Little et al., 2004; Stat et al., 2008b). The endosymbiont community may grant varying degrees of fitness to the coral host depending on the holobiont's capability to tolerate environmental stressors and bleaching (Baker, 2001; Stat et al., 2011).

Symbiodiniaceae endosymbiont community composition has been shown to vary between biogeographic regions, host species, reef depth, light accessibility and shifting environmental dynamics, among other factors (Rowan and Knowlton, 1995; Rowan et al., 1997; Stat et al., 2008a; Rouzé et al., 2016; Eckert et al., 2020; Hume et al., 2020). In particular, the diversity of Symbiodiniaceae in various geographic locations and host taxa has been studied extensively (LaJeunesse, 2002; LaJeunesse et al., 2004; Huang et al., 2011; Keshavmurthy et al., 2014; Hume et al., 2015; Leveque et al., 2019; Terraneo et al., 2019; Teschima et al., 2019; Tan et al., 2020). For example, latitudinal variation in Symbiodiniaceae genus dominance has been observed in the Saudi Arabian Red Sea, with shifts from *Cladocopium* dominance to *Durusdinium* dominance in *Porites* colonies along a north-south gradient (Terraneo et al., 2019; see also Chen et al., 2019). Fundamentally, with *Cladocopium* and *Durusdinium* known to be the most abundant endosymbionts in tropical reefs, corals hosting *Durusdinium* were initially thought to be more tolerant against thermal stress and turbidity fluctuations (Stat and Gates, 2011; Silverstein et al., 2015), whereas *Cladocopium* was generally

considered the more stress-sensitive genus (Chen et al., 2003; Stat and Gates, 2011). However, it is now well understood that *Cladocopium* is found in corals throughout a large depth range and among multiple host species, and even when present in marginal conditions, there may be taxon-specific associations and local adaptations that result in it being the dominant genus (Hume et al., 2015; Rouzé et al., 2016; Innis et al., 2018). For example, corals in the Red Sea exhibit strong species-specific associations and display *Cladocopium* dominance despite a strong latitudinal gradient and facing high temperatures (Ziegler et al., 2017; Osman et al., 2020). Similarly, corals withstanding extreme temperatures in the Persian Gulf maintain predominant associations with *Cladocopium* (Howells et al., 2020).

The diversity and functioning of specific coral-Symbiodiniaceae relationships rely on the sensitivity of symbionts to thermal stress, irradiance and/or host-specificity (LaJeunesse et al., 2004). The composition of the symbionts within the host can be influenced by changing environments and driven by various host or symbiont processes (Kemp et al., 2014). Community alterations are achieved via "switching" (changes in the endosymbiont community composition via exchange of symbionts from the environment) or "shuffling" (shifts in the relative abundances of present symbionts) (Baker, 2003). The holobiont's capacity to undergo these "switching" or "shuffling" processes is vital for its resilience against environmental stress (Baker, 2004; Sampayo et al., 2008; Kemp et al., 2014). More generally, the persistence of coral reefs and the survival of its associated organisms depend greatly on the responses of the coral-Symbiodiniaceae relationship to environmental change (Arif et al., 2014). Seeing as temperature anomalies due to global warming are predicted to occur more frequently (Hughes et al., 2017a,b), studying the diversity of symbionts in different regions is critical for understanding geographic variations in coral reef persistence.

The zooxanthellate coral, *Pachyseris speciosa*, is one of the most common and abundant corals found in the Central Indo-Pacific region with a wide distribution through various depths (DeVantier and Turak, 2017; Bongaerts et al., 2021). Symbiodiniaceae communities hosted by *P. speciosa* have been examined in the Great Barrier Reef, Red Sea, French Polynesia, and Singapore (LaJeunesse et al., 2004; Bongaerts et al., 2011; Ziegler et al., 2015b; Tanzil et al., 2016; Goulet et al., 2019; Meistertzheim et al., 2019; Jain et al., 2020; Smith et al., 2020). However, little is known about the biogeographic variabilities of its endosymbionts across the Central Indo-Pacific as comparisons among localities are limited.

Despite chronically high sediment deposition, turbidity and low light levels, the hyper-urbanized shores of Singapore have

been home to 255 stony coral species (Huang et al., 2009). *Pachyseris speciosa* is one of the most common corals dominating the shallow reefs here (Wong et al., 2018; Chow et al., 2019) and is associated with *Cladocopium* and *Durisdinium* (Tanzil et al., 2016; Jain et al., 2020; Smith et al., 2020). By contrast, Papua New Guinea, which is generally much less affected by urbanization, has a greater coral diversity and is part of the Coral Triangle (Allen et al., 2003; Veron et al., 2011, 2015). Its reefs hold more than 500 stony species that are of vital importance to the local communities and their self-sustainable lifestyles (Allen et al., 2003; Nicholls, 2004; The Nature Conservancy, 2004). Apart from a study investigating the response of endosymbiont communities to elevated carbon dioxide, little is known about the Symbiodiniaceae communities associated with *P. speciosa* here (Noonan et al., 2013).

In this study, we characterize the relative abundances of *Cladocopium* and *Durisdinium* across various sites in Singapore and Papua New Guinea using two distinct quantification methods, quantitative polymerase chain reaction (qPCR) and high-throughput sequencing (HTS). The universal presence and known association of *Pachyseris speciosa* with *Cladocopium* and *Durisdinium* allow their relative abundances to be examined among coral colonies from the two regions. Here, we quantify genus abundances and dominance by the relative concentrations of the nuclear ribosomal internal transcribed spacer 1 (ITS1) region for *Durisdinium* and *Cladocopium* as evaluated by qPCR, and by the relative HTS read abundances of the internal transcribed spacer 2 (ITS2) region for the two genera. In accordance with the SymPortal framework (Hume et al., 2019), we also report on the ITS2 type profiles of *P. speciosa* that account for intragenomic variation and are representative of putative Symbiodiniaceae species. Our data on the relative abundances of the endosymbiont taxa between the western and eastern Central Indo-Pacific highlight the regional biogeographic drivers of similarities and differences in Symbiodiniaceae diversity. Furthermore, a sympatric species complex representing three distinct lineages of *P. speciosa* has been discovered recently (Bongaerts et al., 2021; Feldman et al., 2021). Using a cleaved amplified polymorphic sequence (CAPS) assay, we uncover the different *P. speciosa* lineages from our collections and determine whether they affect Symbiodiniaceae genus dominance. Additionally, we test the interchangeability of using qPCR and HTS to detect relative abundances of *Cladocopium* and *Durisdinium* based on a larger and geographically wider set of samples relative to our previous study (Jain et al., 2020).

## MATERIALS AND METHODS

### Field Collections

Reefs at Singapore and Papua New Guinea were accessed via SCUBA and *Pachyseris speciosa* colonies were haphazardly sampled using a hammer and chisel. A total of 266 colonies were sampled, including 146 from seven different sites in Singapore between 25th and 31st May 2018. Between 18 and 25 samples were collected each from Terumbu Pempang Tengah (1°13'45.1"N 103°43'50.5"E), St. John's Island (01°13'09.0"N

103°50'44.0"E), Pulau Semakau (01°12'11.5"N 103°45'15.0"E), Sisters' Island (or Pulau Subar Laut; 01°12'49.0"N 103°49'59.0"E), Pulau Hantu (01°13'36.5"N 103°44'47.0"E), Raffles Lighthouse (or Pulau Satumu; 01°09'36.5"N 103°44'24.0"E) and Kusu Island (or Pulau Tembakul; 01°13'33.0"N 103°51'34.0"E). From Papua New Guinea, 120 samples were taken, comprising 20 colonies from each of six sites – Kimbe Bay (5°09'55.2"S 150°30'00.2"E), Rabaul (4°12'13.9"S 152°09'54.6"E), Kavieng (2°33'02.1"S 150°47'42.2"E), Madang (5°13'54.0"S 145°48'05.3"E), Milne Bay (10°25'50.5"S 150°43'13.4"E) and Port Moresby (9°27'54.0"S 147°08'34.5"E) – between 1st and 28th September 2018 (Figure 1). All sampled fragments were transported to the laboratory in seawater and fixed in 100% molecular grade ethanol, or stored in 20% salt-saturated DMSO immediately following collection.

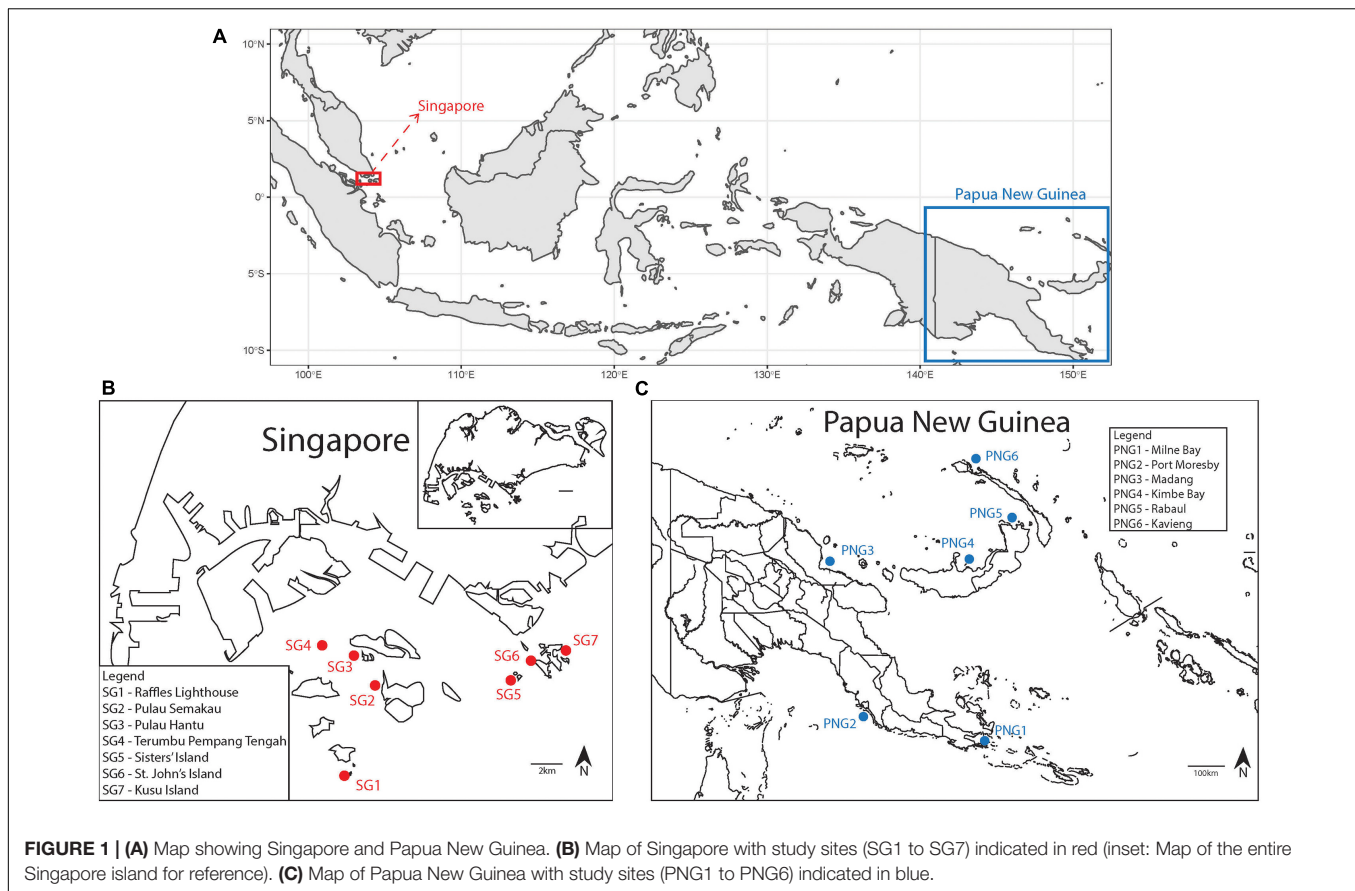
### DNA Extraction

Total genomic DNA was extracted from all the 146 Singapore samples and 120 Papua New Guinea samples using the DNeasy Blood and Tissue Kit (Qiagen Inc., Hilden, Germany) according to the manufacturer's protocol. A 2–4 cm<sup>2</sup> fragment of coral tissue was used for each sample extraction. Fragments were cut into smaller pieces using sterile forceps and scissors prior to addition of buffers. DNA was eluted in 150 µL nuclease-free water. Extracted DNA samples were stored at –80°C until further processing.

### Quantitative Polymerase Chain Reaction

The ITS1 region, located between the 18S and 5.8S rRNA genes, was targeted for the quantification of relative *Cladocopium* and *Durisdinium* rDNA copy numbers. Two samples from a previous study were used to generate concentration standards for the ITS1 amplicons of *Cladocopium* and *Durisdinium* (Jain et al., 2020). The amplicons were quantified using Qubit dsDNA HS Assay Kit (Thermo Fisher Scientific, MA, United States) with the Life Technologies Qubit 3.0 Fluorometer (Thermo Fisher Scientific, MA, United States) and then diluted to 50 ng/µL. For amplification of *Cladocopium*, the universal forward primer [5'-AAG GAG AAG TCG TAA CAA GGT TTC C-3' (Ulstrup and Van Oppen, 2003)] and *Cladocopium*-specific reverse primer [5'-AAG CAT CCC TCA CAG CCA AA-3' (Ulstrup and Van Oppen, 2003)] were used. For *Durisdinium*, the universal forward primer and the *Durisdinium*-specific reverse primer [5'-CAC CGT AGT GGT TCA CGT GTA ATA G-3' (Ulstrup and Van Oppen, 2003)] were used. The amplification profile consisted of an initial denaturation at 95°C for 3 min, followed by 40 cycles of 95°C for 30 s, 53°C for 45 s, 72°C for 45 s and a 5 min extension step at 72°C. The size of the PCR products (~100 bp) was confirmed with gel electrophoresis. The products were then purified using SureClean Plus (Bioline Inc., London, United Kingdom) and quantified with the Qubit assay as mentioned above. Amplicon concentration standards were prepared by diluting the purified PCR product to 1 ng/µL, and then serially diluting to get 10 standards (1 to 10<sup>-9</sup> ng/µL) each for *Cladocopium* and *Durisdinium*. All standards were run alongside each qPCR experiment.





**FIGURE 1 | (A)** Map showing Singapore and Papua New Guinea. **(B)** Map of Singapore with study sites (SG1 to SG7) indicated in red (inset: Map of the entire Singapore island for reference). **(C)** Map of Papua New Guinea with study sites (PNG1 to PNG6) indicated in blue.

All DNA extracts were quantified and diluted to 1 ng/ $\mu$ L. SsoAdvanced SYBR Green SuperMix (Bio-Rad, CA, United States), the above-mentioned primers (Ulstrup and Van Oppen, 2003) and diluted standardized DNA template were used for qPCR using the CFX96 Touch<sup>TM</sup> Real-Time PCR Detection System (Bio-Rad, CA, United States). All standards and samples were run in triplicates. The thermocycling profile used consists of an initial denaturation at 98°C for 3 min followed by 40 cycles of 95°C for 15 s and 60°C for 30 s. A melt curve analysis from 65 to 95°C (0.5°C increase per 5 s) was subsequently performed to verify the specificity of the amplification.

CFX Manager Software (Bio-Rad, CA, United States) was used to analyze the efficiency of standards and to enumerate the relative quantities of *Cladocopium* and *Durisdinium* (expressed as log-scaled ratio of *Durisdinium* concentration to *Cladocopium* concentration) in each sample based on the standard curve, following Jain et al. (2020).

## Illumina Library Preparation, Sequencing and Bioinformatics

The ITS2 region, located between the 5.8S and 28S rRNA genes, was targeted for conventional PCR and HTS. All DNA extracts were quantified and diluted to 1 ng/ $\mu$ L. Reagent volumes, PCR cycling conditions and PCR clean-up protocols followed the 16S Metagenomic Sequencing Library Preparation guide for the Illumina MiSeq System (Illumina, 2013). This

two-step protocol included an amplicon PCR (1st step) with the ITS2-specific SYM\_VAR primer pair [SYM\_VAR\_5.8S2: 5'-GAATTGCAGAACTCCGTGAACC-3' (Hume et al., 2015), SYM\_VAR\_REV: 5'-CGGGTTCWCTTGTYTGACTTCATGC-3' (Hume et al., 2013)]. The index PCR (2nd step) added unique dual indexes (see **Supplementary Table 1**) and adapters complementary to the MiSeq flow cell for binding. Indexed PCR products were normalized using the SequalPrep<sup>TM</sup> Normalization Plate Kit (Thermo Fisher Scientific, MA, United States), pooled and sequenced on the Illumina MiSeq sequencing platform (V3 chemistry; 30% PhiX spike-in) for 300-bp paired-end reads.

Demultiplexed paired fastq.gz files containing Symbiodiniaceae ITS2 reads were analyzed using the SymPortal framework (Hume et al., 2019), run locally. Briefly, sequence filtering and a standardized quality control pipeline were conducted using mothur 1.39.5 (Schloss et al., 2009), the BLAST + suite (Camacho et al., 2009) and minimum entropy decomposition (MED; Eren et al., 2015).

## Identifying Distinct Lineages of *Pachyseris speciosa*

Bongaerts et al. (2021) discovered distinct lineages within *Pachyseris speciosa* that represented a sympatric species complex and developed a CAPS assay to identify each of the lineages. The three lineages were referred to as “green,” “blue” and “red”

(see also Feldman et al., 2021). To determine whether the different lineages influenced Symbiodiniaceae genus dominance in the corals studied here, we performed the CAPS assay on our *P. speciosa* samples.

DNA extracted from all the colonies from Singapore ( $n = 146$ ) was assigned to one of the three lineages using the CAPS assay following Bongaerts et al. (2021). As we found no link between host lineage and Symbiodiniaceae genus dominance in the Singapore samples (see below), up to five randomly chosen samples from each site in Papua New Guinea ( $n = 21$ ) were tested. Briefly, total DNA extracted from each sample was amplified using lineage-specific primers (PsPe-Green, PsPe-Blue and PsPe-Red) and purified using SureClean Plus. Purified products were then digested with the associated restriction enzyme (Green-*Hha*I, Blue-*Hae*III, and Red-*Taq*α1, respectively) and digestion verified on a 3% gel. Following enzymatic digestion, the “green” or “blue” lineage was determined with positive digestion observed using the associated *Hha*I and *Hae*III restriction enzyme. The “red” lineage was assigned to samples showing no digestion using the *Taq*α1 restriction enzyme. To verify digestion of PCR amplicons that could not be visualized through gel imaging, the purified PCR products were sequenced using Sanger sequencing. The sequences were analyzed in Geneious Prime 2020.2.4 (Kearse et al., 2012) and a virtual digest was performed to determine the lineages.

## Statistical Analyses

Data were analyzed using R 3.6.1 (R Core Team, 2017). Two separate runs of the nested analysis of variance (ANOVA) were performed to assess the differences in ITS1 and ITS2 *Durusdinium* to *Cladocopium* ratios among sites in each locality and between the two localities. Specifically, the ratio of *Durusdinium* to *Cladocopium* ITS1 concentrations for each sample obtained from the qPCR experiments were compared between localities (Singapore vs. Papua New Guinea) with sites nested within localities. Separately, the ratios of *Durusdinium* to *Cladocopium* ITS2 HTS read abundances were also compared between the two localities with sites nested within localities. The Tukey test was further performed to resolve statistical differences between sites in each locality.

To determine if and how the qPCR tests and HTS reads were comparable in the relative *Durusdinium* vs. *Cladocopium* levels obtained, we ran a linear model to quantify the relationship between relative (*Durusdinium* divided by *Cladocopium*) ITS1 concentrations and ITS2 read abundances at the sample level. Data were log-transformed for normality and homoscedasticity.

To characterize the geographical variation of Symbiodiniaceae communities at different localities and sites, we report the ITS2 type profiles obtained from SymPortal.

## RESULTS

### Quantitative Polymerase Chain Reaction

The qPCR quantification of the relative abundances of *Durusdinium* vs. *Cladocopium* ITS1 in the 146 colonies sampled

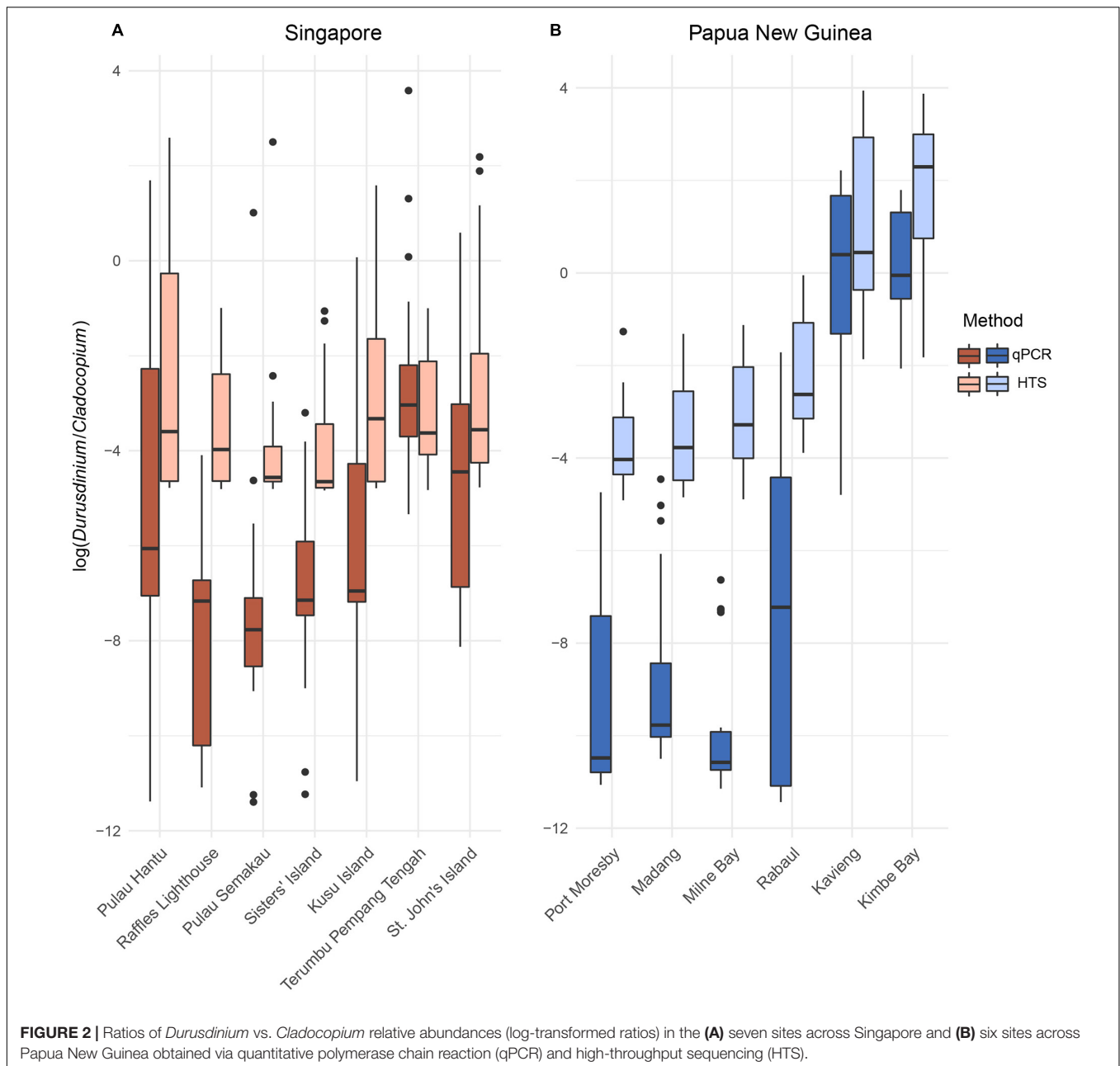
across Singapore showed limited variation among the seven sites examined (Terumbu Pempang Tengah, St. John's Island, Pulau Semakau, Sisters' Island, Pulau Hantu, Raffles Lighthouse and Kusu Island;  $p = 0.392$ ,  $df = 6$ ,  $F = 1.056$ ; **Figure 2**). *Post hoc* Tukey tests further revealed insignificant pairwise site differences in the ratios of the relative abundances of *Durusdinium* vs. *Cladocopium* ( $p$  values ranging from 0.4 to 1).

Among the 120 Papua New Guinea colonies, the ITS1 ratios were significantly different between sites (Port Moresby, Madang, Milne Bay, Rabaul, Kavieng, and Kimbe Bay;  $p < 0.001$ ,  $df = 5$ ,  $F = 7.136$ ) with *post hoc* Tukey tests revealing significantly greater proportions of *Durusdinium* in colonies sampled from Kavieng compared to the other four sites (Madang, Milne Bay, Rabaul and Port Moresby;  $p < 0.001$ ). There were no significant differences in the relative abundances of *Cladocopium* and *Durusdinium* between samples from Madang, Milne Bay, Rabaul and Port Moresby. Overall, ITS1 *Durusdinium* to *Cladocopium* ratios between Singapore and Papua New Guinea were not significantly different ( $p = 0.494$ ,  $df = 1$ ,  $F = 0.470$ ).

### High-Throughput Sequencing

Illumina sequencing reads of the 146 *Pachyseris speciosa* colonies sampled across the seven sites in Singapore yielded a total of 19,721,036 raw reads, resulting in 9,860,518 contigs. Following quality control and sequence filtering, a total of 8,113,743 Symbiodiniaceae ITS2 sequences comprising 77,067 unique sequences were retained. The relative abundances of *Durusdinium* vs. *Cladocopium* ITS2 reads within the 146 coral colonies were not significantly different between the seven sites in Singapore ( $p = 0.118$ ,  $df = 6$ ,  $F = 1.732$ ; **Figure 2**). *Post hoc* Tukey tests indicated higher proportions of *Durusdinium* in colonies from Pulau Hantu compared to Raffles Lighthouse ( $p = 0.131$ ), although no statistically significant differences were detected among all sites. These statistical similarities and differences between the sites in Singapore were generally consistent with patterns obtained with ITS1 ratios.

Illumina sequencing reads of the 120 *Pachyseris speciosa* colonies sampled across the six sites in Papua New Guinea yielded a total of 20,018,361 raw reads, resulting in 10,365,381 raw contigs. Following quality control and sequence filtering, a total of 7,688,010 Symbiodiniaceae ITS2 sequences comprising 93,003 unique sequences were retained. The relative abundances of *Durusdinium* vs. *Cladocopium* ITS2 reads were significantly different among the six Papua New Guinea sites ( $p = 0.0032$ ,  $df = 5$ ,  $F = 3.801$ ). *Post hoc* Tukey test showed larger proportions of *Durusdinium* detected in colonies from Kavieng compared to those from Madang, Milne Bay, Rabaul and Port Moresby ( $p < 0.05$ ). There were no significant differences in the relative abundances of *Cladocopium* and *Durusdinium* between samples from Madang, Milne Bay, Rabaul and Port Moresby. Colonies from Kimbe Bay and Kavieng had similar proportions of *Durusdinium*. These results were consistent with the relative abundances derived from qPCR. However, the ITS2 *Durusdinium* vs. *Cladocopium* ratios based on HTS showed significant differences



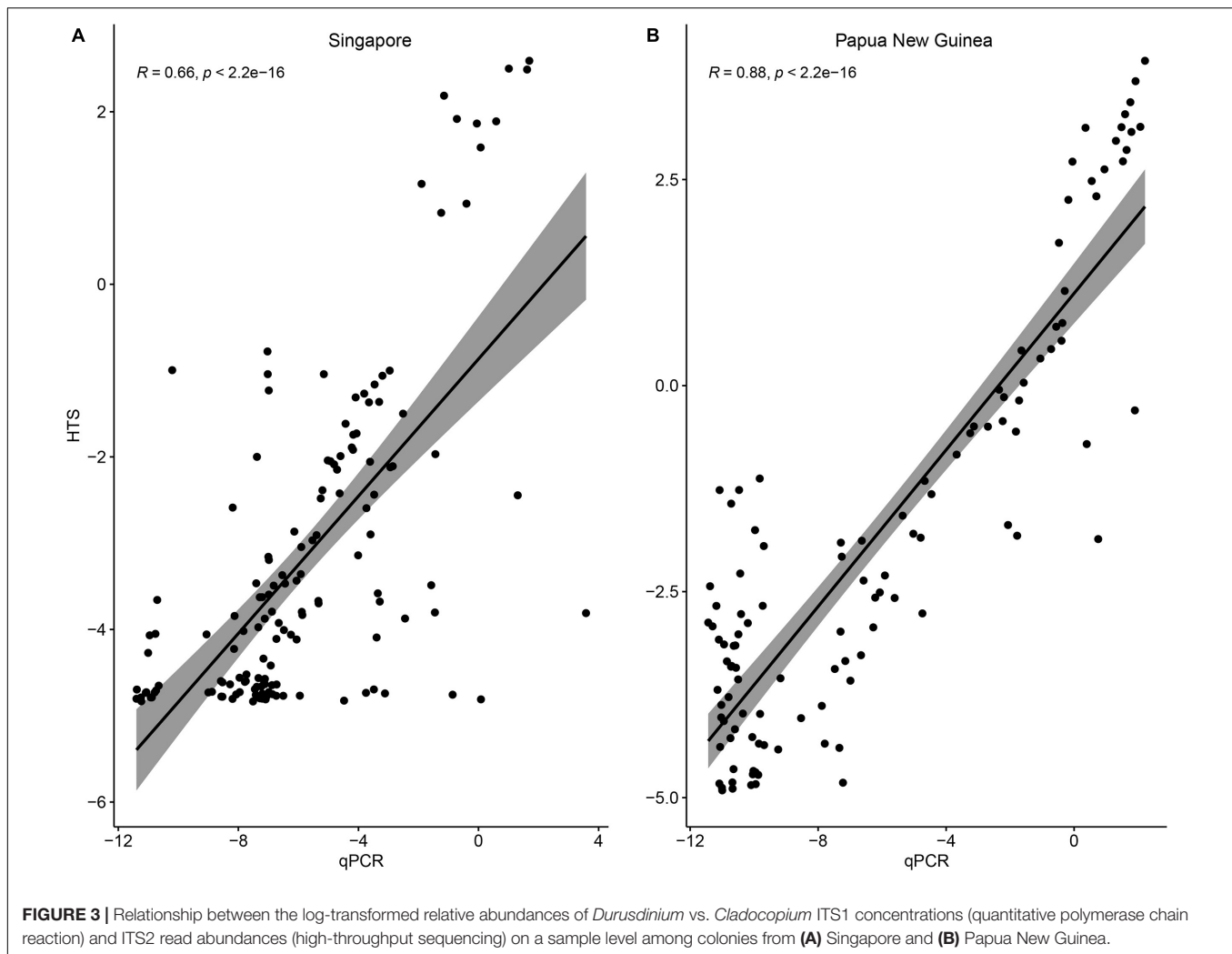
between Singapore and Papua New Guinea ( $p = 0.0015$ ,  $df = 1$ ,  $F = 10.352$ ).

### Methodological and Lineage Variations

Overall, the patterns of relative *Durusdinium* vs. *Cladocopium* abundances were consistent between the qPCR tests and HTS reads (Figure 2). At the sample level, relative ITS1 concentrations determined via qPCR and ITS2 HTS read abundances could be explained by a significant linear relationship at each locality (Singapore:  $R^2 = 0.435$ ,  $p < 0.001$ ; Papua New Guinea:  $R^2 = 0.778$ ,  $p < 0.001$ ; Figure 3). However, six and 15 colonies from Singapore and Papua New Guinea, respectively, recorded as having *Durusdinium*-dominated communities

with HTS were actually *Cladocopium*-dominated according to qPCR. Furthermore, three colonies each from Singapore and Papua New Guinea were recorded as *Durusdinium*-dominated with qPCR but actually showed *Cladocopium* dominance using HTS.

Based on the CAPS assay following Bongaerts et al. (2021), two lineages (“green” and “blue”) occur sympatrically within Singapore and Papua New Guinea. No “red” lineage was identified. To associate the host lineages with the Symbiodiniaceae communities, we compared *Cladocopium* and *Durusdinium* dominance in each colony with the assigned lineage (Supplementary Table 2). Colonies that showed a dominance of *Durusdinium* were assigned to either a “green” or “blue”



lineage. There was no clear association of the “green” lineage with dominance of *Durusdinium*, so we surmised that there was no discernible link between host lineage and endosymbiont community composition.

### ITS2 Type Profiles

Based on the SymPortal framework, nine ITS2 type profiles were found in Singapore *P. speciosa*, including five *Cladocopium* and four *Durusdinium* profiles (Figure 4). The five profiles of *Cladocopium* were associated with eight unique ITS2 sequences and the four profiles of *Durusdinium* were also associated with eight unique ITS2 sequences. The profile C27-C3-1319-C27a was detected in colonies across all sites except for St. John’s Island where only C27-C3-C27a was detected, suggesting the absence of the *Cladocopium* sequence “1319” at this particular site. Colonies from Raffles Lighthouse, Terumbu Pempang Tengah and Sisters’ Island showed none of the *Durusdinium* profiles. Colonies from the other sites contained *Durusdinium* type profiles, with D1/D4-D1c detected predominantly in colonies from Pulau Hantu and St. John’s Island, and D1-D4-D4c-D4f-D1l detected in colonies from Pulau Semakau and Kusu Island.

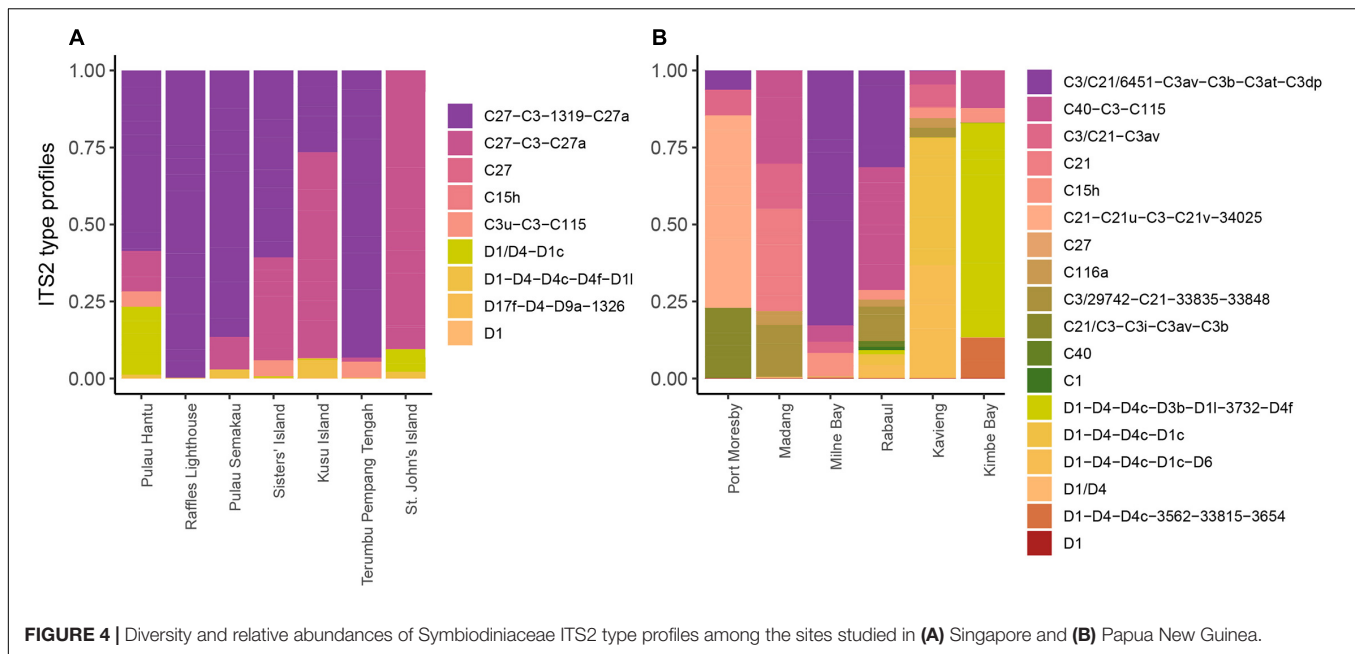
Colonies from Papua New Guinea showed a higher number of ITS2 type profiles (18) as compared to colonies from Singapore. There were 12 ITS2 type profiles assigned to *Cladocopium* and six type profiles assigned to *Durusdinium* across all the six sites sampled (Figure 4). Each site showed dominance of a distinct ITS2 type profile. The dominant type profile detected in colonies from Port Moresby, Madang, Milne Bay and Rabaul belonged to *Cladocopium* whereas colonies from Kavieng and Kimbe Bay showed dominance by *Durusdinium* type profiles (Port Moresby: C21-C21u-C3-C21v-34025; Madang: C21; Milne Bay: C3/C21/6451-C3av-C3b-C3at-C3dp; Rabaul: C40-C3-C115; Kavieng: D1-D4-D4c-D1c and Kimbe Bay: D1-D4-D4c-D3b-D1l-3732-D4f).

## DISCUSSION

### Geographical Variation

In this study, the relative abundances of Symbiodiniaceae genera and ITS2 type profiles hosted by the common reef-building stony coral, *Pachyseris speciosa*, were compared among colonies





**FIGURE 4 |** Diversity and relative abundances of Symbiodiniaceae ITS2 type profiles among the sites studied in **(A)** Singapore and **(B)** Papua New Guinea.

from Singapore and Papua New Guinea. *Cladocopium* C27-C3-1319-C27a was the most abundant ITS2 type profile found in all colonies across sites in Singapore with the exception of St. John's Island where C27-C3-C27a was detected (**Figure 4**). This is expected as previous studies have recorded similar results across multiple sites in Singapore (Jain et al., 2020; Smith et al., 2020) with C27 dominating most *P. speciosa* colonies. However, the type profile C27/C3/C3u-C115 was the most dominant across all six sites examined by Smith et al. (2020). This marginal difference may be the result of 3 years separating the sampling by Smith et al. (2020) in 2015 and the present study in 2018. In particular, a global-scale coral bleaching event (GCBF) occurred here in 2016 (Toh et al., 2018), leading to a shift in the Symbiodiniaceae communities in at least one of the sites, Pulau Hantu (Jain et al., 2020), even as the corals had recovered by 2018 (Ng et al., 2020).

Generally, ITS2 type profiles of *Cladocopium* were more abundant among colonies in Singapore compared to type profiles of *Durussdinium*, corroborating the findings at Pulau Hantu by Jain et al. (2020). While there were five *Cladocopium* and four *Durussdinium* type profiles, the dominant *Cladocopium* type profiles included the sequence of C27 and all the *Durussdinium* type profiles included the sequence of D1. These were also the dominant sequences detected for each of the genera in Jain et al. (2020). High *Durussdinium* abundance was detected in 26% of colonies from Pulau Hantu (Jain et al., 2020), with fewer colonies from Pulau Semakau (5%), Kusu Island (6%), and St. John's Island (14%). There were no *Durussdinium*-dominated colonies at Raffles Lighthouse, Sisters' Island and Terumbu Pempang Tengah.

The increased relative abundances of *Durussdinium* in colonies from Pulau Hantu compared to others could be a result of thermal or urbanization-related stress (Jain et al., 2020), given that certain *Durussdinium* species are commonly associated with resistance to high temperatures and turbidity

fluctuations (Baker, 2003; Ulstrup and Van Oppen, 2003; Jones et al., 2008). *Durussdinium* has been suggested to play an important role in the survival of Singapore's corals (Poquita-Du et al., 2020). The warm, turbid environment subject corals growing here with challenges not usually ideal for coral health (e.g., close proximity to a major urban center and high sedimentation rates), and furthermore, these reefs are susceptible to major bleaching events (Guest et al., 2016; Ng et al., 2020). Indeed, *Durussdinium* has mostly been associated with other marginal reefs comparable to those of Singapore (LaJeunesse et al., 2010; Keshavmurthy et al., 2014). Slight changes in the endosymbiont communities are known to be influenced by various environmental stressors (Buddemeier and Fautin, 1993; Baker, 2001). The limited differences in endosymbiont communities between various sites in Singapore suggest the stresses (e.g., thermal, sediment) that *P. speciosa* is exposed to may be similar among sites.

In colonies from Papua New Guinea, *Cladocopium* type profiles were the most abundant at all sites except Kimbe Bay and Kavieng, where *Durussdinium* dominated most colonies. Rather than the C27-C3-1319-C27a dominance exhibited by corals in Singapore, colonies from Papua New Guinea hosted mostly distinct *Cladocopium* type profiles at different sites. Colonies from Kimbe Bay and Rabaul had the most abundant C40-C3-C115, whereas colonies from Kavieng, Milne Bay, Madang and Port Moresby hosted C3/C21-C3av, C3/C21/6451-C3av-C3b-C3at-C3dp, C21 and C21-C21u-C3-C21v-34025, respectively. These *Cladocopium* type profiles included sequences of either C3 or C21, or both. Notably, *Cladocopium* C3, C21, and C40 are regarded as generalists due to their associations with a wide range of reef coral taxa in the tropics at various depths (LaJeunesse et al., 2003, 2004). In fact, the C3 group comprises many divergent lineages that are symbiotic with distinct host taxa

(LaJeunesse, 2005; Thornhill et al., 2014). The relatively high variability in the dominant type profile between sites observed at Papua New Guinea suggests a certain level of local adaptation even as *Cladocopium* C3, C21 and C40 share very similar ITS2 sequences (LaJeunesse et al., 2003).

*Pachyseris speciosa* colonies from Kimbe Bay and Kavieng were dominated by *Durisdinium*. The distinction of these two sites based on *Durisdinium* dominance does not appear to be spatially driven, although Kimbe Bay, Rabaul and Kavieng are on the islands of New Britain and New Ireland off the New Guinea mainland and samples from these sites contained higher *Durisdinium* levels than the others. It is known that the abundance of *Durisdinium* may be elevated in corals undergoing bleaching, and may not revert to the pre-bleaching community post-recovery (Tye Pettaya et al., 2015; Boulotte et al., 2016; LaJeunesse et al., 2016). However, these sites do not appear to have bleached in recent years (Mana, R. R., unpublished data), suggesting that local environmental factors such as light intensity, sea surface temperature and currents may promote *Durisdinium* dominance in Kimbe Bay and Kavieng. In particular, Kavieng faces the Pacific Ocean and is directly exposed to the South Equatorial Current, likely experiencing distinct local conditions compared to the other more sheltered sites to the south. Further tests and environmental measurements are needed to explain the Symbiodiniaceae dominance patterns at Papua New Guinea.

Comparison of the type profiles between Singapore and Papua New Guinea showed highly diverse endosymbiont communities within and between localities (Figure 4). In particular, the SymPortal framework revealed 18 type profiles throughout Papua New Guinea, which is twice the number detected in Singapore. It remains unclear why the endosymbiont compositions between Singapore and Papua New Guinea differ (LaJeunesse et al., 2004; Bongaerts et al., 2011; Cooper et al., 2011; Ziegler et al., 2015b), but these biogeographical patterns could be a consequence of different environmental factors and thermal regimes as discussed above (Tonk et al., 2013; Ziegler et al., 2015a, 2017). We note that the spatial distances between sampling sites in Papua New Guinea (~100 km) are considerably greater than those in Singapore (~10 km). This could mean greater connectivity and/or more similar environmental conditions among sites in Singapore, and may explain the relatively homogenized Symbiodiniaceae communities within Singapore compared to Papua New Guinea.

## Methodological Variation

Clearly there is a need to extend our comparisons of the endosymbiont communities to more localities in the Central Indo-Pacific using complementary approaches. As we have demonstrated, several colonies recorded as having *Durisdinium*-dominated communities with HTS were actually *Cladocopium*-dominated according to qPCR (Figure 3). Therefore, it may even be necessary to revisit samples that have been used in the past with HTS to infer that symbiosis with *Durisdinium* is associated with thermal tolerance (Baker, 2001; Baker et al., 2004; Stat et al., 2013). Similarly, in our previous study which explored the Symbiodiniaceae community patterns in *P. speciosa*

during and after the 2016 GCBE (Jain et al., 2020), three colonies were found to be *Durisdinium*-dominant based on HTS and *Cladocopium*-dominant based on qPCR. Nevertheless, overall patterns in the relative abundances of *Durisdinium* vs. *Cladocopium* remained consistent.

In this study, differences between localities in the levels of *Durisdinium* vs. *Cladocopium* appeared to be magnified with HTS. Our results showed significant differences in the relative abundances of *Durisdinium* and *Cladocopium* between Singapore and Papua New Guinea for the HTS results but not for qPCR, likely driven by the higher richness of ITS2 type profiles detected in corals from Papua New Guinea. qPCR is a sensitive method for detecting endosymbionts at a much higher resolution compared to more traditional methods like DGGE. While the technology of HTS has allowed us to detect sequence variants much more easily, it needs to be validated further for the purpose of understanding coral-algal symbiosis as the PCR step may be prone to amplification bias (Neilson et al., 2013). PCR may also pick up free-living Symbiodiniaceae in the corals' immediate external environment (Santos, 2004; Coffroth et al., 2006; Sze et al., 2018; Fujise et al., 2021). Hence, further exploration of the Symbiodiniaceae community around the coral is important to quantify the coral-algal symbiosis more precisely by accounting for environmental DNA signals. We suggest that water and sediment surrounding the coral colony of interest should be sampled at the same time for Symbiodiniaceae characterization. Overall, since the inferences of Symbiodiniaceae dominance differ at a sample level, we urge caution when examining endosymbiont abundances, and suggest verifying HTS results with qPCR for more precise estimates.

Indeed, precise characterization of the roles of different Symbiodiniaceae taxa would provide insights on the adaptation of coral reefs as global stressors exacerbate. The large colony-level variations of the coral-Symbiodiniaceae relationship even within a small reef area suggest that local adaptation is ongoing that may allow certain colonies to persist despite the accelerating environmental change (McClanahan et al., 2004; Hoogenboom et al., 2017). Such mosaicism of coral fitness at the reef level would be important for forecasting the performance of local reefs amid global climate change.

## DATA AVAILABILITY STATEMENT

All sequencing reads associated with this work have been deposited at the National Center for Biotechnology Information under the BioProject Accession PRJNA754701.

## AUTHOR CONTRIBUTIONS

SJ, BW, and DH contributed to conception and design of the study. SJ performed the molecular analyses and analyzed the data. SJ and DH wrote the first draft of the manuscript. All authors contributed to the collection of samples, contributed to manuscript revision, read, and approved the submitted version.

## FUNDING

This research was supported by the National Research Foundation (NRF), Prime Minister's Office, Singapore and the Israel Science Foundation under their 2nd Joint Grant Call (NRF2017NRF-ISF002-2658; Grant Number 2658/17), as well as the Ocean Park Conservation Foundation, Hong Kong (OT01.1819).

## ACKNOWLEDGMENTS

We thank Allen Chen and SK for sharing the initial protocol and discussions, as well as members of the Reef Ecology

Laboratory for assistance and support. We are also grateful to Nalini Puniamoorthy, Peter Todd, SK, HH and DT for constructive comments and suggestions. Coral collections were performed under a Singapore National Parks Board research permit (NP/RP16-156) and a Papua New Guinea research permit (AA927408).

## SUPPLEMENTARY MATERIAL

The Supplementary Material for this article can be found online at: <https://www.frontiersin.org/articles/10.3389/fmars.2021.759744/full#supplementary-material>

## REFERENCES

- Al-Horani, F. A., Al-Moghrabi, S. M., and De Beer, D. (2003). The mechanism of calcification and its relation to photosynthesis and respiration in the scleractinian coral *Galaxea fascicularis*. *Mar. Biol.* 142, 419–426. doi: 10.1007/s00227-002-0981-8
- Allen, G. R., Kinch, J., McKenna, S. A., and Seeto, P. (2003). *A Rapid Marine Biodiversity Assessment of Milne Bay Province, Papua New Guinea—Survey II (2000)*. RAP Bulletin of Biological Assessment 29. Washington, DC: Conservation International.
- Arif, C., Daniels, C., Bayer, T., Banguera-Hinestroza, E., Barbrook, A., Howe, C. J., et al. (2014). Assessing *Symbiodinium* diversity in scleractinian corals via next-generation sequencing-based genotyping of the ITS2 rDNA region. *Mol. Ecol.* 23, 4418–4433. doi: 10.1111/mec.12869
- Baker, A. C. (2001). Reef corals bleach to survive change. *Nature* 411, 765–766. doi: 10.1038/35081151
- Baker, A. C. (2003). Flexibility and specificity in coral-algal symbiosis: diversity, ecology, and biogeography of *Symbiodinium*. *Annu. Rev. Ecol. Syst.* 34, 661–689. doi: 10.1146/annurev.ecolsys.34.011802.132417
- Baker, A. C. (2004). “Symbiont diversity on coral reefs and its relationship to bleaching resistance and resilience,” in *Coral Health and Disease*, eds E. Rosenberg and Y. Loya (Berlin: Springer), 177–194.
- Baker, A. C., Starger, C. J., McClanahan, T. R., and Glynn, P. W. (2004). Corals' adaptive response to climate change. *Nature* 430, 741–741. doi: 10.1038/430741a
- Banin, E., Vassilakos, D., Orr, E., Martinez, R. J., and Rosenberg, E. (2003). Superoxide dismutase is a virulence factor produced by the coral bleaching pathogen *Vibrio shiloi*. *Curr. Microbiol.* 46, 418–422. doi: 10.1007/s00284-002-3912-5
- Boillard, A., Dubé, C. E., Gruet, C., Mercière, A., Hernandez-Agreda, A., and Derome, N. (2020). Defining coral bleaching as a microbial dysbiosis within the coral holobiont. *Microorganisms* 8:1682. doi: 10.3390/microorganisms8111682
- Bongaerts, P., Cooke, I. R., Ying, H., Wels, D., den Haan, S., Hernandez-Agreda, A., et al. (2021). Morphological stasis masks ecologically divergent coral species on tropical reefs. *Curr. Biol.* 31, 2286–2298. doi: 10.1016/j.cub.2021.03.028
- Bongaerts, P., Sampayo, E. M., Bridge, T. C. L., Ridgway, T., Vermeulen, F., Englebert, N., et al. (2011). *Symbiodinium* diversity in mesophotic coral communities on the Great Barrier Reef: a first assessment. *Mar. Ecol. Prog. Ser.* 439, 117–126. doi: 10.3354/meps09315
- Boulotte, N. M., Dalton, S. J., Carroll, A. G., Harrison, P. L., Putnam, H. M., Peplow, L. M., et al. (2016). Exploring the *Symbiodinium* rare biosphere provides evidence for symbiont switching in reef-building corals. *ISME J.* 10, 2693–2701. doi: 10.1038/ismej.2016.54
- Buddemeier, R. W., and Fautin, D. G. (1993). Coral bleaching as an adaptive mechanism. *Bioscience* 43, 320–326. doi: 10.2307/1312064
- Camacho, C., Coulouris, G., Avagyan, V., Ma, N., Papadopoulos, J., Bealer, K., et al. (2009). BLAST+: architecture and applications. *BMC Bioinformatics* 10:421. doi: 10.1186/1471-2105-10-421
- Chen, B., Yu, K., Liang, J., Huang, W., Wang, G., Su, H., et al. (2019). Latitudinal variation in the molecular diversity and community composition of *Symbiodiniaceae* in coral from the South China Sea. *Front. Microbiol.* 10:1278. doi: 10.3389/fmicb.2019.01278
- Chen, C. A., Lam, K. K., Nakano, Y., and Tsai, W. S. (2003). A stable association of the stress-tolerant zooxanthellae, *Symbiodinium* clade D, with the low-temperature-tolerant coral, *Oulastrea crispata* (Scleractinia: Faviidae) in subtropical non-reefal coral communities. *Zool. Stud.* 42, 540–550.
- Chow, G. S. E., Chan, Y. K. S., Jain, S. S., and Huang, D. (2019). Light limitation selects for depth generalists in urbanised reef coral communities. *Mar. Environ. Res.* 147, 101–112. doi: 10.1016/j.marenvres.2019.04.010
- Coffroth, M. A., Lewis, C. F., Santos, S. R., and Weaver, J. L. (2006). Environmental populations of symbiotic dinoflagellates in the genus *Symbiodinium* can initiate symbioses with reef cnidarians. *Curr. Biol.* 16, 985–987. doi: 10.1016/j.cub.2006.10.049
- Cooper, T. F., Ulstrup, K. E., Dandan, S. S., Heyward, A. J., Kühl, M., Muirhead, A., et al. (2011). Niche specialization of reef-building corals in the mesophotic zone: metabolic trade-offs between divergent *Symbiodinium* types. *Proc. R. Soc. B Biol. Sci.* 278, 1840–1850. doi: 10.1098/rspb.2010.2321
- DeVantier, L., and Turak, E. (2017). Species richness and relative abundance of reef-building corals in the Indo-West Pacific. *Diversity* 9:25. doi: 10.3390/d9030025
- Eckert, R. J., Reaume, A. M., Sturm, A. B., Studivan, M. S., and Voss, J. D. (2020). Depth influences *Symbiodiniaceae* associations among *Montastraea cavernosa* corals on the Belize Barrier Reef. *Front. Microbiol.* 11:518. doi: 10.3389/fmicb.2020.00518
- Eren, A. M., Morrison, H. G., Lescault, P. J., Reveillaud, J., Vineis, J. H., and Sogin, M. L. (2015). Minimum entropy decomposition: unsupervised oligotyping for sensitive partitioning of high-throughput marker gene sequences. *ISME J.* 9, 968–979. doi: 10.1038/ismej.2014.195
- Falkowski, P. G., Dubinsky, Z., Muscatine, L., and Porter, J. W. (1984). Light and the bioenergetics of a symbiotic coral. *Bioscience* 34, 705–709. doi: 10.2307/1309663
- Feldman, B., Afriq-Rosli, L., Simon-Blecher, N., Bollati, E., Wainwright, B. J., Bongaerts, P., et al. (2021). Distinct lineages and population structure of the coral *Pachyseris speciosa* in the small equatorial reef system of Singapore. *Coral Reefs*. doi: 10.1007/s00338-021-02160-4
- Fujise, L., Suggett, D. J., Stat, M., Kahlke, T., Bunce, M., Gardner, S. G., et al. (2021). Unlocking the phylogenetic diversity, primary habitats, and abundances of free-living *Symbiodiniaceae* on a coral reef. *Mol. Ecol.* 30, 343–360. doi: 10.1111/mec.15719
- Goulet, T. L., Lucas, M. Q., and Schizas, N. V. (2019). “*Symbiodiniaceae* genetic diversity and symbioses with hosts from shallow to mesophotic coral ecosystems,” in *Coral Reefs of the World*, eds Y. Loya, K. Puglise, and T. Bridge (Cham: Springer), 537–551.
- Guest, J. R., Low, J., Tun, K., Wilson, B., Ng, C., Raingeard, D., et al. (2016). Coral community response to bleaching on a highly disturbed reef. *Sci. Rep.* 6:20717. doi: 10.1038/srep20717
- Hoogenboom, M. O., Frank, G. E., Chase, T. J., Jurriaans, S., Álvarez-Noriega, M., Peterson, K., et al. (2017). Environmental drivers of variation in bleaching severity of *Acropora* species during an extreme thermal anomaly. *Front. Mar. Sci.* 4:376. doi: 10.3389/fmars.2017.00376



- Howells, E. J., Bauman, A. G., Vaughan, G. O., Hume, B. C. C., Voolstra, C. R., and Burt, J. A. (2020). Corals in the hottest reefs in the world exhibit symbiont fidelity not flexibility. *Mol. Ecol.* 29, 899–911. doi: 10.1111/mec.15372
- Huang, D., Tun, K., Chou, L. M., and Todd, P. A. (2009). An inventory of zooxanthellate scleractinian corals in Singapore, including 33 new records. *Raffles Bull. Zool.* 22, 69–80.
- Huang, H., Dong, Z., Huang, L., Yang, J., Di, B., Li, Y., et al. (2011). Latitudinal variation in algal symbionts within the scleractinian coral *Galaxea fascicularis* in the South China Sea. *Mar. Biol. Res.* 7, 208–211. doi: 10.1080/17451000.2010.489616
- Hughes, T. P., Barnes, M. L., Bellwood, D. R., Cinner, J. E., Cumming, G. S., Jackson, J. B. C., et al. (2017a). Coral reefs in the *Anthropocene*. *Nature* 546, 82–90. doi: 10.1038/nature22901
- Hughes, T. P., Kerry, J. T., Álvarez-Noriega, M., Álvarez-Romero, J. G., Anderson, K. D., Baird, A. H., et al. (2017b). Global warming and recurrent mass bleaching of corals. *Nature* 543, 373–377. doi: 10.1038/nature21707
- Hume, B. C. C., D'Angelo, C., Burt, J. A., Baker, A. C., Riegl, B., and Wiedenmann, J. (2013). Corals from the Persian/Arabian Gulf as models for thermotolerant reef-builders: prevalence of clade C3 *Symbiodinium*, host fluorescence and ex situ temperature tolerance. *Mar. Pollut. Bull.* 72, 313–322. doi: 10.1016/j.marpolbul.2012.11.032
- Hume, B. C. C., D'Angelo, C., Smith, E. G., Stevens, J. R., Burt, J. A., and Wiedenmann, J. (2015). *Symbiodinium thermophilum* sp. nov., a thermotolerant symbiotic alga prevalent in corals of the world's hottest sea, the Persian/Arabian Gulf. *Sci. Rep.* 5:8562. doi: 10.1038/srep08562
- Hume, B. C. C., Mejia-Restrepo, A., Voolstra, C. R., and Berumen, M. L. (2020). Fine-scale delineation of Symbiodiniaceae genotypes on a previously bleached central Red Sea reef system demonstrates a prevalence of coral host-specific associations. *Coral Reefs* 39, 583–601. doi: 10.1007/s00338-020-01917-7
- Hume, B. C. C., Smith, E. G., Ziegler, M., Warrington, H. J. M., Burt, J. A., LaJeunesse, T. C., et al. (2019). SymPortal: a novel analytical framework and platform for coral algal symbiont next-generation sequencing ITS2 profiling. *Mol. Ecol. Resour.* 19, 1063–1080. doi: 10.1111/1755-0998.13004
- Illumina (2013). *16S Metagenomic Sequencing Library Preparation*. Available online at: [http://support.illumina.com/content/dam/illumina-support/documents/documentation/chemistry\\_documentation/16s/16s-metagenomic-library-prep-guide-15044223-b.pdf](http://support.illumina.com/content/dam/illumina-support/documents/documentation/chemistry_documentation/16s/16s-metagenomic-library-prep-guide-15044223-b.pdf) (accessed January 15, 2020).
- Innis, T., Cunniff, R., Ritson-Williams, R., Wall, C. B., and Gates, R. D. (2018). Coral color and depth drive symbiosis ecology of *Montipora capitata* in Kāne'ohe Bay, O'ahu, Hawai'i. *Coral Reefs* 37, 423–430. doi: 10.1007/s00338-018-1667-0
- Jain, S. S., Afiq-Rosli, L., Feldman, B., Levy, O., Phua, J. W., Wainwright, B. J., et al. (2020). Homogenization of endosymbiont communities hosted by equatorial corals during the 2016 mass bleaching event. *Microorganisms* 8:1370. doi: 10.3390/microorganisms8091370
- Jones, L., Acolado, P., Cala, Y., Cobi Án, D., Coelho, V., Hernández, A., et al. (2008). "The effects of coral bleaching in the northern Caribbean and western Atlantic," in *Status of Caribbean Coral Reefs after Bleaching and Hurricanes in 2005*, eds C. Wilkinson and D. Souter (Townsville, Qld: Global Coral Reef Monitoring Network), 73–84.
- Kearse, M., Moir, R., Wilson, A., Stones-Havas, S., Cheung, M., Sturrock, S., et al. (2012). Geneious basic: an integrated and extendable desktop software platform for the organization and analysis of sequence data. *Bioinformatics* 28, 1647–1649. doi: 10.1093/bioinformatics/bts199
- Kemp, D. W., Hernandez-Pech, X., Iglesias-Prieto, R., Fitt, W. K., and Schmidt, G. W. (2014). Community dynamics and physiology of *Symbiodinium* spp. before, during, and after a coral bleaching event. *Limnol. Oceanogr.* 59, 788–797. doi: 10.4319/lo.2014.59.3.0788
- Keshavmurthy, S., Meng, P. J., Wang, J. T., Kuo, C. Y., Yang, S. Y., Hsu, C. M., et al. (2014). Can resistant coral-*Symbiodinium* associations enable coral communities to survive climate change? A study of a site exposed to long-term hot water input. *PeerJ* 2:e327. doi: 10.7717/peerj.327
- LaJeunesse, T. C. (2002). Diversity and community structure of symbiotic dinoflagellates from Caribbean coral reefs. *Mar. Biol.* 141, 387–400. doi: 10.1007/s00227-002-0829-2
- LaJeunesse, T. C. (2005). "Species" radiations of symbiotic dinoflagellates in the Atlantic and Indo-Pacific since the Miocene-Pliocene transition. *Mol. Biol. Evol.* 22, 570–581. doi: 10.1093/molbev/msi042
- LaJeunesse, T. C. (2020). Zooxanthellae. *Curr. Biol.* 30, R1110–R1113. doi: 10.1016/j.cub.2020.03.058
- LaJeunesse, T. C., Bhagooli, R., Hidaka, M., DeVantier, L., Done, T., Schmidt, G. W., et al. (2004). Closely related *Symbiodinium* spp. differ in relative dominance in coral reef host communities across environmental, latitudinal and biogeographic gradients. *Mar. Ecol. Prog. Ser.* 284, 147–161. doi: 10.3354/meps284147
- LaJeunesse, T. C., Forsman, Z. H., and Wham, D. C. (2016). An Indo-West Pacific 'zooxanthella' invasive to the western Atlantic finds its way to the Eastern Pacific via an introduced Caribbean coral. *Coral Reefs* 35, 577–582. doi: 10.1007/s00338-015-1388-6
- LaJeunesse, T. C., Loh, W. K. W., Van Woesik, R., Hoegh-Guldberg, O., Schmidt, G. W., and Fitt, W. K. (2003). Low symbiont diversity in southern Great Barrier Reef corals, relative to those of the Caribbean. *Limnol. Oceanogr.* 48, 2046–2054. doi: 10.4319/lo.2003.48.5.2046
- LaJeunesse, T. C., Parkinson, J. E., Gabrielson, P. W., Jeong, H. J., Reimer, J. D., Voolstra, C. R., et al. (2018). Systematic revision of Symbiodiniaceae highlights the antiquity and diversity of coral endosymbionts. *Curr. Biol.* 28, 2570.e–2580.e. doi: 10.1016/j.cub.2018.07.008
- LaJeunesse, T. C., Pettay, D. T., Sampayo, E. M., Phongsuwan, N., Brown, B., Obura, D. O., et al. (2010). Long-standing environmental conditions, geographic isolation and host-symbiont specificity influence the relative ecological dominance and genetic diversification of coral endosymbionts in the genus *Symbiodinium*. *J. Biogeogr.* 37, 785–800. doi: 10.1111/j.1365-2699.2010.02273.x
- Leveque, S., Afiq-Rosli, L., Ip, Y. C. A., Jain, S. S., and Huang, D. (2019). Searching for phylogenetic patterns of Symbiodiniaceae community structure among Indo-Pacific Merulinidae corals. *PeerJ* 7:e7669. doi: 10.7717/peerj.7669
- Little, A. F., Van Oppen, M. J. H., and Willis, B. L. (2004). Flexibility in algal endosymbioses shapes growth in reef corals. *Science* 304, 1492–1494. doi: 10.1126/science.1095733
- McClanahan, T. R., Baird, A. H., Marshall, P. A., and Toscano, M. A. (2004). Comparing bleaching and mortality responses of hard corals between southern Kenya and the Great Barrier Reef, Australia. *Mar. Pollut. Bull.* 48, 327–335. doi: 10.1016/j.marpolbul.2003.08.024
- Meisterzheim, A. L., Pochon, X., Wood, S. A., Ghiglione, J. F., and Hédouin, L. (2019). Development of a quantitative PCR–high-resolution melting assay for absolute measurement of coral-Symbiodiniaceae associations and its application to investigating variability at three spatial scales. *Mar. Biol.* 166:13. doi: 10.1007/s00227-018-3458-0
- Neilson, J. W., Jordan, F. L., and Maier, R. M. (2013). Analysis of artifacts suggests DGGE should not be used for quantitative diversity analysis. *J. Microbiol. Methods* 92, 256–263. doi: 10.1016/j.mimet.2012.12.021
- Ng, C. S. L., Huang, D., Toh, K. B., Sam, S. Q., Kikuzawa, Y. P., Toh, T. C., et al. (2020). Responses of urban reef corals during the 2016 mass bleaching event. *Mar. Pollut. Bull.* 154:111111. doi: 10.1016/j.marpolbul.2020.111111
- Nicholls, S. (2004). *The Priority Environmental Concerns of Papua New Guinea*. Samoa: SPREP.
- Noonan, S. H. C., Fabricius, K. E., and Humphrey, C. (2013). *Symbiodinium* community composition in scleractinian corals is not affected by life-long exposure to elevated carbon dioxide. *PLoS One* 8:e63985. doi: 10.1371/journal.pone.0063985
- Osman, E. O., Suggett, D. J., Voolstra, C. R., Pettay, D. T., Clark, D. R., Pogoreutz, C., et al. (2020). Coral microbiome composition along the northern Red Sea suggests high plasticity of bacterial and specificity of endosymbiotic dinoflagellate communities. *Microbiome* 8:8. doi: 10.1186/s40168-019-0776-5
- Poquita-Du, R. C., Huang, D., Chou, L. M., and Todd, P. A. (2020). The contribution of stress-tolerant endosymbiotic dinoflagellate *Durussdinium* to *Pocillopora acuta* survival in a highly urbanized reef system. *Coral Reefs* 39, 745–755. doi: 10.1007/s00338-020-01902-0
- R Core Team (2017). *R: A Language and Environment for Statistical Computing*. Available online at: <http://www.R-project.org> (accessed March 1, 2021)
- Rouzé, H., Lecellier, G., Saulnier, D., and Berteaux-Lecellier, V. (2016). *Symbiodinium* clades A and D differentially predispose *Acropora cytherea* to disease and *Vibrio* spp. colonization. *Ecol. Evol.* 6, 560–572. doi: 10.1002/ece3.1895



- Rowan, R., and Knowlton, N. (1995). Intraspecific diversity and ecological zonation in coral-algal symbiosis. *Proc. Natl. Acad. Sci. U.S.A.* 92, 2850–2853. doi: 10.1073/pnas.92.7.2850
- Rowan, R., Knowlton, N., Baker, A. C., and Jara, J. (1997). Landscape ecology of algal symbionts creates variation in episodes of coral bleaching. *Nature* 388, 265–269. doi: 10.1038/40843
- Sampayo, E. M., Ridgway, T., Bongaerts, P., and Hoegh-Guldberg, O. (2008). Bleaching susceptibility and mortality of corals are determined by fine-scale differences in symbiont type. *Proc. Natl. Acad. Sci. U.S.A.* 105, 10444–10449. doi: 10.1073/pnas.0708049105
- Santos, S. R. (2004). Phylogenetic analysis of a free-living strain of *Symbiodinium* isolated from Jiaozhou Bay, P.R. China. *J. Phycol.* 40, 395–397. doi: 10.1111/j.1529-8817.2004.03186.x
- Schloss, P. D., Westcott, S. L., Ryabin, T., Hall, J. R., Hartmann, M., Hollister, E. B., et al. (2009). Introducing mothur: open-source, platform-independent, community-supported software for describing and comparing microbial communities. *Appl. Environ. Microbiol.* 75, 7537–7541. doi: 10.1128/AEM.01541-09
- Silverstein, R. N., Cunning, R., and Baker, A. C. (2015). Change in algal symbiont communities after bleaching, not prior heat exposure, increases heat tolerance of reef corals. *Glob. Change Biol.* 21, 236–249. doi: 10.1111/gcb.12706
- Smith, E. G., Gurskaya, A., Hume, B. C. C., Voolstra, C. R., Todd, P. A., Bauman, A. G., et al. (2020). Low Symbiodiniaceae diversity in a turbid marginal reef environment. *Coral Reefs* 39, 545–553. doi: 10.1007/s00338-020-01956-0
- Stanley, G. D., and Fautin, D. G. (2001). The origins of modern corals. *Science* 291, 1913–1914. doi: 10.1126/science.1056632
- Stat, M., Bird, C. E., Pochon, X., Chasqui, L., Chauka, L. J., Concepcion, G. T., et al. (2011). Variation in *Symbiodinium* ITS2 sequence assemblages among coral colonies. *PLoS One* 6:e15854. doi: 10.1371/journal.pone.0015854
- Stat, M., and Gates, R. D. (2011). Clade D *Symbiodinium* in scleractinian corals: a “nugget” of hope, a selfish opportunist, an ominous sign, or all of the above? *J. Mar. Biol.* 2011:730715. doi: 10.1155/2011/730715
- Stat, M., Loh, W. K. W., Hoegh-Guldberg, O., and Carter, D. A. (2008a). Symbiont acquisition strategy drives host-symbiont associations in the southern Great Barrier Reef. *Coral Reefs* 27, 763–772. doi: 10.1007/s00338-008-0412-5
- Stat, M., Morris, E., and Gates, R. D. (2008b). Functional diversity in coral-dinoflagellate symbiosis. *Proc. Natl. Acad. Sci. U.S.A.* 105, 9256–9261. doi: 10.1073/pnas.0801328105
- Stat, M., Pochon, X., Franklin, E. C., Bruno, J. F., Casey, K. S., Selig, E. R., et al. (2013). The distribution of the thermally tolerant symbiont lineage (*Symbiodinium* clade D) in corals from Hawaii: correlations with host and the history of ocean thermal stress. *Ecol. Evol.* 3, 1317–1329. doi: 10.1002/ece3.556
- Sze, Y., Miranda, L. N., Sin, T. M., and Huang, D. (2018). Characterising planktonic dinoflagellate diversity in Singapore using DNA metabarcoding. *Metabarcoding Metagenom.* 2:e25136. doi: 10.3897/mbmg.2.25136
- Tan, Y. T. R., Wainwright, B. J., Afq-Rosli, L., Ip, Y. C. A., Lee, J. N., Nguyen, N. T. H., et al. (2020). Endosymbiont diversity and community structure in *Porites lutea* from Southeast Asia are driven by a suite of environmental variables. *Symbiosis* 80, 269–277. doi: 10.1007/s13199-020-00671-2
- Tanzil, J. T. I., Ng, A. P. K., Tey, Y. Q., Tan, B. H. Y., Yun, E. Y., and Huang, D. (2016). A preliminary characterisation of *Symbiodinium* diversity in some common corals from Singapore. *Cosmos* 12, 15–27. doi: 10.1142/s0219607716500014
- Terraneo, T. I., Fusi, M., Hume, B. C. C., Arrigoni, R., Voolstra, C. R., Benzoni, F., et al. (2019). Environmental latitudinal gradients and host-specificity shape Symbiodiniaceae distribution in Red Sea *Porites* corals. *J. Biogeogr.* 46, 2323–2335. doi: 10.1111/jbi.13672
- Teschima, M. M., Garrido, A., Paris, A., Nunes, F. L. D., and Zilberberg, C. (2019). Biogeography of the endosymbiotic dinoflagellates (Symbiodiniaceae) community associated with the brooding coral *Favia graxida* in the Atlantic Ocean. *PLoS One* 14:e0213519. doi: 10.1371/journal.pone.0213519
- The Nature Conservancy (2004). *Designing a Resilient Network of Marine Protected Areas in Kimbe Bay, West New Britain, Papua New Guinea*. Papua New Guinea: The Nature Conservancy.
- Thornhill, D. J., Lewis, A. M., Wham, D. C., and LaJeunesse, T. C. (2014). Host-specialist lineages dominate the adaptive radiation of reef coral endosymbionts. *Evolution* 68, 352–367. doi: 10.1111/evo.12270
- Toh, T. C., Huang, D., Tun, K., and Chou, L. M. (2018). “Summary of coral bleaching from 2014 to 2017 in Singapore,” in *Status of Coral Reefs in East Asian Seas Region: 2018*, eds T. Kimura, K. Tun, and L. M. Chou (Tokyo: Ministry of the Environment of Japan and Japan Wildlife Research Center), 21–23.
- Tonk, L., Sampayo, E. M., Weeks, S., Magno-Canto, M., and Hoegh-Guldberg, O. (2013). Host-Specific interactions with environmental factors shape the distribution of *Symbiodinium* across the Great Barrier Reef. *PLoS One* 8:e68533. doi: 10.1371/journal.pone.0068533
- Tye Pettaya, D., Wham, D. C., Smith, R. T., Iglesias-Prieto, R., and LaJeunesse, T. C. (2015). Microbial invasion of the Caribbean by an Indo-Pacific coral zooxanthella. *Proc. Natl. Acad. Sci. U.S.A.* 112, 7513–7518. doi: 10.1073/pnas.1502283112
- Ulstrup, K. E., and Van Oppen, M. J. H. (2003). Geographic and habitat partitioning of genetically distinct zooxanthellae (*Symbiodinium*) in *Acropora* corals on the Great Barrier Reef. *Mol. Ecol.* 12, 3477–3484. doi: 10.1046/j.1365-294X.2003.01988.x
- Veron, J., DeVantier, L., Turak, E., Green, A. L., Kininmonth, S., Stafford-Smith, M., et al. (2011). “The Coral Triangle,” in *Coral Reefs: An Ecosystem in Transition*, eds Z. Dubinsky and N. Stambler (Dordrecht: Springer), 47–55.
- Veron, J., Stafford-Smith, M., DeVantier, L., and Turak, E. (2015). Overview of distribution patterns of zooxanthellate Scleractinia. *Front. Mar. Sci.* 1:81. doi: 10.3389/fmars.2014.00081
- Wong, J. S. Y., Chan, Y. K. S., Ng, C. S. L., Tun, K., Darling, E. S., and Huang, D. (2018). Comparing patterns of taxonomic, functional and phylogenetic diversity in reef coral communities. *Coral Reefs* 37, 737–750. doi: 10.1007/s00338-018-1698-6
- Ziegler, M., Arif, C., Burt, J. A., Dobretsov, S., Roder, C. M., LaJeunesse, T. C., et al. (2017). Biogeography and molecular diversity of coral symbionts in the genus *Symbiodinium* around the Arabian Peninsula. *J. Biogeogr.* 44, 674–686. doi: 10.1111/jbi.12913
- Ziegler, M., Roder, C., Bchel, C., and Voolstra, C. R. (2015a). Niche acclimatization in Red Sea corals is dependent on flexibility of host-symbiont association. *Mar. Ecol. Prog. Ser.* 533, 163–176. doi: 10.3354/meps11365
- Ziegler, M., Roder, C. M., Büchel, C., and Voolstra, C. R. (2015b). Mesophotic coral depth acclimatization is a function of host-specific symbiont physiology. *Front. Mar. Sci.* 2:4. doi: 10.3389/fmars.2015.00004

**Conflict of Interest:** The authors declare that the research was conducted in the absence of any commercial or financial relationships that could be construed as a potential conflict of interest.

**Publisher’s Note:** All claims expressed in this article are solely those of the authors and do not necessarily represent those of their affiliated organizations, or those of the publisher, the editors and the reviewers. Any product that may be evaluated in this article, or claim that may be made by its manufacturer, is not guaranteed or endorsed by the publisher.

Copyright © 2021 Jain, Afq-Rosli, Feldman, Kunning, Levy, Mana, Wainwright and Huang. This is an open-access article distributed under the terms of the Creative Commons Attribution License (CC BY). The use, distribution or reproduction in other forums is permitted, provided the original author(s) and the copyright owner(s) are credited and that the original publication in this journal is cited, in accordance with accepted academic practice. No use, distribution or reproduction is permitted which does not comply with these terms.



# Integrated Population Genomic Analysis and Numerical Simulation to Estimate Larval Dispersal of *Acanthaster cf. solaris* Between Ogasawara and Other Japanese Regions

Mizuki Horoiwa<sup>1,2</sup>, Takashi Nakamura<sup>3</sup>, Hideaki Yuasa<sup>4</sup>, Rei Kajitani<sup>4</sup>, Yosuke Ameda<sup>5</sup>, Tetsuro Sasaki<sup>5</sup>, Hiroki Taninaka<sup>6</sup>, Taisei Kikuchi<sup>7</sup>, Takehisa Yamakita<sup>8</sup>, Atsushi Toyoda<sup>9</sup>, Takehiko Itoh<sup>4</sup> and Nina Yasuda<sup>10\*</sup>

## OPEN ACCESS

### Edited by:

Charles Alan Jacoby,  
St. Johns River Water Management  
District, United States

### Reviewed by:

Maria Byrne,  
The University of Sydney, Australia  
Gretchen Goodbody-Gringley,  
Central Caribbean Marine Institute,  
Cayman Islands

### \*Correspondence:

Nina Yasuda  
nina27@cc.miyazaki-u.ac.jp

### Specialty section:

This article was submitted to  
Coral Reef Research,  
a section of the journal  
Frontiers in Marine Science

**Received:** 30 March 2021

**Accepted:** 07 December 2021

**Published:** 17 January 2022

### Citation:

Horoiwa M, Nakamura T, Yuasa H, Kajitani R, Ameda Y, Sasaki T, Taninaka H, Kikuchi T, Yamakita T, Toyoda A, Itoh T and Yasuda N (2022) Integrated Population Genomic Analysis and Numerical Simulation to Estimate Larval Dispersal of *Acanthaster cf. solaris* Between Ogasawara and Other Japanese Regions. *Front. Mar. Sci.* 8:688139. doi: 10.3389/fmars.2021.688139

<sup>1</sup> Graduate School of Agriculture, University of Miyazaki, Miyazaki, Japan, <sup>2</sup> Graduate School of Engineering and Science, University of the Ryukyus, Nishihara, Japan, <sup>3</sup> School of Environment and Society, Tokyo Institute of Technology, Tokyo, Japan, <sup>4</sup> Department of Life Science and Technology, School of Life Sciences and Technology, Tokyo Institute of Technology, Tokyo, Japan, <sup>5</sup> Institute of Boninology, Ogasawara, Japan, <sup>6</sup> Interdisciplinary Graduate School of Agriculture and Engineering, University of Miyazaki, Miyazaki, Japan, <sup>7</sup> Faculty of Medicine, University of Miyazaki, Miyazaki, Japan, <sup>8</sup> Japan Agency for Marine-Earth Science and Technology, Yokosuka, Japan, <sup>9</sup> Department of Genomics and Evolutionary Biology, National Institute of Genetics, Shizuoka, Japan, <sup>10</sup> Faculty of Agriculture, University of Miyazaki, Miyazaki, Japan

The estimation of larval dispersal on an ecological timescale is significant for conservation of marine species. In 2018, a semi-population outbreak of crown-of-thorns sea star, *Acanthaster cf. solaris*, was observed on a relatively isolated oceanic island, Ogasawara. The aim of this study was to assess whether this population outbreak was caused by large-scale larval recruitment (termed secondary outbreak) from the Kuroshio region. We estimated larval dispersal of the coral predator *A. cf. solaris* between the Kuroshio and Ogasawara regions using both population genomic analysis and simulation of oceanographic dispersal. Population genomic analysis revealed overall genetically homogenized patterns among Ogasawara and other Japanese populations, suggesting that the origin of the populations in the two regions is the same. In contrast, a simulation of 26-year oceanographic dispersal indicated that larvae are mostly self-seeded in Ogasawara populations and have difficulty reaching Ogasawara from the Kuroshio region within one generation. However, a connectivity matrix produced by the larval dispersal simulation assuming a Markov chain indicated gradual larval dispersal migration from the Kuroshio region to Ogasawara in a stepping-stone manner over multiple years. These results suggest that the 2018 outbreak was likely the result of self-seeding, including possible inbreeding (as evidenced by clonemate analysis), as large-scale larval dispersal from the Kurishio population to the Ogasawara population within one generation is unlikely. Instead, the population in Ogasawara is basically sustained by self-seedings, and the outbreak in 2018 was also most likely caused

by successful self-seedings including possible inbreeding, as evidenced by clonemate analysis. This study also highlighted the importance of using both genomic and oceanographic methods to estimate larval dispersal, which provides significant insight into larval dispersal that occurs on ecological and evolutionary timescales.

**Keywords:** crown-of-thorn starfish, Kuroshio Current, larval dispersal, Ogasawara (Bonin) Islands, population genetic analyses, population genetics, secondary outbreak, oceanographic dispersal simulation

## INTRODUCTION

Many benthic marine invertebrates in coral reef ecosystems exhibit planktonic larval dispersal during their early life histories. Such larval dispersal connects different populations and forms a meta-population structure (Shanks, 2009). Thus, for effective conservation and management of benthic marine invertebrates, assessment of larval dispersal is important (Almany et al., 2009; Botsford et al., 2009). Because it is challenging to directly track the movement of numerous larvae that are smaller than 1 mm in the field, several different indirect methods, including population genetic analysis (e.g., Arndt and Smith, 1998; Yasuda et al., 2009), oceanographic simulation (e.g., Miyake et al., 2009; Storlazzi et al., 2017), towed nets (e.g., Uthicke et al., 2015; Yasuda et al., 2015a; Suzuki et al., 2016), and drifting buoys (e.g., Fukuda and Hanamura, 1996), have been used to estimate larval dispersal. Although each method has advantages and disadvantages, the first two methods can be applied to relatively large spatial scales and thus have been used more frequently than the other methods. On the one hand, the data obtained by population genetic analysis reflect the biological processes of larval dispersal and recruitment. However, these results not only include larval dispersal occurring on an ecological timescale but also reflect historical gene flow and genetic breaks caused by past climate change and plate tectonics (Benzie, 1999a; Crandall et al., 2014). Oceanographic simulation, on the other hand, can capture snapshots of larval dispersal, although even a sophisticated biophysical model cannot accurately simulate larval behavior, recruitment, and survival in the ocean (White et al., 2019). It is therefore important to integrate different methods to estimate larval dispersal (Marko and Hart, 2017), although few studies have attempted to do so (but see Alberto et al., 2011; Schunter et al., 2011; Nakabayashi et al., 2019; Taninaka et al., 2019).

In this study, we examined larval dispersal of a species of crown-of-thorns sea star, *Acanthaster cf. solaris*, which is a notorious predator of reef-building corals in the Pacific. Recent chronic outbreaks of crown-of-thorns sea stars have destroyed coral reef ecosystems in the Indian and Pacific oceans (Baird et al., 2013). For example, more than 90% of coral reefs over 38 km<sup>2</sup> in area were lost due to the feeding damage of crown-of-thorns sea star in Guam (Chesher, 1969). On Australia's Great Barrier Reef (GBR), more than half of the coral reefs have been reduced by 50% in size in the last 27 years and 42% of the decline of corals was due to population outbreaks of crown-of-thorns starfish (De'ath et al., 2012). The crown-of-thorns starfish is a species complex consisting of four genetically different lineages (Haszprunar et al., 2017); Pacific crown-of-thorns sea star (which is considered to be *Acanthaster cf. solaris*), and three other Indian

ocean crown-of-thorns sea stars (*Acanthaster planci* in the north Indian Ocean and two more *Acanthaster* spp. in Red Sea and south Indian Ocean). Population outbreaks of crown-of-thorns sea star in the Indian and Pacific Oceans are largely categorized into two types. One is called "primary outbreak," which is defined as an independent, sudden increase of crown-of-thorns sea star population at a location. The other is called "secondary outbreak," which is defined as an outbreak caused by the spread of larvae released by another outbreak in neighboring regions. While the causes of primary outbreaks are still controversial, the mechanisms of secondary outbreaks are more obvious. With high fecundity and a larval stage that lasts a few to several weeks (Lucas, 1973; Yamaguchi, 1977), once a population outbreak takes place at a population, the large number of larvae produced and dispersed from the population can cause successive population outbreaks at neighboring sites, especially in the western Pacific regions that are impacted by strong warm currents (reviewed in Birkeland and Lucas, 1990; Pratchett et al., 2014; Yasuda, 2018). Given that early monitoring and control are key for management of *A. cf. solaris* (Birkeland and Lucas, 1990), assessment of the spatial range of secondary outbreaks of *A. cf. solaris* is necessary for predicting successive outbreaks and thus important for coral reef conservation.

Many population genetic and phylogeographic studies of *A. cf. solaris* have been conducted using various molecular markers (e.g., Benzie, 1992, 1999a; Yasuda et al., 2009, 2015b; Timmers et al., 2011; Vogler et al., 2013). These studies have indicated strong gene flow over a long distance along western boundary currents such as the Kuroshio Current region (genetic homogeneity from across the Ryukyu Islands to the temperate Pacific coast of mainland Japan) and the Eastern Australian Current region (the GBR, Nash et al., 1988; Benzie, 1999b; Vogler et al., 2013; Harrison et al., 2017), while relatively limited gene flow and genetic differentiation were observed among distant Pacific islands (Yasuda et al., 2009; Timmers et al., 2012; Vogler et al., 2013). Overall, the studies found strong gene flow and genetic homogeneity in regions with strong currents. Genetic data, however, strongly reflect historical gene flow that occurred during past climate change, and the spatial extent of secondary outbreaks could be overestimated (Benzie, 1999b; Yasuda et al., 2009, Yasuda et al., 2015b). Larval dispersal simulation studies in the GBR have indicated southward larval dispersal along the Eastern Australian Current, which is consistent with historically observed patterns of secondary outbreaks of *A. cf. solaris* (Dight et al., 1990a,b; James and Scandol, 1992; Scandol and James, 1992). Net surveys also have shown evidence of large-scale larval dispersal of *A. cf. solaris* along the GBR (Uthicke et al., 2015). While intensive studies of connectivity for *A. cf. solaris*

have been conducted at the Indo-Pacific scale and in some localized regions where secondary outbreaks were suspected (e.g., the Kuroshio region and the GBR), connectivity between such regions and some relatively isolated oceanic island regions has yet to be examined.

In 2018, a population outbreak of *A. cf. solaris* on Ogasawara Island was reported (Biodiversity Center, Natural Environment Bureau, Ministry of the Environment, 2021), which was the second population outbreak on Ogasawara since 1979 (Kurata, 1984). Ogasawara Island is an oceanic island situated ca. 1,000 km south of the Tokyo urban center, and it is out of the mainstream of the Kuroshio Current. It is therefore still unknown whether this population outbreak is caused by mass larval recruitment produced by the outbreaks in the Kuroshio region.

The aim of this study was to estimate larval dispersal between the Kuroshio region and Ogasawara to determine whether the population outbreak in Ogasawara was successively caused by outbreaks in the Kuroshio region. To meet this aim, we used two different methods to estimate larval dispersal; population genomic analysis called multiplexed ISSR genotyping by sequencing (MIG-seq) and oceanographic larval dispersal simulation based on the Global HYbrid Coordinate Ocean Model (HYCOM).

## MATERIALS AND METHODS

### Sampling and DNA Extraction

A total of 187 starfish samples were collected from six Kuroshio regions (Tatsukushi, Miyazaki, Sakurajima, Onna Village, Miyako, and Sekisei Lagoon) and Ogasawara via scuba diving (Table 1 and Figure 1). The tube feet were preserved in 99.5% ethanol prior to DNA extraction. Genomic DNA extraction was carried out using a modified heat alkaline method (Meeker et al., 2007; Nakabayashi et al., 2019).

### Whole-Genome Sequencing and Assembly of a Reference Genome

We obtained a new high-quality whole-genome sequence for mapping. Whole-genome sequencing of the sample collected from Miyazaki (BioSample ID, SAMD00056692) was performed using Sequel, which is a single-molecule real-time sequencer from Pacific Biosciences (PacBio; Menlo Park, CA, United States),

according to the manufacturer's protocol. Previously published whole-genome short-read sequencing data (Wada et al., 2020) were downloaded from the BioProject PRJDB4009 in the ENA/Genbank/DDBJ database. Briefly, we obtained two paired-end (PE) libraries (insert sizes: 300 and 500 bp) and six mate-pair (MP) libraries (insert sizes: 3k, 5k, 8k, 10k, 12k, and 15k).

For the *in silico* procedures in this section, default parameters were used except where otherwise noted. Illumina PE and MP reads were filtered and trimmed using Platanus\_trim v1.0.7.<sup>1</sup> We assembled trimmed PE and MP reads using Platanus v1.2.5 (Kajitani et al., 2014) with the commands “assemble,” “scaffold,” and “gap\_close,” resulting in the scaffolds.

In addition to the short-read assembly, PacBio long-read assembly was conducted using Canu v1.7 (Koren et al., 2017). We polished the Canu contigs with the PacBio long reads using Pbalig v0.3.1<sup>2</sup> and Arrow in the GenomicConsensus package v2.2.2.<sup>3</sup> We additionally polished the contigs with Illumina (Illumina, San Diego, CA, United States) short reads using Bowtie2 v2.3.5.1 (Langmead and Salzberg, 2012) and Pilon v1.22 (Walker et al., 2014). The short read-based polishing was iterated until the number of corrected sites did not increase (number of iterations: 18).

Gaps in the short read-based scaffolds (Platanus result) were filled with polished long read-based contigs using an in-house program. The procedure is as follows (Supplementary Figure 1):

- (1) Fixed-length regions flanking the gaps in scaffolds were extracted.
- (2) The flanking sequences were aligned (queried) to the long read-based contigs using Minimap2 v2.17 (Li, 2018) with the options of “-c -k 19.”
- (3) The alignment results were filtered out if sequence identity < 90%, query coverage < 25%, or multiple best-scoring hits were identified.
- (4) Each gap was filled with a region between the alignments in the contig if the following conditions were satisfied:
  - (i) The flanking region pair was aligned to the same contig.
  - (ii) The distance between alignments < 50 kbp.

<sup>1</sup>[http://platanus.bio.titech.ac.jp/platanus\\_trim](http://platanus.bio.titech.ac.jp/platanus_trim)

<sup>2</sup><https://www.pacb.com/support/software-downloads/>

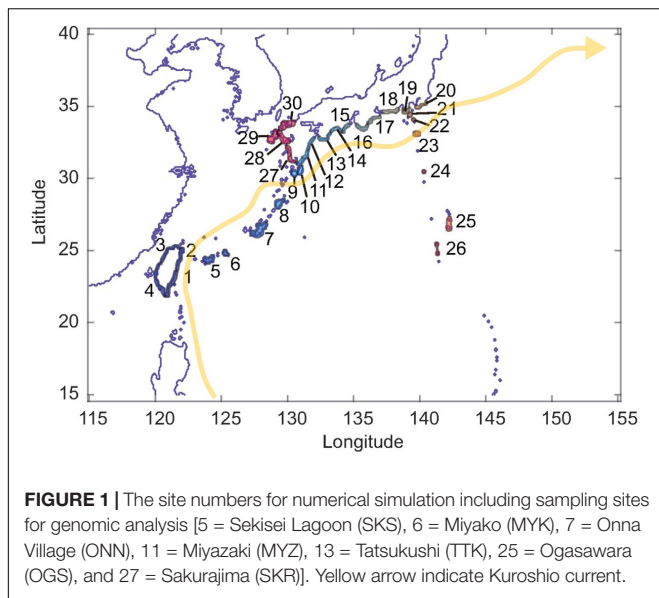
<sup>3</sup><https://github.com/PacificBiosciences/GenomicConsensus>

**TABLE 1** | Sample information and genetic diversity inbreeding coefficient.

Location	N	Site code	Year	Latitude	Longitude	Ho	He	F	N. clones	Div. clones	PI
Tatsukushi	12	TTK	2006	N32.785	E132.865	0.04	0.04	−0.01	1	0.985	5.67E-17
Miyazaki	26	MYO	2019	N31.532	E131.392	0.04	0.04	0.02	0	1	2.01E-18
Sakurajima	23	SKR	2005	N31.529	E130.648	0.04	0.04	0.01	0	1	2.28E-18
Onna Vil.	41	ONN	2013	N23.302	E127.511	0.04	0.04	0.02	1	0.999	3.94E-18
Miyako Is.	22	MYK	2013	N25.101	E125.145	0.04	0.04	0.01	0	1	1.76E-17
Sekisei	28	SKS	2013	N24.317	E124.068	0.04	0.05	0.03	0	1	3.1E-19
Ogasawara	30	OGS	2018–2020	N27.534	E142.115	0.04	0.04	0.03	3	0.993	5.32E-18

N, number of individuals analyzed; Ho, observed heterozygosity; He, expected heterozygosity; F, inbreeding coefficient; N. clones, number of possible clonemates; Div. clones, observed clonal diversity under random; PI, probability of identity.





- (iii) The strands of the alignments were consistent.
- (iv) There was no “N” in the corresponding regions in the contig.

- (5) Steps (1) to (4) were iterated eight times. Here, the specific length of the flanking regions was applied for each iteration (500, 1k, 5k, 10k, 20k, 40k, 80k, and 160k).
- (6) Step (5) was iterated twice.

Finally, to eliminate contamination, we performed homology searches of the assembly against the NCBI genome database (human, bacteria, and virus), the mitochondrial genome of *A. planci* (accession no. NC007788), and the chromosome sequence of the COTS symbiont (COTS27, accession no. AP019861) using BLASTN v2.7.1 (Altschul et al., 1990). The assembled sequences (scaffolds or contigs) were eliminated as contamination if sequence identity  $\geq 90\%$  and query coverage  $\geq 50\%$  (Supplementary Table 1). We assessed the completeness of the draft genome using BUSCO v4.0.6 with the Metazoa Odb10 dataset (Seppey et al., 2019). K-mer-based ( $k = 17$ ) estimations of the sizes of the genome and duplicated regions were also conducted using Jellyfish v2.2.10 (Marçais and Kingsford, 2011) and GenomeScope v2.0 (Ranallo-Benavidez et al., 2020).

## Multiplexed ISSR Genotyping by Sequencing Analysis

MIG-seq is a population genomic method that can easily detect a moderate number of neutral single nucleotide polymorphisms (SNPs) (Suyama and Matsuki, 2015). Previous studies using MIG-seq on marine species successfully discovered species boundaries and genetic structures that were undetectable using traditional genetic markers such as mitochondrial DNA and nuclear ribosomal internal transcribed spacer 2 (Nakabayashi et al., 2019; Takata et al., 2019).

We used eight pairs of multiplex ISSR primers (MIG-seq primer set 1; Suyama and Matsuki, 2015) with the Multiplex PCR Assay Kit Ver. 2 (TaKaRa Bio Inc., Shiga, Japan) for the first polymerase chain reaction (PCR). We slightly modified the protocol by Suyama and Matsuki (2015) and used a total reaction volume of 7  $\mu$ L in a T100™ Thermal Cycler (Bio-Rad, Hercules, CA, United States) under the following conditions: initial denaturation at 94°C for 1 min; followed by 25 cycles of 94°C for 30 s, 38°C for 1 min, and 72°C for 1 min; and final extension at 72°C for 10 min. The samples were indexed in the second PCR, which was performed with PrimeSTAR GXL DNA polymerase (TaKaRa Bio Inc.) using a total reaction volume of 12  $\mu$ L in a thermal cycler under the following conditions: 21 cycles of 98°C for 10 s, 54°C for 15 s, and 68°C for 1 min. PCR products were run on an agarose gel, and 350–800 bp PCR products were extracted from the gel. The gel-extracted DNA was pooled and sequenced using MiSeq Control Software v2.0.12 (Illumina) with the MiSeq Reagent v3 150 cycle kit (Illumina). Image analysis and base calling were performed using Real-Time Analysis Software v1.17.21 (Illumina).

To eliminate low-quality reads and primer sequences from the raw data, we used the FASTX-Toolkit v 0.0.14 (Gordon and Hannon, 2012)<sup>4</sup> with a fastq-quality-filter setting of  $-q\ 30\ -p\ 40$ . We removed adapter sequences for the Illumina MiSeq run from both the 5' end (GTCA GATCGGAAGAGCACACGTCTGAACTCCAGTCAC) and the 3' end (CAGAGATCGGAAGAGCGTCGTGTAGGGAAAGAC) using Cutadapt v1.13 (Martin, 2011), and then we excluded short reads less than 80 bp. We used Stacks v2.2 (Catchen et al., 2013; Rochette and Catchen, 2017) to stack the reads and extract the SNPs. We used the newly sequenced *A. cf. solaris* genome as a reference, as described below. We used the Gstacks option (-rm, -pcr, -duplicates) in Stacks v2.2 to remove PCR duplicates by randomly discarding all but one pair of each set of reads. We used population software in Stacks to prepare the dataset. We used the minimum percentage of individuals required to process a locus across all data ( $r$ ) equal to 0.95. After excluding individuals missing more than 10% of SNP data, we used a single SNP option to avoid strong linkage between loci for Structure analysis. We used all SNPs for the remaining genetic analyses.

## Population Genetics

BayeScan v2.1 (Narum and Hess, 2011) was used to detect possible SNPs under natural selection with a default setting. Genetic diversity (expected and observed heterozygosity,  $H_E$  and  $H_O$ , respectively), Hardy–Weinberg Equilibrium, global  $F_{ST}$  including and excluding Ogasawara samples, and pairwise  $F_{ST}$  values across different populations were calculated using GenAlEx v6.502 (Peakall and Smouse, 2012) with 9,999 permutations.

GenoDive v. 3.0 (Meirmans, 2020) was used to estimate possible clones within each population. Because the maximum pairwise genetic distance across all the samples ignoring missing data was 62 and there was a clear disjunction between a few

<sup>4</sup>[http://hannonlab.cshl.edu/fastx\\_toolkit/index.html](http://hannonlab.cshl.edu/fastx_toolkit/index.html)

possible clonemates and normal distribution histogram of non-clonemates that start from pairwise genetic distance of 13 (Supplementary Figure 2), we heuristically set a limit of possible clonemate as genetic distance of six to identify clones. Probability of Identify (Table 1) using all loci for each population was also estimated using GenAEx 6.5 (Peakall and Smouse, 2012).

To test whether the Ogasawara population is genetically different from other populations, a hierarchical analysis of molecular variance was conducted with prior grouping (Ogasawara vs. other populations) using Arlequin v3.5 (Excoffier and Lischer, 2010).

Bayesian clustering analysis was conducted using Structure software v2.3.4 (Pritchard et al., 2000) with 500,000 burn-in followed by 500,000 steps of Markov chain Monte Carlo simulations and 10 iterations. We used admixture- and allele frequency-correlated models that were expected to best explain the data set. The LOCPRIOR model (Hubisz et al., 2009) was used with Ogasawara vs. other populations and without prior regional grouping, and the number of putative clusters ( $K$ ) was set from 1 to 7. The online software Structure Harvester (Earl and von Holdt, 2012) was used to summarize the likelihood value. Structure plots were summarized using the online software CLUMPAK (Kopelman et al., 2015). To further visualize the genetic relationships among different populations, principal coordinate analysis was conducted using GenAEx v6.502 based on pairwise genetic distances among populations. PGDspider v2.0.8.3 (Lischer and Excoffier, 2012) was used to convert the data formats.

## Simulation of Larval Dispersal

We conducted a Lagrangian larval dispersal simulation to elucidate the oceanographic connectivity between the regions. For this simulation, we used Connectivity Modeling System v2.0 (Paris et al., 2013) with the ocean analysis/reanalysis products produced by the Global Ocean Forecasting System 3.0 of Global HYCOM (Chassignet et al., 2007), which are 1/12° resolution (~9 km) daily products archived from 1993 to 2018.<sup>5</sup> We extracted the surface water current and sea surface temperature (SST) datasets from the Global HYCOM products ranged from 115°E–155°E longitude and 15°N–40°N latitude. Thirty source and sink sites were chosen to create source sink polygons that fit purpose of this study (see Figure 1). The particles regarded as COTS larvae were numerically released from ocean areas inside the polygons and tracked. Once a particle passed more than 14 days after release entered a polygon, the particle was removed and judged as successful settlement, and the connection between the source polygon and sink polygon was counted. If a particle passed 35 days without entering a polygon, it was removed and scored as failure to recruit. The timing of particle release (start time of COTS mass spawning) and duration of spawning at each site were determined by the following rules using a history of SST at the site provided by Global HYCOM analysis/reanalysis products based on Yasuda et al. (2010): (1) If SST at the site rose above 28°C, the particles were released until SST dropped below 26°C or 30 days passed; (2) If SST at the site did not reach 28°C, the particles were released while SST was higher than 26°C. A total

of 100 particles per day were released from each source polygon under the above conditions. Finally, we obtained a connectivity matrix that was created from larval dispersal simulations over 26 years (1993–2018).

Because the connectivity based on simulated larval dispersal is a one-generation direct linkage, indicating that stepping-stone migration had not been considered, we conducted back-tracing to the origin through a discrete-time Markov chain using the connectivity matrix. To this end, we first set the following form of the connectivity matrix  $\mathbf{N}(m \times m)$ :

$$\mathbf{N} = \begin{matrix} & \begin{matrix} \text{Source} \end{matrix} \\ \begin{pmatrix} n_{1,1} & \cdots & n_{1,j} & \cdots & n_{1,m} \\ \vdots & & & & \vdots \\ n_{i,1} & & n_{i,j} & & n_{i,m} \\ \vdots & & & \ddots & \vdots \\ n_{m,1} & \cdots & n_{m,j} & \cdots & n_{m,m} \end{pmatrix} & \begin{matrix} \text{Sink} \end{matrix} \end{matrix} \quad (1)$$

The matrix elements were normalized by the total number of sink particles as follows:

$$\mathbf{P} = \begin{pmatrix} p_{1,1} & \cdots & p_{1,j} & \cdots & p_{1,m} \\ \vdots & & & & \vdots \\ p_{i,1} & & p_{i,j} & & p_{i,m} \\ \vdots & & & \ddots & \vdots \\ p_{m,1} & \cdots & p_{m,j} & \cdots & p_{m,m} \end{pmatrix}, \quad (2)$$

Where

$$p_{i,j} = \frac{n_{i,j}}{\sum_{j=1}^m n_{i,j}} \quad (3)$$

The normalized connectivity matrix can be regarded as the transition matrix of the Markov chain. The  $n$ -th power of the transition matrix  $\mathbf{P}^n$  represents the  $n$  time-step back-trace to the origin source.

## RESULTS

### Sequencing and Single Nucleotide Polymorphism Metrics

In total, 11,461,866 raw reads ranging from 9,190 to 281,474 reads per sample were obtained for 187 *A. cf. solaris* samples. After filtering out the low-quality reads, 6,125,996 reads ranging from 5,996 to 107,468 reads per sample remained. On average, 189,536 reads per individual remained after two-step filtering. We excluded seven samples missing more than 10% data and used a total of 182 samples for analysis. Using all SNP options, we obtained a total of 464 SNPs, which were used for all subsequent analyses except for Structure analysis. For Structure analysis, 115 SNPs using a single SNP option were used. BayeScan indicated that all loci were neutral ( $q$ -values > 0.05).

### Genetic Diversity and Genetic Differentiation

Genetic diversity ( $H_O$  and  $H_E$ ) of the studied populations, including that from Ogasawara, were comparable and ranged

<sup>5</sup><https://www.hycom.org/>

from 0.039 to 0.044 and 0.039–0.045 for  $H_O$  and  $H_E$ , respectively (Table 1). In total five pairs of possible clonemates were found in Tatsukushi (TTK, one pair out of 12), Onna Village (ONN; one pair out of 41), and Ogasawara (OGS; three pairs out of 30) populations (Table 1). Global  $F_{ST}$  values were significant ( $P < 0.001$ ) but small both for groups including ( $F_{ST} = 0.005$ ) and excluding the Ogasawara population ( $F_{ST} = 0.006$ ). Likewise, analysis of molecular variance with prior grouping (Ogasawara vs. other populations) indicated that  $F_{CT}$  was low and not significant (0.00167,  $P = 0.219$ ). Pairwise  $F_{ST}$  values across the studied populations were also small, and only two pairs [Sekisei Lagoon (SKS) and Tatsukushi (TTK), Miyazaki (MYZ), and Ogasawara (OGS)] became significant after sequential Bonferroni correction ( $\alpha < 0.05$ ) (Table 2).

Mean log likelihood values [mean  $\ln P(D)$ ] were highest at  $K = 1$  without prior grouping and comparable at  $K$  from 1 to 7 with prior grouping, with the lowest standard deviation value of mean  $\ln P(D)$  found at  $K = 1$  (Supplementary Table 2). Structure bar plots with and without prior geographic grouping suggested genetic homogeneity across the populations (Figure 2A and Supplementary Figure 4). Principal coordinate analysis indicated that, along the  $x$ -axis, SKS, MYK, and Sakurajima (SKR) were divided from the others, although it was not related to geographic location or the year of sampling (Figure 2B).

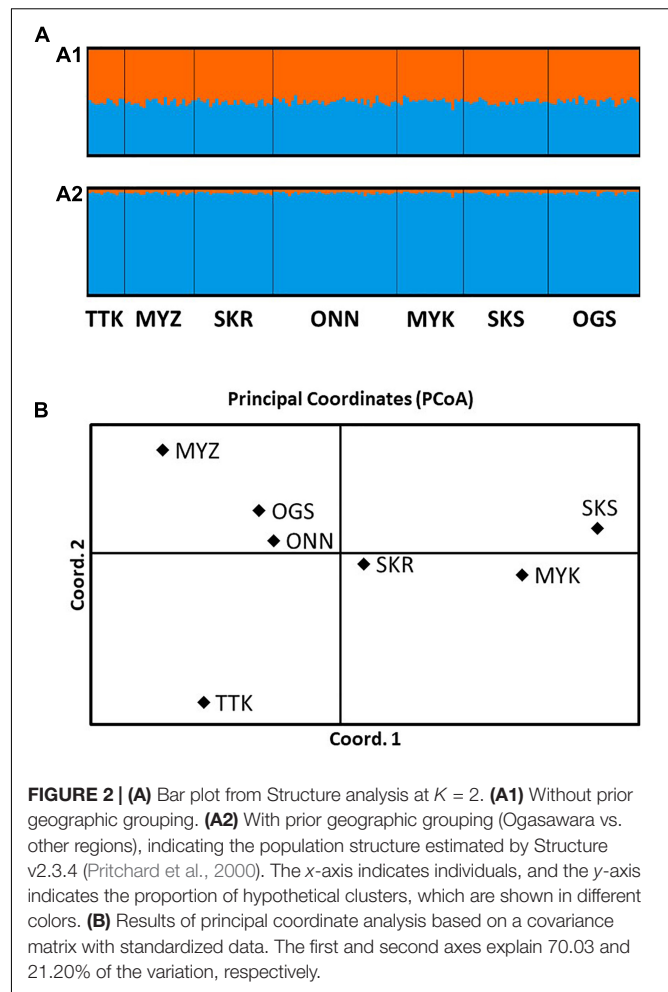
## The Larval Dispersal Simulation

The results of the larval dispersal simulations are shown as a connectivity matrix (Supplementary Figure 3). The diagonal elements of the matrix indicate self-seeding. Basically, site numbers from 1 to 20 were assigned from south to north along the Kuroshio Current; site numbers from 21 to 25 were assigned from Nii-Jima and Shikine islands, which are closer to Japan's main island, to the Ogasawara and Iwo-Jima Islands, which are further; and site numbers from 26 to 30 were assigned along the Tsushima Warm Current. The linkage of the site numbers for numerical simulation to site names for genomic analysis was as follows: 5 = Sekisei Lagoon (SKS), 6 = Miyako (MYK), 7 = Onna Village (ONN), 11 = Miyazaki (MYZ), 13 = Tatsukushi (TTK), 25 = Ogasawara (OGS), and 27 = Sakurajima (SKR). The results of this analysis confirmed that the larvae were transported from south to north by following the Kuroshio Current. However, they

**TABLE 2 |** Pairwise  $F_{ST}$  values (below) and their probability values (above).

	TTK	MYZ	SKR	ONN	MYK	SKS	OGS
TTK		0.295	0.224	0.105	0.003	<b>0.000</b>	0.107
MYZ	0.003		0.400	0.142	0.023	<b>0.000</b>	0.141
SKR	0.004	0.001		0.465	0.484	0.21	0.473
ONN	0.006	0.002	0.000		0.370	0.031	0.447
MYK	0.018	0.007	0.000	0.001		0.355	0.045
SKS	<b>0.028</b>	<b>0.014</b>	0.002	0.004	0.001		0.004
OGS	0.006	0.003	0.000	0.000	0.005	0.008	

Significantly differentiated pairs after sequential Bonferroni correction ( $\alpha < 0.05$ ) are shown in bold face.



**FIGURE 2 |** (A) Bar plot from Structure analysis at  $K = 2$ . (A1) Without prior geographic grouping. (A2) With prior geographic grouping (Ogasawara vs. other regions), indicating the population structure estimated by Structure v2.3.4 (Pritchard et al., 2000). The  $x$ -axis indicates individuals, and the  $y$ -axis indicates the proportion of hypothetical clusters, which are shown in different colors. (B) Results of principal coordinate analysis based on a covariance matrix with standardized data. The first and second axes explain 70.03 and 21.20% of the variation, respectively.

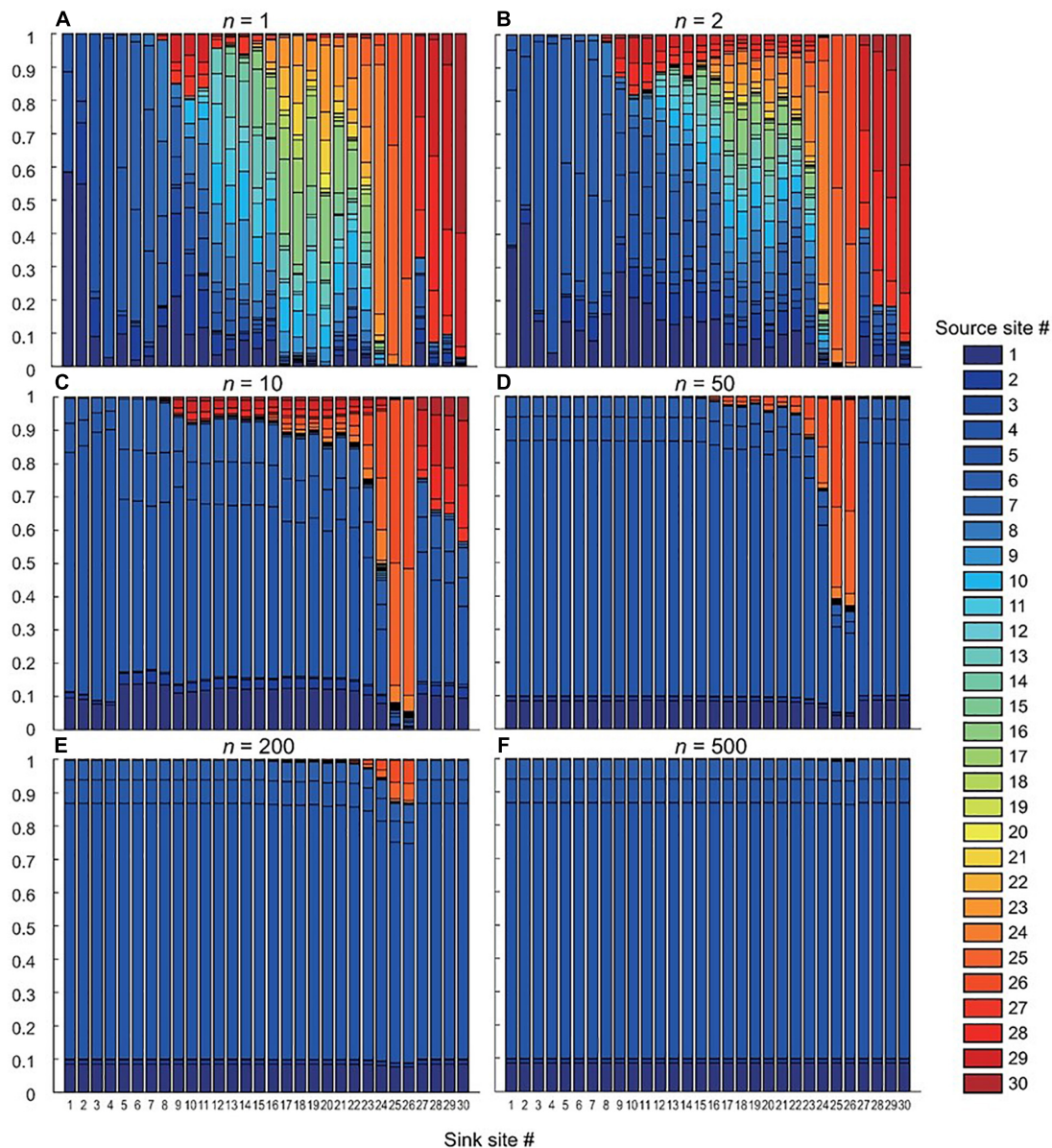
also confirmed that self-seeding dominated in the Ogasawara area, and it is very rare for larvae from the other sites to reach the Ogasawara area directly or for larvae from the Ogasawara area to reach the other sites directly.

Figure 3 shows the back-tracing results obtained using Markov chains. The bar of each site indicates the ratio of the number of particles released from the source site (laws of transition matrix  $P^n$ ). The results indicate that the origin sites gradually converged with some of the upstream sites of the Kuroshio Current. The population in the Ogasawara area is not well mixed with that of the Kuroshio region, but the 200–500 time-steps, which may be regarded as representing over a few hundred generations, confirmed that the populations in the Kuroshio region and the Ogasawara region are almost mixed.

## DISCUSSION

This study examined larval dispersal of the coral predator *A. cf. solaris* between the Kuroshio region and Ogasawara using population genomic analysis and oceanographic simulation to test the secondary outbreak hypothesis. Contrasting results were obtained using different methods. Population genomic analysis





**FIGURE 3 |** The ratio of the number of particles originating from each source site. (A) Simulation of 26-year larval dispersal (see sites, **Figure 1** and connectivity matrix, **Supplementary Figure 3**). The ratio determined by Markov chains with (B) time-step  $n = 2$ , (C)  $n = 10$ , (D)  $n = 50$ , (E)  $n = 200$ , and (F)  $n = 500$ . Site numbers are assigned as follows: 5 = Sekisei Lagoon (SKS), 6 = Miyako (MYK), 7 = Onna Village (ONN), 11 = Miyazaki (MYZ), 13 = Tatsukushi (TTK), 25 = Ogasawara (OGS), and 27 = Sakurajima (SKR).

indicated genetic homogeneity between the populations of the two regions, and oceanographic numerical simulation indicated that multiple-generation stepping-stone migration was required to disperse larvae from the Kurshio region to Ogasawara. These results indicate that the Ogasawara population of *A. cf. solaris* has the same genetic origin as that of the Kuroshio region, but a large amount of one-generation larval dispersal, such as a secondary outbreak from the Kuroshio region to Ogasawara, is unlikely. Rather, the data suggest that the population outbreak in Ogasawara might have been caused by successful self-seeding. This study highlights the importance of an integrated

approach for estimating larval dispersal, including its timescale, for conservation purposes.

## Potential of Secondary Outbreak Between Ogasawara and Kuroshio Region

In this study, all population genomic results indicated genetic similarity and no genetic structure between *A. cf. solaris* populations in the Ogasawara and Kuroshio regions. The analysis of molecular variance and Structure results indicate that the



origins of *A. cf. solaris* populations in the Ogasawara and Kuroshio regions are genetically similar. Low  $F_{ST}/F_{CT}$  values between the Ogasawara and Kuroshio regions indicate (1) a contemporary, large amount of larval dispersal, (2) accumulation of stepping-stone migrants over multiple years, or (3) recent separation of a population with no or limited ongoing gene flow. Based on the oceanographic numerical simulation analysis results and historical records of *A. cf. solaris* in Ogasawara, the latter two are more likely than contemporary, large amounts of larval dispersal.

The result of the 26-year oceanographic simulation suggests that the chance of direct one-generation larval dispersal between the Kuroshio region and Ogasawara is very low, although stepping-stone migration (e.g., via Hachijyo-jima in Izu islands) between the two regions over multiple generations is physically possible. The Markov chain simulation, which simulated stepping-stone migration over multiple generations, indicated that the Ogasawara population is dominated by migrants from the Kuroshio region after 200–500 generations. This implies that the accumulation of larvae from low levels of migration between the Kuroshio and Ogasawara regions over multiple years would result in genetic homogeneity. Given that there are no observed reports of population outbreaks of *A. cf. solaris* in stepping-stone regions (e.g., Izu islands) in the last 40 years (Yasuda, 2018), genetic homogeneity between the Ogasawara and Kuroshio regions observed by  $F$ -statistics and Structure analysis could be attributed to stepping-stone larval migration over multiple generations. Crandall et al. (2018) demonstrated observed results of the marine species along Hawaii archipelagos where  $F_{ST}$  is not significantly different from zero were not actually panmictic but having weak hierarchical structure of isolation-by-distance caused by stepping-stone migration. Coalescent simulation including *A. cf. solaris* samples from Izu islands would confirm this hypothesis.

Alternatively, it is possible that the observed strong gene flow resulted from recent colonization. According to a literature survey, there was no record of *A. cf. solaris* in the Ogasawara region before 1945, and the first record of this species in Ogasawara was in 1968 (Kurata, 1984; Yasuda, 2018). Since then, the density of *A. cf. solaris* in Ogasawara has been low (Yasuda, 2018). However, a lack of a record of *A. cf. solaris* in Ogasawara before 1945 does not necessarily mean a complete absence of this species in the region, given that almost no studies or surveys were conducted before 1945. In addition, crown-of-thorns sea stars are cryptic, and it would have been difficult to detect a few individuals that have been colonized for the first time. Recent migration with a small population size would predict low genetic diversity due to the founder effect, although we observed almost the same genetic diversity in the Ogasawara and Kuroshio regions. Therefore, high genetic diversity in Ogasawara and strong gene flow between the Ogasawara and Kuroshio regions is more likely caused by stepping-stone larval migration over multiple generations, as suggested by the oceanographic simulation.

Whichever may be the case, the oceanographic simulation suggests that contemporary, one-generation larval dispersal between the Ogasawara and Kuroshio regions is limited, and

thus, direct secondary population outbreaks that require a large amount of larval dispersal within a generation from the Kuroshio region to Ogasawara are unlikely.

Kurata (1984) speculated that *A. cf. solaris* in Ogasawara might have colonized either from the Kuroshio region or from Mariana regions such as Guam. According to a population genetics analysis using microsatellite markers, genetic differentiation between the Kuroshio and Guam regions has been identified (Tusso et al., 2016), implying that colonization and/or secondary population outbreaks from Guam to the Ogasawara region are less likely than those from the Kuroshio region.

Only one previous study examined the genetic connectivity of coral reef organisms between the Kuroshio and Ogasawara regions. A reef-building coral species, *Acropora* sp., which has a shorter (average 3–4 days) larval stage than that of *A. cf. solaris*, showed genetic differentiation between the Ogasawara and Kuroshio regions (Nakajima et al., 2012). This implies that larval dispersal from the Kuroshio region to the Ogasawara region of coral reef organisms with short larval stages is quite limited.

## Possible Causes of Population Outbreak in Ogasawara

Oceanographic simulation suggests that many larvae are self-recruited in Ogasawara compared with other *A. cf. solaris* populations in the Kuroshio region (**Supplementary Table 3**). This fact indicates that the observed population outbreak in Ogasawara in 2018 was caused by a sudden increase in regional self-seeding (namely “primary outbreak” as opposed to “secondary outbreak”). While several hypotheses have been proposed to explain the primary outbreak of *A. cf. solaris*, the causes of primary outbreaks are still unclear (Pratchett et al., 2014). The causes of outbreak would also depend on several regional environmental conditions being met simultaneously (Pratchett et al., 2017; Okaji et al., 2019): elevated levels of larval nutrition and subsequent higher survival rates supported by favorable physical, chemical, and biological conditions such as lower predation on larvae and juveniles; and physical processes acting on larvae that increase their survival (e.g., weather conditions and current patterns) (Keesing and Halford, 1992; Okaji et al., 2019).

The population outbreak in Ogasawara in 2018 could be attributed to successful local larval recruitment in 2016, given that it takes 2 years for *A. cf. solaris* larvae to become adults (Birkeland and Lucas, 1990). Oceanographic simulation also suggests that the number of self-recruited larvae in Ogasawara was larger (397) in 2016, which exceeded the average (252) over 26 years (**Supplementary Table 4**). The large number of self-recruited larvae might be partly due to the smaller number of typhoons during the larval period (July to October, estimated by the spawning period associated with water temperature; Yasuda et al., 2010); in 2016, three typhoons passed through the Ogasawara region, which is below the 70-year average (4.47) (data from Japan Meteorological Agency, **Supplementary Table 5**). A previous field survey discovered dense clouds of *A. cf. planci* larvae before one typhoon, but they were scattered and

disappeared from the coral reef area after the typhoon (Suzuki et al., 2016), implying that typhoons prevent mass settlement of larvae. However, in some years with a higher number of self-recruits and fewer typhoons, no population outbreak was observed in Ogasawara.

Recently, self-fertilization and/or clonal propagation hypothesis has been proposed by Guerra et al. (2020) to explain the cause of primary outbreak as evidenced by the existence of hermaphrodites and the finding of possible larval cloning of *A. cf. solaris* (Allen et al., 2019). In the present study, we found three pairs of individuals in Ogasawara population were possible clonal or genetically very close individual (Table 1 and Supplementary Figure 2). It is also notable that we also found one pair of possible clonemates in Tatsukushi population where previous study found hermaphrodites (Guerra et al., 2020). Although we need more precise analysis to identify true clonemates, it is possible that inbreeding including self-fertilization or larval cloning also partly facilitated the initiation of population outbreak in the oceanographically isolated Ogasawara populations.

Other factors such as increased success of cross-fertilization (Rogers et al., 2017), lower salinity, and higher phytoplankton biomass during the larval stage (Lucas, 1973), and reduced predation during the post-settlement stage (McCallum, 1987; Keesing and Halford, 1992) also may be associated with the demographic fluctuation of *A. cf. solaris* in the Ogasawara area. An Allee threshold of three starfish  $\text{ha}^{-1}$  (below which reproductive capacity is greatly reduced regardless of the aggregation level) is proposed and aggregation during spawning period is key in causing population outbreaks (Rogers et al., 2017). Laboratory experiments indicated that lower salinity and increased phytoplankton biomass that are often caused by territorial run-off enhances the survival rate of *A. cf. solaris* (Lucas, 1973; Birkeland, 1982; Fabricius et al., 2010). Keesing and Halford (1992) also suggested that juveniles of *A. cf. solaris* would be strongly influenced by predation because of their slow growth and movement, underlining the importance of posttreatment processes for population outbreak. All these factors may influence the population dynamics of *A. cf. solaris* in Ogasawara.

## Multiple Approaches to Estimate Larval Dispersal in Marine Organisms

This study estimated larval dispersal of *A. cf. solaris* between Kuroshio and Ogasawara using two different approaches: population genomic analysis and larval dispersal simulation. Gene flow estimation by the population genomic approach often reflects both contemporary and evolutionary processes, rendering the interpretation of the amount of contemporary dispersal difficult because of the long evolutionary timescale. Genetic homogeneity can be observed due to a large amount of contemporary larval dispersal (secondary population outbreak) or stepping-stone migrants over multiple generations or recent divergence with no contemporary dispersal. Our study is unique in that it included an oceanographic model with Markov chain simulation. Such a simulation was useful for testing these alternative hypotheses. A simple oceanographic simulation averaged over 26 years first rejected the secondary

population outbreak hypothesis by indicating limited physical larval transport from the Kuroshio to the Ogasawara region within a generation. This result supports the idea that stepping-stone migrants over multiple generations is responsible for the genetic homogeneity observed in the  $F_{ST}$  and Structure analysis between the Kuroshio and Ogasawara populations.

This may give the impression that oceanographic simulation alone is enough for testing the secondary population hypothesis; however, it is generally imperfect for estimating larval dispersal. Our model regarded larvae as neutral passive particles without any of the biological characteristics of larvae that may influence actual larval dispersal, such as vertical movement, natural selection, food availability, and mortality. In addition, the model only simulates the dispersal process, which does not include post-settlement survival. In some marine species, genetic connectivity is quite limited despite having long pelagic larval duration possibly caused by several biological features of larvae and juveniles (e.g., Barber et al., 2000, 2002). Thus, a comparison with genetic connectivity that reflects all the biological characteristics of the species is also important. While several previous studies have reported good agreement between oceanographic models and genetic analysis and have provided robust and straightforward interpretations of larval dispersal occurring on an ecological timescale (e.g., Galindo et al., 2006; White et al., 2010; Sunday et al., 2014; Taninaka et al., 2019), only a few have discussed the usefulness of oceanographic modeling for identifying alternative hypotheses or provided additional insights into the causes of observed population genetic structure (Galindo et al., 2010; Crandall et al., 2014). By applying Markov chain simulation in the numerical simulation, we could also include the effect of migration over multiple generations, which is easier to compare with genetic results than a single generation simulation result in terms of timescale. This method underlines the usefulness and importance of using both genetic and oceanographic methods to estimate larval dispersal and provides significant insight into larval dispersal that occurs on ecological and evolutionary timescales.

## Conservation Implications

This study indicated that population outbreaks of *A. cf. solaris* in the Ogasawara Islands are independent of successive outbreaks in the Kuroshio region and that outbreaks are more likely caused by local self-seedings. Considering it takes at least 2 years for *A. cf. solaris* to reach adulthood (Birkeland and Lucas, 1990), caution and early monitoring should be taken 2 years following the observation of local ocean current system retention and other preferable conditions for the survival during early life stage of *A. cf. solaris*. For example, a large amount of terrestrial run-off will increase the survival rate of *A. cf. solaris* by increasing food available for larvae. In addition, high levels of larvae aggregation were observed only before a typhoon (Suzuki et al., 2016), and thus, a fewer number of typhoons during spawning periods may increase the chance of high levels of larval aggregation and settlement. Local monitoring of juvenile starfish 2 years after such preferable conditions would be useful for early detection and

predicting population outbreaks and to avoid being too late for coral reef management (Okaji et al., 2019).

## DATA AVAILABILITY STATEMENT

The datasets presented in this study can be found in online repositories. The names of the repository/repositories and accession number(s) can be found below: DDBJ (accession: DRA011826).

## AUTHOR CONTRIBUTIONS

NY conceived the study. MH, NY, RK, HY, and TY drafted the manuscript. RK, HY, TI, and AT sequenced, assembled, and reconstructed the reference genome. NY, YA, and TS collected the *Acanthaster* samples. MH, HT, HY, TK, and NY conducted the MIG-seq analysis. TN and TY conducted oceanographic simulations. All authors edited the draft and approved it for publication.

## REFERENCES

- Alberto, F., Raimondi, P. T., Reed, D. C., Watson, J. R., Siegel, D. A., Mitarai, S., et al. (2011). Isolation by oceanographic distance explains genetic structure for *Macrocystis pyrifera* in the Santa Barbara channel. *Mol. Ecol.* 20, 2543–2554. doi: 10.1111/j.1365-294X.2011.05117.x
- Allen, J. D., Richardson, E. L., Deaker, D., Agüera, A., and Byrne, M. (2019). Larval cloning in the crown-of-thorns sea star, a keystone coral predator. *Mar. Ecol. Prog. Ser.* 609, 271–276. doi: 10.3354/meps12843
- Almany, G. R., Connolly, S. R., Heath, D. D., Hogan, J. D., Jones, G. P., McCook, L. J., et al. (2009). Connectivity, biodiversity conservation and the design of marine reserve networks for coral reefs. *Coral Reefs* 28, 339–351. doi: 10.1007/s00338-009-0484-x
- Altschul, S. F., Gish, W., Miller, W., Myers, E. W., and Lipman, D. J. (1990). Basic local alignment search tool. *J. Mol. Biol.* 215, 403–410. doi: 10.1016/S0022-2836(05)80360-2
- Arndt, A., and Smith, M. J. (1998). Genetic diversity and population structure in two species of sea cucumber: differing patterns according to mode of development. *Mol. Ecol.* 7, 1053–1064. doi: 10.1046/j.1365-294x.1998.00429.x
- Baird, A. H., Pratchett, M. S., Hoey, A. S., Herdiana, Y., and Campbell, S. J. (2013). *Acanthaster planci* is a major cause of coral mortality in Indonesia. *Coral Reefs* 32, 803–812. doi: 10.1007/s00338-013-1025-1
- Barber, P. H., Palumbi, S. R., Erdmann, M. V., and Moosa, M. K. (2000). A marine Wallace's line? *Nature* 406, 692–693. doi: 10.1038/35021135
- Barber, P. H., Palumbi, S. R., Erdmann, M. V., and Moosa, M. K. (2002). Sharp genetic breaks among populations of *Haplosquilla pulchella* (Stomatopoda) indicate limits to larval transport: patterns, causes, and consequences. *Mol. Ecol.* 11, 659–674. doi: 10.1046/j.1365-294x.2002.01468.x
- Benzie, J. A. H. (1992). Review of the genetics, dispersal and recruitment of crown-of-thorns starfish (*Acanthaster planci*). *Mar. Freshw. Res.* 43, 597–610. doi: 10.1071/MF9920597
- Benzie, J. A. H. (1999a). Genetic structure of coral reef organisms: ghosts of dispersal past. *Am. Zool.* 39, 131–145. doi: 10.1093/icb/39.1.131
- Benzie, J. A. H. (1999b). Major genetic differences between crown-of-thorns starfish (*Acanthaster planci*) populations in the Indian and Pacific Oceans. *Evolution* 53, 1782–1795. doi: 10.1111/j.1558-5646.1999.tb04562.x
- Biodiversity Center, Natural Environment Bureau, Ministry of the Environment (2021). *Monitoring Site 1000 Coral Reef Survey Report*. Available online at:

## FUNDING

Funding for this study was provided by the Environmental Research and Technology Development Fund (4RF–1501 and 4–1304) of the Ministry of the Environment, Japan; a Grant-in-Aid for Young Scientists (A) (17H04996), JSPS KAKENHI 221S0002, 16H06279 (PAGS) Grant-in-Aid for Research Fellows (19J21342 and 18J23317) and Bilateral Joint Research (JPJSBP120209929) from the Japan Society for the Promotion of Science (JSPS).

## ACKNOWLEDGMENTS

We express our gratitude to Eriko Nagahiro for her help in the molecular experiment.

## SUPPLEMENTARY MATERIAL

The Supplementary Material for this article can be found online at: <https://www.frontiersin.org/articles/10.3389/fmars.2021.688139/full#supplementary-material>

[http://www.biodic.go.jp/moni1000/findings/reports/pdf/2019\\_coral\\_reef.pdf](http://www.biodic.go.jp/moni1000/findings/reports/pdf/2019_coral_reef.pdf) (accessed December 16, 2021).

- Birkeland, C. (1982). Terrestrial runoff as a cause of outbreaks of *Acanthaster planci* (Echinodermata: Asteroidea). *Mar. Biol.* 69, 175–185. doi: 10.1007/BF00396897
- Birkeland, C., and Lucas, J. (1990). *Acanthaster planci: Major Management Problem of Coral Reefs*. Boca Raton, FL: CRC Press, 272.
- Botsford, L. W., White, J. W., Coffroth, M. A., Paris, C. B., Planes, S., Shearer, T. L., et al. (2009). Connectivity and resilience of coral reef metapopulations in marine protected areas: matching empirical efforts to predictive needs. *Coral Reefs* 28, 327–337. doi: 10.1007/s00338-009-0466-z
- Catchen, J., Hohenlohe, P. A., Bassham, S., Amores, A., and Cresko, W. A. (2013). Stacks: an analysis tool set for population genomics. *Mol. Ecol.* 22, 3124–3140. doi: 10.1111/mec.12354
- Chassignet, E. P., Hurlburt, H. E., Smedstad, O. M., Halliwell, G. R., Hogan, P. J., Wallcraft, A. J., et al. (2007). The HYCOM (HYbrid Coordinate Ocean Model) data assimilative system. *J. Mar. Syst.* 65, 60–83. doi: 10.1016/j.jmarsys.2005.09.016
- Chesher, R. H. (1969). Destruction of Pacific corals by the sea star *Acanthaster planci*. *Science* 165, 280–283. doi: 10.1126/science.165.3890.280
- Crandall, E. D., Toonen, R. J., ToBo Laboratory, and Selkoe, K. A. (2018). A coalescent sampler successfully detects biologically meaningful population structure overlooked by F-statistics. *Evol. Appl.* 12, 255–265. doi: 10.1111/eva.12712
- Crandall, E. D., Tremblay, E. A., Liggins, L., Gleeson, L., Yasuda, N., Barber, P. H., et al. (2014). Return of the ghosts of dispersal past: historical spread and contemporary gene flow in the blue sea star *Linckia laevigata*. *Bull. Mar. Sci.* 90, 399–425. doi: 10.5343/bms.2013.1052
- De'ath, G., Fabricius, K. E., Sweatman, H., and Puotinen, M. (2012). The 27-year decline of coral cover on the Great Barrier Reef and its causes. *Proc. Natl. Acad. Sci. U.S.A.* 109, 17995–17999. doi: 10.1073/pnas.1208909109
- Dight, I. J., Bode, L., and James, M. K. (1990a). Modelling the larval dispersal of *Acanthaster planci* I. Large scale hydrodynamics, Cairns Section, Great Barrier Reef Marine Park. *Coral Reefs* 9, 115–123. doi: 10.1007/BF00258222
- Dight, I. J., James, M. K., and Bode, L. (1990b). Modelling the larval dispersal of *Acanthaster planci*. II. Patterns of reef connectivity. *Coral Reefs* 9, 125–134. doi: 10.1007/BF00258224
- Earl, D. A., and von Holdt, B. M. (2012). STRUCTURE HARVESTER: a website and program for visualizing STRUCTURE output and implementing the Evanno method. *Conserv. Genet. Resour.* 4, 359–361. doi: 10.1007/s12686-011-9548-7



- Excoffier, L., and Lischer, H. E. L. (2010). Arlequin suite ver 3.5: a new series of programs to perform population genetics analyses under Linux and Windows. *Mol. Ecol. Resour.* 10, 564–567. doi: 10.1111/j.1755-0998.2010.02847.x
- Fabricius, K. E., Okaji, K., and De'ath, G. (2010). Three lines of evidence to link outbreaks of the crown-of-thorns seastar *Acanthaster planci* to the release of larval food limitation. *Coral Reefs* 29, 593–605. doi: 10.1007/s00338-010-0628-z
- Fukuda, M., and Hanamura, Y. (1996). Small scale distribution and transport of the Japanese anchovy, *Engraulis japonica*, larvae determined from a free-drifting buoy survey in Iyo-Nada, Seto Inland Sea [Japan] [1995]. *J. Agric. Sci. Technol.* 28, 9–20.
- Galindo, H. M., Olson, D. B., and Palumbi, S. R. (2006). Seascape genetics: a coupled oceanographic-genetic model predicts population structure of Caribbean corals. *Curr. Biol.* 16, 1622–1626. doi: 10.1016/j.cub.2006.06.052
- Galindo, H. M., Pfeiffer-Herbert, A. S., McManus, M. A., Chao, Y. I., Chai, F. E. I., and Palumbi, S. R. (2010). Seascape genetics along a steep cline: using genetic patterns to test predictions of marine larval dispersal. *Mol. Ecol.* 19, 3692–3707. doi: 10.1111/j.1365-294X.2010.04694.x
- Gordon, A., and Hannon, G. J. (2012). *FASTX-toolkit. FASTQ/A Short-Reads Pre-Processing Tools*. Available online at: [http://hannonlab.cshl.edu/fastx\\_toolkit/](http://hannonlab.cshl.edu/fastx_toolkit/) (accessed August 30, 2020).
- Guerra, V., Haynes, G., Byrne, M., Yasuda, N., Adachi, S., Nakamura, M., et al. (2020). Non-specific expression of fertilization genes in the crown-of-thorns *Acanthaster cf. solaris*: unexpected evidence of hermaphroditism in a coral reef predator. *Mol. Ecol.* 29, 363–379. doi: 10.1111/mec.15332
- Harrison, H. B., Pratchett, M. S., Messmer, V., Saenz-Agudelo, P., and Berumen, M. L. (2017). Microsatellites reveal genetic homogeneity among outbreak populations of crown-of-thorns starfish (*Acanthaster cf. solaris*) on Australia's Great Barrier Reef. *Diversity* 9:16. doi: 10.3390/d9010016
- Haszprunar, G., Vogler, C., and Wörheide, G. (2017). Persistent gaps of knowledge for naming and distinguishing multiple species of crown-of-thorns seastar in the *Acanthaster planci* species complex. *Diversity* 9:22. doi: 10.3390/d9020022
- Hubisz, M. J., Falush, D., Stephens, M., and Pritchard, J. K. (2009). Inferring weak population structure with the assistance of sample group information. *Mol. Ecol. Resour.* 9, 1322–1332. doi: 10.1111/j.1755-0998.2009.02591.x
- James, M. K., and Scandol, J. P. (1992). Larval dispersal simulations: correlation with the crown-of-thorns starfish outbreaks database. *Mar. Freshw. Res.* 43, 569–581. doi: 10.1071/MF9920569
- Kajitani, R., Toshimoto, K., Noguchi, H., Toyoda, A., Ogura, Y., Okuno, M., et al. (2014). Efficient de novo assembly of highly heterozygous genomes from whole-genome shotgun short reads. *Genome Res.* 24, 1384–1395. doi: 10.1101/gr.170720.113
- Keesing, J. K., and Halford, A. R. (1992). Importance of postsettlement processes for the population dynamics of *Acanthaster planci* (L.). *Mar. Freshw. Res.* 43, 635–651. doi: 10.1071/MF9920635
- Kopelman, N. M., Mayzel, J., Jakobsson, M., Rosenberg, N. A., and Mayrose, I. (2015). CLUMPAK: a program for identifying clustering modes and packaging population structure inferences across K. *Mol. Ecol. Resour.* 15, 1179–1191. doi: 10.1111/1755-0998.12387
- Koren, S., Walenz, B. P., Berlin, K., Miller, J. R., Bergman, N. H., and Phillippy, A. M. (2017). Canu: scalable and accurate long-read assembly via adaptive k-mer weighting and repeat separation. *Genome Res.* 27, 722–736. doi: 10.1101/gr.215087.116
- Kurata, Y. (1984). Crown-of-thorns starfish of Ogasawara Island [in Japanese]. *Mar. Park Inf.* 61, 7–9.
- Langmead, B., and Salzberg, S. L. (2012). Fast gapped-read alignment with Bowtie 2. *Nat. Methods* 9, 357–359. doi: 10.1038/nmeth.1923
- Li, H. (2018). Minimap2: pairwise alignment for nucleotide sequences. *Bioinformatics* 34, 3094–3100. doi: 10.1093/bioinformatics/bty191
- Lischer, H. E. L., and Excoffier, L. (2012). PGDSpider: an automated data conversion tool for connecting population genetics and genomics programs. *Bioinformatics* 28, 298–299. doi: 10.1093/bioinformatics/btr642
- Lucas, J. S. (1973). Reproductive and larval biology and *Acanthaster planci* (L.) in Great Barrier Reef. *Micronesica* 9, 197–203.
- Marçais, G., and Kingsford, C. (2011). A fast, lock-free approach for efficient parallel counting of occurrences of k-mers. *Bioinformatics* 27, 764–770. doi: 10.1093/bioinformatics/btr011
- Marko, P. B., and Hart, M. W. (2018). “Genetic analysis of larval dispersal, gene flow, and connectivity,” in *Evolutionary Ecology of Marine Invertebrate Larvae* (Oxford: Oxford University Press), 165–166.
- Martin, M. (2011). Cutadapt removes adapter sequences from high-throughput sequencing reads. *EMBnet J.* 17:10. doi: 10.14806/ej.17.1.200
- McCallum, H. I. (1987). Predator regulation of *Acanthaster planci*. *J. Theor. Biol.* 127, 207–220. doi: 10.1016/S0022-5193(87)80131-5
- Meeker, N. D., Hutchinson, S. A., Ho, L., and Trede, N. S. (2007). Method for isolation of PCR-ready genomic DNA from zebrafish tissues. *Biotechniques* 43, 610, 612, 614. doi: 10.2144/000112619
- Meirns, P. G. (2020). GenoDive version 3.0: easy-to-use software for the analysis of genetic data of diploids and polyploids. *Mol. Ecol. Resour.* 20, 1126–1131. doi: 10.1111/1755-0998.13145
- Miyake, Y., Kimura, S., Kawamura, T., Horii, T., Kurogi, H., and Kitagawa, T. (2009). Simulating larval dispersal processes for abalone using a coupled particle-tracking and hydrodynamic model: implications for refugium design. *Mar. Ecol. Prog. Ser.* 387, 205–222. doi: 10.3354/meps08086
- Nakabayashi, A., Yamakita, T., Nakamura, T., Aizawa, H., Kitano, Y. F., Iguchi, A., et al. (2019). The potential role of temperate Japanese regions as refugia for the coral *Acropora hyacinthus* in the face of climate change. *Sci. Rep.* 9:1892. doi: 10.1038/s41598-018-38333-5
- Nakajima, Y., Nishikawa, A., Iguchi, A., and Sakai, K. (2012). Regional genetic differentiation among northern high-latitude island populations of a broadcast-spawning coral. *Coral Reefs* 31, 1125–1133. doi: 10.1007/s00338-012-0932-x
- Narum, S. R., and Hess, J. E. (2011). Comparison of  $F_{ST}$  outlier tests for SNP loci under selection. *Mol. Ecol. Resour.* 11(Suppl. 1), 184–194. doi: 10.1111/j.1755-0998.2011.02987.x
- Nash, W. J., Goddard, M., and Lucas, J. S. (1988). Population genetic studies of the crown-of-thorns starfish, *Acanthaster planci* (L.), in the Great Barrier Reef region. *Coral Reefs* 7, 11–18. doi: 10.1007/BF00301976
- Okaji, K., Ogasawara, K., Yamakita, E., Kitamura, M., Kumagai, N., Nakatomi, N., et al. (2019). Comprehensive management program of crown-of-thorns starfish outbreaks in Okinawa [in Japanese]. *J. Jpn. Coral Reef Soc.* 21, 91–110. doi: 10.3755/jcrs.21.91
- Paris, C. B., Helgers, J., van Sebille, E., and Srinivasan, A. (2013). Connectivity modeling system: a probabilistic modeling tool for the multi-scale tracking of biotic and abiotic variability in the ocean. *Environ. Model. Softw.* 42, 47–54. doi: 10.1016/j.envsoft.2012.12.006
- Peakall, R., and Smouse, P. E. (2012). GenAlEx 6.5: genetic analysis in excel. Population genetic software for teaching and research: an update. *Bioinformatics* 28, 2537–2539. doi: 10.1093/bioinformatics/bts460
- Pratchett, M. S., Caballes, C. F., Rivera-Posada, J., and Sweatman, H. P. A. (2014). Limits to understanding and managing outbreaks of crown-of-thorns starfish (*Acanthaster* spp.). *Oceanogr. Mar. Biol.* 52, 133–200. doi: 10.1201/b17143-4
- Pratchett, M. S., Caballes, C. F., Wilmes, J. C., Matthews, S., Mellin, C., Sweatman, H., et al. (2017). Thirty years of research on crown-of-thorns starfish (1986–2016): scientific advances and emerging opportunities. *Diversity* 9:41. doi: 10.3390/d9040041
- Pritchard, J. K., Stephens, M., and Donnelly, P. (2000). Inference of population structure using multilocus genotype data. *Genetics* 155, 945–959. doi: 10.1093/genetics/155.2.945
- Ranallo-Benavidez, T. R., Jaron, K. S., and Schatz, M. C. (2020). GenomeScope 2.0 and Smudgeplot for reference-free profiling of polyploid genomes. *Nat. Commun.* 11:1432. doi: 10.1038/s41467-020-14998-3
- Rochette, N. C., and Catchen, J. M. (2017). Deriving genotypes from RAD-seq short-read data using Stacks. *Nat. Protoc.* 12, 2640–2659. doi: 10.1038/nprot.2017.123
- Rogers, J. G. D., Plágyani, É.E., and Babcock, R. C. (2017). Aggregation, Allee effects and critical thresholds for the management of the crown-of-thorns starfish *Acanthaster planci*. *Mar. Ecol. Prog. Ser.* 578, 99–114. doi: 10.3354/meps12252
- Scandol, J. P., and James, M. K. (1992). Hydrodynamics and larval dispersal: a population model of *Acanthaster planci* on the Great Barrier Reef. *Mar. Freshw. Res.* 43, 583–595. doi: 10.1071/MF9920583
- Schunter, C., Carreras-Carbonell, J., Macpherson, E., Tintoré, J., Vidal-Vijande, E., Pascual, A., et al. (2011). Matching genetics with oceanography: directional gene flow in a Mediterranean fish species. *Mol. Ecol.* 20, 5167–5181. doi: 10.1111/j.1365-294X.2011.05355.x



- Seppey, M., Manni, M., and Zdobnov, E. M. (2019). BUSCO: assessing genome assembly and annotation completeness. *Methods Mol. Biol.* 1962, 227–245. doi: 10.1007/978-1-4939-9173-0\_14
- Shanks, A. L. (2009). Pelagic larval duration and dispersal distance revisited. *Biol. Bull.* 216, 373–385. doi: 10.1086/BBLv216n3p373
- Storlazzi, C. D., van Ormondt, M., Chen, Y.-L., and Elias, E. P. L. (2017). Modeling fine-scale coral larval dispersal and interisland connectivity to help designate mutually supporting coral reef marine protected areas: insights from Maui Nui, Hawaii. *Front. Mar. Sci.* 4:381. doi: 10.3389/fmars.2017.00381
- Sunday, J. M., Popovic, I., Palen, W. J., Foreman, M. G. G., and Hart, M. W. (2014). Ocean circulation model predicts high genetic structure observed in a long-lived pelagic developer. *Mol. Ecol.* 23, 5036–5047. doi: 10.1111/mec.12924
- Suyama, Y., and Matsuki, Y. (2015). MIG-seq: an effective PCR-based method for genome-wide single-nucleotide polymorphism genotyping using the next-generation sequencing platform. *Sci. Rep.* 5:16963. doi: 10.1038/srep16963
- Suzuki, G., Yasuda, N., Ikehara, K., Fukuoka, K., Kameda, T., Kai, S., et al. (2016). Detection of a high-density Brachiolaria-stage larval population of crown-of-thorns sea star (*Acanthaster planci*) in Sekisei Lagoon (Okinawa, Japan). *Diversity* 8:9. doi: 10.3390/d8020009
- Takata, K., Taninaka, H., Nonaka, M., Iwase, F., Kikuchi, T., Suyama, Y., et al. (2019). Multiplexed ISSR genotyping by sequencing distinguishes two precious coral species (Anthozoa: Octocorallia: Coralliidae) that share a mitochondrial haplotype. *PeerJ* 7:e7769. doi: 10.7717/peerj.7769
- Taninaka, H., Bernardo, L. P. C., Saito, Y., Nagai, S., Ueno, M., Kitano, Y. F., et al. (2019). Limited fine-scale larval dispersal of the threatened brooding corals *Heliopora* spp. as evidenced by population genetics and numerical simulation. *Conserv. Genet.* 20, 1449–1463. doi: 10.1007/s10592-019-01228-7
- Timmers, M. A., Andrews, K. R., Bird, C. E., de Maitention, M. J., Brainard, R. E., and Toonen, R. J. (2011). Widespread dispersal of the crown-of-thorns sea star, *Acanthaster planci*, across the Hawaiian archipelago and Johnston Atoll. *Mar. Sci.* 2011:934269. doi: 10.1155/2011/934269
- Timmers, M. A., Bird, C. E., Skillings, D. J., Smouse, P. E., and Toonen, R. J. (2012). There's no place like home: crown-of-thorns outbreaks in the central Pacific are regionally derived and independent events. *PLoS One* 7:e31159. doi: 10.1371/journal.pone.0031159
- Tusso, S., Morcinek, K., Vogler, C., Schupp, P. J., Caballes, C. F., Vargas, S., et al. (2016). Genetic structure of the crown-of-thorns seastar in the Pacific Ocean, with focus on Guam. *PeerJ* 4:e1970. doi: 10.7717/peerj.1970
- Uthicke, S., Doyle, J., Duggan, S., Yasuda, N., and McKinnon, A. D. (2015). Outbreak of coral-eating crown-of-thorns creates continuous cloud of larvae over 320 km of the Great Barrier Reef. *Sci. Rep.* 5:16885. doi: 10.1038/srep16885
- Vogler, C., Benzie, J. A. H., Tenggardjaja, K., Ambariyanto, Barber, P. H., and Wörheide, G. (2013). Phylogeography of the crown-of-thorns starfish: genetic structure within the Pacific species. *Coral Reefs* 32, 515–525. doi: 10.1007/s00338-012-1003-z
- Wada, N., Yuasa, H., Kajitani, R., Gotoh, Y., Ogura, Y., Yoshimura, D., et al. (2020). A ubiquitous subcuticular bacterial symbiont of a coral predator, the crown-of-thorns starfish, in the Indo-Pacific. *Microbiome* 8:123. doi: 10.1186/s40168-020-00880-3
- Walker, B. J., Abeel, T., Shea, T., Priest, M., Abouelliel, A., Sakthikumar, S., et al. (2014). Pilon: an integrated tool for comprehensive microbial variant detection and genome assembly improvement. *PLoS One* 9:e112963. doi: 10.1371/journal.pone.0112963
- White, C., Selkoe, K. A., Watson, J., Siegel, D. A., Zacherl, D. C., and Toonen, R. J. (2010). Ocean currents help explain population genetic structure. *Proc. Biol. Sci.* 277, 1685–1694. doi: 10.1098/rspb.2009.2214
- White, J. W., Carr, M. H., Caselle, J. E., Palumbi, S. R., Warner, R. R., Menge, B. A., et al. (2019). Empirical approaches to measure connectivity. *Oceanography* 32, 60–61. doi: 10.5670/oceanog.2019.311
- Yamaguchi, M. (1977). Larval behavior and geographic distribution of coral reef asteroids in the Indo-west Pacific. *Micronesica Ser.* 13, 283–296.
- Yasuda, N. (2018). “Distribution expansion and historical population outbreak patterns of crown-of-thorns starfish, *Acanthaster planci* sensu lato, in Japan from 1912 to 2015,” in *Coral Reefs of the World*, eds A. Iguchi and C. Hongo (Singapore: Springer), 125–148. doi: 10.1007/978-981-10-6473-9\_9
- Yasuda, N., Kajiwar, K., Nagai, S., Ikehara, K., and Nadaoka, K. (2015a). First report of field sampling and identification of crown-of-thorns starfish larvae. *J. Coral Reef Stud.* 17, 15–16. doi: 10.3755/galaxea.17.15
- Yasuda, N., Taquet, C., Nagai, S., Yoshida, T., and Adjeroud, M. (2015b). Genetic connectivity of the coral-eating sea star *Acanthaster planci* during the severe outbreak of 2006–2009 in the Society Islands, French Polynesia. *Mar. Ecol.* 36, 668–678. doi: 10.1111/maec.12175
- Yasuda, N., Nagai, S., Hamaguchi, M., Okaji, K., Gérard, K., and Nadaoka, K. (2009). Gene flow of *Acanthaster planci* (L.) in relation to ocean currents revealed by microsatellite analysis. *Mol. Ecol.* 18, 1574–1590. doi: 10.1111/j.1365-294X.2009.04133.x
- Yasuda, N., Ogasawara, K., Kajiwar, K., Ueno, M., Oki, K., Taniguchi, H., et al. (2010). Latitudinal differentiation in the reproduction patterns of the crown-of-thorns starfish *Acanthaster planci* through the Ryukyu Island Archipelago. *Plankton Benthos Res.* 5, 156–164. doi: 10.3800/pbr.5.156

**Conflict of Interest:** The authors declare that the research was conducted in the absence of any commercial or financial relationships that could be construed as a potential conflict of interest.

**Publisher's Note:** All claims expressed in this article are solely those of the authors and do not necessarily represent those of their affiliated organizations, or those of the publisher, the editors and the reviewers. Any product that may be evaluated in this article, or claim that may be made by its manufacturer, is not guaranteed or endorsed by the publisher.

Copyright © 2022 Horoiwa, Nakamura, Yuasa, Kajitani, Ameda, Sasaki, Taninaka, Kikuchi, Yamakita, Toyoda, Itoh and Yasuda. This is an open-access article distributed under the terms of the Creative Commons Attribution License (CC BY). The use, distribution or reproduction in other forums is permitted, provided the original author(s) and the copyright owner(s) are credited and that the original publication in this journal is cited, in accordance with accepted academic practice. No use, distribution or reproduction is permitted which does not comply with these terms.



# Bacterial Communities in Coral Offspring Vary Between *in situ* and *ex situ* Spawning Environments

Jia-Ho Shiu<sup>1\*</sup>, Che-Hung Lin<sup>1</sup>, Aziz Jabir Mulla<sup>1,2</sup>, Viet Do Hung Dang<sup>1,3</sup>, Chia-Ling Fong<sup>1,2</sup> and Yoko Nozawa<sup>1\*</sup>

<sup>1</sup> Biodiversity Research Center, Academia Sinica, Taipei, Taiwan, <sup>2</sup> Biodiversity Program, Taiwan International Graduate Program, Biodiversity Research Center, Academia Sinica and National Taiwan Normal University, Taipei, Taiwan, <sup>3</sup> Institute of Marine Environment and Resources, Vietnam Academy of Science and Technology, Haiphong, Vietnam

## OPEN ACCESS

### Edited by:

Nina Yasuda,  
University of Miyazaki, Japan

### Reviewed by:

Chuya Shinzato,  
The University of Tokyo, Japan  
Hironobu Fukami,  
University of Miyazaki, Japan  
Cecilia Conaco,  
University of the Philippines Diliman,  
Philippines

### \*Correspondence:

Jia-Ho Shiu  
jiasr18@gmail.com  
Yoko Nozawa  
nozaway@gate.sinica.edu.tw

### Specialty section:

This article was submitted to  
Coral Reef Research,  
a section of the journal  
Frontiers in Marine Science

**Received:** 17 October 2021

**Accepted:** 14 January 2022

**Published:** 16 February 2022

### Citation:

Shiu J-H, Lin C-H, Mulla AJ,  
Dang VDH, Fong C-L and Nozawa Y  
(2022) Bacterial Communities in Coral  
Offspring Vary Between *in situ* and  
*ex situ* Spawning Environments.  
Front. Mar. Sci. 9:796514.  
doi: 10.3389/fmars.2022.796514

Examining the bacterial communities of offspring is key to understanding the establishment of coral-bacteria associations. Although high sensitivity to the environment is expected, previous studies have only examined bacterial communities of coral offspring in *ex situ* (laboratory) environments, not in *in situ* (field) environments. Here, we examined and compared the effect of *ex situ* and *in situ* environments on bacterial communities of newly released offspring (eggs and larvae) and their maternal colonies in two phylogenetically distant coral species with different reproductive modes: *Dipsastraea speciosa* (Scleractinia; spawner) and *Heliopora coerulea* (Octocorallia; brooder). Our results demonstrated that the spawning environments do not affect the bacterial composition in maternal colonies, but influence that of the offspring (eggs of *D. speciosa* and larvae of *H. coerulea*). Dominant bacterial operational taxonomic units (OTUs) varied between *in situ* and *ex situ* environments in the eggs of *D. speciosa*. The composition of bacterial communities among larvae of *H. coerulea* samples was more diverse in *in situ* environments than in *ex situ* environments. This study provides the first information on *in situ* bacterial communities in coral eggs and larvae and highlights their sensitivities to the local environment. Future studies must take into consideration the influence of *ex situ* environments on bacterial communities in coral offspring.

**Keywords:** bacterial communities, coral offspring, sampling method, alpha diversity, beta diversity

## INTRODUCTION

Resident bacterial communities are known to profoundly influence the physiology and health of both flora and fauna (Thompson et al., 2015; Wang et al., 2017; Douglas, 2019; van Oppen and Blackall, 2019; Apprill, 2020). Likewise, in reef-building corals, recent studies have found that coral-associated bacteria play important functional roles, such as protection against pathogens and the provision of nutrients (carbon, nitrogen, and sulfur). For example, diazotrophs that inhabit within the coral tissue or skeleton (Rohwer et al., 2002; Radecker et al., 2015) provide fixed nitrogen products that are crucially limiting resources in oligotrophic coral reef waters, sustaining their high productivity (Lesser et al., 2007).

Despite the importance of coral-bacteria associations, we know very little about the mechanisms relating to the establishment. Studying microbial communities in coral offspring is key to understanding the establishment of the coral-microbe association, but nevertheless, the majority of knowledge comes from studies on coral endosymbiotic algae (Symbiodiniaceae) in coral offspring, closely related to the reproductive mode of coral host. Most brooding corals release larvae with endosymbiotic algae, whereas spawning corals release eggs without those (Bright and Bulgheresi, 2010; Hartmann et al., 2017). However, such information has not been studied well in coral-bacteria associations.

Previous studies have examined coral-associated bacteria in coral offspring (eggs and larvae) in *ex situ* (laboratory) environments, not in *in situ* (field) environments (Supplementary Table 1). This difference could lead to there being a bias of real bacterial communities in coral offspring as a few studies have demonstrated that environmental conditions are an important factor that affects the bacterial communities in coral offspring (Lema et al., 2016; Leite et al., 2017; Zhou et al., 2017; Bernasconi et al., 2019; Damjanovic et al., 2020a). In adult corals, there was a study recently published showing the difference in bacterial communities between *ex situ* and *in situ* environments (Damjanovic et al., 2020b). However, no such *ex situ* and *in situ* comparisons were studied for the bacterial communities in coral offspring, in spite of that bacteria and coral offspring are sensitive to the environment (Chan et al., 2019; Epstein et al., 2019).

Here we examined the effect of *in situ* and *ex situ* environments on bacterial communities of coral offspring and maternal corals in two coral species with different reproductive modes; *Dipsastraea speciosa* (Scleractinia; spawner) and *Heliopora coerulea* (Octocorallia; brooder). Our results indicate that bacterial communities vary between *in situ* and *ex situ* environments in coral offspring, but not in maternal corals. The results highlight the sensitivity of bacterial communities in coral offspring to the environment and bring to light a potential bias introduced by customary *ex situ* sampling methods that may affect studies on bacteria associated with coral offspring.

## MATERIALS AND METHODS

We examined bacterial communities of offspring (eggs or larvae) and maternal corals in two coral species with different reproductive modes, *D. speciosa* (spawner) and *H. coerulea* (brooder, branching morphotype; Yasuda et al., 2014). *D. speciosa* is hermaphroditic spawner that releases buoyant egg-sperm bundles into the water column for external fertilization during annual spawning events (Lin and Nozawa, 2017). *H. coerulea* is a gonochoric brooder, which releases planula larvae in early summer, that is neutral to negative buoyancy (Babcock, 1990; Harii et al., 2002). Larvae of *H. coerulea* are brooded for up to 2 weeks inside polyps and then moved to the surface of maternal colonies for “surface brooding” for  $\approx 4$  days before detaching for dispersal (Babcock, 1990; Harii and Kayanne, 2003). Two sampling methods were employed in this study; *ex*

*situ* (laboratory) sampling and *in situ* (field) sampling (Table 1). Sampling was conducted at Lyudao (Green Island), Taiwan in April and May 2018 (Figure 1A).

### Ex situ Sampling

Seawater used in the experiment was collected from Gongguan and stored in a 1,500-L tank at the beginning of the experiment (April 26; 4 days before the full moon). The seawater stock tank was placed in the hallway of the Green Island Marine Research Station (GIMRS) in the shade, and seawater was aerated with air stones. Seawater from the stock tank was used for coral rearing for the *ex situ* sampling.

For *D. speciosa*, one fragment ( $\approx 10$  cm in diameter) with mature pigmented eggs (violet gray) was collected from five colonies using a hammer and a chisel at 3–8 m depth in Gongguan, Lyudao on April 27 (3 days before the full moon; Figure 1A). The fragments were kept in a Gongguan harbor ( $\approx 3$  m depth) for 1 day to allow for recovery and then transferred to GIMRS (Figure 1A). The five fragments were placed separately in 20-L rearing tanks with aerated filtered seawater (100  $\mu\text{m}$ ) in the laboratory. Seawater temperature was maintained at  $\approx 26^\circ\text{C}$  by an air-conditioner. The rearing tanks were kept under fluorescent light (6,000 lux) during daytime (6:00–18:00) and kept in darkness during nighttime (18:00–6:00) to induce spawning (Lin et al., 2021). A quarter of the seawater in the rearing tank was changed every 3 days with filtered seawater (100  $\mu\text{m}$ ) from the seawater stock tank.

The spawning of *D. speciosa* fragments was monitored daily by using a plastic cup placed upside down on the top of each fragment. When fragments spawned at  $\approx 22:00$ , egg-sperm bundles were released from polyps, floated to the water surface, and gradually disintegrated into eggs and sperm. As eggs have strong buoyancy, eggs were trapped inside the reversed cup, while sperm dispersed into the water. Spawning of *D. speciosa* occurred on May 1 and 2 [1 and 2 days after the full moon (AFM)] and spawned eggs ( $\approx 200$  eggs) were collected at 7:00 the following morning ( $\approx 9$  h after spawning). Egg samples from 2 fragments were collected on the first day (sample ID: ds2l and ds4l) and others on the second day. After spawning, a small tissue sample ( $\approx 1$  cm in diameter) was collected from each maternal coral (fragment).

For *H. coerulea*, one branch (2 cm in diameter, 5–8 cm in length) that had many brooded larvae partially emerge from polyps on the branch surface was collected from each of the five female colonies using a hammer and a chisel at 5–8 m depth at Daibaisa, Lyudao on May 1 (1 day AFM; Figure 1A). Each branch was kept in a zip-lock bag with seawater, transferred to GIMRS, and placed in a 3-L rearing tank with aerated filtered seawater (100  $\mu\text{m}$ ). Seawater from the 1,500-L seawater tank was used in the rearing tank, and filtered seawater was changed every 1–2 days. During the rearing period, larvae of *H. coerulea* gradually appeared, detached from polyps, and drifted into the water column (Harii and Kayanne, 2003). Ten to fifteen larvae from each branch that were released on May 5 (5 days AFM) were collected in the rearing tank by a dropper. After collecting larvae, a small tissue sample ( $\approx 1$  cm in diameter) was collected from each branch using a nipper as a sample of the maternal

**TABLE 1** | Summary of samples used in the present study.

Species	Reproductive mode	Taxon (subclass/order/family)	Sampling method	Sample name	
				Offspring	Mother
<i>Dipsastraea speciosa</i>	Spawner	Hexacorallia/Scleractinia/Marulinidae	<i>In situ</i>	ds1f, ds2f, ds3f, ds4f, ds5f	DS1F, DS2F, DS3F, DS4F, DS5F
			<i>Ex situ</i>	ds1l, ds2l, ds3l, ds4l, ds5l	DS1L, DS2L, DS3L, DS4L, DS5L
<i>Heliopora coerulea</i>	Brooder	Octocorallia/Helioporacea/Helioporidae	<i>In situ</i>	hc1f, hc2f, hc3f, hc4f, hc5f	HC1F, HC2F, HC3F, HC4F, HC5F
			<i>Ex situ</i>	hc1l, hc2l, hc3l, hc4l, hc5l	HC1L, HC2L, HC3L, HC4L, HC5L

Abbreviations in sample names denote as follows; the first 2 characters represent coral species (DS for *Dipsastraea speciosa*, HC for *Heliopora coerulea*); the number (1–5) is replicate colony number; the last character is sampling method [F for the *in situ* (field) samples and L for the *ex situ* (laboratory) samples]; capital letters for maternal coral samples and small letters for offspring samples.

colony. A 1-L seawater sample was collected from the 1,500-L seawater tank for reference of environmental microbes for the *ex situ* samples of both species on May 1 (1 day AFM).

### In situ Sampling

The spawning timing of *D. speciosa* is well-documented at the study location and was expected between 21:00 and 22:00 around 5–7 days AFM from April to June (Lin and Nozawa, 2017). Colonies of *D. speciosa* that had matured pigmented eggs (violet gray) were selected by visually examining small fragments of colonies broken off using a hammer and a chisel at 3–7 m depth at Gongguan on May 3 (3 days AFM). A gamete trap consisting of a funnel and a 50 ml falcon tube was positioned on each of the 5 selected colonies (**Figure 1B**). Spawning of the colonies was monitored daily from 21:00 to 22:00 using scuba from May 3 (3 days AFM) and was observed from 21:00 to 22:00 on May 5 (5 days AFM). Egg-sperm bundles were released from colonies, floated toward the water surface, and were captured by the gamete trap (**Figure 1B**). Spawned gametes in the falcon tube were collected at 22:00 on the spawning night. A tissue sample was taken from the five colonies using a hammer and a chisel and kept in a zip-lock bag with seawater. A 1-L seawater sample was also collected as a sample of environmental bacteria at 3-m depth.

For *H. coerulea*, larvae loosely attached to the colony surface were collected *in situ* from five colonies at 1–3 m depth in Gongguan on May 5 (5 days AFM; **Figure 1B**). Larvae from each colony were collected using a dropper and kept in a 15-ml falcon tube. A tissue sample from each colony was collected using a hammer and a chisel and kept in a zip bag with seawater. One-liter seawater sample was collected as a sample of environmental bacteria at 3-m depth.

### Total DNA Extraction and Amplification

All *ex situ* and *in situ* samples of gametes, larvae, and maternal coral tissue were washed twice with filtered seawater (0.22  $\mu$ m), and the sperms were filtered out during washing, then coral samples were stored in 99% ethanol at  $-20^{\circ}\text{C}$  at GIMRS. The seawater samples were filtered through cellulose acetate membranes with 0.2- $\mu$ m pores (Aventec, Tokyo, Japan) and the membranes were stored at  $-20^{\circ}\text{C}$ . All coral samples were washed with tris-EDTA (TE) buffer (10 mM Tris-HCl and 1 mM

EDTA, pH 8) before DNA extraction. Egg and larval samples were frozen in liquid nitrogen and then homogenized using a sterile plastic pestle in 1.5 ml tubes. Coral tissue samples that contained skeletons were grounded using a sterile stainless mortar and pestle with liquid nitrogen. The homogenized tissues and membranes of seawater samples were suspended in TE buffer for total DNA extraction using the modified traditional cetyltrimethylammonium bromide (CTAB) method (Wilson, 2001; Hong et al., 2009).

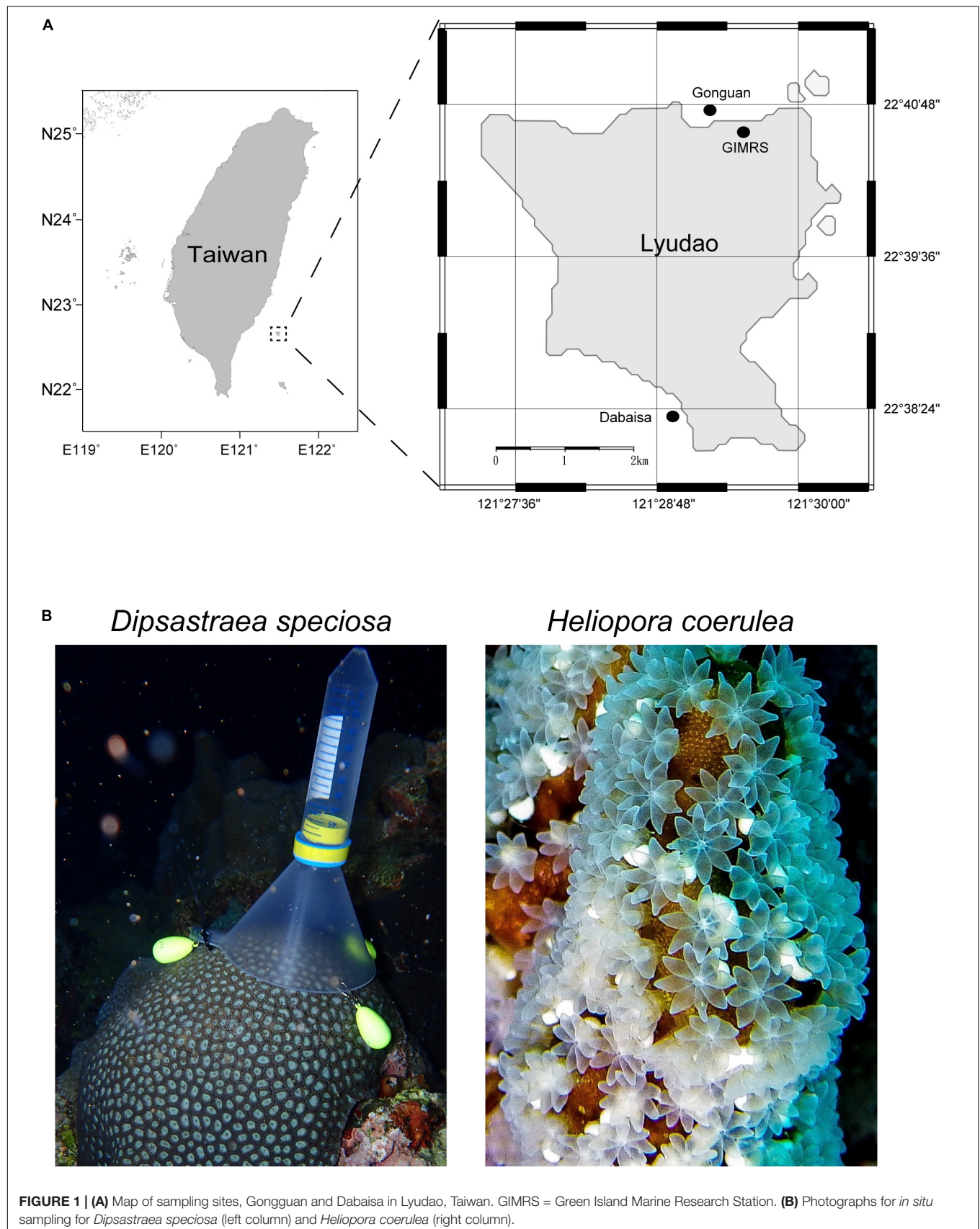
Amplification of the 16S ribosomal RNA gene was performed by PCR using a pair of universal bacterial primers: 968F (5'-AACGCGAAGAACCCTTAC-3') and Uni1391R (5'-ACGGGCGGTGWGTRC-3') for the bacterial V6–V8 hypervariable regions (Nubel et al., 1996; Jorgensen et al., 2012). The PCR was performed in 50  $\mu$ l reaction volumes, consisting of 2.5 U TaKaRa Ex Taq (Takara Bio, Otsu, Japan), 1X TaKaRa Ex Taq buffer, 0.2 mM deoxynucleotide triphosphate mixture (dNTP), 0.2 mM of each primer, and more than 20 ng of total DNA. The thermocycler was set to an initial step of  $94^{\circ}\text{C}$  for 3 min, 30 cycles of  $94^{\circ}\text{C}$  for 30 s,  $55^{\circ}\text{C}$  for 10 s,  $72^{\circ}\text{C}$  for 15 s, and a final extension of  $72^{\circ}\text{C}$  for 5 min. Target DNA bands ( $\approx 420$  bp) were examined on 1.5% agarose gel after electrophoresis and eluted using QIAEX II Gel Extraction Kit (Qiagen, Valencia, CA, United States).

To tag each of the bacterial V6–V8 amplicon with a unique barcode sequence, each tag primer was designed with four overhanging nucleotides at 5' ends of the common primers (**Supplementary Table 2**). The tagging reaction was performed with a 5-cycle PCR, each cycle was run at  $94^{\circ}\text{C}$  for 30 s,  $56^{\circ}\text{C}$  for 10 s, and  $72^{\circ}\text{C}$  for 20 s with the modified primers. End products were purified by the same gel elution method described above, and DNA concentration was determined with the Qubit dsDNA HS assay (Invitrogen, Carlsbad, CA, United States).

### Sequencing and Data Processing

We pooled all V6–V8 amplicons of coral and seawater samples equally for  $2 \times 250$  pair-end reads in Illumina NovaSeq paired-end sequencing (BIOTools Co., Taipei, Taiwan). High-quality reads that were produced after raw reads were merged, sorted, and trimmed using mothur (Schloss et al., 2009) based on the following criteria: (1) reads of 350–500 bp long, (2) average





**FIGURE 1 | (A)** Map of sampling sites, Gongguan and Dabaisa in Lyudao, Taiwan. GIMRS = Green Island Marine Research Station. **(B)** Photographs for *in situ* sampling for *Dipsastraea speciosa* (left column) and *Heliopora coerulea* (right column).

quality score > 27, (3) homopolymer length < 8 bp, and (4) reads with any ambiguous base (N) removed. Then the four base tags and primer sequences were removed.

For the operational taxonomic unit (OTU) analysis, quality-filtered reads were pooled together and OTUs were assigned at 97% identity with the UPARSE pipeline (Edgar, 2013). In UPARSE, de-replication was performed and singletons were excluded (options: `-derep_prefix` and `-minsize 2`). Each OTU was classified with a bootstrap value set to 0.8 using a classifier (Wang et al., 2007) against the SILVA database (release 128) implemented in mothur. OTUs that were not assigned to a *Bacteria* domain or those that were assigned to Chloroplast were removed in subsequent analyses.

## Data Analyses

Alpha-diversity and beta-diversity of bacterial communities were calculated after rarefying to an even 8,000 sequence depth in each sample by USEARCH (v10; options: `-otutab_norm`). For alpha-diversity, the Shannon index, Chao1 richness, and Species Evenness were calculated. Kruskal-Wallis tests were conducted to detect significant differences in the indexes of each coral species. Comparisons were made between the *in situ* and *ex situ* samples of eggs, larvae, and maternal colonies and between offspring (eggs or larvae) and maternal colonies within the *in situ* or *ex situ* samples. Statistical analyses were performed using R ver. 3.6.2 (R Core Team, 2019).

For beta-diversity, relative abundances of bacterial families (Supplementary Figure 1) and OTUs were calculated for individual samples (Chen et al., 2011), and then the Bray-Curtis distance was estimated between samples (Bray and Curtis, 1957). Based on the Bray-Curtis distance, the non-metric multidimensional scaling (nMDS) analysis and the agglomerative hierarchical clustering (CLUSTER) with complete-linkage were performed using the Primer 6 software (PRIMER-E, Lutton, Ivybridge, United Kingdom). nMDS plot with 95% CIs around each group was visualized with the “stat\_ellipse” function in R. Significant variations between *in situ* and *ex situ* samples were examined using Analysis of Similarity (ANOSIM) in the Primer 6 software.

## Data Availability Statement

The data sets generated for this study can be found in the NCBI SRA PRJNA706097.

## RESULTS

The data set of bacterial communities consisted of 2,361,933 reads from a total of 40 samples of offspring and maternal corals and three seawater samples after quality control and removal of no-*Bacteria* and *Chloroplast* OTUs. The number of reads per sample ranged between 8,277 and 179,418, with an average of 54,928 reads per sample, representing 6,601 OTUs. The data set was rarefied to the lowest number reads (8,000 reads) across samples, resulting in 5,181 OTUs for the analysis (Supplementary Figure 2 and Supplementary Table 3).

Alpha diversity of bacterial communities was compared using the Shannon, Chao1, and Evenness indices (Figure 2). There was no significant variation in alpha diversity of bacterial communities between *in situ* and the *ex situ* samples in maternal corals and offspring of each coral species (Kruskal-Wallis tests;  $p > 0.05$ ). Although there was a tendency of higher alpha diversity in offspring than maternal colonies in *D. speciosa* and the opposite in *H. coerulea*, these were not statistically significant (Kruskal-Wallis tests;  $p > 0.05$ ).

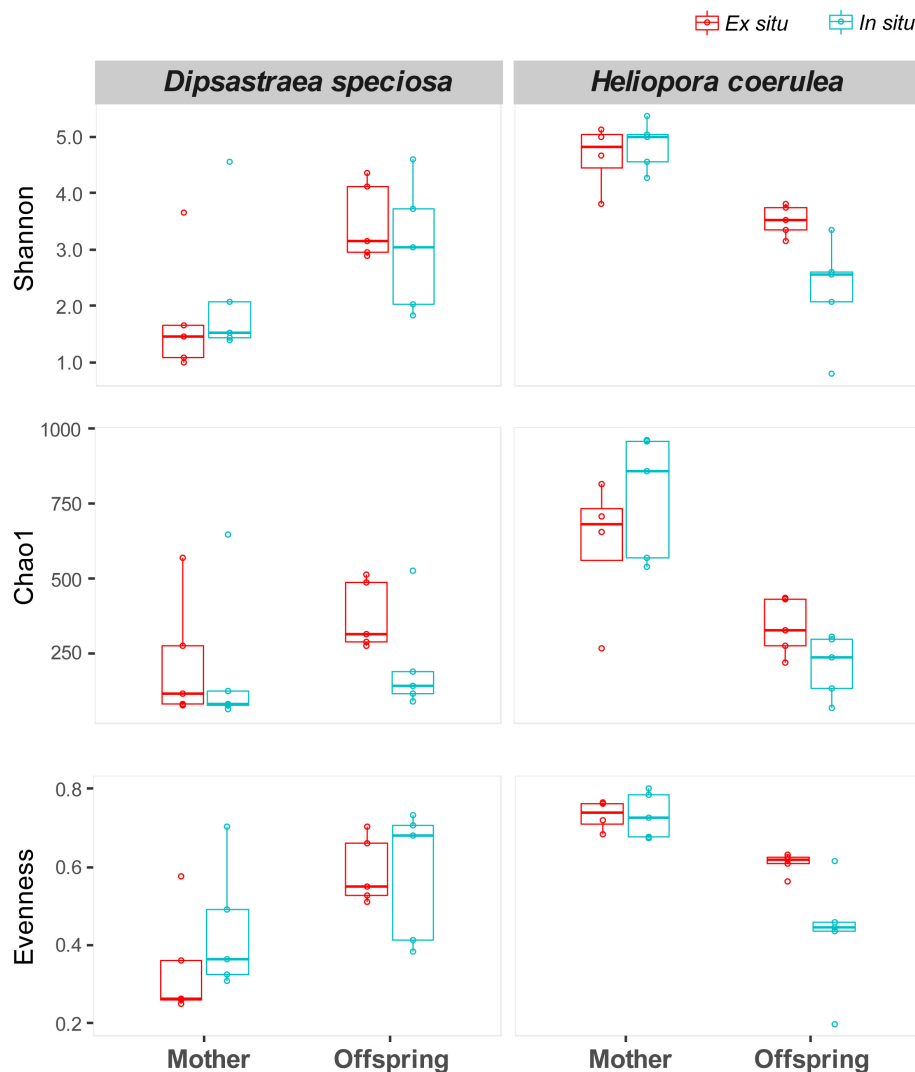
Beta diversity of bacterial communities was grouped into three clusters; maternal corals, offspring, and seawater samples (ANOSIM,  $R = 0.56$ ,  $p < 0.001$ ; Figure 3A). The bacterial communities of maternal corals were clustered by species (2-way crossed ANOSIM,  $R = 0.97$ ,  $p < 0.001$ ), except for sample “DS4F” (Figure 3A), whereas the bacterial communities of offspring were primarily grouped by the *in situ* and *ex situ* sampling environments (2-way crossed ANOSIM,  $R = 0.71$ ,  $p < 0.001$ ). The nMDS analysis indicated similar patterns, with a wide distribution of *in situ* samples of offspring, especially for *H. coerulea* larvae (Figure 3B).

The top 30 OTUs (> 0.09% in cumulative relative abundance) of bacteria in the maternal corals and offspring were compared between the *in situ* and *ex situ* samples for each species (Figure 4 and Supplementary Table 4). *D. speciosa* had three OTU clusters, Groups 1–3 (Figure 4A and Supplementary Table 4A): The maternal coral samples were dominated by OTU Group 2. However, the offspring samples were dominated by OTU Group 1 for the *in situ* samples, and OTU Group 3 for the *ex situ* samples. Dominant bacterial OTUs in Group 2 were almost absent in both offspring and seawater samples, whereas some dominant OTUs in the offspring samples were detected in maternal corals.

In *H. coerulea*, there were four OTU clusters, Groups 4–7 (Figure 4B and Supplementary Table 4B). The maternal corals were dominated almost evenly by OTUs in Groups 4, 5, and 7, irrespective of sampling environments. The OTUs dominated in maternal corals were also dominant in offspring, except for sample “hc2f.” The offspring samples were dominated by OTUs in all four OTU groups: OTUs in Group 6 were more abundant in *in situ* samples, whereas OTUs in Group 4 were more common in *ex situ* samples (Figure 4B). Four OTUs were detected in offspring samples of both coral species; OTU1 and OTU5 in *in situ* samples and OTU12 and OTU18 in *ex situ* samples (Figure 4).

## DISCUSSION

This study examined the effect of *in situ* and *ex situ* environments on bacterial communities of both offspring (eggs and larvae) and maternal corals in two phylogenetically distant coral species, with different reproductive modes; *D. speciosa* and *H. coerulea*. Our results demonstrate that spawning environments influence the composition of bacterial communities in offspring, but not in maternal corals. These findings are in agreement with previous studies that conclude bacterial communities in coral offspring are sensitive to local environments (Apprill et al., 2009; Zhou et al., 2017; Chan et al., 2019; Epstein et al., 2019) and highlight



**FIGURE 2 |** Alpha-diversity indices of bacterial communities (Shannon diversity, Chao 1 richness, and evenness) for the *in situ* (cyan) and *ex situ* samples (red) of maternal corals and offspring (eggs or larvae) in *Dipsastraea speciosa* and *Heliopora coerulea*. No significant variation was detected between the *in situ* and *ex situ* samples of maternal corals and offspring and between maternal corals and offspring within the *in situ* and *ex situ* samples of each species (Kruskal-Wallis test;  $p > 0.05$ ).

that sensitivity is higher than bacterial communities of their maternal colonies.

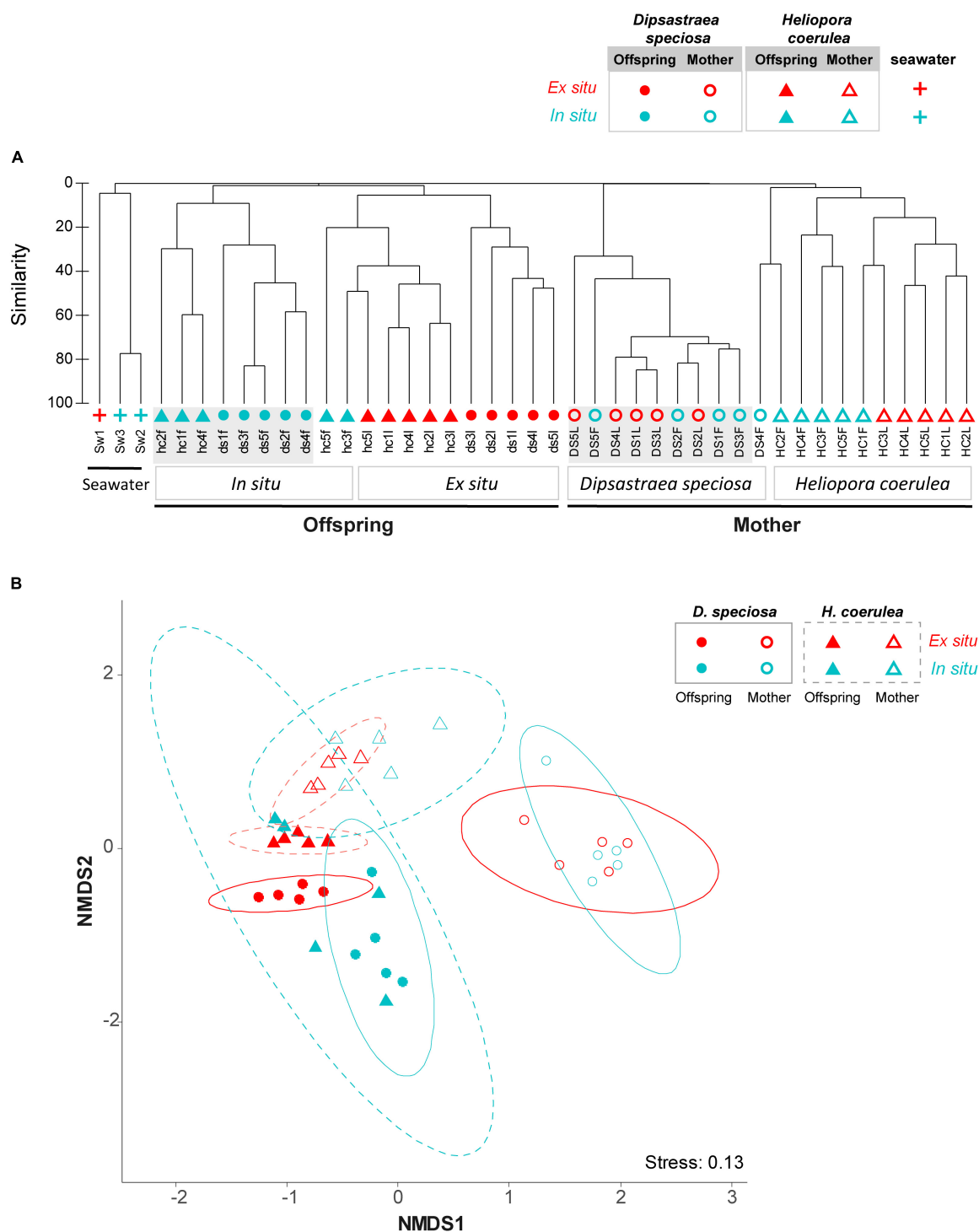
## Alpha Diversity and the Winnow Process Hypothesis

While the alpha-diversity of bacterial communities was similar between the *in situ* and *ex situ* environments, they showed different trends between offspring and maternal corals in the two coral species: Alpha-diversity tended to be higher in offspring compared to maternal corals in *D. speciosa*, whereas this tendency was opposite in *H. coerulea*. The result for the spawning coral *D. speciosa* supports the “winnow process” hypothesis which proposes that alpha-diversity of bacterial communities is initially higher in early life stages and declines in later life

(Littman et al., 2009). However, such a hypothesis could not explain the opposite trend of bacterial community for brooding coral, *H. coerulea*. Although Damjanovic et al. (2020a) reported higher alpha-diversity of bacterial communities in larvae than in maternal corals in brooding scleractinian coral, *Pocillopora acuta*, two of the five sample pairs showed similar alpha-diversity between them. Therefore, the currently limited information does not support the winnow process hypothesis for brooding corals.

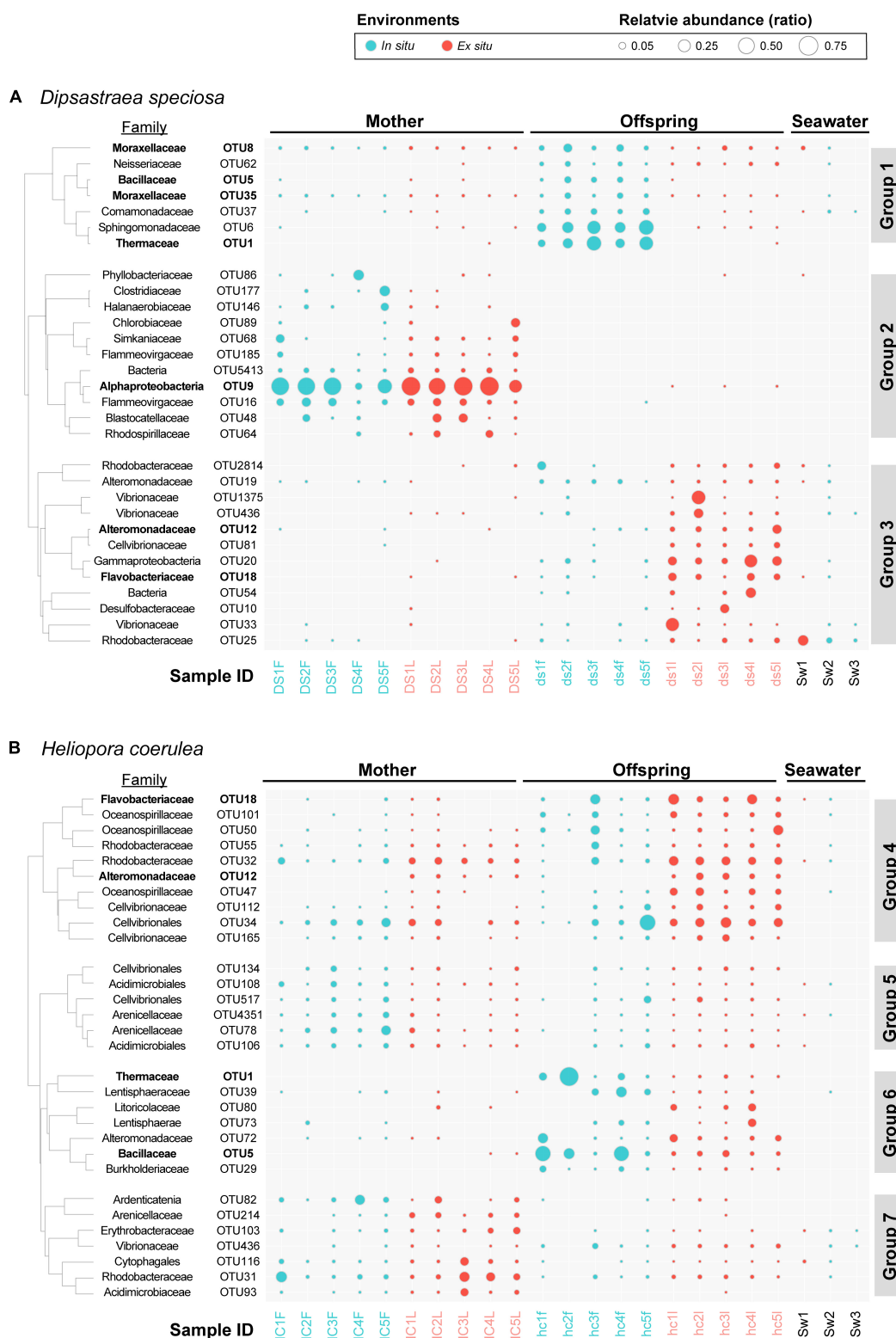
## Bacterial Communities in Eggs of *Dipsastraea speciosa*

The dominant bacterial OTUs (the top 30 OTUs) in eggs of *D. speciosa* were different between *in situ* and the *ex situ* environments and inconsistent with their maternal colonies. The



**FIGURE 3 |** Bacterial community composition in **(A)** clustering and **(B)** nMDS plots. The symbols and colors denote; *Dipsastraea speciosa* (circles), *Heliopora coerulea* (triangles), and seawater (crosses); offspring (filled symbols) and maternal corals (blank symbols); *in situ* (cyan) and *ex situ* (red) environments. 95% CI ellipses are also shown in the nMDS plot for *D. speciosa* (solid line) and *H. coerulea* (dashed line). Abbreviations in sample names denote as follows; the first 2 characters represent coral species (DS for *D. speciosa*, HC for *H. coerulea*); the number (1–5) is replicate colony number; the last character is sampling method [F for the *in situ* (field) samples and L for the *ex situ* (laboratory) samples]; capital letters for maternal coral samples and small letters for offspring samples. nMDS, non-metric multidimensional scaling.





**FIGURE 4 |** Bubble charts of the top 30 bacterial OTUs at the family level in **(A)** *Dipsastraea speciosa* and **(B)** *Heliopora coerulea*, with clusters based on Pearson's correlations. Colors represent *in situ* (cyan) and *ex situ* (red) samples. Sample IDs are listed on the x-axis, and bacterial family and OTUs are shown on the y-axis. For sample IDs, refer to **Figure 3** and **Table 1**. The size of the bubble indicates the relative abundance of OTUs in each sample. Bacterial families (OTUs) discussed in the text are highlighted in bold. OTUs, operational taxonomic units.

same dominant bacterial OTUs between *in situ* and *ex situ* mother samples (Group 2 in **Figure 4A**) indicate that *ex situ* maternal colonies were not under stress, because many studies have shown that the bacterial communities in adult coral were changed under stress (Bourne et al., 2008). However, unlike maternal colonies, this stability was absent in the offspring samples, and the dominant bacterial group in the mother was not vertically transmitted to their offspring.

The dominant bacteria in *in situ* and *ex situ* offspring (Groups 1 and 3 in **Figure 4A**) can be detected in both maternal colonies and seawater samples, so that it is difficult to suggest that these groups were vertically transmitted from mother or horizontally transmitted from environments. Interestingly, both Group 1 and Group 3 dominant bacteria can be detected in *in situ* and *ex situ* offspring samples, but with different relative abundance.

In *ex situ* offspring samples, we had similar results in *D. speciosa* offspring with previous studies. Many of the dominant bacteria in *ex situ* samples (Group 3 in **Figure 4A**) have been previously reported from other studies which collected offspring samples under *ex situ* conditions; e.g., *Rhodobacteraceae*, *Alteromonadaceae*, *Vibrionaceae*, and *Flavobacteriaceae* (Apprill et al., 2009, 2012; Lema et al., 2016; Zhou et al., 2017; Bernasconi et al., 2019; Chan et al., 2019; Damjanovic et al., 2019a, 2020a). Of these, *Rhodobacteraceae* and *Alteromonadaceae* have been detected in eggs of other spawning scleractinian coral species (Apprill et al., 2009; Zhou et al., 2017; Bernasconi et al., 2019; Damjanovic et al., 2019a).

In contrast, the majority of dominant bacteria detected in *in situ* offspring samples in the present study were newly recorded in bacterial communities in the eggs of spawning scleractinian coral species [e.g., *Anoxybacillus* (OTU5; family *Bacillaceae*), *Meiothermus* (OTU1; family *Thermaceae*), and *Enhydrobacter* (OTU35; family *Moraxellaceae*)], except *Acinetobacter* (OTU8; family *Moraxellaceae*). *Acinetobacter* was reported as core bacteria and suggested vertically transmitted from mother to offspring through the mucus in coral *Mussismilia hispida* (Leite et al., 2017). This finding indicates the bacteria group might be horizontally transmitted from the *in situ* environments of this study but more likely have existed already in other studies but was previously not noted due to low relative abundance in *ex situ* samples.

The variance in relative abundance between *in situ* and *ex situ* offspring samples may come from that the *ex situ* environment had smaller water volume and water exchange rate. Among *ex situ* offspring-dominated bacteria (Group 3), *Vibrionaceae*, *Alteromonadaceae*, and *Rhodobacteraceae* have been reported to be uptaken from the environment by coral recruits (Lema et al., 2016; Damjanovic et al., 2019a,b). In addition, *Alteromonas* (OTU19; belonged to Family *Alteromonadaceae*) was reported that it was released from maternal colony to seawater with offspring when spawning, and the offspring would uptake the bacteria from seawater (Ceh et al., 2013). Therefore, smaller water volume and exchange rate of the *ex situ* environment may increase the probability of the bacteria in seawater being uptaken by coral offspring. On the other hand, the two *in situ* dominated bacterial OTUs, *Acinetobacter* (OTU8) and *Enhydrobacter* (OTU35), that appeared in all the sample pairs of

*D. speciosa* from both *in situ* and *ex situ* environments indicate that some bacteria are also vertically transmitted via mucus-covered egg-sperm bundles.

## Bacterial Communities in Larvae of *Heliopora coerulea*

Brooding coral *H. coerulea* shared more common dominant bacteria between maternal colonies and their offspring samples compared to spawning coral *D. speciosa* (**Figure 4**). This may be due to the longer incubation time of brooder offspring developing to larvae inside mother than that of spawner offspring. However, in previous studies, only a small number of bacterial strains were shared between mother and their offspring in brooding scleractinian coral *Pocillopora damicornis* and *P. acuta* (Epstein et al., 2019; Damjanovic et al., 2020a). These dissimilarities are most likely caused by the super-dominant (>90% relative abundance) bacteria (taxa) in maternal colonies that were not dominant in the offspring of *P. damicornis* and *P. acuta*. *H. coerulea* is phylogenetically distant (Class Octocorallia) from scleractinians (Class Hexacorallia) and the phylogenetic difference might affect these results. The other possibility may come from the difference in contact time between maternal corals and offspring: Larvae of *H. coerulea* have a longer brooding (contact) time including the unique “surface brooding” (Babcock, 1990; Harii and Kayanne, 2003) compared to eggs of *D. speciosa* and larvae of *P. damicornis* and *P. acuta* (Epstein et al., 2019; Damjanovic et al., 2020a).

Although the majority of the dominant bacteria in larvae of *H. coerulea* was consensus with their maternal colonies and may be vertically transmitted from maternal corals (irrespective of *in situ* or *ex situ* environments), the spawning environment also affected the beta diversity of bacterial communities in the larvae. The larvae from the *in situ* environment had more diverse bacterial communities among samples than those from the *ex situ* environment (**Figure 3B**). The higher beta diversity of bacterial communities in the offspring from the *in situ* environment may indicate the prevalence of horizontal transmission of bacteria from environment to coral offspring and flexibility of bacterial communities in coral offspring in nature. Previous studies demonstrated that coral recruits under different planulation environments had different bacterial communities in four *Acropora* species and *Pocillopora damicornis* (Chan et al., 2019; Damjanovic et al., 2019b; Epstein et al., 2019). Our results further demonstrate that the spawning environment affects bacterial communities in coral offspring before the planulation stage.

## CONCLUSION AND IMPLICATION

This study provides the first report on *in situ* bacterial communities from coral offspring (eggs of the scleractinian coral, *D. speciosa*, and larvae of the octocoral, *H. coerulea*). We demonstrated that different environments influence bacterial communities in coral offspring, but not in maternal colonies, highlighting the sensitivity of bacterial communities to local environments for offspring compared to maternal corals.

Bacterial communities between maternal colonies and offspring were more similar in *H. coerulea* than in *D. speciosa*, which suggest a higher ratio of vertically transmitted bacteria in *H. coerulea*, probably due to the longer contact time between offspring and maternal corals. Our findings on the sensitivity of bacterial communities in coral offspring to the local environment call attention to future studies when bacterial communities in coral offspring are sampled from *ex situ* environments.

## DATA AVAILABILITY STATEMENT

The datasets presented in this study can be found in online repositories. The names of the repository/repositories and accession number(s) can be found below: <https://www.ncbi.nlm.nih.gov/>, SRA PRJNA706097.

## AUTHOR CONTRIBUTIONS

YN and J-HS contributed to the study design and wrote the manuscript. C-HL, YN, C-LF, VDHD, and AJM performed the coral sampling. J-HS and C-HL performed the experiment. J-HS

analyzed the data. YN and AJM contribute to the manuscript revision. All authors contributed to the article and approved the submitted version.

## FUNDING

This work was financially supported by the internal research grant of Academia Sinica to YN.

## ACKNOWLEDGMENTS

We would like to thank GIMRS that provided technical support in Lyudao, Taiwan. We thank J.-Y. Ding and Y.-L. Chen for their comments and suggestions.

## SUPPLEMENTARY MATERIAL

The Supplementary Material for this article can be found online at: <https://www.frontiersin.org/articles/10.3389/fmars.2022.796514/full#supplementary-material>

## REFERENCES

- Apprill, A. (2020). The role of symbioses in the adaptation and stress responses of marine organisms. *Ann. Rev. Mar. Sci.* 12, 291–314.
- Apprill, A., Marlow, H. Q., Martindale, M. Q., and Rappe, M. S. (2009). The onset of microbial associations in the coral *Pocillopora meandrina*. *ISME J.* 3, 685–699. doi: 10.1038/ismej.2009.3
- Apprill, A., Marlow, H. Q., Martindale, M. Q., and Rappe, M. S. (2012). Specificity of associations between bacteria and the coral *Pocillopora meandrina* during Early Development. *Appl. Environ. Microbiol.* 78, 7467–7475. doi: 10.1128/AEM.01232-12
- Babcock, R. (1990). Reproduction and development of the blue coral *Heliopora coerulea* (Alcyonaria Coenothecalia). *Mar. Biol.* 104, 475–481.
- Bernasconi, R., Stat, M., Koenders, A., Paparini, A., Bunce, M., and Huggett, M. J. (2019). Establishment of coral-bacteria symbioses reveal changes in the core bacterial community with host ontogeny. *Front. Microbiol.* 10:1529. doi: 10.3389/fmicb.2019.01529
- Bourne, D., Iida, Y., Uthicke, S., and Smith-Keune, C. (2008). Changes in coral-associated microbial communities during a bleaching event. *ISME J.* 2, 350–363. doi: 10.1038/ismej.2007.112
- Bray, J. R., and Curtis, J. T. (1957). An Ordination of the Upland Forest Communities of Southern Wisconsin. *Ecol. Monogr.* 27, 326–349.
- Bright, M., and Bulgheresi, S. (2010). A complex journey: transmission of microbial symbionts. *Nat. Rev. Microbiol.* 8, 218–230.
- Ceh, J., Kilburn, M. R., Cliff, J. B., Raina, J.-B., van Keulen, M., and Bourne, D. G. (2013). Nutrient cycling in early coral life stages: *Pocillopora damicornis* larvae provide their algal symbiont (*Symbiodinium*) with nitrogen acquired from bacterial associates. *Ecol. Evol.* 3, 2393–2400. doi: 10.1002/ece3.642
- Chan, W. Y., Peplow, L. M., Menendez, P., Hoffmann, A. A., and van Oppen, M. J. H. (2019). The roles of age, parentage and environment on bacterial and algal endosymbiont communities in *Acropora* corals. *Mol. Ecol.* 28, 3830–3843.
- Chen, C. P., Tseng, C. H., Chen, C. A., and Tang, S. L. (2011). The dynamics of microbial partnerships in the coral *Isopora palifera*. *ISME J.* 5, 728–740. doi: 10.1038/ismej.2010.151
- Damjanovic, K., Menéndez, P., Blackall, L. L., and van Oppen, M. J. H. (2019a). Early life stages of a common broadcast spawning coral associate with specific bacterial communities despite lack of internalized bacteria. *Microb. Ecol.* 79, 706–719. doi: 10.1007/s00248-019-01428-1
- Damjanovic, K., van Oppen, M. J. H., Menendez, P., and Blackall, L. L. (2019b). Experimental inoculation of coral recruits with marine bacteria indicates scope for microbiome manipulation in *Acropora tenuis* and *Platygyra daedalea*. *Front. Microbiol.* 10:1702.
- Damjanovic, K., Menéndez, P., Blackall, L. L., and van Oppen, M. J. H. (2020a). Mixed-mode bacterial transmission in the common brooding coral *Pocillopora acuta*. *Environ. Microbiol.* 22, 397–412.
- Damjanovic, K., Blackall, L. L., Peplow, L. M., and van Oppen, M. J. H. (2020b). Assessment of bacterial community composition within and among *Acropora loripes* colonies in the wild and in captivity. *Coral Reefs* 39, 1245–1255. doi: 10.1007/s00338-020-01958-y
- Douglas, A. E. (2019). Simple animal models for microbiome research. *Nat. Rev. Microbiol.* 17, 764–775. doi: 10.1038/s41579-019-0242-1
- Edgar, R. C. (2013). UPARSE: Highly accurate otu sequences from microbial amplicon reads. *Nat. Methods* 10, 996–998. doi: 10.1038/nmeth.2604
- Epstein, H. E., Torda, G., Munday, P. L., and van Oppen, M. J. H. (2019). Parental and early life stage environments drive establishment of bacterial and dinoflagellate communities in a common coral. *ISME J.* 13, 1635–1638. doi: 10.1038/s41396-019-0358-3
- Harii, S., and Kayanne, H. (2003). Larval dispersal, recruitment, and adult distribution of the brooding stony octocoral *Heliopora coerulea* on Ishigaki Island, Southwest Japan. *Coral Reefs* 22, 188–196.
- Harii, S., Kayanne, H., Takigawa, H., Hayashibara, T., and Yamamoto, M. (2002). Larval survivorship, competency periods and settlement of two brooding corals, *Heliopora coerulea* and *Pocillopora damicornis*. *Mar. Biol.* 141, 39–46.
- Hartmann, A. C., Baird, A. H., Knowlton, N., and Huang, D. (2017). The paradox of environmental symbiont acquisition in obligate mutualisms. *Curr. Biol.* 27, 3711–3716e3713. doi: 10.1016/j.cub.2017.10.036
- Hong, M. J., Yu, Y. T., Chen, C. A., Chiang, P. W., and Tang, S. L. (2009). Influence of species specificity and other factors on bacteria associated with the coral *Stylophora pistillata* in Taiwan. *Appl. Environ. Microbiol.* 75, 7797–7806.
- Jorgensen, S. L., Hannisdal, B., Lanzen, A., Baumberger, T., Flesland, K., Fonseca, R., et al. (2012). Correlating microbial community profiles with geochemical data in highly stratified sediments from the Arctic Mid-Ocean Ridge. *Proc. Natl. Acad. Sci. U. S. A.* 109, E2846–E2855. doi: 10.1073/pnas.1207574109
- Leite, D. C., Leao, P., Garrido, A. G., Lins, U., Santos, H. F., Pires, D. O., et al. (2017). Broadcast spawning coral *Mussismilia hispida* can vertically transfer its associated bacterial core. *Front. Microbiol.* 8:176. doi: 10.3389/fmicb.2017.00176

- Lema, K. A., Clode, P. L., Kilburn, M. R., Thornton, R., Willis, B. L., and Bourne, D. G. (2016). Imaging the uptake of nitrogen-fixing bacteria into larvae of the coral *Acropora millepora*. *ISME J.* 10, 1804–1808. doi: 10.1038/ismej.2015.229
- Lesser, M. P., Falcon, L. I., Rodriguez-Roman, A., Enriquez, S., Hoegh-Guldberg, O., and Iglesias-Prieto, R. (2007). Nitrogen fixation by symbiotic cyanobacteria provides a source of nitrogen for the scleractinian coral *Montastraea cavernosa*. *Mar. Ecol. Prog. Ser.* 346, 143–152.
- Lin, C. H., and Nozawa, Y. (2017). Variability of spawning time (lunar day) in *Acropora* versus merulinid corals: a 7-yr record of in situ coral spawning in Taiwan. *Coral Reefs* 36, 1269–1278. doi: 10.1007/s00338-017-1622-5
- Lin, C. H., Takahashi, S., Mulla, A. J., and Nozawa, Y. (2021). Moonrise timing is key for synchronized spawning in coral *Dipsastraea speciosa*. *Proc. Natl. Acad. Sci. U. S. A.* 118:34. doi: 10.1073/pnas.2101985118
- Littman, R. A., Willis, B. L., and Bourne, D. G. (2009). Bacterial communities of juvenile corals infected with different *Symbiodinium* (dinoflagellate) clades. *Mar. Ecol. Prog. Ser.* 389, 45–59. doi: 10.3354/meps08180
- Nubel, U., Engelen, B., Felske, A., Snaidr, J., Wieshuber, A., Amann, R. I., et al. (1996). Sequence heterogeneities of genes encoding 16S rRNAs in *Paenibacillus polymyxa* detected by temperature gradient gel electrophoresis. *J. Bacteriol.* 178, 5636–5643. doi: 10.1128/jb.178.19.5636-5643.1996
- R Core Team (2019). *R: A language and environment for statistical computing*. Vienna: R Foundation for Statistical Computing.
- Radecker, N., Pogoreutz, C., Voolstra, C. R., Wiedenmann, J., and Wild, C. (2015). Nitrogen cycling in corals: the key to understanding holobiont functioning? *Trends Microbiol.* 23, 490–497. doi: 10.1016/j.tim.2015.03.008
- Rohwer, F., Seguritan, V., Azam, F., and Knowlton, N. (2002). Diversity and distribution of coral-associated bacteria. *Mar. Ecol. Prog. Ser.* 243, 1–10.
- Schloss, P. D., Westcott, S. L., Ryabin, T., Hall, J. R., Hartmann, M., Hollister, E. B., et al. (2009). Introducing mothur: open-source, platform-independent, community-supported software for describing and comparing microbial communities. *Appl. Environ. Microbiol.* 75, 7537–7541. doi: 10.1128/AEM.01541-09
- Thompson, J. R., Rivera, H. E., Closek, C. J., and Medina, M. (2015). Microbes in the coral holobiont: partners through evolution, development, and ecological interactions. *Front. Cell. Infect. Microbiol.* 4:176. doi: 10.3389/fcimb.2014.00176
- van Oppen, M. J. H., and Blackall, L. L. (2019). Coral microbiome dynamics, functions and design in a changing world. *Nat. Rev. Microbiol.* 17, 557–567.
- Wang, Q., Garrity, G. M., Tiedje, J. M., and Cole, J. R. (2007). Naive Bayesian classifier for rapid assignment of rRNA sequences into the new bacterial taxonomy. *Appl. Environ. Microbiol.* 73, 5261–5267.
- Wang, Y., Kuang, Z., Yu, X., Ruhn, K. A., Kubo, M., and Hooper, L. V. (2017). The intestinal microbiota regulates body composition through NFIL3 and the circadian clock. *Science* 357, 912–916. doi: 10.1126/science.aan0677
- Wilson, K. (2001). Preparation of genomic DNA from bacteria. *Curr. Protoc. Mol. Biol.* 2001, 2–4. doi: 10.1002/0471142727.mb0204s56
- Yasuda, N., Taquet, C., Nagai, S., Fortes, M., Fan, T. Y., Phongsuwan, N., et al. (2014). Genetic structure and cryptic speciation in the threatened reef-building coral *Heliopora coerulea* along Kuroshio Current. *Bull. Mar. Sci.* 90, 233–255.
- Zhou, G., Cai, L., Yuan, T., Tian, R., Tong, H., Zhang, W., et al. (2017). Microbiome dynamics in early life stages of the scleractinian coral *Acropora gemmifera* in response to elevated pCO<sub>2</sub>. *Environ. Microbiol.* 19, 3342–3352. doi: 10.1111/1462-2920.13840

**Conflict of Interest:** The authors declare that the research was conducted in the absence of any commercial or financial relationships that could be construed as a potential conflict of interest.

**Publisher's Note:** All claims expressed in this article are solely those of the authors and do not necessarily represent those of their affiliated organizations, or those of the publisher, the editors and the reviewers. Any product that may be evaluated in this article, or claim that may be made by its manufacturer, is not guaranteed or endorsed by the publisher.

Copyright © 2022 Shiu, Lin, Mulla, Dang, Fong and Nozawa. This is an open-access article distributed under the terms of the Creative Commons Attribution License (CC BY). The use, distribution or reproduction in other forums is permitted, provided the original author(s) and the copyright owner(s) are credited and that the original publication in this journal is cited, in accordance with accepted academic practice. No use, distribution or reproduction is permitted which does not comply with these terms.





# A Protocol for Extracting Structural Metrics From 3D Reconstructions of Corals

Eoghan A. Aston<sup>1,2,3\*</sup>, Stephanie Duce<sup>2</sup>, Andrew S. Hoey<sup>1</sup> and Renata Ferrari<sup>3</sup>

<sup>1</sup> Australian Research Council (ARC) Centre of Excellence for Coral Reef Studies, James Cook University, Townsville, QLD, Australia, <sup>2</sup> College of Science and Engineering, James Cook University, Townsville, QLD, Australia, <sup>3</sup> Healthy and Resilient Reefs, Australian Institute of Marine Science, Townsville, QLD, Australia

## OPEN ACCESS

### Edited by:

Shashank Keshavmurthy,  
Academia Sinica, Taiwan

### Reviewed by:

Christopher Goatley,  
University of New England, Australia  
Nadav Shashar,  
Ben-Gurion University of the Negev,  
Israel

### \*Correspondence:

Eoghan A. Aston  
eoghan.aston@my.jcu.edu.au

### Specialty section:

This article was submitted to  
Coral Reef Research,  
a section of the journal  
Frontiers in Marine Science

**Received:** 13 January 2022

**Accepted:** 02 March 2022

**Published:** 07 April 2022

### Citation:

Aston EA, Duce S, Hoey AS and  
Ferrari R (2022) A Protocol for  
Extracting Structural Metrics From 3D  
Reconstructions of Corals.  
Front. Mar. Sci. 9:854395.  
doi: 10.3389/fmars.2022.854395

The 3D structure of individual coral colonies provides insights into their ecological functioning. While structure from motion techniques make it possible to reconstruct 3D models of coral colonies based on overlapping images, the extraction of relevant metrics of complexity in a reproducible way remains challenging. We present a method and associated scripts for the 3D reconstruction of coral colonies from *in-situ* images and the automatic extraction of eleven structural complexity metrics, designed to be run in widely-used software packages. The metrics are designed to capture aspects of complexity relating to the colony's size and shape that are related to their ecological function. We explored the potential ecological applications of some of these metrics using linear models, comparing aspects of complexity among colonies of different size and morphotaxa (combined information on morphology and taxa). Our results showed that a metric as simple as colony diameter explained 95% of the variation in shelter provisioning capability when paired with information on colony morphotaxa. Further, the habitat provisioning of colonies of comparable size was similar among the six of the seven morphotaxa examined. During the current period of rapid uptake of photogrammetry among ecologists, the results of our study provide a basis to use data derived from 3D models to further explore the nuances of the relationship between structure and function of corals at the colony scale in a replicable and standardised way.

**Keywords:** photogrammetry, structural complexity, spatial refuge, automation, structure-from-motion

## INTRODUCTION

Structural complexity is an important component in the functioning of ecosystems, with the abundance and diversity of species generally being positively related to structural complexity of the habitat, especially at low levels of complexity (MacArthur, 1958). The presence of structure creates protected environments that moderate environmental conditions and creates a wide breadth of

ecological niches for animals to exploit (Bruno et al., 2003; Alvarez-Filip et al., 2011; Tokeshi and Arakaki, 2012). As the abundance and diversity of complex physical structures in an ecosystem increases, so does the ability of that ecosystem to support animals with different microhabitat needs (Willis et al., 2005). Whilst the effects of structural complexity are often confounded by differences in the taxonomic composition of habitat-forming organisms, its importance transcends any particular ecosystem and is applicable in almost every natural habitat, from terrestrial coniferous forests (Franklin and Van Pelt, 2004) and savannahs (Gigliotti et al., 2020) to freshwater rivers (Warfe and Barmuta, 2006) and coral reefs (Graham and Nash, 2013).

On coral reefs, one of the world's most biodiverse ecosystems, the importance of structural complexity has long been recognized (Risk, 1972; Vine, 1974). The availability of complex structure provides refugia from predators (Ménard et al., 2012; Rogers et al., 2014; González-Rivero et al., 2017), reduces competition for habitat space through the formation of diverse and abundant ecological niches or microhabitats (Graham and Nash, 2013) and increases the surface area available for foraging (Vine, 1974). Whilst the abundance, density and spatial arrangement of habitat-providing structures are important in shaping fish communities (Pygas et al., 2020), the structural characteristics of individual coral colonies can also play an important role for many small-bodied, site-attached fishes (Quadros et al., 2019). For example, structurally complex colonies are good providers of habitat because they generally supply a large amount of physical refugia from larger bodied predators (Hixon and Beets, 1993; Noonan et al., 2012). As such, fish-habitat relationships vary according to the species of coral and fish, and also change over time according to colony growth and/or erosion (Graham and Nash, 2013; Ferrari et al., 2017). The physical structure provided by individual coral colonies has been related to differences among coral species and/or growth forms (Komyakova et al., 2013; Richardson et al., 2017; Urbina-barreto et al., 2020), among colony sizes (Noonan et al., 2012; Agudo-Adriani et al., 2016; Urbina-barreto et al., 2020), and with environmental setting (Todd, 2008; Ow and Todd, 2010; Doszpot et al., 2019). Despite the importance of the structural complexity of coral colonies, accurately quantifying the physical structure of individual colonies is challenging.

At the scale of individual coral colonies, technical limitations have led to simplified measurements of structural complexity, including the manual measurement of the space between colony branches (Noonan et al., 2012), measurements of colony morphometrics such as height and diameter (Harborne et al., 2011; Harborne et al., 2012), as well as estimates of surface area from foil-wrapping or wax-dipping branches (Veal et al., 2010). However, these methods are generally imprecise, cannot be easily repeated *in situ*, and often damage the colonies (Naumann et al., 2009; Ferrari et al., 2016). Recent advances in computer vision and processing have allowed the full dimensionality of objects to be recorded and analyzed through 3D reconstructions of high-resolution imagery (i.e., close-range photogrammetry; Lavy et al.,

2015; Bayley and Mogg, 2020), which is becoming popular among ecologists.

Underwater close-range photogrammetry offers enormous potential to investigate the physical structure of coral colonies, however there is a need to explore and develop new, ecologically relevant metrics that can be compared among and within coral taxa. The process of analyzing reconstructed objects is now readily accessible and the structure of coral colonies can be analyzed in numerous ways (Figueira et al., 2015; Ferrari et al., 2016). Several metrics offer valuable insights into the structure of colonies including 3D surface area, colony volume, and a variety of ratios, including surface area to volume ratio, and colony rugosity (a ratio of the 3D to 2D surface area) (Bythell et al., 2001; Agudo-Adriani et al., 2016; Ferrari et al., 2016; Doszpot et al., 2019; Zawada et al., 2019a). However, metrics that focus on the delivery of an ecological function, such as shelter provisioning, are somewhat rare (but see Madin et al., 2016; Urbina-barreto et al., 2020). Given the rapidly changing ecological composition of global reef communities due to the combined effects of climate change (Hughes et al., 2017b; Hughes et al., 2018; Richardson et al., 2018; Dietzel et al., 2021) and local anthropogenic stressors (Cheal et al., 2017; Suchley and Alvarez-Filip, 2018), metrics that reflect the ecological functions of corals are required (Madin et al., 2016; Doszpot et al., 2019; Streit et al., 2019). Progress has been made to this end recently, as ecologists are exploring the structural traits of coral colonies in more detail. Quantification of the shelter provisioning capability and size structure of available refuge spaces have been discussed in specific types of coral (Urbina-barreto et al., 2020), as well as how this metric changes over time with coral growth (Million et al., 2021). Underwater close-range photogrammetric reconstructions have also revealed complex, non-linear relationships between simple coral growth measurements, such as linear extension rates, and higher order traits, such as shelter provisioning (Million et al., 2021).

Several aspects of the process of underwater photogrammetry have been assessed to date, including the effects of various parameters such as photograph density and resolution (Marre et al., 2019), camera systems (Guo et al., 2016), lenses and housings (Menna et al., 2016), water turbidity (Bryson et al., 2017) and flying elevation (Marre et al., 2019). Whilst it is of critical importance to understand how models may be affected by user-decisions, comparability between studies could and should be improved by the adoption of standardised workflow procedures. Given that there exist multiple studies based on photogrammetry and deriving estimates of complexity from corals (Agudo-Adriani et al., 2016; Reichert et al., 2016; Doszpot et al., 2019; Vivian et al., 2019; Million et al., 2021), there is great incentive to adopt reproducible methods *via* the use of standardised workflows at key parts in the processing pipeline. This applies both to the reconstruction of coral models (Lange and Perry, 2020) and the extraction of structural complexity metrics.

The aim of this study is to ensure repeatability among users by using a python script to serially process 3D reconstructions of coral colonies and extract a suite of three-dimensional complexity metrics. Following manual isolation of colonies from the

surrounding benthos in the models, we developed a second python script that automatically extracts a suite of three-dimensional structural complexity metrics from each model, saving time and increasing repeatability among users. To investigate the utility of these metrics as ecological indicators, we compared two of these key metrics among 69 colonies of varying size and morphotaxa using Bayesian linear regression models.

## METHODS

### Data Collection and Classification of Corals

Images of 69 colonies were collected from seven reefs on the Great Barrier Reef (GBR) and in the Coral Sea during February 2020 (GBR: Hickson, and Tiger Reefs; Coral Sea: Saumarez, Cato, Wreck, Frederick, and Marion Reefs). The imaged colonies were located at depths between 3 to 13m in sheltered, back reef environments on each reef. Colonies with partial mortality, disease or algal overgrowth were avoided, as this may have affected structural characteristics.

Given the difficulties in identifying coral colonies to species in the field, we used morphotaxa to allow relevant comparisons. Individual colonies from each of the following seven morphotaxa were haphazardly selected and imaged: corymbose *Acropora*, digitate *Acropora*, tabular *Acropora*, branching *Isopora*, branching *Pocillopora*, branching *Porites* and ‘massive’ corals (**Figure 1**). Massive and submassive corals from different genera (mainly *Porites* and *Favia*) were aggregated into a single category (i.e., ‘massive’ corals) due to their structurally comparable morphologies and because none of the massive coral colonies imaged had overhangs contributing to their refuge space. To classify coral morphology, we followed the CATAMI scheme (Althaus et al., 2015), which includes visual guides to broad-level morphologies.

### Field and Laboratory Equipment

Camera system choice has been shown to play an important role in the quality of the final model (Marre et al., 2019). Resultant models from different camera/computer systems can be of comparable quality, however these should always be reported since the resolution (i.e., the smallest resolvable details) can be affected. All images used in this study were taken using a Canon 5D MK IV body (Canon USA Inc.) Ikelite housing (Ikelite Underwater Systems), fitted with an 8” dry lock dome port. A Canon 35mm f/2 IS USM prime lens was used to minimize perspective distortion in photographs while a dome port was chosen to reduce barrel distortion near the edges of images (Menna et al., 2018). Each photograph was a 30.2 Megapixel JPEG image. Relevant PC system specifications were as follows: Intel Core i9 9900K 3.6GHz CPU, 64GB RAM, 1x NVIDIA GeForce RTX 2080Ti Graphics card. High resolution 3D models are possible using cheaper, more compact cameras and off-the-shelf laptops (Lange and Perry, 2020). However, changes in model resolution and processing times associated with different cameras and processing settings affect surface measurements and

may hinder comparisons if not given appropriate consideration. At the colony scale, flying elevation is low (i.e., the sensor is very close to the object of interest), so sufficient overlap is likely to result in comparable model qualities regardless of sensor size (see Menna et al., 2016; Marre et al., 2019 for discussions of camera systems and flying elevation).

Agisoft recommends the use of coded targets for model scaling purposes. We mounted these in pairs (12-bit, printed on waterproof paper) on to two galvanized steel bars at known measured distances apart, ready for automatic detection by the software.

### Data Collection Protocols

The two scale bars were first placed adjacent to the coral colony prior to taking images and were included in a minimum of 20 photographs per colony. For each colony, 100-250 images (depending on colony size and morphotaxa) were taken. The goal was to collect a set of overlapping images taken from multiple angles such that the entire colony was imaged (Bythell et al., 2001; Million et al., 2021). We used an orbital swimming motion – three to four 360 degree passes around the colony at different heights. Imaging for a colony generally took 3-5 minutes (based on 100-250 images plus time before for testing camera settings). It is not critical that swimming motion is identical to generate comparable data, only that the entire colony is imaged with sufficient overlap to resolve all required details in the resultant model.

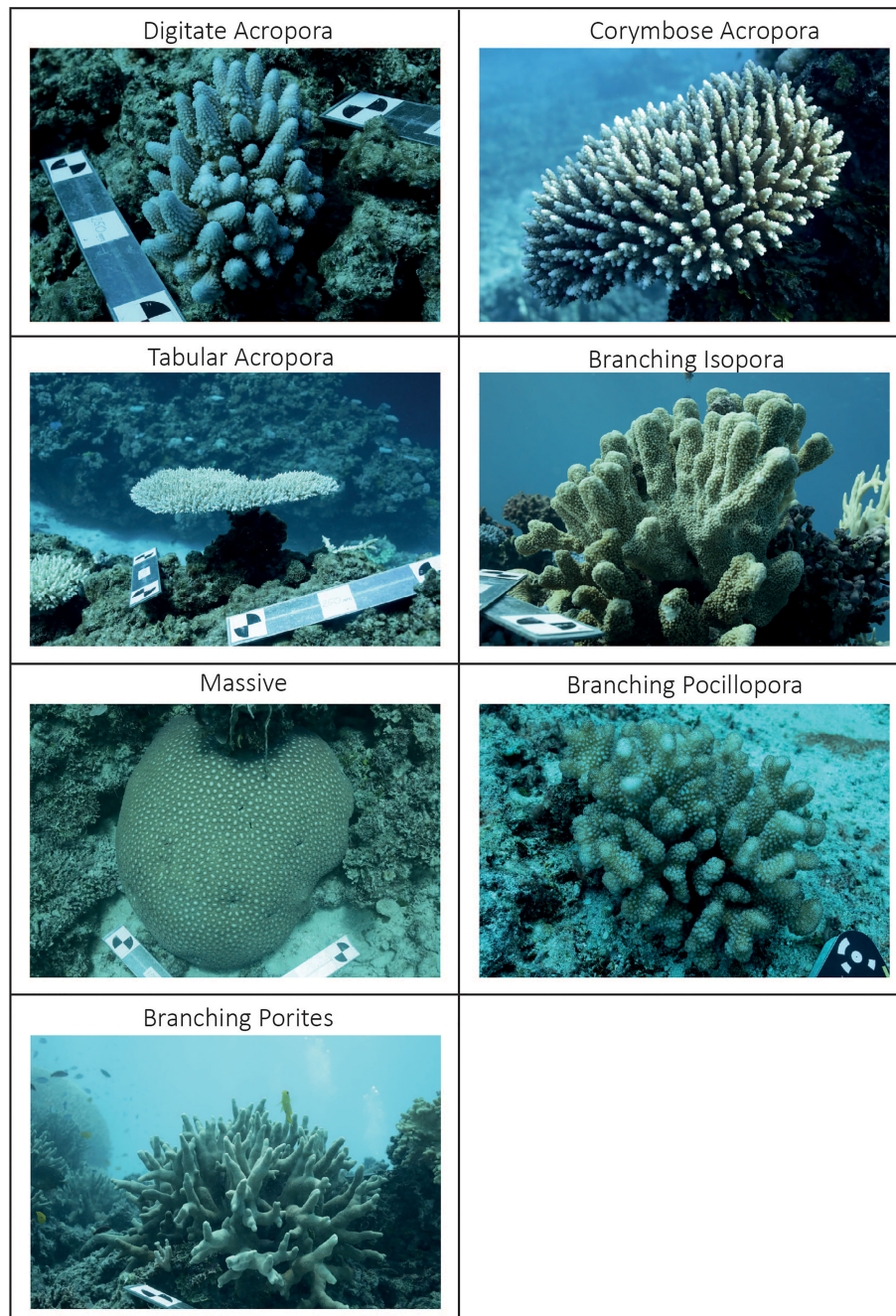
Camera settings were chosen based on local light conditions, but aperture was fixed at f/10 to ensure the entire colony was in focus during imaging.

### Model Reconstructions and Extraction of Structural Complexity Metrics

A variety of paid and free options are available to generate structure from motion models. The choice of software has been shown to lead to differences in the measured characteristics, affecting repeatability and potentially comparability between model data from different studies (Forsmoo et al., 2019). Agisoft Metashape (formerly Photoscan) is the most popular choice of software among ecologists for generating coral reconstructions (Agisoft LLC, St. Petersburg, Russia). 3D models were constructed using Agisoft Metashape Professional Ver 1.7. Total processing time for models varied; massive morphologies with ~150 images per colony took approximately 10-20 minutes to process, whereas larger and complex colonies with image sets numbering over 200 required several hours of processing. Steps for model generation have been discussed extensively, including error reduction, photograph selection, model scaling and accuracy metrics (Green et al., 2014; Forsmoo et al., 2019; Lange and Perry, 2020).

A single python script to reconstruct colonies using the same processing workflow is available (<https://github.com/E-Aston/CoralGeometry>). This script comes with detailed instructions and is interactive within Metashape, designed to be run from within the graphical user interface using the “Run Script” command. These instructions are also provided as **Supplementary Material**. For the use of this script, no





**FIGURE 1** | *In situ* examples of the seven distinct modelled morphotaxa. Note the galvanised scale bars present in several panels used to scale the reconstructions.

knowledge or installation of python is required, only installation of Metashape Professional. On execution of the script, a series of dialogue boxes prompt users to input the settings to be used in serial processing of the models, including the quality threshold for the disabling of photographs, photo alignment accuracy, and dense cloud quality. We provide the settings used to reconstruct the colonies used in this study (**Table 1**), and strongly recommend that others use the same settings when following this

reconstruction protocol, since processing settings affect model resolution and thus final measured characteristics.

Following the reconstruction of models, some manual preparation is needed for metrics extraction. Given the *in-situ* nature of our data collection, some of the benthos to which corals are attached is also reconstructed and needs to be removed manually. This includes “isolating”, i.e., removing any benthos from the reconstruction using metashape such



**TABLE 1 |** Beginning to end of reconstruction pipeline in Metashape.

Workflow Step	Details
1. Remove low-quality images (A)	Disable photos with quality score <0.5
2. Detect markers (A)	Tolerance value is set to 30 by default
3. Align Photos (A)	High Accuracy, generic preselection, Key Point Limit: 40,000 Tie Point Limit: 4,000
4. Clean Sparse cloud and optimize cameras (A)	Three-step automatic iterative process to remove the worst tie points based on reprojection error, reconstruction uncertainty and projection accuracy. Recommended setting: 95 (removes the worst 5% of points at each step in the process).
5. Build Dense Cloud (A)	Quality: Medium Depth filtering: Mild Calculate point colors
6. Build Mesh (A)	Source data: Dense cloud Surface type: Arbitrary (3D) Face count: High Interpolation: Enabled Calculate vertex colors: Yes
7. Build Texture (A)	Mapping mode: Generic Blending mode: Mosaic Texture size/count: 4096 x 1 Enable hole filling: Yes Enable ghosting filter: yes
8. Isolate model (M)	Free-form selection tool Select and delete all faces in the model that are not part of the reconstructed colony
9. Model scaling (M)	Manually delete incorrectly detected markers. Enter distance between targets in reference pane. Update model to apply scaling
10. Object orientation (M)	Use the navigator tool to manipulate the colony to a top-down view (perpendicular to the orientation of upwards growth). Generate report for model with projection set to 'current view'. Planar area is found as 'coverage area' on page 2 of the.pdf which will automatically open on generation. Metric is given in m <sup>2</sup>
11. Export object	Export each completed isolated mesh to a single folder in preparation for metrics extraction

*These settings were the same for each model in the dataset. Within the workflow steps, (M) refers to manual steps needed to be performed by the user, (A) refers to steps automated using the python script.*

that they are ready for automatic metric extraction (**Table 1**). The only measure of colony geometry to be extracted from metashape is planar area, which is automatically calculated using a top-down view upon generation of the model report (**Table 1**; Step 9).

## Extraction of Structural Complexity Metrics

Ten further metrics of the surface geometry or structural complexity were extracted from each colony, using a custom-coded python script utilizing the package *pymeshlab* (Muntoni and Cignoni, 2021), which integrates with the open source 3D software MeshLab v2016.12 (Cignoni et al., 2008). This package contains the full capability of MeshLab without the need to manually obtain surface measurements for each mesh. Our script 'cleans' the mesh (i.e., removes any unwanted faces that are not attached to the colony itself, which are often still present following the export of the model), then applies a series of scripts to measure and calculate several geometric complexity metrics automatically. These higher order complexity metrics were: 3D surface area, colony volume, convex hull volume (the simplest polygon that fully encloses the colony), absolute spatial refuge (a volumetric measurement of the space generated by the interstices of each colony), surface area to volume ratio, shelter size factor (fragmentation of shelter volume), proportion occupied (the ratio of the convex hull volume occupied by the colony), colony maximum diameter and colony height. A detailed summary of these metrics is presented below as well

as how each is calculated (**Table 2**), in addition to a graphical representation of metrics (**Figure S1**).

Given a set of reconstructions in the form of .obj files (the standard output from Metashape), the code returns a .csv file populated with the value of each metric for every coral, saving up to several hours of manual calculations. The use of the metrics extraction script assumes zero knowledge of python programming on the part of the user. All that is required is installation of python and the ability to run scripts from an interpreter. We provide detailed instructions on how to do this in **Supplementary Material**. For further analysis, we investigated a small subset of these (diameter, absolute spatial refuge and shelter size factor), however depending on the research questions, any of the described metrics are extracted and available for analysis.

## Statistical Models for Methods Validation

To assess the validity of the calculated complexity metrics extracted using our python script we selected two of the higher order and popularly used metrics and compared them among colonies of different size and morphotaxa. We chose absolute spatial refuge and shelter size factor. Although any of the 3D metrics presented in this study may be ecologically informative depending on the research question, quantifying the shelter capacity of corals and how this shelter is delivered (i.e. the fragmentation of the shelter) is broadly applicable for ecological purposes, including measuring the functional capacity of corals to provide habitat (Urbina-barreto et al.,

**TABLE 2 |** Summary of metrics calculated for each colony using a combination of Metashape and MeshLab.

Metric name	Description	Unit	Software	Ecological reasoning/application
Colony diameter ( <i>D</i> )	Length along X axis of bounding box (the longest horizontal axis) enclosing each colony	cm	Python/ Meshlab	Widely used in the literature as a basic size metric. Also used to relate to higher order complexity metrics (House et al., 2018; Urbina-barreto et al., 2020)
Height ( <i>H</i> )	Length along Z-axis of bounding box enclosing each colony	cm	Python/ Meshlab	Identified as important for fish abundance (Harborne et al., 2011; Harborne et al., 2012; Agudo-Adriani et al., 2016)
Planar area ( <i>A<sub>2D</sub></i> )	Total area of reef floor occupied by each colony	cm <sup>2</sup>	Metashape	Important metric of spatial occupancy of the reef floor by each colony. Used to calculate popular metrics such as percent cover and useful for examining how different colonies fit together within a patch of reef. Also useful for growth rates (Ferrari et al., 2016; Dornelas et al., 2017)
3D Surface area ( <i>A<sub>3D</sub></i> )	Total surface area of colony	cm <sup>2</sup>	Python/ Meshlab	Relevant metric of potential foraging area provided to corallivores (González-Rivero et al., 2017). Also related to metabolic processes in corals such as photosynthesis (Naumann et al., 2009) Also used to measure 3D growth of colonies (Ferrari et al., 2017a)
Volume ( <i>V</i> )	Total volume of colony	dm <sup>3</sup> (litres)	Python/ Meshlab	Metric related to biomass, size and carbonate production. Also used over time to infer growth rates (Lavy et al., 2015; House et al., 2018)
Convex hull volume ( <i>V<sub>CH</sub></i> )	Volume of the simplest polygon which fully encloses the coral	dm <sup>3</sup> (litres)	Python/ MeshLab	Intermediary step for calculating other metrics related to interstitial space generated by colonies (Dospot et al., 2019; Urbina-barreto et al., 2020).
Absolute spatial refuge ( <i>R</i> )	Volume of the total amount of space generated by each coral ( $R = V_{CH} - V$ )	dm <sup>3</sup> (litres)	Python/ Meshlab	Quantifies interstitial space, with potentially important links to inhabitant fish (Urbina-barreto et al., 2020). Can potentially be used over time to track coral growth in an ecologically relevant manner (Million et al., 2021). Higher values of <i>R</i> indicate more overall shelter volume. This metric is calculated by subtracting the volume of the colony itself from the volume of its enclosing convex hull, leaving a volumetric measure of the interstitial space generated by each colony.
Surface area to volume ratio	Ratio between 3D surface area of a colony to its volume ( $A_{3D} \div V$ )	Ratio	Python/ Meshlab	Ecologically important metric of colony surface complexity that can be used to compare corals of different morphology (Dospot et al., 2019). Higher surface area to volume ratios indicate greater surface complexity.
Shelter size factor ( <i>S</i> )	Ratio of Absolute spatial refuge ( <i>R</i> ) to 3D surface area ( $S = R \div A_{3D}$ )	Ratio	Python/ Meshlab	Quantifies the level of fragmentation of habitat space, useful for comparing the size structure of refugia among colonies of different size and morphology (Urbina-barreto et al., 2020). Higher values indicate comparatively more “open” structures and larger spaces due to the higher volume of shelter space relative to colony surface area.
Proportion occupied ( <i>ProCC</i> )	Ratio of colony volume to convex hull volume ( $ProCC = V \div V_{CH}$ )	Ratio	Python/ Meshlab	Quantifies compactness, a particularly useful metric for branching colonies (Dospot et al., 2019). A higher proportion occupied indicates a more compact branching structure. Also referred to as convexity (Zawada et al., 2019a).

A graphical representation of metrics is available in **Figure S1**.

2020) and tracking how this changes over time with colony growth (Million et al., 2021). We hypothesized that due to differences in the physical structure of colonies of different morphotaxa, the rate of increase in absolute spatial refuge volume with colony size would vary among morphotaxa. We also hypothesized that the differences in physical structure would result in variation in the size-structure of spatial refuges among colonies of different size, again with parameters specific to each morphotaxa considered.

To determine whether 3D metrics of complexity (in this case spatial refuge) could be predicted by simpler linear metrics (i.e., colony diameter) we fitted two Bayesian linear regression models using the package ‘*brms*’ (Bürkner, 2017), both using colony diameter to predict the value of a 3D complexity metric. The first was absolute spatial refuge and the second was shelter size factor. For each of these models, morphotaxa was included as a predictor, so we could also infer how the scaling relationships between these variables differed among morphotaxa.

Appropriately informative Gaussian priors were used to inform the model and restrict to a reasonable outcome space (Banner et al., 2020). Assumptions about the underlying data distribution and prior predictive distributions were chosen based on visual exploration of the data following transformations as well as previous studies that have used similar data in the same way (Urbina-Barreto et al., 2020). Priors for all models were assessed visually using randomly sampled lines from the prior probability distribution (**Figure S2**). Posterior distributions were obtained using four Markov Chain Monte Carlo (MCMC), with 20,000 iterations and a warmup period of 10,000 samples. Inferences about the strength of the relationships between variables in both models were based on 95% highest density probability intervals around means predicted from the posterior distribution of the models. Analyses were carried out using R 4.0.1 (<https://r-project.org>). Initial data exploration of 2D and 3D variables was carried out using a scatterplot matrix on raw data generated using the ‘*Ggally*’ package (**Figure S2**) (Schloerke et al., 2020,

<https://cran.r-project.org/package=Ggally>). Plotting was carried out using the package *ggplot2* (Wickham, 2015). Bayesian  $R^2$  values were obtained to assess how well the regression models fitted the data in each case.

### Model 1: Absolute Spatial Refuge (R) vs. Diameter (D)

Prior predictive distributions were set using the results of regression models previously fit to this data type (Urbina-Barreto et al., 2020). Our data encompassed a similar size range of colonies; the main difference was that we chose to classify based on morphotaxa, a combination of taxonomic identity (genus) and morphology, rather than just morphology. We used log colony diameter  $Dlog_i$  and an indicator variable for morphotaxa (colony ID = CID) to predict log absolute spatial refuge for each colony  $Rlog_i$ , with the following model structure:

$$Rlog_i \sim \text{Normal}(\mu_i, \sigma)$$

$$\mu_i = \alpha_{CID[i]} + \beta_{CID[i]} Dlog_i$$

$$\alpha_{CID} = \text{Normal}(-9, 0.5)$$

$$\beta_{CID} = \text{Normal}(3, 0.5)$$

$$\sigma = \text{Exponential}(1)$$

We assumed a normal distribution with mean  $\mu_i$  and standard deviation  $\sigma$ . The prior values for the intercept  $\alpha$  was the same for each morphotaxa, as was the slope value  $\beta$ , reflective of Urbina-Barreto et al. (2020). An intercept of -9 on the log scale is close to 0 on the natural scale, so scientifically this prior made sense. This subverted the need to attach uninformative priors to the slope and intercept values or to rescale the data in a way that would result in a loss of information in the posterior distribution. These priors were relaxed enough to allow data to drive any differences in the posterior predictions between morphotaxa. An exponential prior with mean 1 was assigned to the standard deviation  $\sigma$ , given that we knew little about this parameter beforehand.

This model was compared to one without the morphotaxa variable using pareto-smoothed importance sampling leave-one-out (PSIS-LOO), to determine whether splitting

colonies into morphotaxa resulted in an improved fit to the data (Yao et al., 2018).

### Model 2: Shelter Size Factor (S) vs. Diameter (D)

Because shelter size factor is a new metric, we used less informative priors to allow the data to drive the model fit. We used colony diameter to predict shelter size factor for each morphotaxa. The model structure was:

$$S_i \sim \text{Normal}(\mu_i, \sigma)$$

$$\mu_i = \alpha_{CID[i]} + \beta_{CID[i]} D_i$$

$$\alpha_{CID} = \text{Normal}(0, 0.5)$$

$$\beta_{CID} = \text{Normal}(4, 2)$$

$$\sigma = \text{Exponential}(1)$$

Where  $S_i$  is the shelter size factor of each colony  $i$ , normally distributed with mean  $\mu_i$  and standard deviation  $\sigma$ .  $D_i$  is the diameter of each colony  $i$ , and this model. The morphotaxa indicator CID was the same as the previous model. Since shelter size factor is dimensionless, we did not log-transform any of the variables for this model. The same exponential prior was assigned to the standard deviation  $\sigma$  as in the previous regression model. To see whether morphotaxa and colony diameter were useful predictors of shelter size factor, and to check for overfitting, models with and without morphotype were compared, again using PSIS-LOO (Yao et al., 2018).

## RESULTS OF STATISTICAL MODELS

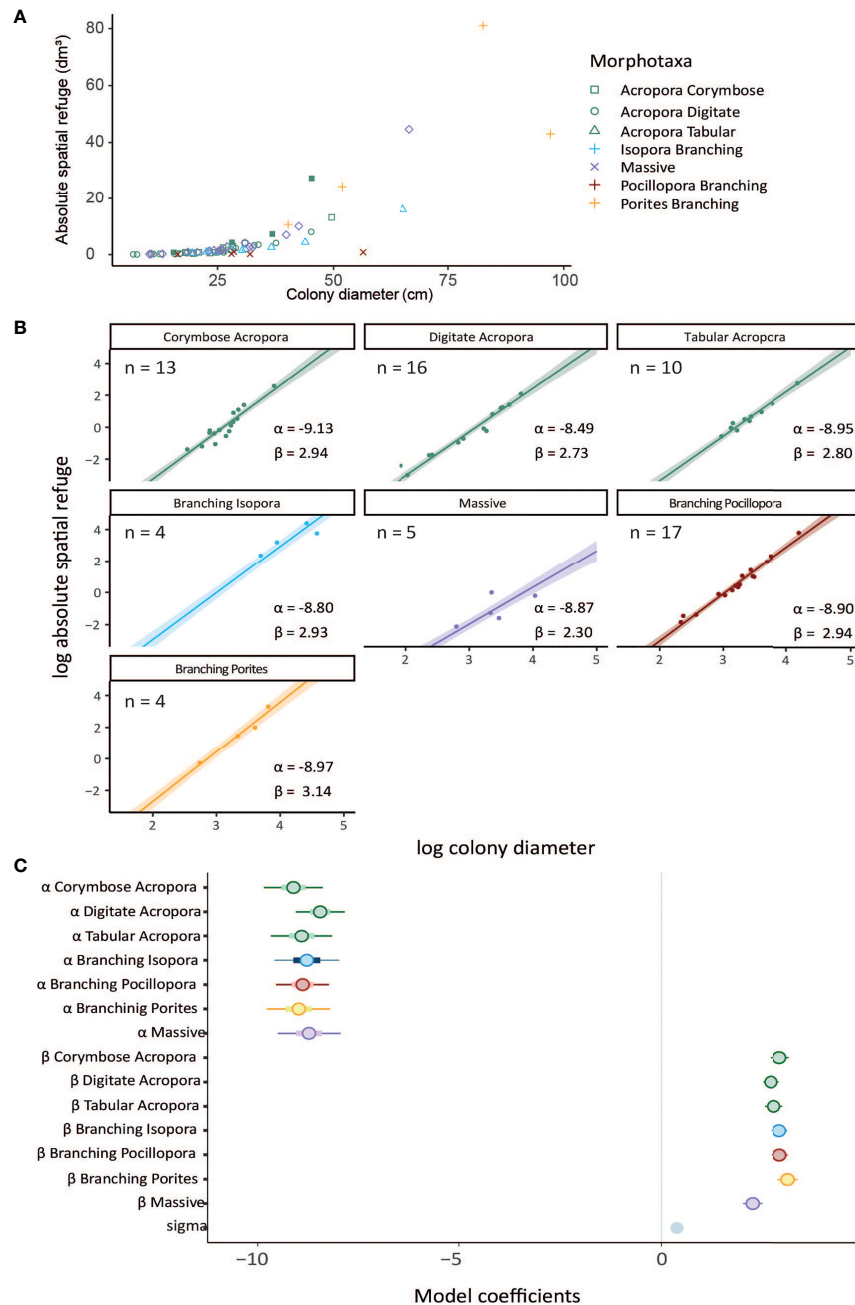
Sixty-nine colonies across the seven morphotaxa (range: 4-17 colonies per morphotaxa) were used for morphometric analysis (Table 3). Colonies ranged in diameter from 6.8 to 97.1 cm [mean diameter:  $29.6 \pm 2.0$  cm (s.e.)] though size distribution was skewed towards smaller colony sizes with 44 of the 69 colonies being < 30cm in diameter. Measurement error was very low across the dataset, with a maximum scaling error of 0.5mm across the entire sample. Most were considerably lower and fell in the range of 0.1-0.3mm scaling error.

**TABLE 3** | Summary of representation and dimensions among the seven unique morphotaxa used for colony reconstructions.

Morphotaxa	<i>n</i>	Mean Diameter ( <i>D</i> ) (cm ± se)	Mean Absolute spatial refuge ( <i>R</i> ) (dm <sup>3</sup> ± se)	Mean Shelter size factor ( <i>S</i> ) (± se)
Branching Pocillopora	17	27.6 ± 3.2	4.923 ± 2.559	0.85 ± 0.11
Digitate Acropora	16	24.2 ± 2.1	2.0129 ± 0.794	0.80 ± 0.08
Corymbose Acropora	13	23.2 ± 3.4	1.8682 ± 0.653	0.67 ± 0.09
Tabular Acropora	10	32.5 ± 4.3	3.1685 ± 1.470	0.95 ± 0.16
Massive	5	32.3 ± 6.6	0.4842 ± 0.177	0.21 ± 0.06
Branching Isopora	4	68.0 ± 13.2	39.758 ± 15.271	3.96 ± 0.69
Branching Porites	4	31.4 ± 6.4	9.940 ± 5.955	2.31 ± 0.06

Note that these are summary statistics only and were not tested statistically for between-group differences.

Shelter size factor is a ratio of the overall spatial refugia volume to the 3D surface area of the colony and is thus unitless. Units for absolute spatial refuge are given in cubic decimetres. One cubic decimetre is equivalent to one litre.



**FIGURE 2 | (A)** Scaling of absolute spatial refuge with increasing colony diameter across all morphotaxa. **(B)** Plotted posteriors from log-log linear model of absolute spatial refuge (mean centred) from the interaction model containing colony diameter as a predictor for each of the seven coral morphotaxa as well as intercept ( $\alpha$ ) and slope ( $\beta$ ) estimates. Shaded regions are 95% highest density probability distribution. **(C)** Posterior predictions for intercept  $\alpha$  and  $\beta$  parameters in the model. Straight line slope parameters indicate the existence of power-law relationships, with steeper slopes corresponding to higher power-scaling. Points indicate means, thick bars are 50% credible intervals, thin blue lines are 95% credible intervals. Numerical values of all model coefficients including posterior uncertainty are included in **Table S1**.

## Model 1 Predictions: Log-Absolute Spatial Refuge (R) vs. Log-Diameter (D)

The best model for predicting absolute spatial refuge included the interaction between morphotaxa and colony diameter (PSIS-LOO model weighting = 1, Bayes  $R^2 = 0.95$ ) (**Table S2**). Most

morphotaxa appeared to fall within a somewhat similar range of increasing spatial refuge with increasing colony diameter (**Figures 2A, C** and **Table S1**). For most morphotaxa, posterior credible intervals were narrow and most colonies fell near the mean prediction slope (**Figure 2B**). The linear model



determined that the scaling of absolute spatial refuge with colony diameter was broadly similar among almost most of the morphotaxa included in this study (95% credible intervals for the posterior estimates of slope overlapped between morphotaxa in most cases, **Table S2**), but there were some differences in the scaling relationships among morphotaxa. The exception was ‘massive’ corals, where the increase in spatial refuge was considerably lower than the six other morphotaxa with increasing colony diameter.

The relationships in the models indicate that there is a power-law relationship between colony diameter and spatial refuge provisioning such that as colonies grow and increase in size, the rate of increase of spatial refuge rises exponentially. Thus, subtle differences in slope gradients on the log-scale become larger when converted back to the natural scale, particularly in larger colonies (**Figure 2A**). For example, absolute spatial refuge in digitate and corymbose *Acropora* scaled to the power of 2.73 and 2.94 respectively (maximum likelihood estimate). For a colony of diameter 25cm, the expected spatial refuge volume would be 1.34 and 1.39dm<sup>3</sup> (1dm<sup>3</sup> = 1000cm<sup>3</sup> or 1 litre) for digitate and corymbose *Acropora* respectively. Following the same scaling law, by the time colonies reach a diameter of 50cm, the expected values of refuge volume would be approximately 8.85dm<sup>3</sup> and 10.59dm<sup>3</sup>, a difference of approximately 20%. For large colonies of diameter 75cm for example, a digitate *Acropora* colony would provide an estimated 27 dm<sup>3</sup> (27 litres equivalent) whilst a comparable corymbose *Acropora* colony would provide an estimated 35.5 dm<sup>3</sup>, a comparatively large difference (36% larger). By contrast, at this large colony size, a branching *Pocillopora* colony, which was also captured well in this study, would have an expected absolute spatial refuge of 44.7dm<sup>3</sup>, scaling at a greater rate with increasing diameter than any of the *Acropora* morphotaxa.

For ‘massive’ colonies, the increase in spatial refuge with increasing colony diameter was the lowest, this group consistently providing the lowest volumes of absolute spatial refuge. A colony with diameter 50cm would have an expected spatial refuge of just 1.13dm<sup>3</sup>, or just over 1.1 litres. Whilst there was relatively little data for this morphotaxa, massive corals clearly provide the least spatial refuge among all morphologies considered in this study.

## Model 2 Predictions: Shelter Size Factor (S) vs. Diameter (D)

The best model was again the interaction model containing morphotaxa (PSIS-LOO model weighting = 1, Bayes  $R^2$  = 0.84) (**Table S4**). Whilst shelter size factor was predicted well by the combination of colony diameter and morphotaxa, (branching *Acropora*, *Pocillopora*, digitate *Acropora* and tabular *Acropora*, there were no strong differences in the rate of increase of shelter size factor with increasing colony diameter in the posterior predictive distributions (**Figure 3** and **Table S3**), with the rate of increase estimates ( $\beta$ ) overlapping in all cases. For all morphotaxa except ‘Massive’ corals, shelter size factor ( $S$ ) and colony diameter ( $D$ ) were positively correlated (**Figure 3**). ‘Massive’ corals had the lowest values of shelter size factor across all colony sizes and a very small increase in shelter size factor with colony diameter. For branching *Isopora* and *Porites*, which respectively had high values

for  $\alpha$  and  $\beta$ , we could not make valid statistical inferences since the sample sizes were too low.

## DISCUSSION

### Metrics Extraction From Reconstructed 3D Models

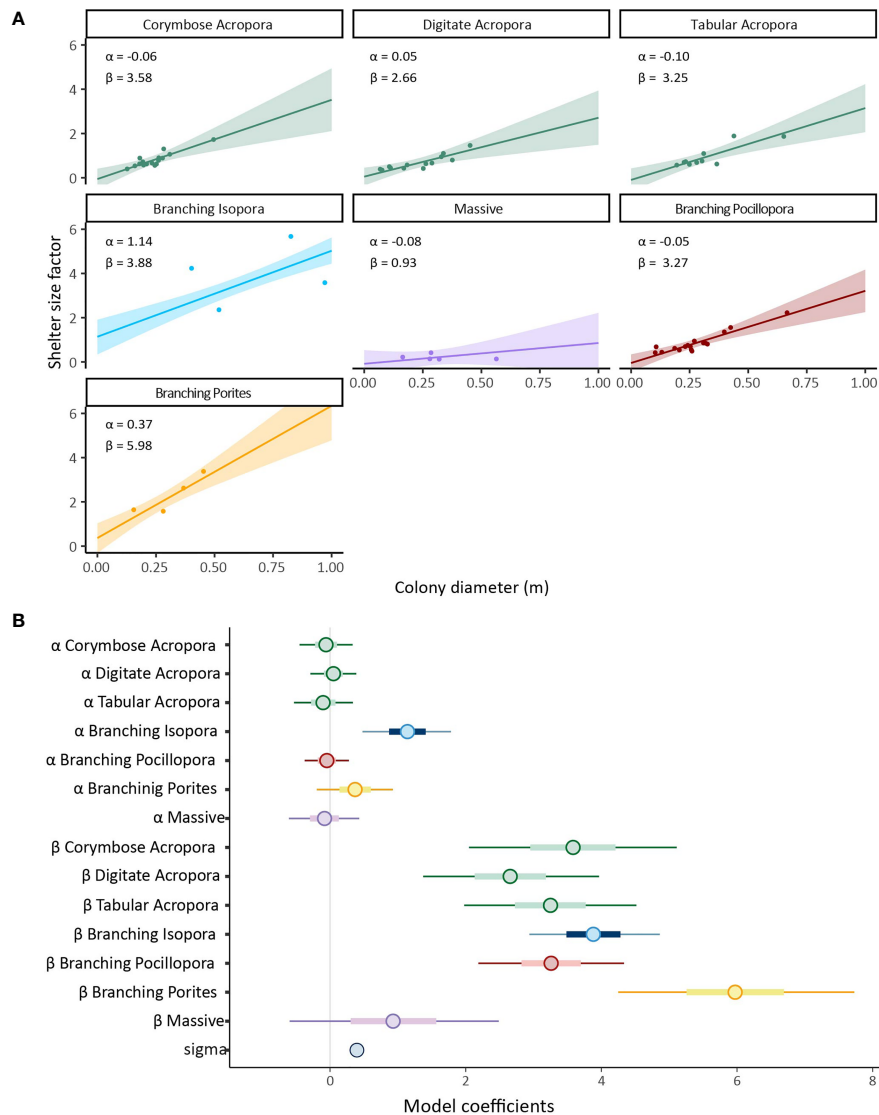
The methods developed in this study allow for the automated extraction of a suite of informative structural complexity metrics from digital reconstructions of coral colonies (or other objects). Applying novel technologies to create 3D reconstructions is accessible, accurate and requires little training. Yet, there is limited guidance on how to apply these technologies for ecological studies. Much of the recent literature deals with the accuracy, precision and repeatability of the resultant models, as well as how to make the reconstructions themselves, laying a critical foundation for the broad uptake of this method (Figueira et al., 2015; Shortis, 2015; Bryson et al., 2017; Raoult et al., 2017; Bayley et al., 2019; Marre et al., 2019). Ecological applications of photogrammetry, whilst rare, show that the accuracy and information-richness of resultant metrics affords more explanatory power of associated biotic communities than comparable manual methods such as chain-and-tape rugosity (Ferrari et al., 2017; González-Rivero et al., 2017; Urbina-barreto et al., 2020; Million et al., 2021). Therefore, it is an ideal time to establish practices of transparency of processing methods as well as standardization. Our routines are designed extract metrics simply and quickly minimizing manual input and decision-making on the part of the user.

Whilst we did not statistically analyze all the calculated metrics, the utility of each of these has been documented in the literature. Thus, researchers can select the most appropriate metrics for research questions from the suite provided by our code (see **Table 3**).

### Establishing the Ecological Utility of Structural Metrics

The metrics presented in this study can be used to compare various aspects of reef functionality by relating aspects of the shape of colonies to their size among different categorical growth forms simultaneously. Such approaches have been shown to be effective in estimating the functional capacity of reefs at the assemblage-scale (Urbina-barreto et al., 2020), predicting higher-order traits of corals using simple morphometrics (House et al., 2018), tracking reef responses to disturbance events (Zawada et al., 2019b), and measuring functional changes associated with colony growth (Million et al., 2021).

Comparison of two metrics of refuge provisioning among our sampled colonies revealed subtle differences in spatial refuge provisioning among a range of morphotaxa (**Figure 3**). We found that absolute spatial refuge could be predicted as a function of colony diameter and morphotaxa, despite a relatively small sample size for some coral groups. The power-law scaling relationships present among colonies are in agreement with other studies of 3D geometry at the colony



**FIGURE 3 | (A)** Plotted posteriors from linear model of shelter size factor from the interaction model containing colony diameter as a predictor for each of the seven morphotaxa. Shaded regions are 95% highest density probability intervals and solid lines are mean slopes of the mean from the posterior probability distribution. **(B)** Posterior predictions for intercept ( $\alpha$ ) and slope ( $\beta$ ) parameters in the same model. Circles indicate means, thick blue bars are 50% credible intervals, thin blue line are 95% credible intervals. All model coefficients including posterior uncertainty are available numerically in **Table S3**.

scale (Dornelas et al., 2017; Urbina-barreto et al., 2020). It is promising that historical data, collected when only 2D metrics were available, may be usefully compared with modern data to document changes overtime. It also suggests that where resource and time limitations prevent the gathering and processing of comprehensive suites of 3D data, for example in small-scale community reef management or citizen science scenarios, ecologically meaningful inferences could be drawn from the measurement of colony diameter and morphotaxa alone. However, whilst we found evidence here for strong scaling relationships between two and three-dimensional elements of colony geometry, our dataset was relatively small, and many

more colonies will be needed to solidify these relationships. Given enough data, a combination of the metrics presented here could be used as a platform to relate colony geometry not only to morphotaxa (as we did here) but also to environmental variables such as depth or exposure. This is arguably necessary as such variables have been shown to influence the phenotype of different coral taxa in the past (Todd, 2008; Ow and Todd, 2010; Doszpot et al., 2019).

Our results indicated that, contrary to Urbina-Barreto et al. (2020), tabular colonies did not provide greater volumes of spatial refuge among colonies of similar size from other morphotaxa. Further, the high surface area created by the

finely branching structure of the canopy itself depresses slightly the estimate of shelter size factor. Their generation of a single, large and continuous overhanging space below the ‘canopy’ has been shown to be a keystone reef structure, capable of supporting high biomass of a range of sizes of fish and other biota (Kerry and Bellwood, 2015). Whilst our generation of estimates for absolute spatial refuge and shelter size factor do capture in part the shaded overhang generated by tabular colonies (Figure S1), it is a conservative estimate of the space they generate. Depending on the growth orientation, vertical distance between the canopy and the benthos and canopy size, the refuge space generated by such morphotaxa can be considered highly variable, which should be a consideration when applying these metrics extraction routines in the future.

## Future Uses of Structural Complexity Metrics

Coral reefs are undergoing substantial change due to a combination of global (Hoegh-Guldberg et al., 2007; Hughes et al., 2017a; Hughes et al., 2017b; Williams and Graham, 2019), and local stressors (Suchley and Alvarez-Filip, 2018). Temperature-induced bleaching events cause differential mortality among coral taxa, with structurally complex taxa such as tabular and branching *Acropora* often being the most adversely affected (Wilson et al., 2006; Madin et al., 2014; Álvarez-Noriega et al., 2016; Hughes et al., 2019). It is expected that as shifts in community composition occur and the relative abundance of stress-tolerant, structurally simple species such as massive and submassive corals increases, reefs may have a reduced capacity to provide shelter spaces for fishes (Karkarey et al., 2017). Our hope is that others will generate data using the routines presented in this study to begin to build a repository of data containing information on many aspects of 3D colony geometry so that such contemporary questions as these can be answered effectively.

Some of the most practical future uses of the photogrammetry derived metrics presented here will be to measure colony growth and to relate aspects of their structure and size to the inhabitant fish species assemblages. Previous studies have found larger colonies support larger and more diverse fish assemblages even at these fine spatial scales, but these relationships are nuanced (Noonan et al., 2012; Agudo-Adriani et al., 2016). The use of photogrammetry scans to relate the full 3D structure of colonies to inhabitant fish is lacking (but see Agudo-Adriani et al., 2016) and establishing reliable relationships across the diverse suite of corals and fish will require large amounts of data from different study groups. Such information will be valuable to management and restoration efforts, where it is useful to know which specific combination of structural parameters leads to maximal biomass of the inhabitant fauna. Selection of coral species in restoration efforts should be tailored to include species that balance hardiness and survivorship with the ability to support fish through the provision of quality refugia (e.g. Shaish et al., 2010). There is a paucity of data across the literature on the 3D nature of growth among different colony morphotypes (but

see Million et al., 2021). Reimaging the same colonies at different time points and extracting a full suite of metrics such as those in this study could provide good insights into how various elements of coral structure changes over time when paired with suitable structural complexity metrics beyond simple linear extension.

## Considerations and Limitations of Photogrammetry-Based Metrics

Photogrammetry scans are, at present, the only way to obtain estimates of surface measurements of corals and the volume of generated habitat refuge at sub-centimetric resolution without disturbing/killing colonies. We were not able to compare underwater scans to control references due to the *in-situ* nature of this study, and thus could not empirically validate the accuracy of our surface measurements. However, studies validating the method using laser and/or computerized tomography (CT) scans of dead coral skeletons have found highly realistic representations (>90% similarity to laser scans) can be obtained even when scanning complex branching corals (McKinnon et al., 2011).

Most of the colonies in this study were <50cm maximum diameter, which does not capture the full range of sizes able to be obtained by all the included morphotaxa, so more data is needed these larger sized colonies. However, the larger reconstructed colonies (~1m diameter) that had associated photosets of >250 photographs were still well modelled in a few hours. The main constraint on the reliability of estimates of the generated in this study is the likely to be the complexity of the branching structures of complex colony shapes (Figueira et al., 2015). Photogrammetry scans are unable to model what is not seen by the camera lens, so occlusions caused by excessively complex/fine branching structures lead to incorrect representations of the 3D structure. The addition of more photographs overcomes this to an extent as excessive overlap between photographs leads to more detail in the surfaces of models, but as colonies become larger and more structurally complex, the model representations are susceptible to a reduction in accuracy (Bythell et al., 2001; Figueira et al., 2015; Zawada et al., 2019a).

## CONCLUSIONS

Photogrammetry is a suitable tool for assessing structural complexity at the colony scale. We show here the information richness and wide utility of photogrammetry by extracting 11 metrics of surface geometry and structural complexity using a single method. The semi-automated workflow presented in this study provides both new and experienced photogrammetry users with a tool to reconstruct corals at the colony scale, then extract an extensive suite of 3D structural complexity metrics. By automating processing at key steps, we aim to facilitate replicability and thus comparisons between studies, boosting the predictive power of statistical models over time

and building a repository of shareable 3D data. As more studies incorporate such routines into their 3D processing workflow, the potential to uncover the nature of how structure relates to function among coral morphotaxa to aid ecological interpretation is immense.

## DATA AVAILABILITY STATEMENT

The raw data supporting the conclusions of this article will be made available by the authors, without undue reservation.

## AUTHOR CONTRIBUTIONS

EA designed the study under the supervision of SD and AH. Fieldwork was carried out by EA. EA performed statistical analyses, coded processing scripts and wrote the manuscript. All authors provided feedback and contributed to the editing of the manuscript, and approved the final submitted version.

## REFERENCES

- Agudo-Adriani, E. A., Cappelletto, J., Cavada-Blanco, F., and Croquer, A. (2016). Colony Geometry and Structural Complexity of the Endangered Species *Acropora Cervicornis* Partly Explains the Structure of Their Associated Fish Assemblage. *PeerJ* 4, e1861. doi: 10.7717/peerj.1861
- Althaus, F., Hill, N., Ferrari, R., Edwards, L., Przeslawski, R., Schönberg, C. H. L., et al. (2015). A Standardised Vocabulary for Identifying Benthic Biota and Substrata From Underwater Imagery: The CATAMI Classification Scheme. *PLoS One* 10, 1–18. doi: 10.1371/journal.pone.0141039
- Alvarez-Filip, L., Gill, J. A., and Dulvy, N. K. (2011). Complex Reef Architecture Supports More Small-Bodied Fishes and Longer Food Chains on Caribbean Reefs. *Ecosphere* 2, art118. doi: 10.1890/ES11-00185.1
- Álvarez-Noriega, M., Baird, A. H., Dornelas, M., Madin, J. S., Cumbo, V. R., and Connolly, S. R. (2016). Fecundity and the Demographic Strategies of Coral Morphologies. *Ecology* 97, 3485–3493. doi: 10.1002/ecy.1588
- Banner, K. M., Irvine, K. M., and Rodhouse, T. J. (2020). The Use of Bayesian Priors in Ecology: The Good, the Bad and the Not Great. *Methods Ecol. Evol.* 11, 882–889. doi: 10.1111/2041-210X.13407
- Bayley, D. T. I., and Mogg, A. O. M. (2020). A Protocol for the Large-Scale Analysis of Reefs Using Structure From Motion Photogrammetry. *Methods Ecol. Evol.* 11, 1410–1420. doi: 10.1111/2041-210X.13476
- Bayley, D. T. I., Mogg, A. O. M., Koldewey, H., and Purvis, A. (2019). Capturing Complexity: Field-Testing the Use of 'Structure From Motion' Derived Virtual Models to Replicate Standard Measures of Reef Physical Structure. *PeerJ* 7, e6540. doi: 10.7717/peerj.6540
- Bruno, J. F., Stachowicz, J. J., and Bertness, M. D. (2003). Inclusion of Facilitation Into Ecological Theory. *Trends Ecol. Evol.* 18, 119–125. doi: 10.1016/S0169-5347(02)00045-9
- Bryson, M., Ferrari, R., Figueira, W., Pizarro, O., Madin, J., Williams, S., et al. (2017). Characterization of Measurement Errors Using Structure-From-Motion and Photogrammetry to Measure Marine Habitat Structural Complexity. *Ecol. Evol.* 7, 5669–5681. doi: 10.1002/ece3.3127
- Bürkner, P. C. (2017). brms: An R Package for Bayesian Multilevel Models Using Stan. *J. Stat. Softw.* 80, 1–28. doi: 10.18637/jss.v080.i01
- Bythell, J., Pan, P., and Lee, J. (2001). Three-Dimensional Morphometric Measurements of Reef Corals Using Underwater Photogrammetry Techniques. *Coral Reefs* 20, 193–199. doi: 10.1007/s003380100157
- Cheal, A. J., MacNeil, M. A., Emslie, M. J., and Sweatman, H. (2017). The Threat to Coral Reefs From More Intense Cyclones Under Climate Change. *Glob. Chang. Biol.* 23, 1511–1524. doi: 10.1111/gcb.13593

## FUNDING

Funding for field work was provided by the Director of National Parks.

## ACKNOWLEDGMENTS

We would like to thank the relevant staff at Parks Australia, particularly Andy Warmbrunn, Mitchell Baskys and Martin Russell, and Rob Benn and the crew of the MV Iron Joy for logistical support. RF was funded through the Reef Restoration and Adaptation Program and other internal projects within the Australian Institute of Marine Science.

## SUPPLEMENTARY MATERIAL

The Supplementary Material for this article can be found online at: <https://www.frontiersin.org/articles/10.3389/fmars.2022.854395/full#supplementary-material>

- Cignoni, P., Callieri, M., Corsini, M., Dellepiane, M., Ganovelli, F., and Ranzuglia, G. (2008). *MeshLab: An Open-Source Mesh Processing Tool*. 6th Eurographics Ital Chapter Conf 2008 - Proc. 129–136.
- Dietzel, A., Bode, M., Connolly, S. R., and Hughes, T. P. (2021). The Population Sizes and Global Extinction Risk of Reef-Building Coral Species at Biogeographic Scales. *Nat. Ecol. Evol.* 5, 663–669. doi: 10.1038/s41559-021-01393-4
- Dornelas, M., Madin, J. S., Baird, A. H., and Connolly, S. R. (2017). Allometric Growth in Reef-Building Corals. *Proc. R. Soc. B Biol. Sci.* 284, 1–7. doi: 10.1098/rspb.2017.0053
- Doszpot, N., McWilliam, M., Pratchett, M., Hoey, A., and Figueira, W. (2019). Plasticity in Three-Dimensional Geometry of Branching Corals Along a Cross-Shelf Gradient. *Diversity* 11, 44. doi: 10.3390/d11030044
- Ferrari, R., Malcolm, H. A., Byrne, M., Friedman, A., Williams, S. B., Schultz, A., et al. (2017). Habitat Structural Complexity Metrics Improve Predictions of Fish Abundance and Distribution. *Ecography (Cop)* 41, 1077–1091. doi: 10.1111/ecog.02580
- Ferrari, R., McKinnon, D., He, H., Smith, R. N., Corke, P., González-Rivero, M., et al. (2016). Quantifying Multiscale Habitat Structural Complexity: A Cost-Effective Framework for Underwater 3D Modelling. *Remote Sens* 8, rs8020113. doi: 10.3390/rs8020113
- Figueira, W., Ferrari, R., Weatherby, E., Porter, A., Hawes, S., and Byrne, M. (2015). Accuracy and Precision of Habitat Structural Complexity Metrics Derived From Underwater Photogrammetry. *Remote Sens* 7, 16883–16900. doi: 10.3390/rs71215859
- Forsmo, J., Anderson, K., Macleod, C. J. A., Wilkinson, M. E., DeBell, L., and Brazier, R. E. (2019). Structure From Motion Photogrammetry in Ecology: Does the Choice of Software Matter? *Ecol. Evol.* 9, 12964–12979. doi: 10.1002/ece3.5443
- Franklin, J. F., and Van Pelt, R. (2004). Spatial Aspects of Structural Complexity in Old-Growth Forests. *J. For* 102, 22–28. doi: 10.1093/jof/102.3.22
- Gigliotti, L. C., Slotow, R., Hunter, L. T. B., Fattebert, J., Sholto-Douglas, C., and Jachowski, D. S. (2020). Habitat Complexity and Lifetime Predation Risk Influence Mesopredator Survival in a Multi-Predator System. *Sci. Rep.* 10, 1–10. doi: 10.1038/s41598-020-73318-3
- González-Rivero, M., Harborne, A. R., Herrera-Reveles, A., Bozec, Y. M., Rogers, A., Friedman, A., et al. (2017). Linking Fishes to Multiple Metrics of Coral Reef Structural Complexity Using Three-Dimensional Technology. *Sci. Rep.* 7, 1–15. doi: 10.1038/s41598-017-14272-5
- Graham, N. A. J., and Nash, K. L. (2013). The Importance of Structural Complexity in Coral Reef Ecosystems. *Coral Reefs* 32, 315–326. doi: 10.1007/s00338-012-0984-y



- Green, S., Bevan, A., and Shapland, M. (2014). A Comparative Assessment of Structure From Motion Methods for Archaeological Research. *J. Archaeol. Sci.* 46, 173–181. doi: 10.1016/j.jas.2014.02.030
- Guo, T., Capra, A., Troyer, M., Gruen, A., Brooks, A. J., Hench, J. L., et al. (2016). Accuracy Assessment of Underwater Photogrammetric Three Dimensional Modelling for Coral Reefs. *Int. Arch. Photogramm Remote Sens Spat Inf Sci. - ISPRS Arch.* 41, 821–828. doi: 10.3929/ethz-b-000118990
- Harborne, A. R., Mumby, P. J., and Ferrari, R. (2012). The Effectiveness of Different Meso-Scale Rugosity Metrics for Predicting Intra-Habitat Variation in Coral-Reef Fish Assemblages. *Environ. Biol. Fishes* 94, 431–442. doi: 10.1007/s10641-011-9956-2
- Harborne, A. R., Mumby, P. J., Kennedy, E. V., and Ferrari, R. (2011). Biotic and Multi-Scale Abiotic Controls of Habitat Quality: Their Effect on Coral-Reef Fishes. *Mar. Ecol. Prog. Ser.* 437, 201–214. doi: 10.3354/meps09280
- Hixon, M., and Beets, J. (1993). Predation, Prey Refuges, and the Structure of Coral-Reef Fish Assemblages. *Ecol. Monogr.* 63, 77–101. doi: 10.2307/2937124
- Hoegh-Guldberg, O., Mumby, P. J., Hooten, A. J., Steneck, R. S., Greenfield, P., Gomez, E., et al. (2007). Coral Reefs Under Rapid Climate Change and Ocean Acidification. *Science* 318, 1737–1742. doi: 10.1126/science.1152509
- House, J. E., Brambilla, V., Bidaut, L. M., Christie, A. P., Pizarro, O., Madin, J. S., et al. (2018). Moving to 3D: Relationships Between Coral Planar Area, Surface Area and Volume. *PeerJ* 6, e4280. doi: 10.7717/peerj.4280
- Hughes, T., Barnes, M., Bellwood, D. R., Cinner, J., Cumming, G., Jackson, J. B., et al. (2017a). Coral Reefs in the Anthropocene. *Nature* 546, 82–90. doi: 10.1038/nature22901
- Hughes, T. P., Kerry, J. T., Álvarez-Noriega, M., Álvarez-Romero, J. G., Anderson, K. D., Baird, A. H., et al. (2017b). Global Warming and Recurrent Mass Bleaching of Corals. *Nature* 543, 373–377. doi: 10.1038/nature21707
- Hughes, T. P., Kerry, J. T., Baird, A. H., Connolly, S. R., Dietzel, A., Eakin, C. M., et al. (2018). Global Warming Transforms Coral Reef Assemblages. *Nature* 556, 492–496. doi: 10.1038/s41586-018-0041-2
- Hughes, T. P., Kerry, J. T., Connolly, S. R., Baird, A. H., Eakin, C. M., Heron, S. F., et al. (2019). Ecological Memory Modifies the Cumulative Impact of Recurrent Climate Extremes. *Nat. Clim. Chang* 9, 40–43. doi: 10.1038/s41558-018-0351-2
- Karkarey, R., Alcoverro, T., Kumar, S., and Arthur, R. (2017). Coping With Catastrophe: Foraging Plasticity Enables a Benthic Predator to Survive in Rapidly Degrading Coral Reefs. *Anim. Behav.* 131, 13–22. doi: 10.1016/j.anbehav.2017.07.010
- Kerry, J. T., and Bellwood, D. R. (2015). Do Tabular Corals Constitute Keystone Structures for Fishes on Coral Reefs? *Coral Reefs* 34, 41–50. doi: 10.1007/s00338-014-1232-4
- Komyakova, V., Munday, P. L., and Jones, G. P. (2013). Relative Importance of Coral Cover, Habitat Complexity and Diversity in Determining the Structure of Reef Fish Communities. *PLoS One* 8, 1–12. doi: 10.1371/journal.pone.0083178
- Lange, I. D., and Perry, C. T. (2020). A Quick, Easy and non-Invasive Method to Quantify Coral Growth Rates Using Photogrammetry and 3D Model Comparisons. *Methods Ecol. Evol.* 11, 714–726. doi: 10.1111/2041-210X.13388
- Lavy, A., Eyal, G., Neal, B., Keren, R., Loya, Y., and Ilan, M. (2015). A Quick, Easy and Non-Intrusive Method for Underwater Volume and Surface Area Evaluation of Benthic Organisms by 3D Computer Modelling. *Methods Ecol. Evol.* 6, 521–531. doi: 10.1111/2041-210X.12331
- MacArthur, R. (1958). Population Ecology of Some Warblers of Northeastern Coniferous Forests. *Ecology* 39, 599–619. doi: 10.2307/1931600
- Madin, J. S., Baird, A. H., Dornelas, M., and Connolly, S. R. (2014). Mechanical Vulnerability Explains Size-Dependent Mortality of Reef Corals. *Ecol. Lett.* 17, 1008–1015. doi: 10.1111/ele.12306
- Madin, J. S., Hoogenboom, M. O., Connolly, S. R., Darling, E. S., Falster, D. S., Huang, D., et al. (2016). A Trait-Based Approach to Advance Coral Reef Science. *Trends Ecol. Evol.* 31, 419–428. doi: 10.1016/j.tree.2016.02.012
- Marre, G., Holon, F., Luque, S., Boissery, P., and Deter, J. (2019). Monitoring Marine Habitats With Photogrammetry: A Cost-Effective, Accurate, Precise and High-Resolution Reconstruction Method. *Front. Mar. Sci.* 6, 1–15. doi: 10.3389/fmars.2019.00276
- McKinnon, D., He, H., Upcroft, B., and Smith, R. N. (2011). Towards Automated and in-Situ, Near-Real Time 3-D Reconstruction of Coral Reef Environments. *Ocean - MTS/IEEE Kona Progr. B.* doi: 10.23919/OCEANS.2011.6106982
- Ménard, A., Turgeon, K., Roche, D. G., Binning, S. A., and Kramer, D. L. (2012). Shelters and Their Use by Fishes on Fringing Coral Reefs. *PLoS One* 7, e38450. doi: 10.1371/journal.pone.0038450
- Menna, F., Nocerino, E., Drap, P., Remondino, F., Murtiyoso, A., Grussenmeyer, P., et al. (2018). Improving Underwater Accuracy by Empirical Weighting of Image Observations. *Int. Arch. Photogramm Remote Sens Spat Inf Sci. XLII-2*, 699–705. doi: 10.3929/ethz-b-000271676
- Menna, F., Nocerino, E., Fassi, F., and Remondino, F. (2016). Geometric and Optic Characterization of a Hemispherical Dome Port for Underwater Photogrammetry. *Sensors* 16, 1–21. doi: 10.3390/s16010048
- Million, W. C., O'Donnell, S., Bartels, E., and Kenkel, C. D. (2021). Colony-Level 3d Photogrammetry Reveals That Total Linear Extension and Initial Growth Do Not Scale With Complex Morphological Growth in the Branching Coral, *Acropora Cervicornis*. *Front. Mar. Sci.* 8, 1–12. doi: 10.3389/fmars.2021.646475
- Muntoni, A., and Cignoni, P. (2021). PyMeshlab. *Zenodo*. doi: 10.5281/zenodo.4438750
- Naumann, M. S., Niggel, W., Laforsch, C., Glaser, C., and Wild, C. (2009). Coral Surface Area Quantification-Evaluation of Established Techniques by Comparison With Computer Tomography. *Coral Reefs* 28, 109–117. doi: 10.1007/s00338-008-0459-3
- Noonan, S. H. C., Jones, G. P., and Pratchett, M. S. (2012). Coral Size, Health and Structural Complexity: Effects on the Ecology of a Coral Reef Damselfish. *Mar. Ecol. Prog. Ser.* 456, 127–137. doi: 10.3354/meps09687
- Ow, Y. X., and Todd, P. A. (2010). Light-Induced Morphological Plasticity in the Scleractinian Coral *Goniastrea Pectinata* and Its Functional Significance. *Coral Reefs* 29, 797–808. doi: 10.1007/s00338-010-0631-4
- Pygas, D. R., Ferrari, R., and Figueira, W. F. (2020). Review and Meta-Analysis of the Importance of Remotely Sensed Habitat Structural Complexity in Marine Ecology. *Estuar. Coast Shelf Sci.* 235, 106468. doi: 10.1016/j.jecss.2019.106468
- Quadros, A. L. S., Barros, F., Blumstein, D. T., Meira, V. H., and Nunes, J. A. C. C. (2019). Structural Complexity But Not Territory Sizes Influences Flight Initiation Distance in a Damselfish. *Mar. Biol.* 166, 65. doi: 10.1007/s00227-019-3508-2
- Raoult, V., Reid-Anderson, S., Ferri, A., and Williamson, J. (2017). How Reliable Is Structure From Motion (SfM) Over Time and Between Observers? A case study using coral reef bommies. *Remote Sens* 9, 740. doi: 10.3390/rs9070740
- Reichert, J., Schellenberg, J., Schubert, P., and Wilke, T. (2016). 3D Scanning as a Highly Precise, Reproducible, and Minimally Invasive Method for Surface Area and Volume Measurements of Scleractinian Corals. *Limnol. Oceanogr. Methods* 14, 518–526. doi: 10.1002/lom3.10109
- Richardson, L. E., Graham, N. A. J., and Hoey, A. S. (2017). Cross-Scale Habitat Structure Driven by Coral Species Composition on Tropical Reefs. *Sci. Rep.* 7, 7557. doi: 10.1038/s41598-017-08109-4
- Richardson, L. E., Graham, N. A. J., Pratchett, M. S., Eurich, J. G., and Hoey, A. S. (2018). Mass Coral Bleaching Causes Biotic Homogenization of Reef Fish Assemblages. *Glob. Chang. Biol.* 24, 3117–3129. doi: 10.1111/gcb.14119
- Risk, M. (1972). Fish Diversity on a Coral Reef in the Virgin Islands. *Atoll Res. Bull.* 153, 1–5. doi: 10.5479/si.00775630.153.1
- Rogers, A., Blanchard, J. L., and Mumby, P. J. (2014). Vulnerability of Coral Reef Fisheries to a Loss of Structural Complexity. *Curr. Biol.* 24, 1000–1005. doi: 10.1016/j.cub.2014.03.026
- Schloerke, B., Cook, D., Larmanange, J., Briatte, F., Marbach, M., Thoen, E., et al. (2020). Package: GGally ver 2.1.2. Available at: <https://cran.r-project.org/web/packages/GGally/>
- Shaish, L., Levy, G., Katzir, G., and Rinkevich, B. (2010). Employing a Highly Fragmented, Weedy Coral Species in Reef Restoration. *Ecol. Eng.* 36, 1424–1432. doi: 10.1016/j.ecoleng.2010.06.022
- Shortis, M. (2015). Calibration Techniques for Accurate Measurements by Underwater Camera Systems. *Sensors* 15, 30810–30826. doi: 10.3390/s151229831
- Streit, R. P., Cumming, G. S., and Bellwood, D. R. (2019). Patchy Delivery of Functions Undermines Functional Redundancy in a High Diversity System. *Funct. Ecol.* 33, 1144–1155. doi: 10.1111/1365-2435.13322
- Suchley, A., and Alvarez-Filip, L. (2018). Local Human Activities Limit Marine Protection Efficacy on Caribbean Coral Reefs. *Conserv. Lett.* 11, 1–9. doi: 10.1111/conl.12571

- Todd, P. A. (2008). Morphological Plasticity in Scleractinian Corals. *Biol. Rev.* 83, 315–337. doi: 10.1111/j.1469-185X.2008.00045.x
- Tokeshi, M., and Arakaki, S. (2012). Habitat Complexity in Aquatic Systems: Fractals and Beyond. *Hydrobiologia* 685, 27–47. doi: 10.1007/s10750-011-0832-z
- Urbina-barreto, I., Pinel, R., Fr, L., Mahamadaly, V., Elise, S., Kulbicki, M., et al. (2020). Quantifying the Shelter Capacity of Coral Reefs Using Photogrammetric 3D Modeling : From Colonies to Reefscapes. *Ecol. Indic.* 121, 107151. doi: 10.1016/j.ecolind.2020.107151
- Veal, C. J., Holmes, G., Nunez, M., Hoegh-Guldberg, O., and Osborn, J. (2010). A Comparative Study of Methods for Surface Area and Three Dimensional Shape Measurement of Coral Skeletons. *Limnol. Oceanogr. Methods* 8, 241–253. doi: 10.4319/lom.2010.8.241
- Vine, P. (1974). Effects of Algal Grazing and Aggressive Behaviour of the Fishes *Pomacentrus Lividus* and *Acanthurus Sohal* on Coral-Reef Ecology. *Mar Biol.* 24, 131–136. doi: 10.1007/BF00389347
- Vivian, D. N., Yee, S. H., Courtney, L. A., and Fisher, W. S. (2019). Estimating 3-Dimensional Surface Areas of Small Scleractinian Corals. *Caribb J. Sci.* 49, 192. doi: 10.18475/cjos.v49i2.a8
- Warfe, D. M., and Barmuta, L. A. (2006). Habitat Structural Complexity Mediates Food Web Dynamics in a Freshwater Macrophyte Community. *Oecologia* 150, 141–154. doi: 10.1007/s00442-006-0505-1
- Wickham, H. (2015). *Ggplot2: Create Elegant Data Visualisations Using the Grammar of Graphics. Version 2* (New York: Springer-V), 1–189.
- Williams, G. J., and Graham, N. A. J. (2019). Rethinking Coral Reef Functional Futures. *Funct. Ecol.* 33, 942–947. doi: 10.1111/1365-2435.13374
- Willis, S. C., Winemiller, K. O., and Lopez-Fernandez, H. (2005). Habitat Structural Complexity and Morphological Diversity of Fish Assemblages in a Neotropical Floodplain River. *Oecologia* 142, 284–295. doi: 10.1007/s00442-004-1723-z
- Wilson, S. K., Graham, N. A. J., Pratchett, M. S., Jones, G. P., and Polunin, N. V. C. (2006). Multiple Disturbances and the Global Degradation of Coral Reefs: Are Reef Fishes at Risk or Resilient? *Glob Chang Biol.* 12, 2220–2234. doi: 10.1111/j.1365-2486.2006.01252.x
- Yao, Y., Vehtari, A., Simpson, D., and Gelman, A. (2018). Using Stacking to Average Bayesian Predictive Distributions (With Discussion). *Bayesian Anal.* 13, 917–1007. doi: 10.1214/17-BA1091
- Zawada, K. J., Dornelas, M., and Madin, J.S. (2019a). Quantifying Coral Morphology. *Coral Reefs* 38, 1281–1292. doi: 10.1101/553453
- Zawada, K. J. A., Madin, J. S., Baird, A. H., Bridge, T. C. L., and aDornelas, M. (2019b). Morphological Traits Can Track Coral Reef Responses to the Anthropocene. *Funct. Ecol.*, 962–975. doi: 10.1111/1365-2435.13358

**Conflict of Interest:** The authors declare that the research was conducted in the absence of any commercial or financial relationships that could be construed as a potential conflict of interest.

**Publisher's Note:** All claims expressed in this article are solely those of the authors and do not necessarily represent those of their affiliated organizations, or those of the publisher, the editors and the reviewers. Any product that may be evaluated in this article, or claim that may be made by its manufacturer, is not guaranteed or endorsed by the publisher.

Copyright © 2022 Aston, Duce, Hoey and Ferrari. This is an open-access article distributed under the terms of the Creative Commons Attribution License (CC BY). The use, distribution or reproduction in other forums is permitted, provided the original author(s) and the copyright owner(s) are credited and that the original publication in this journal is cited, in accordance with accepted academic practice. No use, distribution or reproduction is permitted which does not comply with these terms.



# Consideration of Genetic Structure in the Ecologically or Biologically Significant Marine Areas Criteria: A Review of Convention on Biological Diversity Regional Workshops and A Case Study of Coral Reef Conservation Planning

Takehisa Yamakita<sup>1\*</sup>, Fumiaki Sodeyama<sup>1</sup>, Akira Iguchi<sup>2,3</sup>, Yuko F. Kitano<sup>4,5</sup>, Kosuke M. Teshima<sup>6</sup>, Akifumi Shimura<sup>7</sup>, Aki Nakabayashi<sup>7</sup>, Satoshi Nagai<sup>8</sup>, Takashi Nakamura<sup>9</sup>, Hiroaki Aizawa<sup>9</sup> and Nina Yasuda<sup>7,10</sup>

## OPEN ACCESS

### Edited by:

Andrew M Fischer,  
University of Tasmania, Australia

### Reviewed by:

Ana Carolina de Azevedo Mazzuco,  
Federal University of Espírito Santo,  
Brazil  
Cong Zeng,  
Shanghai Jiao Tong University, China

### \*Correspondence:

Takehisa Yamakita  
yamakitat@jamstec.go.jp

### Specialty section:

This article was submitted to  
Coral Reef Research,  
a section of the journal  
Frontiers in Marine Science

**Received:** 26 November 2021

**Accepted:** 04 April 2022

**Published:** 27 May 2022

### Citation:

Yamakita T, Sodeyama F, Iguchi A, Kitano YF, Teshima KM, Shimura A, Nakabayashi A, Nagai S, Nakamura T, Aizawa H and Yasuda N (2022) Consideration of Genetic Structure in the Ecologically or Biologically Significant Marine Areas Criteria: A Review of Convention on Biological Diversity Regional Workshops and A Case Study of Coral Reef Conservation Planning. *Front. Mar. Sci.* 9:823009. doi: 10.3389/fmars.2022.823009

<sup>1</sup> Marine Biodiversity and Environmental Assessment Research Center, Research Institute for Global Change, Japan Agency for Marine-Earth Science and Technology (JAMSTEC), Yokosuka, Japan, <sup>2</sup> Marine Geology Research Group, Research Institute of Geology and Geoinformation, National Institute of Advanced Industrial Science and Technology, Tsukuba, Japan, <sup>3</sup> Research Laboratory On Environmentally-Conscious Developments and Technologies [E-Code], National Institute of Advanced Industrial Science and Technology (AIST), Tsukuba, Japan, <sup>4</sup> Biodiversity Division, National Institute for Environmental Studies, Tsukuba, Japan, <sup>5</sup> Japan Wildlife Research Center, Tokyo, Japan, <sup>6</sup> Department of Biology, Kyushu University, Fukuoka, Japan, <sup>7</sup> Faculty of Agriculture, University of Miyazaki, Miyazaki, Japan, <sup>8</sup> Coastal and Inland Fisheries Ecosystems Division, Fisheries Technology Institute, Japan Fisheries Research and Education Agency, Yokohama, Japan, <sup>9</sup> Department of Transdisciplinary Science and Engineering, School of Environment and Society, Tokyo Institute of Technology, Tokyo, Japan, <sup>10</sup> Graduate School of Agricultural and Life Sciences, The University of Tokyo, Tokyo, Japan

In this study we reviewed the use of genetic information in the Ecologically or Biologically Significant Marine Areas (EBSA) of Convention on Biological Diversity (CBD). We also evaluated genetic indicators for each criterion of important marine areas. We proposed five genetic indices, mainly based on microsatellite analysis (e.g., private allele frequency and number of cryptic species), then selected EBSAs in tropical and temperate zones of Japan based on eight coral species as a case study. Finally, we compared the results with the findings from conventional species-based EBSAs. In the EBSAs genetic information was mainly used in the Northern Hemisphere, particularly in the Baltic Sea; it was rarely applied in the Southern Hemisphere and Asian regions. Although typically applied to large organisms, genetic information is used to various organisms, including benthic and bacterial communities. Genetic data are used as indicators of diversity and endemism. Genetic indices were available for all seven EBSA criteria, but only five indices of three criteria were used. Examination of important areas of corals in the temperate zone using these indices showed that the indices without genetic indicators extracted a large number of important areas in the tropics; however, the use of genetic indicators identified important locations, including in temperate zones. Comparison with conventional, mainly species-based non-genetic methods showed less than 50% agreement, although particularly important sites in marine protected areas were identified by both methods. While there is still more work to be done, such as consideration of the number of survey sites or target species, one reason is

that species-based methods tend to evaluate tropical areas higher. Therefore, these genetic indices are useful for examining important regions, particularly in temperate zones; they revealed cryptic lineages, indicating that many unknown marine taxa should be considered in vulnerable marine areas. Some indicators could be extracted with additional effort, such as population size estimation, immigration, or the use of next-generation sequencing, thus guiding future studies. Because limited genetic information was available in the early stages of EBSA selection, there is a need for systematic surveys and evaluations, particularly in the Southern hemisphere, Asian region, and in small organisms.

**Keywords:** marine protected area (MPA), phylogeny, coral, spatial planning, Aichi 2020 target, biogeography, macro ecology

## INTRODUCTION

The seven Ecologically or Biologically Significant Marine Areas (EBSA) criteria were introduced for identification of important areas for biodiversity at high sea under the Convention on Biological Diversity (CBD) (DFO, 2004; CBD Secretariat, 2008; Dunn et al., 2014). In 2010, numerical targets for protected areas were adopted in the CBD-COP10 as the Aichi Biodiversity Targets. Subsequently, discussions of important marine areas based on EBSA and other similar indicators have been underway in the open ocean, as well as the territorial waters and Exclusive Economic Zones of various countries (CBD, 2010; Bax et al., 2016; Asaad et al., 2017; Yamakita et al., 2017). Some of the indicators used for EBSA are based on genetic data. For example, the biodiversity criterion explicitly describes genetic diversity. In addition, the use of field genetic information (e.g., environmental DNA; eDNA) has become popular after the COP10. The application of such genetic methods is not limited to surveys of species distribution; it includes the collection of population genetic information (Ficetola et al., 2008; Tsuji et al., 2020; Miya et al., 2020). Therefore, the importance of managing genetic information for various types of ecosystem monitoring and assessment should be increased (Muller-Karger et al., 2018; Hoban et al., 2020).

Many marine taxa do not have clear correspondence between morphological species and genetic species. Recent genetic analyses of some common species have revealed cryptic species (Parsons, 1996; Bennetts et al., 1999; Krück et al., 2013; DeBiasse and Hellberg, 2015; Tyler et al., 2020). In particular, morphological identification of scleractinian corals (i.e., main constituents of coral reefs) is hampered by the paucity of species-specific morphological features and high morphological plasticity (Muko et al., 2000; Todd, 2008) accompanied by genetic complexes caused by hybridization, as well as incomplete lineage sorting (e.g., reticulate evolution) (Kenyon, 1997; Willis et al., 2006; Fukami, 2008; Richards and Hobbs, 2015). There may be many cryptic coral species in the Japanese temperate region (Fukami, 2008). Thus, it is difficult to identify species with high certainty, either using morphological features or individual-based phylogenetic analysis methods; it is essential to utilize population genetic information to evaluate hidden species boundaries and species diversity (Filatov et al., 2013; Yasuda et al., 2014; Kitano et al., 2015; Nakabayashi et al., 2019; Zawada

et al., 2019). Considering the above complexity and the difficulty of using morphospecies as indicators, accurate estimation of coral biodiversity and important marine areas is difficult without geological genetic information. Therefore, we propose population genetic indicators of major coral species to fit the EBSA criteria; we performed a case study to identify important locations in the North West Pacific around the Japanese Archipelago (Yasuda et al., 2019). In addition, there is a lack of quantitative evaluations using genetic information to select important areas. To assess the utility and representativeness of genetic information as an indicator of important areas, case studies are needed to compare the results of genetic index-based methods and classical species or community-level methods. This would allow better identification of important areas for conservation from the perspective of land/seascapes and biogeography.

Here, we systematically review the use of genetic information in the reports of the EBSA regional workshops under the CBD. We focus on bias according to region, criteria, and organism. We also describe the genetic indices used for EBSA proposed by Yasuda et al. (2019), as well as the correspondence between genetic indices and the EBSA criteria; we perform a spatial comparison of the results. Finally, we compare the proposed genetic EBSA indicators and existing indicators, which are typically based on conventional biological community information.

## METHODS

### Review of Studies Used for the EBSA Criteria, Including Genetic Indices

All 17 EBSA regional workshop reports published on the CBD website as of April 2020 (15 regions including two updates regarding the northeast Atlantic) were investigated (<https://www.cbd.int/ebsa/>). A list of target areas, criteria, and target organisms referring to “genetic\*” was extracted. In particular, when a reference contained “genetic\*,” we examined whether the genetic information was reflected in the text. We also extracted information regarding target ecosystems and organisms to assess potential target biases. To show regional differences concerning the relative number of areas that use genetic information, we conducted statistical tests using the Base and RVAideMemoire packages (v. 0.9-80) in R software. Fisher pairwise multiple



comparison was applied to the comparison of each regional data. For hypothesis testing, we evaluated the difference between Asian regions and other areas, and the difference between the Northern and Southern Hemispheres. We performed Fisher's exact test for this purpose. For the analysis of the regional difference, we limited the data only for the areas approved by CBD and recent candidate (OSPAR/North East Atlantic).

## Potential Indicators and Proposed Important Marine Areas

We reanalyzed population genetics indicators to select EBSA of coral reefs on the Japanese coast (Yasuda et al., 2019). To understand the background of the indicators, we listed and ranked potentially applicable indicators based on expert discussion, then described the reasons for selecting specific indicators.

For the genetic indicators we used the number of unique alleles as criterion 1 (uniqueness or rarity). The cloning rate and the presence of environmental adaptive genes served as criterion 4 (vulnerability, fragility, sensitivity, or slow recovery). The number of cryptic species and the allelic richness constituted criterion 6 (biological diversity).

Specimens were collected in 31 regions from more than 4000 colonies, including 18 regions in temperate areas (**Figure 1**). Among these regions, Tatsukushi in Tosa-shimizu City, Kouchi in western Shikoku Island, and Sekisei Lagoon in Ishigaki City in western Okinawa were selected for restoration area of coral reefs based on the Law for the Promotion of Nature Restoration. Locations at the tip of the Japanese peninsula, on the Pacific side of Japan, have large coral reefs, even in temperate areas.

The genetic values of indicators based on microsatellite analysis were extracted for *Acropora pruinosa* (Brook, 1892), *Acropora solitaryensis* (Veron and Wallace, 1984), *Acropora cf. glauca* (Brook, 1893), *Acropora hyacinthus* complex (Dana, 1846) (Kitano et al., 2020), *Pocillopora damicornis* (Linnaeus, 1758), *Pocillopora acuta* (Lamarck, 1816), *Pocillopora verrucosa* (Ellis and Solander, 1786), and *Heliopora coerulea* (Pallas, 1766) (Published data from Yasuda et al., 2014; Kitano et al., 2015; Nakabayashi et al., 2019; Yasuda et al., 2019; Pipithkul et al., 2021, unpublished raw data also available at <https://doi.org/10.5061/dryad.7pvmcxdv3> and original values of estimated indicators are available on the **Supplementary Table Data Sheet 1**); most of these are dominant taxa, particularly in temperate areas.

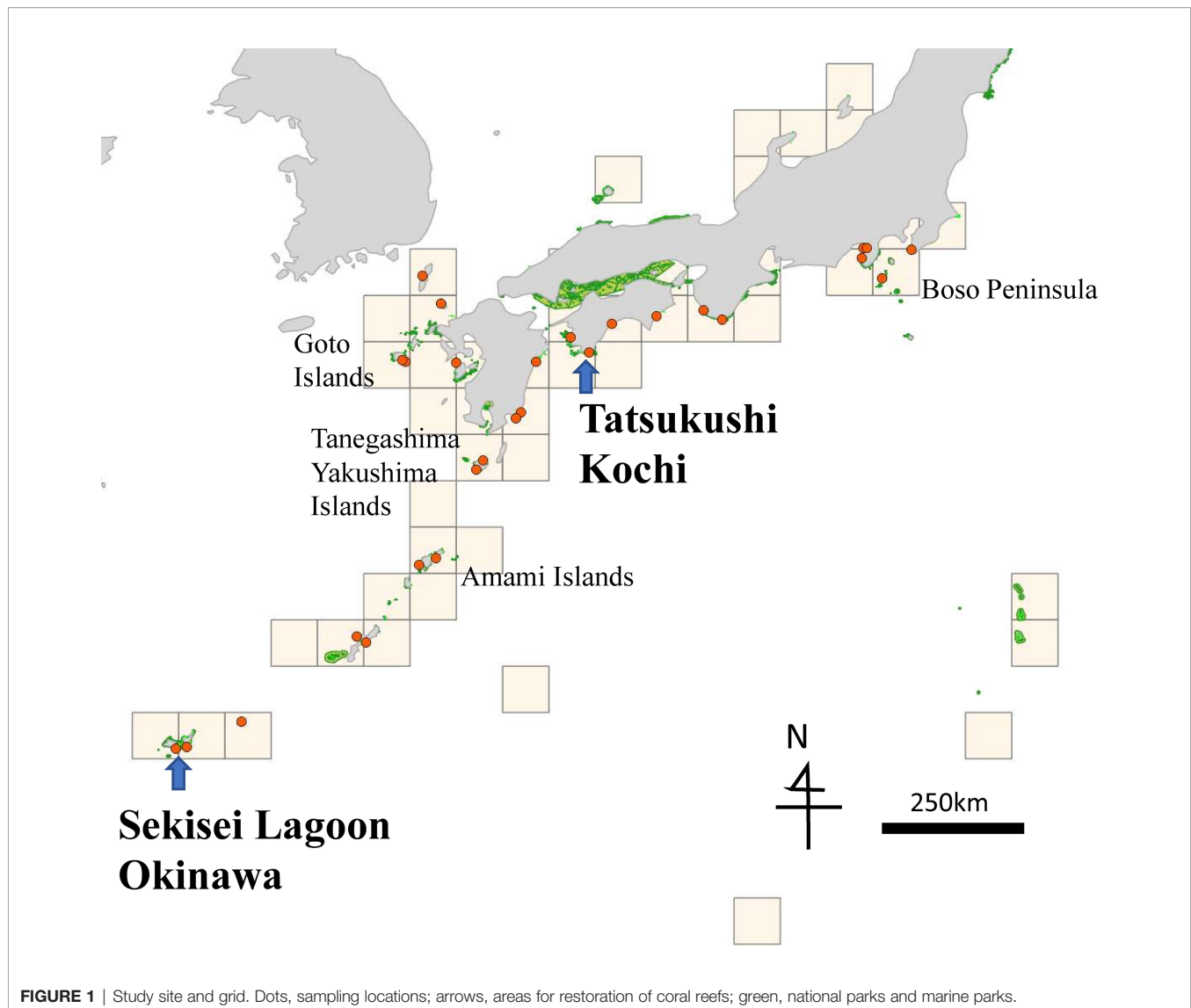
To extract each indicator, we considered the mean number of unique alleles for each (newly identified) subspecies of the above taxa, except *H. coerulea*, which exists in a particularly limited area. We averaged the clone rate of two species with sufficient specimens—*A. hyacinthus* and *A. pruinosa*. We evaluated the presence/absence of allele G at C29226S281 which previously applied for *Acropora* species (Jin et al., 2016) for the species *A. hyacinthus* is the only one species with sufficient genetic information and most widely distributed species not limited to temperate like other species. We counted the number of taxa, including newly identified subspecies (cryptic species). We considered the mean allelic richness, standardized according to

genus. Allelic richness was calculated as the percentage per genet in the sampled regions. We used FSTAT ver. 2.9.3.212 (Goudet, 2002) to calculate allelic richness for each population. This program uses rarefaction to standardize allelic richness to the smallest N in a comparison.

For the indicators which were not used genetic information we used latter variables (details of some indicators are explained in **Supplementary Document Data Sheet 2**). For Criterion 2 (special importance for life history stages of species), we used the center of connectivity networks according to ocean currents (Nakabayashi et al., 2019). For Criterion 3 (importance for threatened, endangered, or declining species and/or habitats), we used the number of endangered coral species habitat using range of each species (Ministry of the Environment Japan, 2009; Sugihara et al., 2015). For Criterion 5 (biological productivity), we used the mean of current coral area (Nature Conservation Bureau Environment Agency and Marine Parks Center of Japan, 1994) and predicted future coral area (Yamakita, 2018). For Criterion 7 (naturalness), we used the length of natural coast (Nature Conservation Bureau Environment Agency and Asia Air Survey Co. Ltd., 1994). To predict future coral area, we applied a model that used the generalized linear method for the areas of corals in an approximately 10-km mesh. As environmental variables, we used the winter sea-surface temperature, chlorophyll a, particulate inorganic carbon, water depth, coastline length, wave height, and tidal range (Kumagai et al., 2022). The predicted area was limited to existing areas of coral reefs and algal beds. The correlation of the model with the current status was 0.64.

EBSA extraction was conducted in two regions of the Japanese Archipelago (**Figure 1**). One region comprised all areas both temperate and tropical zones (areas with tropical zones hereafter); the other region comprised only temperate zones. This is because other studies have shown a biogeographic boundary due to the Kuroshio Current (Kai et al., 2022), and our results also show a boundary of genetic differences between temperate and tropical zones for several coral species. The values of each indicator were ranked as low, middle, or high, in accordance with the EBSA selection process by the calculation described in Yamakita et al. (2015). Although the highly evaluated places met the EBSA criteria, we conducted further prioritization using multiple criteria that have been proposed for systematic EBSA selection (Ardron et al., 2014; Yamakita et al., 2015; Yamakita et al., 2017). Data used for this calculation of was provided as **Supplementary Table Data Sheet 1**.

For prioritization we used the mean of seven criteria, number of highly evaluated criteria (count Max hereafter) among seven criteria, means of three criteria that used genetic variables, and count Max among the three criteria. The result of prioritization was ranked as low, middle, or high. Other prioritization methods such as complementarity analysis using Maxan were not used (Ball and Possingham, 2000) because of the difficulty comparing result of areas with tropical zones and temperate zones only which has different number of no data places by this analysis. The analysis was conducted using 1° grids. For grids with multiple sample sites, the mean value after ranking was used for analysis.



**FIGURE 1** | Study site and grid. Dots, sampling locations; arrows, areas for restoration of coral reefs; green, national parks and marine parks.

We evaluated differences in the proportion of highly evaluated grids between tropical and temperate zones. Fisher's exact test was conducted for each criterion, with Bonferroni correction for multiple comparisons. Next, the sums of the numbers of highly evaluated grids for criteria-based (Criteria 1, 4, and 6) or non-criteria-based (Criteria 2, 3, 5, and 7) genetic indicators were used to compare highly evaluated grids between tropical and temperate zones. We used the exact conditional test of independence, a test for three-way categorical table runs, with the Cochran-Mantel-Haenszel chi-squared test function in R software.

### Comparison of Important Marine Areas According to Genetic and Species Diversity

Important areas selected by genetic indicators were compared with areas selected by conventional assessment based on species (Yamano et al. in preparation and partly published in the latter

reports [Shirayama, 2016; Kitano et al., 2020]; compiled data also available in the appendix). The conventional species-based assessment used the following indices for important corals off the coast of Japan.

Criterion 1 (uniqueness or rarity) was ranked *via* complementarity analysis of endemic species. Criterion 2 (special importance for life history stages of species) was evaluated according to ocean current connectivity using the larvae transport model of Marine Geospatial Ecology Tools (Roberts et al., 2010; Trembl et al., 2012). Criterion 3 (importance for threatened, endangered, or declining species and/or habitats) was based on the number of Red List species in Japan and ranked *via* complementarity analysis ([https://www.env.go.jp/nature/kisho/sango\\_tokusei.html](https://www.env.go.jp/nature/kisho/sango_tokusei.html)). Criterion 4 (vulnerability, fragility, sensitivity or slow recovery) was evaluated using coverage change after bleaching in 1998. Criterion 5 (biological production) was evaluated using coral reef development based on water temperature (18°C, 13°C, and

10°C of the coldest month). For Criterion 6 (biological diversity), the number of species was used. For Criterion 7 (naturalness), the ratio of natural coast was used (Nature Conservation Bureau Environment Agency and Asia Air Survey Co. Ltd., 1994). Although assessment based on species (Shirayama, 2016) considers two methods to integrate seven criteria (i.e., the use of different datasets and the use of distinct thresholds), we considered only the similar method of integration for this analysis (i.e., mean and count Max of seven criteria, and the mean and count Max of the three criteria that used for genetic variables).

To compare the genetic and conventional evaluations, we applied Cohen's kappa statistic, which represents coincidence on a scale of -1 to 1; a value of > 0.6 is considered significant coincidence and a higher value indicates a stronger relationship (Yamakita et al., 2019).

## RESULTS

### Review of Studies Using Genetic Indices in EBSAs

Among the 16 regional reports, genetic information was included in 14 (Table 1). Genetic information was used 40 cases for seven criteria in 347 EBSAs and candidate areas (2%). The percentage was also 2% using five criteria as the denominator, excluding two criteria (Criteria 5 [biological productivity] and 7 [naturalness]) that were not based on genetic information.

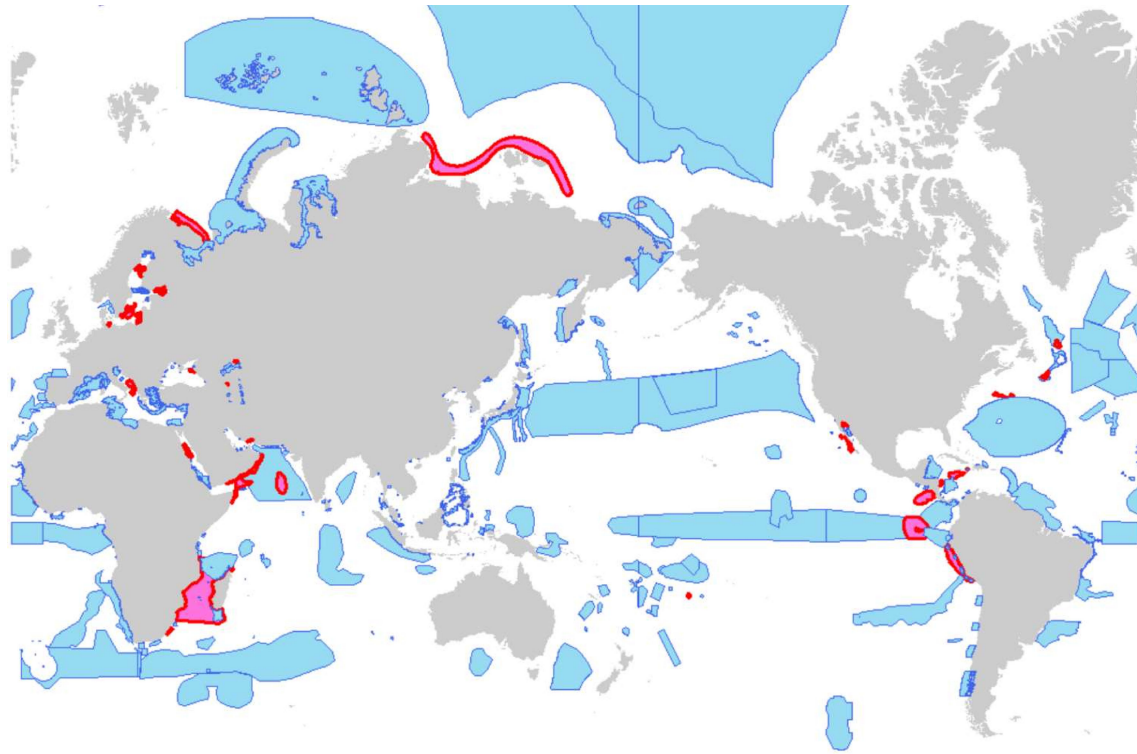
Thirty-five areas had genetic information (10% of 347 EBSAs) (Table 1 and Figure 2). Red shapes indicate areas where genetic indicators were used. Areas with genetic information were in the Baltic Sea, northeast Atlantic, northwest Atlantic (Arctic, Caribbean Sea/western mid-Atlantic), and eastern tropical and temperate Pacific. The differences were significant for Baltic Sea vs. East Asia and Baltic Sea vs. southeastern Atlantic ( $p < 0.05$ ; pairwise comparisons using Fisher's exact test with Hochberg adjustment for multiple comparisons. Note that the 16 regions were regarded as different groups). A significant difference was also detected between the Asia and other regions; Northern and Southern Hemispheres ( $p = 0.01$  and  $p = 0.05$ ; Fisher's exact test).

As target organisms, cetaceans (whales and dolphins) were used most frequently (15 times). Invertebrates (except coral) and fish were used 14 and 12 times, respectively; and general statements about genetic diversity that do not refer to any particular species was tied with birds (9 times). Bacterial communities were used as the target organisms twice, as representatives of hydrothermal and deep habitats. The same study or series of studies by the same authors tended to be cited for a particular region, such as birds in the northeast Atlantic. This is presumably because of insufficient data or because regional workshops are not required to review all genetic research.

Corals were used as target organisms of genetic evaluation seven times including two locations which did not appeared on the CBD approved area. These included three deep sea corals and

TABLE 1 | Regional distribution of genetic parameters.

Regions of workshop	Number of Areas	genetically evaluated criteria	genetically evaluated area	Cr.1:Unique-ness or rarity	Cr.2: Life history/stages of species	Cr.3: Threatened etc. sp. and/or habitats	Cr.4: Vulnerability, slow recovery etc.	Cr.5: Biological productivity	Cr.6: Biological diversity	Cr.7: Naturalness	Others (not in criteria such as in summary and description)	Regions containing Asia	Main targeted hemisphere
APC	11	2	3%	2	18%	1	0	0	0	0	4		N
BALT	9	7	11%	5	56%	3	0	0	0	0	0		N
BSCS	33	3	1%	3	9%	0	1	0	2	0	0		N
EA	34	0	0%	0	0%	0	0	0	0	0	1	Yes	N
ETTP	21	2	1%	2	10%	0	0	0	1	0	4		S
TEMP													
MED	15	1	1%	1	7%	0	1	0	0	0	2		N
NP	20	2	1%	2	10%	0	0	0	2	0	1		N
NEA	17	2	2%	2	12%	0	0	0	0	0	4	Yes	N
NEIO	10	0	0%	0	0%	0	0	0	0	0	0	Yes	N
NWA	7	3	6%	3	43%	2	0	0	0	0	2	Yes	N
NWIO	30	7	3%	5	17%	2	0	0	3	0	0	Yes	N
OS-NEAFC	10	4	6%	4	40%	4	0	0	0	0	1		N
SEA	44	1	0%	1	2%	0	0	0	0	0	0		S
SIO	39	2	1%	2	5%	0	0	0	1	0	6	Yes	S
SP	26	1	1%	1	4%	0	0	0	1	0	3	Yes	S
WC	21	3	2%	2	10%	0	1	0	0	0	4		S
Western Mid-Atlantic													
SUM	347	40	2%	35	10%								



**FIGURE 2** | EBSAs in the CBD repository (added information about OSPAR/North East Atlantic) and distribution of use of genetic information. Red and blue, areas that did and did not, respectively, use genetic information.

two studies that used different criteria in the same areas. The studies demonstrated the distribution of endangered species, genetic isolation, human impact, genetic connectivity, and discontinuity (Le Goff-Vitry and Rogers, 2005; Miller et al., 2008; Magalon et al., 2011; Morrison et al., 2011; Ross et al., 2017).

Genetic evaluation was performed *via* phylogenetic tree construction using mitochondrial 16S DNA and intraspecific analyses of diversity and connectivity that involved microsatellite markers (Le Goff-Vitry and Rogers, 2005; Morrison et al., 2011; Ross et al., 2017). Although most analyses were population-based, two focused on invertebrate communities. No study focused on genetic data for multiple species.

### Case Study of Important Marine Areas: Selection of Indicators

The following genetic indicators are listed in **Table 2**: 1) genetic diversity; 2) genetic structure, determined by simple clustering or structure analysis; 3) inter- and intra-genetic structures of populations; 4) phylogenetic analysis; 5) almost-fixed model of migration; 6) and 7) advanced flexible simulations (e.g., migration and branching); 8) population history; and 9) adaptation, determined by simple detection or using statistics. Use of the zooxanthellae genetic structure was excluded based on data availability and analysis complexity.

Next, we identified indicators that represented the EBSA criteria and indicators that were readily measurable; these were used to assess genetic indicators of EBSA. **Table 3** shows criteria representativeness from one (low) to five (high).

With respect to genetic diversity, the number of private alleles was considered; this potentially represents Criteria 1 and 6. The number of private alleles increases in the presence of genetic structure or local adaptation. Therefore, it was considered an appropriate indicator of diversity or uniqueness.

Allelic richness was also considered as an indicator of Criteria 6 and 4. A higher allelic richness value indicates a larger population and significantly greater population structure. However, when the degree of population structure is high, local diversity may be low despite high overall diversity. Furthermore, harmful alleles may accumulate when the population size decreases.

With respect to genetic structure, genetic structure analysis and identification of hidden lineages was considered. The discovery of hidden species is likely to fall under Criteria 1 and 6. Hidden lineages fell under Criterion 3. The reliability of other analysis methods will be affected by these results because they assume a uniform genetic structure within the local population.

With respect to structure among and within populations, genetic distance ( $F_{st}$ ) was regarded as an indicator of gene flow. By examining the centrality of the network based on the genetic distance, this value indicates Criterion 2 over long periods. In



**TABLE 2 |** Types of genetic indicators and example of methods based on allele or sequence.

Target types	Model types	Method examples allele-based (such as microsatellite)	Sequence (SNP)-based
1) Genetic diversity	Summary Statistics	Number of alleles Heterozygosity(observed, expected) Private alleles	Number of segregating sites Nucleotide diversity in population
	Statistics between populations	Heterozygosity between populations Nei's net-distance(genetic distance)	Private haplotype Nucleotide diversity between populations
2) Genetic structure	Simple clustering (considered as island model) Estimation by almost fixed model (island model based clustering)	STRUCTURE	PCA STRUCTURE
3) Inter- and intra-genetic structures	Estimation by almost fixed model	Fst, Fis, Fit	Fst, Fis, Fit, f3, f4
4) Phylogenetic tree and relationships between populations	Application of molecular evolution model	Phylogenetic tree (sequence information)	Phylogenetic tree
		Haplotype network (sequence information)	Haprotpe network
5) Immigration rate	Estimation using island model (almost fixed model)	Estimate from Fst (variance will be high)	Estimate from Fst (However vatiance will be high)
6) Immigration and branching period	Estimation using more flexible simulation	Several applications, such as IMA2. (Result will be model dependent.)	Several application such as IMA2. (Result will be model dependent.)
7) Immigration and branching and merging	Estimation using more flexible simulation (divergence and admixture)		TreeMix (Massive genome wide data will be needed)
8) Population history	Analysis using neutrality		Testing divergence from neutrality using such as Tajima'sD PSMC, etc.
	Single population based dynamics model (population structure will be absorbed in the difference of population size)		
	Application of user-defined model		ABC, etc.
9) Adaptation	Summary statistics No model needed (many regions needed)	Testing neutrality such as Tajima'sD Individual analysis	Testing neutrality such as Tajima'sD Outlier analysis (such as outlier, genome scan)

addition, the edge of the network contains habitat for endangered species (i.e., Criterion 3). Isolation in the network could be an indicator of Criterion 4 in some instances. Criterion 5 represents the inverse of diversity. A high genetic flow reduces the number of locally specific characteristics but increases overall adaptation in the target area.

Fis, the inbreeding coefficient, was used as an indicator of structure among and within populations. If the inbreeding percentage is high, the target population is likely to have high vulnerability (Criterion 4). A high rate of inbreeding corresponded to Criteria 3 (endangered species), 5, and 6.

With respect to branching relationships between populations or individuals, we did not consider specific indicators for each location. Such analysis involves the visualization of phylogenetic relationships, which are calculated from genetic distances (e.g., Fst). Although the result was used to create clustered zones, it was not a sufficient indicator to show the status of each location. In terms of population differentiation, the numbers of overlapping genetic boundaries between multiple and cryptic species were considered. Because of the plethora of boundaries, we included in the analysis only boundaries between temperate and tropical zones.

The migration rate was calculated by assignment test. Based on the migration rate, the centrality of the network was calculated as an indicator of Criterion 2 (importance in life history). Furthermore, the percentage of self-seeding was regarded as an indicator of biological productivity in the target taxon. The assignment test result is also related to the origin of diversity and the hierarchical structure of differentiation. Therefore, exchange of diversity (overall or local) should be considered when analyzing diversity. Calculation of this index based on Fst results in significant variance and is dependent on the model. Therefore, it is important to specify the target of analysis and establish appropriate assumptions prior to the analysis. Because of these reasons migration rate was not used in our case study.

With respect to population history, clonal structure and effective population size were considered as suitable indicators. Clonal rate was presumed to decrease the value (score) of Criterion 6 (genetic diversity) and increase the score of Criterion 4 (vulnerability). It could also be an indicator of Criterion 5 (productivity) for specific clades such as staghorn corals in a local area. However, most species targeted in this study do not reproduce often. Therefore, regardless of

**TABLE 3** | Considered indicators and representativeness of each criterion.

No. in Table 2	Target	Indicator	Specific method	Representativeness of each criterion (5 is the most suitable)							MS or NGS		
				“+”:actual use “-”:Candidate not used									
				Cr.1	Cr.2	Cr.3	Cr.4	Cr.5	Cr.6	Cr.7			
1)	Genetic diversity	Number of private alleles		5	+	1	1	1	4	1	MS		
1)	Genetic diversity	Allelic richness		1	1	1	4	1	5	+	1	MS	
1)	Population history	Clonal rate		3	2	1	5	+	4	1	1	Depends	
2)	Genetic structure/diversity	Identification of hidden lineages or cryptic species; Genetic structure/clustering		4	1	3	-	2	1	5	+	1	NGS
3)	Inter- and intra-genetic structures of populations	Genetic distance	Pairwise Fst and network analysis	1	5	-	3	2	1	4	1	NGS/MS	
3)	Inter- and intra-genetic structures of populations	Inbreeding coefficient	Fis from heterozygosity (observed, expected)	1	1	3	-	5	3	3	1	MS/NGS	
5)	Immigration rate	Estimated the amount of migration by original population of individual sample	Assinment Test	1	4	1	2	3	4	1	1	MS	
8)	Population history	Demography/Effective population size Ne	PSMC MSMC	1	1	1	4	5	-	4	1	NGS	
9)	Adaptation	Presence of environment adaptive gene		4	1	1	5	+	4	3	1	NGS	

Cr.1, uniqueness or rarity; Cr.2, special importance for life history stages of species; Cr.3, importance for threatened, endangered, or declining species and/or habitats; Cr.4, vulnerability; fragility, sensitivity, or slow recovery; Cr.5, biological productivity; Cr.6, biological diversity; Cr.7, naturalness; MS, microsatellite; NGS, next-generation sequencing.

whether corals are quantitatively increased, productivity does not contribute to their reproduction. Thus, productivity may not be an effective indicator. Some taxa that propagate by fragmentation (e.g., staghorn corals) or a regional colony of large populations may also correspond to Criterion 1 or Criterion 2 in addition to Criterion 5. However, such cases will be specific to species or region. Although fragmentation may increase the clonal rate in corals, sexual reproduction is the main mechanism to maintain their heterozygosity or genetic diversity (Ayre and Hughes, 2004). In addition, the vulnerability of clonal populations to environmental change is situation-dependent (Lasker and Coffroth, 1999).

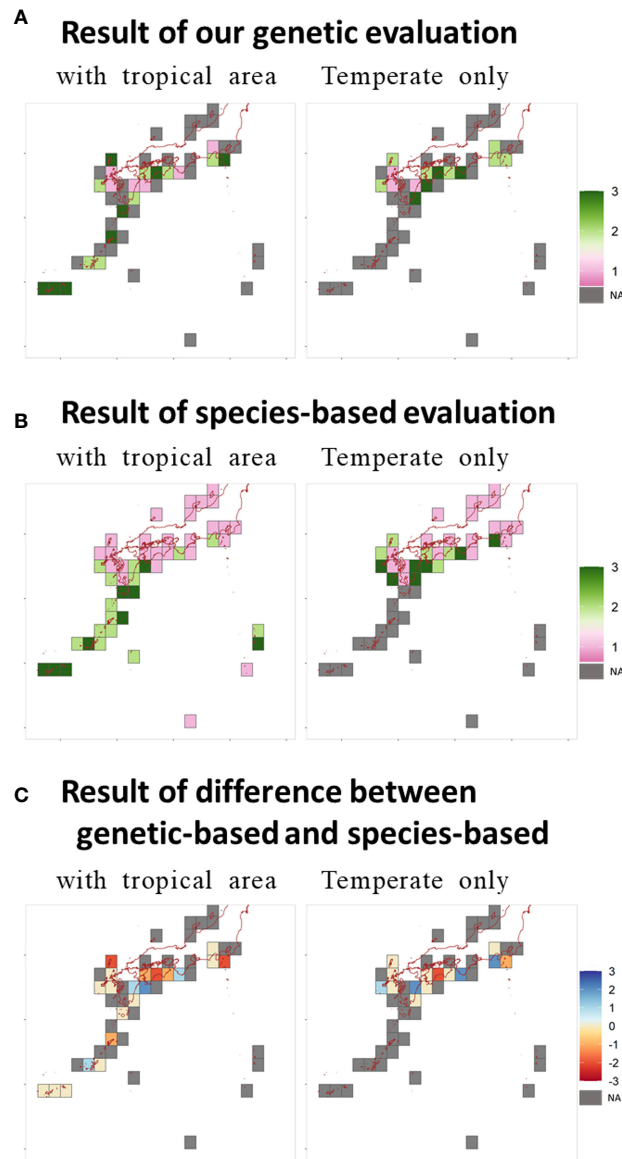
Notably, the effective population size can be estimated based on heterozygosity. Although it is difficult to set the generation time for corals, whole-genome analysis enabled estimation of past population history. Estimated population size can be used as an indicator of Criterion 5. The population history and differentiation size can be used as indicators of Criterion 6. In addition, past changes in the population may enable assessments of vulnerability and susceptibility (Criterion 4). We considered the presence or absence of environment-adaptive genes. We examined stress-tolerance genes (Jin et al., 2016), particularly for high water temperatures, as an indicator of Criterion 4 and uniqueness (Criterion 1). This aspect also might be related to Criterion 5, in terms of adaptation. If different alleles are adaptive in different populations, the diversity (Criterion 6) of the population might also be increased.

We applied five genetic indicators for EBSA Criteria 1, 4, and 6 on the Japanese coast. The number of private alleles was used for Criterion 1. The clonal rate and the presence of environmental adaptive genes were used for Criteria 4. The number of cryptic species and the allelic diversity were used for Criterion 6. We also considered genetic indicators for Criteria 2, 3, and 5; however, we did not use any of these indicators. For Criterion 2, only a weak correlation was observed between

genetic distance and the distance matrix based on ocean currents. In addition, similar geographical distribution were observed between genetic distance and other genetic indices. Therefore, we did not adopt this genetic connectivity indicator; we used a distance matrix based on ocean currents. However, genetic distance was used as a reference to separate areas for analysis (i.e. separation of temperate and tropical was supported by genetic distance). For Criterion 3, we considered allele heterozygosity and the number of cryptic species. However, accuracy was low for allele heterozygosity because of the small sample size; the number of cryptic species was more appropriate as an indicator of biodiversity. For Criterion 5 (productivity), the estimated population according to genetic analysis was not used because availability of data on coral reef area, the inadequate accuracy of heterozygosity-based estimation, and variation in the estimated population, which depends on the model assumptions.

## Case Study of Important Marine Areas: Results

**Figure 3** shows the results of the evaluation of indicators for EBSA criteria. The raw values were ranked high, middle, or low, as instructed in the EBSA protocol (**Figures S-1-3-1A in Supplementary Document Data Sheet 2**). If there were two locations in the same grid, the values were averaged. The tropical zone was highly rated for some indicators. For Criteria 5, 6, and 7, high values were rare in the temperate zone. For Criteria 2 and 4, high values tended to be found in the temperate zone. Comparison of the ratio of highly evaluated grids between the temperate and tropical zones yielded a significant difference for Criterion 5 ( $p < 0.007$ ; significance level after Bonferroni adjustment for multiple comparisons). Furthermore, the numbers of highly evaluated grids significantly differed in the temperate and tropical zones between the genetic (Criteria 1, 4, and 6) and non-genetic (Criteria 2, 3, 5, and 7) criteria ( $p = 0.005$ , exact conditional test of independence in  $2 \times 2 \times 2$  tables).



**FIGURE 3** | Distribution of results for **(A)** integrated result for all criteria, **(B)** integrated result for all criteria for species-based evaluation, and **(C)** difference between genetic and species-based evaluation. NA, not available.

Therefore, the degree of bias in tropical zones differed according to whether criteria were based on genetic information.

Integration of the seven criteria is shown in **Figure 3A**. Areas around the Sekisei Lagoon, Amami Oshima Island, and Yakushima–Tanegashima Island were stably selected in the tropical zone. Upon integration of temperate-zone data alone, Miyazaki and Kochi Prefectures (the southernmost areas affected by the Kuroshio Warm Current) were identified as important. Sekisei Lagoon and Kochi were selected as coral restoration areas (**Figure 1**). Integration of the results of genetic indicators only (**Figures S-1-3-1C**) identified several major discrete coral reef areas from the Boso Peninsula (northern limit of the Pacific Ocean) to the Goto Islands (northwest Kyushu).

## Comparison of Proposed Important Marine Areas Based on Genetic and Species Diversities

**Figure 3B** shows the integrated results for species-based assessment and the difference in the results for species-based and genetic evaluation. Positive values indicate that genetic information was highly valued. Species-based criteria tended to yield a larger number of highly evaluated areas in the tropical zone (**Figures 3B** and **S-1-3-2A**). Comparison of the rates of highly evaluated grids between temperate and tropical zones yielded a significant difference for Criteria 3, 5, 6, and 7 ( $p < 0.007$ ; significance level after Bonferroni adjustment for multiple

comparisons). There was also a significant difference in the number of highly evaluated grids in temperate and tropical zones between criteria that were (Criteria 1, 4, 6) and were not (Criteria 2, 3, 5, and 7) used on genetic indicators for the genetic analysis ( $p < 0.001$ , exact conditional test of independence in  $2 \times 2$  tables).

The results of integrating the seven criteria were compared as the rates of the number of highly evaluated grids identified by both methods (i.e., agreement). For the areas with tropical zone, the rates of agreement were 5/12 and 5/6,  $\kappa = 0.3$  based on the mean (agreement divided by highly evaluated grids by genetic method, the agreement by species based method, and kappa statistic successively); they were 4/6 and 4/8,  $\kappa = 0.4$  based on the count Max (**Figures 3C and S-1-3-2C**). For the temperate zone, the rates of agreement were 3/6 and 3/4,  $\kappa = 0.4$  based on the mean; they were 2/6 and 2/3,  $\kappa = 0.2$  based on the count Max (**Figures 3C and S-1-3-2C**). The agreement of highly evaluated grids was higher for locations evaluated for the areas with tropical zone. However, the kappa value did not indicate high correspondence.

Integration of the three criteria (Criteria 1, 4, 6) using genetic indicators in the areas with tropical zone yielded agreement rates of 3/7 and 3/6,  $\kappa = 0.2$  based on the mean; the rates were 6/13 and 6/10,  $\kappa < 0.1$  based on the count Max (**Figures S-1-3-2D**). For the temperate zone, the rates of agreement were 3/5 and 3/4,  $\kappa = 0.5$  based on the mean, they were 3/7 and 3/5,  $\kappa = 0.3$  based on the count Max.

There were no significant negative or positive relationships between the results of genetic and species-based indicators. This means that there are some differences between methods, and the two are complementary especially in temperate zone. However, important areas such as areas for restoration of coral reefs (Tatsukushi in Kochi and Sekisei Lagoon in Okinawa), were selected in all cases.

## DISCUSSION

### Biases in EBSA Selection and Potential Use of Genetic Variables

Most of the criteria lacked genetic information; few of the areas used such information. The geographical bias of the evaluation toward the Northern Hemisphere and non-Asian regions, and toward larger and/or iconic animals, suggest that research bias is linked to the use of genetic information (Mayer et al., 2007; Webb et al., 2010; Hughes et al., 2021). However, there are cases that consider variety in the types of organisms, suggesting feasibility for the use of such genetic methods in analyses of other organisms and/or ecosystems.

Collection of the species-distribution data used to select EBSAs is facilitated by global databases such as the Ocean Biodiversity Information System (OBIS) and the Global Biodiversity Information Facility (GBIF). In the case of tropical Asia, for which genetic information was lacking, > 49,000 occurrence data were recently updated (Yamakita et al., 2017; Sudo and Nakaoka, 2020; Sudo et al., 2021; Takeuchi et al., 2021).

These contributed increasing-use cases for the analysis of important areas (Beazley et al., 2016; Guijarro et al., 2016; Yamakita et al., 2017; Furushima et al., 2019) and revealed global biodiversity patterns/dynamics (Chaudhary et al., 2016). Several works referred to national/regional spatial planning either directly or indirectly (Gormley et al., 2013; Nature Conservation Bureau Ministry of the Environment Government of Japan, 2014; Shirayama, 2016). Therefore, databases, species distribution data, and species distribution modelling influence the identification of important marine areas, particularly in the context of insufficient data.

For the collection of the genetic data, GenBank and the European Nucleotide Archive were established in 1982; the DNA Data Bank of Japan was established in 1986 (Benson et al., 2013) which is more than 10 years earlier than OBIS and GBIF. Data linked to a geographical location and standardized for a particular marker can be used to identify geographical or temporal differences (e.g., farm crops) (Hijmans and Spooner, 2001; Gratton et al., 2017). Although databases lack useful information regarding marine species that do not use the same marker, the recent increase in the number of readable genes will enable standardization. For example, genome-wide genotyping by MIG-seq (Suyama and Matsuki, 2015) enables the identification of single nucleotide polymorphisms using a universal primer set. Therefore, it can be used to detect cryptic species and other genetic differences as a future perspective (Hoban et al., 2020).

The use of coral DNA is hampered by the lack of variability in mitochondrial DNA (Hellberg, 2007; Shearer and Coffroth, 2008), which is typically used to estimate inter- and intra-species differences (Avice, 2000; Bowen et al., 2014). However, next-generation sequencing enables the assessment of genome-wide genetic variation (Iguchi et al., 2019; Takata et al., 2019). eDNA analysis, which targets mitochondrial DNA, is difficult to apply to corals because of low resolution to identify coral species; nonetheless, trials involving nuclear DNA regions with high resolution are underway (Alexander et al., 2020). eDNA analysis is also capable of detecting adaptive genetic markers, coralline algae that promote coral settlement, and macro algae that compete with corals, thereby enabling the evaluation of coral distribution in terms of interspecies interactions. eDNA analysis also can provide the detailed biodiversity information of bacteria and plankton communities in coral ecosystems, and probably it would be a useful tool to evaluate the healthy and preferable environments for coral propagation.

In addition to the lack of genetic information, the structure of EBSA workshops may lead to bias. The proposed area of each EBSA initially relied on the opinions of a small number of experts. Although the proposal was made after review of potential EBSAs in each geographic unit, there were limited time and information available for the review. This was partly because completion of the EBSA identification work was required soon after the CBD-COP10. The possibility of providing more global data and systematic information was suggested after the first round of the workshop (Ardrón et al., 2014; Bax et al., 2016). Because the aim was to establish protected



areas by negotiation after the identification of scientifically important marine areas, strong evidence, high resolution, and geographically wide genetic and species factors were needed. A flame work for the data accumulation and integrative analysis of such data (especially including genetic data) is needed to elaborate a new strategic plan (CBD Secretariat, 2020; Hoban et al., 2020; Laikre et al., 2020).

## Usefulness of the Proposed Indicators and Perspectives

At least three of seven EBSA criteria can be evaluated using population genetic indicators. Genetic indicators of connectivity, productivity, and naturalness had different feasibilities. Connectivity can be evaluated immediately using pre-existing numerical values. In the future, productivity may be evaluated using genetic measures if an appropriate survey design and analysis of local population structures are employed. Naturalness may not be evaluated using genetic measures. It may need to combine with other measures, such as the use of coral growth rings or human activity itself.

Although it is not essential to evaluate all criteria, nor is it required to use genetic indicators for all criteria, the use of genetic information is expected to increase over time. Genetic data have not been used for indicators of EBSA, other than biodiversity and endemism, partly because of insufficient examples. Each EBSA criterion has an assumed levels of ecological hierarchy; most criteria are considered compatible with community- and species-level indicators (Asaad et al., 2017). However, there were levels in which genetic data contributed to indicators as well as species-level and community-level indicators. In addition, the adaptability of indicators to multiple criteria (Table 3) and the similarity of the criteria suggests that prioritization including weighting of the criteria, or visual representation used in integrated evaluations may be preferable [e.g., ecosystem health or services (Halpern et al., 2013; Yamakita et al., 2020)]. For such representation more amount of systematic sampling will be needed in the future. Recently, the world wide application of eDNA surveys has been considered in future planning for the Asia-Pacific and marine components of The Group on Earth Observations, Biodiversity Observation Network (AP-BON and MBON) (Muller-Karger et al., 2018; Takeuchi et al., 2021). Such efforts have already begun in some places, such as the ANEMONE project in Japan. A much more ideal approach would be to collect specimens directly in many locations. However, water sampling is probably a more easily accessible way to obtain genetic data on dominant corals on a global scale.

The application of genetic indices to the major taxa, including dominant species, allowed the identification of important areas of coral reefs, particularly in the temperate zone. The biogeographic boundary between the Amami Islands of Kagoshima Prefecture and the Tanegashima and Yakushima Islands, which are separated by the Kuroshio Current, has been established (Sato, 1969). Although this boundary is not definitive for marine organisms (Sakai et al., 2009), it was consistent with several genetic boundaries detected in the present study and a previous study (Nakabayashi et al., 2019).

The two types of assessments yielded similar results on a broad spatial scale especially for nature restoration area and

important areas for conservation efforts are identified as well as selection based on species. However, they did not show sufficiently high agreement with the species-based indicators. Therefore, a more detailed study is needed. There is a need to determine whether the proposed indicators adequately reflect the biodiversity of the target taxa. The small number of sites, limitation of used species, and criteria; use of means for integration; and lack of information regarding rare species are the weaknesses of the present study. In addition, some issues remain, such as understanding the regional historical changes in biodiversity (e.g., temporal change and biogeography of species distributions). A notable finding of this study was the selected EBSAs for corals in the temperate zone, which will inform future conservation planning. Integrated assessment of species-based and genetic methods will be complementary and useful for investigations of important marine areas.

In conclusion, genetic surveys have become easier to conduct; species distribution and biodiversity can be assessed. However, the CBD targets did not consider enough for genetic diversity (CBD Secretariat, 2020; Hoban et al., 2020; Laikre et al., 2020). Using the EBSA report of CBD as an example, we quantified the shortfalls in marine biodiversity assessments using genetic information in terms of geographic area, species, and criteria. We also conducted a case study concerning the application of genetic indicators in assessments of important areas using the EBSA criteria and revealed important areas in the temperate zone, particularly for coral reefs. Our findings will enhance assessments based on macro ecological and biogeographic analysis using genetic information.

## DATA AVAILABILITY STATEMENT

The datasets presented in this study can be found in online repositories or **Supplementary Material**. The names of the repository/repositories and accession number(s) can be found in the article/**Supplementary Material**.

## AUTHOR CONTRIBUTIONS

TY, NY, AI, and YK conceived the idea. FS, YK, TY, AN, AS, HA, NY, TN, KT, and SN compiled the data. TY analyzed the compiled data. TY, NY, AI, YK, FS, KT, TN, and SN write and/or commented on the paper. All authors contributed to the article and approved the submitted version.

## FUNDING

We would like to thank the support by the members and/or funding of the Environmental Research and Technology Development Fund (4RF-1501[JPMEERF20154R01], 4-1304, S9, and S15 PANCES [JPMEERF16S11530]) of the Ministry of the Environment; a Grant-in-Aid for Young Scientists (A) (17H04996), JSPS Bilateral Joint

Research (JPJSBP120209929), JSPS KAKENHI Grant Number 20H00653, by Tenure Track Facilitation and Fixing Project of Miyazaki University and support of the Research Laboratory on Environmentally-conscious Developments and Technologies (E-code) at the National Institute of Advanced Industrial Science and Technology (AIST).

## ACKNOWLEDGMENTS

We acknowledge the support of the Research Laboratory on Environmentally-conscious Developments and Technologies (E-

code) at the National Institute of Advanced Industrial Science and Technology (AIST), and the Tenure Track Facilitation and Fixing Project of Miyazaki University. We also would like to thank Hiroya Yamano for providing the information of the part of comparison to conventional way of analysis.

## SUPPLEMENTARY MATERIAL

The Supplementary Material for this article can be found online at: <https://www.frontiersin.org/articles/10.3389/fmars.2022.823009/full#supplementary-material>

## REFERENCES

- Alexander, J. B., Bunce, M., White, N., Wilkinson, S. P., Adam, A. A. S., Berry, T., et al. (2020). Development of a Multi-Assay Approach for Monitoring Coral Diversity Using eDNA Metabarcoding. *Coral Reefs* 39, 159–171. doi: 10.1007/s00338-019-01875-9
- Ardron, J. A., Clark, M. R., Penney, A. J., Hourigan, T. F., Rowden, A. A., Dunstan, P. K., et al. (2014). A Systematic Approach Towards the Identification and Protection of Vulnerable Marine Ecosystems. *Mar. Policy* 49, 146–154. doi: 10.1016/j.marpol.2013.11.017
- Asaad, I., Lundquist, C. J., Erdmann, M. V., and Costello, M. J. (2017). Ecological Criteria to Identify Areas for Biodiversity Conservation. *Biol. Conserv.* 213, 309–316. doi: 10.1016/j.biocon.2016.10.007
- Avise, J. C. (2000). *Phylogeography: The History and Formation of Species*. Cambridge: Harvard University Press. doi: 10.5860/choice.37-5647
- Ayre, D. J., and Hughes, T. P. (2004). Climate Change, Genotypic Diversity and Gene Flow in Reef-Building Corals. *Ecol. Lett.* 7, 273–278. doi: 10.1111/j.1461-0248.2004.00585.x
- Ball, I. R., and Possingham, H. P. (2000). “MARXAN (V1.8.2)”, in *Marine Reserve Design Using Spatially Explicit Annealing, a Manual*. Brisbane: University of Queensland.
- Bax, N. J., Cleary, J., Donnelly, B., Dunn, D. C., Dunstan, P. K., Fuller, M., et al. (2016). Results of Efforts by the Convention on Biological Diversity to Describe Ecologically or Biologically Significant Marine Areas. *Conserv. Biol.* 30, 571–581. doi: 10.1111/cobi.12649
- Beazley, L., Kenchington, E., Murillo, F. J., Lirette, C., Guizarro, J., McMillan, A., et al. (2016). Species Distribution Modelling of Corals and Sponges in the Maritimes Region for Use in the Identification of Significant Benthic Areas. *Canadian Technical Report of Fisheries and Aquatic Sciences* 3172 Nova Scotia: Fisheries and Oceans Canada.
- Bennetts, R. Q., Grady, J. M., Rohde, F. C., and Quattro, J. M. (1999). Discordant Patterns of Morphological and Molecular Change in Broadtail Madtoms (Genus *Noturus*). *Mol. Ecol.* 8, 1563–1569. doi: 10.1046/j.1365-294x.1999.00709.x
- Benson, D. A., Cavanaugh, M., Clark, K., Karsch-Mizrachi, L., Lipman, D. J., Ostell, J., et al. (2013). GenBank. *Nucleic Acids Res.* 41, D36–D42. doi: 10.1093/nar/gks1195
- Bowen, B. W., Shanker, K., Yasuda, N., Maria, M. C., Von Der Heyden, S., Paulay, G., et al. (2014). Phylogeography Unplugged: Comparative Surveys in the Genomic Era. *Bull. Mar. Sci.* 90, 13–46. doi: 10.5343/bms.2013.1007
- CBD (2010). “Strategic Plan for Biodiversity 2011–2020,” in *Montreal: Secretariat of the Convention on Biological Diversity* (Canada: Secretariat of the Convention on Biological Diversity Montreal), 10–11.
- CBD Secretariat (2008). “COP 9 Decision IX/20. Marine and Coastal Biodiversity,” in *Ninth Meet. Conf. Parties to Conv. Biol. Divers.* 19–30 May 2008. 113–124. Available at: <https://www.cbd.int/decisions/cop/?m=cop-09>.
- CBD Secretariat (2020) *Zero Draft of the Post-2020 Global Biodiversity Framework, CBD/Wg2020/2/3*. Available at: <https://www.cbd.int/doc/c/efb0/1f84/a892b98d2982a829962b6371/wg2020-02-03-en.pdf>.
- Chaudhary, C., Saeedi, H., and Costello, M. J. (2016). Bimodality of Latitudinal Gradients in Marine Species Richness. *Trends Ecol. Evol.* 31, 670–676. doi: 10.1016/j.tree.2016.06.001
- DeBiasse, M. B., and Hellberg, M. E. (2015). Discordance Between Morphological and Molecular Species Boundaries Among Caribbean Species of the Reef Sponge *Callyspongia*. *Ecol. Evol.* 5, 663–675. doi: 10.1002/ece3.1381
- DFO (2004). “Identification of Ecologically and Biologically Significant Areas,” in *Can. Sci. Advis. Sec. Ecosystem Status Rep. 2004/006* [Canda: Fisheries and Oceans Canada (DFO)], 15.
- Dunn, D. C., Ardron, J., Bax, N., Bernal, P., Cleary, J., Cresswell, I., et al. (2014). The Convention on Biological Diversity’s Ecologically or Biologically Significant Areas: Origins, Development, and Current Status. *Mar. Policy* 49, 137–145. doi: 10.1016/j.marpol.2013.12.002
- Ficetola, G. F., Miaud, C., Pompanon, F., and Taberlet, P. (2008). Species Detection Using Environmental DNA From Water Samples. *Biol. Lett.* 4, 423–425. doi: 10.1098/rsbl.2008.0118
- Filatov, M. V., Frade, P. R., Bak, R. P. M., Vermeij, M. J. A., and Kaandorp, J. A. (2013). Comparison Between Colony Morphology and Molecular Phylogeny in the Caribbean Scleractinian Coral Genus *Madracis*. *PLoS One* 8, e71287. doi: 10.1371/journal.pone.0071287
- Ellis, J., and Solander, D. (1786). *The Natural History of Many Curious and Uncommon Zoophytes*. London: Benjamin White and Son. 208 pp.
- Fukami, H. (2008). Short Review: Molecular Phylogenetic Analyses of Reef Corals. *Galaxea J. Coral Reef Stud.* 10, 47–55. doi: 10.3755/galaxea.10.47
- Furushima, Y., Yamakita, T., Miwa, T., Lindsay, D., Fukushima, T., and Shirayama, Y. (2019). “New Techniques for Standardization of Environmental Impact Assessment,” in *Environmental Issues of Deep-Sea Mining* (Cham: Springer International Publishing), 275–313. doi: 10.1007/978-3-030-12696-4\_11
- Gormley, K. S. G., Porter, J. S., Bell, M. C., Hull, A. D., and Sanderson, W. G. (2013). Predictive Habitat Modelling as a Tool to Assess the Change in Distribution and Extent of an OSPAR Priority Habitat Under an Increased Ocean Temperature Scenario: Consequences for Marine Protected Area Networks and Management. *PLoS One* 8, e68263. doi: 10.1371/journal.pone.0068263
- Gratton, P., Marta, S., Bocksberger, G., Winter, M., Trucchi, E., and Kühl, H. (2017). A World of Sequences: Can We Use Georeferenced Nucleotide Databases for a Robust Automated Phylogeography? *J. Biogeogr.* 44, 475–486. doi: 10.1111/jbi.12786
- Guizarro, J., Beazley, L., Lirette, C., Kenchington, E., Wareham, V., Gilkinson, K., et al. (2016). Species Distribution Modelling of Corals and Sponges From Research Vessel Survey Data in the Newfoundland and Labrador Region for Use in the Identification of Significant Benthic Areas. *Canadian Technical Report of Fisheries and Aquatic Sciences* 3171, (Nova Scotia: Fisheries and Oceans Canada).
- Halpern, B. S., Longo, C., Hardy, D., McLeod, K. L., Samhour, J. F., Katona, S. K., et al. (2013). An Index to Assess the Health and Benefits of the Global Ocean. *Nature* 488, 615–620. doi: 10.1038/nature11397
- Hellberg, M. E. (2007). Footprints on Water: The Genetic Wake of Dispersal Among Reefs. *Coral Reefs* 26, 463–473. doi: 10.1007/s00338-007-0205-2
- Hijmans, R. J., and Spooner, D. M. (2001). Geographic Distribution of Wild Potato Species. *Am. J. Bot.* 88, 2101–2112. doi: 10.2307/3558435
- Hoban, S., Bruford, M., D’Urban Jackson, J., Lopes-Fernandes, M., Heuertz, M., Hohenlohe, P. A., et al. (2020). Genetic Diversity Targets and Indicators in the

- CBD Post-2020 Global Biodiversity Framework Must be Improved. *Biol. Conserv.* 248, 108654. doi: 10.1016/j.biocon.2020.108654
- Hughes, A. C., Orr, M. C., Ma, K., Costello, M. J., Waller, J., Provoost, P., et al. (2021). Sampling Biases Shape Our View of the Natural World. *Ecography* 4, 1259–1269. doi: 10.1111/ecog.05926
- Iguchi, A., Yoshioka, Y., Forsman, Z. H., Knapp, I. S. S., Toonen, R. J., Hongo, Y., et al. (2019). RADseq Population Genomics Confirms Divergence Across Closely Related Species in Blue Coral (*Heliopora Coerulea*). *BMC Evol. Biol.* 19, 187. doi: 10.1186/s12862-019-1522-0
- Jin, Y. K., Lundgren, P., Lutz, A., Raina, J. B., Howells, E. J., Paley, A. S., et al. (2016). Genetic Markers for Antioxidant Capacity in a Reef-Building Coral. *Sci. Adv.* 2, 1500842. doi: 10.1126/sciadv.1500842
- Kai, Y., Motomura, H., and Matsuura, K. (2022). *Fish Diversity of Japan: Evolution, Zoogeography, and Conservation*. Eds. Y. Kai, H. Motomura and K. Matsuura (Singapore: Springer Singapore). doi: 10.1007/978-981-16-7427-3
- Kenyon, J. C. (1997). Models of Reticulate Evolution in the Coral Genus *Acropora* Based on Chromosome Numbers: Parallels With Plants. *Evol. (N. Y.)* 51, 756–767. doi: 10.2307/2411152
- Kitano, Y. F., Hongo, C., Yara, Y., Sugihara, K., Kumagai, N. H., and Yamano, H. (2020). Data on Coral Species Occurrences in Japan Since 1929. *Ecol. Res.* 35, 975–985. doi: 10.1111/1440-1703.12136
- Kitano, Y. F., Nagai, S., Ueno, M., and Yasuda, N. (2015). Most Pocillopora Damicornis Around Yaeyama Islands are Pocillopora Acuta According to Mitochondrial ORF Sequences. *Galaxea J. Coral Reef Stud.* 17, 21–22. doi: 10.3755/galaxea.17.21
- Krück, N. C., Tibbetts, I. R., Ward, R. D., Johnson, J. W., Loh, W. K. W., and Ovenden, J. R. (2013). Multi-Gene Barcoding to Discriminate Sibling Species Within a Morphologically Difficult Fish Genus (*Sillago*). *Fish. Res.* 143, 39–46. doi: 10.1016/j.fishres.2013.01.007
- Kumagai, J., Wakamatsu, M., Hashimoto, S., Saito, O., Yoshida, T., Yamakita, T., et al. (2022). Natural Capitals for Nature's Contributions to People: The Case of Japan. *Sustain. Sci.* 17, 919–954. doi: 10.1007/s11625-020-00891-x
- Laike, L., Hoban, S., Bruford, M. W., Segelbacher, G., Allendorf, F. W., Gajardo, G., et al. (2020). Post-2020 Goals Overlook Genetic Diversity. *Sci. (80- )* 367, 1083–1085. doi: 10.1126/science.abb2748
- Lasker, H. R., and Coffroth, M. A. (1999). Responses of Clonal Reef Taxa to Environmental Change. *Am. Zool.* 39, 92–103. doi: 10.1093/icb/39.1.92
- Le Goff-Vitry, M. C., and Rogers, A. D. (2005). "Molecular Ecology of *Lophelia pertusa* in the NE Atlantic," in *Cold-Water Corals and Ecosystems* (Berlin: Springer), 653–662. doi: 10.1007/3-540-27673-4\_32
- Magalon, H., Faure, B., Bigot, L., Guillaume, M., and Bruggemann, H. (2011). "Connectivity of the Coral *Pocillopora meandrina* in the Eparses and Réunion Islands," in 7th Western Indian Ocean Marine Science Association Symposium, Oct 2011 Kenya. (Accession No. hal-00852811)
- Mayer, P. M. R., McCutchen, S. K., Canfield, M. D., and Timothy, J. (2007). Meta-Analysis of Nitrogen Removal in Riparian Buffers. *J. Environ. Qual.* 36, 1172. doi: 10.2134/jeq2006.0462
- Miller, M. W., Halley, R. B., and Gleason, A. C. R. (2008). "Reef Geology and Biology of Navassa Island," in *Coral Reefs of the USA* (Dordrecht: Springer), 407–433. doi: 10.1007/978-1-4020-6847-8\_10
- Ministry of the Environment Japan (2009). *Environmental Characteristics of Red List Corals (Species)*, (Tokyo: Ministry of the Environment Japan).
- Miya, M., Gotoh, R. O., and Sado, T. (2020). MiFish Metabarcoding: A High-Throughput Approach for Simultaneous Detection of Multiple Fish Species From Environmental DNA and Other Samples. *Fish. Sci.* 86, 939–970. doi: 10.1007/s12562-020-01461-x
- Morrison, C. L., Ross, S. W., Nizinski, M. S., Brooke, S., Järnegen, J., Waller, R. G., et al. (2011). Genetic Discontinuity Among Regional Populations of *Lophelia pertusa* in the North Atlantic Ocean. *Conserv. Genet.* 12, 713–729. doi: 10.1007/s10592-010-0178-5
- Muko, S., Kawasaki, K., Sakai, K., Takasu, F., and Shigesada, N. (2000). Morphological Plasticity in the Coral *Porites sillimanianii* and its Adaptive Significance. *Bull. Mar. Sci.* 66, 225–239.
- Muller-Karger, F. E., Miloslavich, P., Bax, N. J., Simmons, S., Costello, M. J., Sousa Pinto, I., et al. (2018). Advancing Marine Biological Observations and Data Requirements of the Complementary Essential Ocean Variables (EOVs) and Essential Biodiversity Variables (EBVs) Frameworks. *Front. Mar. Sci.* 5, doi: 10.3389/fmars.2018.00211
- Nakabayashi, A., Yamakita, T., Nakamura, T., Aizawa, H., Kitano, Y. F., Iguchi, A., et al. (2019). The Potential Role of Temperate Japanese Regions as Refugia for the Coral *Acropora hyacinthus* in the Face of Climate Change. *Sci. Rep.* 9, 1892. doi: 10.1038/s41598-018-38333-5
- Nature Conservation Bureau Environment Agency and Asia Air Survey Co. Ltd (1994). *Coastal Survey Report, the 4th National Survey on the Natural Environment*, Tokyo: Environment Agency.
- Nature Conservation Bureau Environment Agency and Marine Parks Center of Japan (1994). *The Report of the Marine Biotic Environment Survey in the 4th National Survey on the Natural Environment (Coral Reefs) Vol. 3* (Tokyo: Environment Agency).
- Nature Conservation Bureau Ministry of the Environment Government of Japan (2014) *Ecologically or Biologically Significant Marine Area (EBSAs) Identified by Japan*. Available at: <http://www.env.go.jp/en/nature/biodic/kaiyo-hozen/kaiiki/index.html>. [Accessed April 10, 2022]
- Parsons, K. E. (1996). Discordant Patterns of Morphological and Genetic Divergence in the "Austrocochlea constricta" (Gastropoda: Trochidae) Species Complex. *Mar. Freshw. Res.* 47, 981–990. doi: 10.1071/MF9960981
- Pipithkul, S., Shizu, S., Shimura, A., Yokochi, H., Nagai, S., Fukami, H., et al. (2021). High Clonality and Geographically Separated Cryptic Lineages in the Threatened Temperate Coral, *Acropora pruinosa*. *Front. Mar. Sci.* doi: 10.3389/fmars.2021.668043
- Richards, Z. T., and Hobbs, J. P. A. (2015). Hybridisation on Coral Reefs and the Conservation of Evolutionary Novelty. *Curr. Zool.* 61, 132–145. doi: 10.1093/czoolo/61.1.132
- Roberts, J. J., Best, B. D., Dunn, D. C., Trembl, E. A., and Halpin, P. N. (2010). Marine Geospatial Ecology Tools: An Integrated Framework for Ecological Geoprocessing With ArcGIS, Python, R, MATLAB, and C++. *Environ. Model. Software* 25, 1197–1207. doi: 10.1016/j.envsoft.2010.03.029
- Ross, R. E., Nimmo-Smith, W. A. M., and Howell, K. L. (2017). Towards 'Ecological Coherence': Assessing Larval Dispersal Within a Network of Existing Marine Protected Areas. *Deep. Res. Part I Oceanogr. Res. Pap.* 126, 128–138. doi: 10.1016/j.dsr.2017.06.004
- Sakai, Y., Kadota, T., Shimizu, N., Tsuboi, M., Yamaguchi, S., Nakaguchi, K., et al. (2009). Fish Fauna on Reefs of Tokara Islands, Southern Japan, Surveyed By Underwater Census During 2002–2007. *J. Grad. Sch. Biosph. Sci. Hiroshima Univ.* 48, 19–35. doi: 10.15027/39872
- Shearer, T. L., and Coffroth, M. A. (2008). Barcoding Corals: Limited by Interspecific Divergence, Not Intraspecific Variation. *Mol. Ecol. Resour.* 8, 247–255. doi: 10.1111/j.1471-8286.2007.01996.x
- Shirayama, Y. (2016) *Project Final Reports: S-9-5 Quantitative Assessment and Future Projection of Biodiversity Loss in Marine Ecosystems*. Available at: [https://www.env.go.jp/policy/kenkyu/suishin/kadai/kadai\\_ichiran/completed\\_projects.html](https://www.env.go.jp/policy/kenkyu/suishin/kadai/kadai_ichiran/completed_projects.html).
- Sudo, K., and Nakaoka, M. (2020). Fine-Scale Distribution of Tropical Seagrass Beds in Southeast Asia. *Ecol. Res.* 35, 994–1000. doi: 10.1111/1440-1703.12137
- Sudo, K., Quiros, T. E. A. L., Prathep, A., Luong, C., Lin, H. J., Bujang, J. S., et al. (2021). Distribution, Temporal Change, and Conservation Status of Tropical Seagrass Beds in Southeast Asia: 2000–2020. *Front. Mar. Sci.* 8, doi: 10.3389/fmars.2021.637722
- Sugihara, K., Nomura, K., Yokochi, H., Shimoike, K., Kajiura, K., Suzuki, G., et al. (2015). *Zooxanthellate Scleractinian Corals of Tanegashima Island, Japan*, (Tsukuba: National Institute for Environmental Studies).
- Suyama, Y., and Matsuki, Y. (2015). MIG-Seq: An Effective PCR-Based Method for Genome-Wide Single-Nucleotide Polymorphism Genotyping Using the Next-Generation Sequencing Platform. *Sci. Rep.* 5, 16963. doi: 10.1038/srep16963
- Takata, K., Taninaka, H., Nonaka, M., Iwase, F., Kikuchi, T., Suyama, Y., et al. (2019). Multiplexed ISSR Genotyping by Sequencing Distinguishes Two Precious Coral Species (Anthozoa: Octocorallia: Coralliidae) That Share a Mitochondrial Haplotype. *PeerJ* 2019, e7769. doi: 10.7717/peerj.7769
- Takeuchi, Y., Muraoka, H., Yamakita, T., Kano, Y., Nagai, S., Bunthang, T., et al. (2021). The Asia-Pacific Biodiversity Observation Network: 10-Year Achievements and New Strategies to 2030. *Ecol. Res.* 36, 232–257. doi: 10.1111/1440-1703.12212
- Todd, P. A. (2008). Morphological Plasticity in Scleractinian Corals. *Biol. Rev.* 83, 315–337. doi: 10.1111/j.1469-185X.2008.00045.x

- Treml, E. A., Roberts, J. J., Chao, Y., Halpin, P. N., Possingham, H. P., and Riginos, C. (2012). "Reproductive Output and Duration of the Pelagic Larval Stage Determine Seascape-Wide Connectivity of Marine Populations," in *Integrative and Comparative Biology* (Oxford: Oxford University Press), 525–537. doi: 10.1093/icb/ics101
- Tsuji, S., Maruyama, A., Miya, M., Ushio, M., Sato, H., Minamoto, T., et al. (2020). Environmental DNA Analysis Shows High Potential as a Tool for Estimating Intraspecific Genetic Diversity in a Wild Fish Population. *Mol. Ecol. Resour.* 20, 1248–1258. doi: 10.1111/1755-0998.13165
- Tyler, J., Bonfitto, M. T., Clucas, G. V., Reddy, S., and Younger, J. L. (2020). Morphometric and Genetic Evidence for Four Species of Gentoo Penguin. *Ecol. Evol.* 10, 13836–13846. doi: 10.1002/ece3.6973
- Veron, J. E. N., and Wallace, C. C. (1984). Scleractinia of Eastern Australia. Part V. Family Acroporidae. *Monogr. Ser. Aust. Inst. Mar. Sci.* 6, 1–422.
- Webb, T. J., vanden Berghe, E., and O'Dor, R. (2010). Biodiversity's Big Wet Secret: The Global Distribution of Marine Biological Records Reveals Chronic Under-Exploration of the Deep Pelagic Ocean. *PloS One* 5, e10223. doi: 10.1371/journal.pone.0010223
- Willis, B. L., Van Oppen, M. J. H., Miller, D. J., Vollmer, S. V., and Ayre, D. J. (2006). The Role of Hybridization in the Evolution of Reef Corals. *Annu. Rev. Ecol. Syst.* 37, 489–517. doi: 10.1146/annurev.ecolsys.37.091305.110136
- Yamakita, T. (2018). Change of the Ocean After the Great East Japan Earthquake: Utilization of Geographic Information System and GIScience. *e-Research Species Biol.* 2, 20181016. Available at: <http://www.speciesbiology.org/eShuseibutsu/evol2/front.html> [Accessed April 10, 2022]
- Yamakita, T., Nakaoka, M., Yamano, H., Nanami, A., Ishikawa, Y., Sudo, K., et al. (2020). *PANCES Policy Brief, No. 3* (Tsukuba: NIES). Available at: <https://www.nies.go.jp/pances/en/policybrief>. [Accessed April 10, 2022]
- Yamakita, T., Sodeyama, F., Whanpetch, N., Watanabe, K., and Nakaoka, M. (2019). Application of Deep Learning Techniques for Determining the Spatial Extent and Classification of Seagrass Beds, Trang, Thailand. *Bot. Mar.* 62, 291–307. doi: 10.1515/bot-2018-0017
- Yamakita, T., Sudo, K., Jintsu-Uchifune, Y., Yamamoto, H., and Shirayama, Y. (2017). Identification of Important Marine Areas Using Ecologically or Biologically Significant Areas (EBSAs) Criteria in the East to Southeast Asia Region and Comparison With Existing Registered Areas for the Purpose of Conservation. *Mar. Policy* 81, 273–284. doi: 10.1016/j.marpol.2017.03.040
- Yamakita, T., Yamamoto, H., Nakaoka, M., Yamano, H., Fujikura, K., Hidaka, K., et al. (2015). Identification of Important Marine Areas Around the Japanese Archipelago: Establishment of a Protocol for Evaluating a Broad Area Using Ecologically and Biologically Significant Areas Selection Criteria. *Mar. Policy* 51, 136–147. doi: 10.1016/j.marpol.2014.07.009
- Yasuda, N., Shimura, A., Nakabayashi, A., Yamakita, T., Nakamura, T., Aizawa, H., et al. (2019). Does Temperate Japanese Region Provide Refugia for Reef-Building Corals in Face of Climate Change? *DNA Polymorph.* 27, 37–42.
- Yasuda, N., Taquet, C., Nagai, S., Fortes, M., Fan, T.-Y., Phongsuwan, N., et al. (2014). Genetic Structure and Cryptic Speciation in the Threatened Reef-Building Coral *Heliopora Coerulea* Along Kuroshio Current. *Bull. Mar. Sci.* 90, 233–255. doi: 10.5343/bms.2012.1105
- Zawada, K. J. A., Dornelas, M., and Madin, J. S. (2019). Quantifying Coral Morphology. *Coral Reefs* 4, 57–71. doi: 10.1101/553453

**Conflict of Interest:** The authors declare that the research was conducted in the absence of any commercial or financial relationships that could be construed as a potential conflict of interest.

**Publisher's Note:** All claims expressed in this article are solely those of the authors and do not necessarily represent those of their affiliated organizations, or those of the publisher, the editors and the reviewers. Any product that may be evaluated in this article, or claim that may be made by its manufacturer, is not guaranteed or endorsed by the publisher.

Copyright © 2022 Yamakita, Sodeyama, Iguchi, Kitano, Teshima, Shimura, Nakabayashi, Nagai, Nakamura, Aizawa and Yasuda. This is an open-access article distributed under the terms of the Creative Commons Attribution License (CC BY). The use, distribution or reproduction in other forums is permitted, provided the original author(s) and the copyright owner(s) are credited and that the original publication in this journal is cited, in accordance with accepted academic practice. No use, distribution or reproduction is permitted which does not comply with these terms.





## OPEN ACCESS

## EDITED BY

Nina Yasuda,  
The University of Tokyo, Japan

## REVIEWED BY

Mohammad Reza Shokri,  
Shahid Beheshti University, Iran  
Naoki Kumagai,  
National Institute for Environmental  
Studies (NIES), Japan

## \*CORRESPONDENCE

Chaolun Allen Chen  
cac@gate.sinica.edu.tw

## SPECIALTY SECTION

This article was submitted to  
Coral Reef Research,  
a section of the journal  
Frontiers in Marine Science

RECEIVED 15 October 2021

ACCEPTED 08 August 2022

PUBLISHED 27 September 2022

## CITATION

Kuo C-Y, Tsai C-H, Huang Y-Y,  
Heng WK, Hsiao A-T, Hsieh HJ and  
Chen CA (2022) Fine intervals are  
required when using point intercept  
transects to assess coral reef status.  
*Front. Mar. Sci.* 9:795512.  
doi: 10.3389/fmars.2022.795512

## COPYRIGHT

© 2022 Kuo, Tsai, Huang, Heng, Hsiao,  
Hsieh and Chen. This is an open-access  
article distributed under the terms of  
the [Creative Commons Attribution  
License \(CC BY\)](#). The use, distribution  
or reproduction in other forums is  
permitted, provided the original  
author(s) and the copyright owner(s)  
are credited and that the original  
publication in this journal is cited, in  
accordance with accepted academic  
practice. No use, distribution or  
reproduction is permitted which does  
not comply with these terms.

# Fine intervals are required when using point intercept transects to assess coral reef status

Chao-Yang Kuo<sup>1</sup>, Cheng-Han Tsai<sup>2</sup>, Ya-Yi Huang<sup>1</sup>,  
Wei Khang Heng<sup>1</sup>, An-Tzi Hsiao<sup>3</sup>, Hernyi Justin Hsieh<sup>4</sup>  
and Chaolun Allen Chen<sup>1,5,6\*</sup>

<sup>1</sup>Biodiversity Research Center, Academia Sinica, Taipei, Taiwan, <sup>2</sup>College of Science and Engineering, James Cook University, Townsville, QLD, Australia, <sup>3</sup>Department of Biological Science and Technology, National Yang Ming Chiao Tung University, Hsinchu, Taiwan, <sup>4</sup>Penghu Marine Biology Research Center, Fisheries Research Institute, Council of Agriculture, Makung, Taiwan, <sup>5</sup>Department of Life Science, National Taiwan Normal University, Taipei, Taiwan, <sup>6</sup>Department of Life Science, Tunghai University, Taichung, Taiwan

The Point Intercept Transect (PIT) method has commonly been used in recent decades for estimating the status of coral reef benthic communities. It is a simple method that is efficiently performed underwater, as benthic components are recorded only as presence or absence at specific interval points along transects. Therefore, PIT is also popular in citizen science activities such as Reef Check programs. Longer intervals are commonly associated with longer transects, yet sampling interval length can significantly influence benthic coverage calculations. Despite this, the relative accuracy of longer or shorter intervals related to transect length has not been tested for PIT. In this study, we tested the optimum intervals of PIT for several commonly used transect lengths using the bootstrap method on empirical data collected on tropical coral reefs and non-reefal coral communities. Our results recommend fine intervals of 10 cm or shorter, depending on the length of the transect, to increase the accuracy of estimating benthic community status on coral reefs. Permanent transects should also be considered in long-term monitoring programs to improve data quality.

## KEYWORDS

benthic community, reef survey methods, LIT, reef check, citizen science, long-term monitoring

# 1 Introduction

Living coral cover, or coral cover, refers to the proportion of reef surface covered by live corals instead of other sessile organisms such as macroalgae or sponges. It represents the biomass of the coral assemblages, which strongly affects the reef fish biomass (Komyakova et al., 2013; Russ et al., 2021). Coral cover, particularly the hard coral cover, is the most widely used indicator in assessing the health of coral reefs (Wilkinson, 2000; Wilkinson, 2002; Wilkinson, 2004; Wilkinson, 2008). In addition, it might also be the only available index for studying the spatial and temporal changes in the status of coral reefs at regional or global scales (Jackson et al., 2014; Souter et al., 2020; Kimura et al., 2022). In the past few decades, about 11% of the world's hard coral cover was lost due to multiple disturbances, from about 32.3% in the late 1970s to 28.8% in 2018 (Souter et al., 2020), which further resulted in the degradation of biodiversity and ecosystem functioning (Tsai et al., 2022; Obura et al., 2022). The changing patterns of coral cover, regardless of stabilization or the ability to recover in response to disturbances, is one of the main indicators for assessing the effectiveness of the coral reef management strategies (Selig and Bruno, 2010; Hargreaves-Allen et al., 2017; Strain et al., 2019). As a result, it is vital to estimate the coral cover accurately.

A variety of methods have been applied to estimate the status of coral reef benthic communities in recent history. Before the introduction of the Line Intercept Transect (LIT) method by Loya and Slobodkin in the early 1970s (Loya and Slobodkin, 1971; Loya, 1972), most coral reef studies were qualitative, recording only presence/absence or relative abundance of flora and fauna (reviewed in Stoddart, 1969; Stoddart, 1972). Quantitative methods further calculate abundances in percentages of operational taxonomic units (OTUs). Several quantitative methods have been developed and can be divided into three categories. The first are plotless methods that measure OTUs along transects directly, including the LIT (Loya and Slobodkin, 1971; Loya, 1972), Chain Intercept Transect method (Porter, 1972; Hughes and Jackson, 1985; English et al., 1997; Hill and Wilkinson, 2004), and Point Intercept Transect (PIT) method (Dodge et al., 1982; Segal and Castro, 2001; Hill and Wilkinson, 2004). The latter is also called the Line-Point Transect method (Ohlhorst et al., 1988; Nadon and Stirling, 2006). The second group consists of plot or quadrat methods that calculate the abundance of OTUs within each quadrat. Quadrats can be permanently (Hughes, 1996) or randomly placed (Hill and Wilkinson, 2004) on reefs. Operational taxonomic unit (OTU) percentages can be measured manually with the Coral Point Count with Excel extensions (CPCe) software (Kohler and Gill, 2006), or semi-automatically with artificial intelligence techniques such as CoralNet (Beijbom et al., 2015). The latter was recently developed using structure-from-motion and photogrammetry to create 3D images for measuring

the complexity of reefs (Burns et al., 2015; Bryson et al., 2017; Pizarro et al., 2017). However, 3D images cannot be used to measure OTU percentages yet.

The LIT method adapted from plant community studies (Kershaw, 1957) was specifically designed to obtain high resolutions of benthic community structures such as those in the coral reefs (Loya and Slobodkin, 1971; Loya, 1972). This method records transition points on the transect (to the nearest cm) where OTUs change. The number of points per OTU section represents the size of a benthic colony or organism, such as a colony of coral or a sponge. The percentage cover of each OTU on a transect is calculated as the total number of points of each OTU counted divided by the total number of points along the transect. Compared to quadrat methods, the LIT method is not only more applicable and efficient underwater but also more comparable across different reef habitats or studies (reviewed in Loya, 1978). It has been recommended by the Global Coral Reef Monitoring Network (GCRMN) as the standard method for management level monitoring (Hill and Wilkinson, 2004). However, the LIT method has been challenged for its long sampling time underwater (Dodge et al., 1982; Segal and Castro, 2001; Hill and Wilkinson, 2004). In average, it takes 20 to 35 minutes, or even more, depending on the level of identification, to survey a 20 m transect with the LIT method (Ohlhorst et al., 1988; Facon et al., 2016).

The PIT method has been recommended as an alternative transect survey method for simplifying the survey effort and improving underwater working efficiency (Dodge et al., 1982; Segal and Castro, 2001; Hill and Wilkinson, 2004). It records OTUs at points either below or next to the transect at specific intervals, such as the 50 cm interval used by the Tropical Program of Reef Check (Hodgson, 1999; Hodgson et al., 2006). The percentage of each OTU on a PIT transect is calculated as the number of points per OTU divided by the total number of sampling points. In other words, the PIT method is equivalent to the LIT method whenever the point interval is one cm. Cutting down the number of sampling points reduces the ability to detect rare species. Moreover, it cannot measure the size of coral colonies, which is a valuable indicator for representing the status of coral reefs (Hill and Wilkinson, 2004). However, it reduces the time required for surveying a transect (Dodge et al., 1982; Ohlhorst et al., 1988; Facon et al., 2016). For instance, the time required for surveying a 10 m transect with the species-level resolution of corals decreases significantly from 30 minutes with the LIT method to four minutes with the PIT method with 50 cm interval (Dodge et al., 1982). Because using the PIT method increases the ability to survey larger areas using either longer or more transects, which minimizes the problems associated with habitat heterogeneity (Dodge et al., 1982), the PIT method has been widely used for estimating the status of coral reefs.

Point intervals can significantly influence the accuracy of the PIT method, and wider intervals tend to be associated with longer

transects. Common combinations are 10, 25, and 50 cm intervals associated with 10 m (Beenaerts and Berghe, 2005; Harris and Sheppard, 2008; Francini-Filho et al., 2013), 25 m (Adjeroud et al., 2002; Adjeroud et al., 2009), and 50 m transects (Wilson and Green, 2009; Pratchett et al., 2011; Graham et al., 2014), respectively (Supplementary Table 1). One exception is the 50 cm interval associated with the 20 m transects used by the Reef Check's Tropical Program (Hodgson, 1999; Hodgson et al., 2006). However, the accuracy of intervals associated with transect lengths has not been tested properly before now.

To date, only two studies have compared the accuracy of different intervals on the PIT method, and they recommended intervals of 4 cm and 25 cm (Segal and Castro, 2001; Facon et al., 2016). Their difference might be due to variation in reef type. Both studies were restricted to limited types of reefs, such as the less developed reef in the Abrolhos Archipelago, Brazil (Segal and Castro, 2001), and the Indian Ocean Reefs of Réunion Island (Facon et al., 2016), respectively. No study has tested the optimal interval of the PIT method across a variety of reef types.

In this study, we tested for the optimal interval of the PIT method and the correlation between interval and transect length on various types of coral assemblages, including well developed tropical coral reefs and less developed non-reefal coral assemblages in Taiwan. There were three main goals for this study, which were to use a simulated bootstrap method to (1) suggest the optimum sampling interval of the PIT method by determining (a) the standard deviation (SD) of the total coral cover (TCC), including hard and soft coral, estimated by the PIT method using a variety of intervals to generate accumulation curves and (b) the dissimilarity between community composition indices generated by PIT and LIT methods using commonly employed intervals, (2) test whether optimizing sampling intervals are transect length-dependent, and (3) use empirical data to compare the accuracy of the TCC estimated *via* the PIT method.

## 2 Materials and methods

### 2.1 Study sites

This study was carried out at six sites on four reefs across Taiwan's tropical and subtropical regions. The two tropical reefs

are in the south (Tiaoshi, TS) and the southeast (Kihaw, KH) of Taiwan Island, while the two subtropical non-reefal coral communities are in Penghu Archipelago (Chinwan Inner Bay, CIB) in the Taiwan Strait and the north of Taiwan Island (Yehliu, YL) (Table 1 and Figure 1). The six sites included two depths in Yehliu (3 m and 6 m) and Tiaoshi (5 m and 10 m), but only one depth each in Kihaw (3 m) and Chinwan Inner Bay (3 m) because there are no suitable reef communities at deeper than 5 m in the two sites.

### 2.2 Field survey methods

Three transects were placed consecutively, a few meters apart from each other, along depth contours parallel to the shoreline at each site. Alternatively, three transects were deployed in parallel for short reefs. The standard transect length used in this study was 15 m due to underwater topographic limitations and the availability of suitable habitats for corals—continuous hard substrates. However, one transect at the shallow site (5m) of Tiaoshi was 14 m long because of operator error. A total of 18 transects ( $j = 18$ ) at six sites were surveyed for this study between April and July in 2019.

We adopted the concept of the Chain Intercept Transect method to lay out transects according to reef contouring (Porter, 1972; Hughes and Jackson, 1985; English et al., 1997; Hill and Wilkinson, 2004). The benthic community of each transect was recorded by survey divers using Olympus TG-4 camera with a waterproof housing and a video light fixed at the height of ca. 20 cm above substrates. Recording speed was maintained at two meters per minute to ensure a stable and clear visualization of substrates and transect line scales. To minimize the observer bias and to ensure quality and consistency, the identification of the benthic community was conducted by the same most experienced researcher.

### 2.3 Benthic community identification and data processing

We identified hard corals (HC), including the scleractinians, *Heliopora* and *Millepora*, to species level. The rest of the benthos

TABLE 1 The community type, depth and the GPS coordinates of the six survey sites on four reefs.

Community type	Reef	Depth (m)	Latitude	Longitude
Non-reefal coral community	Yehliu	Shallow (3)	25.203963°	121.681284°
Non-reefal coral community	Yehliu	Deep (6)	25.204023°	121.681217°
Non-reefal coral community	Chinwan Inner Bay	Shallow (5)	23.529575°	119.560073°
Tropical coral reef	Kihaw	Shallow (3)	23.116620°	121.397059°
Tropical coral reef	Tiaoshi	Shallow (5)	21.952802°	120.769397°
Tropical coral reef	Tiaoshi	Deep (10)	21.949711°	120.770459°

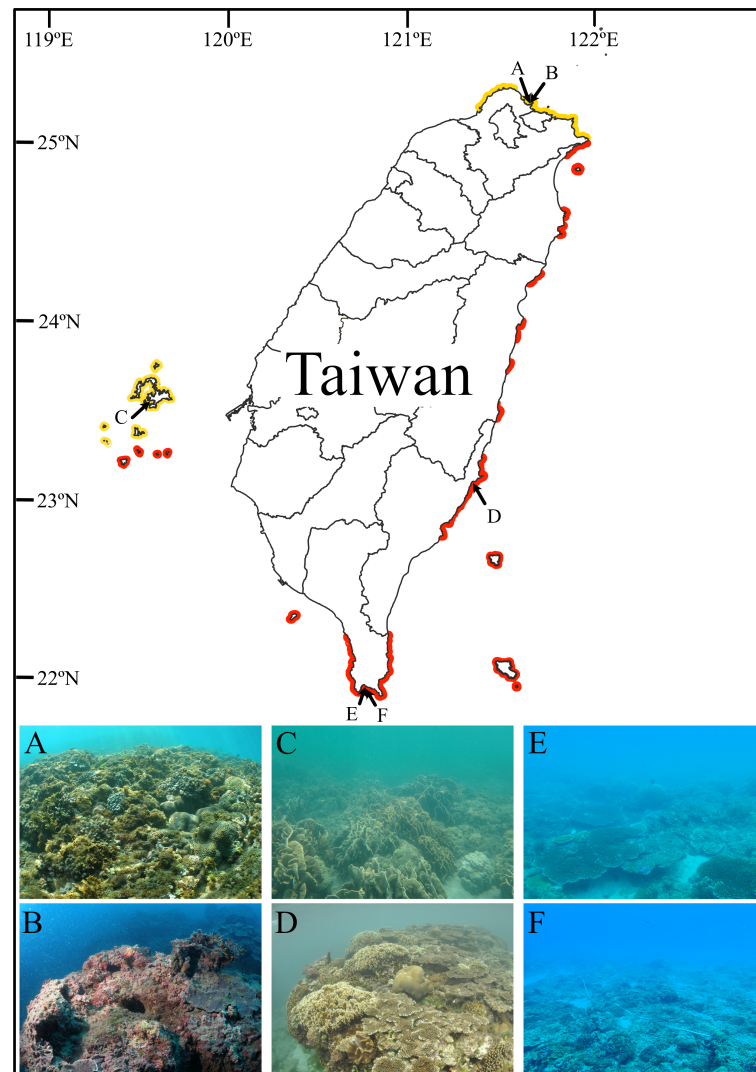


FIGURE 1

Locations of the six survey sites at four reefs in Taiwan. The six sites include the shallow (A) and deep sites (B) in Yehliu, the shallow sites in Chinwan Inner Bay (C) and Kihaw (D), and the shallow (E) and deep sites (F) in Tiaoshi. The red and yellow lines indicate the distribution range of tropical coral reefs (in red) and non-reefal coral communities (in yellow) in Taiwan. The distribution map was modified from Dai (2018); Keshavmurthy et al. (2019), and Kuo et al. (2022a).

and substrates were identified as soft coral (SC), recently killed coral (RKC), nutrient indicator algae (NIA), turf algae (TF), crustose coralline algae (CCA), sponge (SP), rock (RC), rubble (RB), sand (SD), silt/clay (SI), and other substrates (OT). The data is available at <https://doi.org/10.5061/dryad.0rxwdb35>.

The quantification of each category on each transect was first calculated using the LIT method. Briefly, the substrate type at each sampling point with one cm interval was assigned to one of the twelve categories. The percentage cover of each category on each transect was calculated by dividing the cumulative lengths of the category by the total length of the transect (1400 cm or 1500 cm). To further evaluate the compositions of hard and soft

corals along each transect, colony number, average colony size, and species richness of both were calculated. Species evenness and diversity of hard corals were determined by Pielou evenness ( $J$ ) and Shannon-Wiener index ( $H'$ ), respectively. Herein, we term “LIT datasets” and “LIT communities” to represent the data and communities obtained by the LIT method. LIT datasets and LIT communities were used as baselines for comparison with the PIT method.

To reduce the variability caused by observers or transect placement when comparing the two sampling methods, we did not lay out transects explicitly for the PIT method in the field. Instead, the datasets of the PIT method were extracted from our



empirical LIT datasets. The datasets and communities generated using the PIT method are herein referred to as “PIT datasets” and “PIT communities.”

## 2.4 Data analysis

### 2.4.1 The optimum sampling interval for the Point Intercept Transect method

The optimum sampling interval for the PIT method is defined as the minimum number of random sampling points required to generate a PIT community comparable to the coral cover estimated by the LIT method of the same transect. All else being equal, if the number of sampling points used is less than the minimum required, the coral cover among PIT communities generated from the same number of random sampling points results in considerable variation, which implies an unreliable estimate of coral cover. In contrast, an excessive number of sampling points (overly more than the minimum number of sampling points required) may not substantially improve the accuracy of coral cover estimates and thus be a waste of sampling effort, as described in Bros and Cowell (1987).

We first used the bootstrap method (Efron, 1979; Manly, 1992) with Monte Carlo approach to resample PIT communities from LIT datasets. The bootstrap approach is one of the resampling techniques which has been applied in a wide range

of ecological research, from individual species to community-level (summarized by Manly, 2007). One of its applications is to evaluate the sampling sufficiency for sampling design by calculating the confidence interval of the data generated from the limited empirical data (Bros and Cowell, 1987; Manly, 1992; Pillar, 1998). In this study, this produced surrogate samples which serve as proxies for PIT samples that were obtained empirically. The resampling procedure is described as follows (Figure 2):

- (i)  $x$  sampling point was selected without replacement from one of the 18 LIT datasets to form a PIT community. For instance, one sampling point ( $x = 1$ ) was randomly selected from transect  $j_1$  to form a PIT community with one sampling point. Then the selected sampling point(s) was restored to the original LIT dataset before the next resampling. This process was repeated for additional 199 times to form a total of 200 PIT communities ( $n = 200$ ) with one sampling point ( $x = 1$ );
- (ii) calculate the percentage cover of each benthic category for each of the  $n$  PIT communities;
- (iii) repeat procedures (i) and (ii) by selecting  $x$  sampling points to calculate the SD of the TCC of each set of  $n$  PIT communities with the same number of  $x$  points.  $x$  is equal to 2, 3, 4, ...,  $i-2$ ,  $i-1$ , and  $i$ . In total,  $i \times n$  PIT communities were generated.  $i$  is the number of all

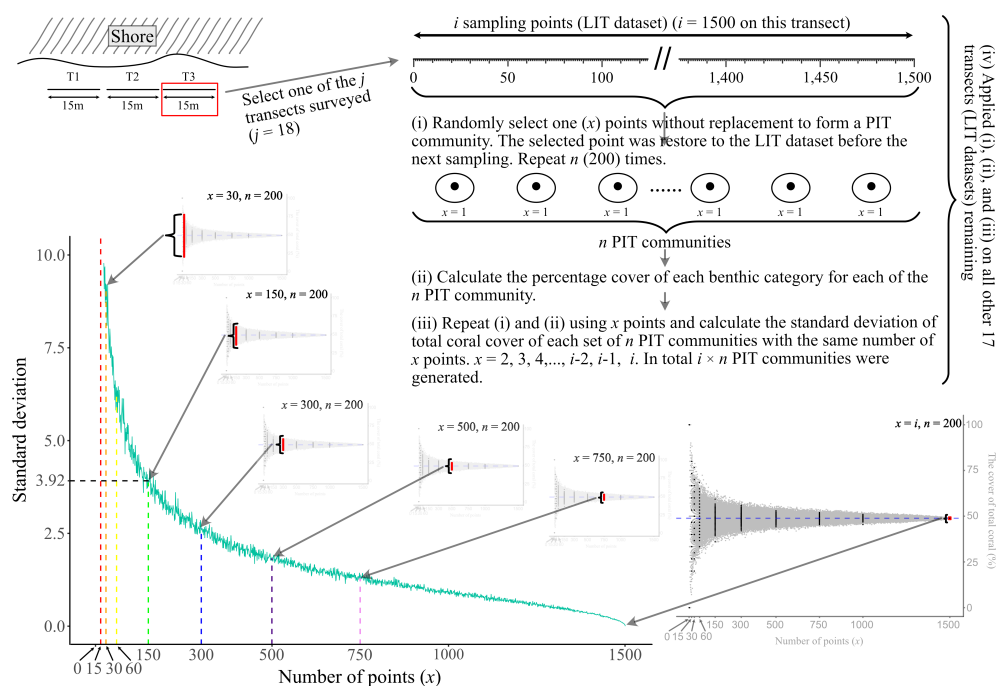


FIGURE 2

The visual guide of the resampling procedure using the bootstrap method with Monte Carlo approach. LIT and PIT are the abbreviation of Line Intercept Transect and Point Intercept Transect.

sampling points of a given transect ( $i = 1,400$  and  $1,500$  for  $14\text{ m}$  and  $15\text{ m}$  transect, respectively). When  $x = i$ , the PIT benthic community composition is equal to the LIT benthic community along the same transect, and

- (iv) apply procedures (i), (ii), and (iii) on all the remaining  $17$  LIT datasets. There were  $i \times n \times j$  PIT communities generated.

Second, scatter plots were used to illustrate the TCC, of the PIT community generated by different sampling points at each LIT transect (Bros and Cowell, 1987). Accumulation curves were used to illustrate the relationship between the number of sampling points and the accuracy, in which the latter was represented by the SD of the TCC of the  $200$  PIT communities with the same number of sampling points ( $x$ ) on each transect (Figure 2). Two hundred times of bootstrap sampling is sufficient as the accumulation curves of  $200$ ,  $500$ , and  $1000$  times of bootstrap sampling were similar (Supplementary Figure 1). Lower SD indicates that the TCC of PIT communities is closer to that of LIT communities, which implies a lesser difference between the two methods. However, as the accumulation curve was fairly smooth without an explicit elbow point, we used the SD of  $3.92$  (95% confidence limit) as a reference criteria to obtain the optimum sampling interval (minimum number of sampling points required) of PIT (Bros and Cowell, 1987). Based on the criteria, the range of the number of sampling points with  $\text{SD} < 3.92$  would fall within the range of accuracy (i.e., the TCC of the PIT method is within the 95% confidence interval of the TCC of the LIT method on the same transect). Those number of points, which are evenly distributed on a transect, would be determined as the optimum sampling interval for the PIT method. In addition, to examine if the optimum sampling interval is influenced by the types of coral community, we compared the optimum sampling intervals for the PIT method between tropical coral reefs and non-reefal coral communities using Mann-Whitney U tests.

Third, other than estimating the optimal sampling interval at the population level using TCC as the index, we also want to estimate it at the community level, considering other sessile organisms such as turf algae, macroalgae, and sponges compete for limited space with corals. For this statistic, we merged the  $12$  categories identified into the ten categories of Reef Check's Tropical Program protocol (Hodgson et al., 2006). We then used multivariable indices (i.e., dissimilarity matrix indices) to estimate the optimum sampling interval at the community level. The compositions of the benthic community generated by the PIT method using the optimum sampling interval should be similar to those by LIT. The Bray-Curtis dissimilarity index (Bray and Curtis, 1957) of individual community composition between each PIT community and LIT community of the same transect was first calculated. Accumulation curves were then used to determine the relationship between the sampling

intervals and the average Bray-Curtis dissimilarity index for each of the  $200$  PIT communities with the same number of random points. This summary statistic used six different numbers of random sampling points ( $15$ ,  $30$ ,  $60$ ,  $150$ ,  $300$ , and  $750$ ) evenly distributed on a  $15\text{ m}$  transect instead of continuous increments. These six numbers of random sampling points were selected to represent the several commonly used sampling intervals in the coral reef benthic survey; i.e.,  $50\text{ cm}$  ( $30$  random points),  $25\text{ cm}$  ( $60$  random points), and  $10\text{ cm}$  ( $150$  random points), with additional very-fine scales –  $2\text{ cm}$  ( $750$  random points) and  $5\text{ cm}$  ( $300$  random points), and very-large-scale –  $100\text{ cm}$  ( $15$  random points), to explore the accuracy across a wide range of intervals. Intervals are cited herein as PIT  $100$ , PIT  $50$ , PIT  $25$ , PIT  $10$ , PIT  $5$ , and PIT  $2$ . The resampling procedure and statistical analyses were performed in R v.  $4.0.3$  (R Core Team, 2020) using the “vegan” package (Oksanen et al., 2020). The R codes of the resampling procedure are provided in the **Supplementary Material**.

## 2.4.2 Testing the dependency between optimum sampling interval and transect length

The procedure to test if the optimum sampling interval depends on transect length is described as follows (Supplementary Figure 2):

- (v) the three transects laid out at each site were attached end-to-end to form a  $45\text{-m}$  (except for one  $44\text{ m}$ ) long virtual transect. The three transects were combined from the same site to reduce the random site effect. A total of six long virtual transects were constructed for the six surveyed sites;
- (vi) five repeated,  $k$  meters long each, subset transects were randomly extracted from each of the six  $45\text{ m}$  virtual transects. A subset transect was formed by selecting continuous sampling points with  $1\text{ cm}$  interval from a random starting point. Continuous sampling, instead of interval sampling, was used to maintain the spatial structure of the benthic community. For instance, a  $10\text{ m}$  subset transect was extracted by randomly selecting  $1000$  continuous sampling points along the  $45\text{ m}$  virtual transect with  $4500$  sampling points. A total of  $30$  subset transects were generated (five transects from each site). Each subset transect served as the LIT dataset with  $i$  sampling points ( $i = 100k$ );
- (vii) apply procedures (i), (ii), and (iii) on the thirty  $k$ -meters subset transects generated from the procedure (vi) to calculate the percentage cover of each benthic category of each of the  $n$  PIT communities; and
- (viii) repeat procedures (vi) and (vii) with  $k = 10, 20, 30$ , and  $40$ , respectively.

The two analyses that applied to the  $15\text{-m}$  transects described earlier, including (1) accumulation curves of the SD

of the TCC of each of the 200 PIT communities generated from the same number of random points on each transect and (2) accumulation curves of the six intervals of interest (PIT 2, PIT 5, PIT 10, PIT 25, PIT 50 and PIT 100) and the average Bray-Curtis dissimilarity index of each set of 200 PIT communities with the same number of random points, were used to determine the optimum sampling intervals for the transect lengths of interest. The actual numbers of random sampling points used for each transect length are provided in [Supplementary Table 2](#). The R codes for attaching transects end-to-end and the resampling procedure is provided in the [Supplementary Material](#).

### 2.4.3 The accuracy of total coral cover estimated by the Point Intercept Transect method compared to the Line Intercept Transect method

To evaluate the performance of each potential optimum interval, we tested those intervals on the empirical dataset. The TCC was calculated from each of the 18 LIT datasets using the PIT method with 100, 50, 25, 10, 5, and 2 cm sampling intervals. Root mean square error (RMSE) was computed and defined as the deviation from the TCC estimated from 18 PIT communities with the same interval to the perfect fit line (i.e., a 1:1 relationship between observed and predicted values). The elbow of the plotted RMSE curve was identified as the minimum interval required.

## 3 Results

### 3.1 Benthic community composition on empirical transects

The total coral (hard and soft), rock, and nutrient indicator algae were the top three major benthic components of the 18 LIT communities surveyed. The average coverages ( $\pm$  SD) were  $35.69 \pm 3.62\%$ ,  $27.17 \pm 4.13\%$ , and  $21.01 \pm 6.02\%$ , respectively ([Figure 3](#) and [Supplementary Table 3](#)). The average coverages of sand and silt/clay were  $7.40 \pm 2.55\%$  and  $4.80 \pm 2.31\%$ , respectively, while the rest components, including recently killed corals, sponges, rubbles, and others, covered less than 5% of the substrates ([Supplementary Table 3](#)).

The TCC on each transect ranged between 7.06% and 68.76% ([Figures 3C, J](#) and [Supplementary Table 3](#)). The average colony number, colony size, species richness, and Pielou evenness (*J*) per transect were  $37.53 \pm 3.38$  colonies,  $14.36 \pm 0.66$  cm,  $15.00 \pm 1.67$  species, and  $0.30 \pm 0.02$ , respectively ([Supplementary Table 3](#)). The highest TCC, the first transect in Kihaw, was contributed by 63 colonies (18 species) with an average colony size and evenness of 16.38 cm and 0.28, respectively ([Supplementary Table 3](#)). In contrast, the third transect at the shallow site in Yehliu featured the lowest TCC, species richness (5 species), and coral colony abundance (7 colonies); however, coral colonies here in average are

larger (15.14 cm) and species evenness is high (0.42) ([Supplementary Table 3](#)). The coral assemblage on the second transect at the Tiaoshi deep site (TCC = 16.99%) was featured with the largest (19.62 cm) average colony size, contributed by 13 colonies (11 species) ([Supplementary Table 3](#)). The smallest (9.24 cm) average colony size was recorded on another transect (the first) of the same site. In addition, the similar TCC (17.85%) was contributed by 29 colonies (19 species), which is two-fold more than that of the previous transect ([Supplementary Table 3](#)).

### 3.2 The optimum sampling interval for the Point Intercept Transect method

The TCC of each PIT community formed a horizontal, bell-shaped distribution, with peak values corresponding to the TCC of their related LIT community ([Figure 3](#)). The distribution was most symmetrical when the TCC of the LIT community was around 50% (e.g., [Figure 3M](#)). It was positively skewed when TCC was higher than 50% (e.g., [Figure 3J](#)) and was negatively skewed, when TCC was lower than 50% (e.g., [Figure 3C](#)). The TCC of PIT communities varied, ranging from 0% to 100% when low numbers of random sampling points were selected. With an increase in the number of random sampling points, the TCC of the PIT community started to converge significantly toward the same level as the TCC of the LIT community on the same transect ([Figure 3](#)).

The SD of the TCC for each set of the 200 PIT communities with different random sampling points decreased rapidly with the increasing number of random sampling points ([Figure 4A](#) and [Supplementary Figure 3](#)). The accumulation curves of the 18 transects surveyed were similar except for one transect with the lowest TCC of 7.06% (transect three at the shallow depth of Yehliu, see [Supplementary Table 3](#)), where its SD decreased faster than the rest of the transects ([Figure 4A](#) and [Supplementary Figure 3](#)). The average (and maximum) SD of the 18 transects was 45.58 (50.12), with one random sampling point selected. The SD declined to 11.62 (13.56), 8.29 (9.18), 5.80 (6.77), 3.54 (4.08), 2.33 (2.77), and 1.16 (1.32) when random sampling point numbers selected were 15 (PIT 100), 30 (PIT 50), 60 (PIT 25), 150 (PIT 10), 300 (PIT 5), and 750 (PIT 2), respectively ([Figure 4A](#) and [Table 2](#)). Of the 18 transects, 14 transects fell within the range of accuracy, i.e., with SD <3.92, when using 150 random sampling points (PIT 10), while three and one transects fell within the range of accuracy when using 300 (PIT 5) and 60 sampling points (PIT 25). All 18 transects showed SD values outside of the range of accuracy for PIT 2, PIT 50, and PIT 100. Therefore, overall, PIT 10 was determined as the optimum sampling interval for PIT ([Supplementary Table 4](#)). Meanwhile, there was no significant difference in the optimum sampling interval recommended between the tropical coral reefs and the non-reefal coral communities (Mann-Whitney Test,  $p = 0.36$ ).

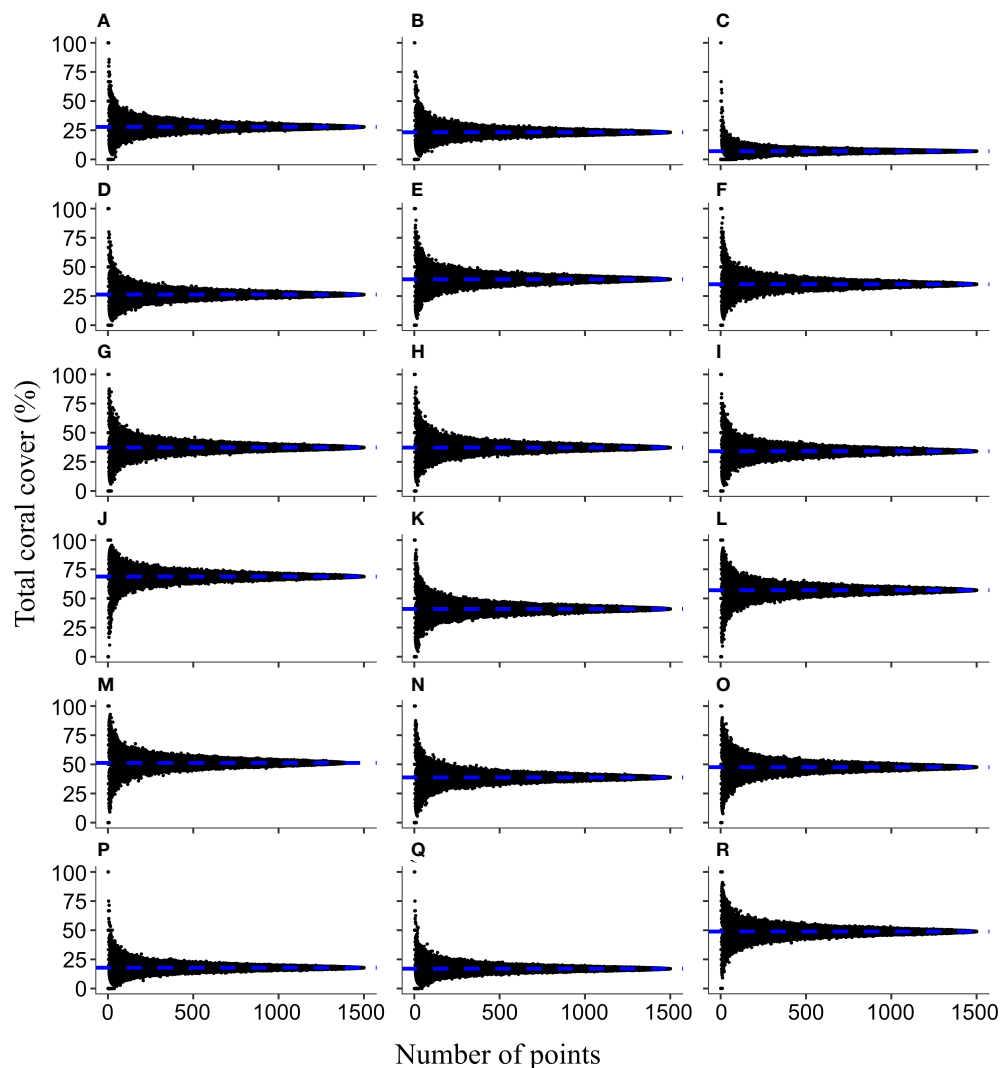


FIGURE 3

The bell-shaped distribution of the total coral cover (TCC) in relation to the number of random sampling points generated by bootstrap sampling on 18 LIT datasets. The eighteen communities were in the shallow (A–C) and deep sites (D–F) in Yehliu, the shallow sites in Chinwan Inner Bay (G–I) and Kihaw (J–L), and the shallow (M–O) and deep sites (P–R) in Tiaoshi. The order of transects within each habitat is synchronized with the order in [Supplementary Table 3](#). The horizontal blue dashed line indicates the TCC of each transect measured with the LIT method.

In terms of dissimilarity of community compositions, there was a decreasing trend with decreasing sampling intervals between the LIT and PIT communities ([Figure 4B](#)). The differences in the average dissimilarity between LIT and PIT communities varied among transects, ranging between 0.06 and 0.60, with an average of 0.29 at PIT 100. The average (and highest) dissimilarity values of the 18 transects were reduced to 0.23 (0.53), 0.17 (0.46), 0.11 (0.29), 0.06 (0.19), and 0.02 (0.05) at PIT 50, PIT 25, PIT 10, PIT 5, and PIT 2, respectively ([Figure 4B](#) and [Supplementary Table 5](#)). From the accumulation curves, three elbow points were detected among the 18 transects, with the majority (11 out of 18 transects) at 10 cm intervals (PIT 10), while only two and five transects at 5 cm intervals (PIT 5) and

2 cm intervals (PIT 2), respectively ([Figure 4B](#) and [Supplementary Table 5](#)).

### 3.3 Testing the dependency between optimum sampling interval and transect length

The average SD of individual 200 PIT communities at the same interval among the 30 equal-length subset transects decreased with increasing transect length ([Figures 5A, C, E, G](#), and [Table 2](#)). The PIT interval where the average SD fell within the range of accuracy ( $SD < 3.92$ ) were PIT 5 for 10-m transects,



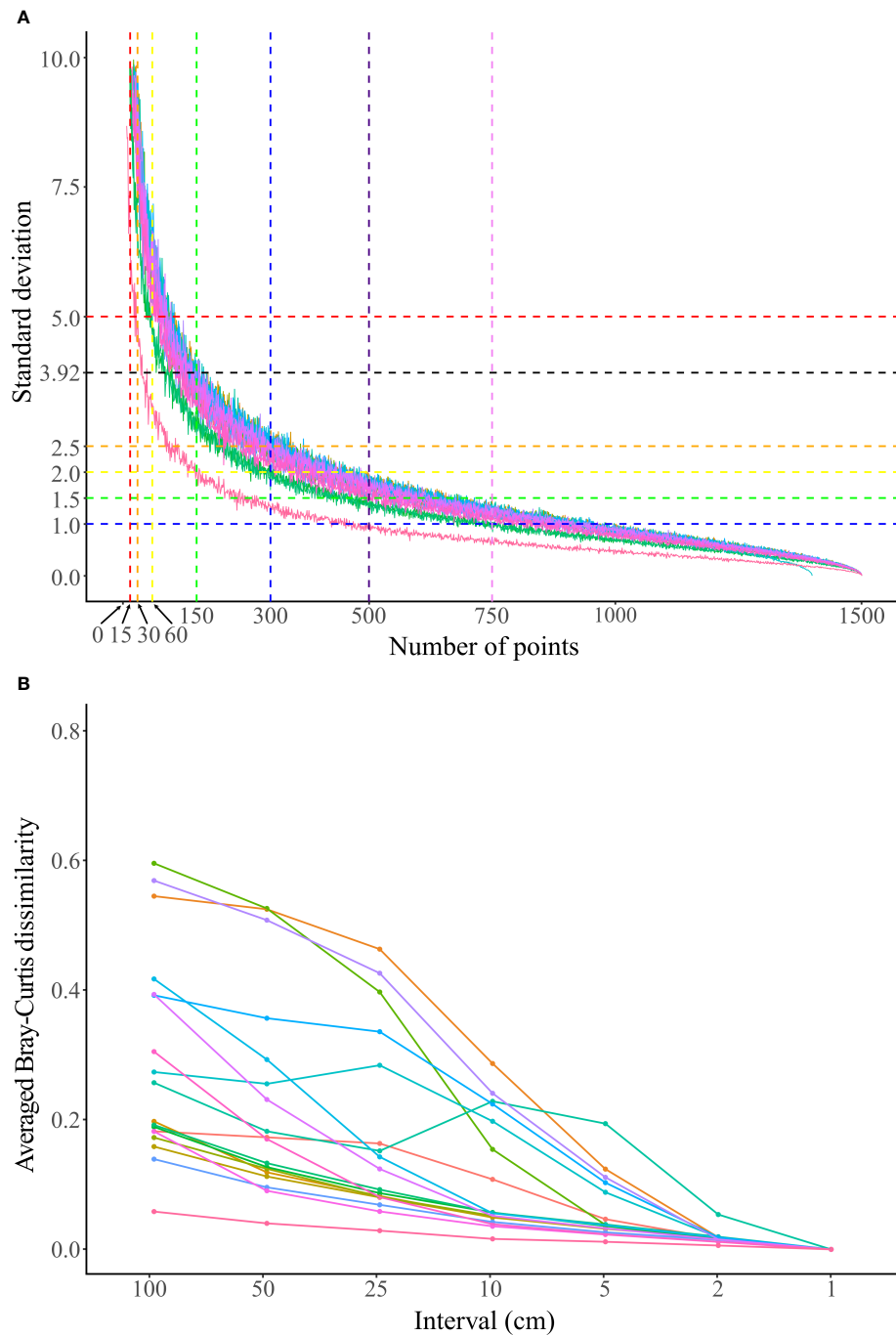


FIGURE 4

(A) The standard deviation (SD) of the TCC of each set of 200 PIT communities with different randomly sampling points from 15 m transects. The horizontal dashed lines mark SDs of 5 (red), 3.92 (black), 2.5 (orange), 2 (yellow), 1.5 (green), and 1 (blue), and the vertical dashed lines mark the number of points using PIT 100 (15 points, red), PIT 50 (30 points, orange), PIT 25 (60 points, yellow), PIT 10 (150 points, green), PIT 5 (300 points, blue), PIT 3 (500 points, indigo), and PIT 2 (750 points, purple). (B) The Bray-Curtis dissimilarity index between the PIT community and the LIT community on the same transect. Each dot represents the average of 200 PIT communities with the same interval. The color of the accumulation curves represent the 18 transects surveyed and are referred to in [Supplementary Figure 3](#).

**TABLE 2** The average (maximum) standard deviation of the total coral cover of 200 PIT communities using six different sampling intervals (PIT 100, PIT 50, PIT 25, PIT 10, PIT 5, and PIT 2) for different lengths of transect.

Transect length (m)	Interval (cm)					
100	50	25	10	5	2	
10	13.78 (16.34)	9.67 (11.88)	6.69 (8.33)	4.07 (4.99)	2.74 (3.50)	1.38 (1.79)
15	11.62 (13.56)	8.29 (9.18)	5.80 (6.77)	3.54 (4.08)	2.33 (2.77)	1.16 (1.32)
20	10.21 (11.59)	7.18 (8.48)	5.04 (5.81)	3.06 (3.61)	2.07 (2.52)	1.02 (1.20)
30	8.34 (10.08)	5.74 (6.67)	4.05 (4.72)	2.53 (3.00)	1.70 (1.96)	0.85 (0.99)
40	7.10 (8.44)	5.10 (5.88)	3.57 (3.97)	2.19 (2.56)	1.46 (1.73)	0.71 (0.83)

PIT 10 for 20-m and 30-m transects, and PIT 25 for the 40-m transect (Table 2). More strictly, by only accounting for the maximum SD <3.92, the optimum sampling intervals were PIT 5 for 10-m transects and PIT 10 for 20-m, 30-m, and 40-m transects (Figures 5A, C, E, G, and Table 2). As shown on the accumulation curves of the average Bray-Curtis dissimilarity index, the elbow points were detected between PIT 10 and PIT 2, regardless of transect length (Figures 5B, D, F, H).

### 3.4 Total coral cover error estimated by the Point Intercept Transect method compared to the Line Intercept Transect method

The TCC measured by the PIT method was closer to those by the LIT method at finer sampling intervals (Figure 6A). The RMSE curve showed a decreasing trend with decreasing sampling intervals, with the elbow identified at the 10 cm sampling interval (PIT 10) (Figure 6B).

## 4 Discussion

Our analysis revealed that current sampling intervals of the PIT method used in the literature could not accurately estimate the status of the benthic community, specifically the TCC, and act as an alternative to replace the LIT method. Instead, the range between 2 cm (PIT 2) and 10 cm (PIT 10) were better options, depending on the transect length and statistics parameters used (Table 2).

A 10 cm interval (PIT 10) is the recommended sampling interval in most of our study combinations of point interval and transect length. It is between the recommended 4 cm and 25 cm intervals in two other studies conducted in Brazil and Réunion Island (Segal and Castro, 2001; Facon et al., 2016). The variation between those studies and our study might be attributed to the taxonomic resolution, statistical methods used, and the reef environment of each study area. Segal and Castro (2001) sought an interval for measuring the cover of individual species rather than TCC. Finer operational taxonomic units

(OTUs) require shorter intervals. For instance, PIT 25 is sufficient for identifying the ten OTUs used by the Tropical Program of Reef Check while PIT 10 is necessary for identifying over 30 OTUs, including identifying corals to the genus level, as reported in the study conducted at Réunion Island (Facon et al., 2016).

The statistical methods also play a role in determining the optimum sampling interval. Both our study and that of Facon et al. (2016) discriminate the optimal sampling interval by identifying the elbow on the accumulation curves of the dissimilarity between PIT and LIT communities with ten OTUs. Yet, our result (PIT 2) was more conservative when using the Bray-Curtis dissimilarity index than the result (PIT 25) of Facon et al. (2016), which used Pearson correlation coefficients (Legendre and Legendre, 1998).

The variation in the status of benthic communities also alters the optimum sampling interval. Theoretically, TCC, coral colony abundance, colony size distribution, and pattern of colonies distributed along the transect would affect how quickly reaching an optimum interval in the PIT method. In our study, it requires the highest number of sampling points to achieve the optimum interval on the transect with 50% of TCC. The number was reduced along with either a decrease or an increase in TCC (Supplementary Table 4). While our study was conducted on reefs across well-developed tropical coral reefs and non-reefal coral communities, Segal and Castro (2001) and Facon et al. (2016)'s work were conducted on the less-developed reefs in the Abrolhos Archipelago, Brazil, and the Indian Ocean reefs on Réunion Island, respectively. It is hard to distinguish what causes the difference in the recommended optimum sampling intervals without the knowledge of the reef status. This highlights the need to further research on how the distribution patterns of the benthic community affect the accuracy of survey methods.

Our study showed that there was no significant difference in optimum intervals between the tropical coral reefs and non-reefal coral communities. The influence of habitat structure on benthic community composition was more significant with an increase in transect length (Figures 4B, 5B, D, F, H). The lack of a similar pattern among transects in the same type of reef indicates that the complexity of the

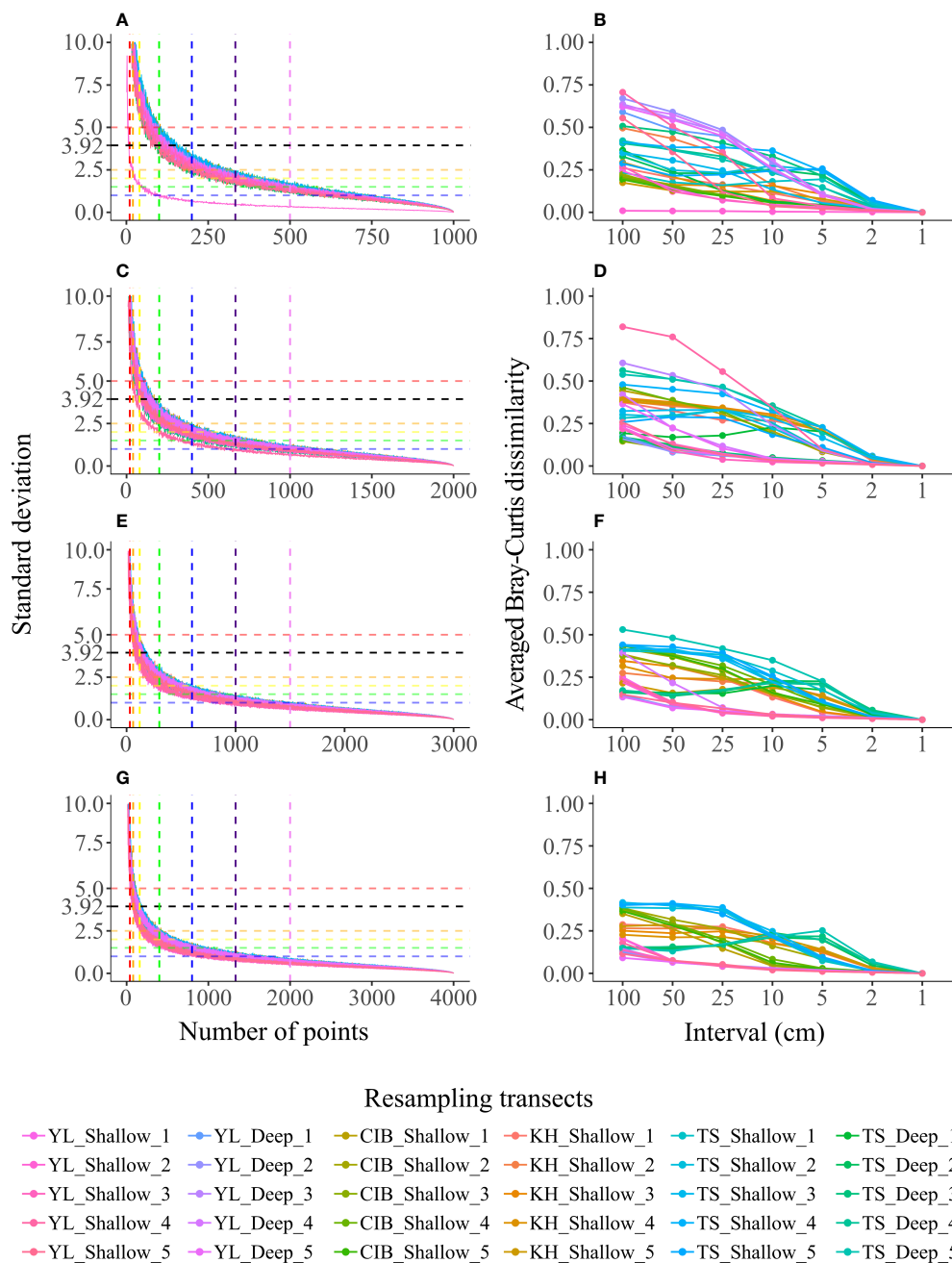


FIGURE 5

The accumulation curves of the standard deviation (SD) of the TCC of each set of 200 PIT communities with different randomly sampled points (A, C, E, G), and the average of the 200 Bray-Curtis dissimilarity indexes between each PIT community at the same interval and LIT community (B, D, F, H) on different transect lengths. The transect lengths were 10 m (A, B), 20 m (C, D), 30 m (E, F), and 40 m (G, H). The horizontal dashed lines in A, C, E, G mark SDs of 5 (red), 3.92 (black), 2.5 (orange), 2 (yellow), 1.5 (green), and 1 (blue), and the vertical dashed lines mark the points used in PIT 100 (red), PIT 50 (orange), PIT 25 (yellow), PIT 10 (green), PIT 5 (blue), PIT 3 (indigo), and PIT 2 (purple).

benthic community within sites is more apparent than among reefs. This also suggests that the historical environmental conditions have significantly changed recently due to increasing natural disturbances and human-induced stresses

at larger and local scales (Ribas-Deulofeu et al., 2016). Local stressors cause declines in reef conditions, reduce resilience, and postpone recovery from natural disturbances (Carilli et al., 2009; Ortiz et al., 2018). Under the stress of climate

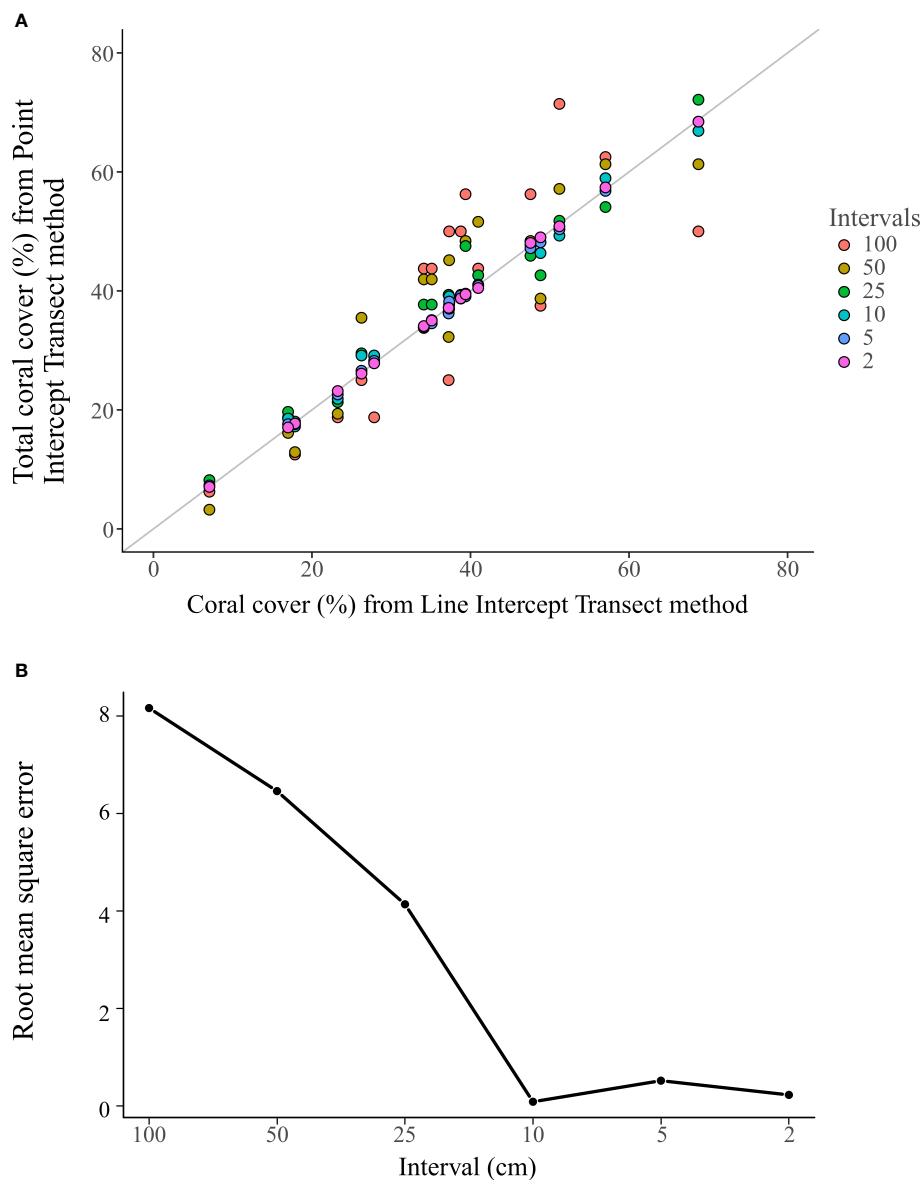


FIGURE 6

The total coral cover (TCC) of PIT communities generated from the 18 LIT communities survey over different sampling intervals. Each dot represents one PIT community, and colors indicate different intervals (A). The root mean square error of the TCC measured using the PIT method to the TCC measured using the LIT method on each of the 18 transects at different sampling intervals (B).

change-induced extreme disturbances, such as more frequent and severe bleaching events (Hughes et al., 2018), typhoons (Tsuboki et al., 2015; Knutson et al., 2020), and the lack of the ability to recover between disturbances will prevent the full recovery of coral reefs and result in further degradation.

Previous coral reef monitoring studies using PIT 50 on non-permanent transects have reported high annual variations in TCC at the same survey sites without major disturbances between survey censuses (Dai et al., 2004; TEIA, 2016; TEIA, 2017). Our finding that the 50 cm sampling interval (PIT 50)

estimates a high variation of TCC might explain the high temporal changes in those studies, as well as emphasize the necessity of using non-permanent transects. Using non-permanent transects for long-term monitoring reduces the effort to set up and maintain the markers and the time consumed in searching for transect markers. This method benefits most when surveyors are familiar with the reef and the benthic community composition is homogeneous within the target survey area. However, several issues need to be considered. First, human errors, such as misidentifying the



starting point and direction of transects, are unavoidable. The issue is more profound on less-developed or patchily distributed coral communities. Even a slight displacement of starting point or direction would result in a significantly different community composition. Second, success in consistently relocating the survey spot is highly reliant on the participation of a few experienced key members. It means the project is exposed to the risk of inconsistency in data collection over the long term. Extra care is necessary for interpreting monitoring results.

Applying the permanent transect method requires extra work on marker maintenance; however, it can benefit monitoring programs. It improves the quality of data because it is more consistent, repeatable, and reliable. The results are comparable across survey censuses, and the changes in benthic communities can be more confidently attributed to environmental changes rather than the errors in the sampling method (summary in Hill and Wilkinson, 2004). In addition, permanent transects set up in the field can be used for a variety of projects from citizen science programs to long-term ecological monitoring projects and fine-scale research such as a demographic approach to understand the dynamics of scleractinians in the reef (Edmunds and Riegl, 2020), which enables the enhancement of the quality of citizen science education and helps improve the management strategies.

A comprehensive understanding of the status of coral reef benthic communities requires cooperation between both coral reef scientists and citizen scientists to conduct the survey with consistent and comparable methods. Our results suggest that a 10 cm sampling interval is the minimum necessary when using the PIT method as an alternative to the LIT method. In addition, our results highlight the need for setting up permanent transects for long-term monitoring purposes, as suggested by Reef Check (Hodgson et al., 2006) and GCRMN (Hill and Wilkinson, 2004), to improve the consistency, repeatability, and reliability of data collection (Hill and Wilkinson, 2004).

## Data availability statement

The datasets presented in this study can be found in online repositories. The names of the repository/repositories and accession number(s) can be found below: Kuo et al. (2022b), Data from: Fine intervals are required when using point intercept transects to assess coral reef status, Dryad, Dataset, <https://doi.org/10.5061/dryad.0rxwdb35>.

## Author contributions

C-YK, C-HT, HH, and CC conceived the study. C-YK, A-TH, Y-YH, and CC conducted the field survey. CC conducted

benthic community component identifications. C-YK and A-TH conducted data wrangling. C-YK and C-HT conceived and performed the statistics. C-YK, Y-YH, and WH wrote the first draft of the manuscript. All authors have read and approved the submitted version.

## Funding

This study was funded by the Ocean Conservation Administration, Ocean Affairs Council, Taiwan (grant no. 108-C-9), and Biodiversity Research Center, Academia Sinica.

## Acknowledgments

Many thanks to Ai-Chi Chung and Meng-Yun Hsieh for helping in conducting the fieldwork and the lab members of the Coral Reef Evolutionary and Ecological Genetic Laboratory of the Biodiversity Research Center, Academia Sinica, Taiwan, and the Penghu Marine Biology Research Center, Fisheries Research Institute, Council of Agriculture, Taiwan, for providing logistical support. We would like to thank Buford C. Pruitt, Jr. for English editing and Dr. Chun-Lin Lee for the comments on the visual guide of resampling procedures. We appreciate the reviewers and editors who assisted in improving this manuscript.

## Conflict of interest

The authors declare that the research was conducted in the absence of any commercial or financial relationships that could be construed as a potential conflict of interest.

## Publisher's note

All claims expressed in this article are solely those of the authors and do not necessarily represent those of their affiliated organizations, or those of the publisher, the editors and the reviewers. Any product that may be evaluated in this article, or claim that may be made by its manufacturer, is not guaranteed or endorsed by the publisher.

## Supplementary material

The Supplementary Material for this article can be found online at: <https://www.frontiersin.org/articles/10.3389/fmars.2022.795512/full#supplementary-material>

## SUPPLEMENTARY FIGURE 1

The accumulation curves of the standard deviation of the TCC of each set of 200 (A), 500 (B), and 1000 (C) PIT communities by the bootstrap method with different randomly sampled points.

## SUPPLEMENTARY FIGURE 2

The visual guide of the resampling procedure to testing if the optimum sampling interval depends on transect length.

## SUPPLEMENTARY FIGURE 3

The standard deviation (SD) of the TCC of each set of 200 PIT communities having different randomly sampled points used on each 15 m transect surveyed. Horizontal dashed lines mark SDs of 5 (red), 3.92 (black), 2.5 (orange), 2 (yellow), 1.5 (green), and 1 (blue), and the vertical dashed lines mark the number of points for PIT 100 (15 points, red), PIT 50 (30 points, orange), PIT 25 (60 points, yellow), PIT 10 (150 points, green), PIT 5 (300 points, blue), PIT 3 (500 points, indigo), and PIT 2 (750 points, purple). The color of the accumulation curves represents the 18 transects surveyed.

## References

- Adjeroud, M., Augustin, D., Galzin, R., and Salvat, B. (2002). Natural disturbances and interannual variability of coral reef communities on the outer slope of Tiahura (Moorea, French Polynesia): 1991 to 1997. *Mar. Ecol. Prog. Ser.* 237, 121–131. doi: 10.3354/meps237121
- Adjeroud, M., Michonneau, F., Edmunds, P. J., Chancerelle, Y., Loma, T. L., Penin, L., et al. (2009). Recurrent disturbances, recovery trajectories, and resilience of coral assemblages on a South Central Pacific reef. *Coral Reefs* 28, 775–780. doi: 10.1007/s00338-009-0515-7
- Beenaerts, N., and Berghe, E. V. (2005). Comparative study of three transect methods to assess coral cover, richness and diversity. *West Ind. Oc. J. Mar. Sci.* 4, 29–38. doi: 10.4314/wiojms.v4i1.28471
- Beijbom, O., Edmunds, P. J., Roelfsema, C., Smith, J., Kline, D. I., Neal, B. P., et al. (2015). Towards automated annotation of benthic survey images: Variability of human experts and operational modes of automation. *PLoS One* 10, e0130312. doi: 10.1371/journal.pone.0130312
- Bray, J. R., and Curtis, J. T. (1957). An ordination of the upland forest communities of southern Wisconsin. *Ecol. Monogr.* 27, 325–349. doi: 10.2307/1942268
- Bros, W. E., and Cowell, B. C. (1987). A technique for optimizing sample size (replication). *J. Exp. Mar. Biol. Ecol.* 114, 63–71. doi: 10.1016/0022-0981(87)90140-7
- Bryson, M., Ferrari, R., Figueira, W., Pizarro, O., Madin, J., Williams, S., et al. (2017). Characterization of measurement errors using structure-from-motion and photogrammetry to measure marine habitat structural complexity. *Ecol. Evol.* 7, 5669–5681. doi: 10.1002/ece3.3127
- Burns, J. H. R., Delparte, D., Gates, R. D., and Takabayashi, M. (2015). Integrating structure-from-motion photogrammetry with geospatial software as a novel technique for quantifying 3D ecological characteristics of coral reefs. *PeerJ* 3, e1077. doi: 10.7717/peerj.1077
- Carilli, J. E., Norris, R. D., Black, B. A., Walsh, S. M., and McField, M. (2009). Local stressors reduce coral resilience to bleaching. *PLoS One* 4, e6324. doi: 10.1371/journal.pone.0006324
- Dai, C.-F. (2018). “Chapter 7. coastal and shallower water ecosystem,” in *Regional Oceanography of Taiwan version II*, ed. S. Jan (Taipei, Taiwan: National Taiwan University Press), 263–299.
- Dai, C.-F., Soong, K., Jeng, M.-S., Chen, C. A., and Fan, T.-Y. (2004). *The Status of Coral Reefs in Taiwan* (Taipei, Taiwan: Council of Agriculture, Executive Yuan).
- Dodge, R. E., Logan, A., and Antonius, A. (1982). Quantitative reef assessment studies in Bermuda: a comparison of methods and preliminary results. *Bull. Mar. Sci.* 32, 745–760.
- Edmunds, P., and Riegl, B. (2020). Urgent need for coral demography in a world where corals are disappearing. *Mar. Ecol. Prog. Ser.* 635, 233–242. doi: 10.3354/meps13205
- Efron, B. (1979). Bootstrap methods: another look at jackknife. *Ann. Stat.* 7, 1–26. doi: 10.1214/aos/1176344552
- English, S. A., Wilkinson, C., and Baker, V. (1997). *Survey Manual for Tropical Marine Resources, 2nd Edn* (Townsville, Australia, Australian Institute of Marine Science).
- Facon, M., Pinault, M., Obura, D., Pioch, S., Pothin, K., Bigot, L., et al. (2016). A comparative study of the accuracy and effectiveness of line and point intercept transect methods for coral reef monitoring in the southwestern Indian ocean islands. *Ecol. Indic.* 60, 1045–1055. doi: 10.1016/j.ecolind.2015.09.005
- Francini-Filho, R. B., Coni, E. O. C., Meirelles, P. M., Amado-Filho, G. M., Thompson, F. L., Pereira-Filho, G. H., et al. (2013). Dynamics of coral reef benthic assemblages of the Abrolhos Bank, Eastern Brazil: inferences on natural and anthropogenic drivers. *PLoS One* 8, e54260. doi: 10.1371/journal.pone.0054260
- Graham, N. A. J., Chong-Seng, K. M., Huchery, C., Januchowski-Hartley, F. A., and Nash, K. L. (2014). Coral reef community composition in the context of disturbance history on the Great Barrier Reef, Australia. *PLoS One* 9, e101204. doi: 10.1371/journal.pone.0101204
- Hargreaves-Allen, V. A., Mourato, S., and Milner-Gulland, E. J. (2017). Drivers of coral reef marine protected area performance. *PLoS One* 12, e0179394. doi: 10.1371/journal.pone.0179394
- Harris, A., and Sheppard, C. (2008). “Status and recovery of the coral reefs of the Chagos Archipelago, British Indian Ocean Territory,” in *CORDIO Status Report 2008*, eds. D. Obura, J. Tamelander and O. Linden (Mombasa: CORDIO: Coastal Oceans Research and Development, Indian Ocean), 61–70.
- Hill, J., and Wilkinson, C. (2004). *Methods for Ecological Monitoring of Coral Reefs* (Townsville, Australia: Australian Institute of Marine Science). Available at: <https://www.cbd.int/doc/case-studies/ttc/ttc-00197-en.pdf>.
- Hodgson, G. (1999). A global assessment of human effects on coral reefs. *Mar. Pollut. Bull.* 38, 345–355. doi: 10.1016/S0025-326X(99)00002-8
- Hodgson, G., Hill, J., Kiene, W., Maun, L., Mihaly, J., Liebler, J., et al. (2006). *Reef Check Instruction Manual: A Guide to Reef Check Coral Reef Monitoring* (Pacific Palisades, California, USA: Reef Check Foundation).
- Hughes, T. P. (1996). Demographic approaches to community dynamics: a coral reef example. *Ecology* 77, 2256–2260. doi: 10.2307/2265718
- Hughes, T. P., Anderson, K. D., Connolly, S. R., Heron, S. F., Kerry, J. T., Lough, J. M., et al. (2018). Spatial and temporal patterns of mass bleaching of corals in the Anthropocene. *Science* 359, 80–83. doi: 10.1126/science.aan8048
- Hughes, T. P., and Jackson, J. B. C. (1985). Population dynamics and life histories of foliaceous corals. *Ecol. Monogr.* 55, 141–166. doi: 10.2307/1942555
- Jackson, J., Donovan, M., Cramer, K., and Lam, V. (2014). *Status and Trends of Caribbean Coral Reefs: 1970-2012* (Gland, Switzerland: Global Coral Reef Monitoring Network, IUCN).
- Kershaw, K. A. (1957). The use of cover and frequency in the detection of pattern in plant communities. *Ecology* 38, 291–299. doi: 10.2307/1931688
- Keshavmurthy, S., Kuo, C.-Y., Huang, Y.-Y., Carballo-Bolaños, R., Meng, P.-J., Wang, J.-T., et al. (2019). Coral reef resilience in Taiwan: lessons from long-term ecological research on the coral reefs of Kenting National Park (Taiwan). *J. Mar. Sci. Eng.* 7, 388. doi: 10.3390/jmse7110388
- Kimura, T., Chou, L. M., Huang, D., Tun, K., and Goh, E. (2022). *Status and Trends of East Asian Coral Reefs: 1983-2019* (Global Coral Reef Monitoring Network, East Asia Region).
- Knutson, T., Camargo, S. J., Chan, J. C. L., Emanuel, K., Ho, C.-H., Kossin, J., et al. (2020). Tropical cyclones and climate change assessment: part II: projected response to anthropogenic warming. *Bull. Am. Meteorol. Soc.* 101, E303–E322. doi: 10.1175/BAMS-D-18-0194.1
- Kohler, K. E., and Gill, S. M. (2006). Coral point count with Excel extensions (CPCe): a visual basic program for the determination of coral and substrate coverage using random point count methodology. *Comput. Geosci.* 32, 1259–1269. doi: 10.1016/j.cageo.2005.11.009
- Komyakova, V., Munday, P. L., and Jones, G. P. (2013). Relative importance of coral cover, habitat complexity and diversity in determining the structure of reef fish communities. *PLoS One* 8, e83178. doi: 10.1371/journal.pone.0083178
- Kuo, C.-Y., Keshavmurthy, S., Huang, Y.-Y., Ho, M.-J., Hsieh, H. J., Hsiao, A.-T., et al. (2022a). “Transitional coral ecosystems of Taiwan in the era of changing climate,” in *Coral Reefs of the Eastern Asia under Anthropogenic Impacts*, eds. I. Takeuchi and H. Yamashiro (Cham, Switzerland: Springer Nature).
- Kuo, C.-Y., Tsai, C.-H., Huang, Y.-Y., Heng, W. K., Hsiao, A.-T., Hsieh, H. J., et al. (2022b). *Data from: Fine intervals are required when using point intercept transects to assess coral reef status, Dryad, Dataset*. doi: 10.5061/dryad.0rxwdb35

- Legendre, P., and Legendre, L. (1998). *Numerical Ecology. 2nd English Edn* (Amsterdam: Elsevier).
- Loya, Y. (1972). Community structure and species diversity of hermatypic corals at Eilat, Red Sea. *Mar. Biol.* 13, 100–123. doi: 10.1007/BF00366561
- Loya, Y. (1978). "Plotless and transect methods," in *Coral Reefs: Research Methods*, eds. D. R. Stoddart and R. E. Johannes (Paris: UNESCO), 197–217.
- Loya, Y., and Slobodkin, L. B. (1971). The coral reefs of Eilat (Gulf of Eilat, Red Sea). *Symp. Zool. Soc. Lond.* 28, 117–139.
- Manly, B. F. J. (1992). Bootstrapping for determining sample sizes in biological studies. *J. Exp. Mar. Biol. Ecol.* 158, 189–196. doi: 10.1016/0022-0981(92)90226-Z
- Manly, B. F. J. (2007). *Randomization, Bootstrap and Monte Carlo Methods in Biology, 3rd Edn* (New York: Chapman and Hall/CRC).
- Nadon, M.-O., and Stirling, G. (2006). Field and simulation analyses of visual methods for sampling coral cover. *Coral Reefs* 25, 177–185. doi: 10.1007/s00338-005-0074-5
- Obura, D., Gudka, M., Samoilys, M., Osuka, K., Mbugua, J., Keith, D. A., et al. (2022). Vulnerability to collapse of coral reef ecosystems in the Western Indian Ocean. *Nat. Sustain.* 5, 104–113. doi: 10.1038/s41893-021-00817-0
- Ohlhorst, S. L., Liddell, W. D., Taylor, R. J., and Taylor, J. M. (1988). "Evaluation of reef census techniques," in *Proceedings of the 6th International Coral Reef Symposium*, Vol. 2, Townsville, QLD, Australia. 319–324.
- Oksanen, J., Blanchet, F. G., Friendly, M., Kindt, R., Legendre, P., McGlinn, D., et al. (2020) *Vegan: Community Ecology package. version 2.5-7*. Available at: <https://CRAN.R-project.org/package=vegan>.
- Ortiz, J.-C., Wolff, N. H., Anthony, K. R. N., Devlin, M., Lewis, S., and Mumby, P. J. (2018). Impaired recovery of the Great Barrier Reef under cumulative stress. *Sci. Adv.* 4, earr6127. doi: 10.1126/sciadv.aar6127
- Pillar, V. D. (1998). Sampling sufficiency in ecological surveys. *Bot. Stud.* 22, 37–48.
- Pizarro, O., Friedman, A., Bryson, M., Williams, S. B., and Madin, J. (2017). A simple, fast, and repeatable survey method for underwater visual 3D benthic mapping and monitoring. *Ecol. Evol.* 7, 1770–1782. doi: 10.1002/ece3.2701
- Porter, J. W. (1972). Patterns of species diversity in Caribbean reef corals. *Ecology* 53, 745–748. doi: 10.2307/1934796
- Pratchett, M. S., Trapon, M., Berumen, M. L., and Chong-Seng, K. (2011). Recent disturbances augment community shifts in coral assemblages in Moorea, French Polynesia. *Coral Reefs* 30, 183–193. doi: 10.1007/s00338-010-0678-2
- R Core Team (2020). *R: A Language and Environment for Statistical Computing* (Vienna, Austria: R Foundation for Statistical Computing). Available at: <https://www.R-project.org/>.
- Ribas-Deulofeu, L., Denis, V., De Palmas, S., Kuo, C.-Y., Hsieh, H. J., and Chen, C. A. (2016). Structure of benthic communities along the Taiwan latitudinal gradient. *PLoS One* 11, e0160601. doi: 10.1371/journal.pone.0160601
- Russ, G. R., Rizzari, J. R., Abesamis, R. A., and Alcala, A. C. (2021). Coral cover a stronger driver of reef fish trophic biomass than fishing. *Ecol. Appl.* 31, e02224. doi: 10.1002/eap.2224
- Segal, B., and Castro, C. B. (2001). A proposed method for coral cover assessment: a case study in Abrolhos, Brazil. *Bull. Mar. Sci.* 69, 487–496.
- Selig, E. R., and Bruno, J. F. (2010). A global analysis of the effectiveness of marine protected areas in preventing coral loss. *PLoS One* 5, e9278. doi: 10.1371/journal.pone.0009278
- Souter, D., Planes, S., Wicquart, J., Logan, M., Obura, D., and Staub, F. (2020). "Chapter 2. Status of coral reefs of the world," in *Status of Coral Reefs of the World: 2020* (The Global Coral Reef Monitoring Network and the International Coral Reef Initiative). <https://gcrmn.net/2020-report/>
- Stoddart, D. R. (1969). Ecology and morphology of recent coral reefs. *Biol. Rev.* 44, 433–498. doi: 10.1111/j.1469-185X.1969.tb00609.x
- Stoddart, D. R. (1972). "Field methods in the study of coral reefs," in *Proceedings of the first international symposium on corals and coral reefs*, Mandapam Camp, India. 71–80.
- Strain, E. M. A., Edgar, G. J., Ceccarelli, D., Stuart-Smith, R. D., Hosack, G. R., and Thomson, R. J. (2019). A global assessment of the direct and indirect benefits of marine protected areas for coral reef conservation. *Divers. Distrib.* 25, 9–20. doi: 10.1111/ddi.12838
- TEIA (2016). *Reef Check Taiwan Annual Survey Report 2016* (Taipei, Taiwan: Taiwan Environmental Information Association). Available at: <https://www.slideshare.net/reefcheck/2016-70458046>.
- TEIA (2017). *Reef Check Taiwan Annual Survey Report 2017* (Taipei, Taiwan: Taiwan Environmental Information Association). Available at: <https://www.slideshare.net/reefcheck/2017-108449450>.
- Tsai, C.-H., Sweatman, H. P. A., Thibaut, L. M., and Connolly, S. R. (2022). Volatility in coral cover erodes niche structure, but not diversity, in reef fish assemblages. *Sci. Adv.* 8, eabm6858. doi: 10.1126/sciadv.abm6858
- Tsuboki, K., Yoshioka, M. K., Shinoda, T., Kato, M., Kanada, S., and Kitoh, A. (2015). Future increase of supertyphoon intensity associated with climate change. *Geophys. Res. Lett.* 42, 646–652. doi: 10.1002/2014GL061793
- Wilkinson, C. (2000). *Status of Coral Reefs of the World: 2000* (Townsville, Australia: Australian Institute of Marine Science). Available at: <https://gcrmn.net/resource/status-coral-reefs-world-2000/>.
- Wilkinson, C. (2002). *Status of Coral Reefs of the World: 2002* (Townsville, Australia: Australian Institute of Marine Science). Available at: <https://gcrmn.net/resource/status-coral-reefs-world-2002/>.
- Wilkinson, C. (2004). *Status of Coral Reefs of the World: 2004, Vol. 1* (Townsville, Australia: Australian Institute of Marine Science). Available at: <https://gcrmn.net/resource/status-coral-reefs-world-2004-volume-1/>.
- Wilkinson, C. (2008). *Status of Coral Reefs of the World: 2008* (Townsville, Australia: Global Coral Reef Monitoring Network and Reef and Rainforest Research Centre). Available at: <https://gcrmn.net/resource/status-coral-reefs-world-2008/>.
- Wilson, J., and Green, A. (2009). *Biological Monitoring Methods for Assessing Coral Reef Health and Management Effectiveness of Marine Protected Areas in Indonesia* (Bali, Indonesia: The Nature Conservancy).

# Advantages of publishing in Frontiers



## OPEN ACCESS

Articles are free to read  
for greatest visibility  
and readership



## FAST PUBLICATION

Around 90 days  
from submission  
to decision



## HIGH QUALITY PEER-REVIEW

Rigorous, collaborative,  
and constructive  
peer-review



## TRANSPARENT PEER-REVIEW

Editors and reviewers  
acknowledged by name  
on published articles

## Frontiers

Avenue du Tribunal-Fédéral 34  
1005 Lausanne | Switzerland

**Visit us:** [www.frontiersin.org](http://www.frontiersin.org)

**Contact us:** [frontiersin.org/about/contact](http://frontiersin.org/about/contact)



## REPRODUCIBILITY OF RESEARCH

Support open data  
and methods to enhance  
research reproducibility



## DIGITAL PUBLISHING

Articles designed  
for optimal readership  
across devices



## FOLLOW US

@frontiersin



## IMPACT METRICS

Advanced article metrics  
track visibility across  
digital media



## EXTENSIVE PROMOTION

Marketing  
and promotion  
of impactful research



## LOOP RESEARCH NETWORK

Our network  
increases your  
article's readership